Analysis of Wildfire Impacts on High Ozone Days in Houston, Beaumont, and Dallas-Fort Worth during 2012 and 2013

Final Report:
WO582-11-10365-FY14-19

Prepared for:
Jonathan Steets
Texas Commission on Environmental Quality
12100 Park 35 Circle MC 164
Austin, TX, 78711

Prepared by:
Sue Kemball-Cook, Thomas Pavlovic, Jeremiah Johnson, Lynsey Parker, DJ Rasmussen, Justin Zagunis, Lan Ma and Greg Yarwood
ENVIRON International Corporation
773 San Marin Drive, Suite 2115
Novato, California, 94998
www.environcorp.com
P-415-899-0700
F-415-899-0707

July 2014

ENVIRON

CONTENTS

TABLES

FIGURES

EXECUTIVE SUMMARY

The purpose of this study was to assess whether the 2012 and 2013 design values for the Houston-Galveston-Brazoria (HGB), Beaumont-Port Arthur (BPA), and Dallas-Fort Worth (DFW) areas may have been influenced by wildfire emissions, and whether any days contributing to the design value might be excluded from comparison with the National Ambient Air Quality Standard (NAAQS) for ozone under the Exceptional Events Rule (EER). For a day to be excluded from comparison with the NAAQS, an event must meet the following four criteria:

1. The event meets the definition of exceptional event (40 CFR §50.1(j); i.e. affects air quality, is a natural event or human activity unlikely to recur in same location and is not reasonably preventable)
2. There was a clear, causal relationship between the 8-hour ozone concentrations at the affected monitors and the specified event;
3. The measured values were in excess of normal historical fluctuations; and
4. No exceedance would have occurred but for the event.

Wildfires are considered by the EPA to meet the first criterion, and prescribed fires may also satisfy this criterion.

We reviewed the four highest 8-hour ozone days in 2012 and 2013 at the monitors with the highest and second-highest design values in the HGB and DFW areas as well as the monitor with the highest design value in the BPA area and two additional days selected by the TCEQ at the Seabrook and La Porte monitors in the HGB area. For each of these high ozone days, we evaluated the potential for fire emissions to have influenced monitored ozone. We reviewed available ambient monitoring data, model data, emission inventories and satellite products, and determined whether emissions from fires are likely to have contributed to high ozone at monitors with high ozone on each day.

For each day where a clear, causal relationship with upwind fire(s) was evident, we determined whether the measured daily maximum 8-hour ozone concentration (MDA8) was in excess of normal historical fluctuations by analyzing the frequency distribution of MDA8 ozone at that monitor for the period 2006-2013 and assessing whether the day in question had MDA8 above the 95th percentile. All days that satisfied EER criteria 1-3 above are listed in Table ES-01. These days were analyzed further by modeling them with the Comprehensive Air Quality Model with Extensions (CAMx; ENVIRON 2014a) photochemical grid model to estimate the contribution to the MDA8 ozone from fire emissions. For each monitor and day, we performed a modeling assessment of whether an exceedance/violation would have occurred but for the event. The results are summarized in Table ES-01.

No day contributing to 2013 design values for HGB, DFW or BPA monitors satisfied all four criteria, and the Seabrook and La Porte monitors do not satisfy all four criteria on the two additional days selected for analysis by the TCEQ, namely 3/24/12 and 9/25/13.

Table ES-01. Comparison of high ozone days showing clear, causal relationship with fire emissions with the remaining three EER criteria.

Date	Monitor Name	CAMS Number	Area	2013 Design Value (ppb)	Exceptional Event Rule Criteria			
					Fire(s) Present Upwind?	Clear Causal Relationship?	Concentration in Excess of Historical Backgound?	Passes "But-For" Test?
6/25/2012	Grapevine Fairway	70	DFW	86	Yes	Yes	Yes	No
6/25/2012	Denton Airport South	56	DFW	87	Yes	Yes	No	No
6/27/2012	Grapevine Fairway	70	DFW	86	Yes	Yes	Yes	No
6/27/2012	Denton Airport South	56	DFW	87	Yes	Yes	Yes	No
7/3/2013	Northwest Harris Co.	26	HGB	82	Yes	Yes	Yes	No
7/4/2013	Manvel Croix	84	HGB	87	Yes	Yes	Yes	No
7/4/2013	Sabine Pass	640	BPA	75	Yes	Yes	Yes	No
9/25/2013	Seabrook	45	HGB	77	Yes	Yes	Yes	No
9/25/2013	La Porte	556	HGB	78	Yes	Yes	Yes	No

The photochemical modeling results showed that none of the 2012 or 2013 days evaluated passed the EER “but-for” test. Modeled impacts on MDA8 ozone due to fire emissions were sufficiently small that no violations or exceedances of the NAAQS would be removed by subtracting the modeled ozone impacts of fire emissions from the observed MDA8. However, it is important to note the uncertainties inherent in photochemical modeling of fires and their impact on ozone.

The modeled ozone impacts of fires depend on accurate characterization of fire emissions and simulation of the transport, chemical transformation, and fate of emitted ozone precursors and the ozone that forms from them. Fire emissions contain uncertainties in both their magnitude and their chemical composition (e.g. Wiedinmyer et al. 2011; Jaffe and Wigder, 2012). The chemical composition of the emissions plays a role in the photochemistry of the resulting fire plume and therefore the resulting ozone impact.

The chemistry of ozone production in fire plumes is an area of active research. Measurement campaigns in which aircraft made transects through fire plumes and measured ozone and other trace gases have produced a range of results regarding the magnitude of ozone production in fire plumes (e.g. Bertschi et al., 2004; Alvarado et al; 2010). Jaffe and Wigder (2012) note that there is not a clear relationship between the quantity of ozone precursor emissions released into the atmosphere and the ozone produced in the plume downwind of the fire. Wigder et al. (2013) hypothesize that plume rise and the altitude of subsequent plume transport can affect ozone production in the plume because temperatures are lower at higher altitudes.

The interaction of fire plumes with anthropogenic emissions is not well understood. Singh et al. (2012) and Wigder et al. (2013) found enhanced ozone in fire plumes that mixed with air containing urban emissions. The presence of aerosols (smoke) in the fire plume can reduce the amount of sunlight available to initiate photochemistry, inhibiting ozone formation (e.g. Parrington et al., 2013). The TCEQ’s SIP modeling is focused on ozone and does not include

simulation of aerosols, so this "aerosol shading" mechanism is absent in our modeling of 2012 and 2013.

Photochemical modeling is one method of carrying out a "but-for" analysis for a candidate exceptional event, and other methods are available. For example, ozone concentrations at a given monitor on a high ozone day can be compared to ozone at that monitor on days when ozone was low but weather conditions were similar. By comparing days with comparable weather, the contribution of fire emissions to ozone at the monitor on a high ozone day can be estimated though comparison with ozone values on all other days with similar weather, implicitly making an assumption that the presence of the fire is the only source of difference.

Because all available methods of carrying out the "but-for" analysis have limitations, a weight of evidence approach may be indicated in which multiple analysis methods are carried out and the results compared. The conclusions from such a comparison would take into account the uncertainties inherent in each method.

The photochemical modeling performed in this study could be refined through the use of day-specific emission inventories. The WRF meteorological modeling of 2013 should be evaluated in more detail and sensitivity testing to determine whether a configuration can be found that better simulates the surface wind shifts on high ozone days should be performed Meteorological model evaluation for 2013 will be undertaken as part of Texas Air Quality Research Program (AQRP) Project 14-016. We did not evaluate the 2012 WRF meteorological model inputs to CAMx, but this should be done as well and further testing undertaken if problems with model performance are found.

The work plan for this project allowed for the Desert Research Institute (DRI) to analyze particulate matter (PM) filters collected at DFW and HGB area monitors for the presence of the biomass burning markers levoglucosan and mannosan in order to provide a definitive conclusion as to whether fire emissions influenced ozone at DFW and HGB monitors on days of interest. No filters were available for the BPA area (Richard Tropp, DRI, personal communication, 2014). Due to equipment malfunction, DRI was unable to carry out this analysis during the time frame of this study. Laboratory analysis of available PM filters for levoglucosan and mannosan will provide an unambiguous determination as to whether a fire plume was present at each monitor for which data are available and should be carried out when possible.

<u>Summary of Recommendations</u>

- Perform PM filter analysis for levoglucosan/mannosan for days listed in Table ES-01
- Carry out a "but-for" analysis using alternate method(s) and compare with photochemical modeling results
- Review the representation of chemistry of ozone formation within fire plumes in CAMx and evaluate whether updates to the model are required to allow accurate simulation of fire plumes in the TCEQ's SIP modeling

- Refine photochemical modeling analysis through the use of day-specific emissions and improvement of WRF model performance in simulating surface winds in the 2013 episodes

- Evaluate WRF model performance for 2012 and improve if necessary

1.0 INTRODUCTION

Wildfires can emit large quantities of trace gases and aerosols into the atmosphere. These emissions undergo chemical and physical changes as they are transported away from the active fire region. Primary emitted species are depleted as they are deposited and chemically processed, while secondary species such as ozone and secondary organic aerosols form within the fire plume. Research shows that both primary and secondary species can influence air quality at local and regional scales (e.g., Junquera et al., 2005; Jaffe et al., 2008, Hu et al., 2008, Jaffe and Wigder, 2012). Ozone and particulates formed in wildfire plumes can be transported to populated regions and can influence measured concentrations at air quality monitors.

The National Ambient Air Quality Standard (NAAQS) for ozone is violated at a monitor if the annual fourth highest daily maximum 8-hour average concentration averaged over three consecutive years exceeds a threshold value. This threshold is currently 0.075 ppm (75 ppb) under the current standard, which was set in 2008. A single year of data is not considered sufficient to demonstrate attainment; instead, the fourth highest value in a given year is used as an indicator of attainment status. Consequently, this statistic is referred to as the annual 8-hour design value.

The U.S. Environmental Protection Agency (EPA) allows the exclusion of monitoring data influenced by exceptional events such as wildfires or dust transport when determining attainment status for the NAAQS. States must demonstrate to the U.S. EPA that a wildfire event satisfies Exceptional Events Rule (EER) requirements. The EER (40 CFR §50.1(j)) defines an exceptional event to have these attributes:

- affects air quality;
- is not reasonably controllable or preventable; and
- is caused by human activity that is unlikely to recur at a particular location or is a natural event.

To exclude data for a given day from a monitor's 8-hour ozone design value calculation, the following must be demonstrated to show that an exceptional event occurred:

1. the event was not reasonably preventable;
2. there was a clear, causal relationship between the 8-hour ozone concentrations at the affected monitors and the specified event;
3. the measured values were in excess of normal historical fluctuations; and
4. no exceedance would have occurred but for the event.

Wildfires are considered by the EPA to meet the criterion of not being reasonably preventable, and prescribed fires may also satisfy this criterion.

The purpose of this project is to determine whether the 2012 and 2013 design values for the Houston-Galveston-Brazoria (HGB), Beaumont-Port Arthur (BPA), and Dallas-Fort Worth (DFW) areas were influenced by fire emissions, and whether any days contributing to the design value should be excluded from comparison with the NAAQS under the EER.

Figure 1-1 summarizes the analysis method and shows the procedure followed for each analyzed day. The purpose of the analysis was to apply the four EER criteria sequentially and eliminate days which did not meet each criterion. The steps in the analysis are shown in the gray shaded boxes and the methods used for each step are shown in the Analysis Method column on the left. First, we reviewed the four highest 8-hour ozone days in 2012 and 2013 at the monitors with the highest and second-highest design values in the HGB and DFW areas as well as the monitor with the highest design value in the BPA area and two days selected by the TCEQ at the Seabrook and La Porte monitors in the HGB area.

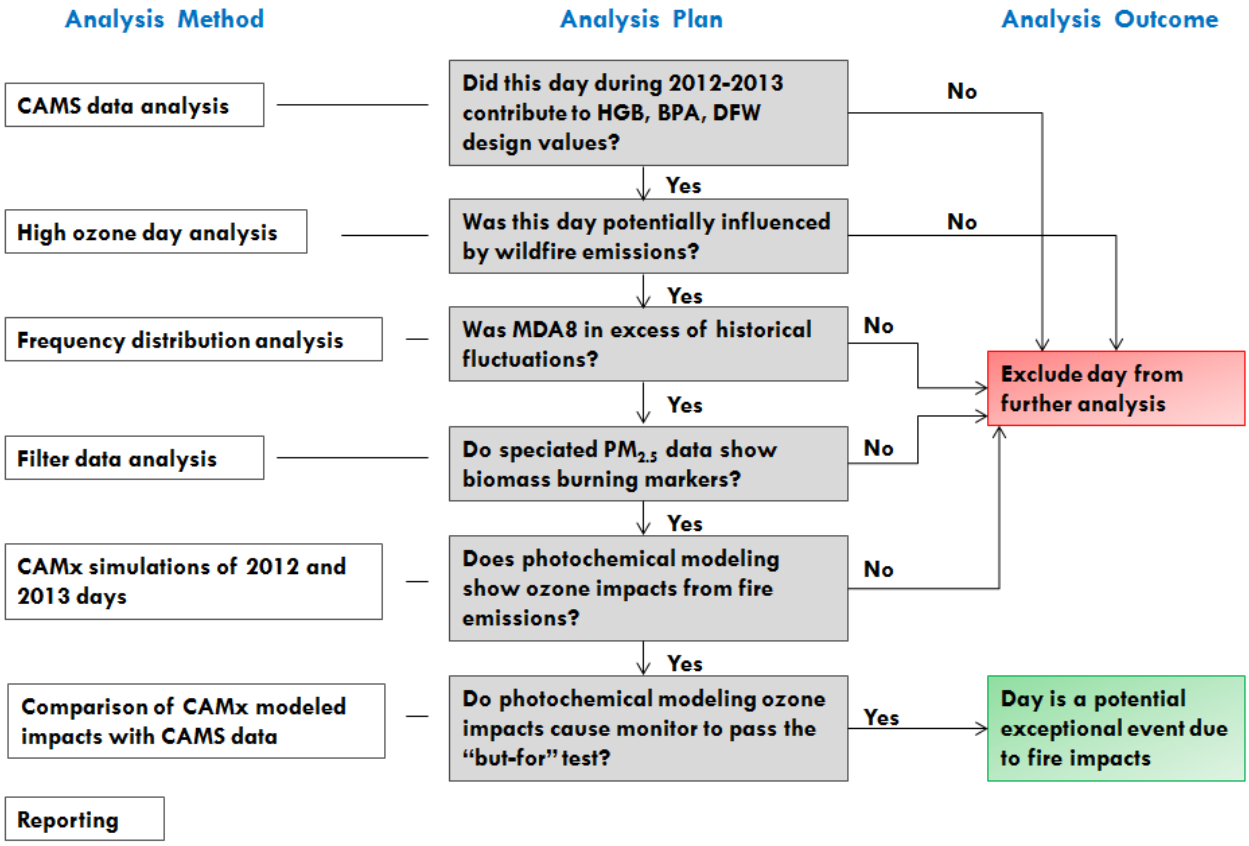

Figure 1-1. Summary of method for determining whether high ozone days meet the four EER criteria.

We selected the days to be reviewed using ozone data collected at regulatory Continuous Air Monitoring Stations (CAMS) in each area and reported on the Texas Commission on Environmental Quality (TCEQ) website[1]. Based on 2012-2013 ozone design values, the monitors shown in Table 1-1 were selected for analysis.

[1] http://www.tceq.state.tx.us/cgi-bin/compliance/monops/8hr_attainment.pl

Table 1-1. HGB, DFW and BPA area monitors selected for analysis.

Area	Monitor	2013 Design Value [ppb]
HGB	***Manvel Croix Park C84**	**87**
HGB	Northwest Harris Co. C26/A110/X154	82
HGB	+La Porte Sylvan Beach C556	78
HGB	+Seabrook Friendship Park C45	77
DFW	***Denton Airport South C56/A163/X157**	**87**
DFW	Grapevine Fairway C70/A301/X182	86
BPA	***SETRPC 40 Sabine Pass C640/C1654**	**75**

Area's design value monitor (highest design value in area's monitoring network)
+Selected for analysis by the TCEQ

The days with the four highest values of the daily maximum 8-hour average ozone (MDA8) during 2012 and 2013 at each monitor listed in Table 1-1 are shown in Table 1-2. These days were evaluated in this study to determine whether there was a clear, causal connection between high ozone at the monitor and fire emissions. For the Seabrook and La Porte monitors, the TCEQ selected the highest MDA8 day only for analysis, so the 2nd-4th high MDA8 days are shown in gray and were not evaluated. In Table 1-3, the days shown in Table 1-2 are listed according to geographic area and listed chronologically. There are a number of days which are among the four highest MDA8 ozone days at multiple monitor. For example, June 26 was one of the four highest MDA8 ozone days at monitors in HGB, DFW and BPA.

A total of thirteen days in 2012 and seventeen in 2013 were evaluated. In Section 2 of this report, we describe the methods and data used to evaluate the potential for fire emissions to have affected ozone on the days shown in black type in Table 1-2. The analysis of each high ozone day is presented in Section 3. Section 3 is organized chronologically (Table 1-3), and on days when multiple monitors had one of its 4 highest MDA8 values, an analysis of each monitor on that day is presented sequentially. In Section 4, we present an analysis of speciated $PM_{2.5}$ data for days determined in Section 3 to have a clear causal relationship between fires and ozone, and in Section 5, we evaluate these days to determine whether their ozone values were in excess of normal historical fluctuations. In Section 6, we present photochemical modeling results that address the question of whether each monitor would have had an exceedance/violation but for the fire emissions. Finally, in Section 7 we present a summary of results and recommendations for future work. The Technical Systems Audit is described in Section 8.

Table 1-2. Four highest 8-hr ozone days for HGB, BPA and DFW monitors and corresponding 8-hr ozone values (in ppb). Days shown in gray type were not analyzed in this study. Shading corresponds to the Air Quality Index (AQI) shown below the table. Data from TCEQ website http://www.tceq.state.tx.us/cgi-bin/compliance/monops/8hr_4highest.pl.

	Monitoring Site	Highest		Second Highest		Third Highest		Fourth Highest	
		Date	Value	Date	Value	Date	Value	Date	Value
2012	Manvel Croix Park C84	6/26/2012	136	6/25/2012	94	5/21/2012	90	9/20/2012	87
	Northwest Harris Co. C26	6/27/2012	99	3/26/2012	85	6/1/2012	84	5/17/2012	82
	La Porte Sylvan Beach C556	3/24/2012	109	3/25/2012	90	8/20/2012	88	6/26/2012	87
	Seabrook Friendship Park C45	3/24/2012	113	3/25/2012	95	8/20/2012	89	5/21/2012	86
	Grapevine Fairway C70	6/26/2012	97	6/25/2012	97	6/27/2012	92	6/24/2012	86
	Denton Airport South C56	6/27/2012	95	9/6/2012	89	5/17/2012	86	6/25/2012	81
	SETRPC 40 Sabine Pass C640	3/24/2012	92	3/25/2012	90	6/26/2012	79	5/22/2012	76
2013	Manvel Croix Park C84	8/16/2013	94	7/4/2013	86	6/3/2013	86	7/2/2013	84
	Northwest Harris Co. C26	8/28/2013	83	10/9/2013	82	5/13/2013	82	7/3/2013	80
	La Porte Sylvan Beach C556	9/25/2013	124	8/29/2013	71	7/13/2013	68	7/3/2013	68
	Seabrook Friendship Park C45	9/25/2013	104	8/29/2013	78	7/13/2013	73	9/26/2013	67
	Denton Airport South C56	7/5/2013	90	9/4/2013	87	9/6/2013	85	8/31/2013	85
	Grapevine Fairway C70	9/6/2013	89	9/4/2013	89	8/30/2013	89	9/12/2013	83
	SETRPC 40 Sabine Pass C640	7/4/2013	74	7/2/2013	72	7/13/2013	67	5/7/2013	67

Table 1-3. 2012 and 2013 days with four highest values of MDA8 ozone and highest MDA8 days at the Seabrook and La Porte monitors in HGB listed by metropolitan area.

Days to Analyze		
HGB	**BPA**	**DFW**
3/24/2012	3/24/2012	5/17/2012
3/26/2012	3/25/2012	6/24/2012
5/17/2012	5/22/2012	6/25/2012
5/21/2012	6/26/2012	6/26/2012
6/1/2012	5/7/2013	6/27/2012
6/25/2012	7/2/2013	9/6/2012
6/26/2012	7/4/2013	7/5/2013
6/27/2012	7/13/2013	8/30/2013
9/20/2012		8/31/2013
5/13/2013		9/4/2013
6/3/2013		9/6/2013
7/2/2013		9/12/2013
7/3/2013		
7/4/2013		
8/16/2013		
8/28/2013		
9/25/2013		
10/9/2013		

2.0 METHODS

This section describes the methods used to analyze the potential for ozone impacts from fire emissions on the HGB, DFW and BPA high ozone days listed in Table 1-3. We review available ambient monitoring data, model data, emission inventories and satellite products, and determine whether there is a clear, causal connection between emissions from fires and high values of monitored ozone on each day. In Section 2.1, we give an overview of how the analysis for each day was carried out, and then in Section 2.2, we describe in more detail each data set and analysis tool that was used.

2.1 Overview of Analysis Method

For each high ozone day, we begin by examining the time series of 1-hour average ozone at the monitor of interest. In addition to the 1-hour ozone time series, we present 1-hour time series for NO, NOx and SO_2 for that monitor, if available. Plumes from wildfires have enhanced levels of NOx and NO, depending on the distance from the fire. Large levels of NO would indicate fresh emissions from a nearby fire, while a plume from a more distant fire may have high levels of NOx, but not NO, due to the conversion of NO to NO_2 during transit. Coal-fired power plant plumes are characterized by the presence of SO_2, which is released into the air during combustion of coal. The presence of SO_2 is used to distinguish between plumes of ozone precursors from fires and coal-fired power plants; high SO_2 levels are present in coal-fired power plant plumes, but not wildfire plumes.

In addition to examining the ozone time series for the monitor of interest, we review the ozone time series for several other monitors located on the periphery of the urban area where the monitor with high ozone is located. This allows us to estimate the background ozone level present in the air arriving in the urban area on that day. Different monitors will be upwind of the urban areas on each day, depending on the wind direction. Once we have estimated the background ozone entering the urban area, we can then estimate the ozone enhancement at the monitor with high ozone due the influence of fires or other emissions sources.

A key question is whether air arriving at a monitor with high ozone has passed in the vicinity of a fire so that ozone precursor emissions from the fire may have influenced ozone levels within the air mass. To answer this question, we calculate back trajectories to estimate the path the air mass travelled prior to arriving at the monitor. A set of back trajectories are calculated for each monitor/day using different tools, which are described in detail in Section 2.2. The tools use different meteorological inputs and have different spatial and temporal resolutions; therefore, they each have strengths and limitations in their estimation of the back trajectories. Analysis of the complete set of back trajectories while taking into account the known strengths and limitations of each method gives a more complete picture of the probable path of the air mass.

Trajectories ending at different altitudes are used to assess the presence of vertical wind shear, which may indicate enhanced uncertainty in the back trajectories. For each monitor with high ozone, we also review surface wind vectors for each hour of the day (plotted along with 1-hour

ozone) for comparison with the back trajectory results. We then examine the set of back trajectories to determine whether the air passed over fire locations, which are derived from satellite fire detections and fire reports. When evaluating the potential for ozone impacts at a monitor, we consider the proximity of the fire location to the back trajectory as well as the magnitude of the fire emissions. Note that the trajectories are plotted as lines, which is an idealization of the actual flow. A fire does not need to be intersected by the back trajectory, but needs only be in the vicinity of the trajectory to be considered as having the potential to influence the air mass. If no fires are present in the vicinity of the back trajectories, we conclude that there is little likelihood that fire emissions contributed to high ozone at the monitor in question and do not proceed further with the analysis.

If we find that a fire is present along the back trajectories, we turn to an examination of its potential impacts. We follow the back trajectory until it enters the urban area where the monitor with high ozone is located. We review figures that display the MDA8 ozone and the daily maximum 1-hour average (MDA1) $PM_{2.5}$ value for each monitor in the urban area and determine whether there is high ozone and/or $PM_{2.5}$ consistent with a fire plume entering the urban area. We also review 1-hour ozone and $PM_{2.5}$ time series for all monitors in the urban area to determine whether unusually high values of ozone and $PM_{2.5}$ are present. If ozone and/or $PM_{2.5}$ are high at monitors in the vicinity of the trajectory as it enters the upwind side of the urban area, we would consider the possibility of a fire impact at the monitor with high ozone. If neither ozone nor $PM_{2.5}$ is enhanced at monitors in the vicinity of the trajectory on the upwind side of the urban area and ozone is high only on the downwind side of the urban area, we conclude that fire impacts most likely played a significantly less important role than local urban emissions in causing high ozone at the monitor.

We also consider the role that fires may play in the development of high regional levels of background ozone. We use satellite fire, smoke and satellite aerosol optical depth (AOD) retrieval products to determine whether fire emissions may have contributed to high levels of background ozone. If there is intense fire activity along with the presence of smoke and enhanced AOD, it is possible that fire emissions may also be contributing to enhanced ozone. The satellite products used in this study provide a vertically-integrated estimate of AOD and smoke through the entire depth of the atmospheric column. A region of enhanced AOD may not necessarily correspond to an area of high surface $PM_{2.5}$, but may be associated with an elevated layer of smoke or dust that does not mix down to the surface (e.g. Duncan et al., 2014). Therefore, we supplement the satellite products with analyses of surface ozone and $PM_{2.5}$ for the continental U.S. prepared by the U.S. EPA. We use these analyses together with the satellite products to diagnose high regional levels of ozone, $PM_{2.5}$ and aerosols that may contribute to high background levels of ozone entering an urban area on a high ozone day. We expect that on a day with high background ozone due to intense but distant fire activity, all monitors in a given urban area will have high 8-hour ozone values. The signature of a nearby fire, on the other hand would be more consistent with a narrow plume that affects only some monitors in an urban area and has high levels of NOx and $PM_{2.5}$ as well as ozone, but not SO_2.

For each high ozone day listed in Table 1-3, we follow the procedure detailed above and make a recommendation as to whether that day should be investigated further to determine whether it may be classified as an exceptional event. Additional study via photochemical modeling and/or analysis of available PM filter data would then be recommended for that day.

2.2 Description of Analysis Tools and Data Sets

2.2.1 Surface Wind Back Trajectories

Surface wind back trajectories were developed using the TCEQ's AQPlot tool (McDonald and Mercado, 2006). AQPlot calculates air parcel trajectories based on CAMS site surface wind speed and direction measurements. The model performs an interpolation using data from specified monitoring sites to calculate a resultant wind field with which to generate trajectories originating from user-defined locations. These trajectories represent motion of a particle advected only by the interpolated horizontal wind field. There is no vertical motion defined in the model and there is no dispersion. Consequently, AQPlot is most useful for examining short trajectories in regions with dense monitoring networks. It is useful when employed in conjunction with trajectory models that include a more refined representation of particle motion, but are limited by their use of gridded, three-dimensional wind fields with relatively coarse spatial resolution.

The temporal resolution in the AQPlot model is 1 hour, and a tick mark appears on the trajectory path every hour. The accuracy of AQPlot increases with the number and spatial coverage of sites selected. Surface wind data were obtained from the TCEQ website (http://tceq.com/agency/air_main.html). In order to improve model accuracy, as well evaluate back trajectories for upwind and downwind monitors, sites on the periphery of the HGB, BPA and DFW areas were identified. For the HGB area, back trajectories for the following monitors were plotted along with the monitor that had high ozone on each day: Hamshire C64 (E), Danciger C618 (W), Jones Forest C698 (N) and Galveston C5005 (S). For DFW, Parker County C76 (W), Greenville C1006 (E) and Italy C1044 (S) were used, and in the BPA area, Beaumont-Downtown C2 (NW), West Orange C9 (NE) and SETRPC Mauriceville 42 C311 (N) were identified as urban perimeter/background sites.

AQPlot was used to develop back trajectories for all days shown in Table 1-3 at all monitor and background site locations. Figure 2-1 shows and example of AQPlot surface wind back trajectories for July 4, 2013 for Manvel Croix Park C84 and four HGB urban area perimeter/background sites. All trajectories originated at the time of MDA1 ozone at Manvel Croix. All times shown in AQPlot trajectory figures refer to local time (i.e. Central Daylight Time).

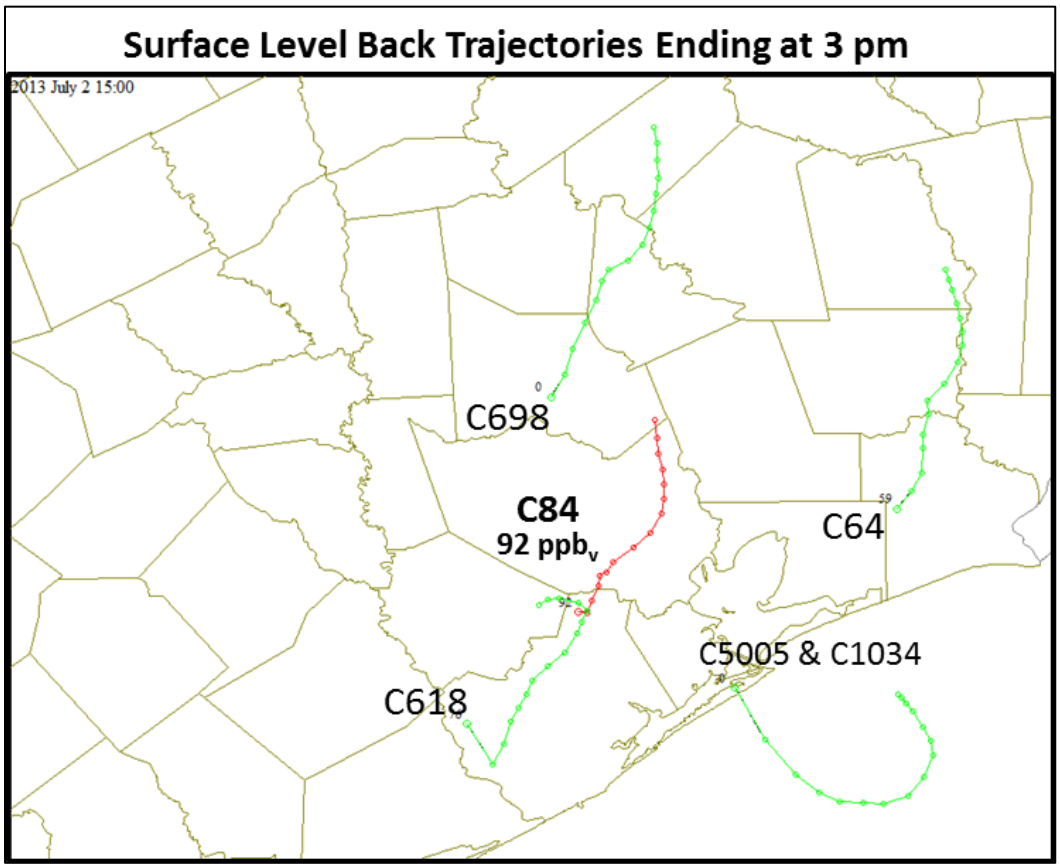

Figure 2-1. July 2, 2013 AQPlot surface wind back trajectories terminating at HGB area ozone monitoring sites outside or on the periphery of the HGB urban area.

2.2.2 Ambient Measurements

TCEQ CAMS data were used to determine the relationship between ozone and other species and between ozone and the wind field on high ozone days. The CAMS data were downloaded from the TCEQ website (http://tceq.com/agency/air_main.html). When multiple measurements of a parameter at one site were available, we used the measurements from the instrument with the smallest number of hours with missing or invalid data. Time-series analysis was conducted for each day for ozone, NO, NO_2, NOy, NOx, $PM_{2.5}$, CO and SO_2, where available. Figure 2-2 shows example of ambient measurements on March 24, 2012 at the Seabrook monitor in Houston.

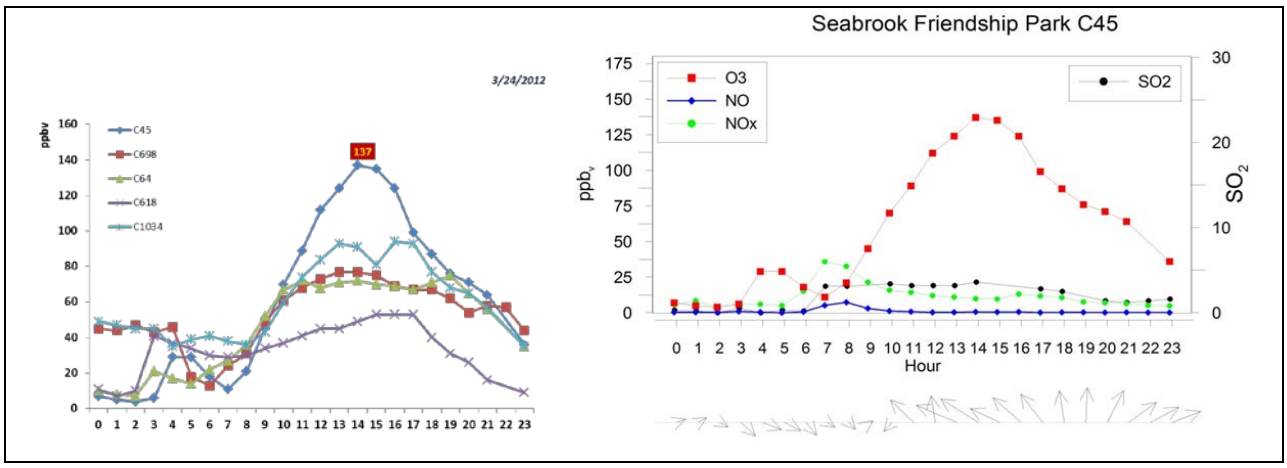

Figure 2-2. Ambient measurements at the Seabrook Friendship Park C45 with background sites (left) coupled with ozone, NO, NOx, SO_2 and wind vectors (right).

The left panel of Figure 2-2 shows 1-hour average ozone time series for the monitor of interest (Seabrook, C45) and monitors located around the perimeter of the urban area. Ozone is much lower at these monitors than at Seabrook, which has a trajectory leading back across the Houston urban area and the heavily industrialized Houston Ship Channel region. A more detailed map of the HGB area showing major roadways, the urban area, the Ship Channel, and monitor locations is provided in Figure 2-3. Similar maps for the DFW and BPA areas are shown in Figure 2-4.

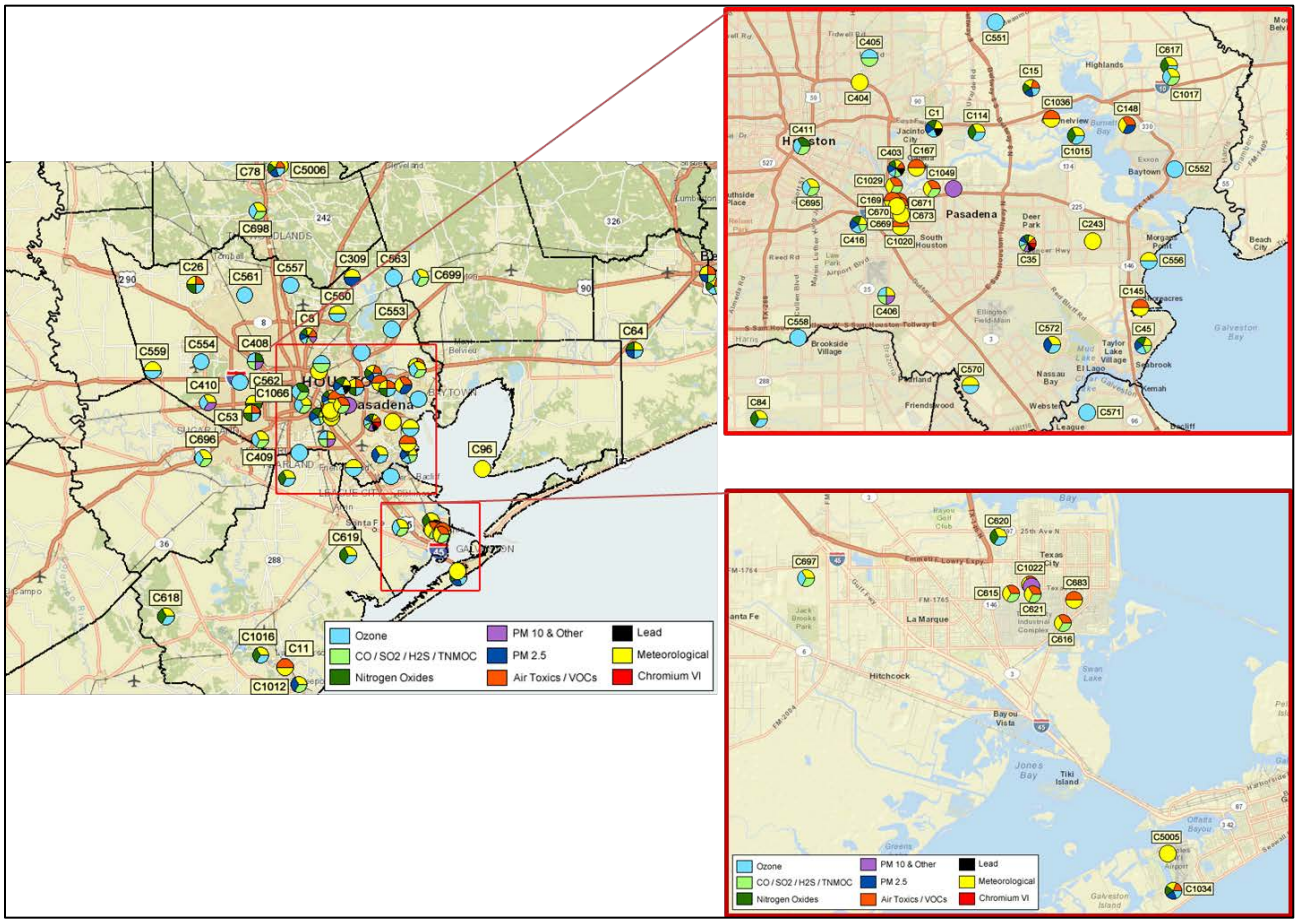

Figure 2-3. HGB area CAMS monitoring locations (left). Inserts showing zoomed locations in the Houston downtown (upper right) and Galveston area (lower right). TCEQ figure from http://www.tceq.state.tx.us/cgi-bin/compliance/monops/select_summary.pl?region12.gif.

DFW Area **BPA Area**

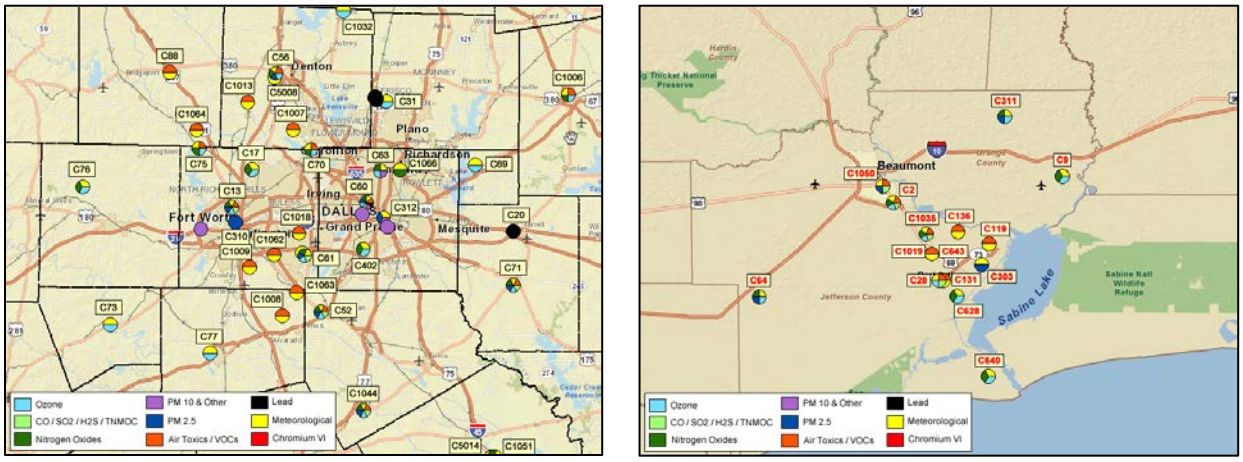

Figure 2-4. TCEQ CAMS monitoring locations in the DFW (left) and BPA areas (right).

The presence of plumes of ozone and $PM_{2.5}$ can be diagnosed by examining the spatial and temporal patterns of ozone and $PM_{2.5}$ concentrations across all monitors in each region. The daily maximum 8-hour average ozone concentration (MDA8) and daily maximum 1-hour average ozone concentration (MDA1) $PM_{2.5}$ for each CAMS monitor are overlaid on the HGB, BPA or DFW area maps.

In addition to spatial analysis, ozone and $PM_{2.5}$ are analyzed time series of hourly ozone and $PM_{2.5}$ concentrations from all monitors in the region. By inspection of the time series plots, it is possible to determine the background ozone level in each metropolitan area and to determine whether the monitor of interest had unusually high ozone for that area on that day. Because many ozone monitors do not measure $PM_{2.5}$, it is important to evaluate the $PM_{2.5}$ time series for monitors nearby the CAMs site that had high ozone. An example of each type of figure is shown in Figure 2-5.

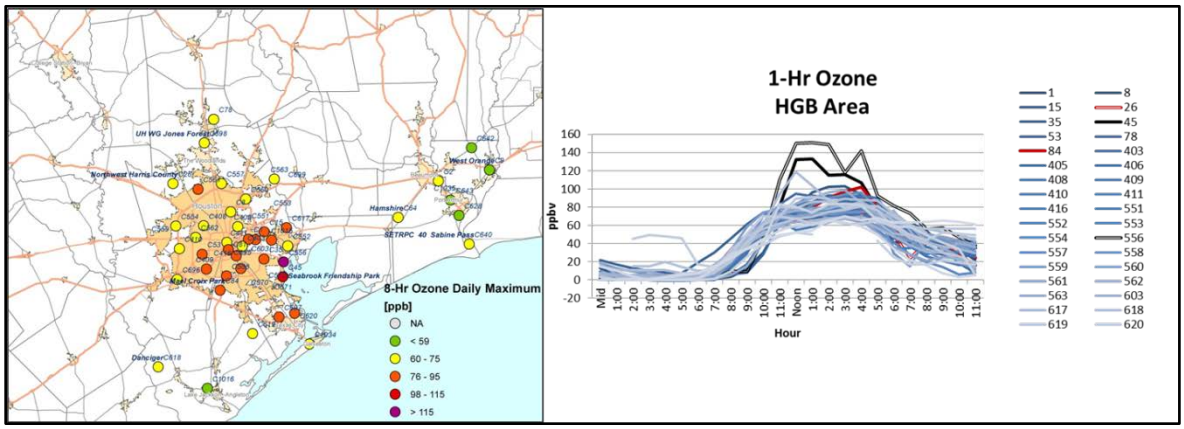

Figure 2-5. Maximum 8-hr ozone on September 25, 2013 (left) coupled with hourly ozone time series from all HGB area ozone monitors (right).

2.2.3 HYSPLIT Analysis

In order to determine possible source regions for air arriving in the HGB, DFW or BPA areas on high ozone days, a back trajectory analysis was performed. 72-hour back trajectories were prepared using on-line tools provided by the National Oceanic and Atmospheric Administration (NOAA) at http://www.arl.noaa.gov/ready/hysplit4.html. These tools are based on application of NOAA's HYSPLIT model (Draxler et al., 2013) with archived weather forecast model data from the National Center for Environmental Prediction's Eta North American Model (NAM) The NAM data have a horizontal resolution of 12 km and the temporal resolution of the data is 3 hours. An interpolation of the wind data is performed by the READY website for trajectory times that fall in between the NAM output intervals. For trajectories that begin at hour 2200 or 2300, the READY website calculates the trajectory using 2100 hours as the endpoint because it is not able to wrap around to the next day. The bias introduced into the results by this change in trajectory start times is expected to be small. Note that back trajectories are a qualitative tool subject to theoretical and data limitations and can only provide approximate information regarding possible source regions for pollutants transported to a monitor. HYSPLIT back trajectories were developed for all monitors and all days in Table 1-2. Figure 2-6 shows an example of a 72-hour back trajectories ending at three different altitudes (500 m, 1,500 m and 2,500 m) above the Seabrook Friendship Park C45 monitor on August 20, 2013. We examine back trajectories ending at different altitudes in order to assess the importance of vertical wind shear within the mixed layer.

HYSPLIT back trajectories are more reliable than the near-surface AQPlot trajectories in regions lacking surface monitoring sites, and provide valuable information about wind patterns aloft, but may not be as reliable at the precise location and time of measured peak ozone, due to their limited spatial and temporal resolution. Uncertainties are introduced by the spatial and temporal resolution of the three-dimensional gridded EDAS meteorological data and also by the inherent uncertainties in the analyzed meteorological data. The meteorological data are derived by assimilating available high frequency observations, such as wind profiler, radar, and aircraft data with modeled predictions. The horizontal spatial resolution is 12 km and the

temporal resolution is 3 hours. Large scale weather patterns are likely well-simulated by the meteorological model, but smaller scale localized weather features may not be captured at the model's spatial and temporal resolution. The HYSPLIT back trajectories are therefore likely to be more accurate on days with strong winds driven by large-scale weather features. Days with light, shifting winds or influence from a local-scale circulation such as a sea breeze are likely to have back trajectories with higher uncertainties.

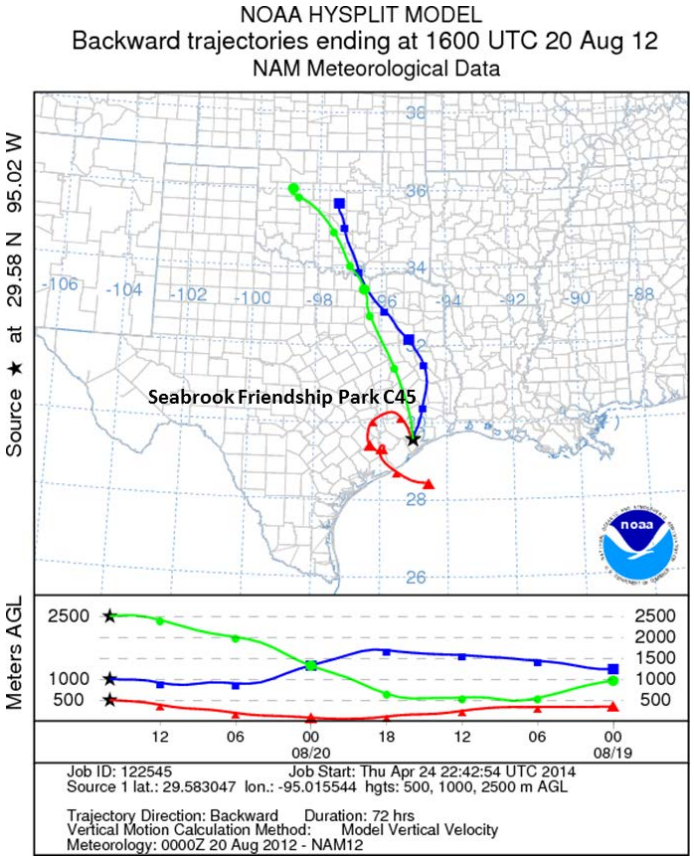

Figure 2-6. HYSPLIT back trajectories terminating at Seabrook Friendship Park C45. Back trajectories are shown for three altitudes (500 m, 1,500 m and 2,500 m) using NAM 12km meteorology.

2.2.4 SmartFire Fire Location and Trajectory Analysis

Fire location analysis was conducted using the online SMARTFIRE tool (http://firesmoke.us/wfdss/index.php?lat=47.5&lon=-115&tool=SmartFire#list). The SmartFire fire information system is a framework for managing wildfire information collected from satellites and ground reports. In addition, the software has the ability to generate back trajectories at user-specified locations and altitudes and to display the back trajectories together with fire location and size. The trajectories are calculated using the HYSPLIT model and Eta Data Assimilation System (EDAS) 40 km resolution input meteorological fields with 3-hourly temporal resolution. For each monitor location and high ozone day listed in Table 1-3, the online SmartFire tool was used to develop 72-hour back trajectories originating near the

surface (10 m). The SmartFire back trajectories ending time point was the first hour of the 8-hour period of the MDA8 at the monitor with high ozone. An example of a SmartFire back trajectory and fire location plot is shown in Figure 2-7. Note that only the fires that were active on the day of high ozone at the monitor are shown. Other fire data (discussed below) are used to evaluate whether there were fires along the back trajectory before the high ozone day under study.

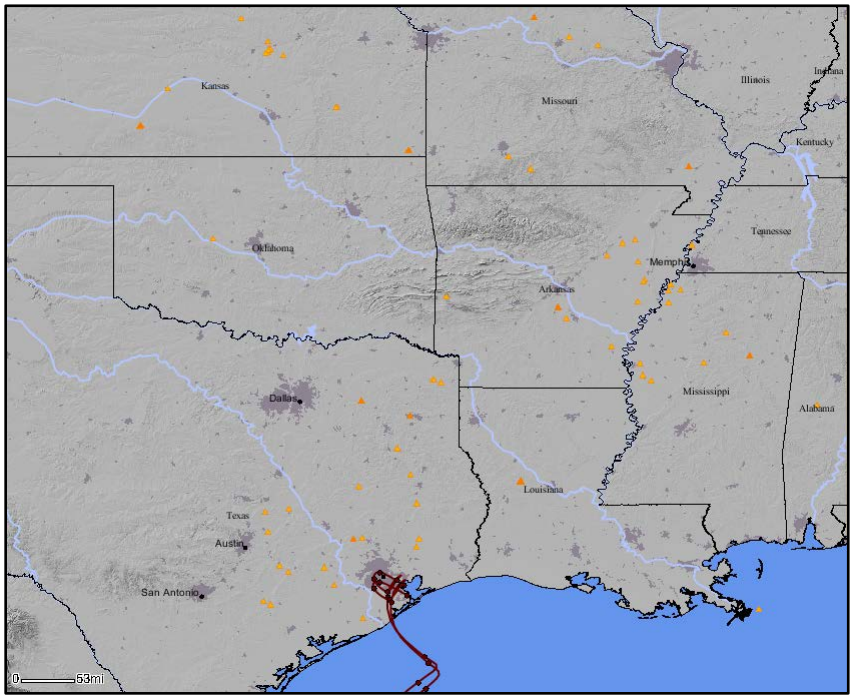

Figure 2-7. August 20, 2013 SmartFire fire locations (orange triangles) plotted together with 72-hour back trajectories ending near the surface (10 m above ground level) at a CAMS monitor in the HGB area. The trajectories are calculated using EDAS meteorology with 40 km horizontal resolution.

Note that the HYSPLIT model is run with EDAS meteorology that has 40 km resolution, which is coarser than the NAM 12 km meteorology used to make the HYSPLIT multi-altitude plots similar to Figure 2-6. The HYSPLIT trajectories calculated using the EDAS 40 km meteorology should be viewed as having a higher uncertainty than those calculated with the NAM winds.

2.2.5 Satellite-Based Fire/Smoke Imagery and Surface $PM_{2.5}$

To determine whether fire emissions may have contributed to high levels of background ozone, we used satellite fire and smoke plume detections from NOAA's Hazard Mapping System (HMS) Fire and Smoke Analysis Product. The HMS product uses data from the GOES Imager, the AVHRR (Advanced Very High Resolution Radiometer) instrument, and MODIS (Moderate Resolution Imaging Spectroradiometer). Fire locations derived by thee algorithms based on different satellite retrievals reviewed by an analyst, who removes false detections and

reconciles the three fire location data sets. The analyst outlines the locations of smoke plumes inferred from satellite aerosol optical depth retrievals. It is important to note that while the HMS smoke visualization is useful in showing the presence of smoke and its relation to active fires, these plumes of smoke may not mix down to the surface and may not affect air quality at ground level. Current HMS images are available from http://www.ospo.noaa.gov/Products/land/fire.html. Archived images for the time period of interest were supplied by the NOAA National Environmental Satellite, Data, and Information Service (NESDIS).

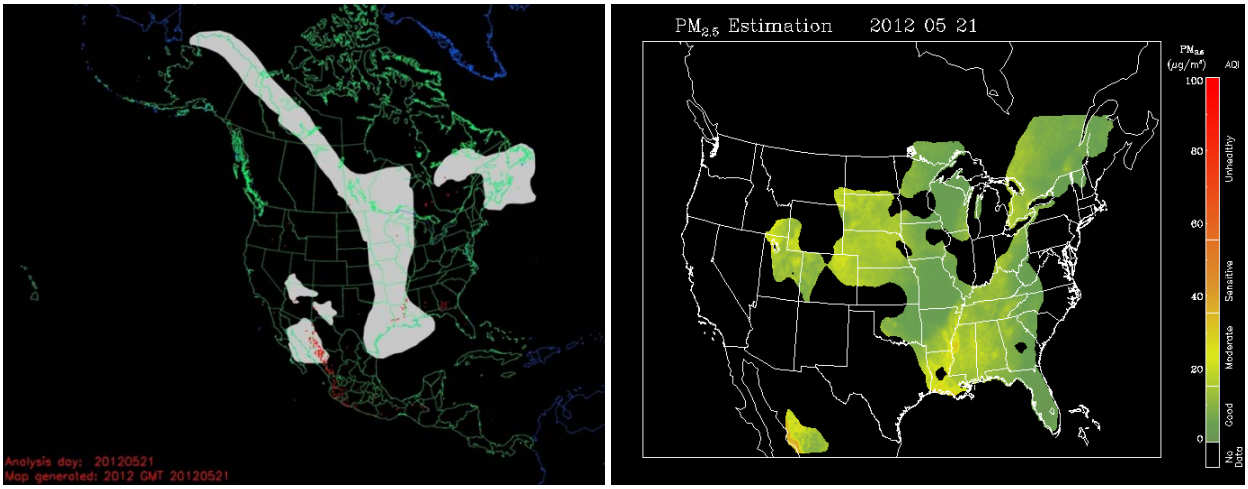

Figure 2-8. Left panel: HMS product showing fire locations (red dots) and smoke plume (gray area). Right panel: IDEA surface $PM_{2.5}$ estimate based on AOD and surface monitoring data.

The left panel of Figure 2-8 is an example HMS plot showing fire locations (red dots) and a smoke plume (gray area) over the continental U.S. A $PM_{2.5}$ surface map is presented alongside the HMS map to show the extent of PM plumes at the surface (right panel). The estimated surface $PM_{2.5}$ concentration is a blend of satellite and surface data and is only available for daylight hours. $PM_{2.5}$ is estimated using satellite retrievals of aerosol optical depth (AOD) together with surface $PM_{2.5}$ measurements. The AOD retrievals are based on measurements from the MODIS instruments. The MODIS instruments fly aboard two polar-orbiting satellites, Terra, and Aqua. These satellites orbit the Earth, traveling from pole to pole while the earth rotates beneath them; a given area of the Earth will have an overpass from Terra and Aqua approximately twice a day. From the retrieved AOD, the surface $PM_{2.5}$ is estimated based on a regression that was developed using air quality model simulations (van Donkelaar et al., 2010). The $PM_{2.5}$ maps were downloaded from the NOAA IDEA (**I**nfusing satellite **D**ata into **E**nvironmental **A**pplication) website[2]. We used this product to complement the surface $PM_{2.5}$ analysis and CAMs site data; the advantage of this $PM_{2.5}$ product comes from the satellite's ability to cover a wide area and to provide additional insight into the $PM_{2.5}$ distribution in areas where surface monitoring networks are sparse.

[2] http://www.star.nesdis.noaa.gov/smcd/spb/aq/

2.2.6 Ozone and $PM_{2.5}$ Analyses Based on Surface Monitoring Data

Surface level air quality index maps for ozone and $PM_{2.5}$ were obtained from the EPA website http://www.airnow.gov/. The maps are based on interpolation of real time surface measurements (EPA, 2004, EPA, 2014) of ozone and $PM_{2.5}$. Figure 2-9 shows example ozone (left) and $PM_{2.5}$ (right) air quality data on May 22, 2012. The color scale in the plots corresponds to the AQI index, which is shown below the maps in Figure 2-9. In contrast to $PM_{2.5}$ shown on Figure 2-8 which is based on satellite AOD retrievals and surface observations, the AQI surface representation of $PM_{2.5}$ concentration shown in Figure 2-9 is based on surface observations and standard interpolation techniques (EPA, 2004, EPA, 2014).

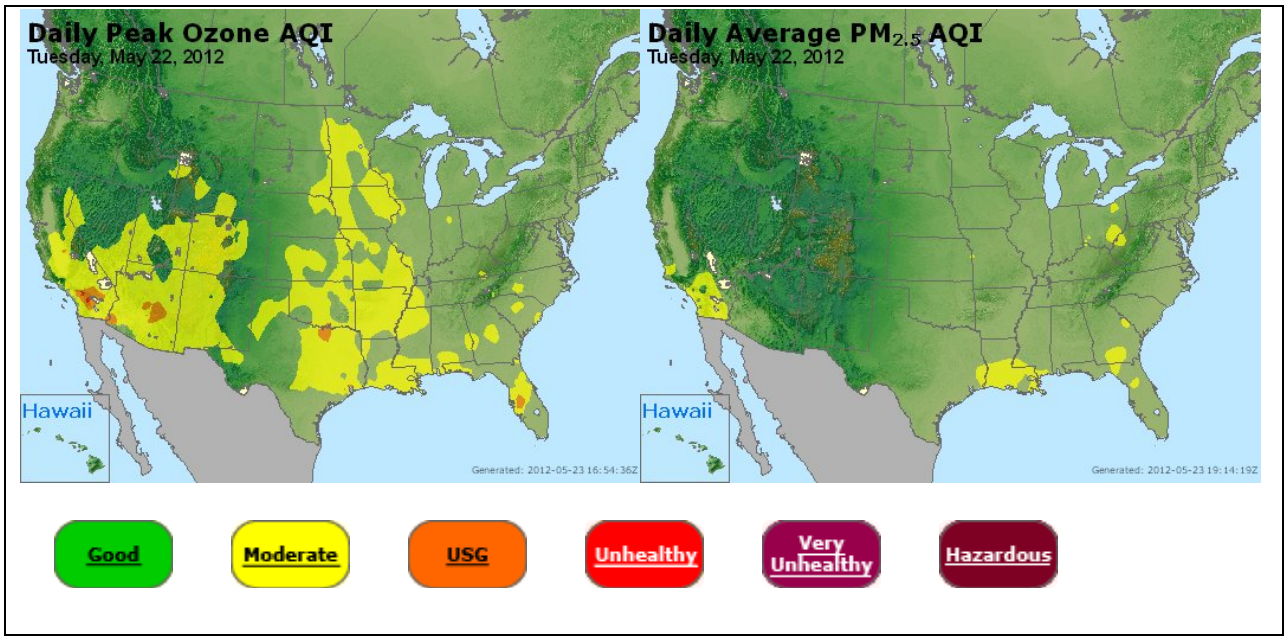

Figure 2-9. EPA showing ozone and $PM_{2.5}$ AQI plots based on analysis of surface measurements (data from: http://www.airnow.gov/).

2.2.7 FINN Emission Plots

ENVIRON obtained estimates of fire emissions for each day of the 2012 and 2013 ozone seasons from the National Center for Atmospheric Research (NCAR) (Wiedinmyer, personal communication, 2014). The Fire Emissions Inventory from NCAR (FINN) is described by Wiedinmyer et al. (2011). The emission estimates are derived from analysis of fire locations determined from MODIS fire detections. MODIS instruments detect fires as thermal anomalies (i.e. hot spots seen against a cooler background) at a spatial resolution of about 1 kilometer. Fire emissions estimated from the MODIS data include NOx, CO, VOC, SO_2 and PM species, along with other compounds (e.g., mercury). While the satellites provide the benefit of daily coverage of the U.S. the MODIS instruments cannot detect small (<1 km^2) fires nor fires located beneath clouds or obscured by thick smoke. Therefore, there may be fires that appear in the SmartFire tool maps that are not present in the FINN inventory. An example of this would be a

fire that occurred on a cloudy day and was not detected by the MODIS instruments but did appear in the ground-based fire report database accessed by SmartFire.

The data record for each fire in the FINN emission inventory consists of location (latitude and longitude), Julian date, acreage burned, biomass burned (fuel loading), and emission estimates. The acreage burned was set to 1 km^2 in almost every record, representing the size of a single satellite pixel. NOx and PM_{10} emissions were extracted for the day-specific fire emission inventory and served as an indicator for fire location and intensity. PM_{10} and NOx emission plots were generated for each high ozone day analyzed, as well as for the three days preceding the high ozone day (i.e. -24 hours, -48 hours and -72 hours). For example, to present March 24 NOx/PM_{10} fire emissions, March 21st (-72 hour), 22nd (-48 hour) and 23rd (-24 hour) emission plots were also developed. This is synchronized with the 72-hour wind back trajectories, and allows us to review fire locations over the 72 hour back trajectory time period. For example, Figure 2-10 depicts fire locations and emissions from March 23 (-72 hour) through March 26, 2012.

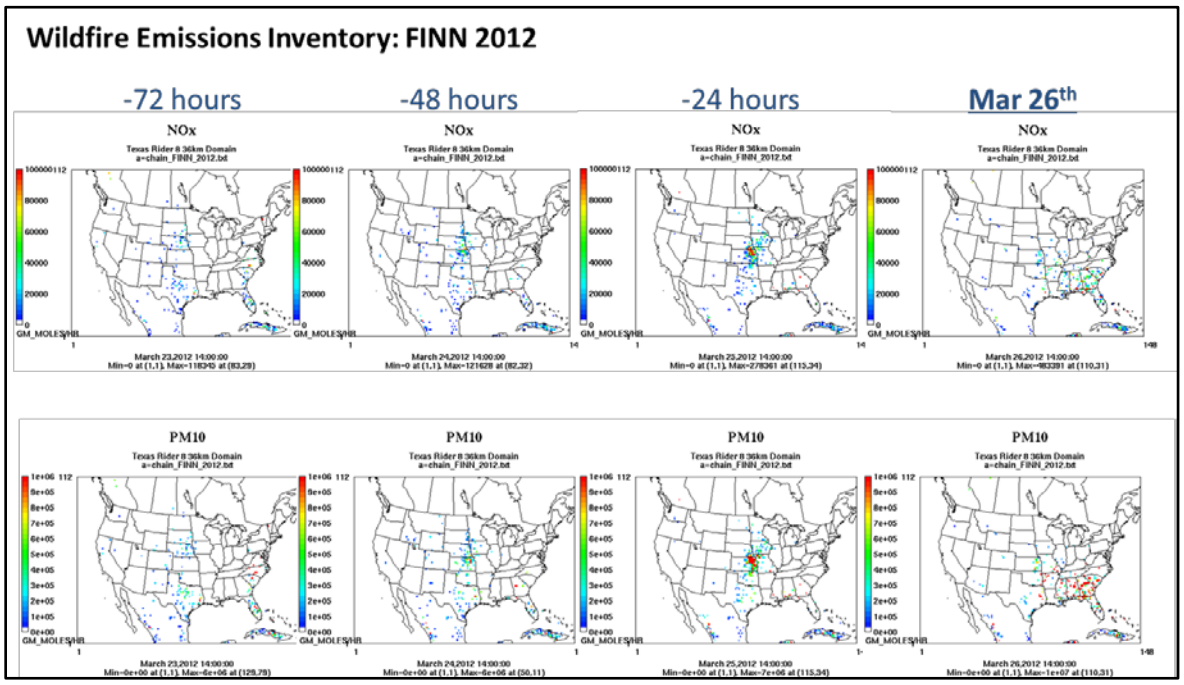

Figure 2-10. March 23 – 26, 2012 NOx and PM_{10} emissions from wildfires based FINN data (Wiedinmyer et al., 2011).

2.2.8 DataFed Exceptional Event Decision Support System Products

We used data from the DataFed Exceptional Event Decision Support System at http://datafed.net/EE_DSS.html. For each high ozone day, we reviewed the MODIS fire location plot and thee model output plots from the Navy Aerosol Analysis and Prediction System (NAAPS). The NAAPS models is described at http://www.nrlmry.navy.mil/aerosol_web/Docs/globaer_model.html and is a tropospheric

chemistry-transport model that uses global meteorology from the Navy Operational Global Atmospheric Prediction System (NOGAPS) model. We use the NAAPS smoke emissions product, which uses satellite data to estimate the location and magnitude of emissions of smoke based on the GOES Wildfire Automated Biomass Burning Algorithm (WF_ABBA). We also use the NAAPS model output surface layer smoke and sulfate aerosol concentrations to estimate the relative contributions of smoke and sulfate aerosols to ambient $PM_{2.5}$ concentrations.

3.0 HIGH OZONE DAY ANALYSIS

In Section 3, we present the analysis of individual days shown in Table 1-3 in chronological order, beginning with 2012 days in Section 3.1 and concluding with 2013 days in Section 3.2.

3.1 2012 Ozone season

In 2012, there were total of thirteen distinct days that contributed to the ozone design values in the HGB, DFW and BPA areas. Monitors analyzed on each day are listed in Table 3-1. In this section, we analyze each of these days for each monitor shown in Table 3-1 using the methods described in Section 2.

Table 3-1. Monitors analyzed by day: 2012.

Day	Monitor(s) Analyzed
3/24/2012	Sabine Pass, Seabrook, La Porte
3/25/2012	Sabine Pass
3/26/2012	NW Harris
5/17/2012	Denton, NW Harris
5/21/2012	Manvel Croix
5/22/2012	Sabine Pass
6/1/2012	NW Harris
6/24/2012	Grapevine Fairway
6/25/2012	Denton, Grapevine Fairway, Manvel Croix
6/26/2012	Sabine Pass, Grapevine Fairway, Manvel Croix
6/27/2012	Denton, Grapevine Fairway, NW Harris
9/6/2012	Denton
9/20/2012	Manvel Croix

3.1.1 March 24, 2012

March 24-26, 2012 was an episode of high 8-hour ozone throughout much of East Texas that occurred during a period of unseasonably warm weather. During March 24-26, temperatures were in the low 80s in the HGB, BPA and DFW areas (Figure 3-1). Figure 3-2 shows areas of ozone AQI of "Moderate" or higher across broad regions of East Texas, including the HGB, DFW and BPA areas. Although ozone was high regionally, the $PM_{2.5}$ AQI reached levels of "Moderate" or higher only in HGB, DFW and BPA.

March 24 was one of the 4 highest MDA8 days in 2012 for the La Porte (C556) and Seabrook Friendship Park (C45) monitors in the HGB area and the Sabine Pass (C640) monitor in the BPA area. The left panel of Figure 3-3 shows AQPlot surface wind back trajectories ending at the Seabrook monitor and the following monitors located outside the central HGB urban area: Jones Forest C698 (north of the urban area), Hamshire C64 (east), Galveston C5005 (south) and Danciger C618 (southwest).

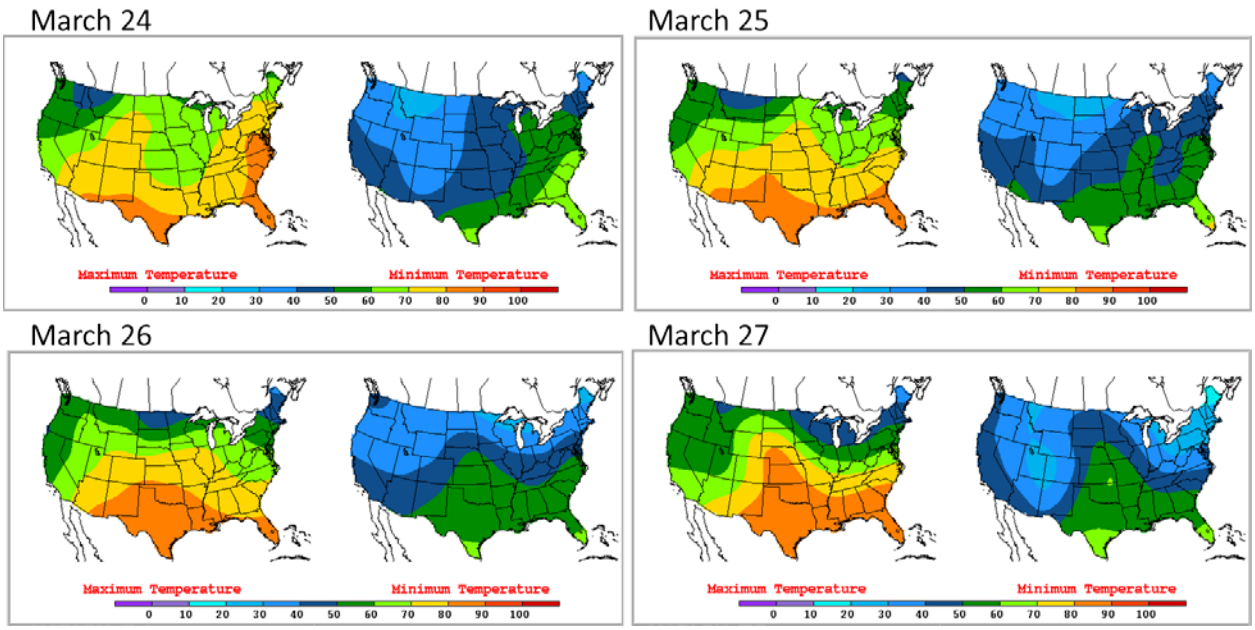

Figure 3-1. Daily maximum surface temperature analysis for March 24-27, 2012. NOAA weather map from http://www.hpc.ncep.noaa.gov/dailywxmap/index_20120324.html.

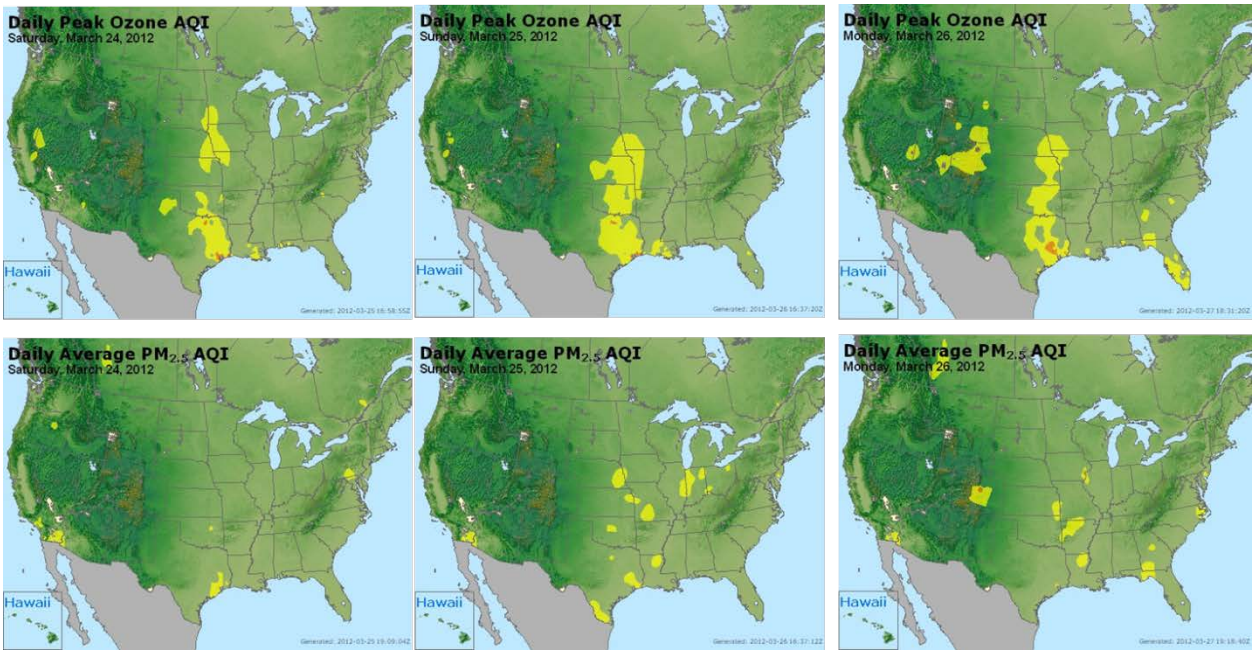

Figure 3-2. EPA AQI index for ozone (upper panels) and $PM_{2.5}$ (lower panels) for March 24-26, 2012.

The upper right panel of Figure 3-3 shows the 1-hour average ozone time series for Seabrook and the three sites shown in the AQPlot back trajectory plot and 1-hour average time series of

ozone, NO, NOx and SO_2 at Seabrook together with Seabrook hourly wind vectors are shown in the lower right panel. The Seabrook monitor has an MDA1 value of 137 ppb, while the three outlying sites have MDA1 values ranging between ~50-80 ppb.

There is a small amount of SO_2 present at Seabrook throughout the daylight hours. The peak value of 1-hour SO_2 is ~5 ppb. This indicates that the Seabrook monitor was influenced by the plume of one or more coal-fired power plants on March 24. However, the relatively low SO_2 concentration and the fact the SO_2 level was constant throughout the daylight hours indicates that this impact is not sufficient to explain the timing and magnitude of peak 1-hour ozone at Seabrook.

Figure 3-4 and Figure 3-5 are analogous to Figure 3-3 for the La Porte and Sabine Pass sites, respectively. Both La Porte and Sabine Pass have 1-hour ozone peaks exceeding 100 ppb in the early afternoon. Peak 1-hour ozone values at the three monitors located in the outskirts of the BPA area range between 55-70 ppb (Figure 3-5). SO_2 is not monitored at Sabine Pass, and the SO_2 and meteorological measurements at the La Porte site were unavailable during this period due to preventive maintenance.

The upper panels of Figure 3-6 depict 72-hour HYSPLIT back trajectories ending at altitudes of 500 m, 1,000 m and 2,500 m at the La Porte, Seabrook and Sabine locations at the time of their respective daily maximum 1-hour average ozone values. In the lower panels of Figure 3-6 are SmartFire back trajectories for the Seabrook and La Porte monitors in HGB area (left panel) and the Sabine Pass monitor in the BPA area (right panel). The HYSPLIT and AQPlot back trajectories all show stagnant, recirculating winds over the HGB and BPA areas. This is consistent with the coastal CAMS site (C45 and C1034) wind vectors, which show morning winds from the north-northwest with a shift to southerly winds around midday. The AQplot back trajectories show winds that are generally northerly in both HGB and BPA, with recirculation and a change to southerly winds at the near-coastal monitoring sites Galveston, La Porte, Seabrook and Sabine Pass. This is consistent with a sea breeze/bay breeze with offshore winds in the morning shifting to onshore winds in the afternoon. The monitors located further inland (e.g. C698) do not show evidence of this recirculation and are beyond the range of the sea breeze circulation. For all three monitors, HYSPLIT 12 km NAM trajectories show winds that are southerly for trajectories ending at 500 m and 1,000 m aloft during the days preceding March 24 rotating to northwesterly winds by the 24th. The trajectory ending at 2,000 m aloft shows only northwesterly flow.

The SmartFire back trajectories ending at 10 m altitude also show stagnant recirculating winds on March 24 with southeasterly flow in the days leading up to March 24. They show that the air arriving at these three monitors did not pass over locations with active fires in the 72 hours leading up to the 1-hour ozone maxima. The HYSPLIT NAM and AQPlot back trajectories agree that air arriving at the three monitors on March 24 did not pass over regions with active fires.

The HMS satellite product (left panel of Figure 3-7) shows an area of enhanced AOD offshore in the Gulf of Mexico. The IDEA $PM_{2.5}$ analysis (right panel of Figure 3-7) is missing data for the region along the Texas coast. The $PM_{2.5}$ AQI (right panel of Figure 3-8) shows moderate but not

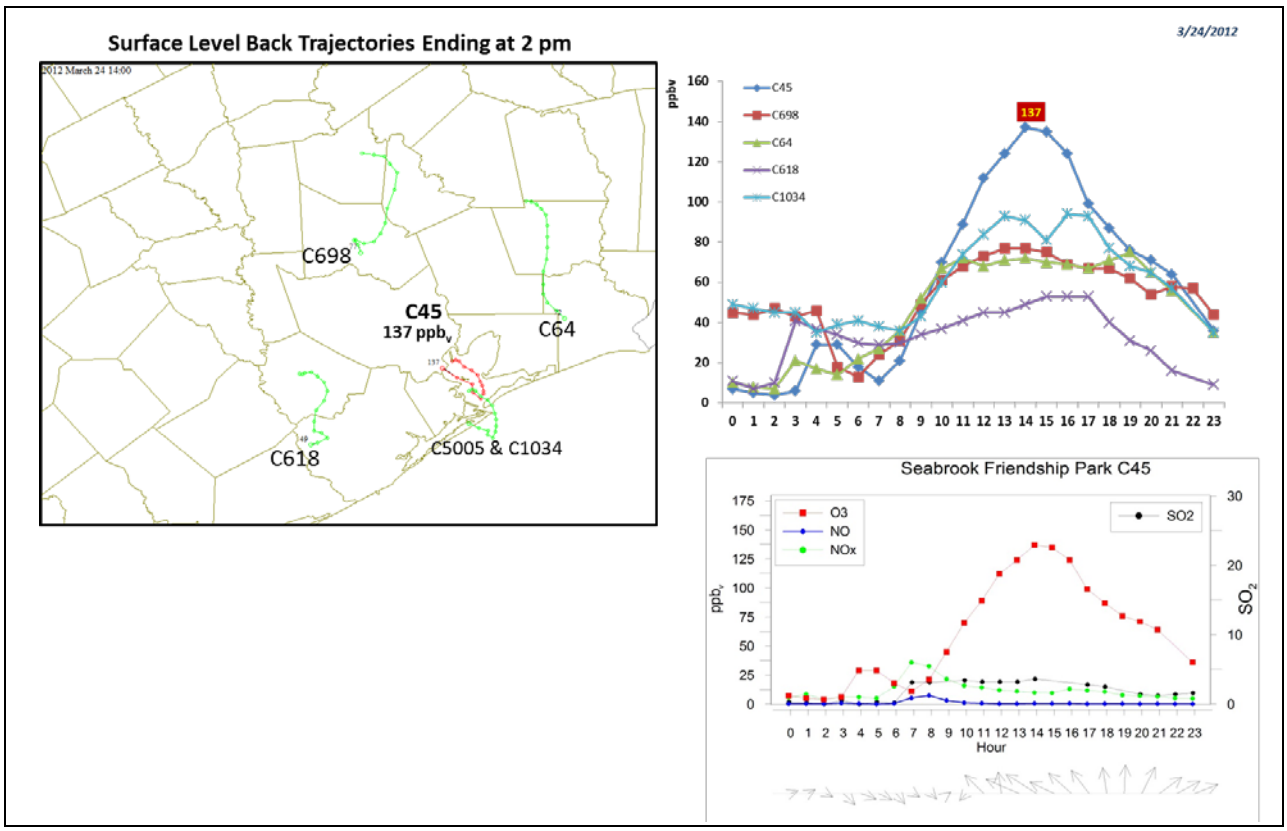

Figure 3-3. March 24, 2012 high ozone day at Seabrook Friendship Park C45. Left panel: AQPlot back trajectories terminating at C45 and four HGB monitors located outside the central urban area at the time of peak 1-hour ozone at C45. Upper right panel: 1-hour average ozone time series for C45 and surrounding HGB monitors. Lower right panel: time series of 1-hour ozone, NO, NO_2, SO_2 and wind vectors at the Seabrook Friendship Park C45 monitor on March 24.

exceptionally high $PM_{2.5}$ in the vicinity of the HGB and BPA areas. It is possible that the region of enhanced AOD in the HMS product did not mix down far enough to affect the air arriving in the HGB and BPA areas on March 24.

The FINN (Figure 3-9) fire emissions and NAAPS smoke emission (Figure 3-10) plots both show fires located to the north of the HGB area. The back trajectories for the La Porte and Seabrook monitors do not intersect the emission locations or region of smoke shown in the NAAPS model analysis (lower right hand panel of Figure 3-10), however the back trajectories for the Sabine Pass monitor pass though the region where the NAAPS analysis indicates the presence of smoke reaching concentrations of 5-8 µg m^{-3}.

Figure 3-11 and Figure 3-12 show maps of the HGB and BPA CAMS monitoring locations. Each monitor is color-coded showing its MDA8 ozone (upper panel) and/or MDA1 $PM_{2.5}$ value. March 24 1-hour time series for ozone and $PM_{2.5}$ time-series measurements are shown on the right side of the figures. Figure 3-11 shows that monitors to the north and west of the HGB area had

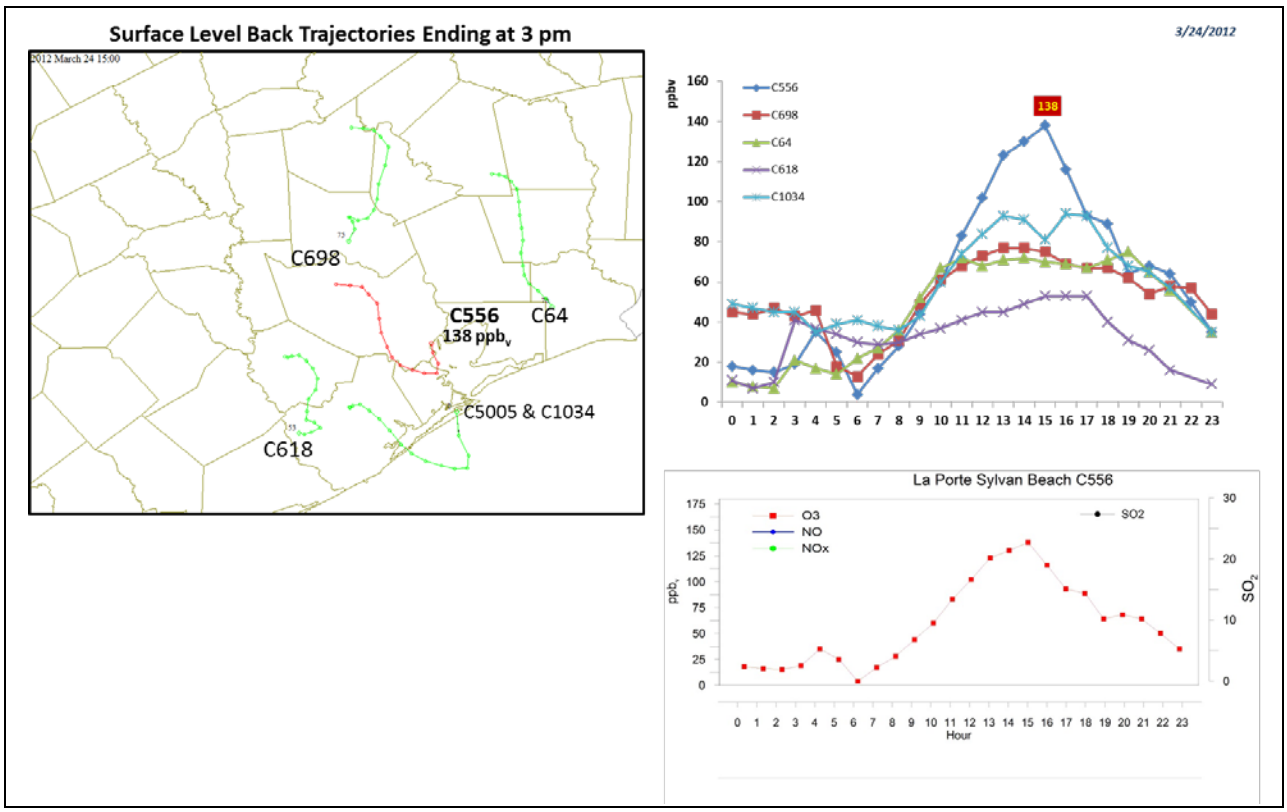

Figure 3-4. March 24, 2012 high ozone day at La Porte C556. Left panel: AQPlot back trajectories terminating at C556 and four HGB monitors located outside the central urban area at the time of peak 1-hour ozone at C556. Upper right panel: 1-hour average ozone time series for C556 and surrounding HGB monitors. Lower right panel: time series of 1-hour ozone at the C556 monitor on March 24. Wind NO, NOx and SO_2 data for the La Porte C556 monitor were not available on this day, as the monitor was undergoing preventive maintenance.

lower MDA8 values than monitors in the southwestern part of the urban area, such as Seabrook and La Porte. This is consistent with the generally northerly flow in the morning of March 24 and recirculating afternoon winds shown at the monitors and the back trajectories. Figure 3-12 shows that the HGB monitors with very high ozone are located in or are generally downwind of an area with high emissions on a relatively stagnant day when back trajectories do not show evidence for transport near fires. The generally low values of $PM_{2.5}$ at monitors in the HGB and BPA areas during the day when ozone values are highest suggest that the area of enhanced AOD seen offshore in the HMS product and the fires located northwest of the BPA area did not have a strong influence onshore during the period of peak ozone on March 24. Both the HGB and BPA area show increases in $PM_{2.5}$ in the evening, but this occurred after the ozone maxima, and suggests that the cause of the $PM_{2.5}$ maxima is not the main contributor to high ozone on March 24.

We conclude that there is no compelling evidence for fire influence on ozone on March 24 for the Seabrook, La Porte or Sabine Pass monitors and recommend no further evaluation of March 24, 2012.

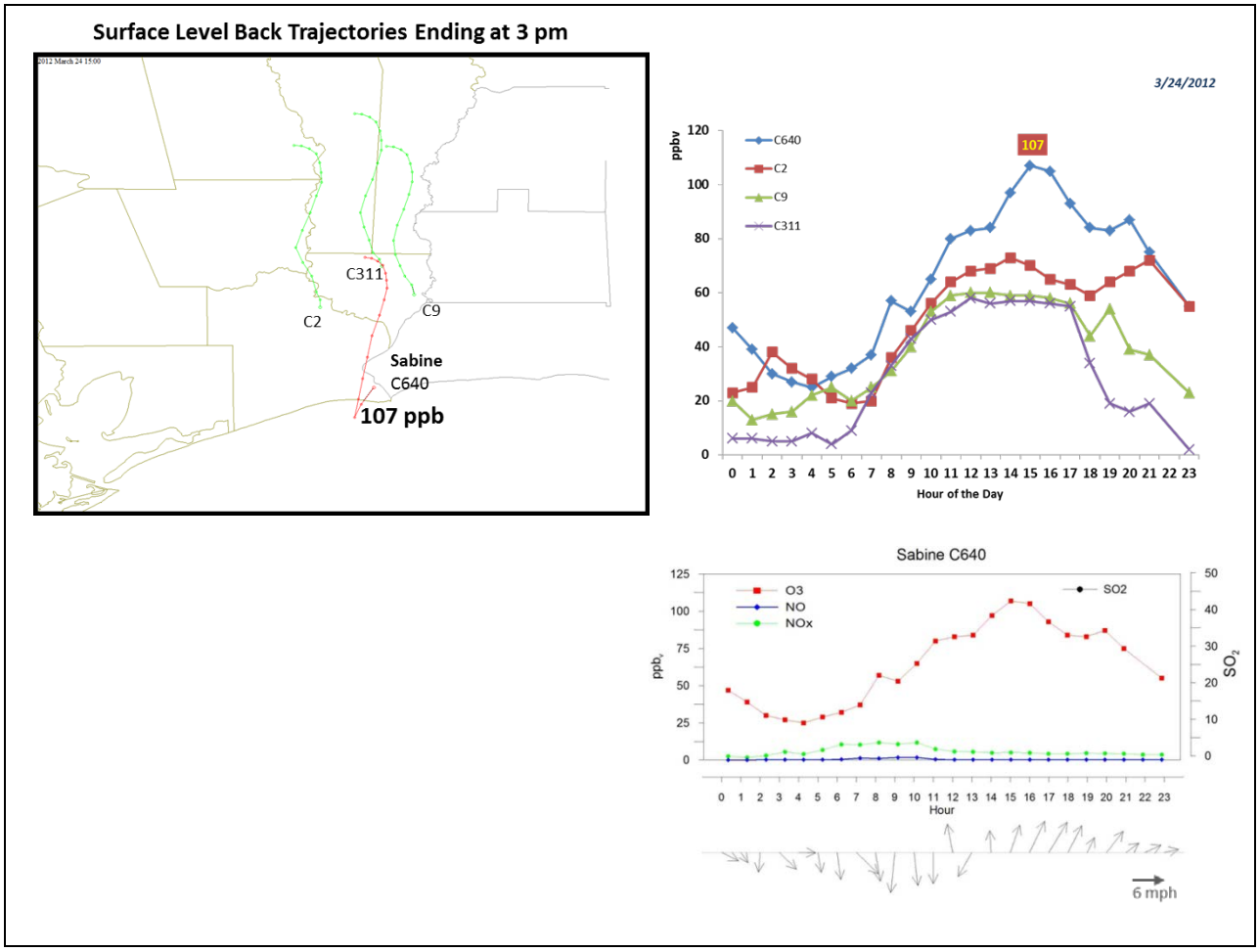

Figure 3-5. March 24, 2012 high ozone day at Sabine Pass C640. Left panel: AQPlot back trajectories terminating at C640 and three BPA monitors located outside the central urban area at the time of peak 1-hour ozone at C640. Upper right panel: 1-hour average ozone time series for C640 and surrounding BPA monitors. Lower right panel: time series of 1-hour ozone at the C640 monitor on March 24. Lower right panel: time series of 1-hour ozone, NO, NO_2 and wind vectors at the Sabine monitor.

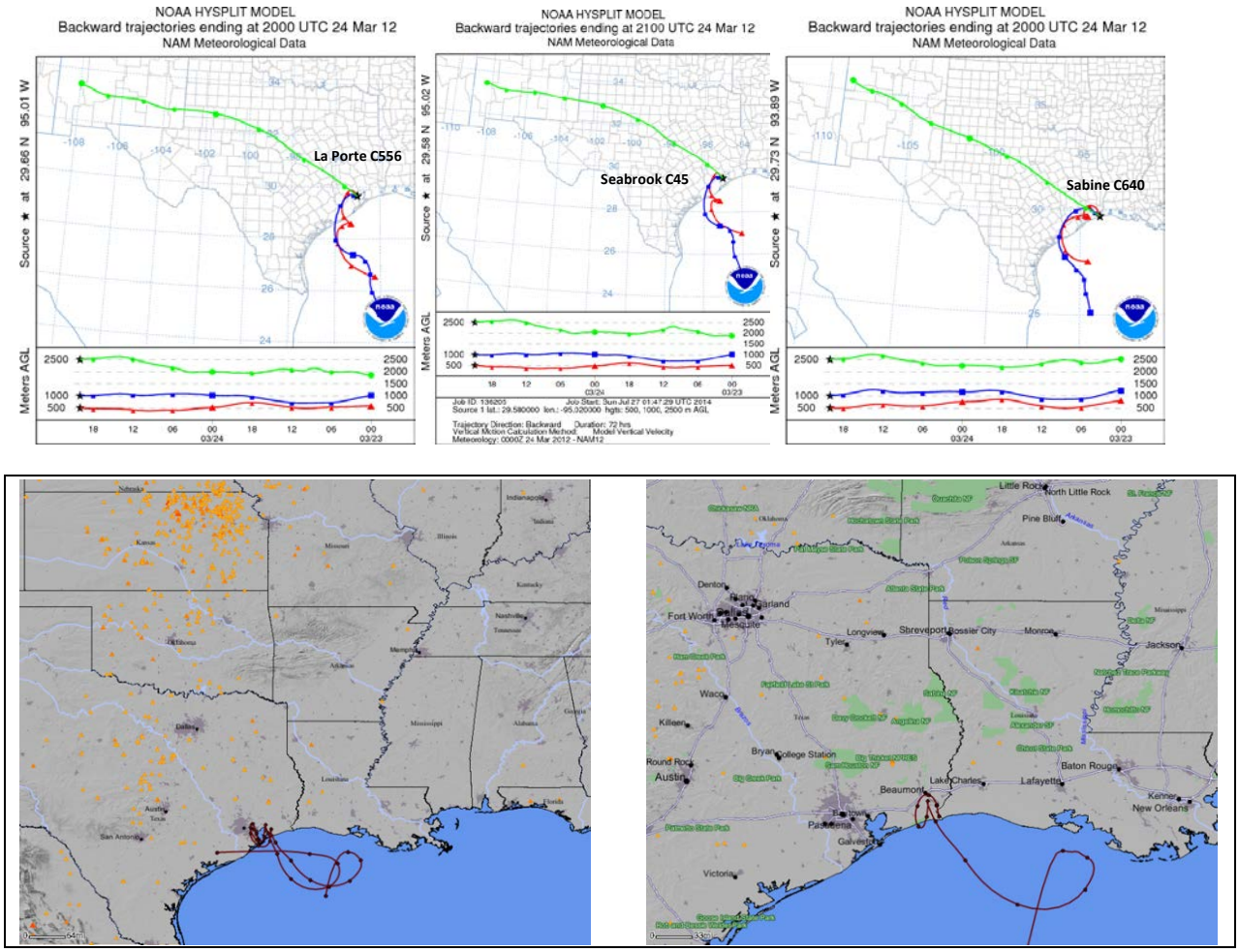

Figure 3-6. March 24 72-hour HYSPLIT back trajectories at La Porte (top left); Seabrook (top middle) and Sabine site (top right); SmartFire plots showing fire locations for March 24 (orange triangles) and 72-hour back trajectories from HGB sites (bottom left) and BPA Sabine C640 site location (bottom right).

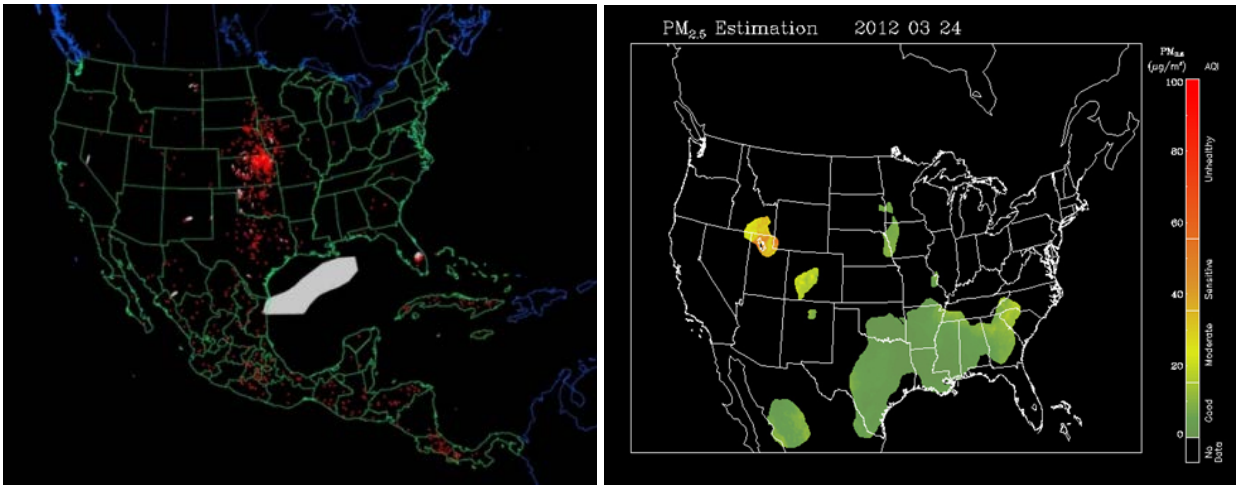

Figure 3-7. Fire locations across the United States on March 24, 2012 (left); red dots correspond to satellite detections indicating active fires, gray areas are smoke plumes inferred from satellite aerosol optical depth (AOD) measurements. Right panel shows nationwide surface $PM_{2.5}$ analysis based on satellite AOD retrievals and surface monitoring data.

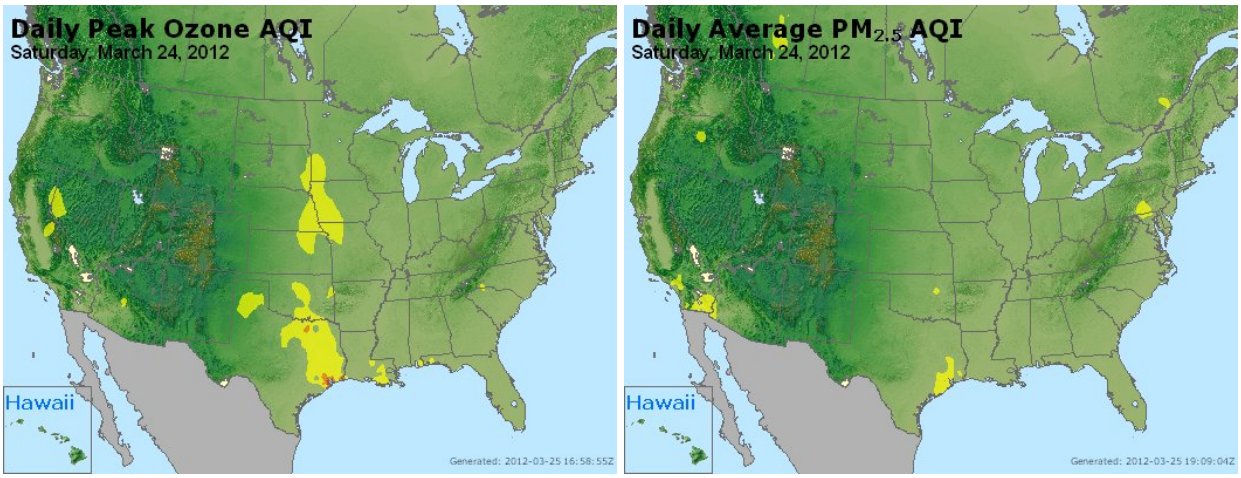

Figure 3-8. March 24 AIRNOW daily average ozone (left) and $PM_{2.5}$ (right) based on observed surface monitoring data. Data from: [http://www.airnow.gov/.](http://www.airnow.gov/)

Wildfire Emissions Inventory: FINN 2012

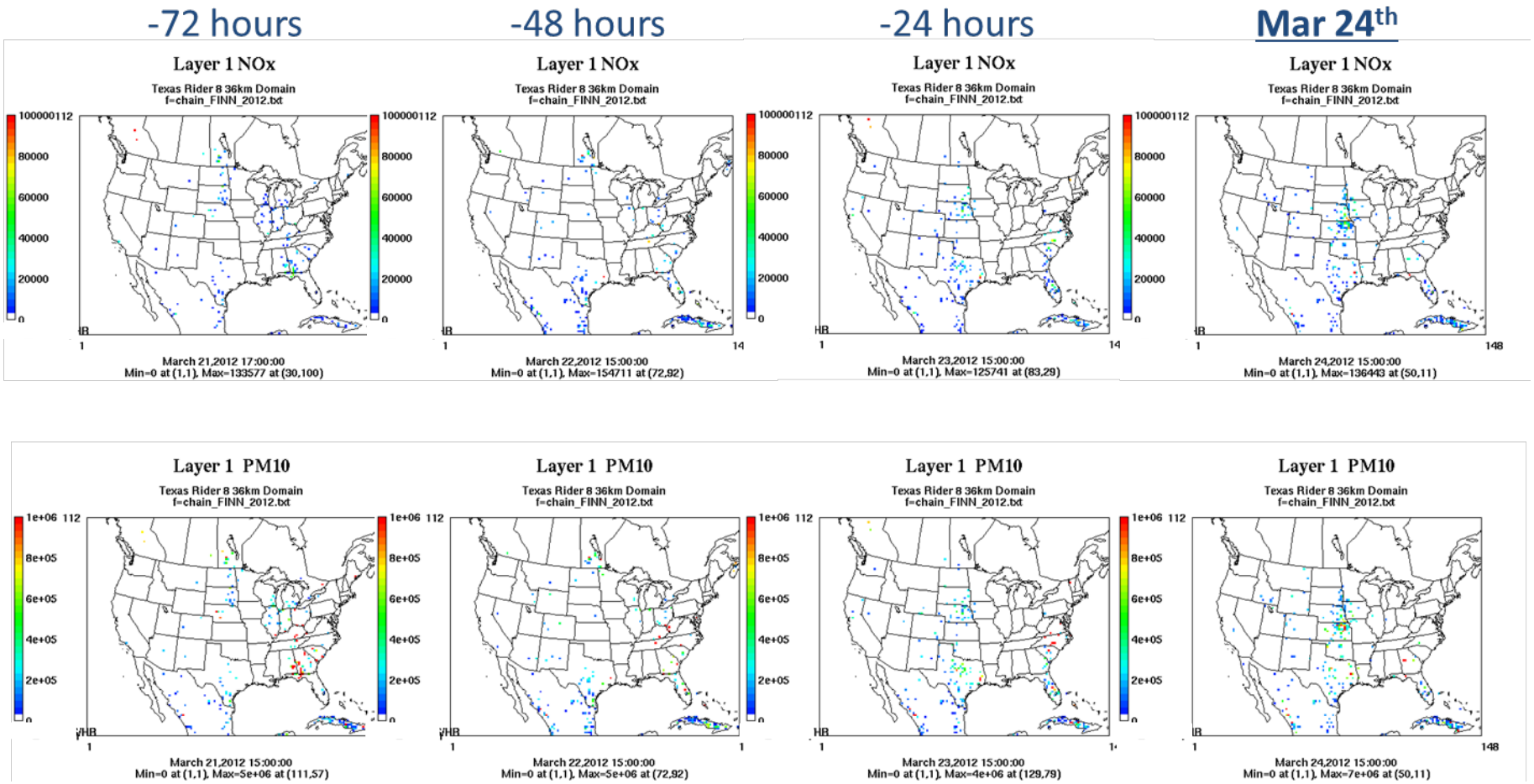

Figure 3-9. March 24, 2012 FINN fire emissions of NOx and PM_{10}. Units for NOx emission in gram mol/hr (10,000 gmol/hr ~ 1 ton/hr). PM_{10} expressed in g/hr.

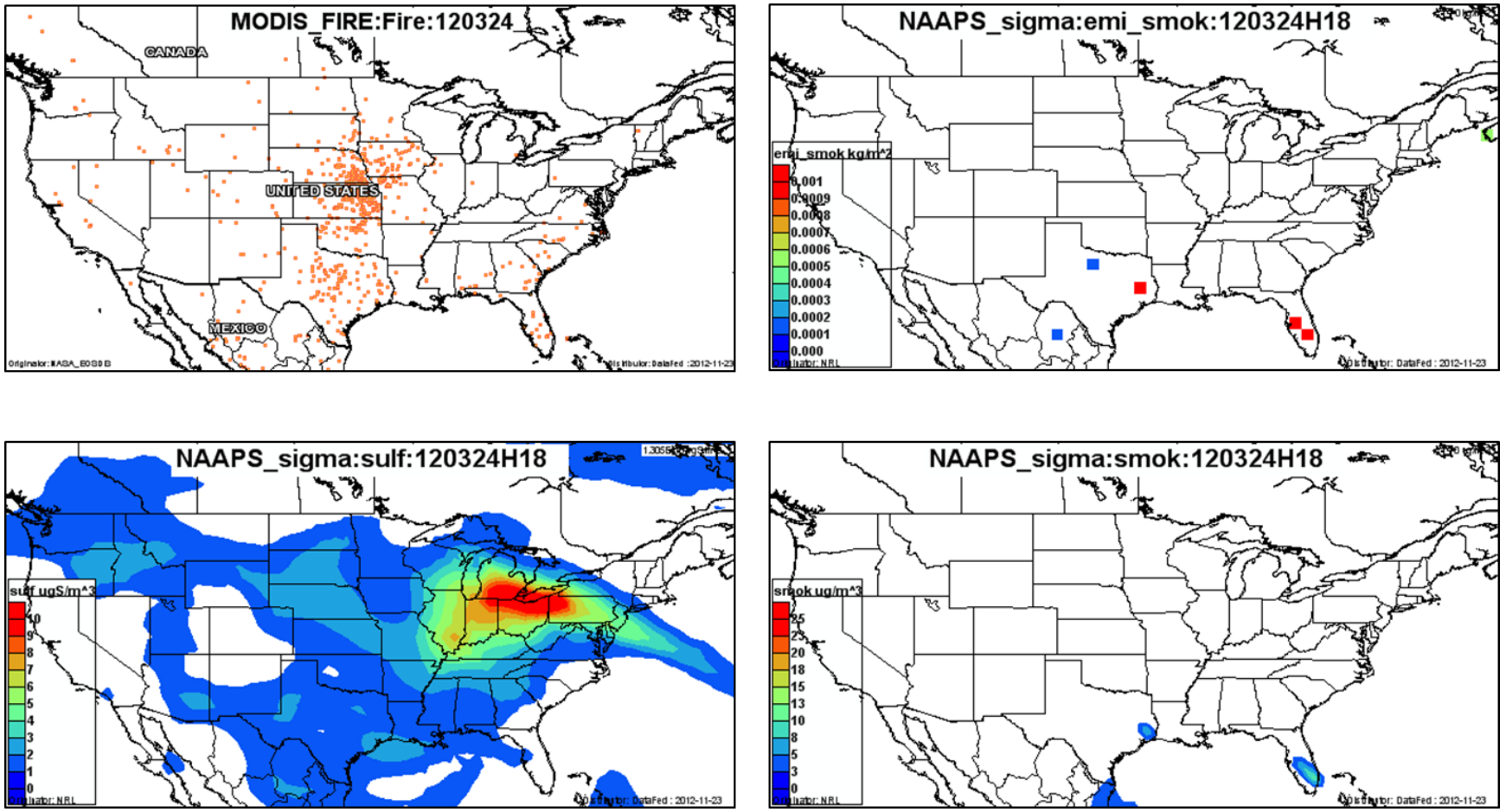

Figure 3-10. March 24, 2012 DataFed analysis. Upper left panel: Locations of active fires from MODIS satellite fire detections. Upper right panel: NAAPS model smoke emissions. Lower left panel: NAAPS model surface layer sulfate concentrations. Lower right panel: NAAPS model surface layer smoke concentrations.

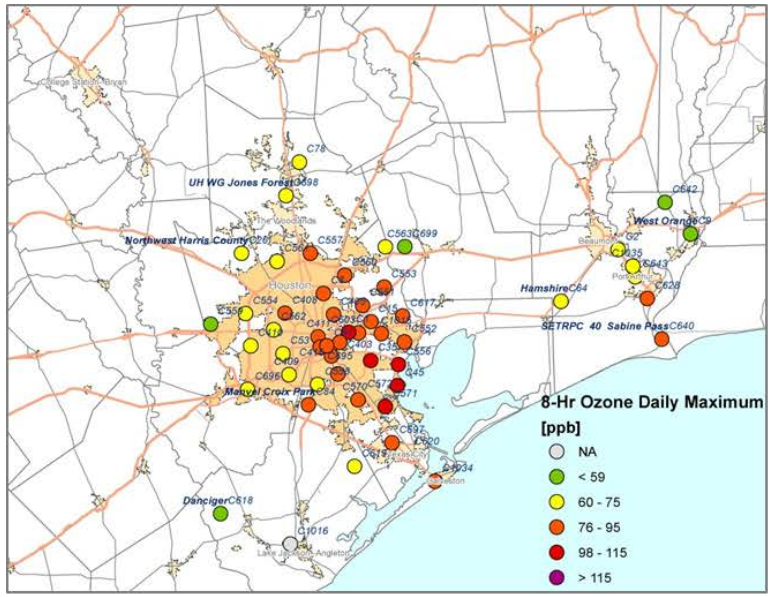

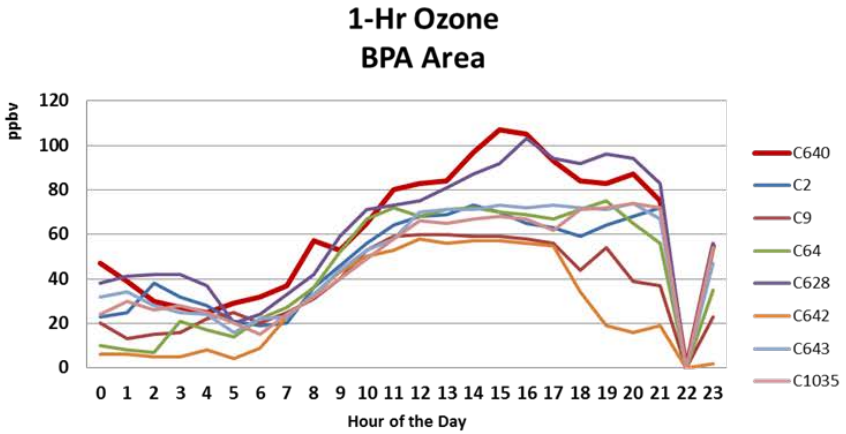

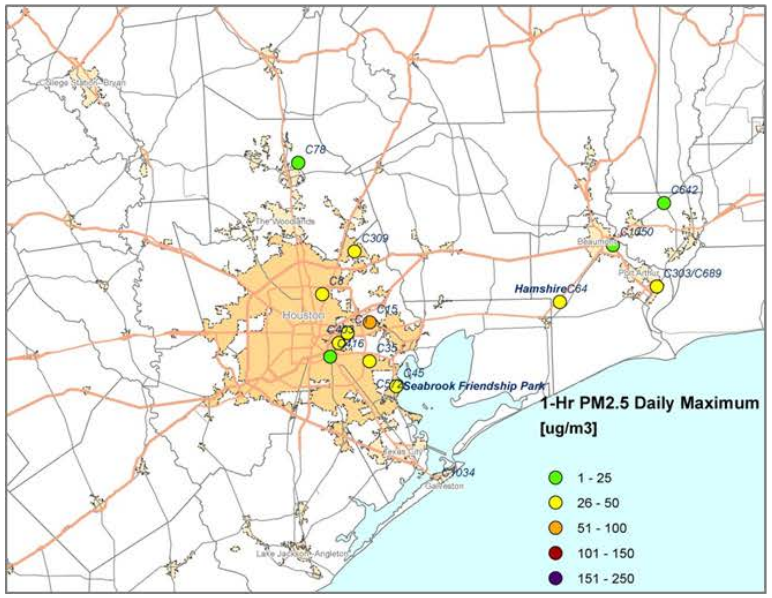

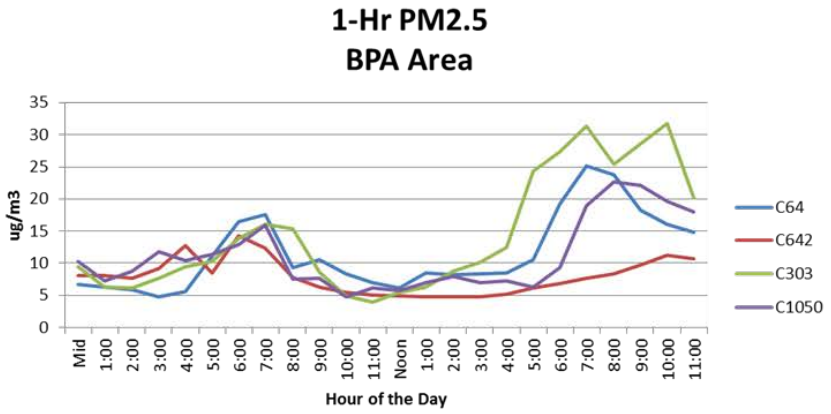

Figure 3-11. Regional ozone (top left and right) and $PM_{2.5}$ (bottom left and right) measurements (BPA area time series).

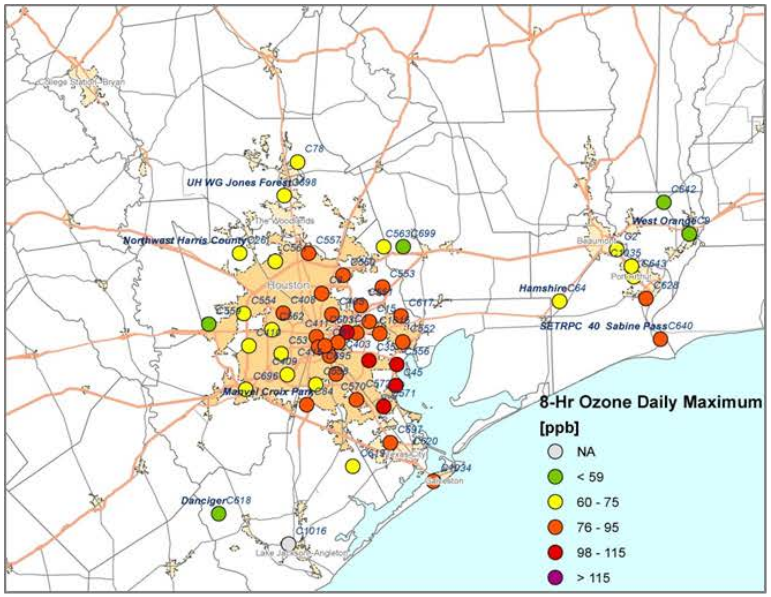

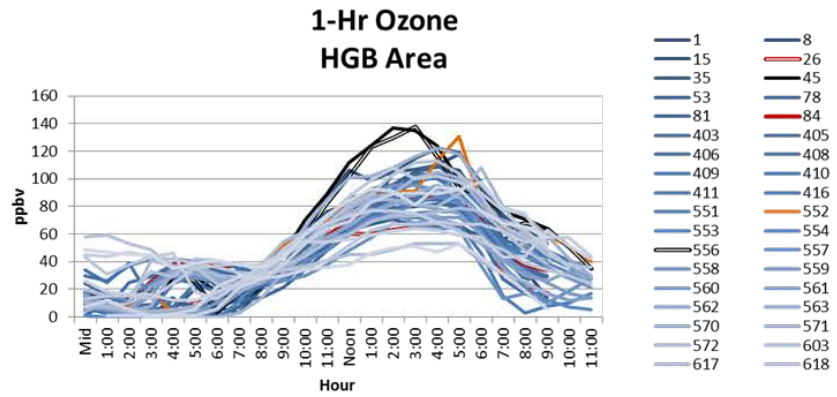

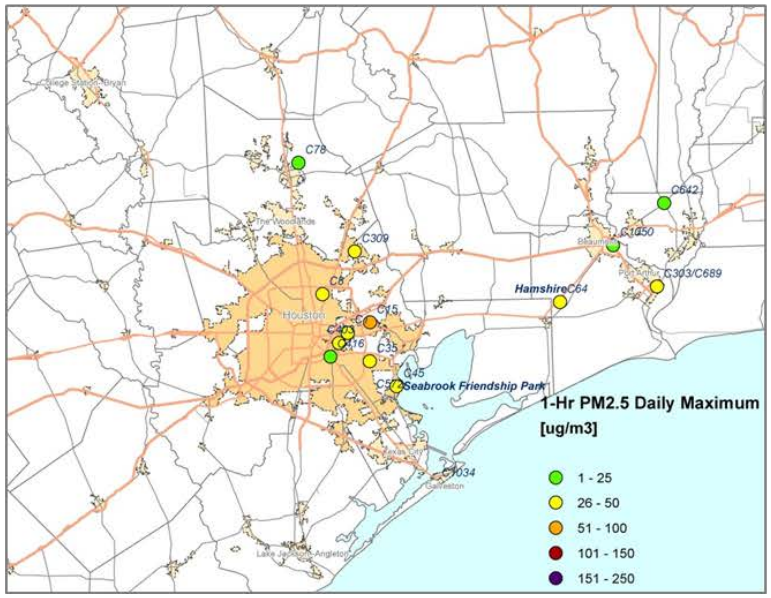

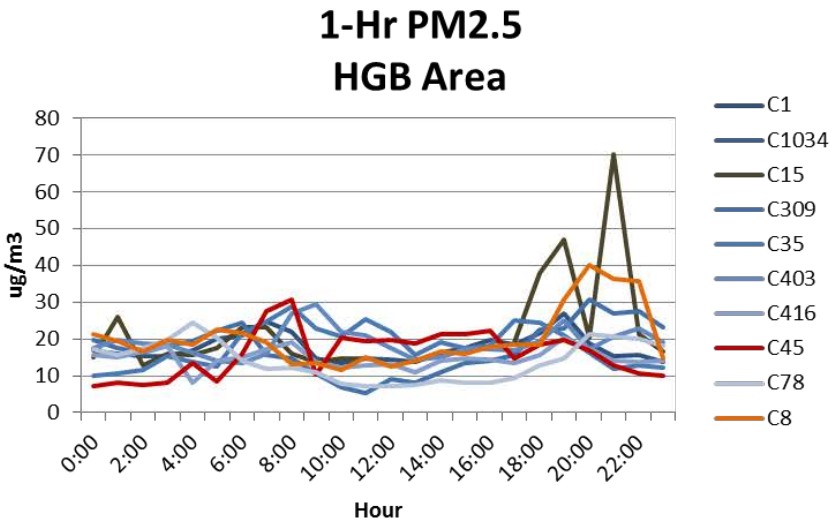

Figure 3-12. Regional ozone (top left and right) and $PM_{2.5}$ (bottom left and right) measurements (HGB area time series).

3.1.2 March 25, 2012

On March 25, 2012, the Sabine Pass monitor recorded its 2nd high MDA8 ozone reading for 2012. The Sabine Pass monitor observed MDA1 ozone of 104 ppb (Figure 3-13). The peak 1-hour ozone is 50 ppb higher at Sabine Pass than at the C311 monitor, located to the north of the BPA urban area. The AQPlot surface wind back trajectory ending at the Sabine Pass monitor at the time of maximum 1-hour ozone (left panel of Figure 3-13) shows a recirculating flow, with northerly winds in the morning with a shift to southerly winds at 2 pm. This is consistent with the wind vectors at the Sabine Pass monitor (lower right panel of Figure 3-13. AQPlot back trajectories for the three other BPA area sites show northerly winds and no evidence of recirculating flow, as seen at the Sabine Pass monitor.

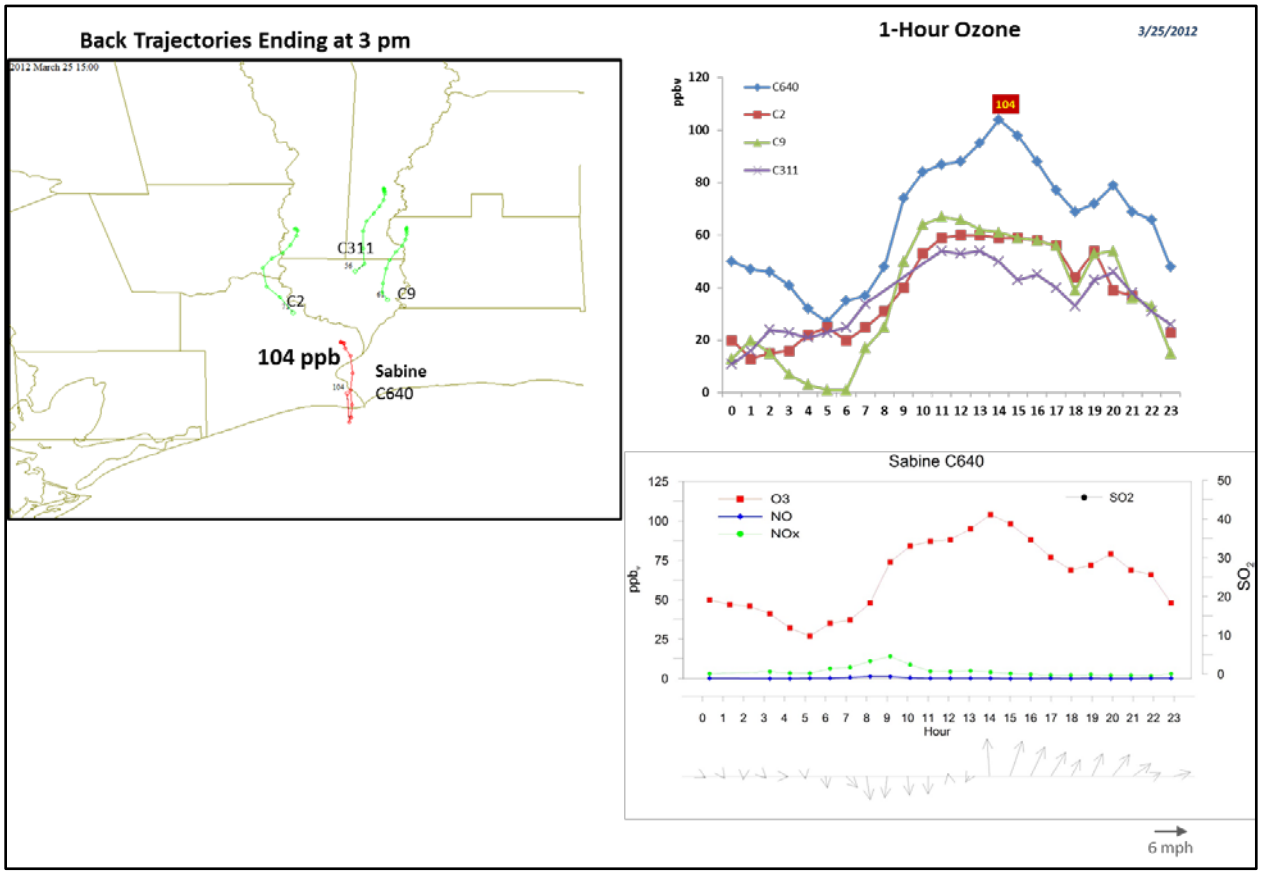

Figure 3-13. March 25, 2012 high ozone day at Sabine Pass C640. Left panel: back trajectories from AQPlot for 3 monitors located outside the central urban area at the time of peak 1-hour ozone at C640. Upper right panel: 1-hour average ozone time series for the C640 and surrounding BPA monitors. Lower right panel: time series of 1-hour ozone, NO, NO_2 and wind vectors at the Sabine monitor on March 25.

Figure 3-14 shows SmartFire and HYSPLIT NAM 72-hour back trajectories ending at Sabine Pass location at the time maximum 1-hour ozone was observed. The back trajectories for low level

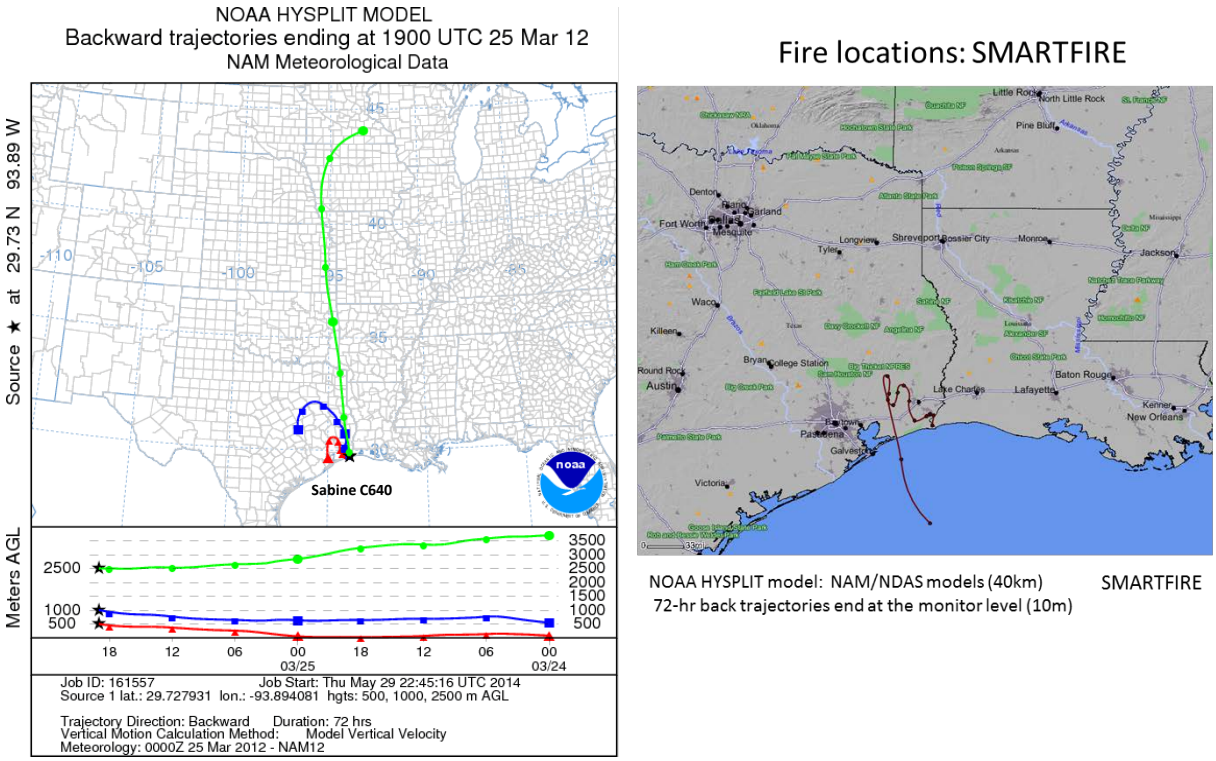

Figure 3-14. March 25 72-hour HYSPLIT back trajectories from Sabine Pass site (left panel) ending at March 25, 2012; SmartFire plot showing fire locations (orange triangles) and 72-hour back trajectories from the BPA site (right panel).

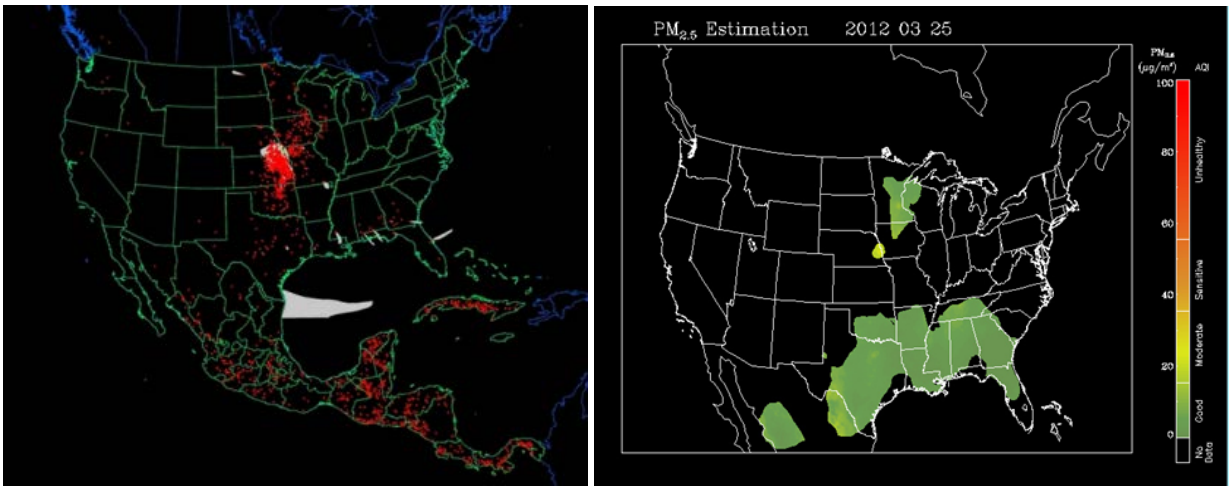

Figure 3-15. Left panel: HMS product showing March 25 fire locations (red dots) and smoke plume (gray area). Right panel: IDEA surface $PM_{2.5}$ estimate based on AOD and surface monitoring data.

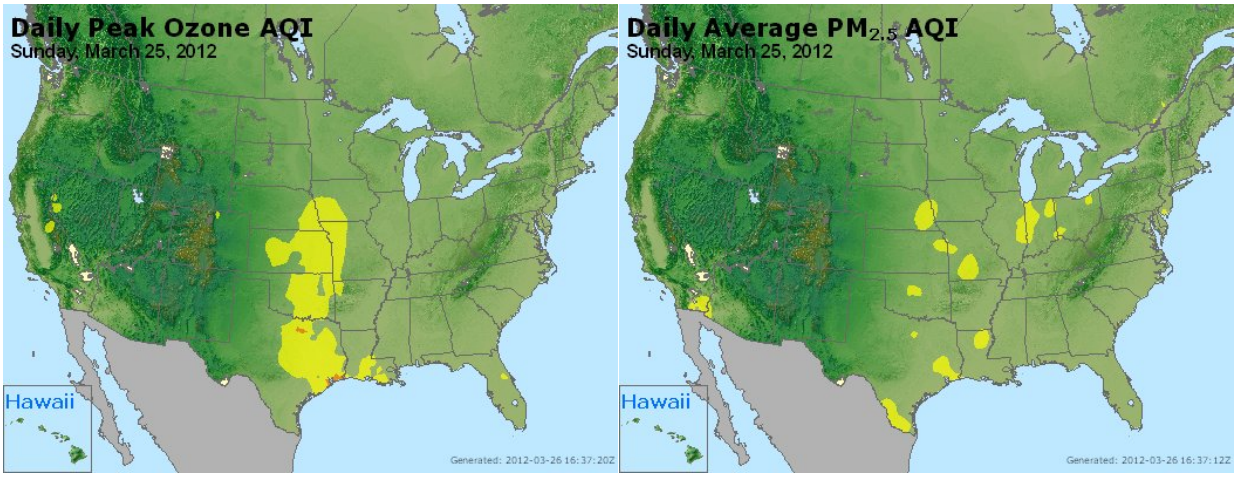

Figure 3-16. March 25 AIRNOW daily average ozone (left) and $PM_{2.5}$ (right) based on observed surface monitoring data. Data from: http://www.airnow.gov/.

winds indicate stagnant flow that did not pass near locations of active fires during the preceding 72 hours. The HMS product (left panel of Figure 3-15) shows an area of enhanced AOD over the Gulf of Mexico that is well south of the trajectories. The IDEA near-surface $PM_{2.5}$ estimate (right panel of Figure 3-15) has no data in the vicinity of the low-level back trajectories on March 25. The $PM_{2.5}$ AQI (Figure 3-16) and the CAMS monitoring sites (Figure 3-19) indicate that there are moderate levels of $PM_{2.5}$ in the BPA area on March 25. The FINN and the NAAPS plots (Figure 3-17; Figure 3-18) agree that there are no fire emissions or smoke along the path of the low-level back trajectories.

$PM_{2.5}$ levels in the BPA area are at relatively low levels during the period when Sabine Pass 1-hour ozone levels are at their maximum values on March 25 (Figure 3-13). Low levels of $PM_{2.5}$ taken together with the fact that there is no NOx peak at the time of maximum 1-hour ozone (Figure 3-13) show that the peak ozone values were unlikely to be the result of a smoke plume impact. Background ozone entering the BPA area from the north is approximately 60 ppb (Figure 3-19). The north-south gradient in MDA8 ozone across the BPA area (Figure 3-19) and the northerly near surface wind flow and subsequent recirculation at the Sabine Pass monitor suggest that local BPA emissions were the primary contributor to the enhancement over background ozone at the Sabine Pass monitor on March 25. The fact that the low-level back trajectories do not pass over active fires and the lac k of evidence of a smoke plume impact leads us to conclude that there is no compelling evidence for fire influence on ozone on March 25 for the Sabine Pass monitor. We recommend no further evaluation of March 25, 2012.

Wildfire Emissions Inventory: FINN 2012

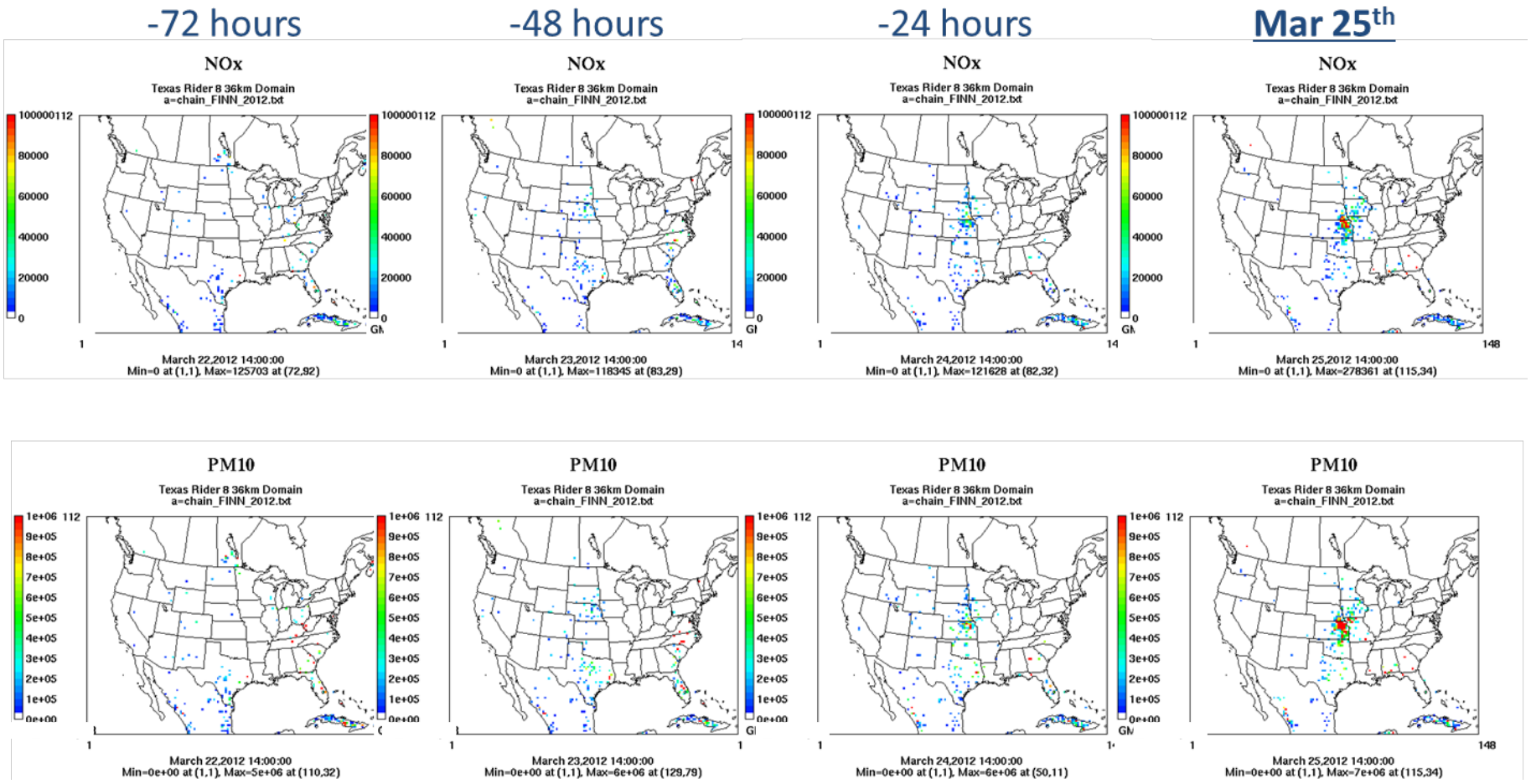

Figure 3-17. March 25 2012 FINN fire emissions of NOx and PM_{10}.

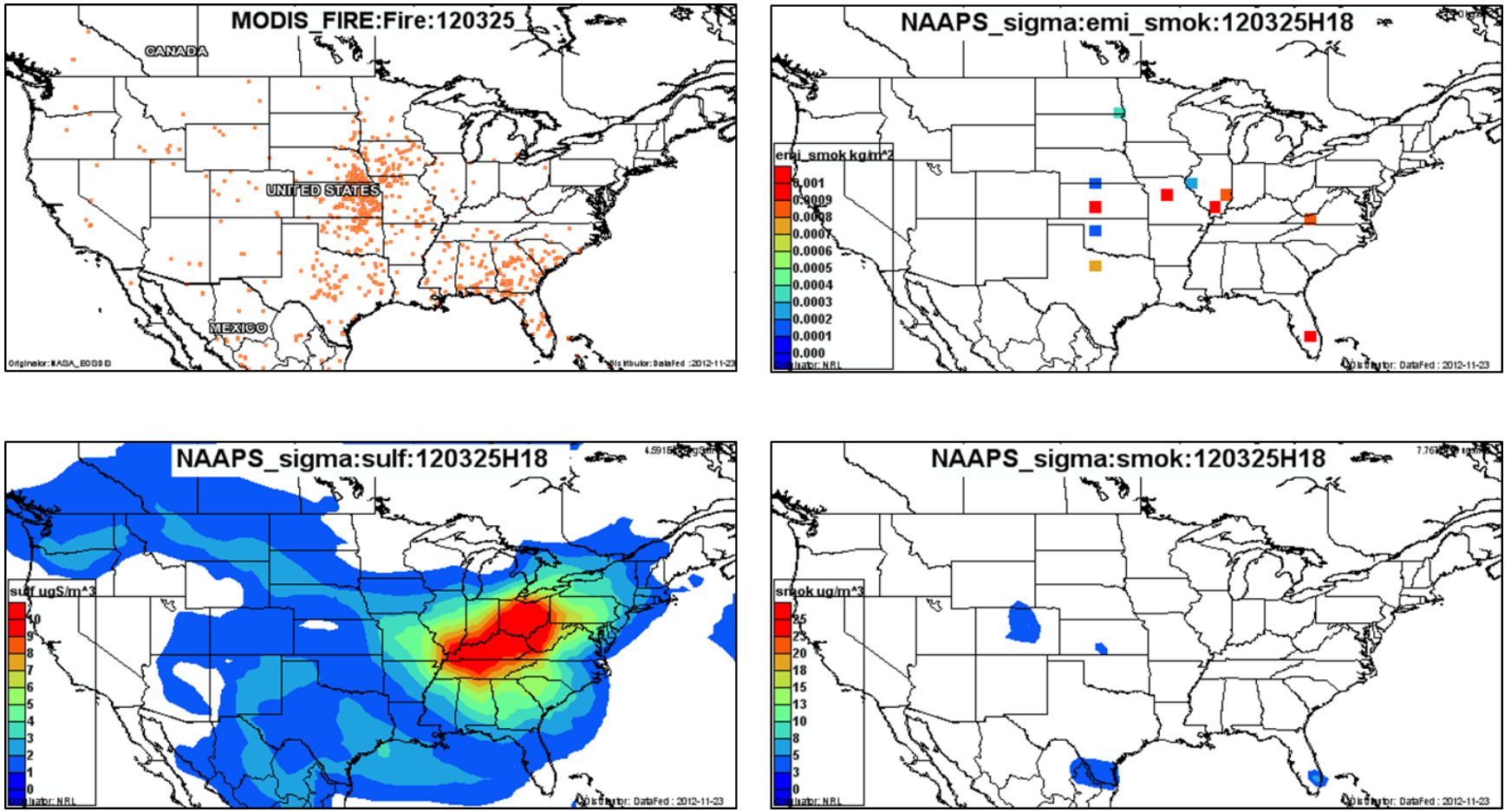

Figure 3-18. March 25, 2012 DataFed analysis. Upper left panel: Locations of active fires from MODIS satellite fire detections. Upper right panel: NAAPS model smoke emissions. Lower left panel: NAAPS model surface layer sulfate concentrations. Lower right panel: NAAPS model surface layer smoke concentrations.

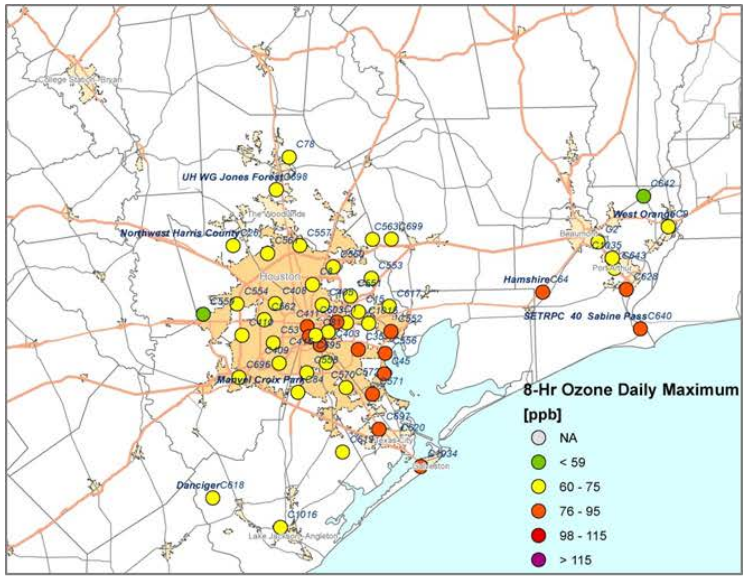

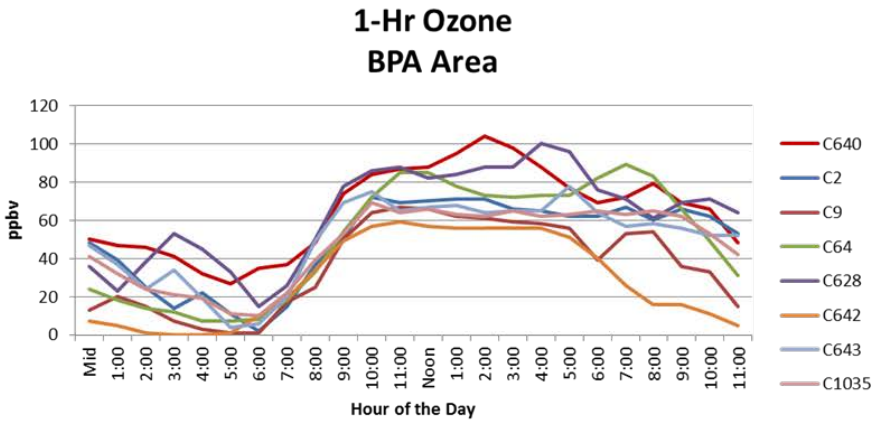

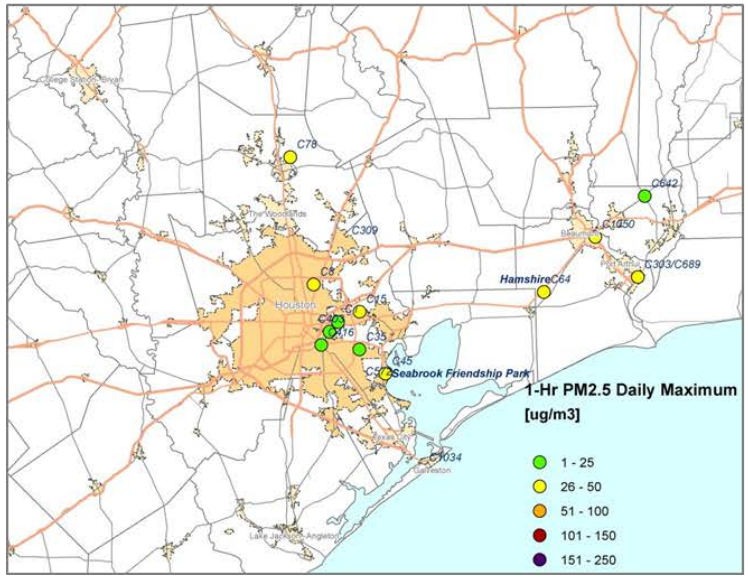

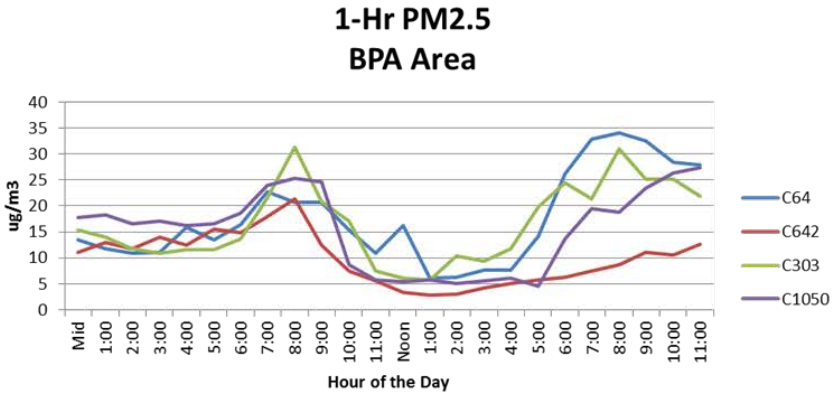

Figure 3-19. March 25 Regional ozone (top left and right) and $PM_{2.5}$ (bottom left and right) measurements (BPA area time series.

3.1.3 March 26, 2012

On March 26, the Northwest Harris County monitor, C26, had its second highest MDA8 value (85 ppb) for 2012, with 1-hour ozone reaching a peak of 91 ppb (Figure 3-20). Values of 1-hour ozone exceeding 100 ppb were recorded at several monitors in the northern HGB area, e.g.: Mercer Arboretum (126 ppb), Atascocita (122 ppb) and Jones Forest (126 ppb) (Figure 3-26). The monitors south of the urban area had lower peak 1-hour values in the range of 60-90 ppb range () Figure 3-26). Figure 3-20 shows AQPlot surface wind back trajectories and NW Harris Count monitor wind vectors indicating that winds were stagnant with recirculation on March 26, and that winds were northerly in the early morning, switching to southerly by late morning.

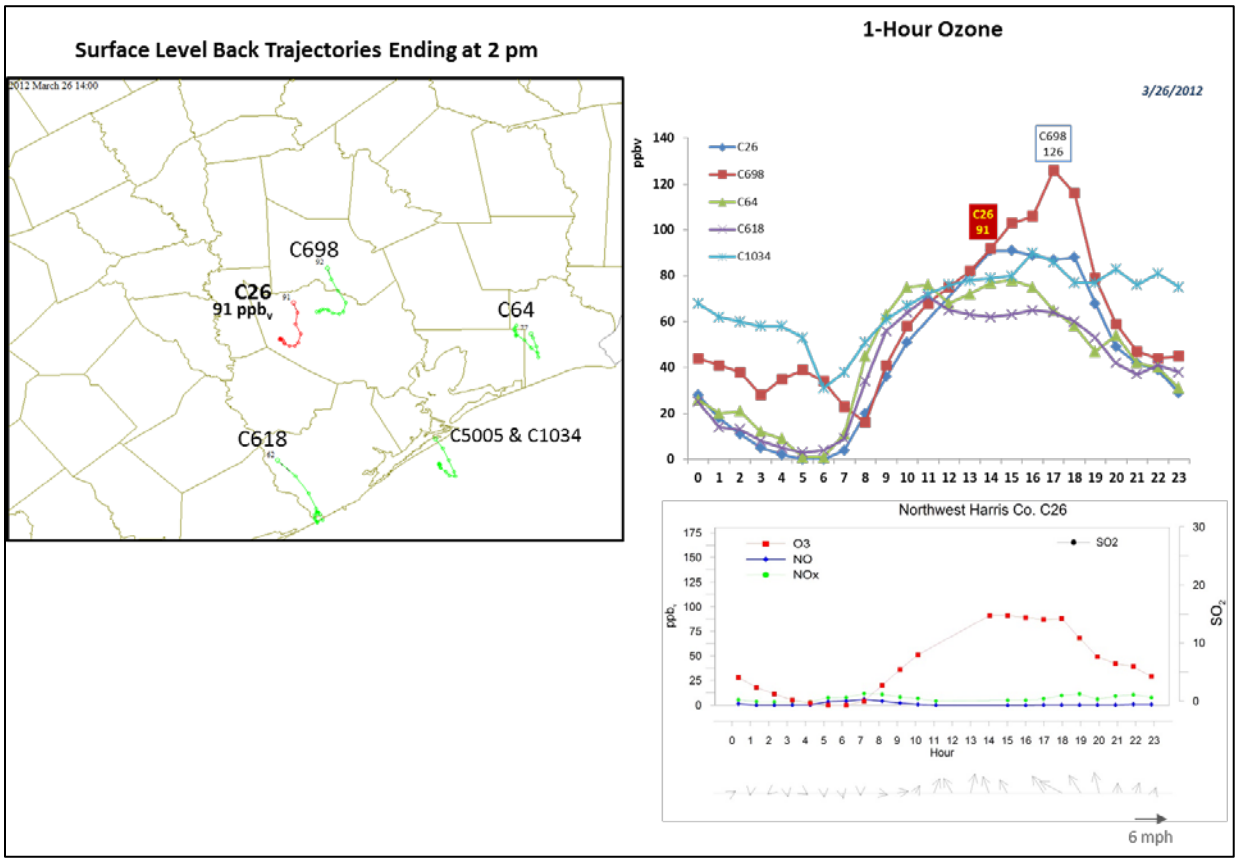

Figure 3-20. March 26, 2012 high ozone day at Northwest Harris County, C26. Left panel: back trajectories from AQPlot for the HGB monitors for March 26 at the time of peak 1-hour ozone at C26. Upper right panel: 1-hour average ozone time series for the C26 and surrounding HGB monitors. Lower right panel: time series of 1-hour ozone, NO, NO_2 and wind vectors at the Northwest Harris monitor on March 26.

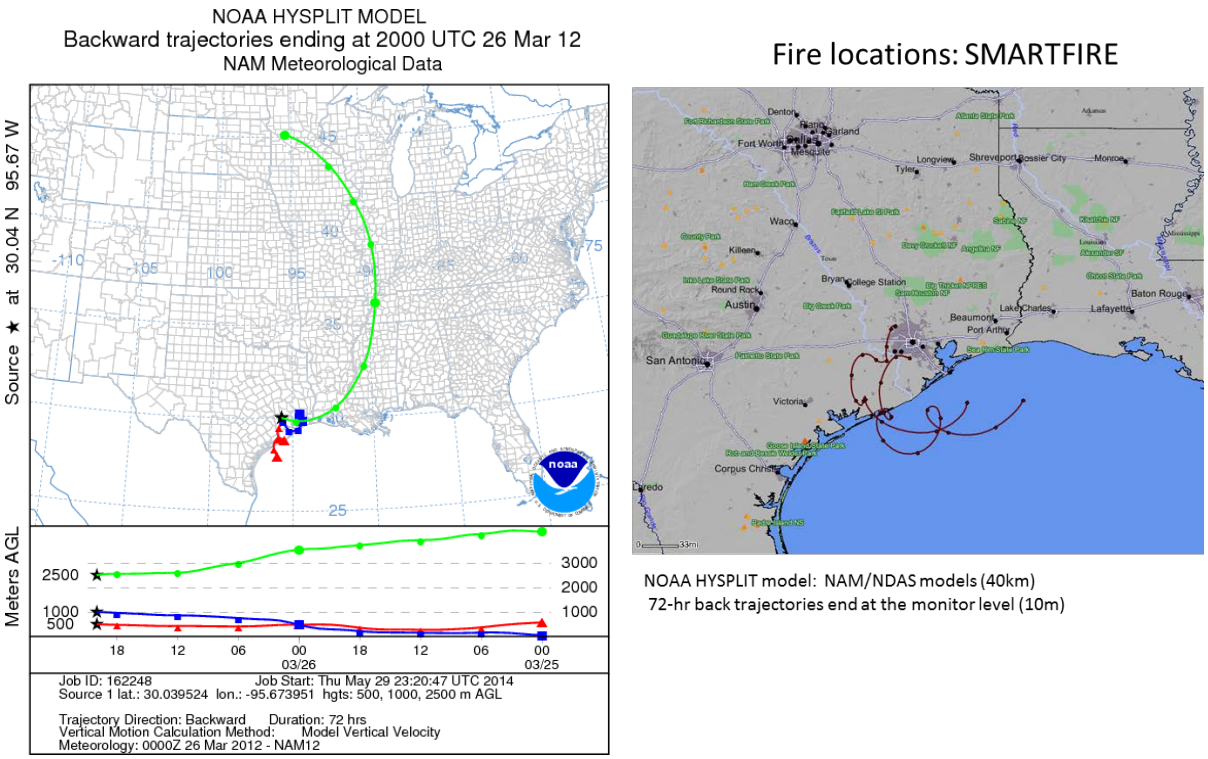

Figure 3-21. 72-hour HYSPLIT back trajectories from the NW Harris County monitor (left panel) ending at March 26, 2012; SmartFire plot showing fire locations (orange triangles) and 72-hour back trajectories from two HGB sites C26 and C84 (right panel).

Figure 3-21 shows 72-hour SmartFire and HYSPLIT NAM back trajectories terminating above the Sabine Pass monitor at the time maximum ozone was observed. Like the AQPlot back trajectories, the SmartFire and HYSPLIT NAM 500 m and 1,000 m back trajectories show stagnant low-level winds and indicate overall southerly flow with back trajectories that lead southward out over the Gulf of Mexico. There are no fires in the immediate vicinity of the back trajectories on the SmartFire plot.

The HMS product (left panel of Figure 3-22) shows no evidence of fires or smoke in the HGB area on March 26, and the IDEA $PM_{2.5}$ surface estimate (right panel of Figure 3-22) is missing data over the HGB area. The $PM_{2.5}$ AQI index (Figure 3-23) and $PM_{2.5}$ time series (Figure 3-26) also show no evidence of enhanced $PM_{2.5}$. The spatial pattern of ozone in Figure 3-26 shows monitors southwest of the HGB area had lower ozone and monitors to the northeast of the urban area had higher ozone. Given the southerly wind direction in the back trajectories, this pattern suggests that ozone formed from local emissions enhanced ozone at the northern monitors. The DataFed analysis (Figure 3-25) shows neither smoke nor fire emissions along the back trajectories, but does show the presence of sulfate aerosol in the HGB area.

The fact that the low-level back trajectories do not pass over active fires together with the lack of evidence for a smoke plume in the HGB area lead us to conclude that there is no compelling evidence for fire influence on ozone on March 26 for the Northwest Harris County monitor.

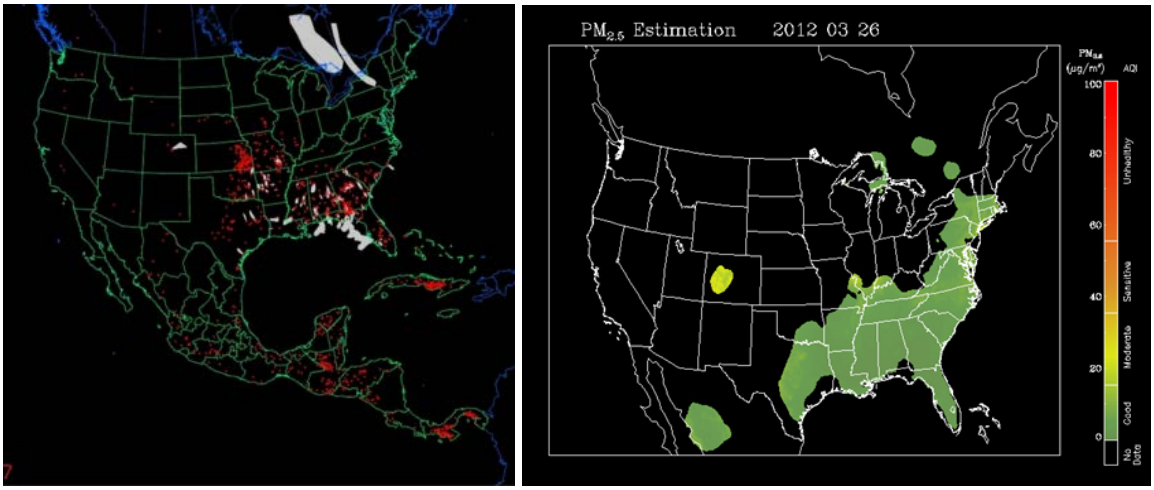

Figure 3-22. Left panel: HMS product showing March 26 fire locations (red dots) and smoke plume (gray area). Right panel: IDEA surface $PM_{2.5}$ estimate based on AOD and surface monitoring data.

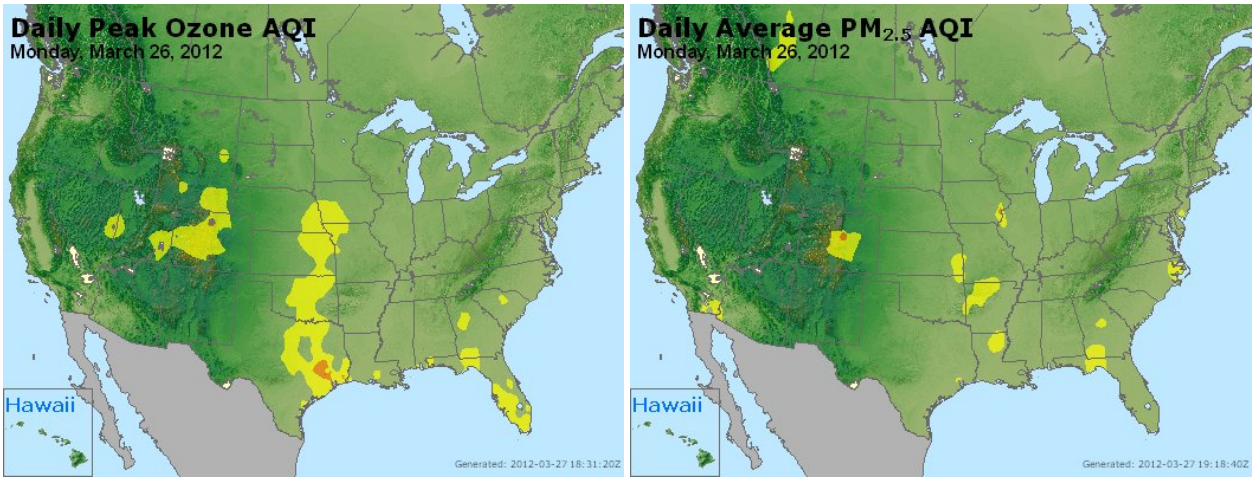

Figure 3-23. March 26 Daily average ozone (left) and $PM_{2.5}$ (right) based on observed values. Data from: [http://www.airnow.gov/.](http://www.airnow.gov/)

High ozone at the NW Harris County monitor is more likely due to the impact of local HGB emissions, consistent with the high readings at several monitors in the north and northeastern parts of the urban area on a day with southerly winds. We recommend no further evaluation of March 26, 2012.

Wildfire Emissions Inventory: FINN 2012

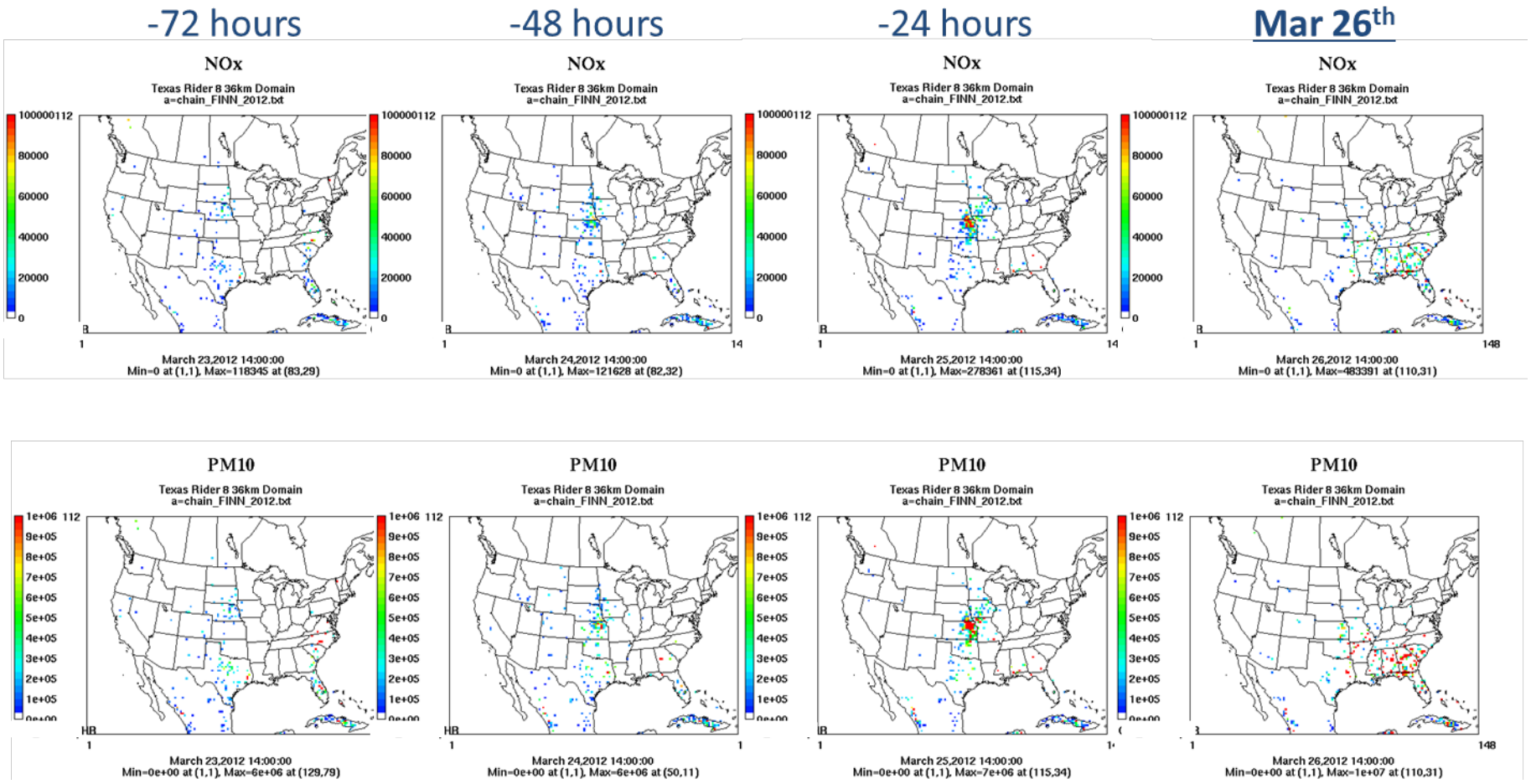

Figure 3-24. March 26 2012 FINN fire emissions of NOx and PM_{10}.

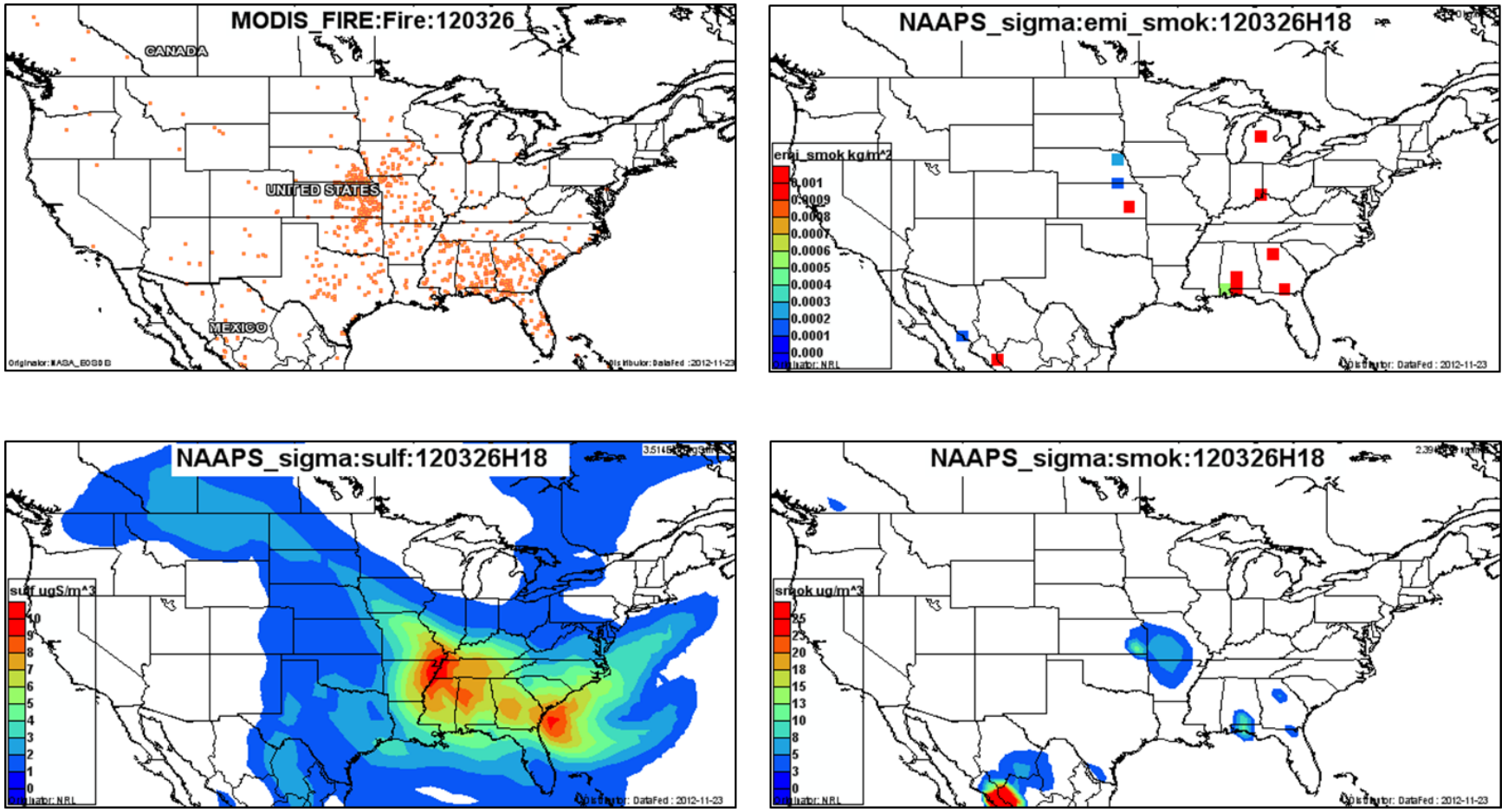

Figure 3-25. March 26, 2012 DataFed analysis. Upper left panel: Locations of active fires from MODIS satellite fire detections. Upper right panel: NAAPS model smoke emissions. Lower left panel: NAAPS model surface layer sulfate concentrations. Lower right panel: NAAPS model surface layer smoke concentrations.

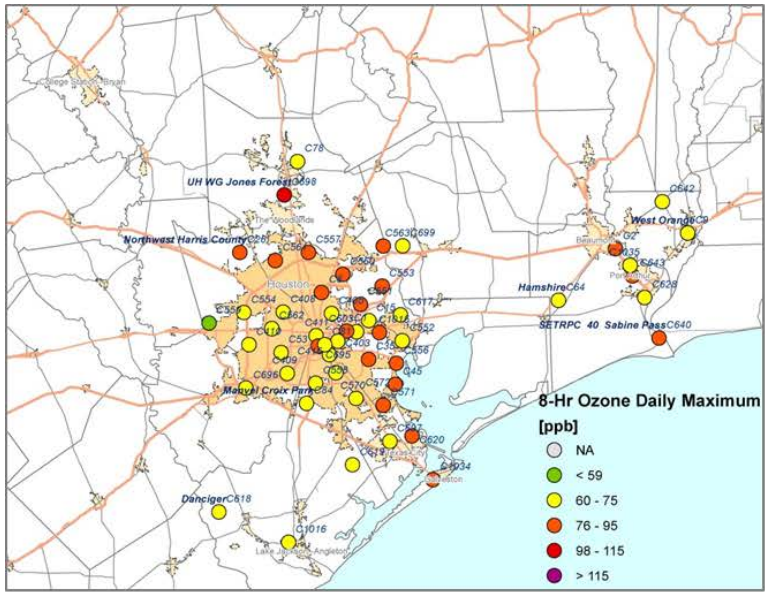

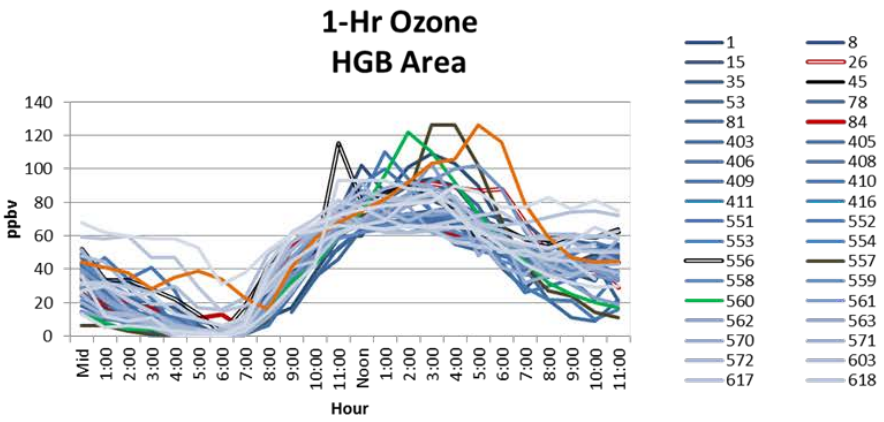

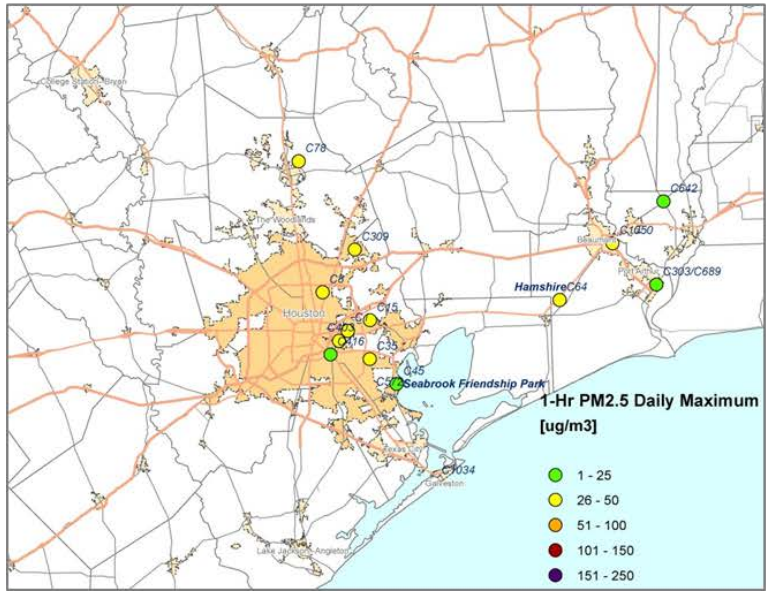

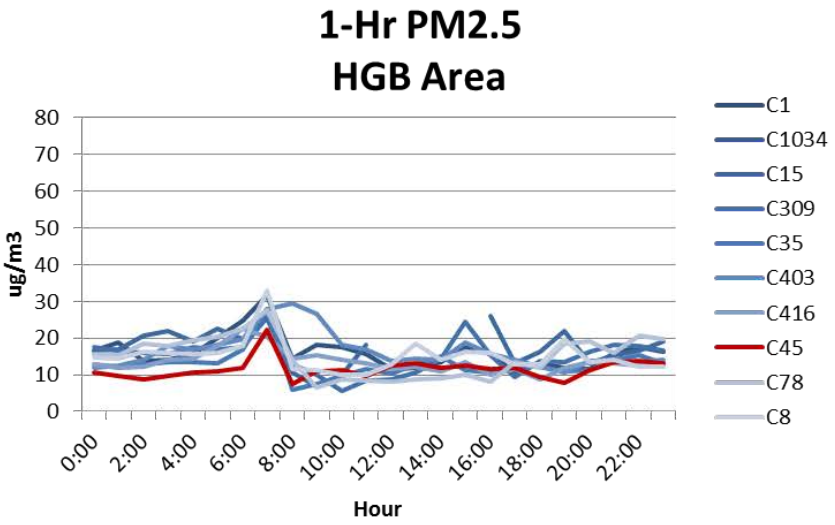

Figure 3-26. Regional ozone (top left and right) and $PM_{2.5}$ (bottom left and right) measurements (HGB area time series).

3.1.4 May 17, 2012

May 14-22, 2012 was a period of high ozone in East Texas. On May 17, the NW Harris County Monitor (C26) in the HGB area recorded its 4th high MDA8 value for 2012 with an MDA8 of 82 ppb. The peak 1-hour ozone value was 92 ppb and occurred at 4 pm (Figure 3-27). Background ozone was high (~60 ppb) on May 17 (Figure 3-34). There is no pronounced NOx or NO peak at the time of the NW Harrison County monitor's peak in 1-hour ozone, and SO_2 is not monitored at this site. The wind vectors at the monitor (lower right panel of Figure 3-27) show a sea breeze circulation pattern, with weak, shifting winds that are generally northerly in the morning and switching to southerly by late afternoon. This is consistent with the AQPlot back trajectory (upper left panel of Figure 3-27) and the HYSPLIT NAM 500 m back trajectory (upper left panel of Figure 3-29).

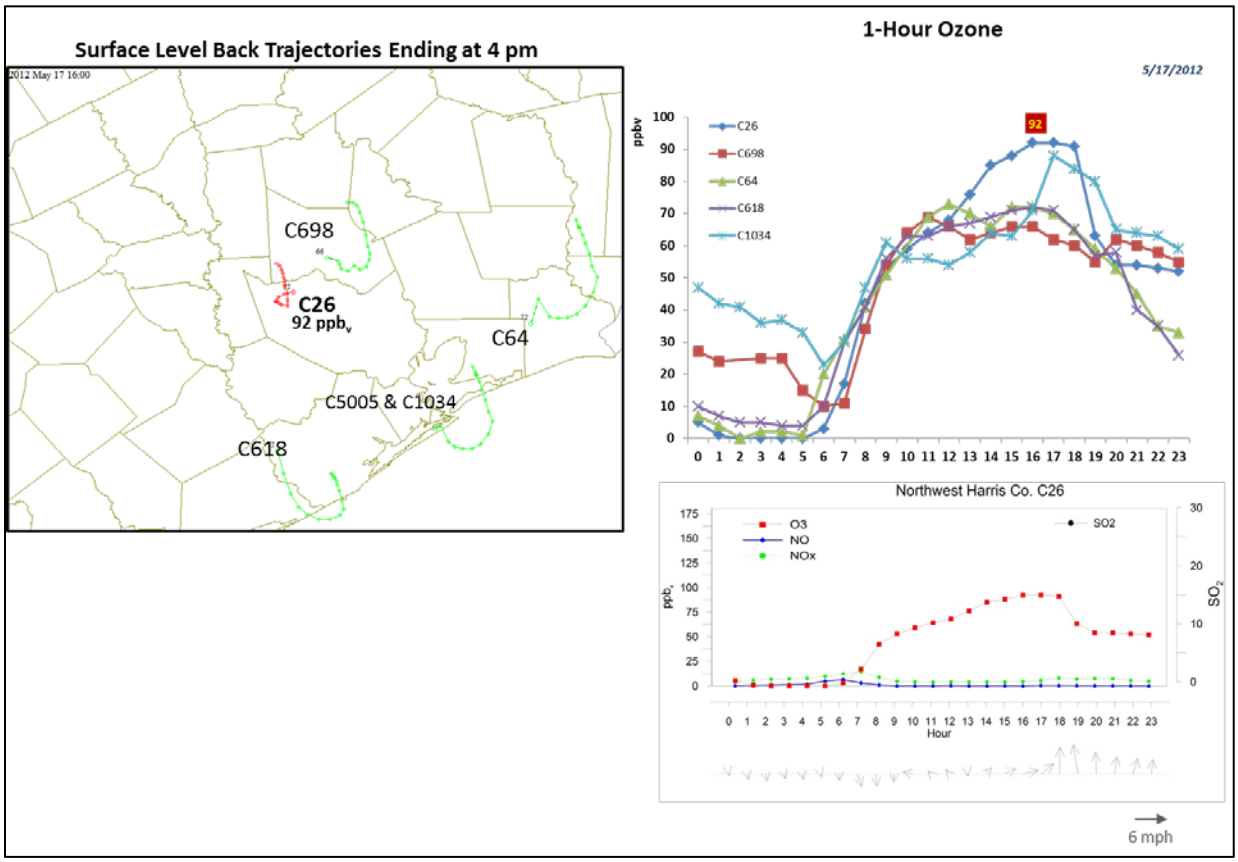

Figure 3-27. May 17, 2012 high ozone day at Northwest Harris Co. C26. Left panel: back trajectories calculated using AQPlot for the HGB monitors at the time of peak ozone impact at C26. Upper right panel: 1-hour average ozone time series for the C26 and surrounding HGB monitors. Lower right panel: time series of 1-hour ozone, NO, NO_2 and wind vectors at the Northwest Harris monitor.

The SmartFire back trajectory indicates a stronger and more northerly flow with less recirculation than is evident in the AQPlot and HYSPLIT NAM 12 km trajectories. The SmartFire back trajectory passes in the vicinity of a fire northeast of College Station (lower

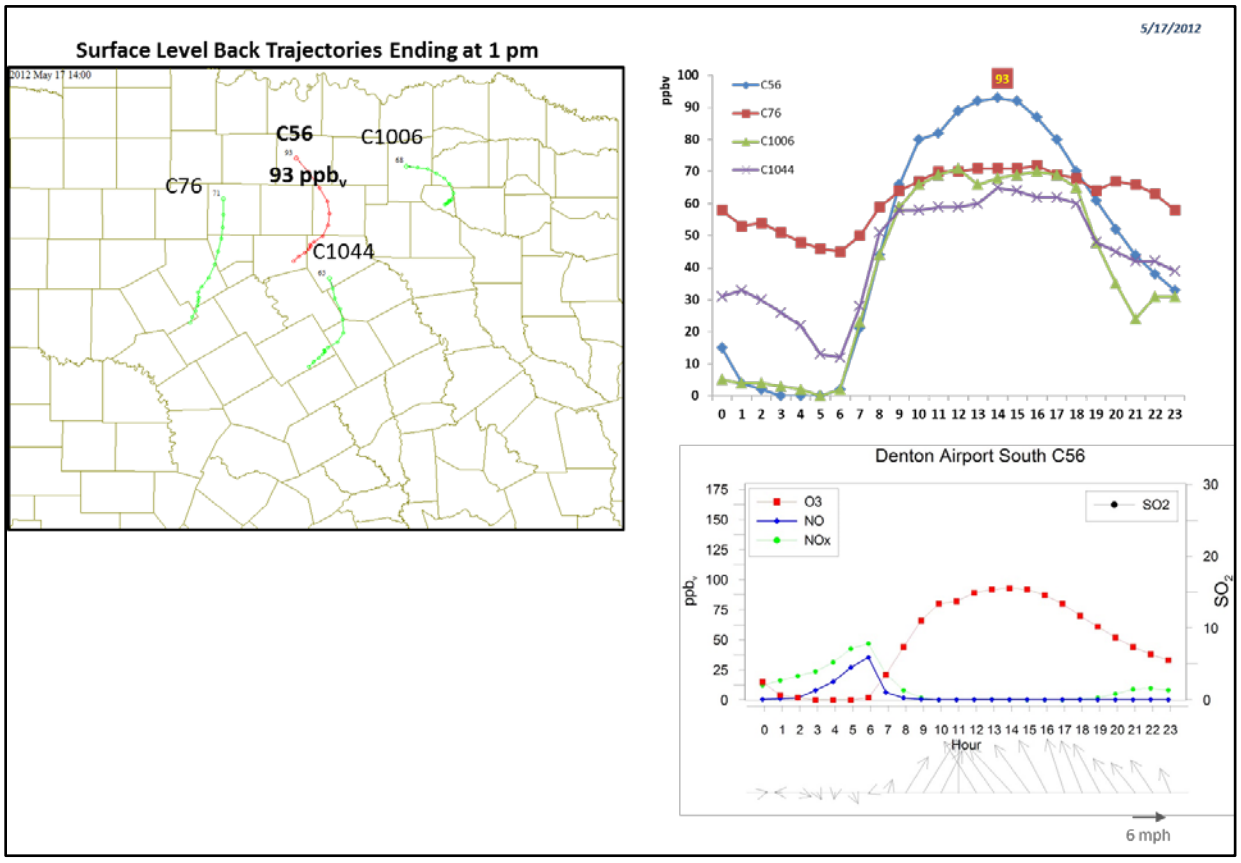

Figure 3-28. May 17, 2012 high ozone day at Denton Airport C56. Left panel: back trajectories calculated using AQPlot for the DFW monitors at the time of peak ozone impact at C56. Upper right panel: 1-hour average ozone time series for the C56 and surrounding DFW monitors. Lower right panel: time series of 1-hour ozone, NO, NO_2 and wind vectors at the Denton Airport C56.

(left panel of Figure 3-29) 48 hours before the air arrives at C26. The FINN fire emissions plots for the days leading up to May 17 (Figure 3-32) show that there are fires north of HGB 24 hours before the time of high ozone at the NW Harris County monitor, but that when the SmartFire trajectories pass in the vicinity of the fires seen at -48 hours, no fire activity is present. The HYSPLIT 12 NAM back trajectory does not reach far enough to the north for the air to have passed in the vicinity of the fire shown in the SmartFire back trajectory. Therefore, the results of the back trajectory analysis are inconclusive.

Inspection of the HMS product (Figure 3-30) shows that no smoke plumes are evident in the vicinity of the May 17 FINN fire emission maxima. The DataFed smoke emissions and smoke analysis plots do not show the presence of smoke in the HGB area (Figure 3-33). The $PM_{2.5}$ AQI is moderate in the vicinity of the fires, but is not extremely high (Figure 3-31). $PM_{2.5}$ monitors are located on the eastern side of the HGB urban area, and the southwestern-most of these monitors within the urban area shows a higher reading than the others (Figure 3-34). All $PM_{2.5}$

monitors in the HGB area have moderate or higher readings, suggesting that PM levels are moderate in the airmass entering the HGB area. While there was enhanced PM in the airmass, the data suggest that the source(s) of the PM did not cause the high ozone values measured at NW Harris County, for the two reasons explained below.

The spatial plots of monitored MDA8 ozone and MDA1 $PM_{2.5}$ (Figure 3-34) show that, while background ozone was high, monitors on the southwest side of the HGB area had higher ozone than monitors on the northeast side. The back trajectories indicate that air entered the urban area from the northeast and then developed an anti-cyclonic curvature so that air passed over the HGB urban area and then moved northward until it reached the NW Harris County monitor. There is a northeast-southwest ozone gradient that is consistent with the AQPlot and HYSPLIT NAM back trajectories, and suggests that the HGB urban plume caused the enhancement in ozone at the monitors downwind of the urban area.

Figure 3-34 shows that a central Houston monitor (C416 – Park Place) has a sharp $PM_{2.5}$ peak of nearly 60 µg m^{-3} at 3 pm. This brief, sharp increase in PM is consistent with the impact of a plume from a local source, rather than the impact of a distant plume generated by a fire; such a plume would be more broadly distributed in space and due to the effects of dispersion in transit, and would likely be detected at more than one monitor. This peak in PM is unlikely to correspond to the high ozone at the NW Harris County monitor. We recommend no further study of May 17, 2012 for the NW Harris County monitor.

On May 17, 2012, the Denton Airport South (C56) in the DFW area had its third highest value of the MDA8 for 2012 (86 ppb). Maximum 1-hour ozone observed was 93 ppb (Figure 3-28). The upper left panel of Figure 3-28 shows AQPlot surface wind back trajectories from Denton Airport C56 monitor location and three other sites located on the periphery of the DFW urban area. There are early morning NO and NOx peaks at the Denton monitor that dissipate well before ozone attains its mid-day maximum (bottom right panel of Figure 3-28). The NOx peak is well-correlated with the morning $PM_{2.5}$ peak at Denton; this $PM_{2.5}$ peak occurs at the same time as $PM_{2.5}$ peaks for other DFW area monitors and is likely the product of emissions from vehicle traffic. The Denton monitor is located 1.5 miles from the I-35 Highway. The wind vectors at the Denton monitor are consistent with the AQPlot back trajectories and the SmartFire and HYSPLIT NAM 500 m trajectories (Figure 3-29), which also show southerly/southeasterly flow.

Figure 3-29 shows that there are fires along the 72-hour back trajectory, and the presence of these fires during the time when the air parcels travelled along this path is also apparent in the FINN fire emissions plots (Figure 3-32) and the MODIS fire location plot for May 17 (Figure 3-33). However, no smoke is evident in the HMS satellite imagery (Figure 3-30) and $PM_{2.5}$ AQI is not elevated regionally (Figure 3-31). The NAAPS emissions and smoke analysis (Figure 3-31) show no evidence of smoke along the back trajectories on May 17 or on the preceding day (not shown).

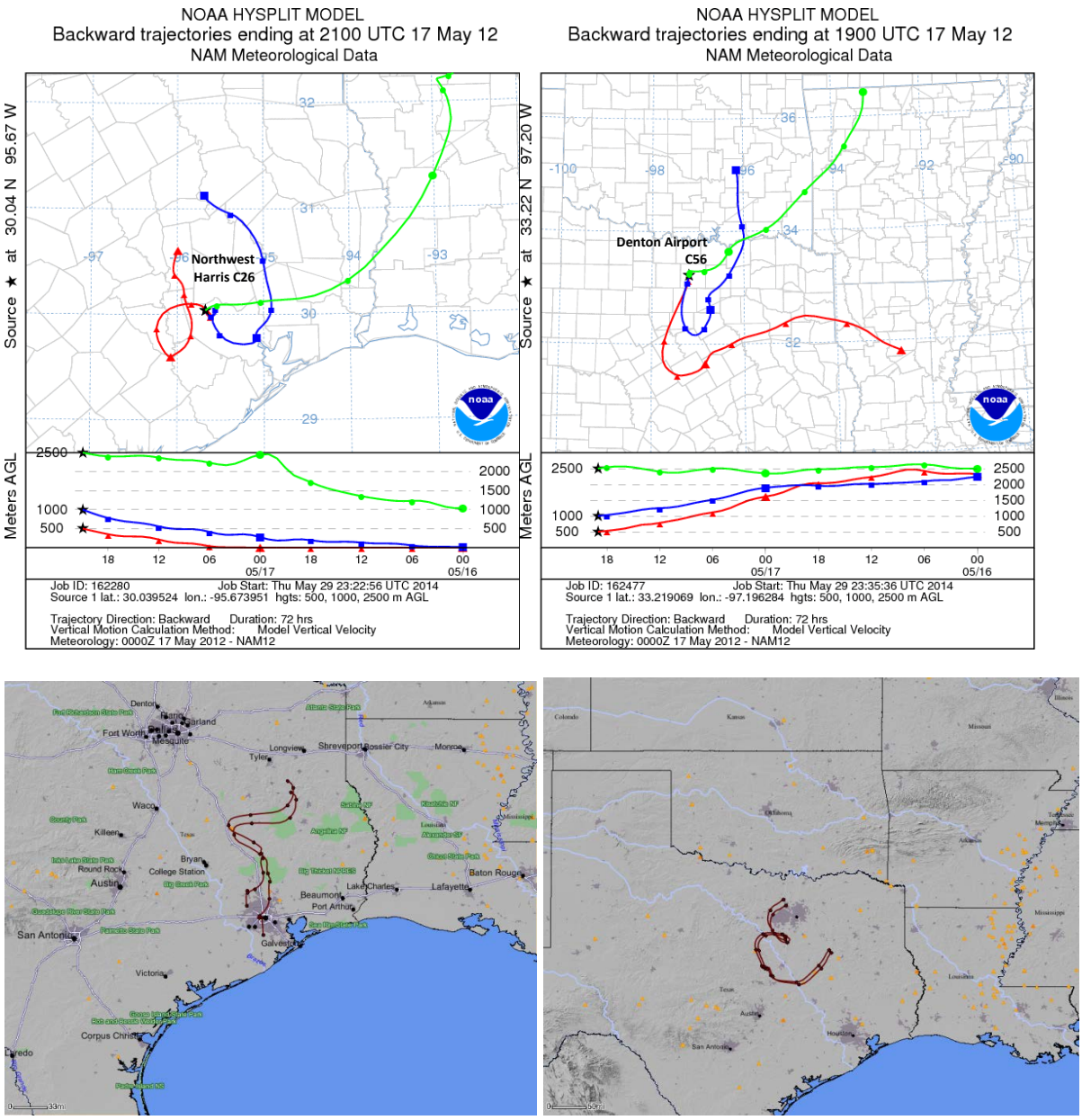

Figure 3-29. 72-hour HYSPLIT back trajectories (NAM 12km) from Northwest Harris and Denton Airport site ending May 17 2012; SMARTFIRE plots showing fire locations (orange triangles) and 72-hour HYSPLIT back trajectories (EDAS 40 km) from two HGB sites, C26 and C84, (bottom left) and two DFW sites C56 and C70 (bottom right).

The ozone MDA8 and $PM_{2.5}$ MDA1 plots (Figure 3-35) show a north-south gradient in ozone across the DFW urban area and low values of $PM_{2.5}$ at all monitors except Kaufman (C71). Peak values of $PM_{2.5}$ at this site occurs after the 1-hour average ozone maximum at Denton and may be due to impacts from the fires, which are relatively close to the Kaufman monitor. If a fire plume were advected into the DFW area from the south and transported to the Denton monitor, we would expect to see enhanced $PM_{2.5}$ at monitors in the vicinity of and south of Denton, but this is not the case. Because no $PM_{2.5}$ or NOx plume is apparent near or at the

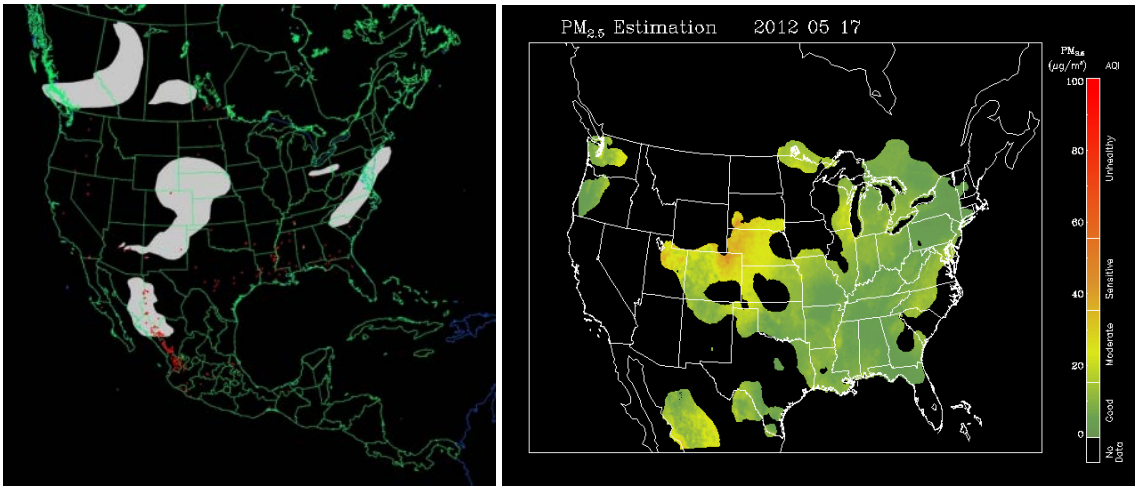

Figure 3-30. Left panel: HMS product showing May 17 fire locations (red dots) and smoke plume (gray area). Right panel: IDEA surface $PM_{2.5}$ estimate based on AOD and surface monitoring data.

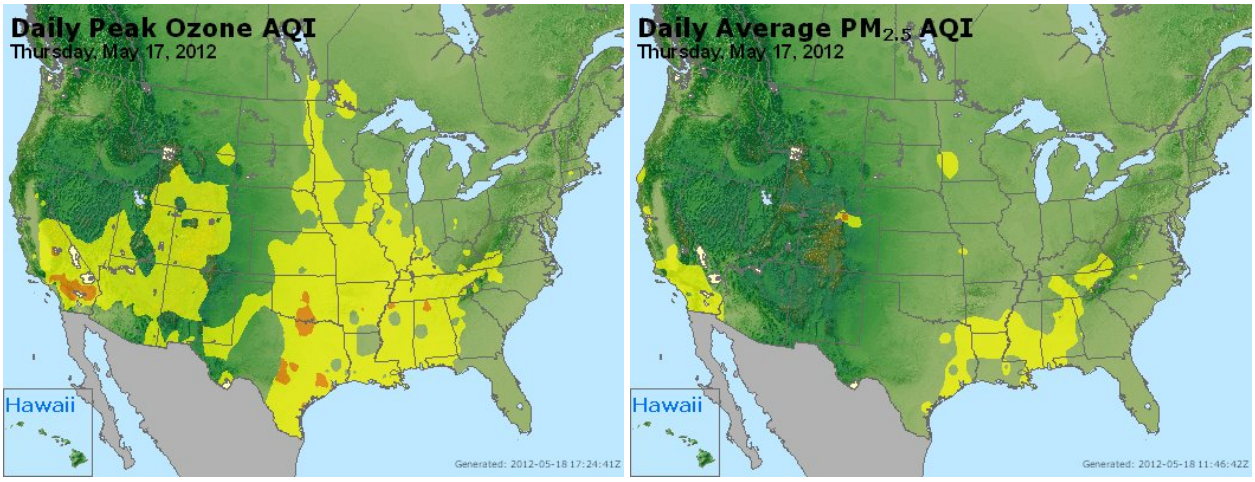

Figure 3-31. Daily average ozone (left) and $PM_{2.5}$ (right) based on observed values. Data from: http://www.airnow.gov/.

monitor, and the spatial pattern of ozone is consistent with high ozone at Denton due to a DFW urban plume impact, we do not recommend further study of May 17, 2012 at the Denton monitor.

Wildfire Emissions Inventory: FINN 2012

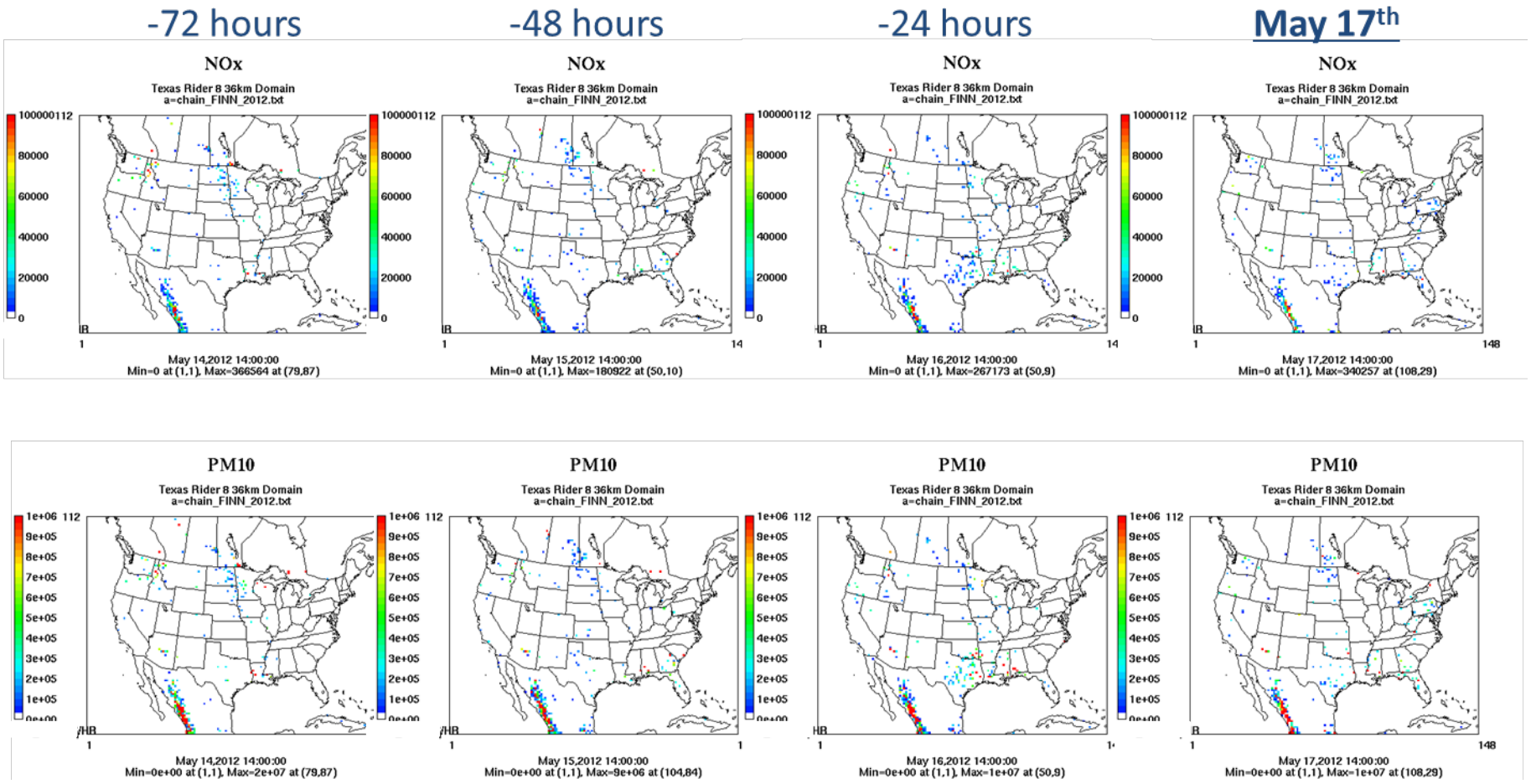

Figure 3-32. May 17, 2012 FINN fire emissions of NOx and PM_{10}.

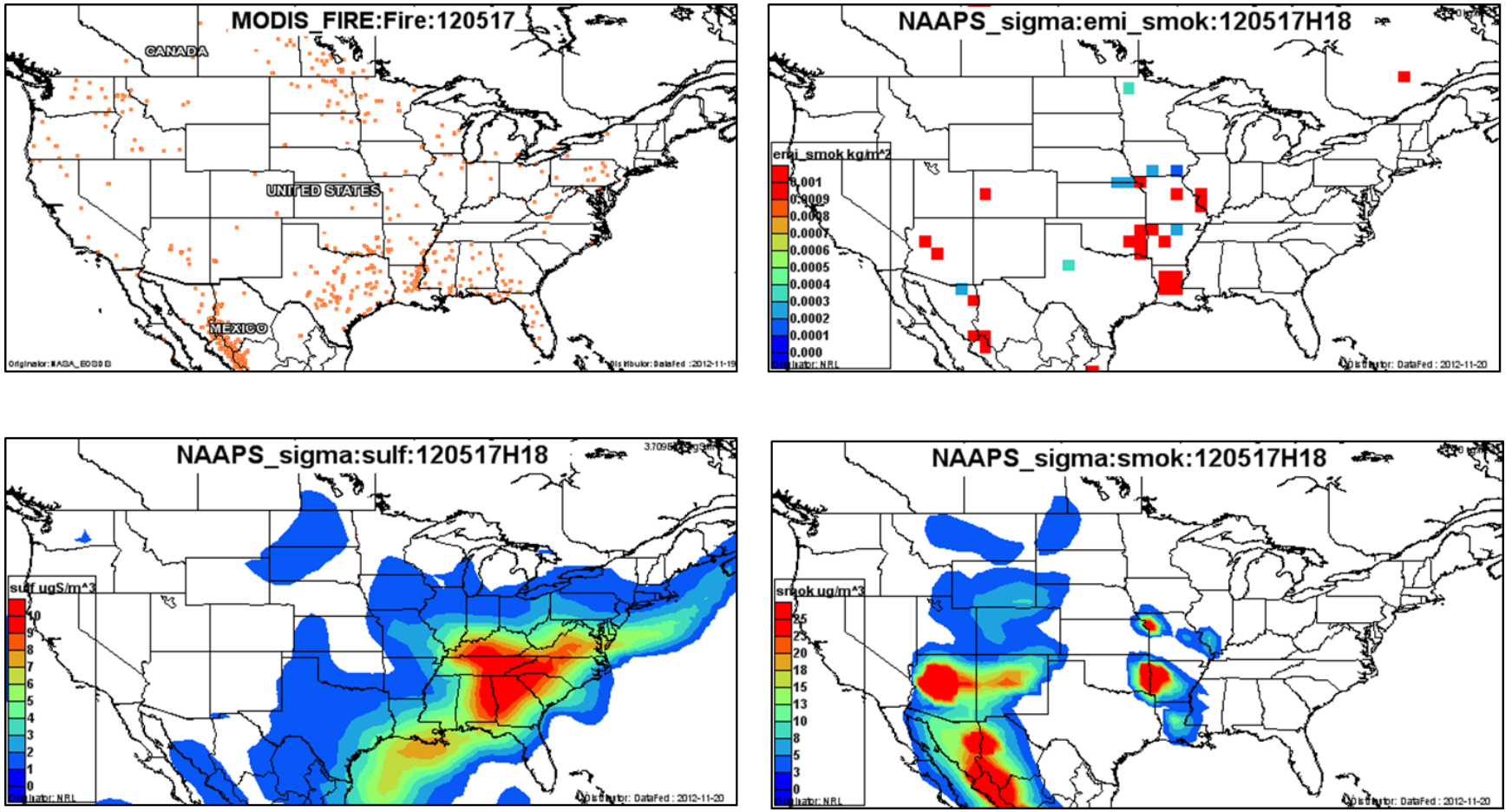

Figure 3-33. May 17, 2012 DataFed analysis. Upper left panel: Locations of active fires from MODIS satellite fire detections. Upper right panel: NAAPS model smoke emissions. Lower left panel: NAAPS model surface layer sulfate concentrations. Lower right panel: NAAPS model surface layer smoke concentrations.

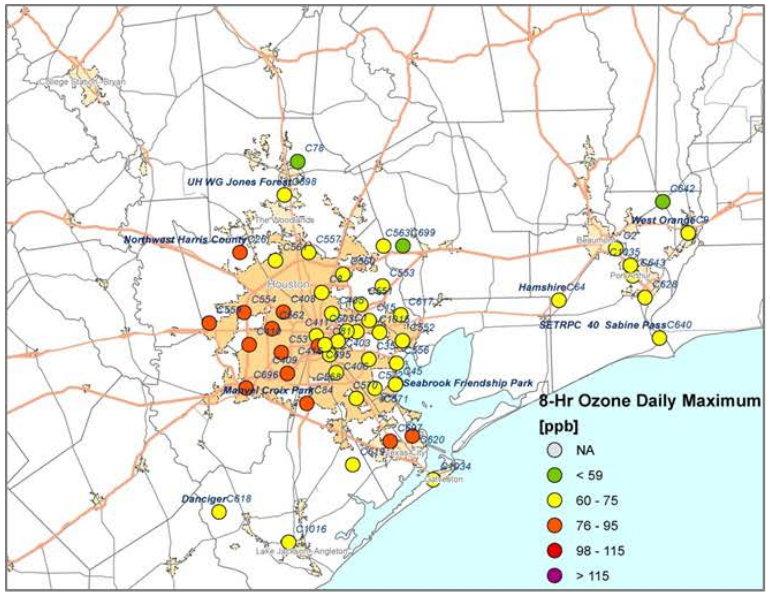

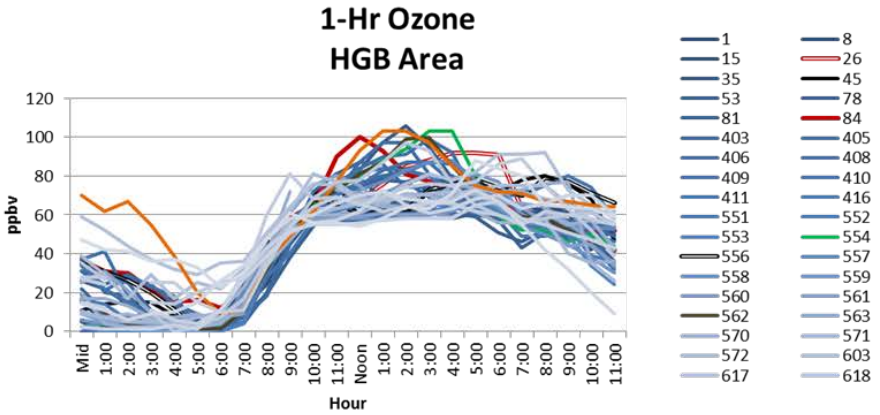

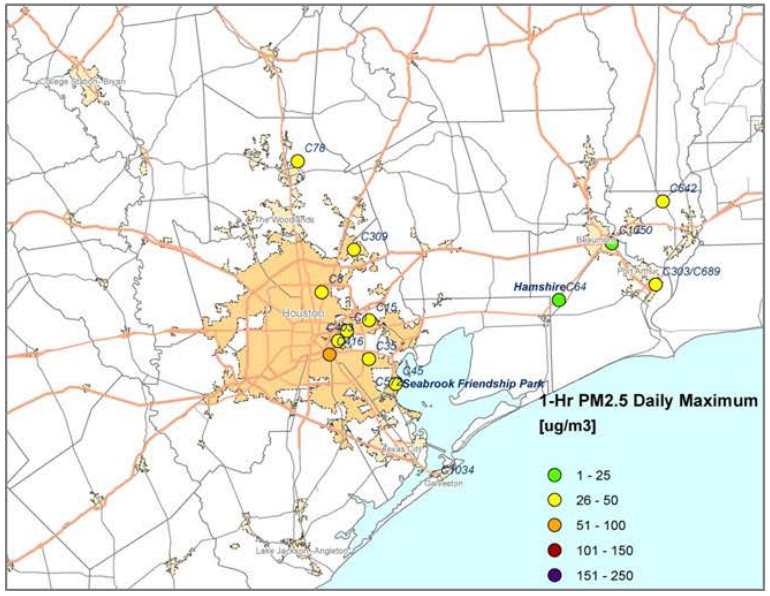

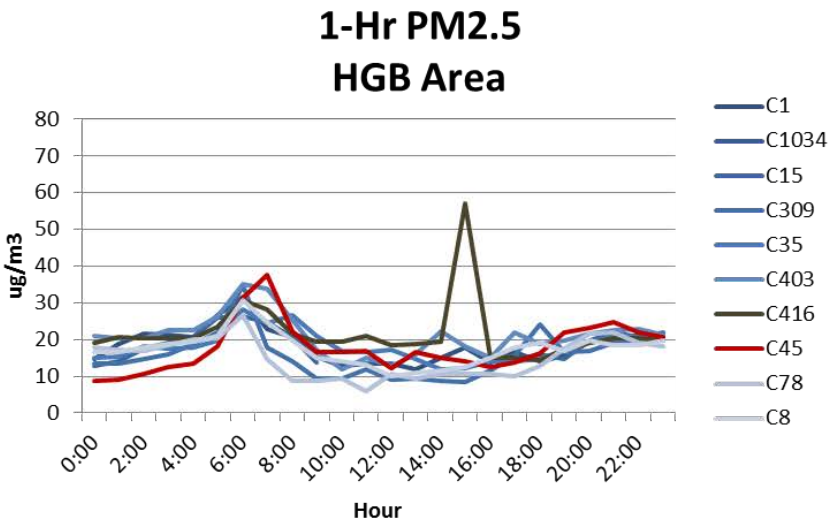

Figure 3-34. May 17 regional ozone (top left and right) and $PM_{2.5}$ (bottom left and right) measurements (HGB area time series).

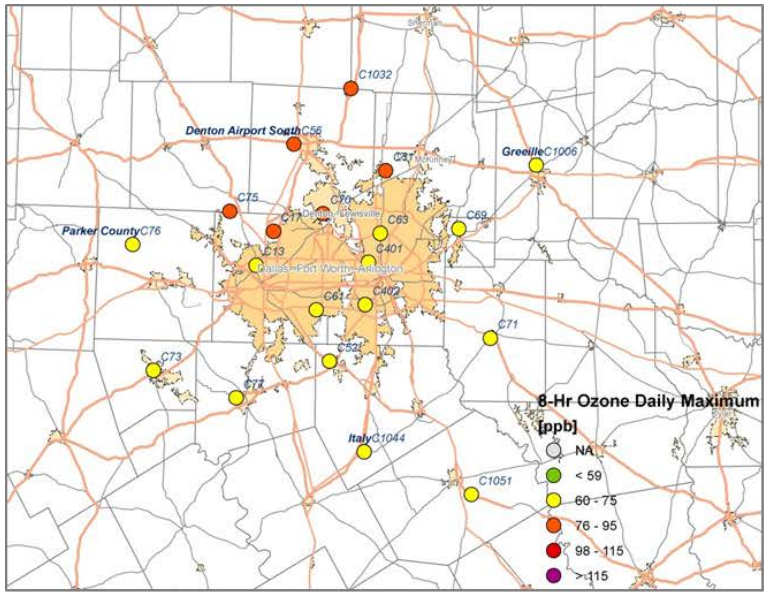

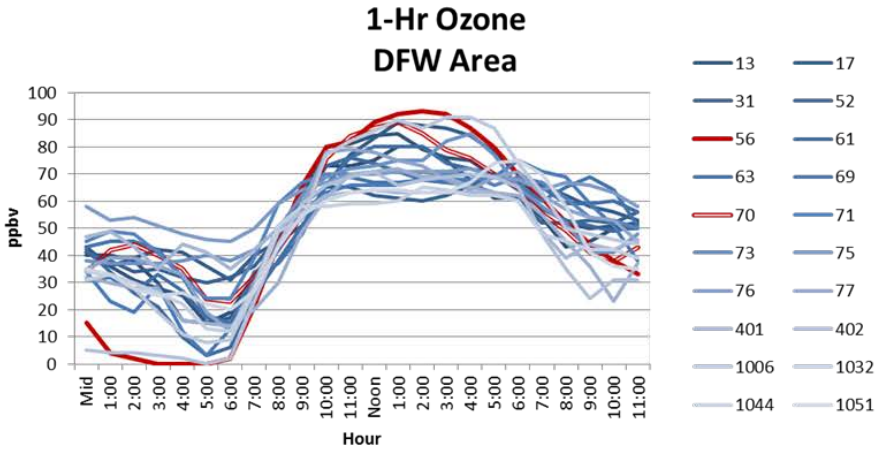

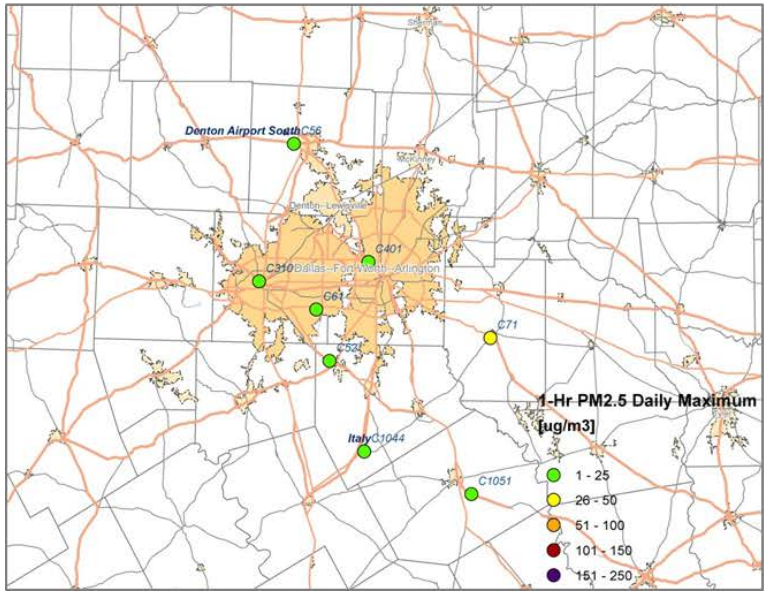

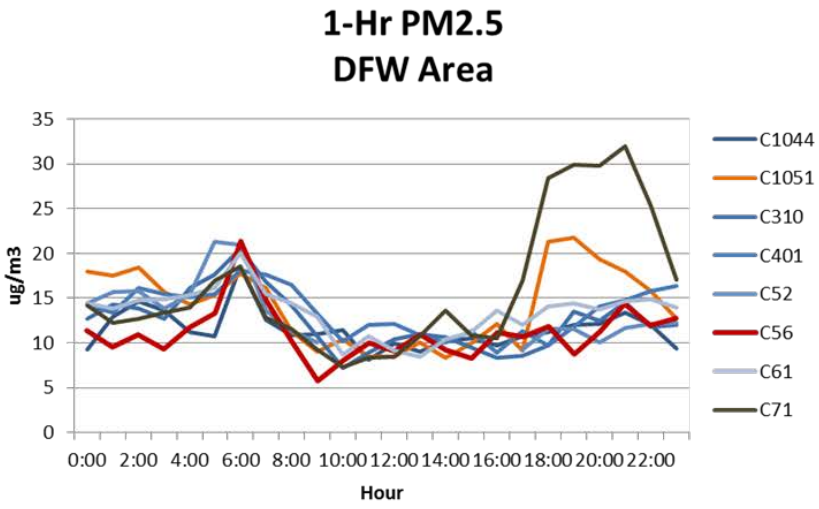

Figure 3-35. Regional ozone (top left and right) and $PM_{2.5}$ (bottom left and right) measurements (DFW area time series).

3.1.5 May 21, 2012

On May 21, the Manvel Croix Park C84 monitor had its 3rd highest MDA8 value of 2012 (90 ppb). The peak 1-hour ozone at Manvel was 101 ppb, which is ~40 ppb higher than the peak daytime 1-hour values recorded at the C698 monitor north of the HGB urban area and the C64 monitor to the east (Figure 3-36). The Galveston monitor (C1034), located on the coast southeast of Manvel Croix, has a 1-hour ozone peak of similar magnitude to Manvel Croix, but the peak occurs two hours later in the day. There is no NOx or NO peak coincident with the ozone peak at Manvel Croix. The AQPlot back trajectories ending at HGB monitors at the time of peak 1-hour ozone at the Manvel Croix monitor show northerly winds switching to southwesterly in the early afternoon, consistent with a sea breeze circulation (Figure 3-36).

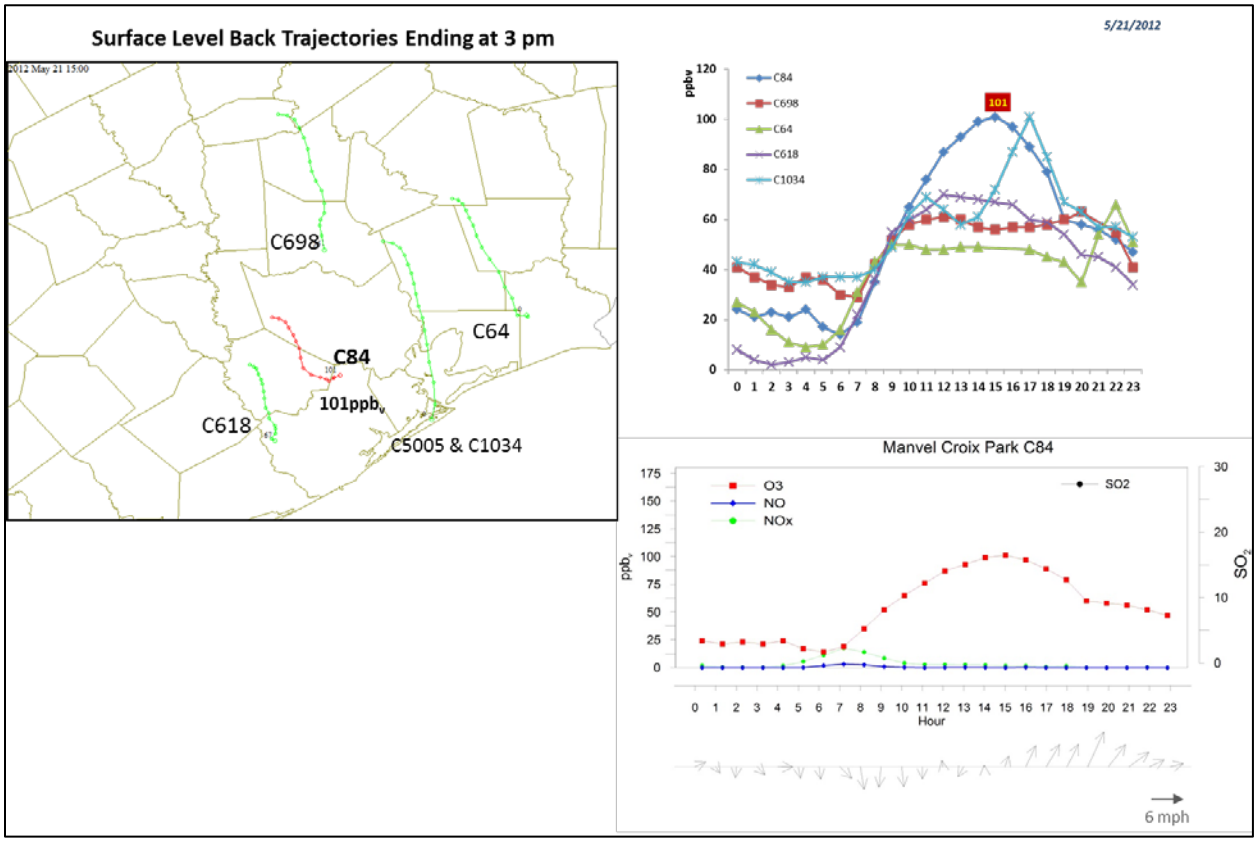

Figure 3-36. May 21, 2012 high ozone day at Manvel Croix Park C84. Left panel: back trajectories from C84 and background HGB monitors at the time of peak 1-hr ozone impact at C84. Upper right panel: 1-hour average ozone time series for the C84 and background monitors. Lower right panel: time series of 1-hour ozone, NO, NO_2 and wind vectors at the Manvel Croix Park. SO_2 is not monitored at the Manvel Croix CAMS.

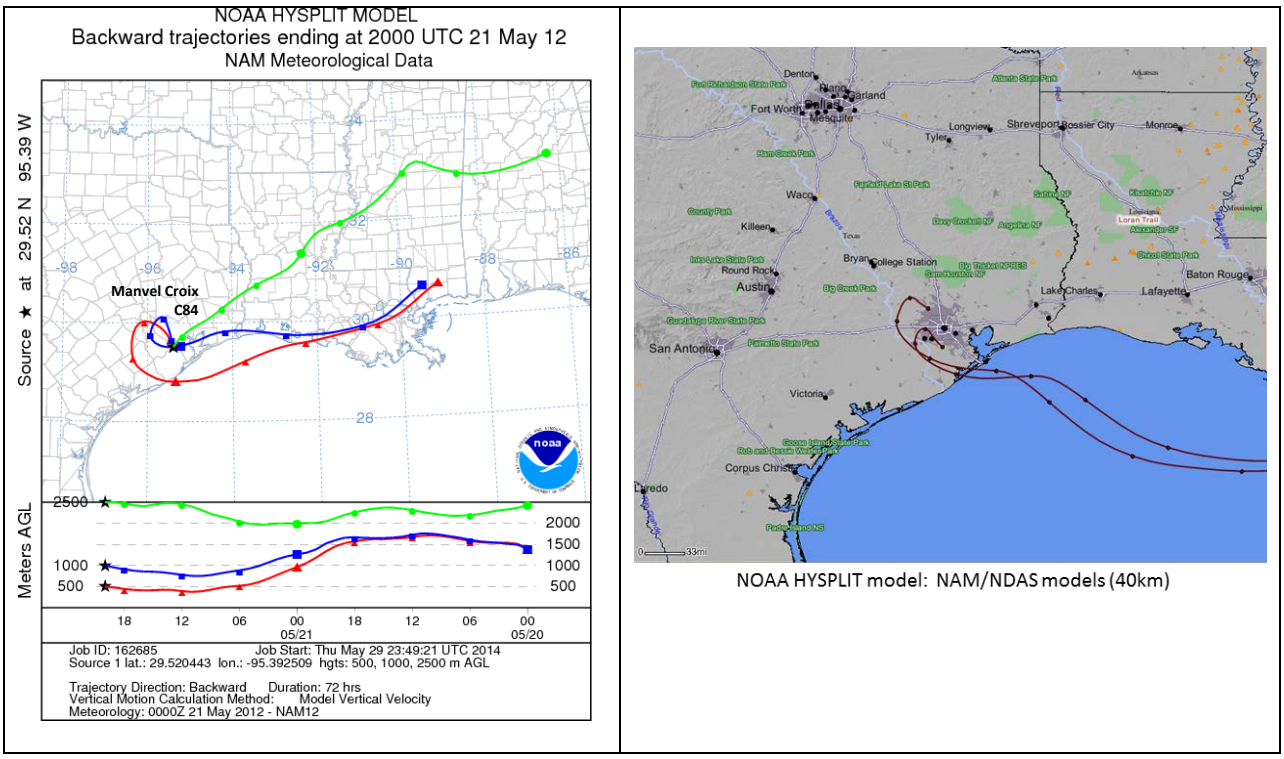

Figure 3-37. 72-hour HYSPLIT back trajectories (NAM 12km) from Manvel Croix Park C84 (left panel) ending May 21, 2012; SmartFire plots showing fire locations (orange triangles) and 72-hour HYSPLIT back trajectories (EDAS 40 km; 10m) for HGB site C26 (right panel).

SmartFire and HYSPLIT NAM back trajectories (Figure 3-37) are consistent with the AQPlot trajectories in showing flow from the north in the morning of May 21. Figure 3-37 indicates that in the days leading up to May 21, the winds were out of the northeast (HYSPLIT NAM) or southeast (SmartFire). As the back trajectories approach the HGB area, they developed an anti-cyclonic curvature, turning to the north and then turning southward and traversing the HGB urban area. The SmartFire trajectories show flow off the Gulf of Mexico and the back trajectories do not pass near any fires. The 500 m and 1,000 HYSPLIT NAM back trajectories pass over a fire located on the Louisiana coast.

Figure 3-38 shows the HMS product for May 21. The fire on the Louisiana coast shown on the SmartFire plot does not appear on the HMS plot, nor does it appear in the FINN emission inventory (Figure 3-40). The Louisiana fire does appear on the DataFed MODIS plot (Figure 3-41). The HMS product smoke extent shows that an area of enhanced AOD was present in the region traversed by both the SmartFire and HYSPLIT NAM back trajectories, and it is possible that aerosols may have prevented detection of this fire by some algorithms. The $PM_{2.5}$ AQI is moderate along the Louisiana coast in the vicinity of the fire as well as in the HGB area (Figure 3-39). The NAAPS fire emission and smoke analysis show neither significant fire emissions nor smoke near the HGB area.

Because the Louisiana fire is distant (>100 miles) from the HGB area, we would expect a plume from the fire to be broad enough to affect multiple monitors in the HGB area. Figure 3-42

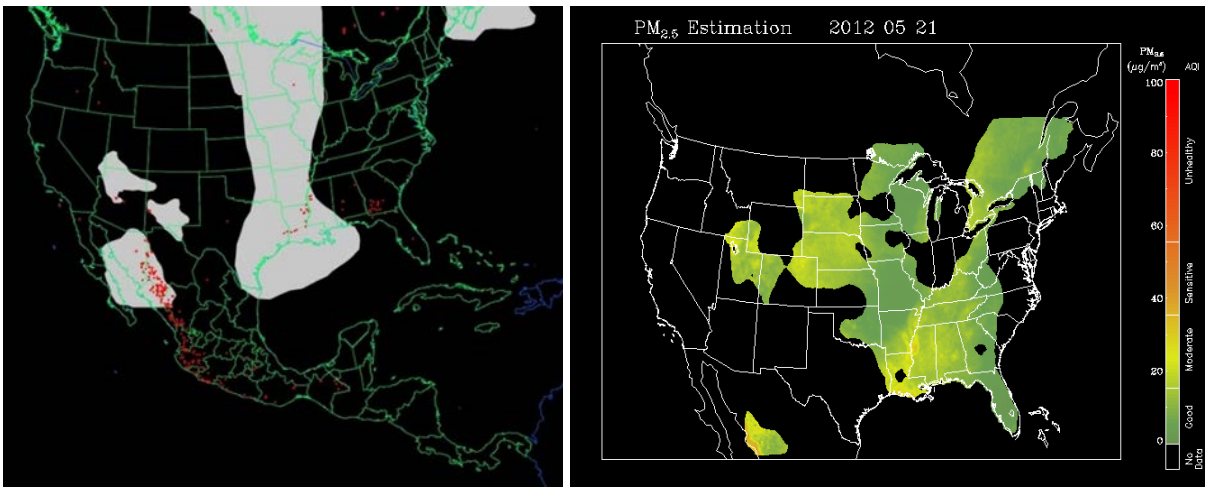

Figure 3-38. Left panel: HMS product showing May 21 fire locations (red dots) and smoke plume (gray area). Right panel: IDEA surface $PM_{2.5}$ estimate based on AOD and surface monitoring data.

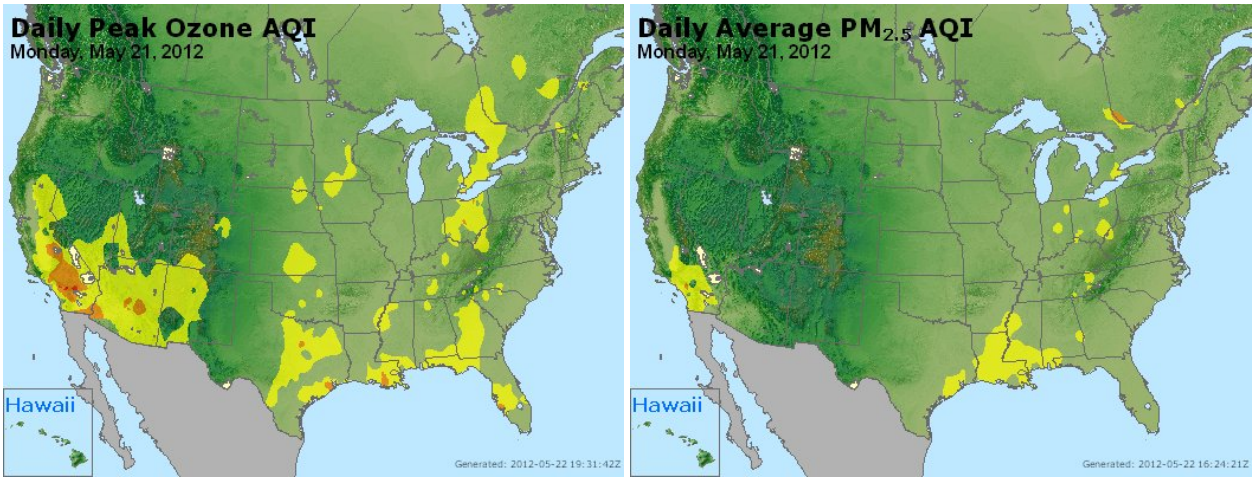

Figure 3-39. Daily average ozone (left) and $PM_{2.5}$ (right) based on observed values. Data from: http://www.airnow.gov/.

shows that $PM_{2.5}$ is not strongly enhanced in the HGB area, and the highest values of $PM_{2.5}$ occur well after the ozone peak at monitors that are located in the central HGB area. The ozone spatial pattern in Figure 3-42 shows a northwest-to-southeast gradient with lower values of MDA8 in the northern side of the HGB area and higher values on the southeastern side. The back trajectories are consistent in showing the winds were northerly in the morning such that sites on the northern side of the area were upwind, while the sites on the southern side of the area that had higher ozone were downwind of the urban area. Given the strong likelihood of a significant contribution from local emissions to Manvel Croix ozone on May 21 and the lack of $PM_{2.5}$ in the HGB area during the hours when ozone was at its maximum, we conclude that high ozone at Manvel Croix was likely due to an HGB urban

ENVIRON

Wildfire Emissions Inventory: FINN 2012

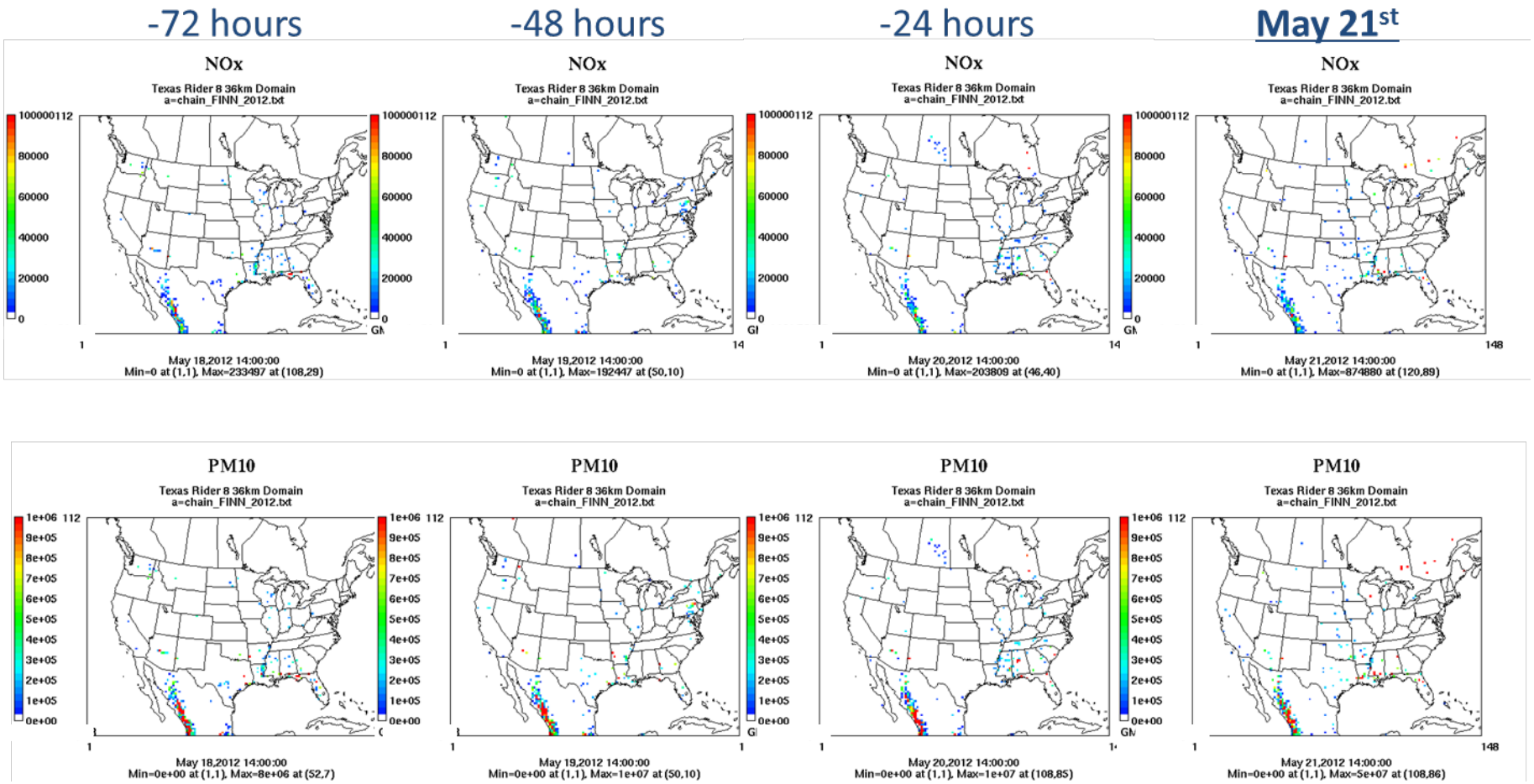

Figure 3-40. May 21, 2012 FINN fire emissions of NOx and PM_{10}.

plume impact and that the influence of the distant Louisiana fire was small to negligible. We do not recommend further analysis of May 21, 2012.

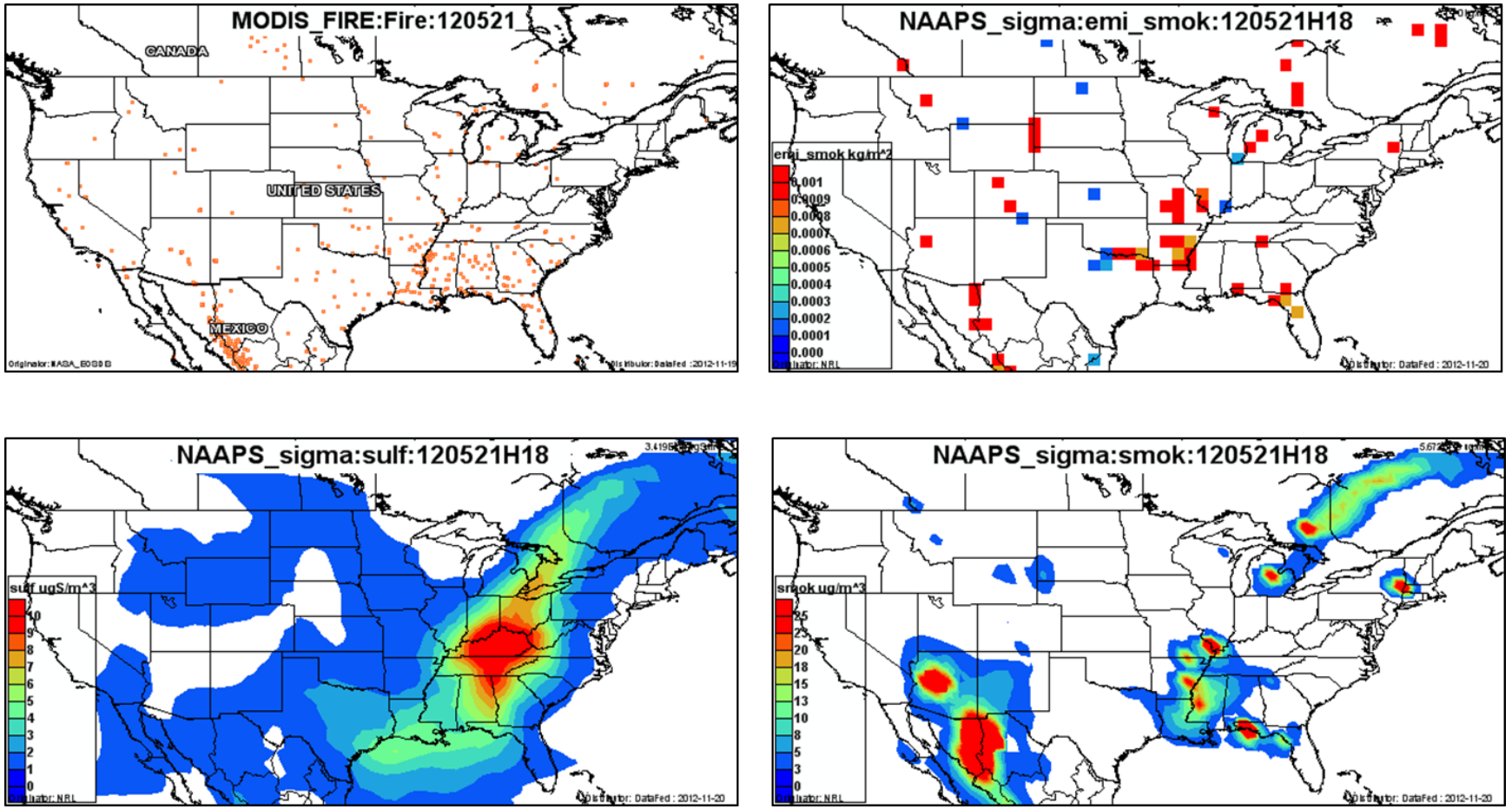

Figure 3-41. May 21, 2012 DataFed analysis. Upper left panel: Locations of active fires from MODIS satellite fire detections. Upper right panel: NAAPS model smoke emissions. Lower left panel: NAAPS model surface layer sulfate concentrations. Lower right panel: NAAPS model surface layer smoke concentrations.

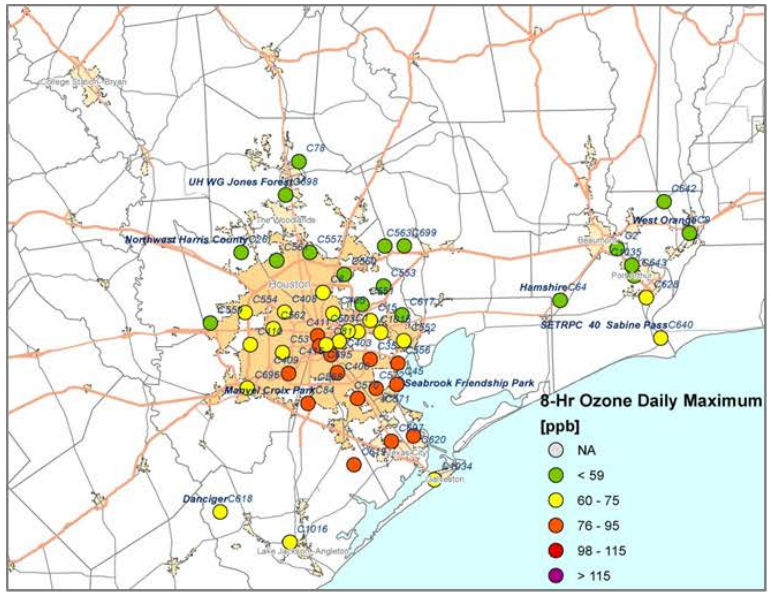

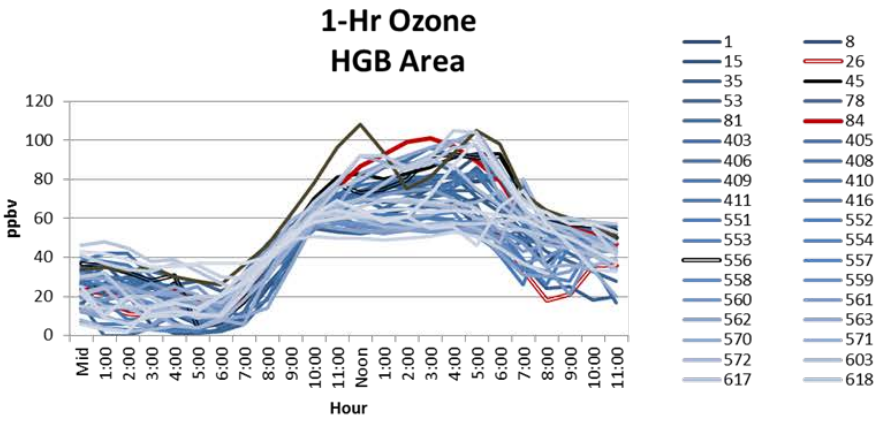

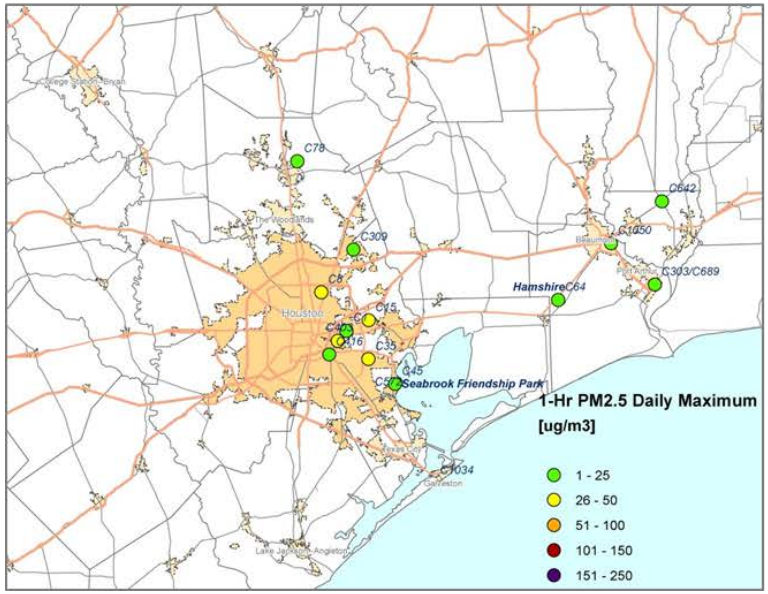

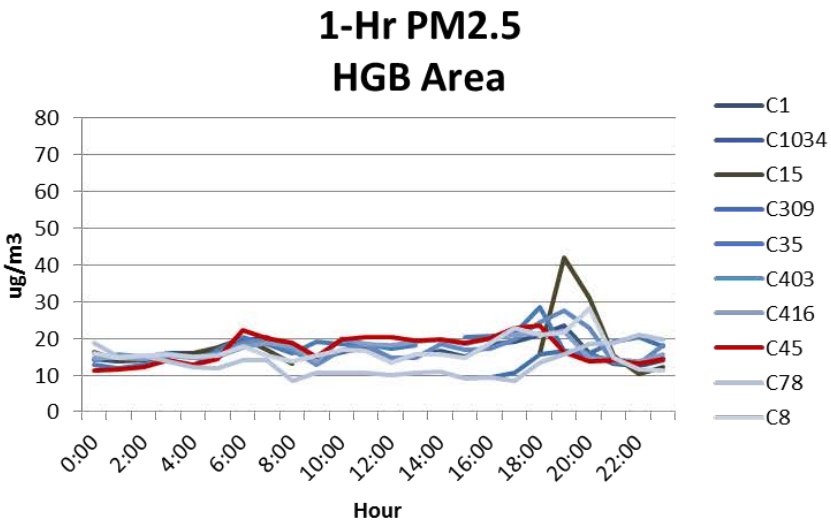

Figure 3-42. Regional ozone (top left and right) and $PM_{2.5}$ (bottom left and right) measurements (HGB area time series).

3.1.6 May 22, 2012

On May 22, 2012, the Sabine Pass (C640) monitor had its 4th highest MDA8 ozone (76 ppb) of 2012. Sabine Pass had higher ozone than all other sites in the BPA area, and background ozone in the BPA area on this day was in the range of 50-60 ppb (Figure 3-43; Figure 3-49). The Sabine Pass monitor had brisk (>10 mph) northwesterly winds until noon, when the wind shifted to southwesterly (Figure 3-43). The AQPlot back trajectory for the Sabine Pass monitor is consistent with the monitored winds, with a back trajectory traversing Galveston Bay before turning northward toward the Sabine monitor. The AQplot back trajectories from the other BPA monitors, which are located further inland than the Sabine Pass monitor, show west-northwesterly winds on June 1 with no shift in wind direction at noon.

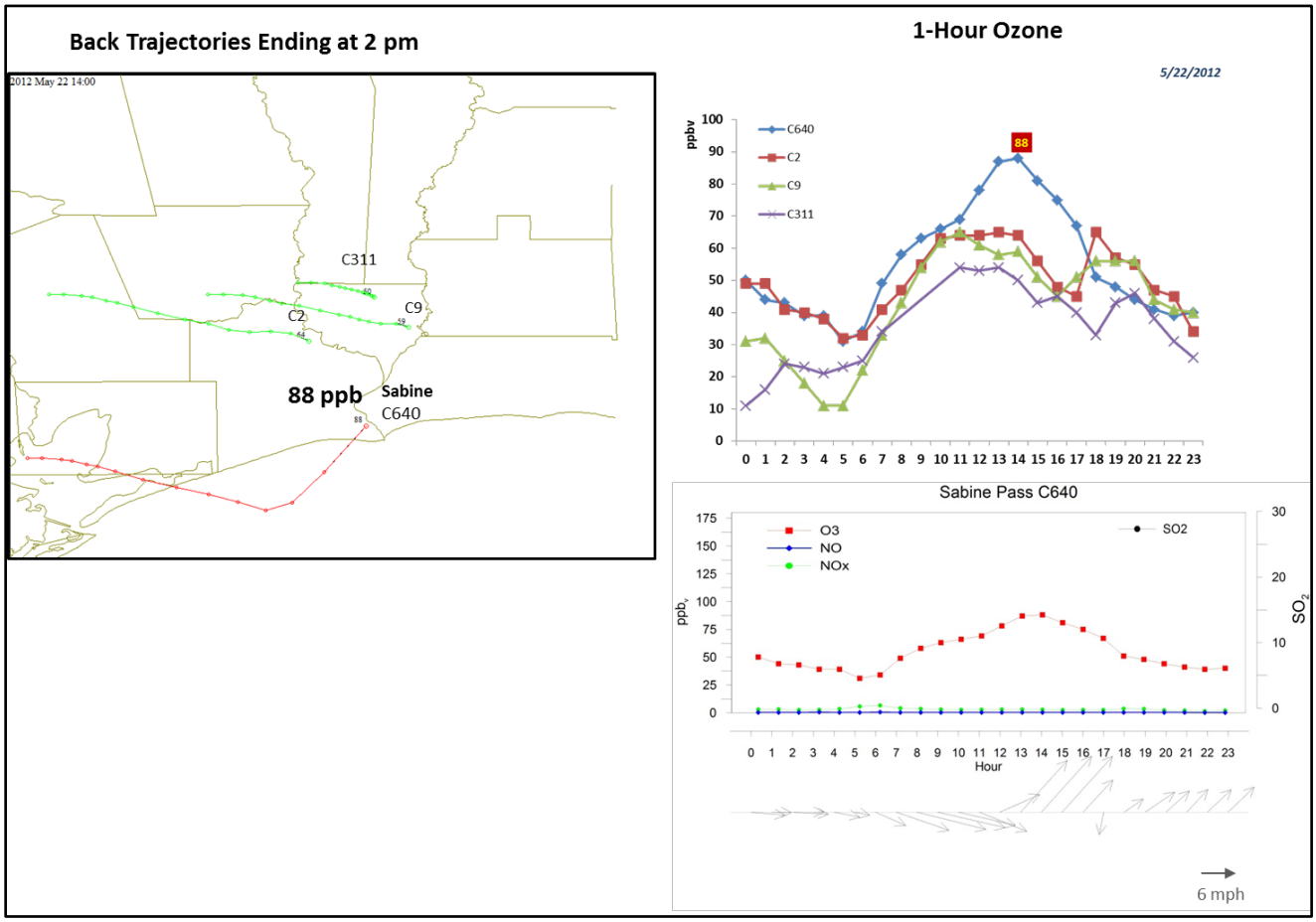

Figure 3-43. May 22, 2012 high ozone day at Sabine Pass C640. Left panel: AQPlot back trajectories ending at C640 and three background sites at the time of peak 1-hr ozone was observed at C640. Upper right panel: 1-hour average ozone time series for the C640 and background monitors. Lower right panel: time series of 1-hour ozone, NO, NO_2 and wind vectors at the Sabine Pass C640.

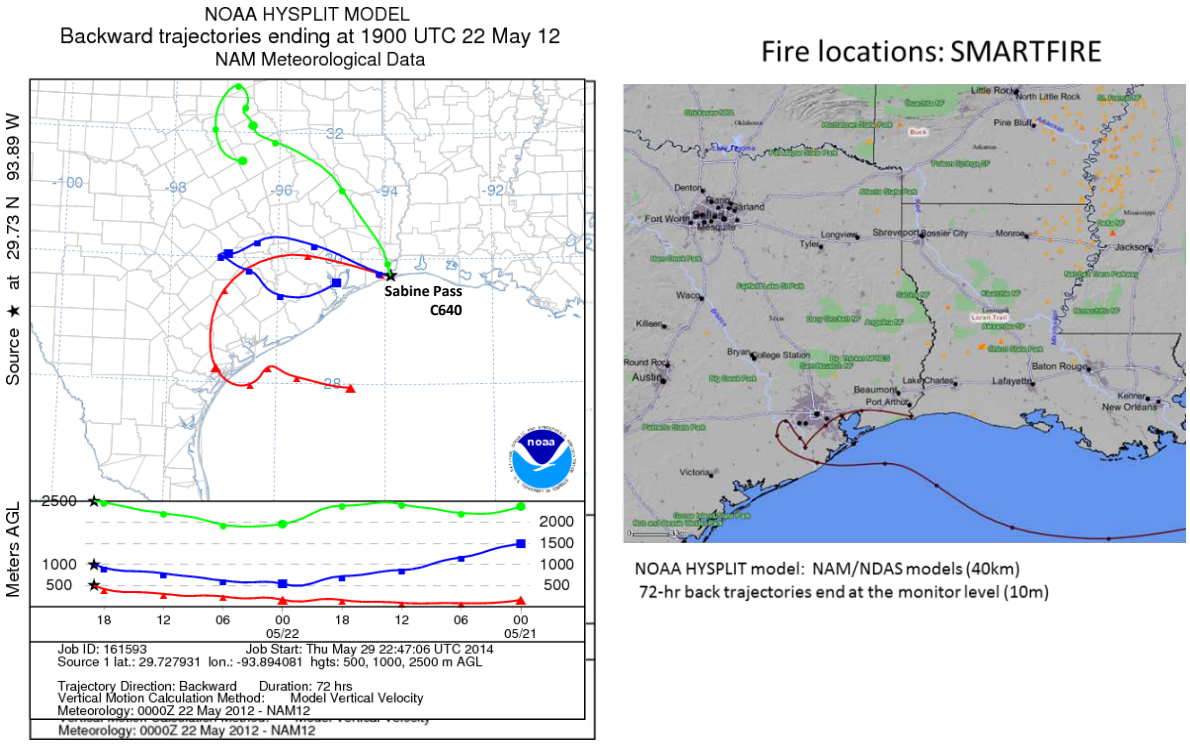

Figure 3-44. 72-hour HYSPLIT back trajectories (NAM 12km) from Sabine Pass C640 ending May 22, 2012; SmartFire plot showing fire locations (orange triangles) and 72-hour HYSPLIT back trajectories (EDAS 40 km) from C640.

The SmartFire and HYSPLIT NAM 500 m back trajectories (Figure 3-44) s did not pass in the vicinity of any fires, but the HYSPLIT NAM 1,000 m back trajectory took a more northerly route that brought it near a fire located just north of the HGB urban area. This fire appears in the HMS product (Figure 3-45), but not in the FINN emissions data (Figure 3-47) or the in DataFed MODIS fire location plot. The HMS plot shows the presence of enhanced AOD over East Texas and Louisiana, and the NAAPS smoke analysis shows the presence of smoke over the BPA area. The NAAPS plots show strong fire emissions in northern Louisiana as well as the presence of sulfate aerosol over the BPA area.

Figure 3-49 shows the spatial distribution of ozone and $PM_{2.5}$ in the BPA area. The southern monitors in the BPA area have higher ozone than the northern monitors. The HYSPLIT and AQplot back trajectories suggest that air arriving at the southern monitors in the BPA area had traversed the HGB area on May 21, which was a high ozone day (i.e., MDA8.75 ppb) at many monitors in the HGB area. High ozone on May 22 at the Sabine Pass monitor, therefore, is likely related to transported ozone from the HGB area. $PM_{2.5}$ levels in the BPA area were ≤20 µg m^{-3} during the period when the Sabine Pass monitor had its 1-hour ozone maximum. $PM_{2.5}$ values rose slightly during the afternoon commute hours, but this occurred well after the ozone maximum at Sabine Pass. There was no NOx peak coincident with peak 1-hour ozone at Sabine Pass. There is no evidence of an impact from a fire emissions plume, so we do not recommend further analysis of May 22, 2012.

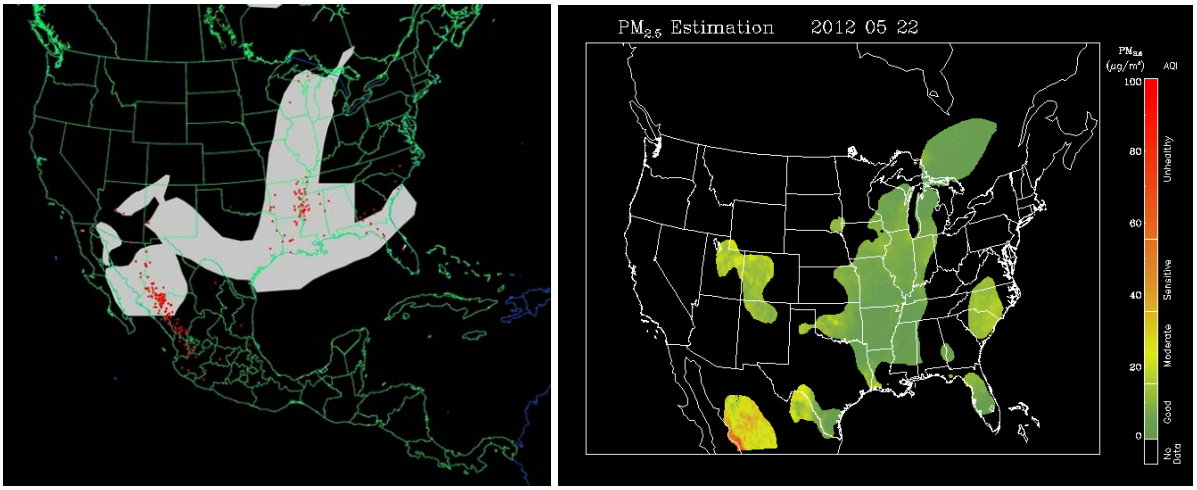

Figure 3-45. Left panel: HMS product showing May 22 fire locations (red dots) and smoke plume (gray area). Right panel: IDEA surface $PM_{2.5}$ estimate based on AOD and surface monitoring data.

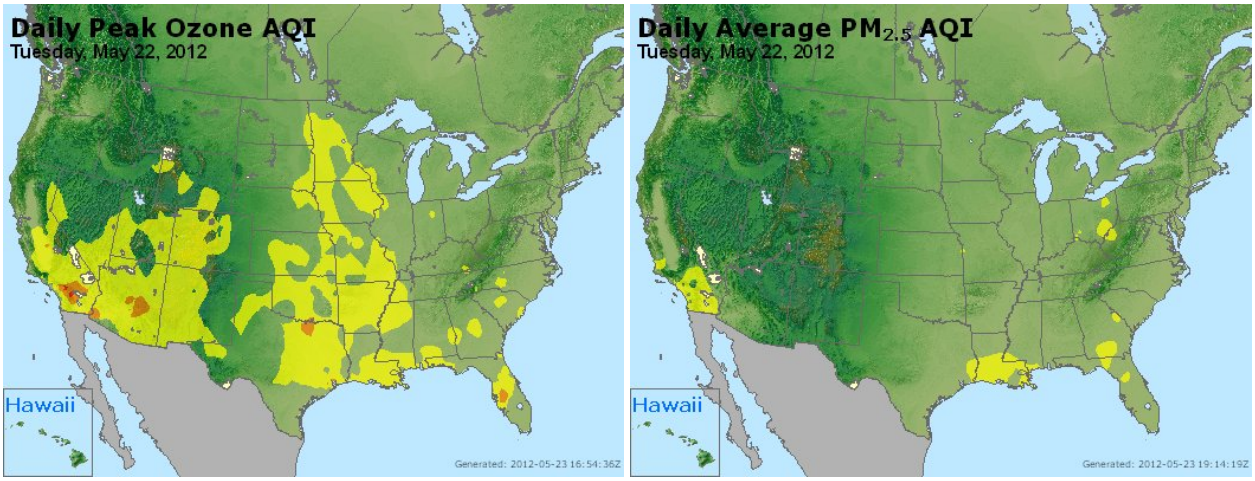

Figure 3-46. May 22 daily average ozone (left) and $PM_{2.5}$ (right) based on observed values. Data from: [http://www.airnow.gov/.](http://www.airnow.gov/)

Wildfire Emissions Inventory: FINN 2012

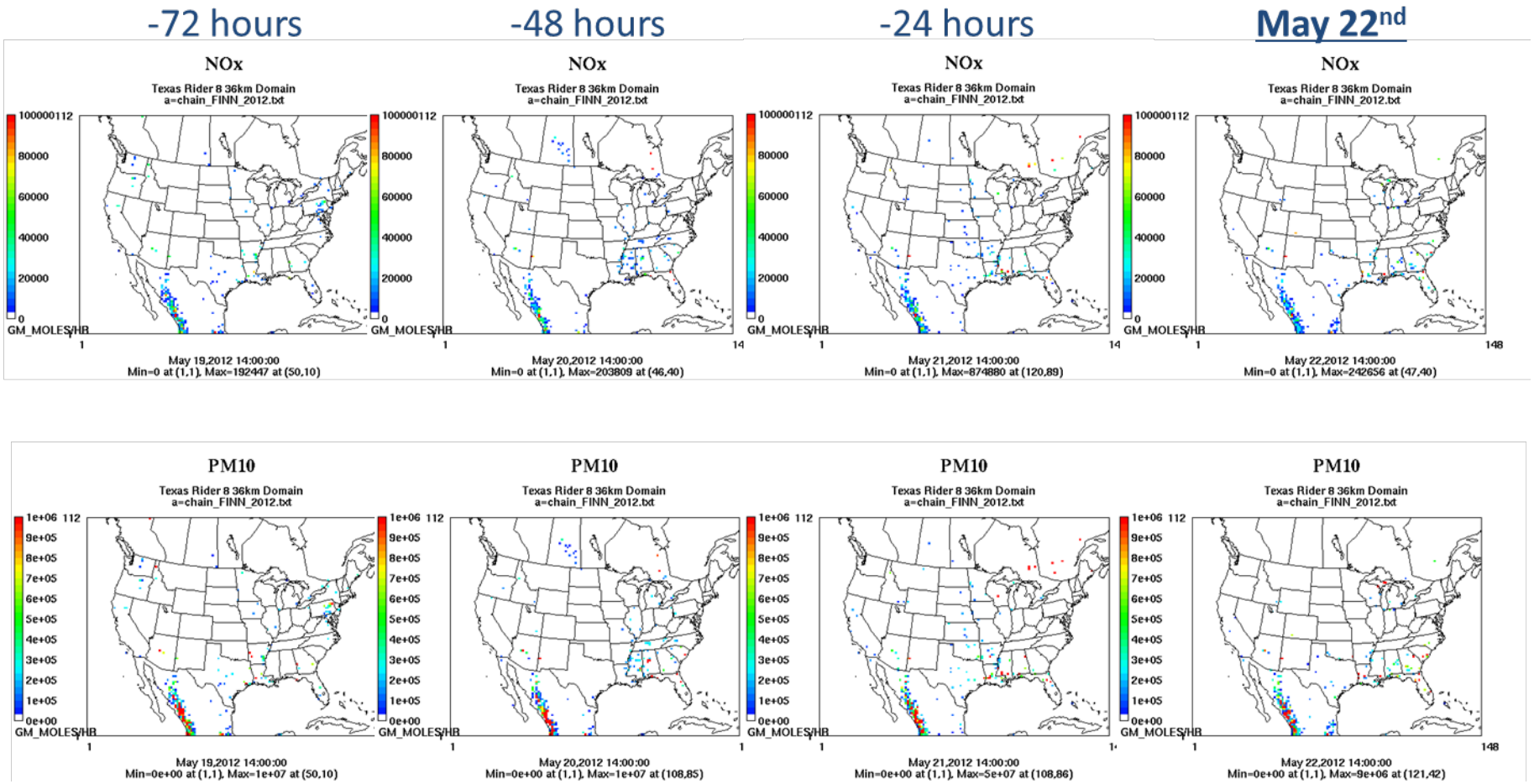

Figure 3-47. May 22, 2012 FINN fire emissions of NOx and PM_{10}.

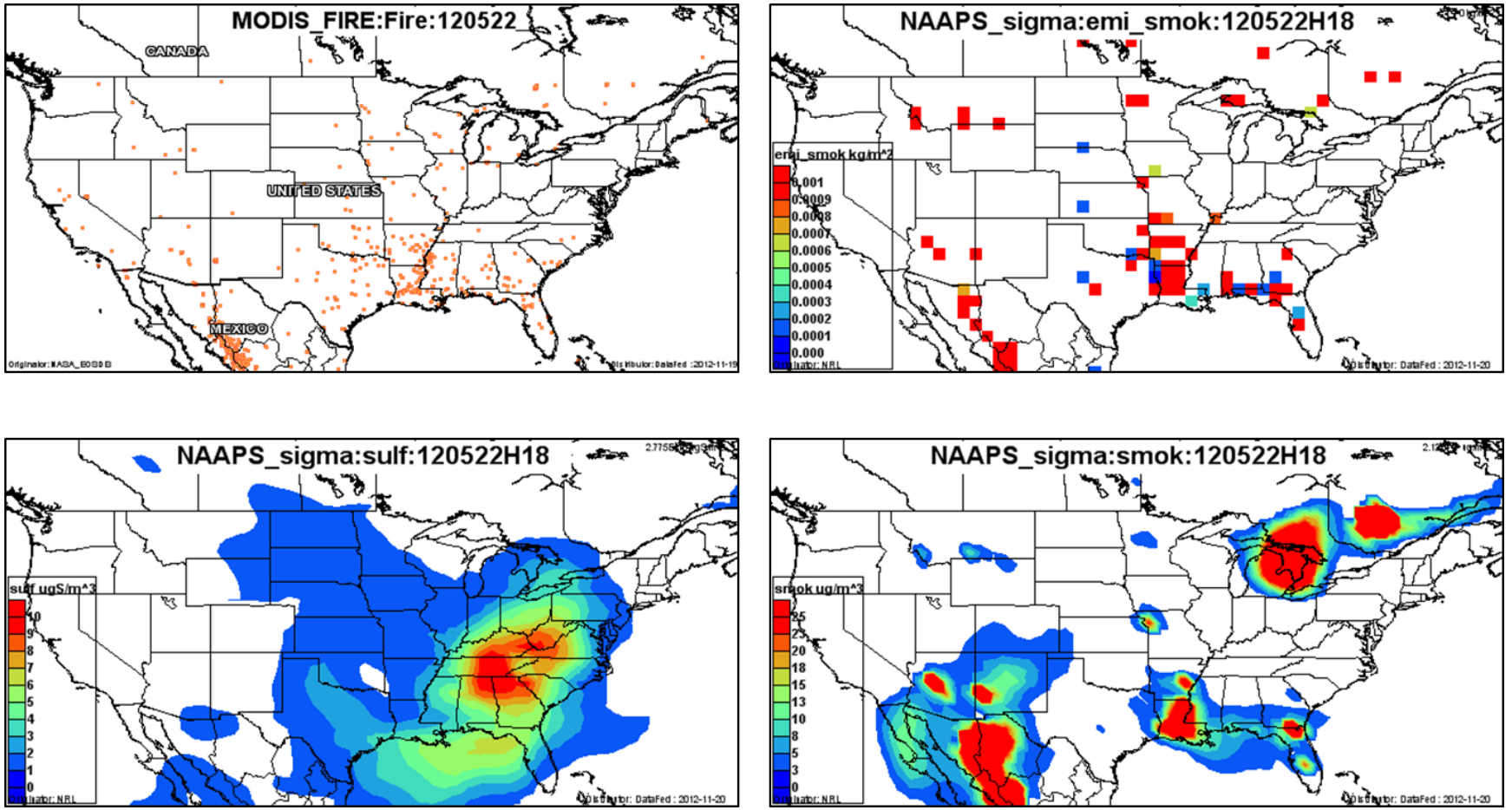

Figure 3-48. May 22, 2012 DataFed analysis. Upper left panel: Locations of active fires from MODIS satellite fire detections. Upper right panel: NAAPS model smoke emissions. Lower left panel: NAAPS model surface layer sulfate concentrations. Lower right panel: NAAPS model surface layer smoke concentrations.

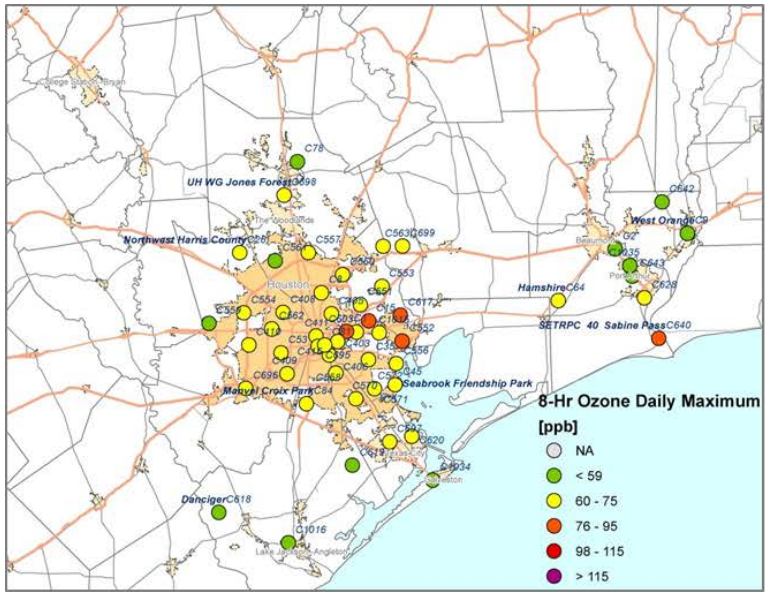

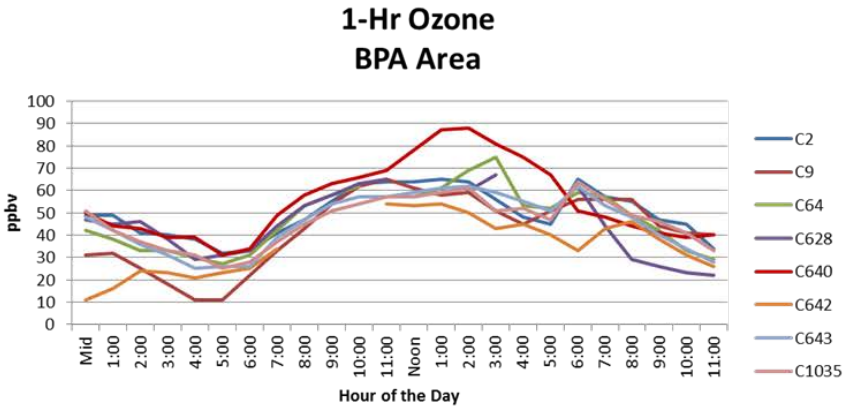

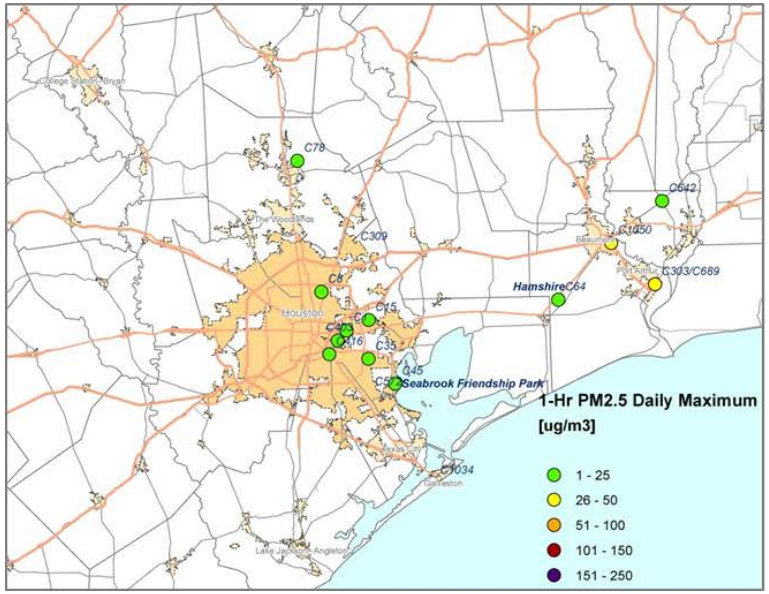

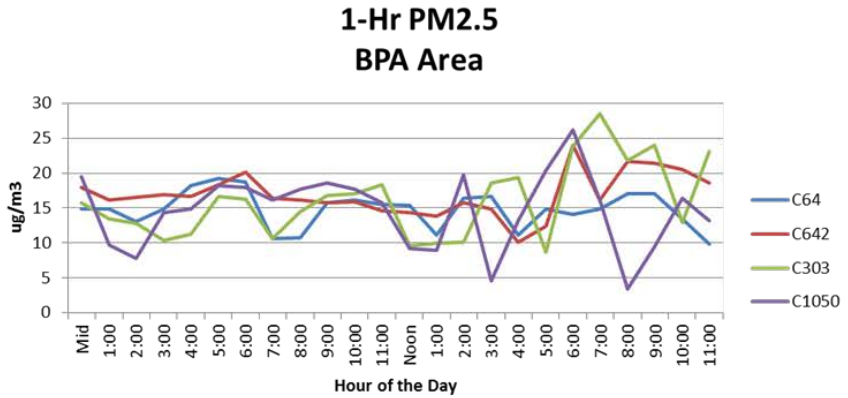

Figure 3-49. May 22 regional ozone (top left and right) and $PM_{2.5}$ (bottom left and right) measurements (HGB area time series).

3.1.7 June 1, 2012

On June 1, the NW Harris County monitor (C26) recorded its third highest MDA8 for 2012 (84 ppb) and the 1-hour average ozone maximum was 96 ppb (Figure 3-50). Although the NW Harris monitor had a higher 1-hour peak than the other monitors shown in Figure 3-50, it had a lower MDA8 and 1-hour ozone peak than many monitors in the HGB area on June 1 (Figure 3-56). The AQPlot back trajectory for the NW Harris monitor (Figure 3-50) shows stagnant conditions near the time of the 1-hour ozone peak with northerly winds in the early morning shifting to very light southerly winds by 10 am. Back trajectories for the other monitors shown in Figure 3-50 show a similar pattern of northerly flow followed by a wind shift as the trajectory approaches the monitor.

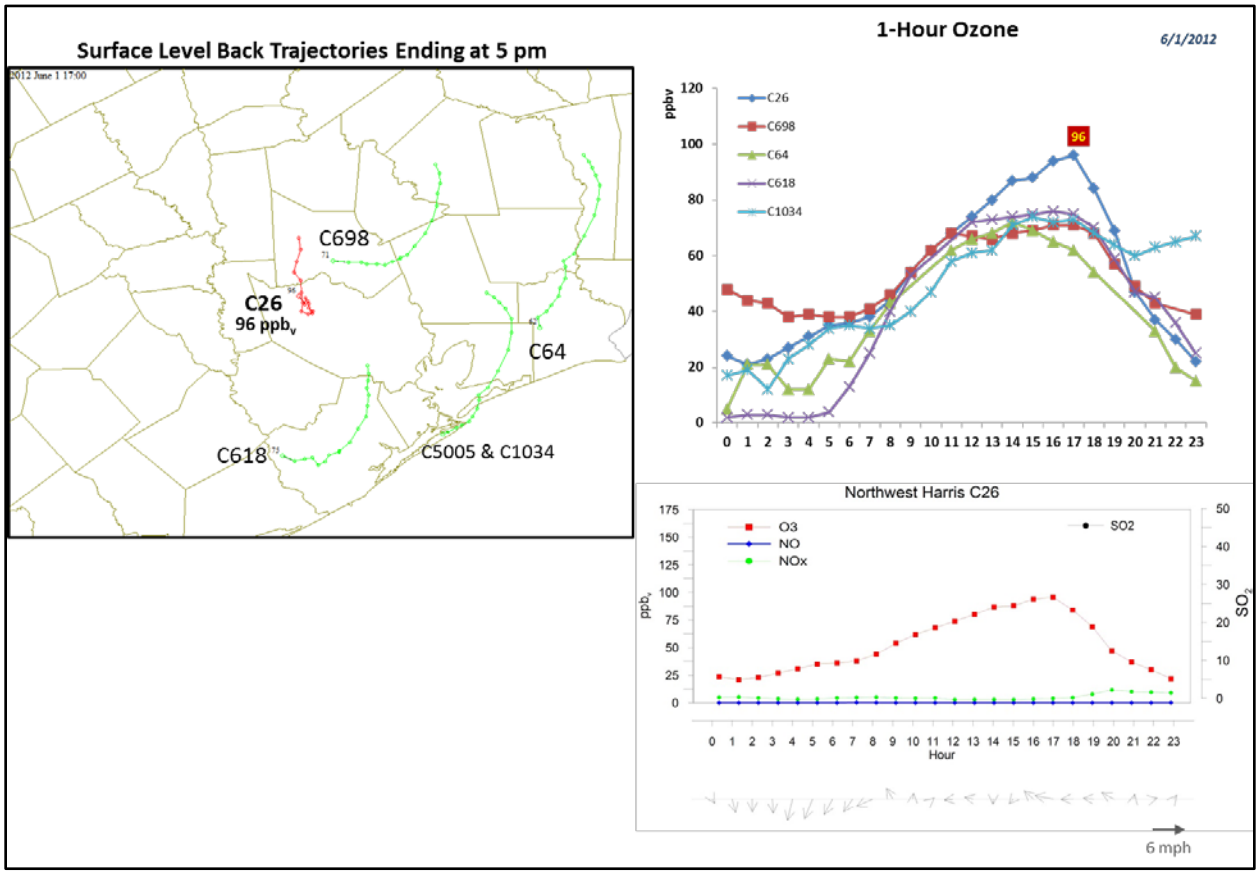

Figure 3-50. June 1, 2012 high ozone day at Northwest Harris C26. Left panel: AQPlot back trajectories ending at C26 and four background sites at the time of peak 1-hr ozone was observed at C26. Upper right panel: 1-hour average ozone time series for the C26 and background monitors. Lower right panel: time series of 1-hour ozone, NO, NO_2 and wind vectors at the Northwest Harris C26.

The SmartFire and HYSPLIT NAM back trajectories (Figure 3-51) both show northerly flow as the trajectories approach the NW Harris monitor, but differ as the trajectories move further

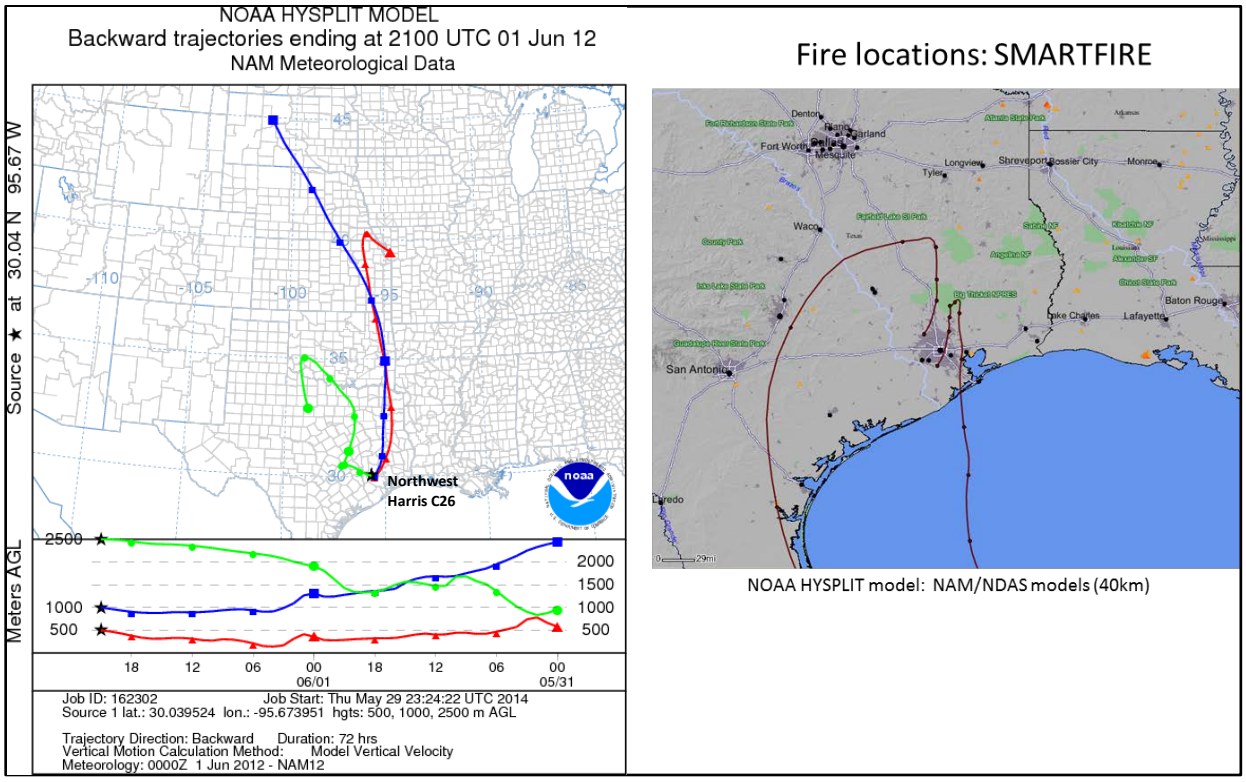

Figure 3-51. 72-hour HYSPLIT back trajectories (NAM 12km) from Northwest Harris C26 ending June 1, 2012; SmartFire plot showing fire locations (orange triangles) and 72-hour HYSPLIT back trajectories (EDAS 40 km) from C26.

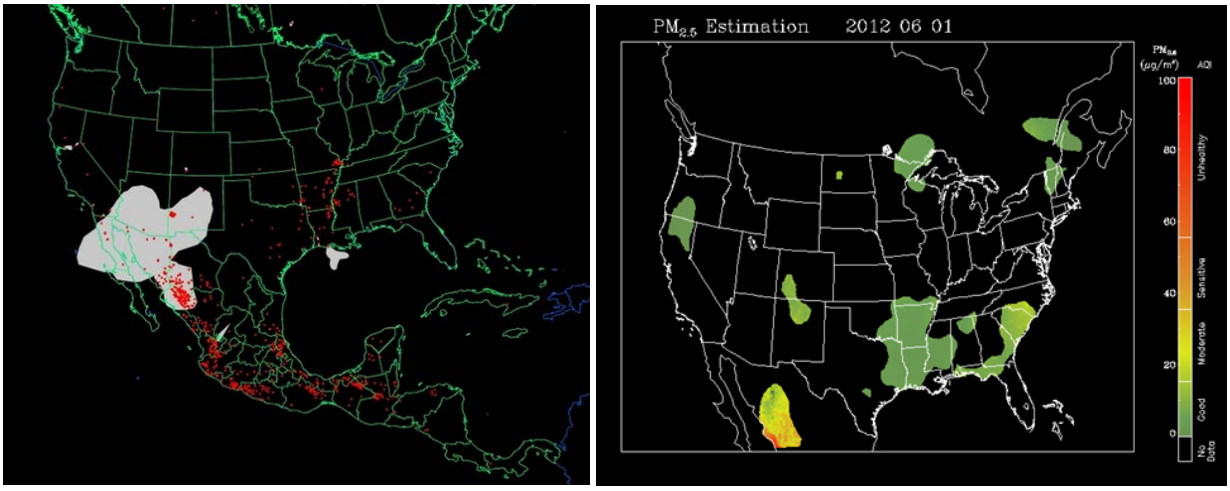

Figure 3-52. Left panel: HMS product showing June 1 fire locations (red dots) and smoke plume (gray area). Right panel: IDEA surface $PM_{2.5}$ estimate based on AOD and surface monitoring data.

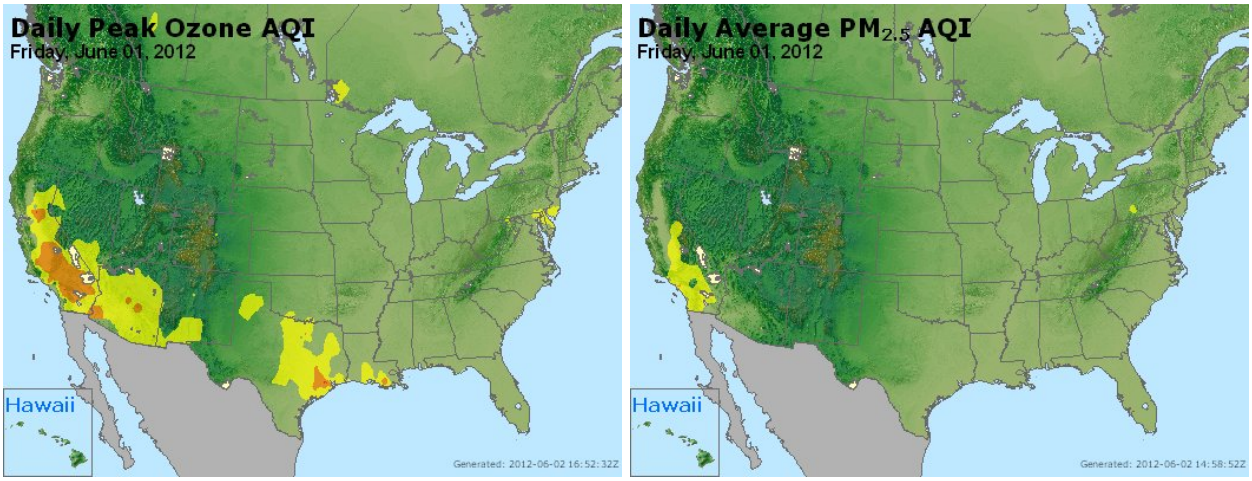

Figure 3-53. June 1 Daily average ozone (left) and $PM_{2.5}$ (right) based on observed values. Data from: [http://www.airnow.gov/.](http://www.airnow.gov/)

back in time. The HYSPLIT NAM low-level trajectories show transport from the north, while the SmartFire trajectory indicates that the airmass arriving at the NW Harris monitor originated over the Gulf of Mexico rather than over the continental U.S. The SmartFire tool shows a fire located near Baytown on Galveston Bay. The HMS product for June 1 (Figure 3-52) and the DataFed MODIS plot (Figure 3-55) do not show a fire or smoke plume in this location, but the FINN maps for -48 hours and -24 hours do show a fire (Figure 3-54). No smoke emissions or smoke appear in the HGB area or along the back trajectories in the NAAPS analyses (Figure 3-55).

While the SmartFire and NAM low-level HYSPLIT back trajectories are not consistent with one another in the days preceding June 1, they all agree that winds were northerly on the morning of June 1 and that the trajectories do not pass in the vicinity of the Baytown area fire. The ozone spatial pattern in Figure 3-56 is consistent with the light northerly wind pattern with a wind reversal during the day. Monitors in the north of the HGB area have lower ozone than those near the urban core to the south. Then ozone spatial pattern is consistent with an impact from local HGB area emissions sources at NW Harris County.

The only $PM_{2.5}$ monitor in the HGB area that shows high values of $PM_{2.5}$ on June 1 is the Houston East (C1) monitor. However, this peak occurs at 1 am and is not associated with high ozone at NW Harris County. During the high ozone period midday on June 1, $PM_{2.5}$ values were less than 25 $\mu g\ m^{-3}$ and are not consistent with a fire plume impact that could cause high ozone. There is no NOx peak coincident with the ozone peak at the NW Harris monitor (Figure 3-50). We therefore conclude that fire emissions did not play an important role in causing high ozone at the NW Harris County monitor on June 1 and recommend that no further evaluation be performed for June 1.

ENVIRON

Wildfire Emissions Inventory: FINN 2012

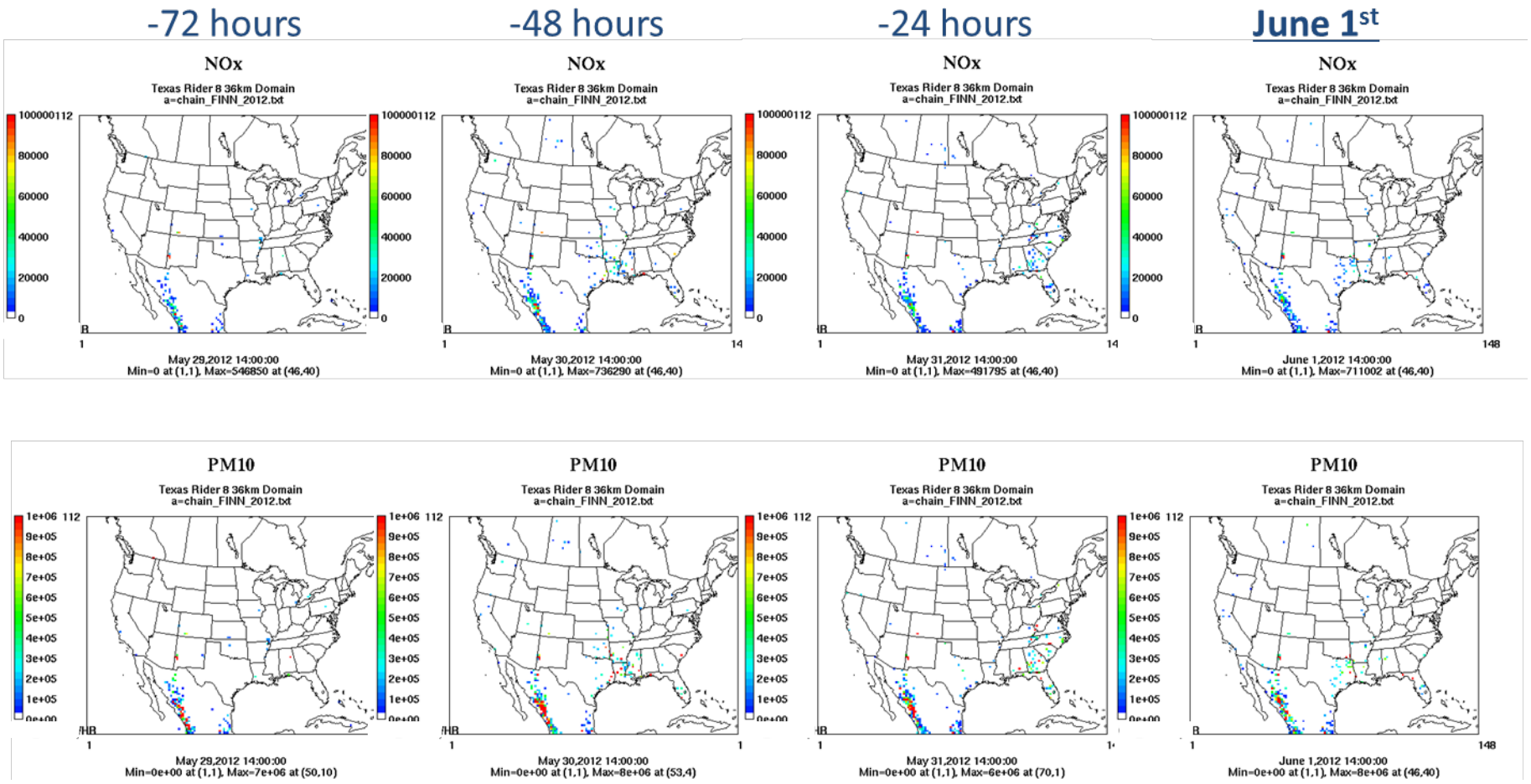

Figure 3-54. June 1, 2012 FINN fire emissions of NOx and PM_{10}.

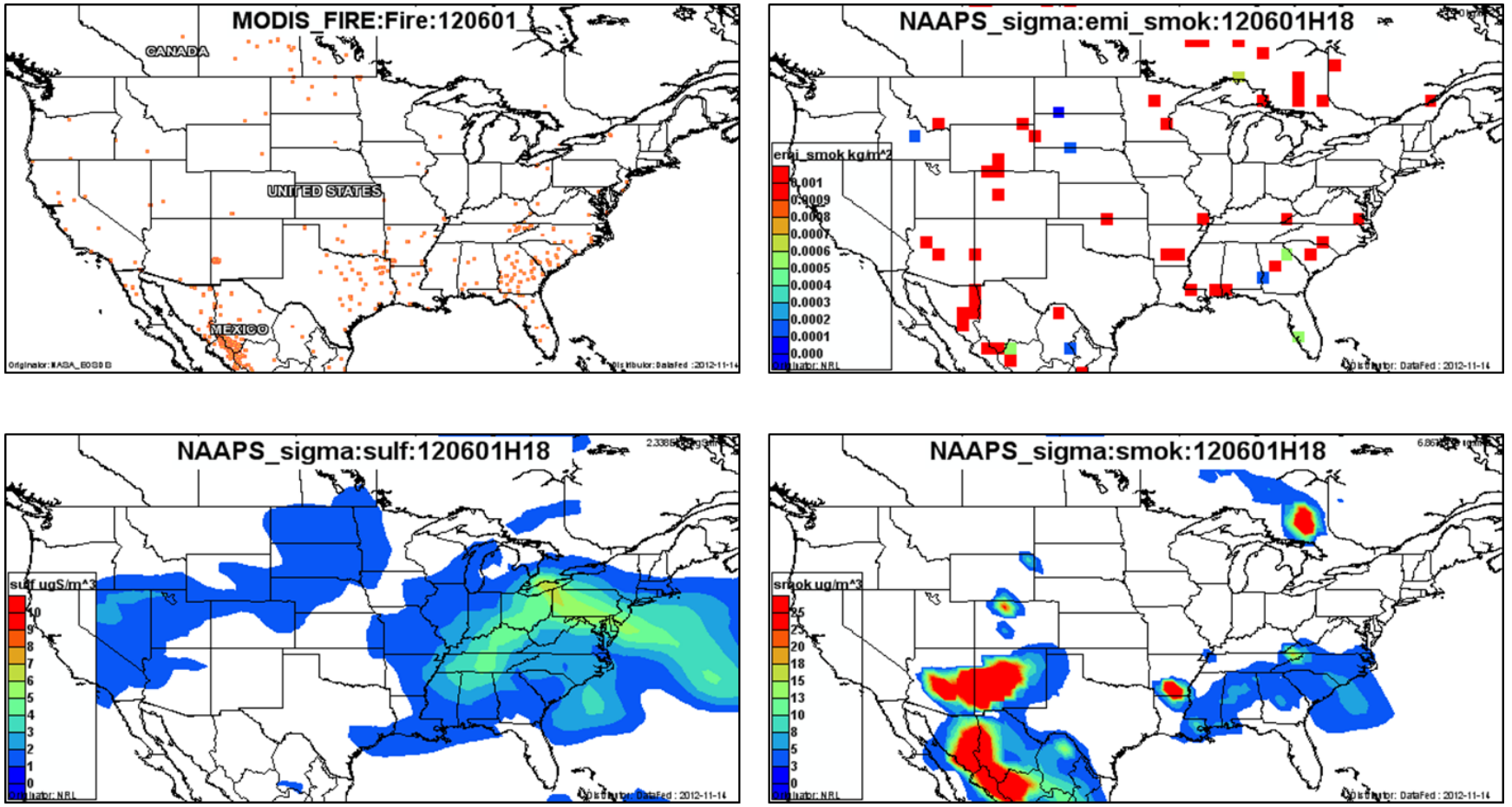

Figure 3-55. June 1, 2012 DataFed analysis. Upper left panel: Locations of active fires from MODIS satellite fire detections. Upper right panel: NAAPS model smoke emissions. Lower left panel: NAAPS model surface layer sulfate concentrations. Lower right panel: NAAPS model surface layer smoke concentrations.

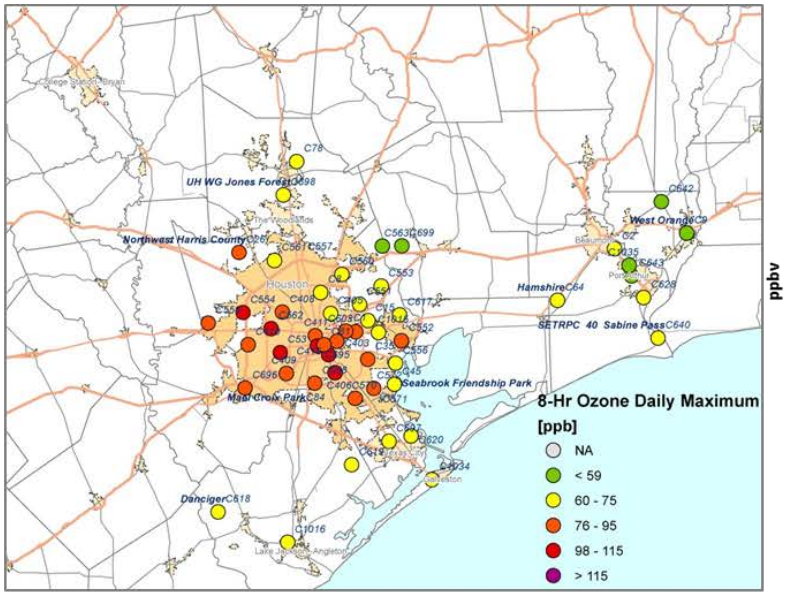

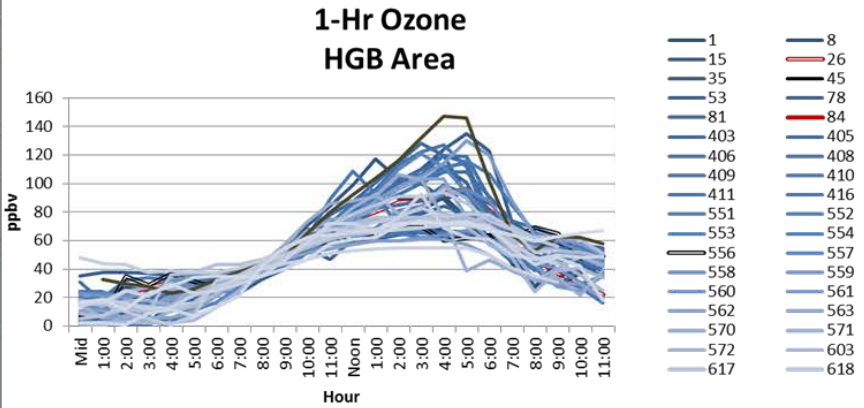

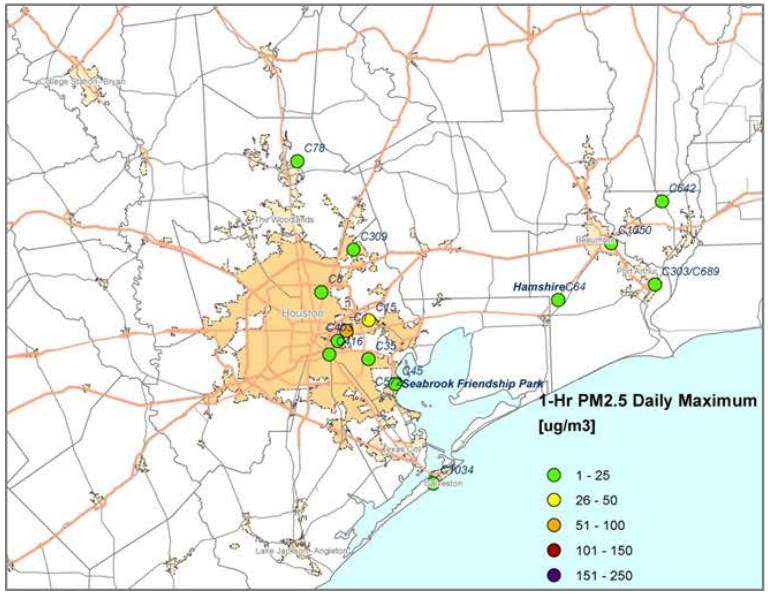

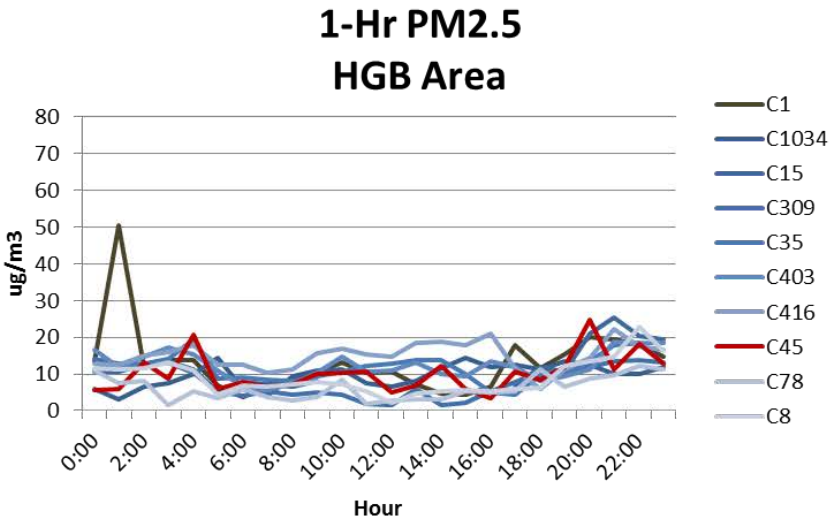

Figure 3-56. Regional ozone (top left and right) and $PM_{2.5}$ (bottom left and right) measurements (HGB area time series).

3.1.8 June 24, 2012

June 24-27, 2012 was a high ozone episode in East Texas. During this episode, temperatures in Texas and the rest of the central U.S. were very high (**Error! Reference source not found.**). There were many large fires active in the central and western U.S. (e.g. Figure 3-58) and much of the region was affected by smoke. By June 27, the eastern half of the U.S. had smoke aloft (Figure 3-91).

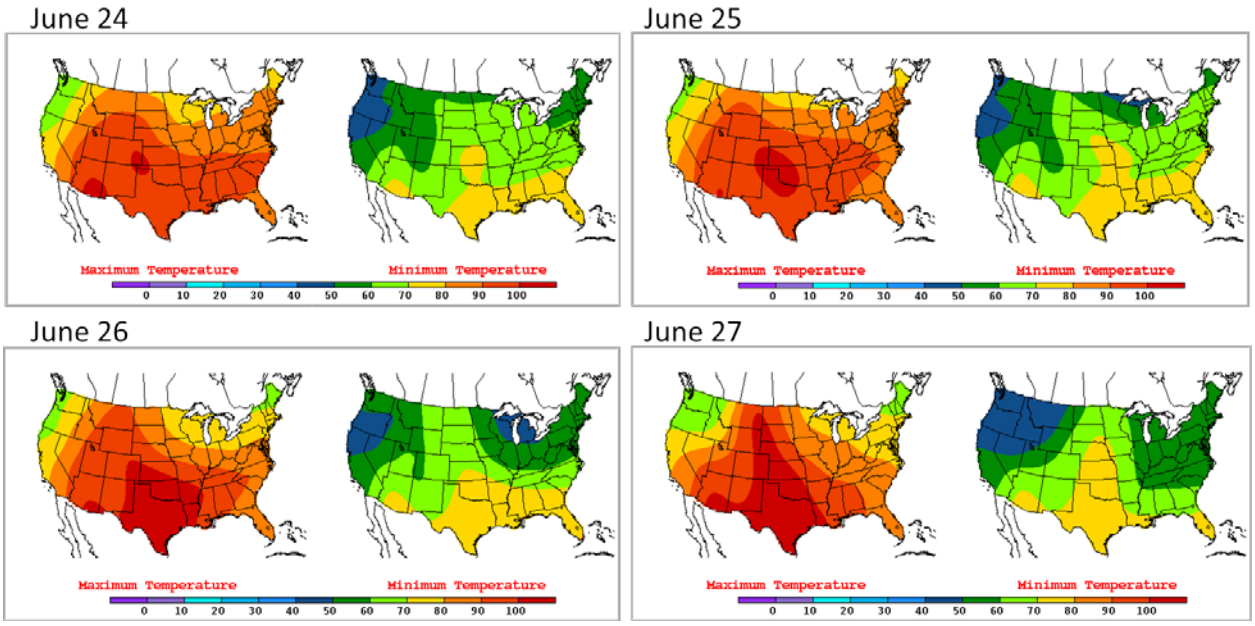

Figure 3-57. Daily maximum surface temperature analysis for June 24-27, 2012. NOAA weather map from http://www.hpc.ncep.noaa.gov/dailywxmap/index_20120627.html.

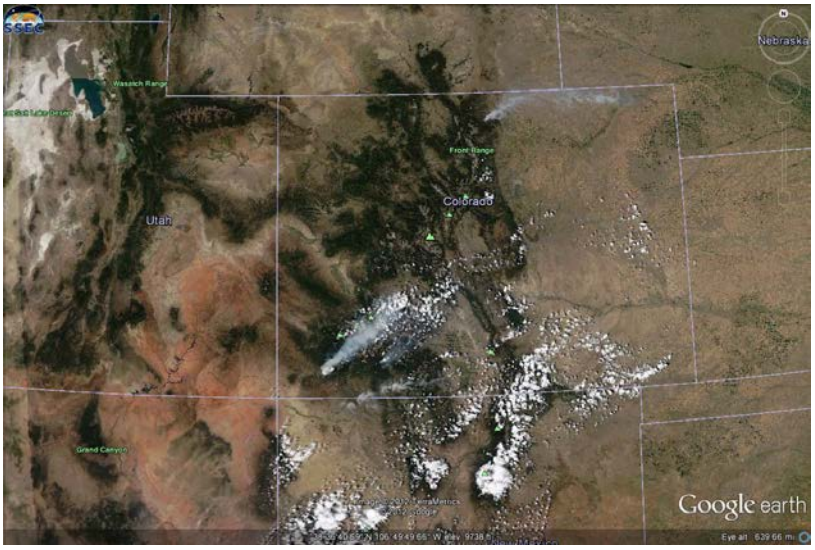

Figure 3-58. MODIS image showing smoke from Colorado fires. June 24, 2012. Image from http://alg.umbc.edu/usaq/archives/2012_06.html.

On June 24, the Grapevine Fairway (C70) monitor in the DFW area had its 4th high MDA8 day (86 ppb). Background ozone in the DFW area was high (~60 ppb) on June 24 and the Grapevine monitor had a peak 1-hour ozone value of 99 ppb (Figure 3-59). The AQPlot back trajectory for the Grapevine monitor (Figure 3-59) shows light southerly winds as do the trajectories for the other three monitors. There is no NOx or NO peak near the time of the 1-hour ozone maximum at the Grapevine Fairway monitor.

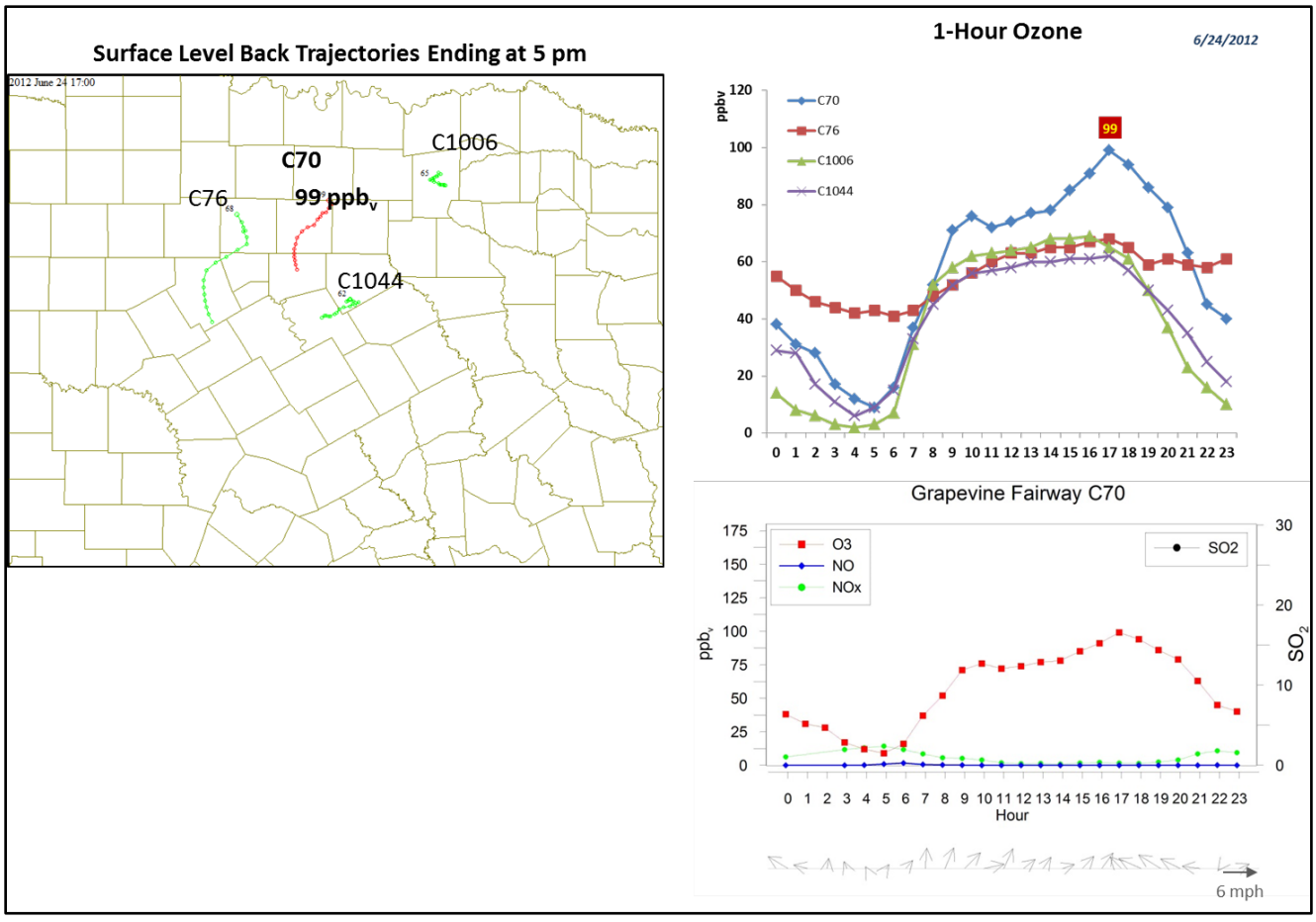

Figure 3-59. June 24, 2012 high ozone day at Grapevine Fairway C70. Left panel: AQPlot back trajectories ending at C70 and four background sites at the time of peak 1-hr ozone was observed. Upper right panel: 1-hour average ozone time series for the C70 and background monitors. Lower right panel: time series of 1-hour ozone, NO, NO_2 and wind vectors at the Grapevine Fairway C70 site.

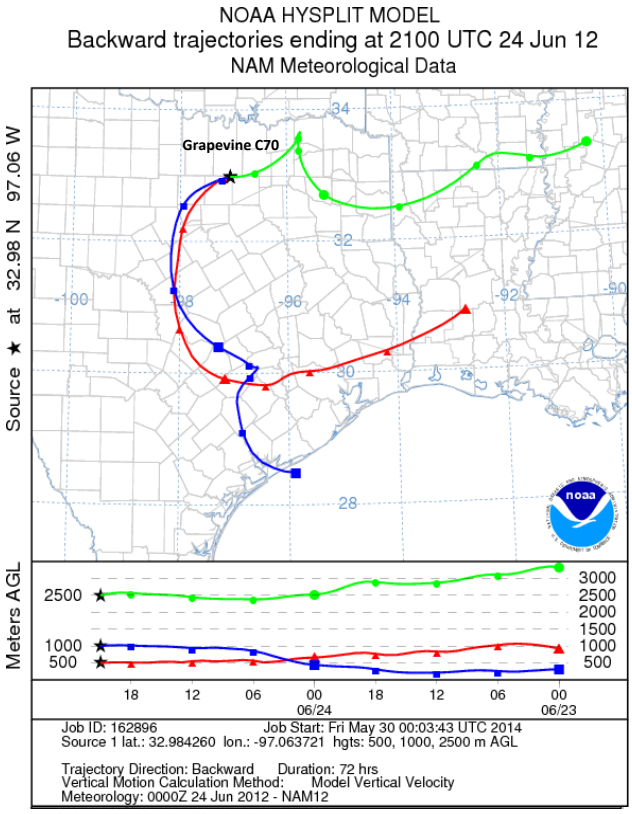

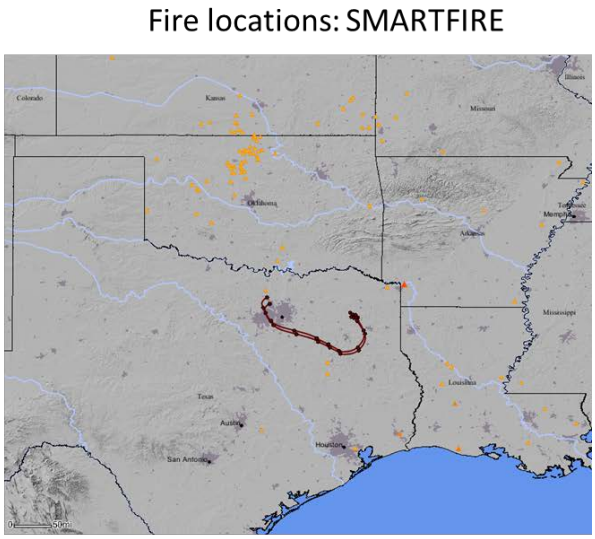

Figure 3-60. 72-hour HYSPLIT back trajectories (NAM 12km) from Grapevine Fairway C70 ending June 24, 2012; SmartFire plot showing fire locations (orange triangles) and 72-hour HYSPLIT surface level back trajectories (EDAS 40 km; 10m) from DFW sites C70 and C56.

The SmartFire and HYSPLIT NAM back trajectories (Figure 3-60) agree that low-level winds were southerly with an anti-cyclonic curvature during the 72-hour period. There is considerable vertical shear on June 24, as indicated by the different paths taken by the HYSPLIT back trajectories ending at 500 m and 1,000 m and the trajectory ending at 2,500 m. The SmartFire map shows a fire east of Austin in the vicinity of the HYSPLIT 500 m and 1,000 m back trajectories and two fires that lie south of the SmartFire back trajectories.

The HMS product Figure 3-61 shows all three fires present in the SmartFire map as do the FINN fire emissions maps (Figure 3-63) and the DataFed MODIS plot (Figure 3-64). The NAAPS model shows low levels (<5 µg m^{-3}) of smoke in the DFW area. However, $PM_{2.5}$ readings are relatively low south of the DFW area (Figure 3-62 and Figure 3-65) and are not consistent with a fire plume entering the DFW area borne on the southerly wind (Figure 3-65). The Kaufman monitor (C71) and Arlington Airport monitor have peaks in the early evening, but these peaks occur after the 1-hour ozone maxima for most monitors in the area and are only moderately high (~25 µ m^{-3}).

The spatial pattern of ozone in the DFW area on June 24 shows that monitors within the urban core had higher ozone than the monitors in outlying areas (Figure 3-65). This is consistent with

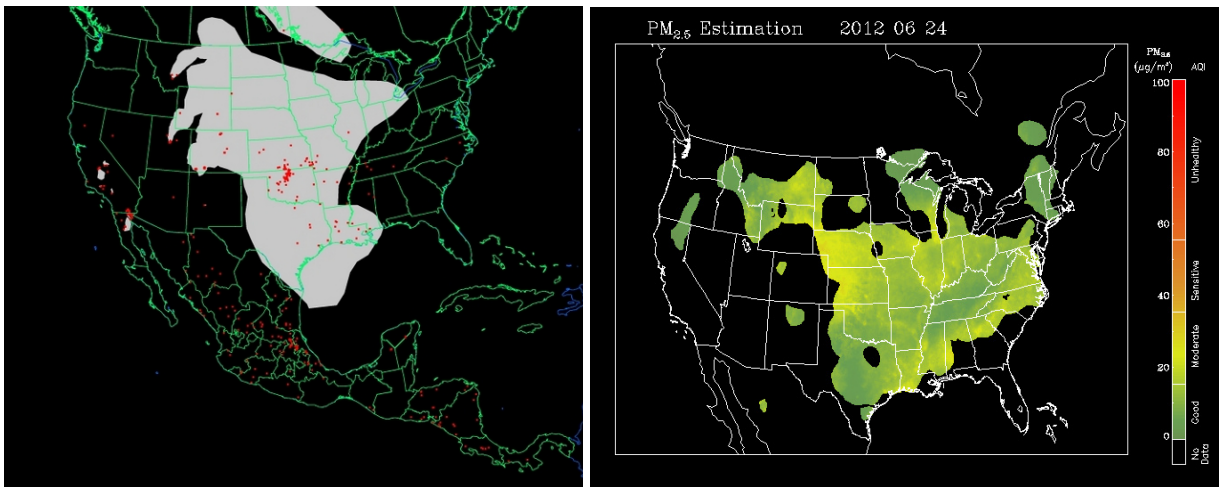

Figure 3-61. Left panel: HMS product showing June 24 fire locations (red dots) and smoke plume (gray area). Right panel: IDEA surface $PM_{2.5}$ estimate based on AOD and surface monitoring data.

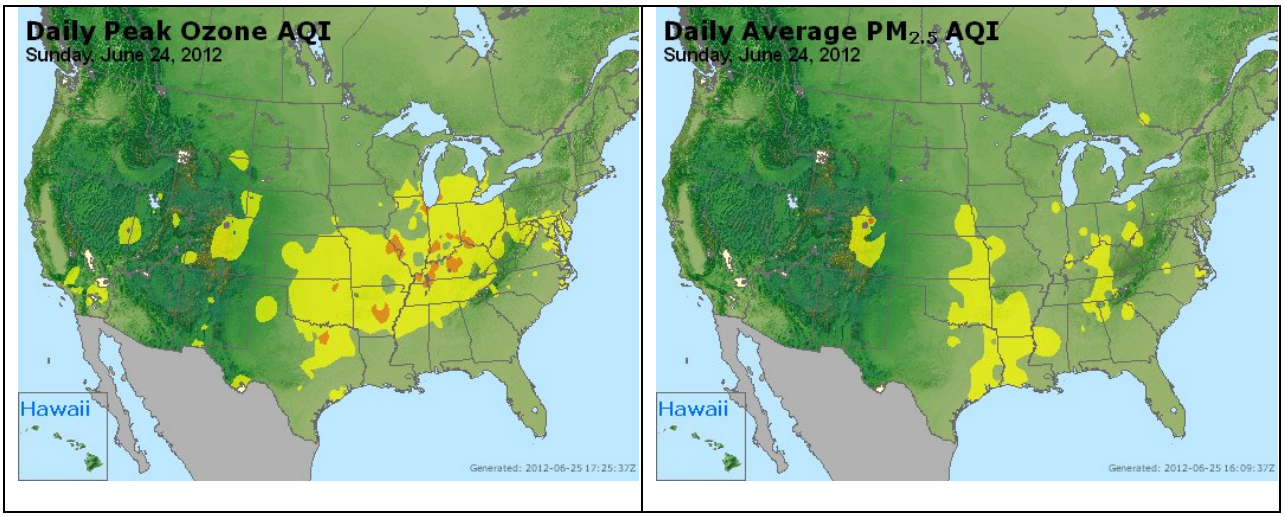

Figure 3-62. Daily average ozone (left) and $PM_{2.5}$ (right) based on observed values. Data from: http://www.airnow.gov/.

the stagnant winds which would tend to keep the DFW emissions and ozone formed from them within the area.

Because there is little evidence that emissions from the distant fires influenced ozone on June 24 and because the likelihood of impact from local sources is far greater, we do not recommend further evaluation for June 24, 2012.

Wildfire Emissions Inventory: FINN 2012

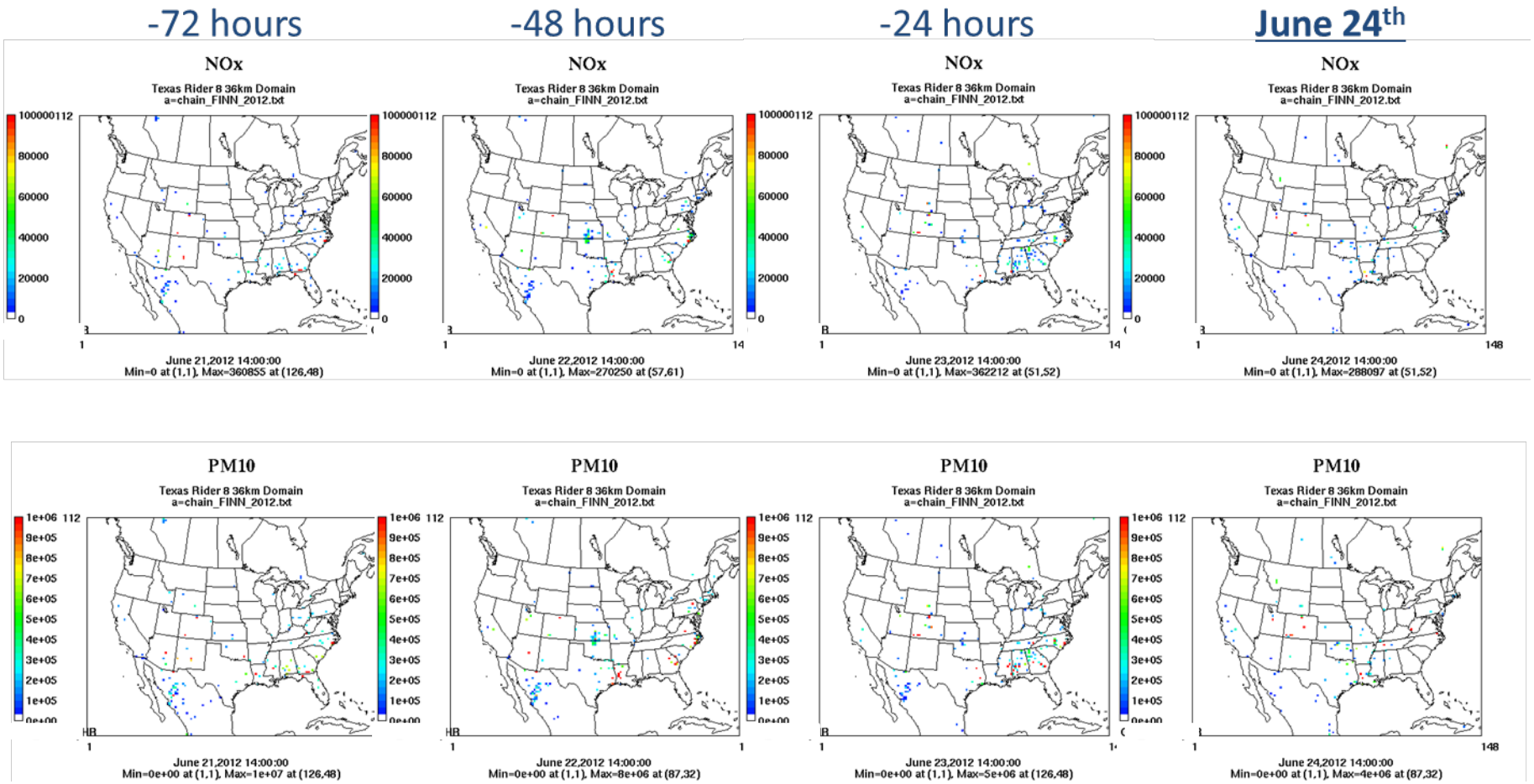

Figure 3-63. June 24, 2012 FINN fire emissions of NOx and PM_{10}.

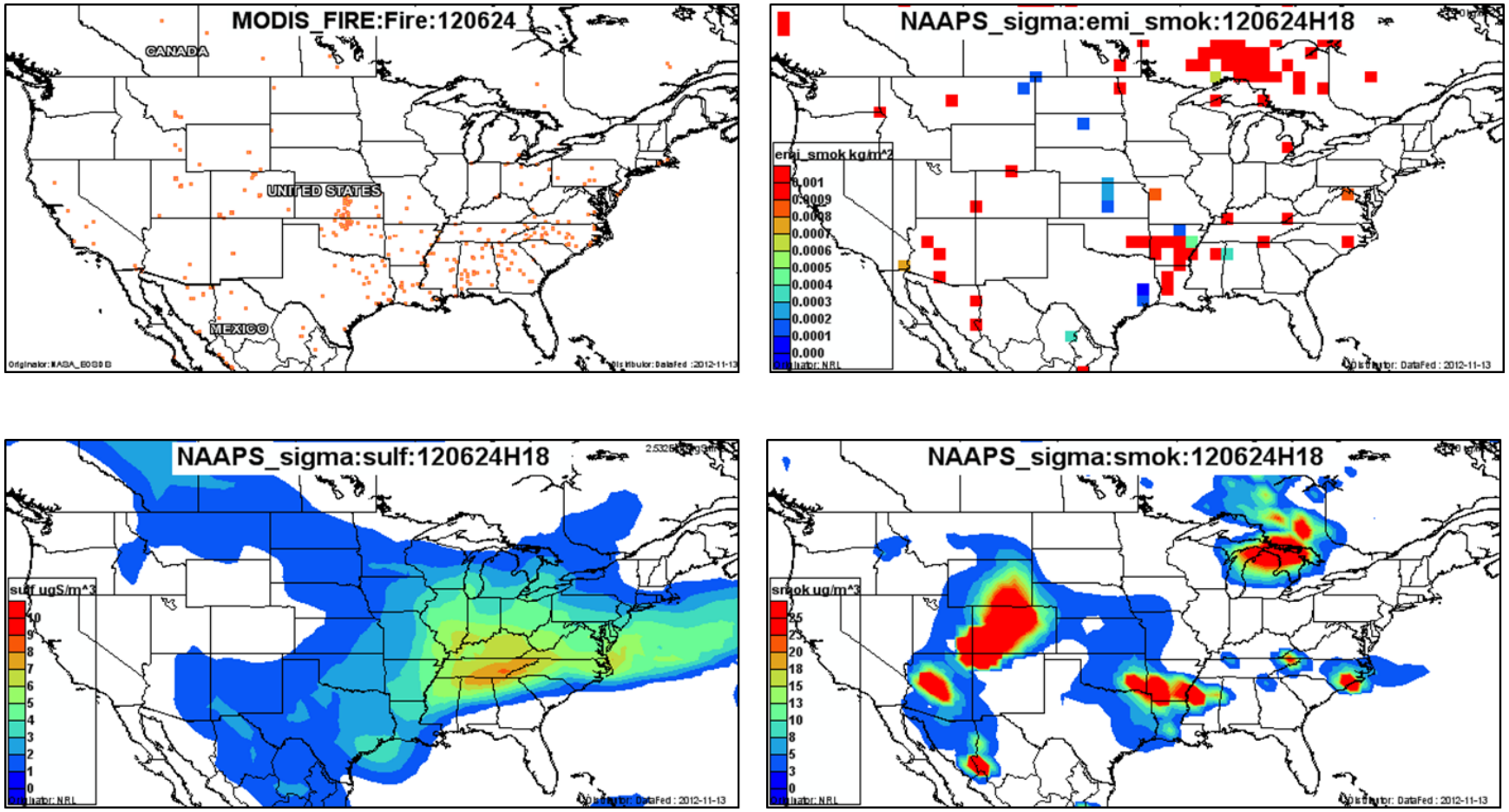

Figure 3-64. June 24, 2012 DataFed analysis. Upper left panel: Locations of active fires from MODIS satellite fire detections. Upper right panel: NAAPS model smoke emissions. Lower left panel: NAAPS model surface layer sulfate concentrations. Lower right panel: NAAPS model surface layer smoke concentrations.

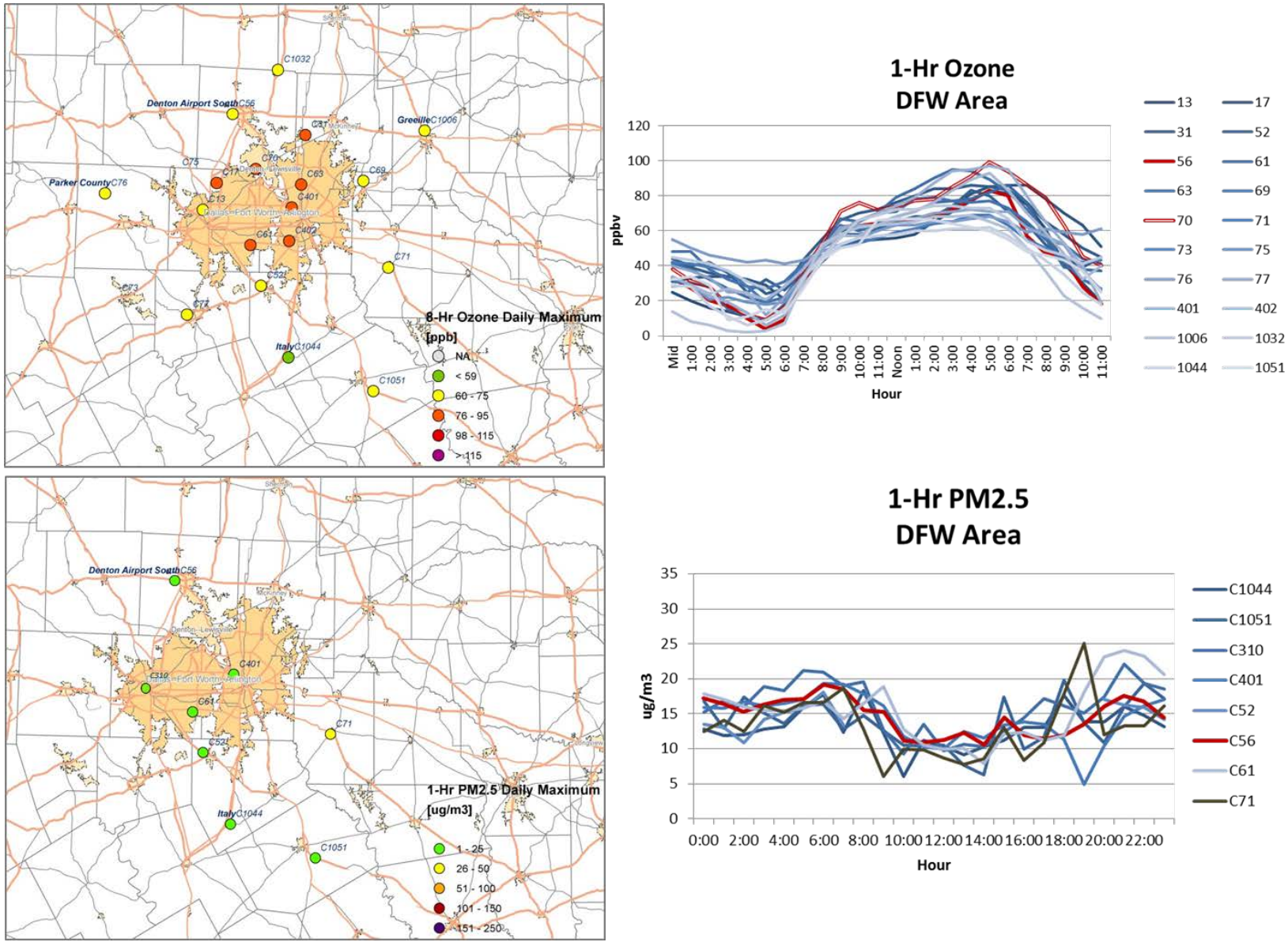

Figure 3-65. June 24 regional ozone (top left and right) and $PM_{2.5}$ (bottom left and right) measurements (DFW area time series).

3.1.9 June 25, 2012

On June 25, 2012, the Denton Airport South (C56) and Grapevine Fairway (C70) monitors in the DFW area recorded their 4th (81 ppb) and 2nd highest (97 ppb) MDA8 values of 2012, respectively. Denton Airport South C56 had a peak 1-hour ozone reading of 88 ppb (Figure 3-66), while Grapevine Fairway C70 had a 1-hour ozone maximum of 111 ppb (Figure 3-67). Wind vectors and AQPlot back trajectories for both monitors show stagnant, shifting winds that are southerly during the midday hours (Figure 3-66 and Figure 3-67). No peaks in NO or NOx are evident at Denton during the daylight hours when ozone is high. However, Grapevine Fairway does show relatively high NOx after the morning peak that coincides with a period of enhanced ozone from 9-10 am. When the NOx subsides at 11 am, ozone falls at 11 am before continuing its rise at 12 pm. SO_2 is not monitored at either Denton or Grapevine Fairway.

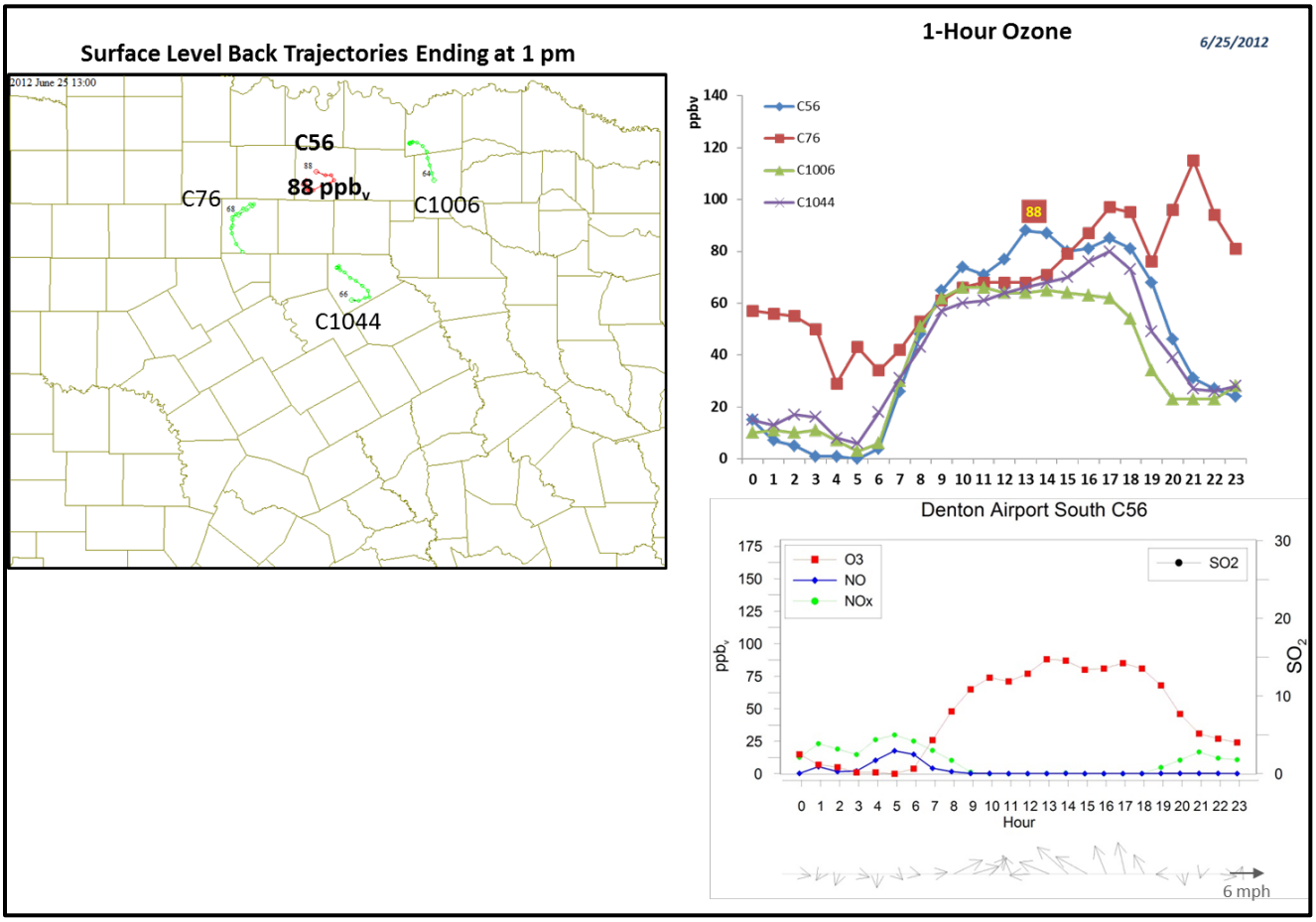

Figure 3-66. June 25, 2012 high ozone day at Denton Airport South C56. Left panel: AQPlot back trajectories ending at C56 and four background sites at the time of peak 1-hr ozone was observed. Upper right panel: 1-hour average ozone time series for the C70 and background monitors. Lower right panel: time series of 1-hour ozone, NO, NO_2 and wind vectors at the Grapevine Fairway C56 site.

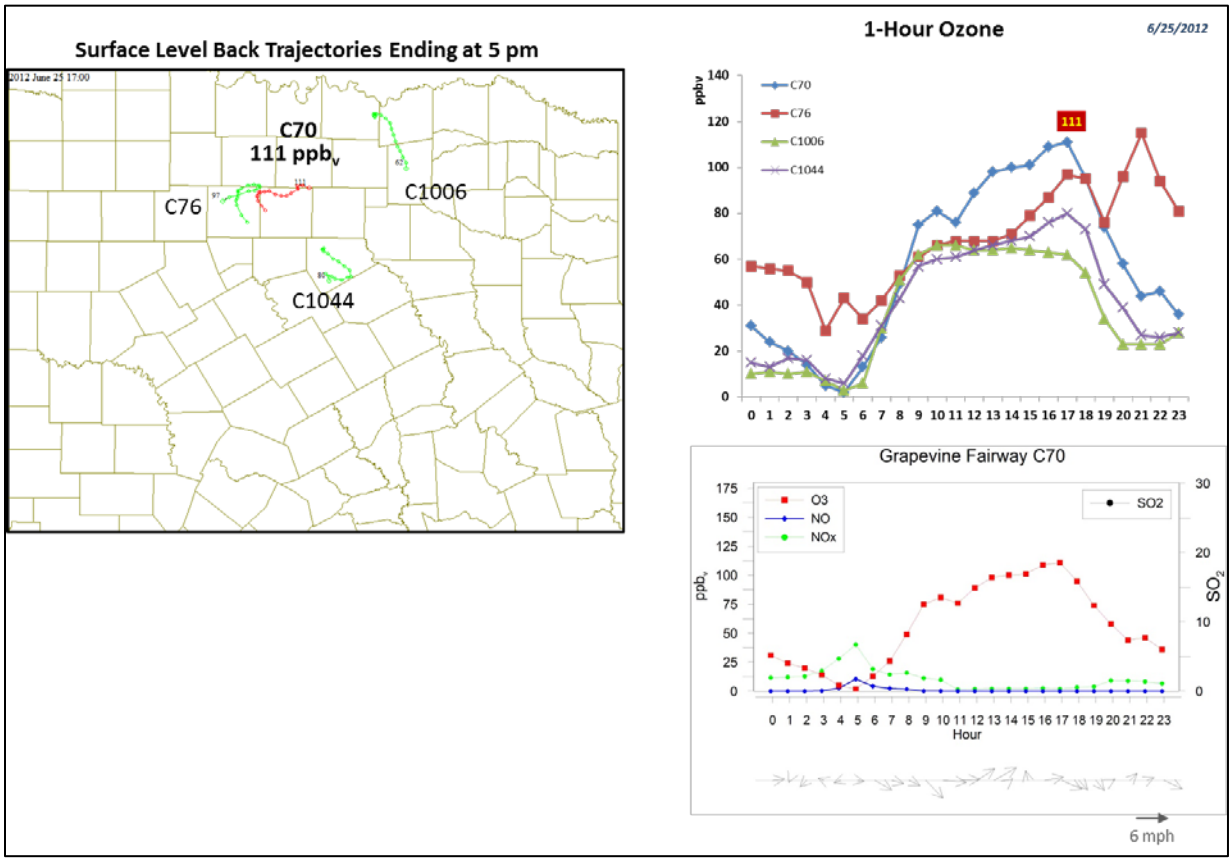

Figure 3-67. June 25, 2012 high ozone day at Grapevine Fairway C70. Left panel: AQPlot back trajectories ending at C70 and four background sites at the time of peak 1-hr ozone was observed. Upper right panel: 1-hour average ozone time series for the C70 and background monitors. Lower right panel: time series of 1-hour ozone, NO, NO_2 and wind vectors at the Grapevine Fairway C70 site.

The SmartFire back trajectory plot (lower panels of Figure 3-69) shows stagnant winds on June 25 and transport from the region south of the DFW area during the preceding two days. The SmartFire back trajectories for Denton and Grapevine pass in the vicinity of two fires at -48 hours and -42 hours. Fires appear south of the DFW area in the FINN emissions plots (Figure 3-72) but not the HMS product (Figure 3-70). The HYSPLIT 12 km NAM back trajectories for both monitors also show stagnant flow on June 25 and stagnant or southerly flow leading up to June 25 for trajectories ending at 500 m and 1,000. However, the HYSPLIT 12 km NAM 500 m trajectories show that air passed well to the west of the fires in the SMARTFIRE plot. The back trajectory analysis, therefore, is not conclusive as to whether there was a fire upwind of the DFW area.

The NAAPS analysis (Figure 3-73) shows that there was smoke present in the DFW area on June 25, consistent with the HMS smoke product (Figure 3-70). The FINN (Figure 3-72) and NAAPS emissions plots (Figure 3-73) show the presence of the fires southeast of the DFW area.

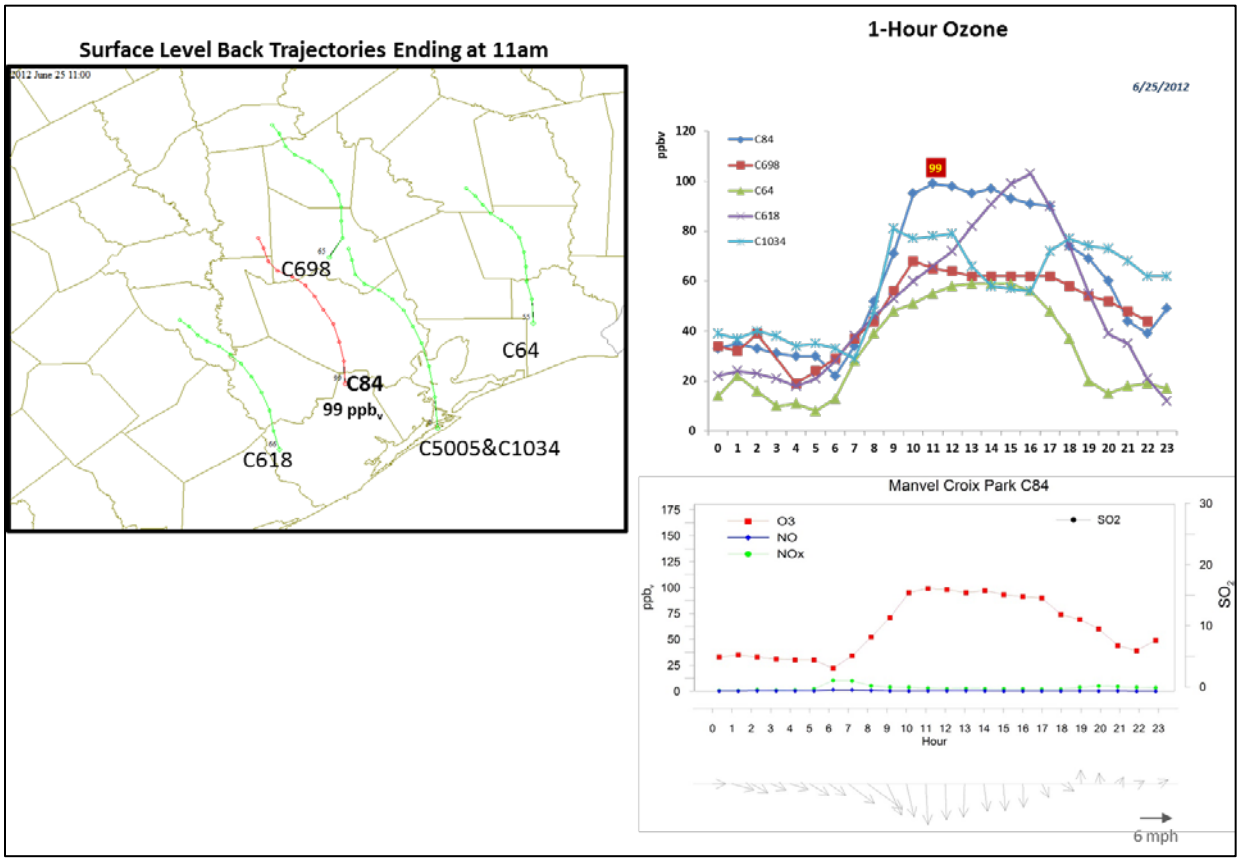

Figure 3-68. June 25, 2012 high ozone day at Manvel Croix Park C84. Left panel: AQPlot back trajectories ending at C84 and four background sites at the time of peak 1-hr ozone was observed. Upper right panel: 1-hour average ozone time series for the C84 and background monitors. Lower right panel: time series of 1-hour ozone, NO, NO_2 and wind vectors at the Grapevine Fairway C84 site.

The spatial plot of ozone in the DFW area (Figure 3-75) is consistent with a stagnation event. In a stagnation event, low wind speeds and shifting wind directions tend to keep emissions of ozone precursors within the urban area; this causes ozone to be higher at sites within the DFW metroplex and lower at outlying monitors. The $PM_{2.5}$ spatial and time series plots do not show enhanced $PM_{2.5}$ at the Denton monitor (C56), indicating that fire emissions likely did not impact the Denton or Grapevine monitors and contributed to high ozone on June 25, 2012. The $PM_{2.5}$ spatial plot indicates that monitors to the south of the DFW area had higher readings; this is consistent with their closer proximity to the fires, although it is not possible to tell given the data at hand whether the fires are the direct cause. (The NAAPS sulfate plot indicates the presence of sulfate aerosol, although concentrations are <3 µg m^{-3}.) The only monitor with a significantly elevated $PM_{2.5}$ values is the C310 monitor, located in downtown Fort Worth. This sharp peak occurred at 6 am and is characteristic of a plume impact, although it is not well-correlated with peak ozone at either the Denton or Grapevine monitors. The $PM_{2.5}$ values are not high along the back trajectories to either monitor or in their vicinity and the spatial pattern of ozone is more consistent with a stagnant day in the

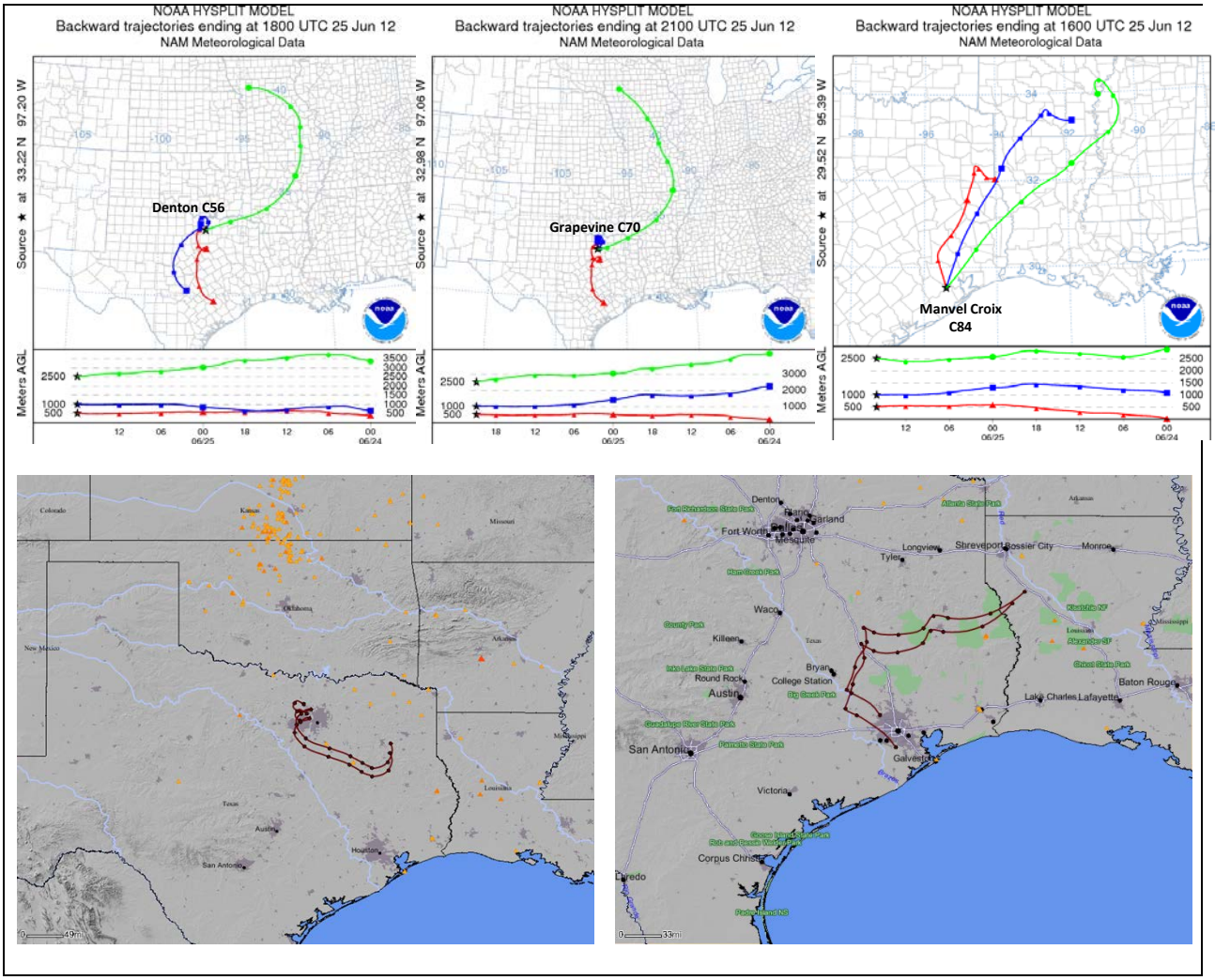

Figure 3-69. 72-hour HYSPLIT back trajectories at Denton C56 (top left); Grapevine C70 (middle) and Manvel Croix C84 (top right); SMARTFIRE plots showing fire locations (orange triangles) and 72-hour HYSPLIT back trajectories from DFW sites (bottom left) and HGB area (bottom right).

midst of a high ozone episode where background levels were high across east Texas than a plume impact. However, it is possible that fires contributed to ozone in the DFW area, and given the magnitude of the 6 am peak at C310 and the diagnosed smoke in the area, further investigation is warranted. We recommend additional evaluation of June 25, 2012 for Denton and Grapevine.

On June 25, the Manvel Croix monitor in the HGB area had its second highest MDA8 of 2012 (94 ppb). The peak 1-hour ozone value at Manvel Croix on June 25 was 99 ppb. The AQPlot back trajectory for Manvel Croix (Figure 3-68) shows northwesterly winds as do the back trajectories

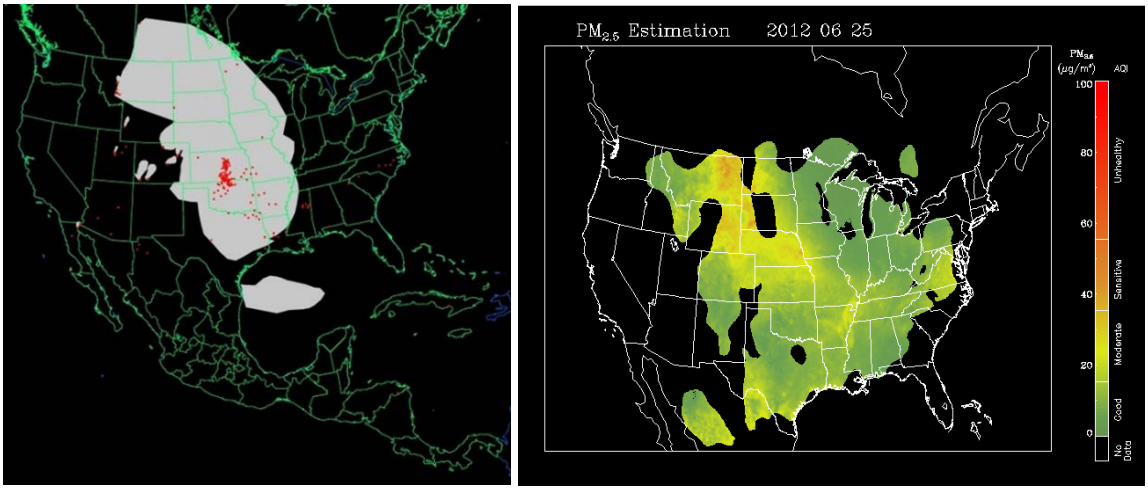

Figure 3-70. Left panel: HMS product showing June 25 fire locations (red dots) and smoke plume (gray area). Right panel: IDEA surface $PM_{2.5}$ estimate based on AOD and surface monitoring data.

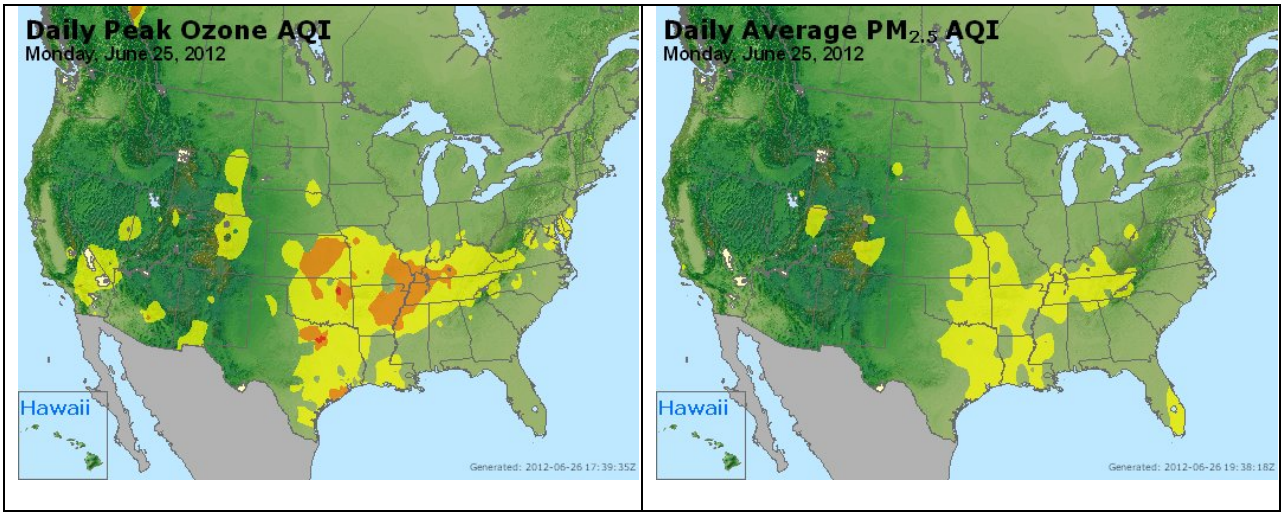

Figure 3-71. Daily average ozone (left) and $PM_{2.5}$ (right) based on observed values. Data from: http://www.airnow.gov/.

for the other monitors. The SmartFire and HYSPLIT NAM back trajectories agree that winds were northerly on June 25 and that the 72-hour back trajectories extend toward Northeast Texas and Arkansas. Both the HYSPLIT and SmartFire trajectories pass to the north of a fire near the Louisiana border at about -66 hours. This fire appears in the HMS map (Figure 3-70) as well as in the FINN emissions (Figure 3-72) and NAAPS smoke emissions (Figure 3-73). Figure 3-71 indicates that the AQI for both ozone and $PM_{2.5}$ were high across East Texas.

The spatial plots of monitors in the HGB area (Figure 3-74) show that although $PM_{2.5}$ values are between 26 and 50 µg m^{-3} at several monitors in the HGB area, the only monitor that appears to show a peak consistent with a plume impact is the Galveston monitor (C1058), for which 12-4 pm $PM_{2.5}$ data were rejected by TCEQ validators. Monitors located upwind of the Manvel

Croix monitor show no such peaks, which suggests that a fire plume was not present at Manvel Croix on June 25. The Manvel Croix monitor shows no NO or NOx plume near the time of the 1-hour average ozone maximum (Figure 3-68).

Figure 3-74 confirms that background ozone was high on June 25 in the HGB area (>60 ppb). Ozone MDA8 values were lower on the northeast (upwind) side of the HGB area than on the southwest (downwind) side. Ozone, $PM_{2.5}$ and wind data therefore, are consistent with an impact from local emissions sources on a day with high background ozone rather than a fire plume impact, and we recommend no further evaluation of June 25, 2012 at the Manvel Croix monitor.

ENVIRON

Wildfire Emissions Inventory: FINN 2012

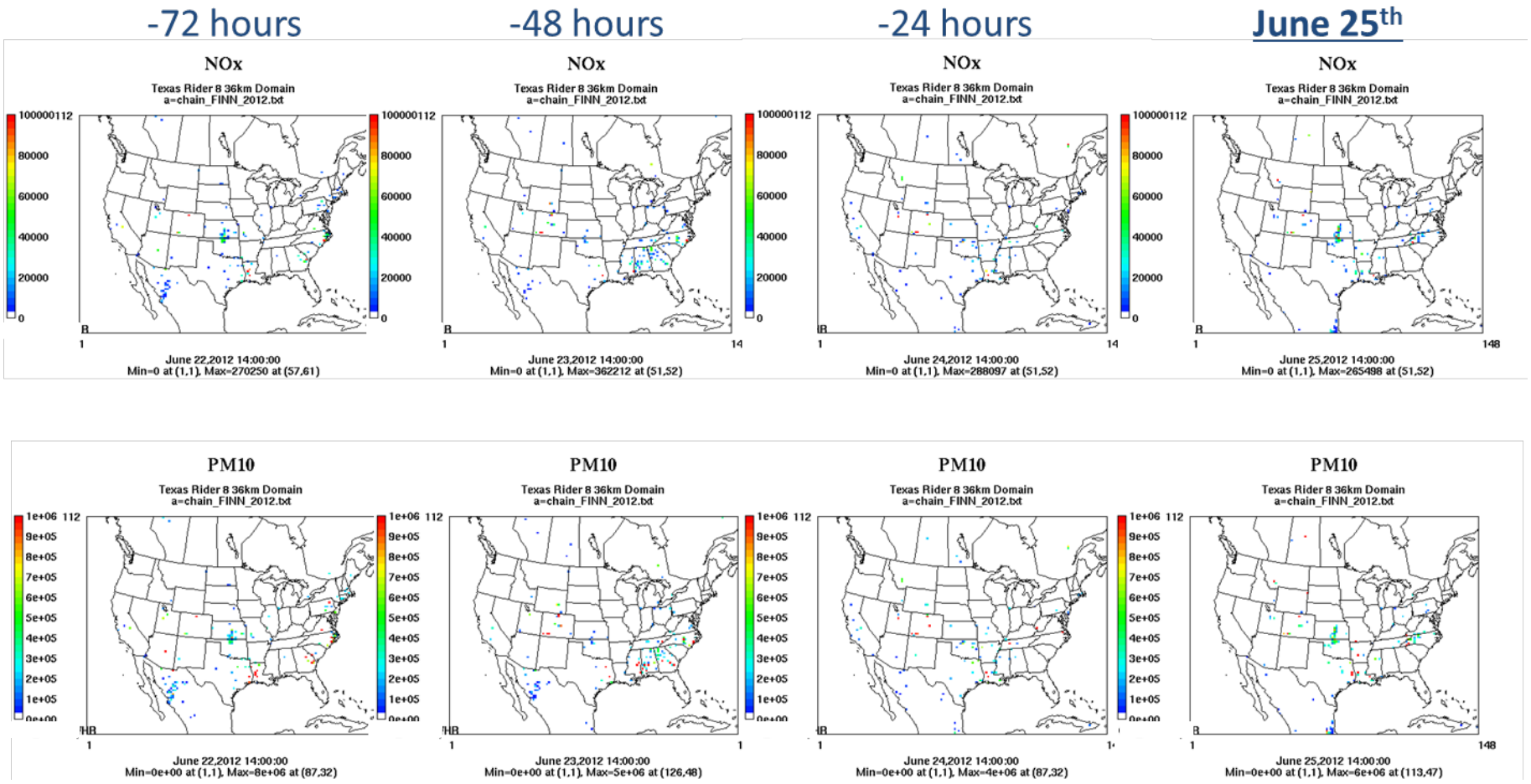

Figure 3-72. June 25, 2012 FINN fire emissions of NOx and PM_{10}.

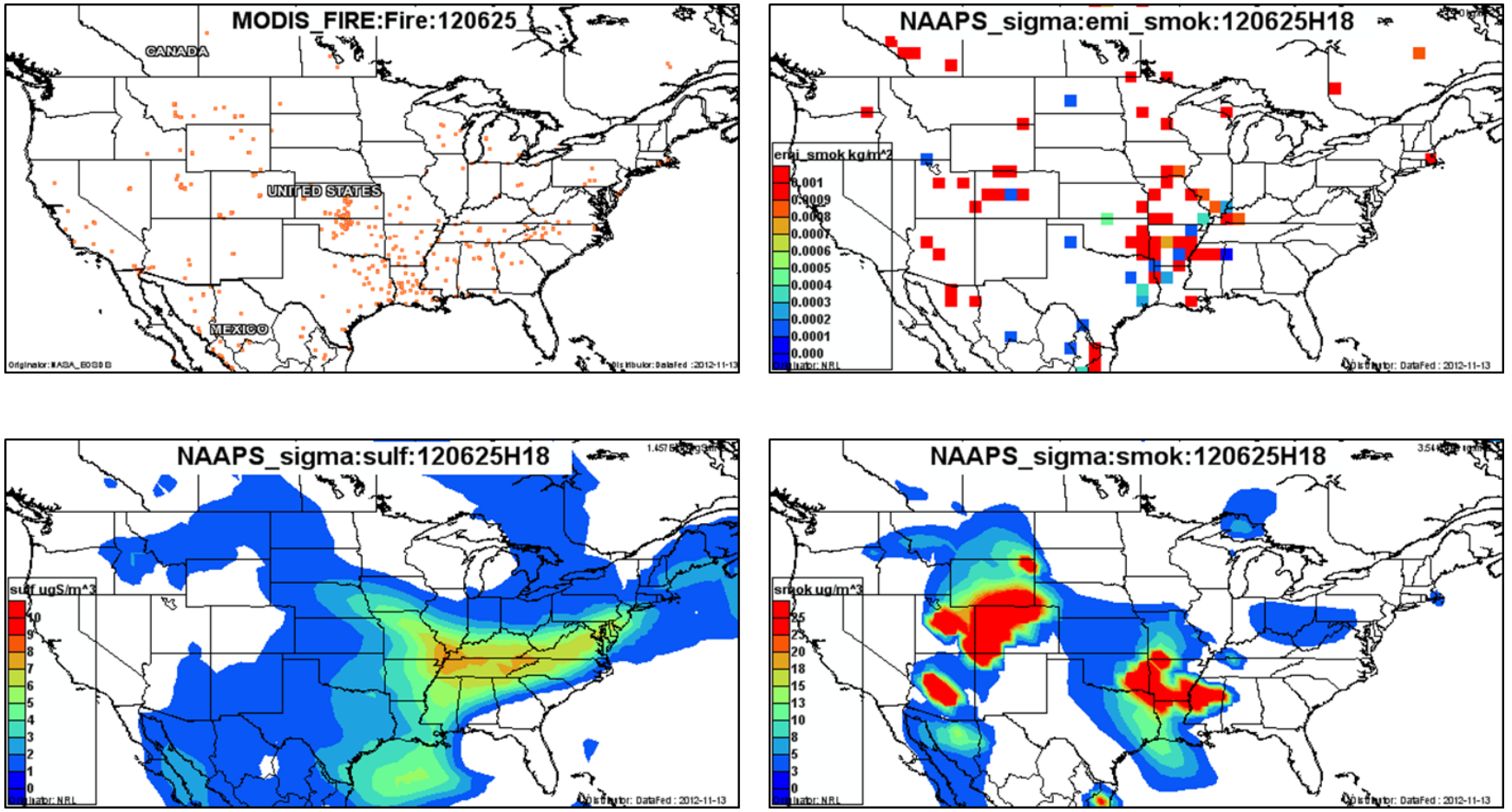

Figure 3-73. June 25, 2012 DataFed analysis. Upper left panel: Locations of active fires from MODIS satellite fire detections. Upper right panel: NAAPS model smoke emissions. Lower left panel: NAAPS model surface layer sulfate concentrations. Lower right panel: NAAPS model surface layer smoke concentrations.

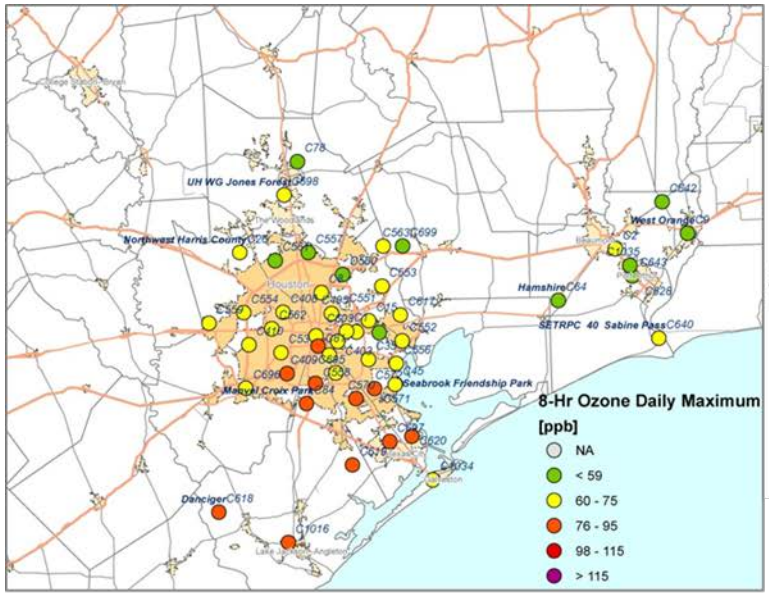

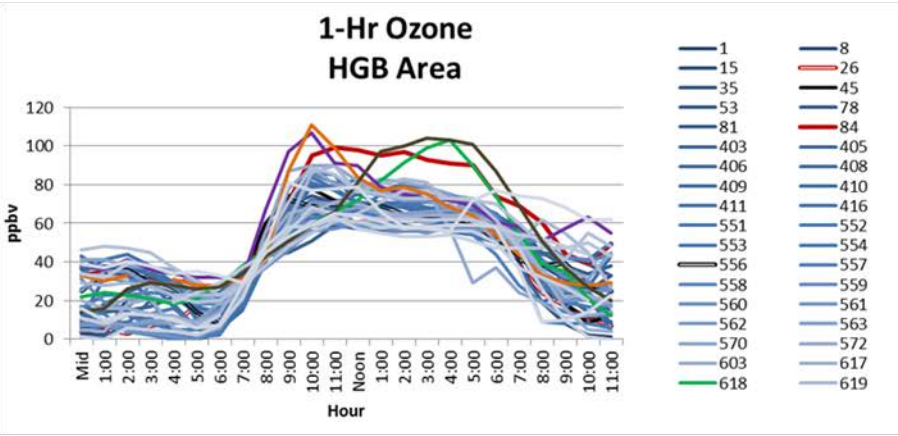

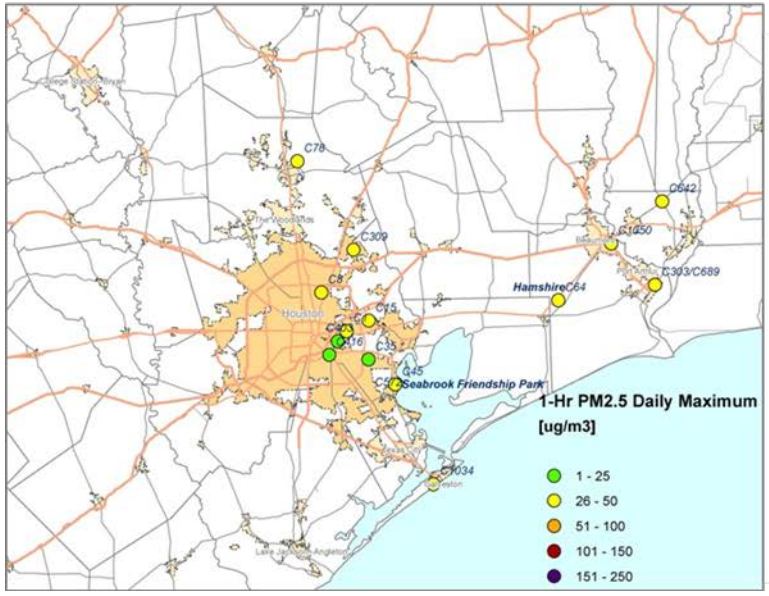

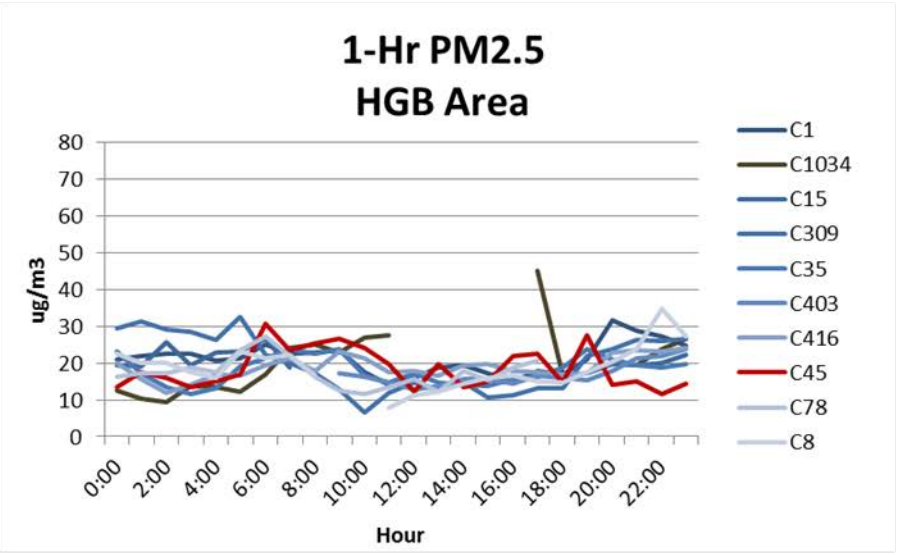

Figure 3-74. Regional ozone (top left and right) and $PM_{2.5}$ (bottom left and right) measurements (HGB area time series).

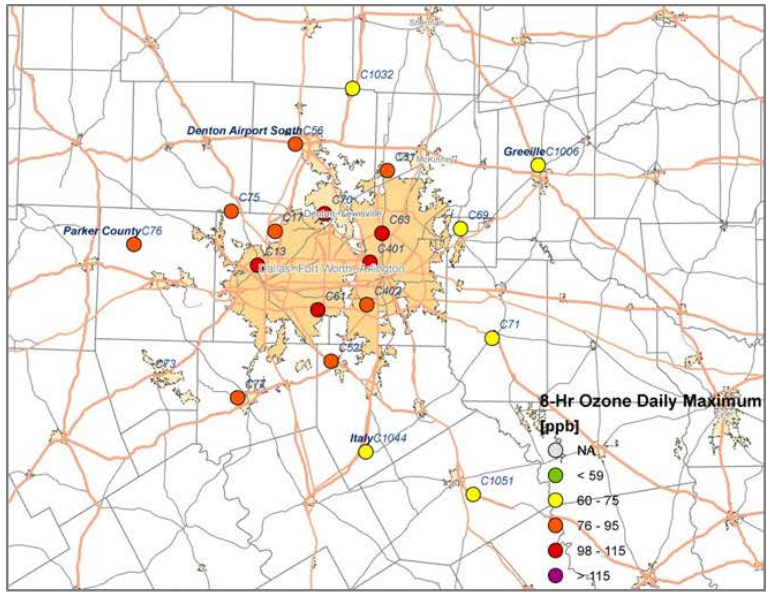

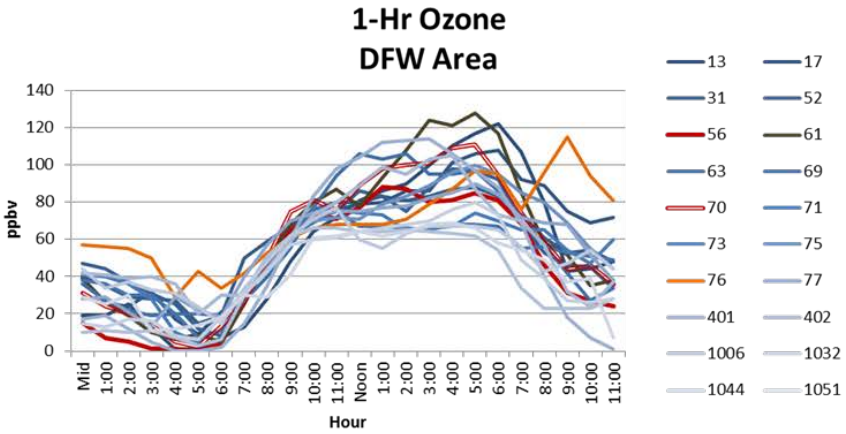

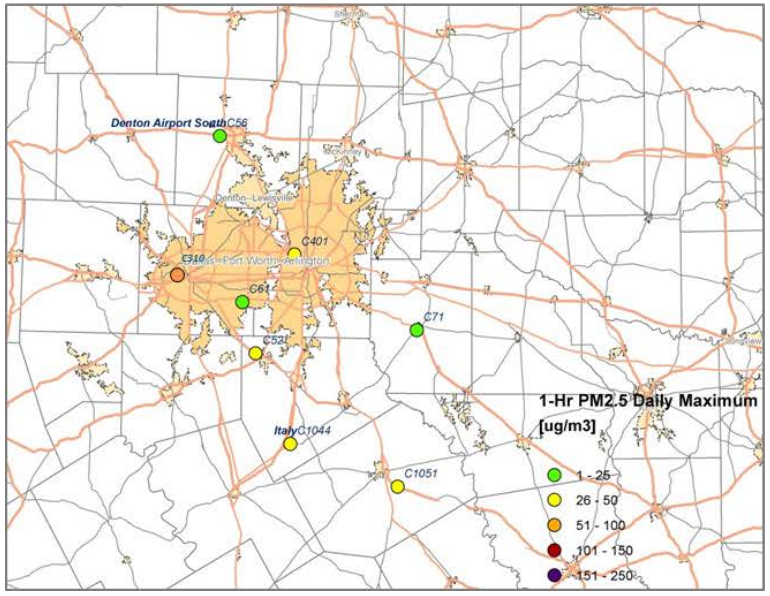

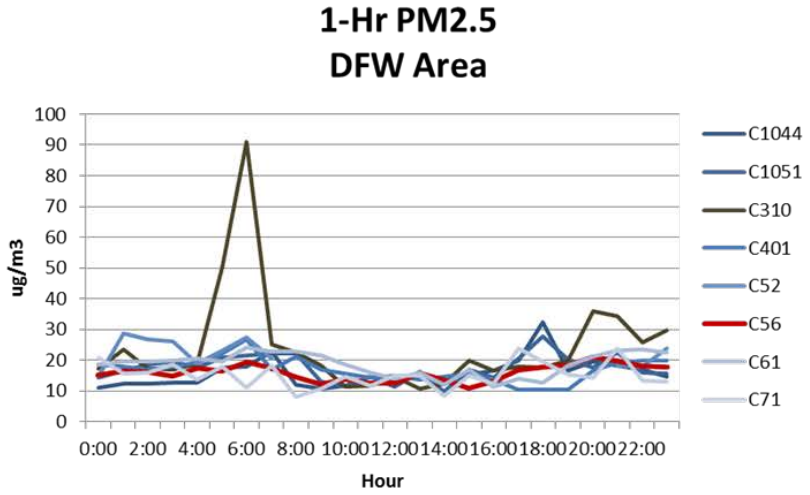

Figure 3-75. Regional ozone (top left and right) and $PM_{2.5}$ (bottom left and right) measurements (DFW area time series).

3.1.10 June 26, 2012

On June 26, 2012, East Texas was in the midst of a multi-day high ozone episode and both ozone and $PM_{2.5}$ levels were high in East Texas (Figure 3-81). The HMS product shows enhanced AOD across East Texas (Figure 3-80). Background ozone levels were ~60 ppb in the HGB area (Figure 3-84). At the Manvel Croix monitor, the highest MDA8 value of 2012 was recorded (136 ppb) and the peak 1-hour ozone value was 166 ppb (Figure 3-76). There is a NOx peak in the morning that dissipates slowly following the end of the morning commute and does not coincide with the 1-hour ozone peak.

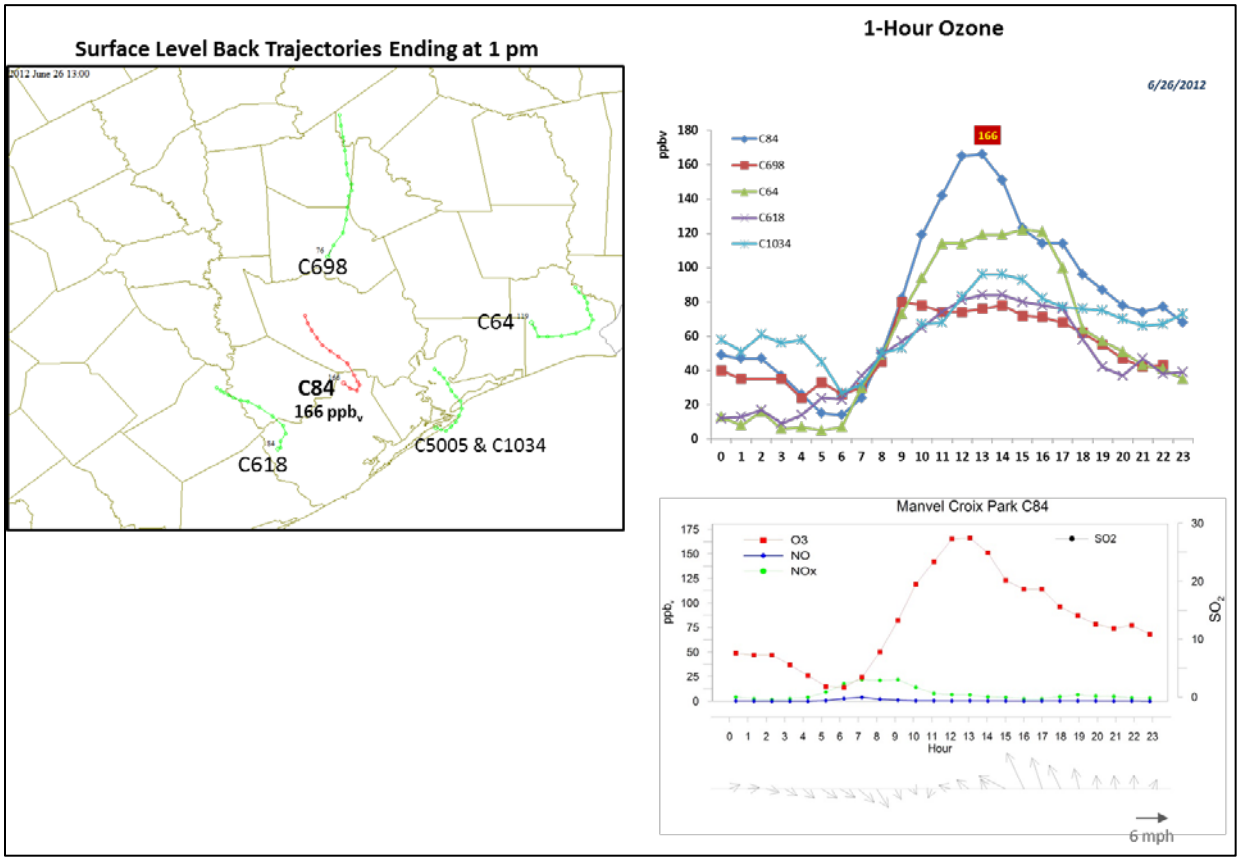

Figure 3-76. June 26, 2012 high ozone day at Manvel Croix Park C84. Left panel: AQPlot back trajectories ending at C84 and four background sites at the time of peak 1-hr ozone was observed. Upper right panel: 1-hour average ozone time series for the C84 and background monitors. Lower right panel: time series of 1-hour ozone, NO, NO_2 and wind vectors at the Manvel Croix Park C84 site.

The AQplot back trajectories for HGB area monitors show winds from the northwest in the morning switching to southerly by late morning for sites near the coast, including Manvel Croix. The SmartFire and HYSPLIT NAM back trajectories do not resolve the sea breeze circulation, but show northerly flow leading up to the time of peak 1-hour ozone at Manvel Croix (left panel of Figure 3-79). The SmartFire plot shows that there are fires upwind of the HGB area. The fires

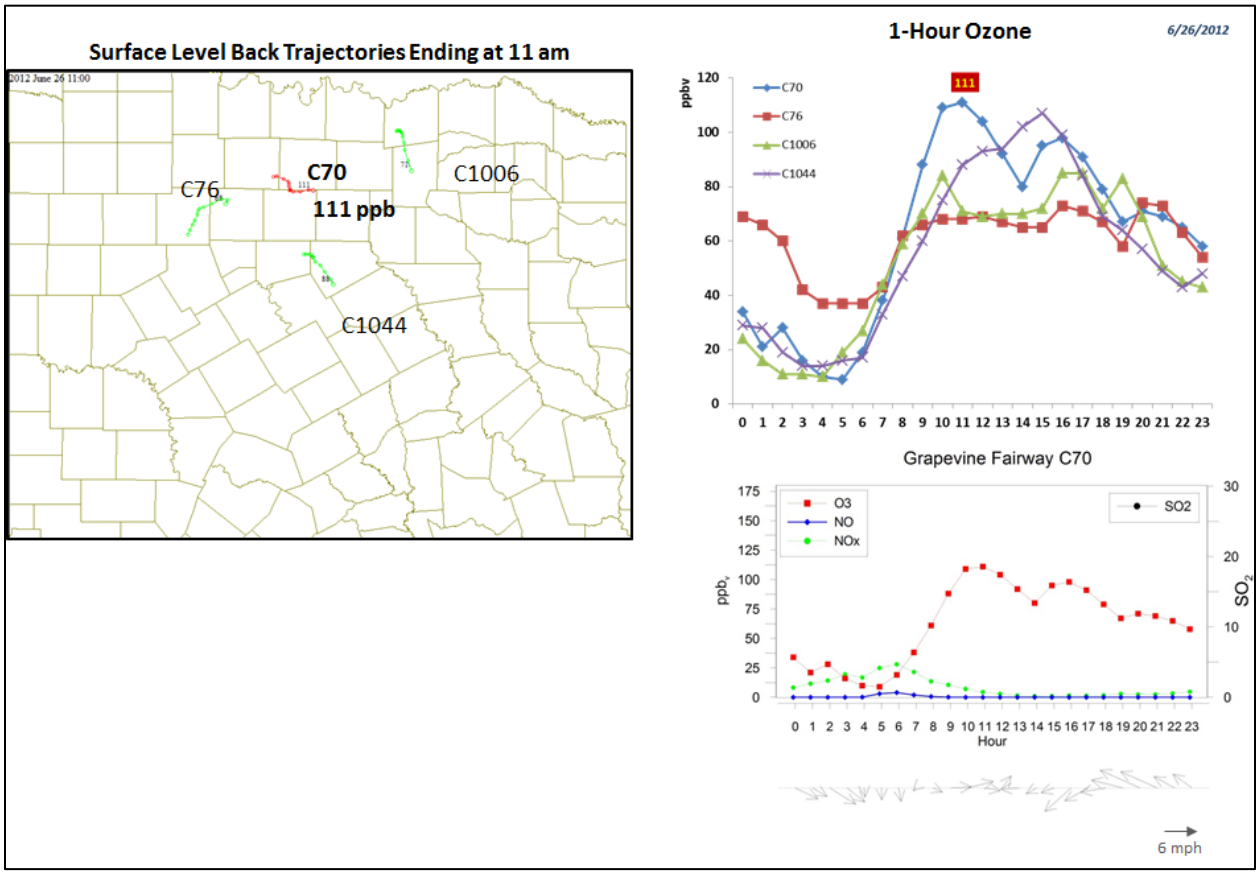

Figure 3-77. June 26, 2012 high ozone day at Grapevine C70. Left panel: AQPlot back trajectories ending at C70 and four background sites at the time of peak 1-hr ozone was observed. Upper right panel: 1-hour average ozone time series for the C70 and background monitors. Lower right panel: time series of 1-hour ozone, NO, NO_2 and wind vectors at the Grapevine Fairway C70 site.

upwind of Houston are also visible in the FINN emissions (Figure 3-82), NAAPS smoke emissions (Figure 3-83) and in the DataFed MODIS fire location plot (Figure 3-83). The NAAPS smoke analysis shows smoke covering East Texas, with concentration 8-10 µg m^{-3} in the HGB area (Figure 3-83).

Similar to June 25, the ozone spatial pattern is consistent with an HGB urban plume impact, with lower ozone at sites on the northeast side of the HGB area and higher ozone at sites on the southern (downwind) side of the area (Figure 3-84). If ozone were enhanced in a plume travelling southward from the fire locations shown in Figure 3-79, high $PM_{2.5}$ and/or ozone would likely have been detected at the monitors on the northern edge of the HGB area such as C78.

The $PM_{2.5}$ time series for several monitors in the HGB area (Figure 3-84) show a peak at 6 am (C45, C35). This peak appears to be a plume impact and dissipates by 7 am. The timing coincides with the morning NOx peak at Manvel Croix, but it is not clear whether they are

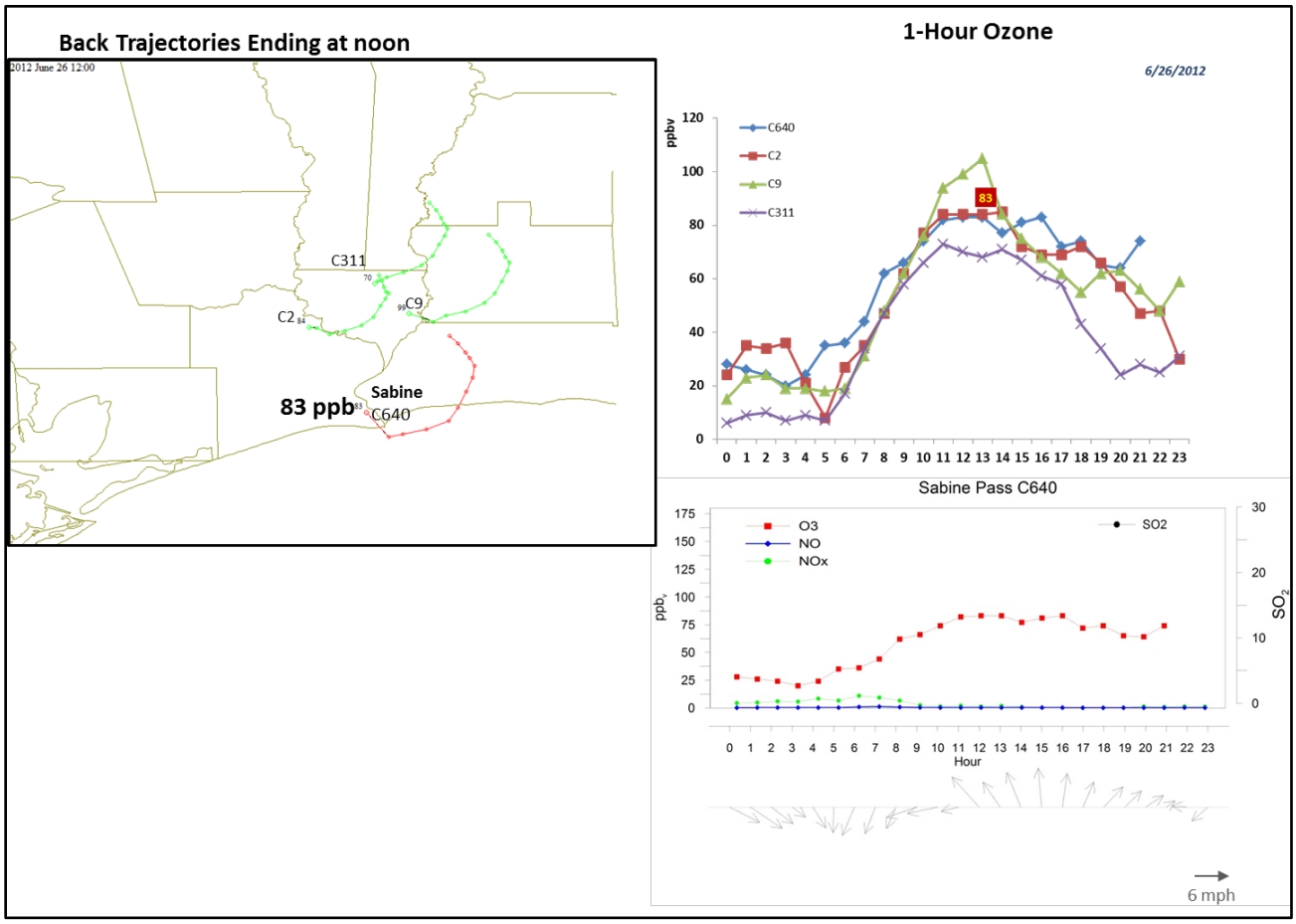

Figure 3-78. June 26, 2012 high ozone day at Sabine Pass C640. Left panel: AQPlot back trajectories ending at C640 and four background sites at the time of peak 1-hr ozone was observed. Upper right panel: 1-hour average ozone time series for the C640 and background monitors. Lower right panel: time series of 1-hour ozone, NO, NO_2 and wind vectors at the Sabine Pass C640 site.

related. High levels of $PM_{2.5}$ are no longer present by the time of maximum 1-hour ozone at Manvel Croix. The spatial gradient in HGB MDA8 ozone values taken together with the northerly wind direction suggests an impact due to local HGB emissions at the Manvel Croix monitor rather an impact from a distant fire. We recommend no further evaluation be done for the Manvel Croix monitor on June 26.

Like Manvel Croix, the Grapevine Fairway monitor in DFW had its 1st high MDA8 ozone on June 26. The 1-hour ozone peak was 111 ppb (Figure 3-77) and background ozone in the DFW area was very high (~70 ppb; Figure 3-86). Figure 3-86 shows values of the MDA8 >90 ppb for many monitors in the area and $PM_{2.5}$ exceeding 26 µg m^{-3}. Winds were extremely stagnant during the 72 hours leading up to the 1-hour ozone maximum at Grapevine on June 26. All back trajectories (Figure 3-77; Figure 3-79) show air to be recirculating over the DFW metroplex during the preceding 72 hours. The SmartFire map (Figure 3-79) shows that there is a fire south of the DFW urban area. The HYSPLIT NAM 500 m trajectory and SmartFire trajectory pass in the

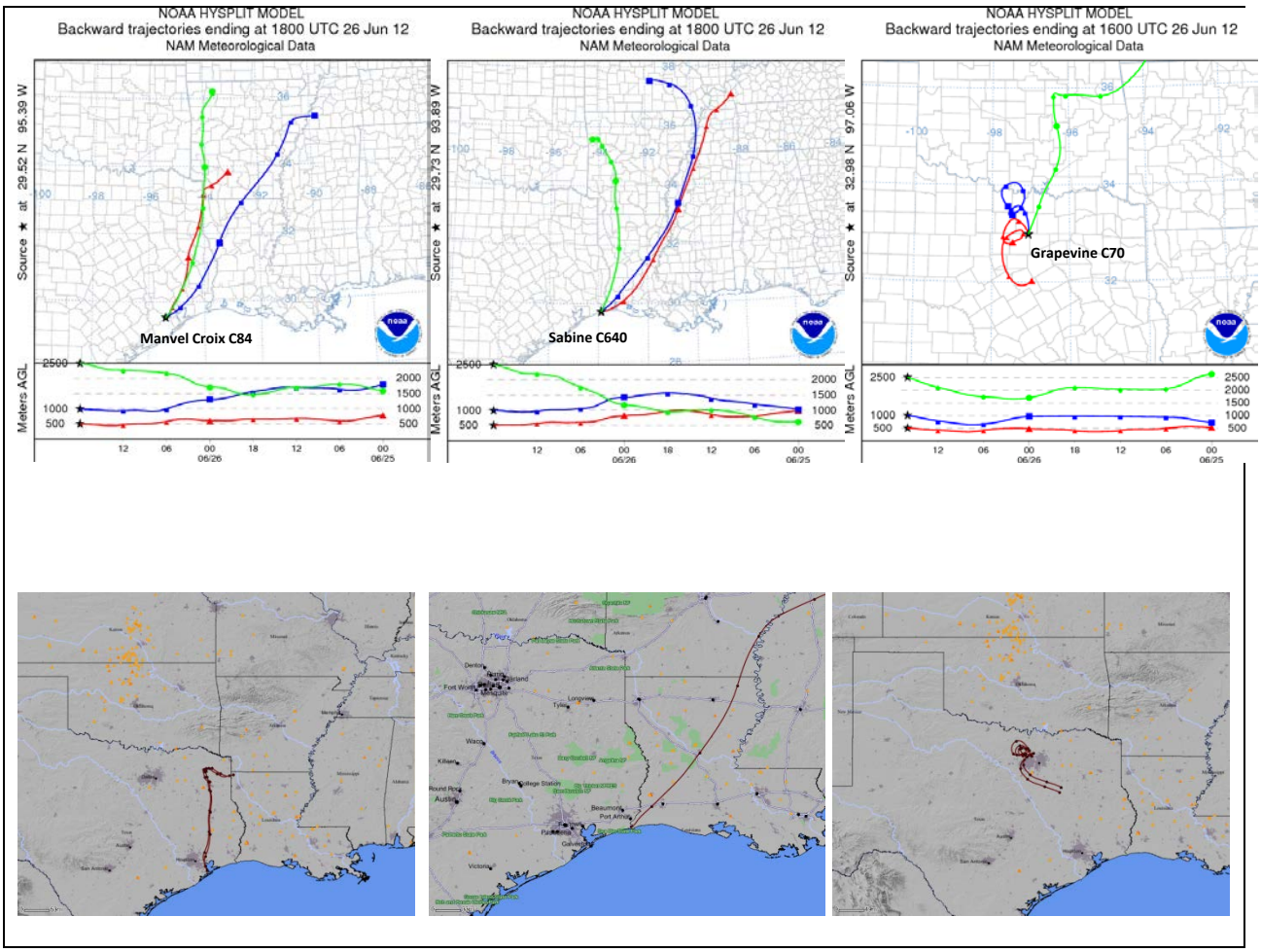

Figure 3-79. 72-hour HYSPLIT back trajectories at Manvel Croix C84 (top left); Sabine Pass C640 (middle) and Grapevine Fairway C70 (top right); SmartFire plots showing fire locations (orange triangles) and 72-hour HYSPLIT back trajectories from HGB (bottom left) and BPA area (bottom center) and DFW (bottom right)

vicinity of this fire between -66 and -60 hours. The FINN fire emissions plot (Figure 3-82) and the NAAPS fire emissions plot (Figure 3-83) show that there was a fire south of DFW during this time. The HMS product (Figure 3-80) and the NAAPS smoke analysis (Figure 3-83) agree that there was smoke throughout East Texas on June 26 and Figure 3-81 indicates that the $PM_{2.5}$ AQI was moderate across the DFW region.

To determine whether the fire south of DFW could have had a strong influence on high ozone at Grapevine on June 26, we examine the timing of the ozone and $PM_{2.5}$ peaks shown in Figure 3-86. The ozone time series show that June 26 was a day of extremely high background ozone consistent with fact that this is the third day of a regional high ozone event. Most of the monitors in the DFW area have MDA1 ozone values between 70-100 ppb. However, there are several monitors with higher peaks: Grapevine (C70), Dallas Executive Airport (C402,) Arlington Municipal Airport (C61), Midlothian (C52), and Cleburne (C77). These monitors lie in a fairly

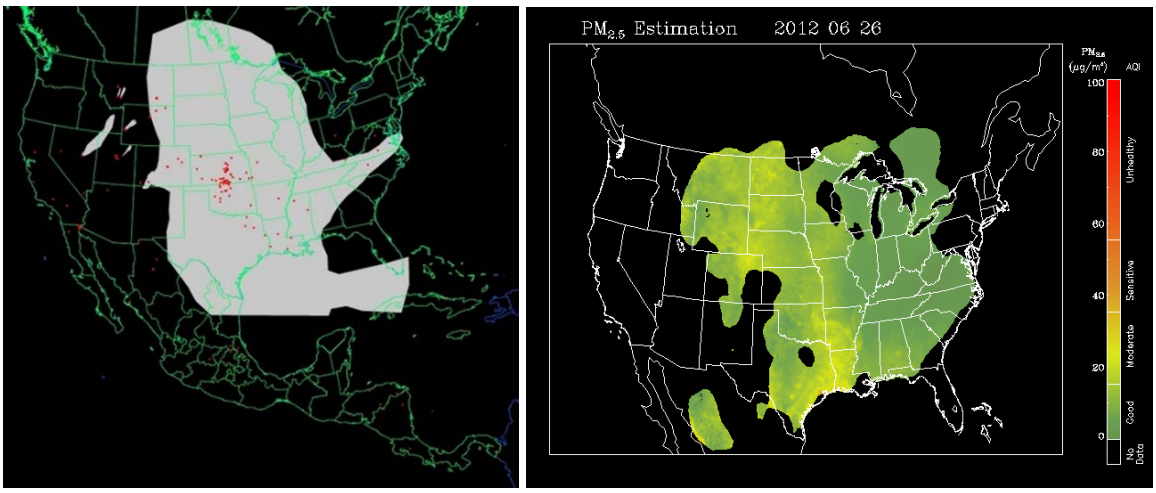

Figure 3-80. Left panel: HMS product showing June 26 fire locations (red dots) and smoke plume (gray area). Right panel: IDEA surface $PM_{2.5}$ estimate based on AOD and surface monitoring data.

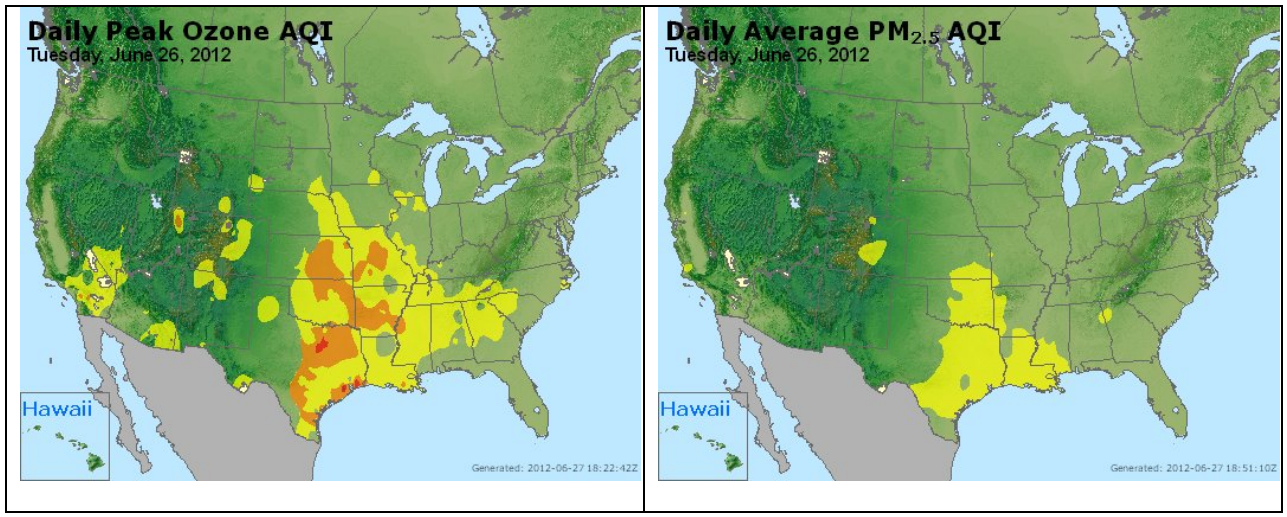

Figure 3-81. Daily average ozone (left) and $PM_{2.5}$ (right) based on observed values. Data from: http://www.airnow.gov/.

narrow north-south oriented band so we examine the timing of the 1-hour ozone peaks at these monitors together with 1-hour $PM_{2.5}$ peaks. We expect that if a fire plume impact were a major contributor to the ozone peaks any at these monitors, a $PM_{2.5}$ peak would occur near the ozone monitor. The possibility of a fire plume in the DFW area during periods of high ozone at these monitors day would then require further investigation through PM filter analysis and/or photochemical modeling.

On June 26, the $PM_{2.5}$ monitors in the DFW area have a morning peak at 6-8 am which corresponds to the time of the morning commute hours. Most of the monitors have a second, larger peak in the 4-7 pm evening commute hour period. However, there are three $PM_{2.5}$ monitors with 1-hour peaks that are ~10 µg m^{-3} higher than the rest of the DFW area monitors:

Midlothian (C52), Kaufman (C71), and Denton (C56). These monitors have narrow, strong peaks that are consistent with fire plume impacts from a source that is relatively nearby.

The peak at the Midlothian (C52) monitor occurs at 2 am on the morning of June 26 and dissipates by the time of the morning commute hours, when the ozone at Grapevine begins to build toward its peak. Midlothian $PM_{2.5}$ data recorded between 8 am and 10 pm were rejected by TCEQ validators. The Kaufman (C71) monitor has the highest MDA1 $PM_{2.5}$ of all DFW area monitors, reaching nearly 50 µg m^{-3} at 5 pm. The Denton Airport monitor (C56) has a peak which is nearly as high and occurs even later in the evening, at 9 pm.

Denton is the $PM_{2.5}$ monitor which is closest to the Grapevine ozone monitor, and Denton does not have its peak value until after sundown, many hours after the Grapevine monitor has its 1-hour ozone peak (11 am) and ozone levels have diminished to ~70 ppb. This suggests that the source of the enhanced $PM_{2.5}$ did not make a significant contribution to high ozone during the day at Grapevine. All ozone monitors within the DFW urban area recorded MDA8>75 ppb on June 26. Although the 1-hour $PM_{2.5}$ peaks indicate that fire plumes could have been present in the DFW area, the timing of the peaks suggests that the likelihood of an urban impact at Grapevine is far higher than that of a fire plume impact. We recommend no further analysis of Grapevine on June 26.

On June 26, the Sabine Pass monitor recorded its 3rd highest MDA8 of 2012 (79 ppb). Figure 3-78 shows that peak 1-hour ozone value at Sabine Pass was 83 ppb, while the West Orange (C9) monitor had a higher 1-hour peak over 100 ppb. The SmartFire back trajectory is consistent with the HYSPLIT NAM back trajectory in showing northeasterly winds that are strong compared to the winds in DFW in June 26 (Figure 3-79). The SmartFire map shows several fires in Louisiana along the SmartFire and HYSPLIT NAM back trajectories. The FINN emissions maps agree that fires were present along the back trajectories from -48 hours through the initiation time of the back trajectories (Figure 3-82). However, the fires detected along the back trajectories are quite distant from the Sabine Pass monitor. The NAAPS smoke analysis shows that there was 8-10 µg m^{-3} smoke concentrations in the Sabine Pass monitor area, consistent with the presence of smoke in the HMS product, and it is possible that fire emissions contribute to background ozone advected into the BPA area on June 26.

The Hamshire monitor (C64) has the highest ozone peak of all monitors in the BPA area on June 26, while the Sabine Pass has ozone that rises and fall together with the majority of the area other BPA monitors. This suggests that the Sabine Pass monitor is influenced by background ozone and similar local emissions as the other BPA monitors that do not show pronounced 1-hour peaks consistent with a plume impact. Therefore, we do not recommend further evaluation of June 26, 2012 for the Sabine Pass monitor.

Wildfire Emissions Inventory: FINN 2012

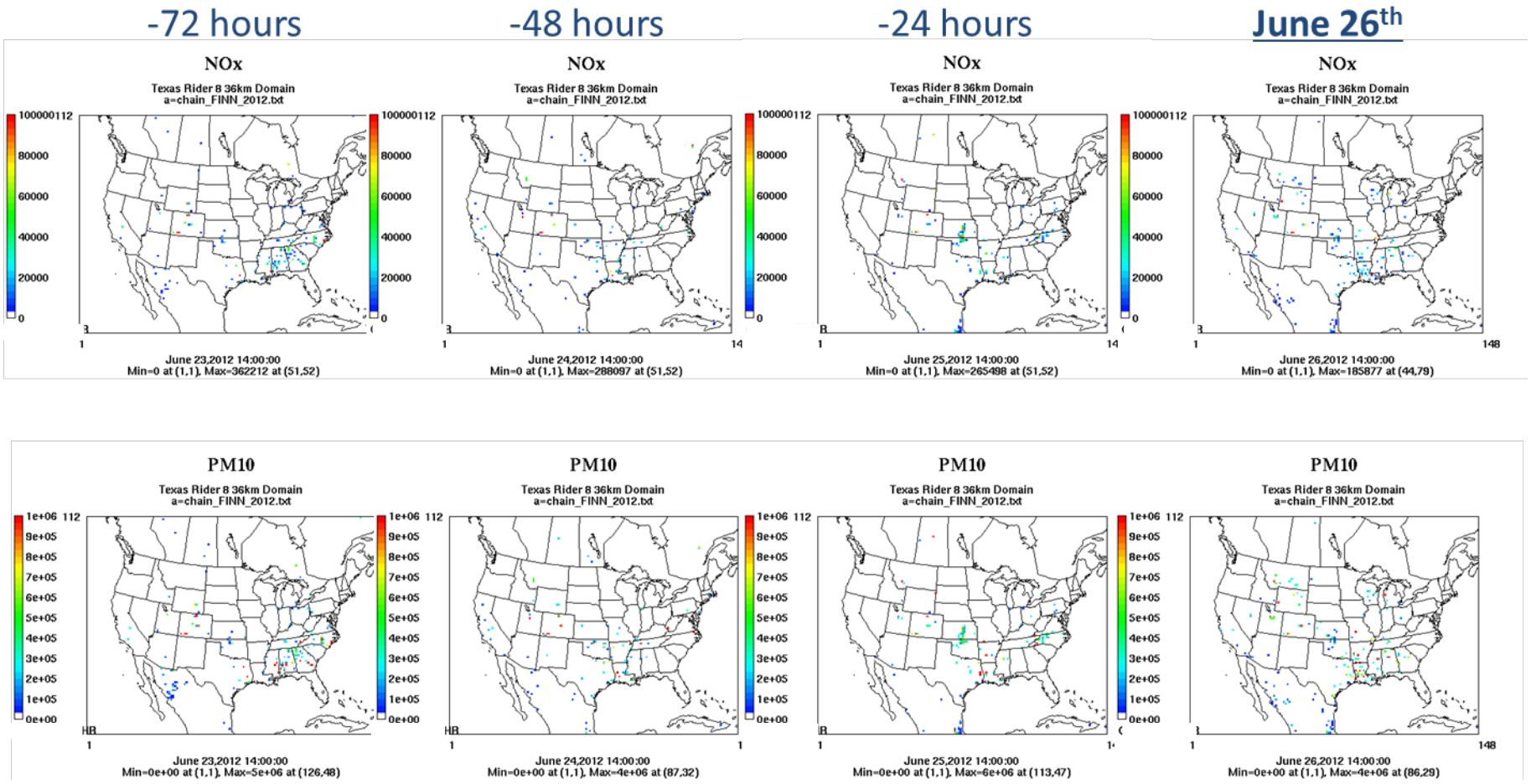

Figure 3-82. June 26, 2012 FINN fire emissions of NOx and PM_{10}.

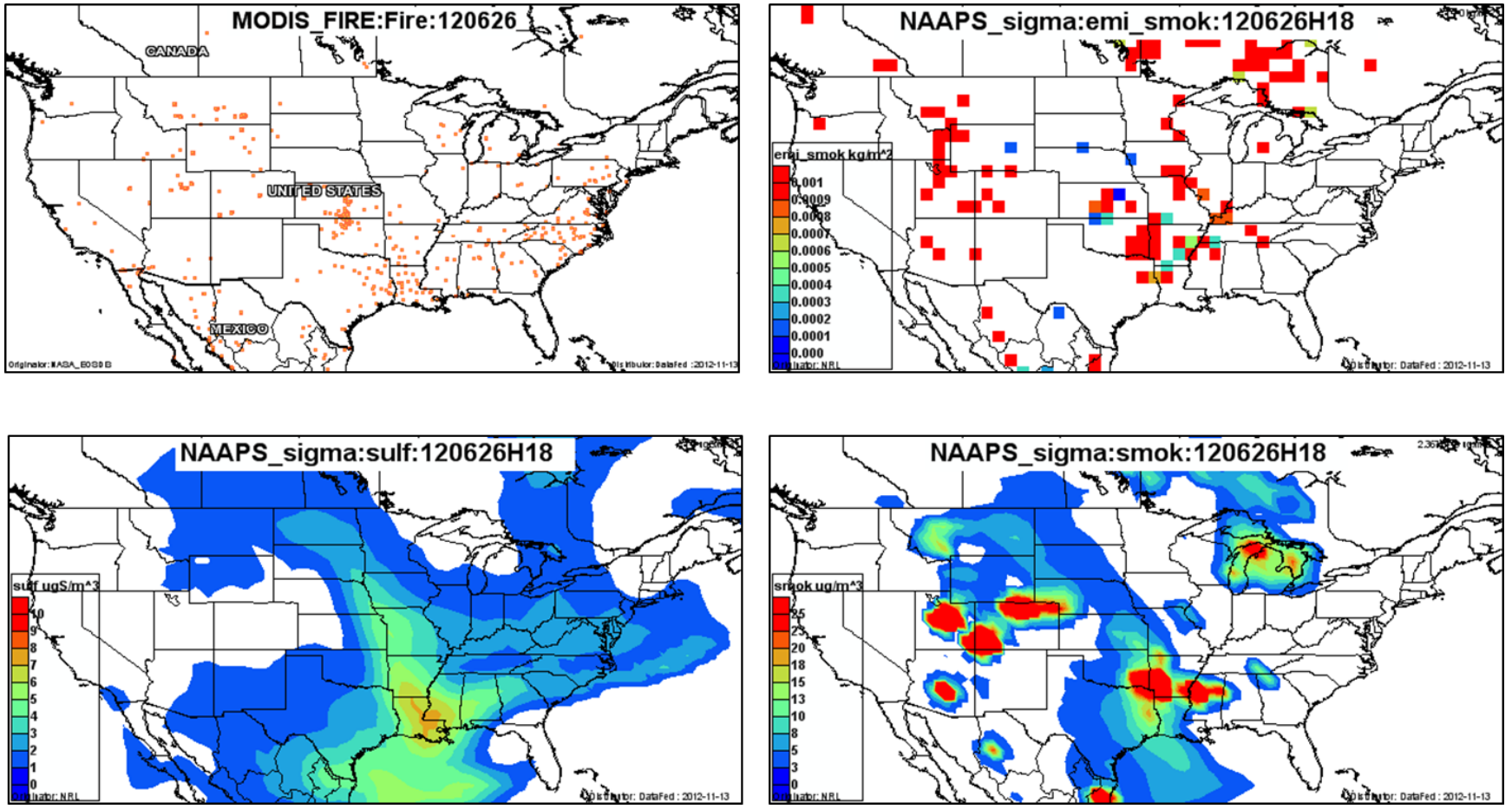

Figure 3-83. June 26, 2012 DataFed analysis. Upper left panel: Locations of active fires from MODIS satellite fire detections. Upper right panel: NAAPS model smoke emissions. Lower left panel: NAAPS model surface layer sulfate concentrations. Lower right panel: NAAPS model surface layer smoke concentrations.

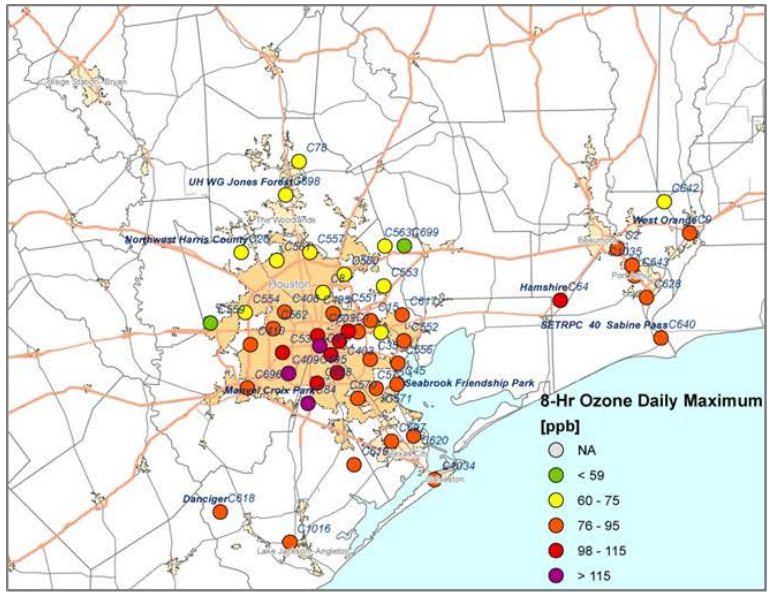

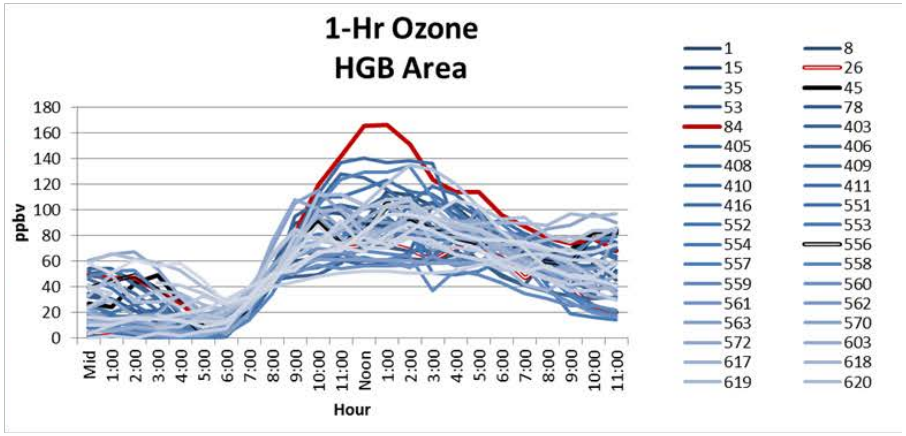

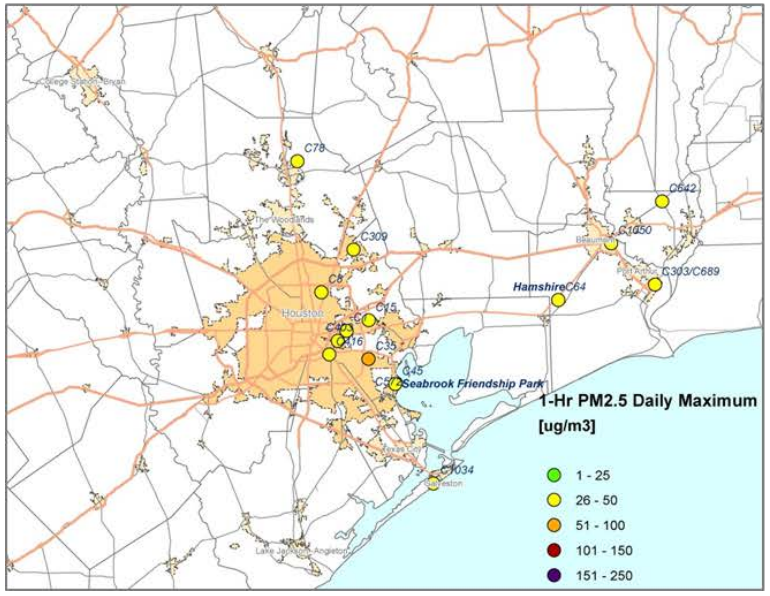

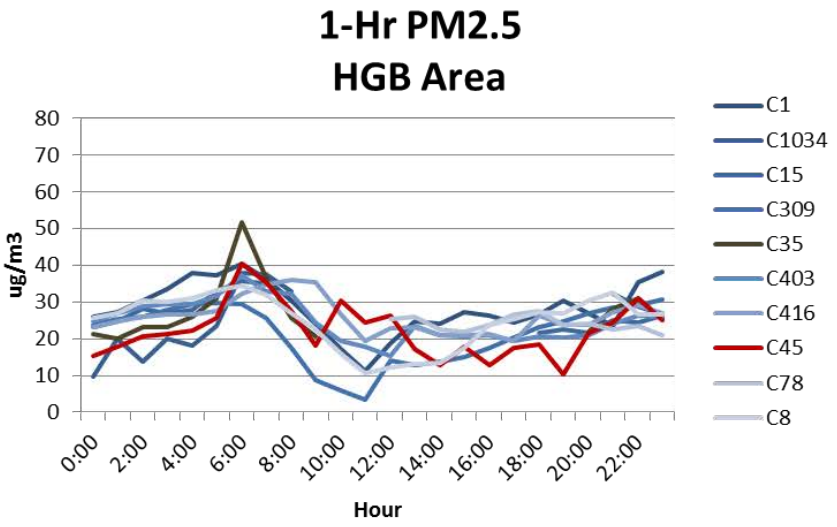

Figure 3-84. Regional ozone (top left and right) and $PM_{2.5}$ (bottom left and right) measurements (HGB area time series).

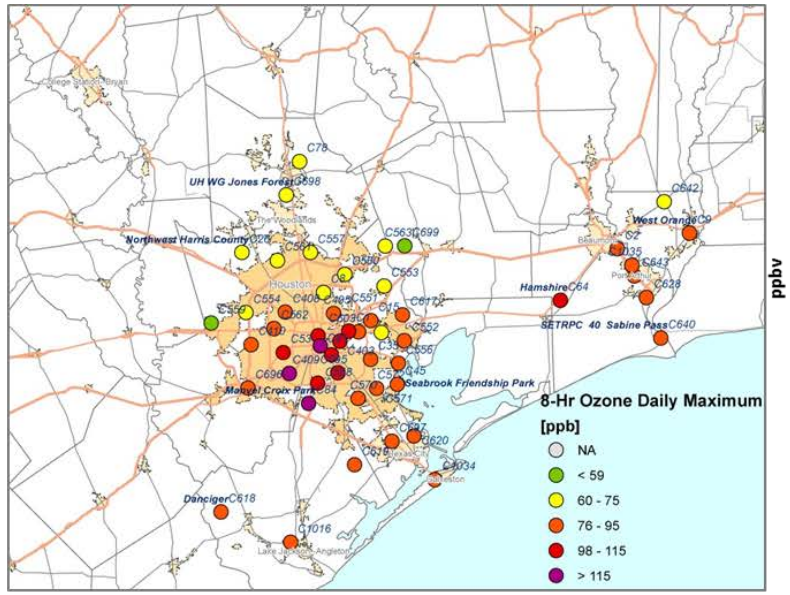

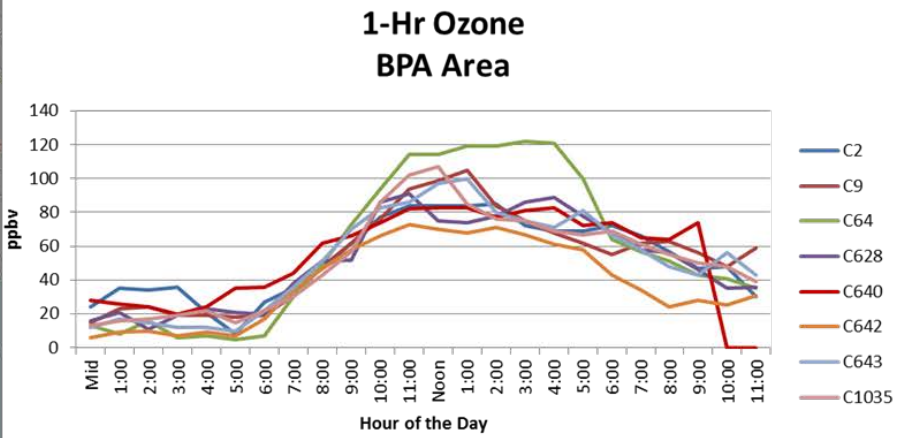

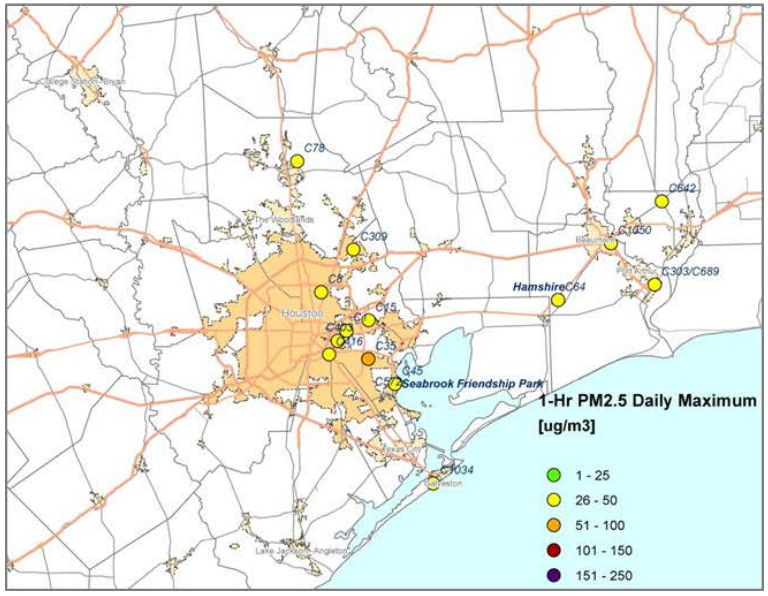

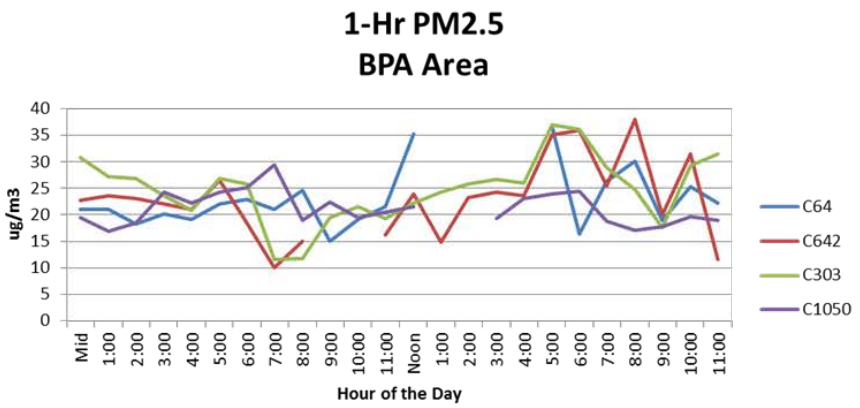

Figure 3-85. Regional ozone (top left and right) and $PM_{2.5}$ (bottom left and right) measurements (BPA area time series).

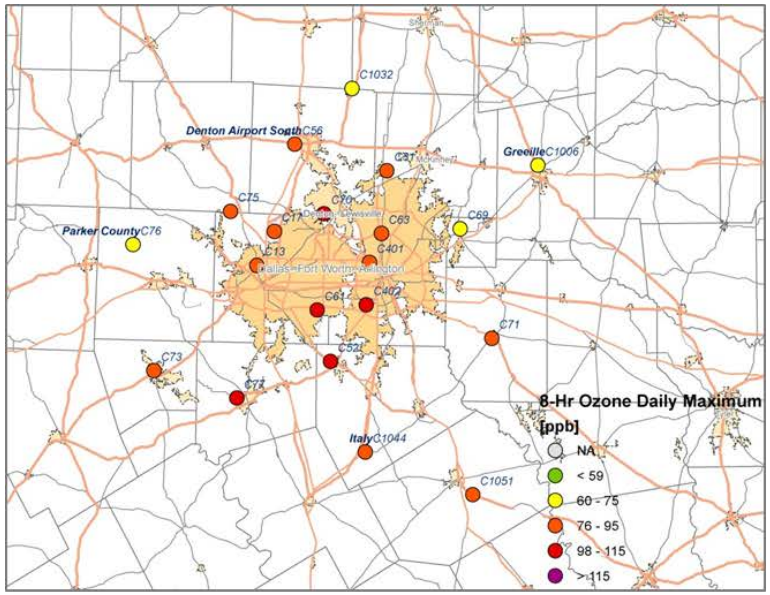

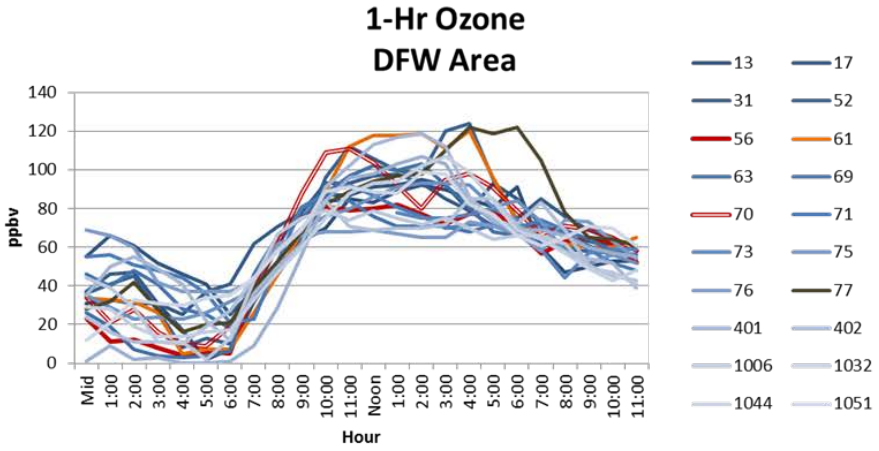

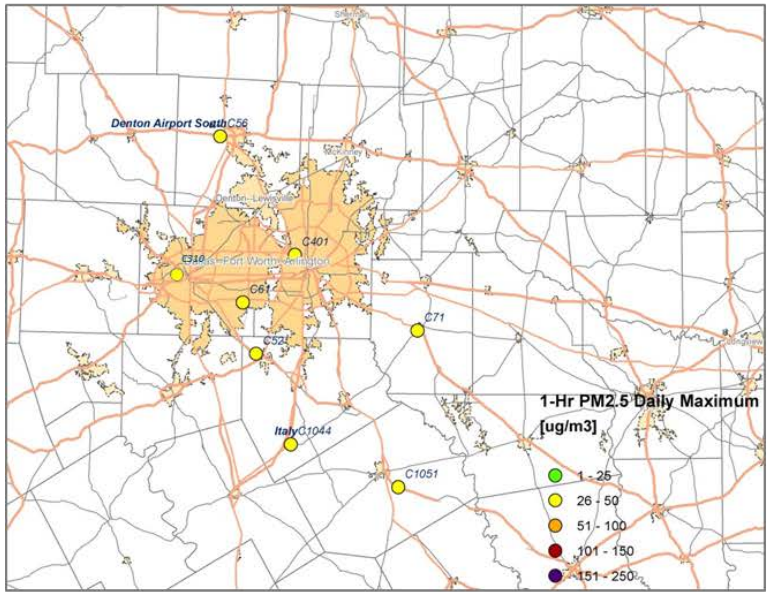

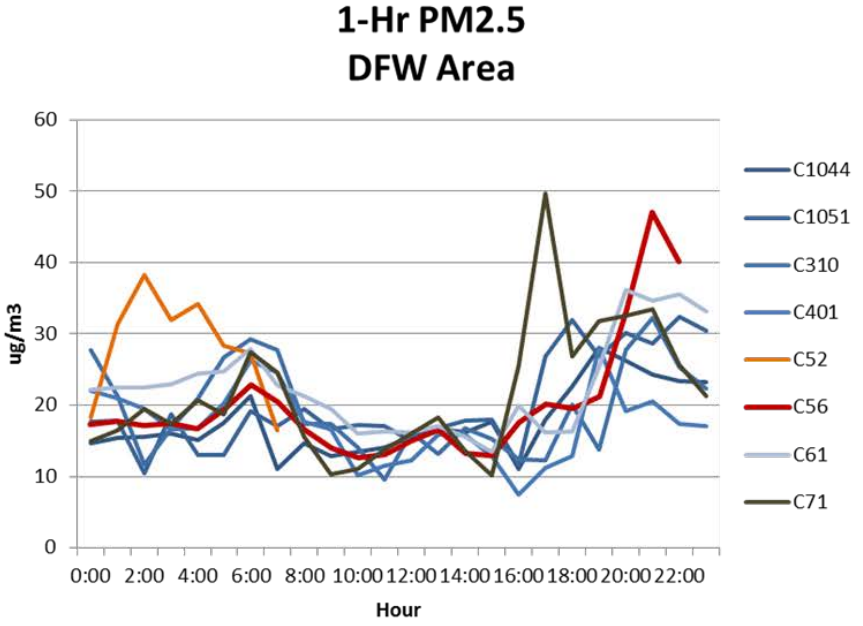

Figure 3-86. Regional ozone (top left and right) and $PM_{2.5}$ (bottom left and right) measurements (DFW area time series).

3.1.11 June 27, 2012

June 27 was the final day of the June 24-27 ozone episode in the HGB area. Background ozone levels in the HGB area were high (>60 ppb;

Figure 3-95) and the AQI index for ozone and $PM_{2.5}$ were moderate or higher across most of East Texas (Figure 3-92). Smoke from wildfires in the western U.S. covered the central and eastern U.S. and East Texas temperatures remained in the triple digits. On June 27, the NW Harris monitor had its highest MDA8 reading of 2012 (99 ppb) and had a peak 1-hour ozone value of 127 ppb at 11 am (Figure 3-87). The AQplot back trajectory and winds at the monitor indicate that winds were southerly during the daylight hours on June 27 (Figure 3-87). The SmartFire and HYSPLIT NAM back trajectories also show south/southeasterly flow on June 27 (Figure 3-90). Both the SmartFire trajectory and the 500 m and 1,000 m HYSPLIT back trajectories extend back over the Gulf of Mexico and into Louisiana. The SmartFire map shows that the back trajectories cross a fire on the Louisiana coast and this fire also appears on the FINN emissions plots (Figure 3-93), in the DataFed MODIS fire location plot (Figure 3-94) and in the HMS product (Figure 3-91).

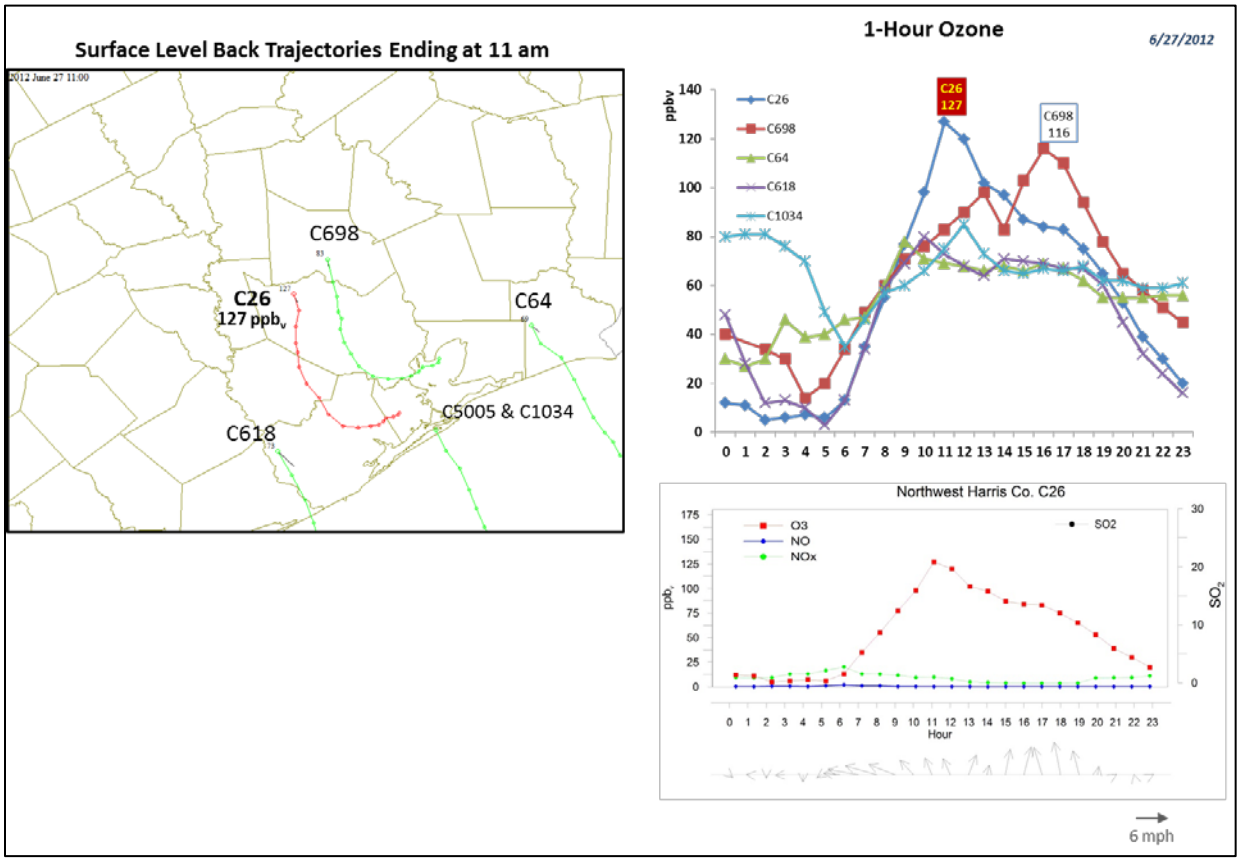

Figure 3-87. June 27, 2012 high ozone day at Northwest Harris C26. Left panel: AQPlot back trajectories ending at C26 and four background sites at the time of peak 1-hr ozone was observed. Upper right panel: 1-hour average ozone time series for the C26 and background

monitors. Lower right panel: time series of 1-hour ozone, NO, NO_2 and wind vectors at the Sabine Pass C26 site.

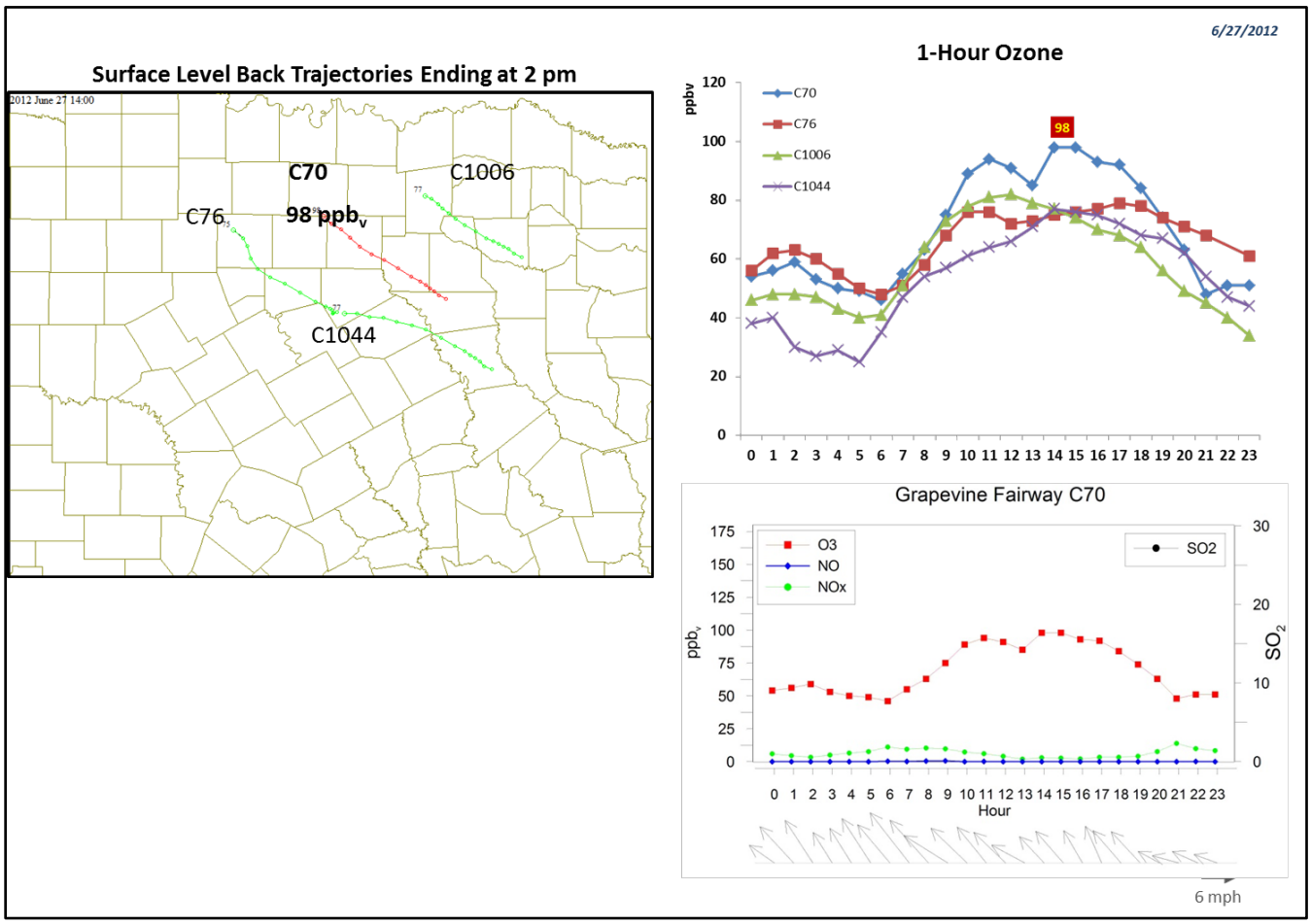

Figure 3-88. June 27, 2012 high ozone day at Grapevine Fairway C70. Left panel: AQPlot back trajectories ending at C70 and four background sites at the time of peak 1-hr ozone was observed. Upper right panel: 1-hour average ozone time series for the C70 and background monitors. Lower right panel: time series of 1-hour ozone, NO, NO_2 and wind vectors at the Grapevine C70 site.

The spatial pattern of ozone in the HGB area on June 27 is consistent with the southerly wind direction, with higher ozone at monitors in the northern part of the urban area and lower ozone at monitors in the southern part (

Figure 3-95). The monitors with the highest 1-hour ozone peaks are Mercer Arboretum (C557), NW Harris County (C26), Houston Aldine (C8), UH WG Jones Forest (C698) and Conroe Relocated (C78). These monitors are all located in the northern end of the HGB urban area and the northernmost monitors, C698 and C78, are the monitors with the late afternoon 1-hour ozone peaks. This spatial pattern is consistent with an HGB urban plume impact, with the plume moving northward during the day.

The HMS smoke product (Figure 3-91) and the NAAPS smoke analysis (Figure 3-94) both indicate the presence of smoke across East Texas on June 27. Figure 3-95 shows that $PM_{2.5}$ AQI is moderate for all HGB area monitors, which is consistent with the HMS and NAAPS analyses. The only HGB monitor with $PM_{2.5}$ greater than ~30 µg m^{-3} is the Houston East monitor (C1),

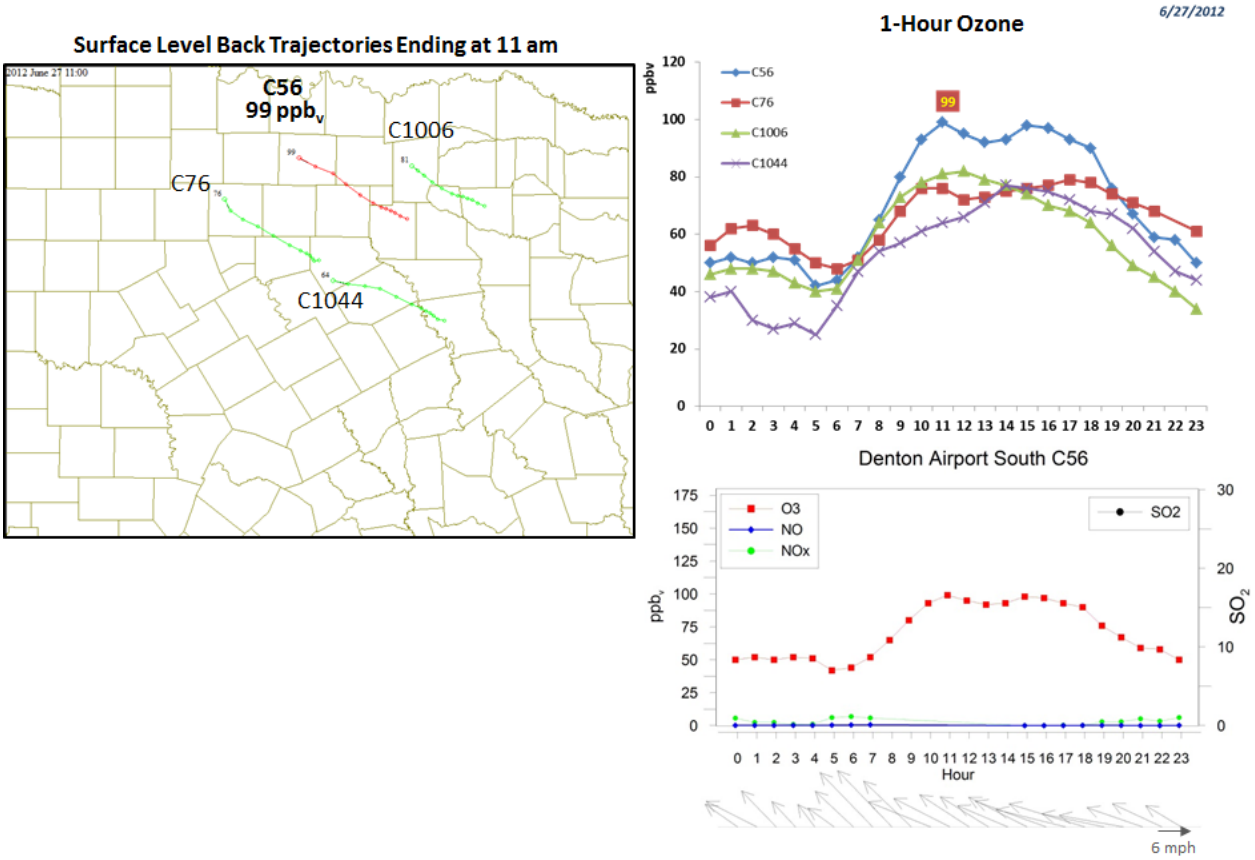

Figure 3-89. June 27, 2012 high ozone day at Denton Airport South C56. Left panel: AQPlot back trajectories ending at C56 and four background sites at the time of peak 1-hr ozone was observed. Upper right panel: 1-hour average ozone time series for the C70 and background monitors. Lower right panel: time series of 1-hour ozone, NO, NO_2 and wind vectors at the Grapevine Fairway C56 site.

which is located in the vicinity of a number of industrial and urban sources, and is not near the NW Harris monitor. No high values of $PM_{2.5}$ are evident at monitors located on the southern end of the HGB area (C45, C35), so, while fires may have contributed to elevated regional background ozone levels, there is no evidence of a fire plume coming ashore in the HGB area on June 27. We recommend no further evaluation of June 27 for the NW Harris County monitor.

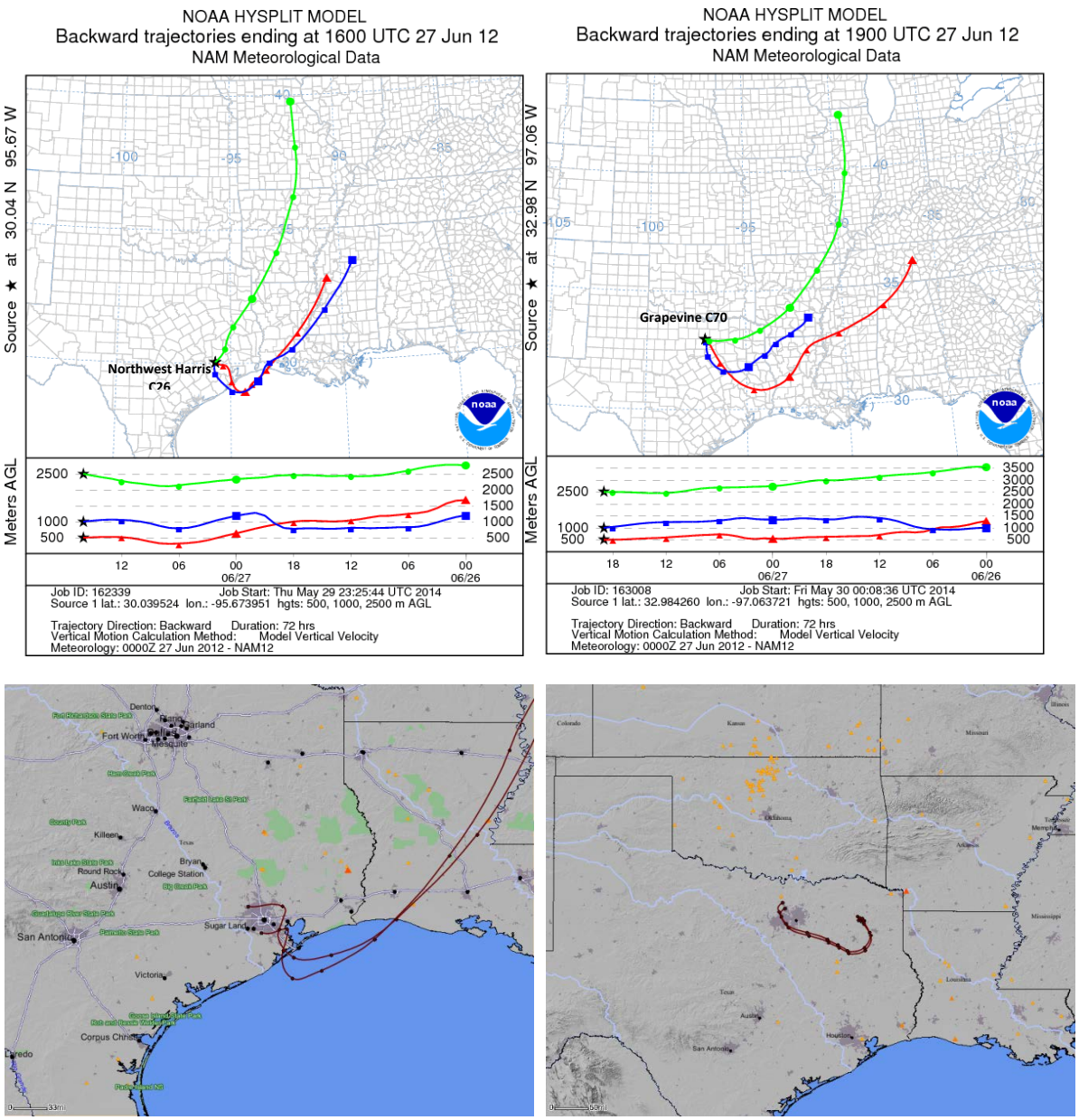

Figure 3-90. 72-hour HYSPLIT back trajectories at Northwest Harris C26 (top left); Grapevine C70 (right); SmartFire plots showing fire locations (orange triangles) and 72-hour HYSPLIT back trajectories from HGB area (bottom left) and DFW area monitors (bottom right).

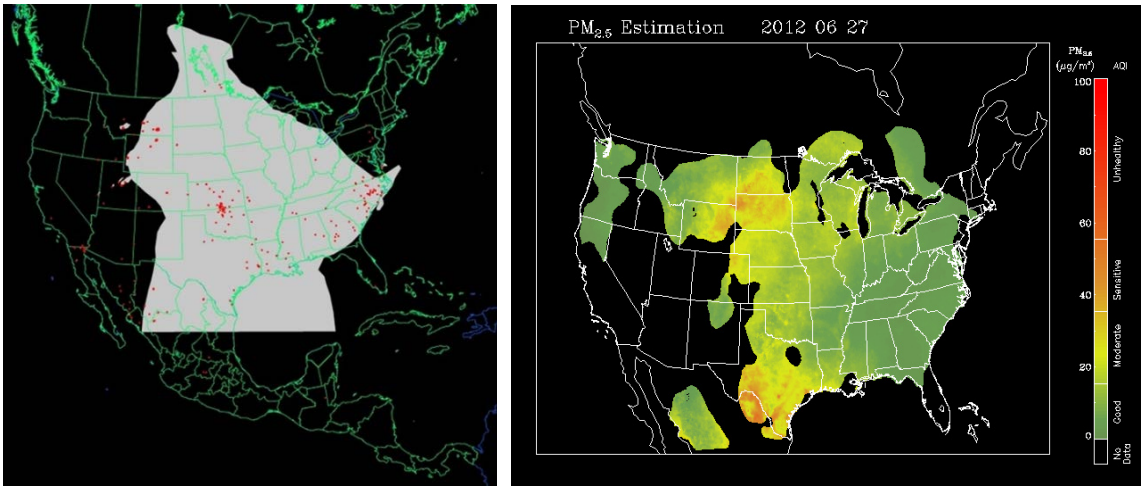

Figure 3-91. Left panel: HMS product showing June 27 fire locations (red dots) and smoke plume (gray area). Right panel: IDEA surface $PM_{2.5}$ estimate based on AOD and surface monitoring data.

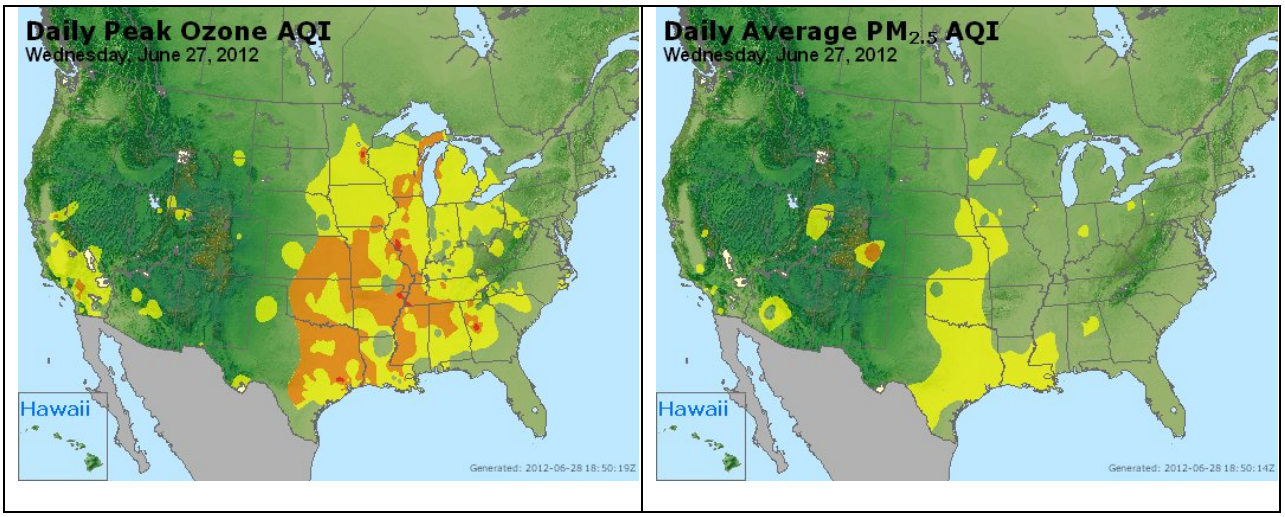

Figure 3-92. Daily average ozone (left) and $PM_{2.5}$ (right) based on observed values. Data from: http://www.airnow.gov/.

The Denton Airport South and Grapevine Fairway monitors in DFW had their 1st and 3rd highest MDA8 days, respectively, on June 27. On this day, winds were southeasterly (Figure 3-88) in the DFW area and the SmartFire and HYSPLIT NAM back trajectories are consistent in showing anti-cyclonic flow in the 72 hours leading up to the ozone maxima for the monitors (Figure 3-90). However, the locations of the SmartFire and HYSPLIT 500 m and 1,000 m back trajectories are quite different. While the SmartFire trajectories terminate in Northeast Texas, the HYSPLIT 500 m and 1,000 m trajectories continue east over a region where fires are present (Figure 3-93). The long-range back trajectory analysis, therefore, is inconclusive.

The 1-hour ozone time series for the DFW area shows that, although the Denton and Grapevine monitors recorded high values of 1-hour ozone, they were not significantly higher than the peak values of the rest of the DFW area monitors, and the shape of the ozone time series is not consistent with a plume impact in which ozone would suddenly increase and then decrease as the plume moves away from the monitor. On this day, background ozone was very high (~70 ppb) and the difference in peak values among the monitors is correlated with their location. Monitors on the northern side of the DFW area had higher ozone than monitors on the southern side, consistent with the AQPlot back trajectories which showed southerly near-surface winds.

The HMS smoke product (Figure 3-91) and the NAAPS smoke analysis (Figure 3-94) agree that smoke was present over the DFW area on June 27. The $PM_{2.5}$ data for this day are missing for several monitors, so it is difficult to assess the $PM_{2.5}$ time series (Figure 3-96). The ozone spatial pattern and time series together with the wind direction suggest that a DFW urban plume impact on a day with very high background ozone is a more likely explanation for high ozone at Denton and Grapevine than direct fire plume impacts. However, because the $PM_{2.5}$ data are missing for several monitors and the back trajectory analysis was inconclusive, we recommend analysis of available PM filter data and photochemical modeling for June 27, 2012 for the Grapevine and Denton monitors to shed light on the causes of high ozone.

Wildfire Emissions Inventory: FINN 2012

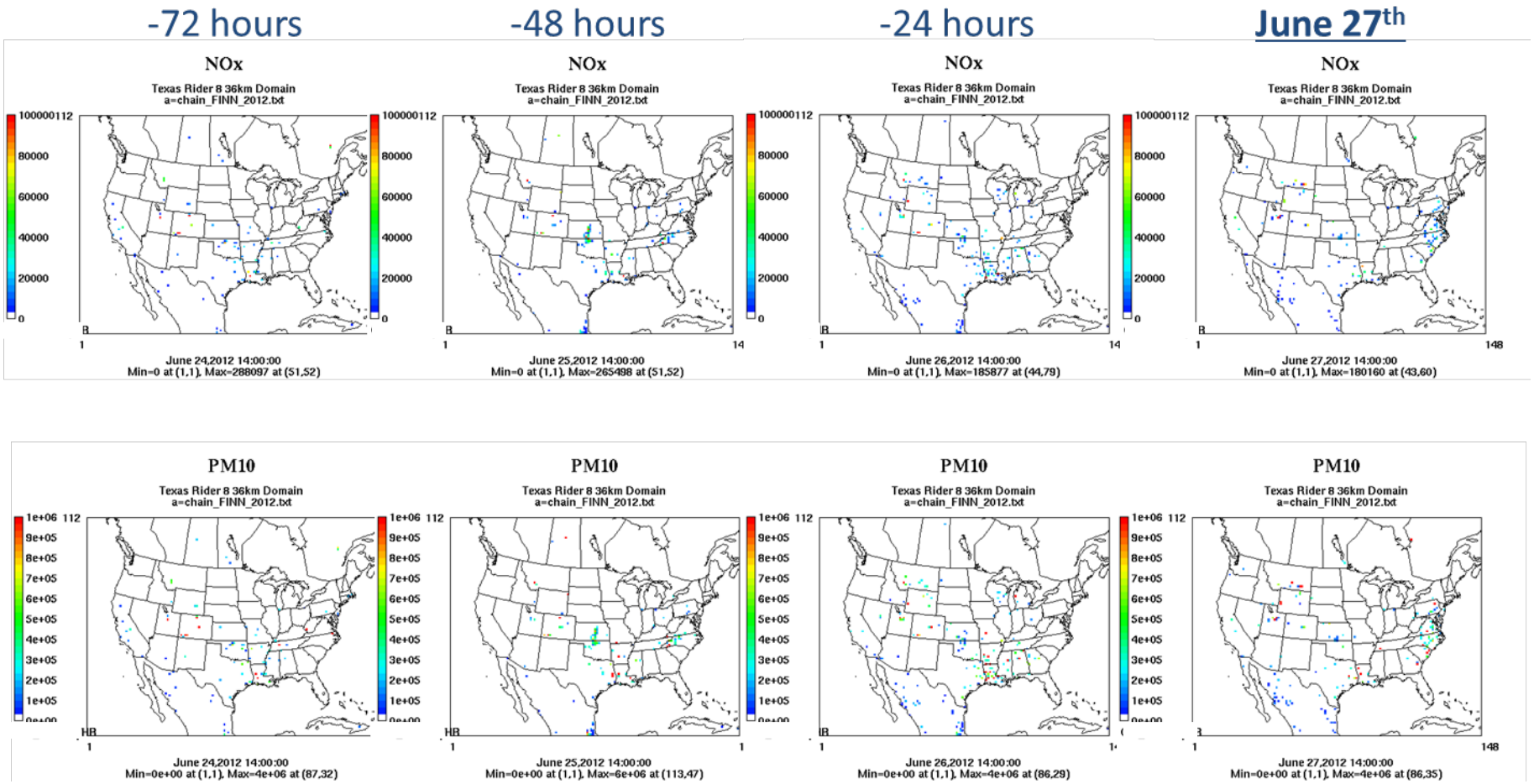

Figure 3-93. June 27, 2012 FINN fire emissions of NOx and PM_{10}.

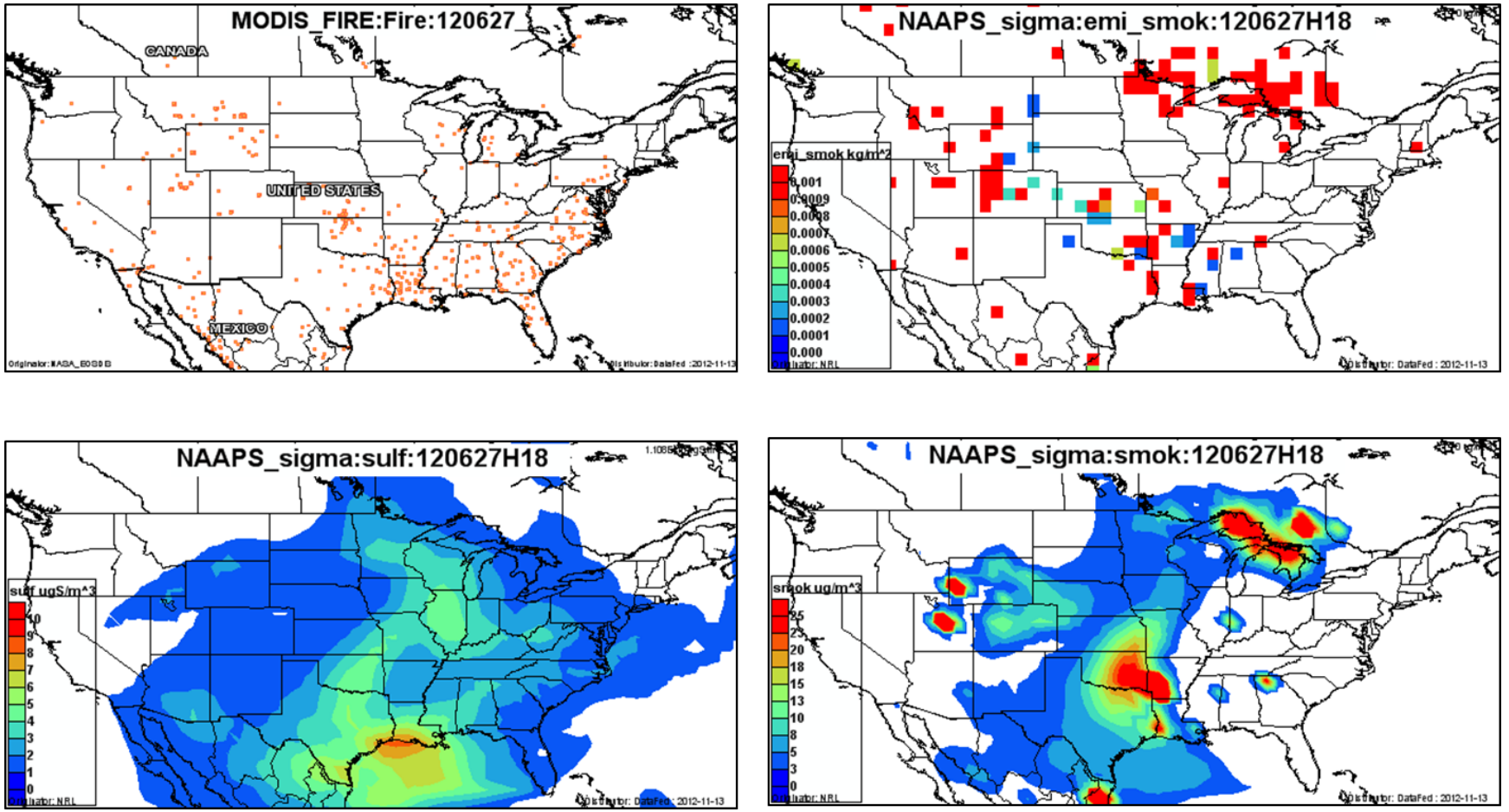

Figure 3-94. June 27, 2012 DataFed analysis. Upper left panel: Locations of active fires from MODIS satellite fire detections. Upper right panel: NAAPS model smoke emissions. Lower left panel: NAAPS model surface layer sulfate concentrations. Lower right panel: NAAPS model surface layer smoke concentrations.

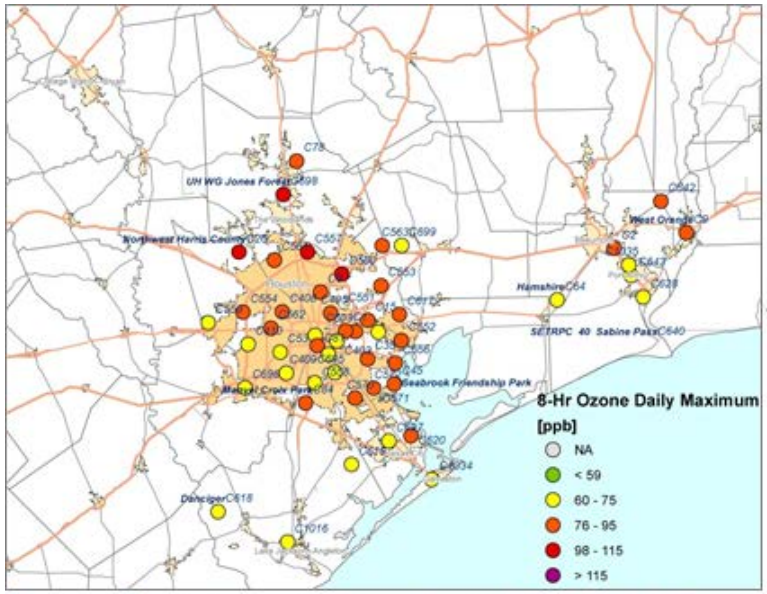

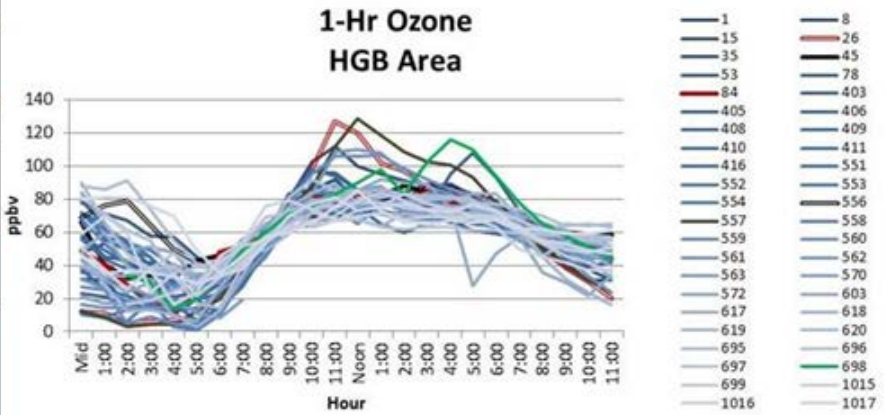

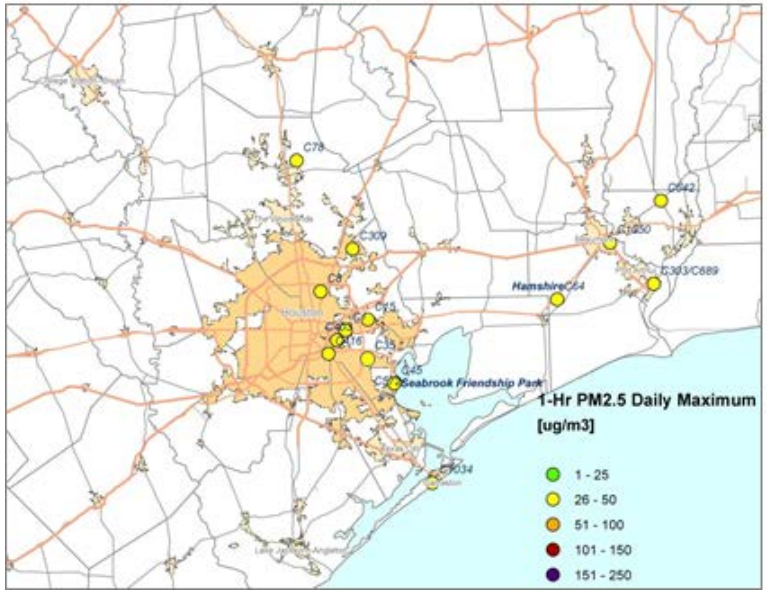

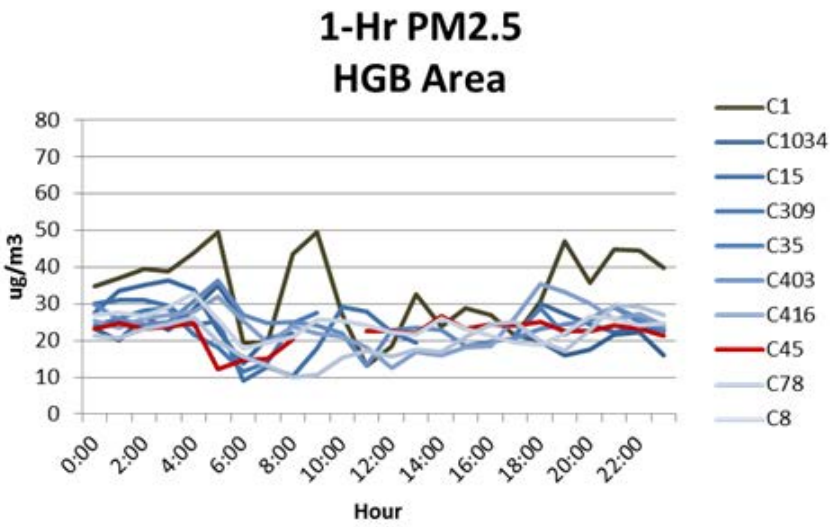

Figure 3-95. Regional ozone (top left and right) and PM2.5 (bottom left and right) measurements (HGB area time series).

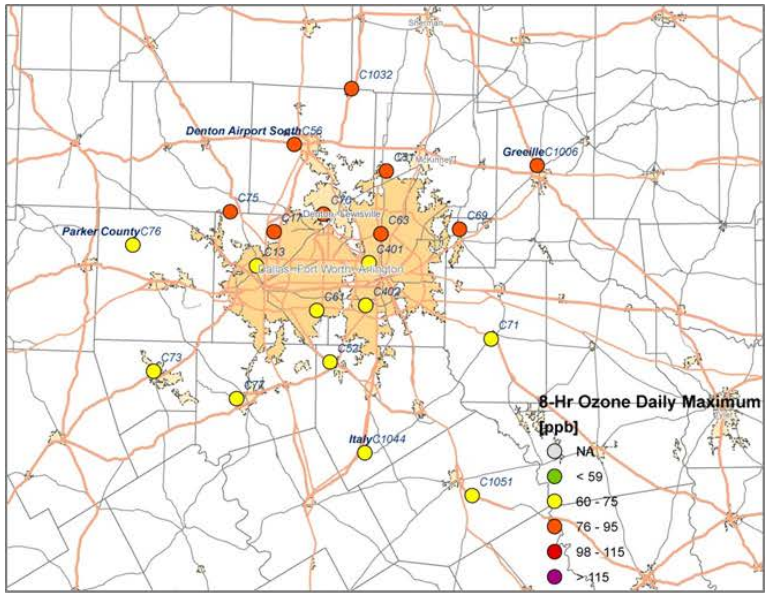

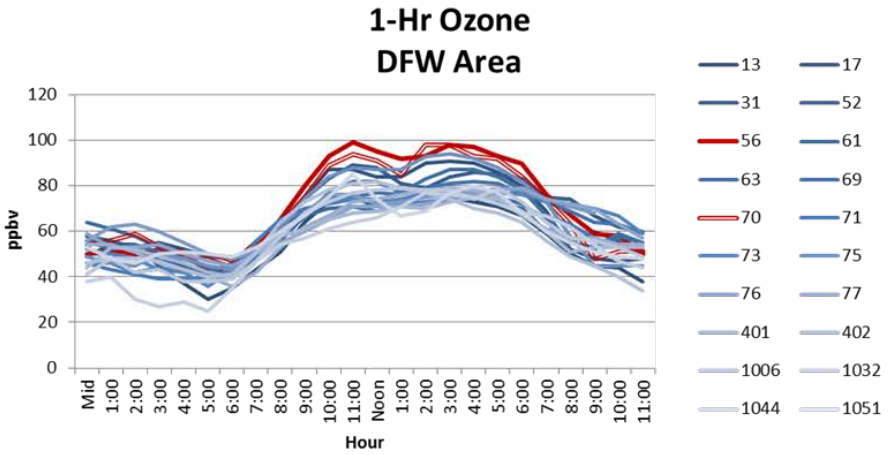

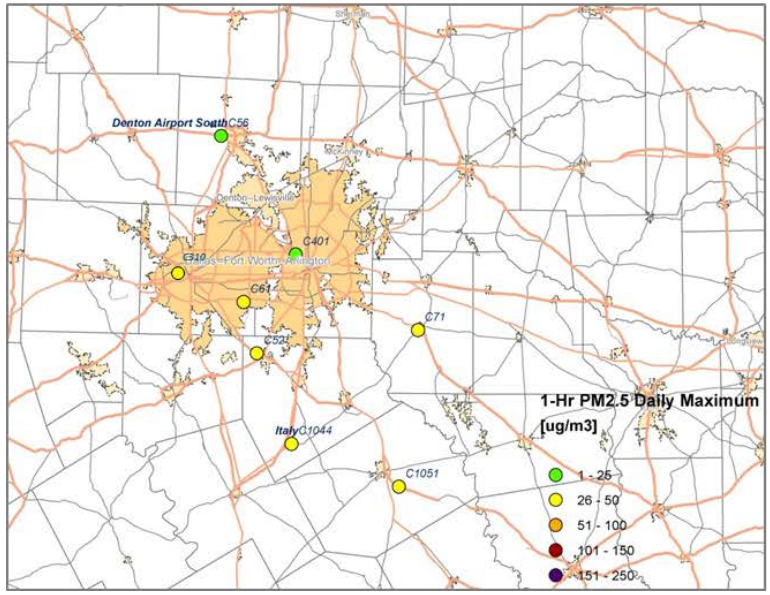

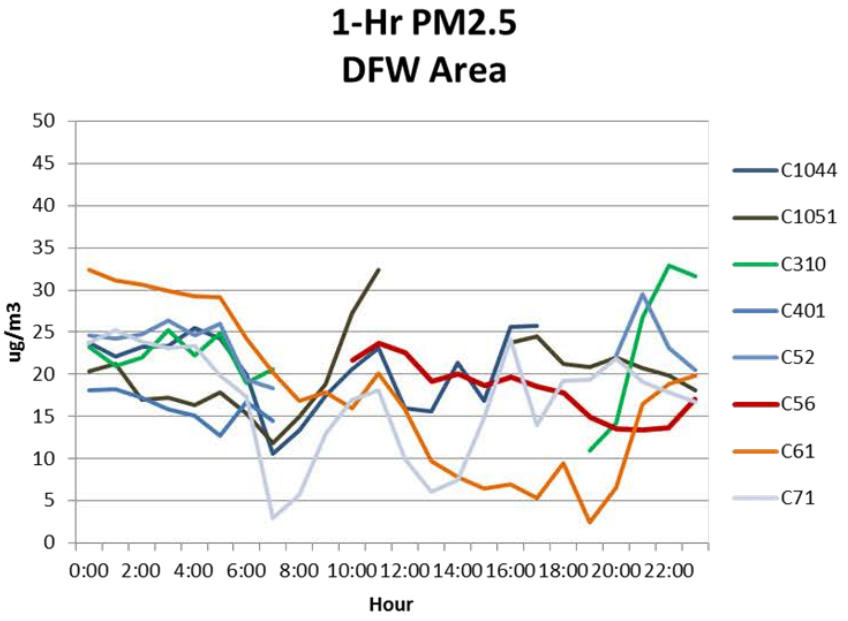

Figure 3-96. Regional ozone (top left and right) and $PM_{2.5}$ (bottom left and right) measurements (DFW area time series).

3.1.12 September 6, 2012

On September 6, 2012, the Denton Airport South (C56) site monitored its second highest MDA8 ozone reading of 2012 (89 ppb). Figure 3-97 shows surface wind back trajectories that indicate that winds were generally southerly in the DFW area on September 6. SmartFire and HYSPLIT NAM back trajectories (Figure 3-98) also show southerly low-level winds on September 6. The HYSPLIT NAM and SmartFire back trajectories agree that transport from south Texas occurred during the 72-hour period leading up to high ozone at Denton. The SmartFire map shows no fire activity near the DFW area, and several fires north of Austin and near the coast. These fires appear in the FINN emission inventory (Figure 3-101) as well as the HMS product (Figure 3-99).

The spatial map of ozone in the DFW area for September 6 (Figure 3-103) shows that monitors on the south side of the DFW area had lower ozone than monitors on the north side of the DFW area. This pattern is consistent with DFW urban plume impacts at northern monitors such as Denton on this day, which has southerly winds. The northernmost monitor, C1032, has the latest 1-hour ozone peak of any monitor in the area.

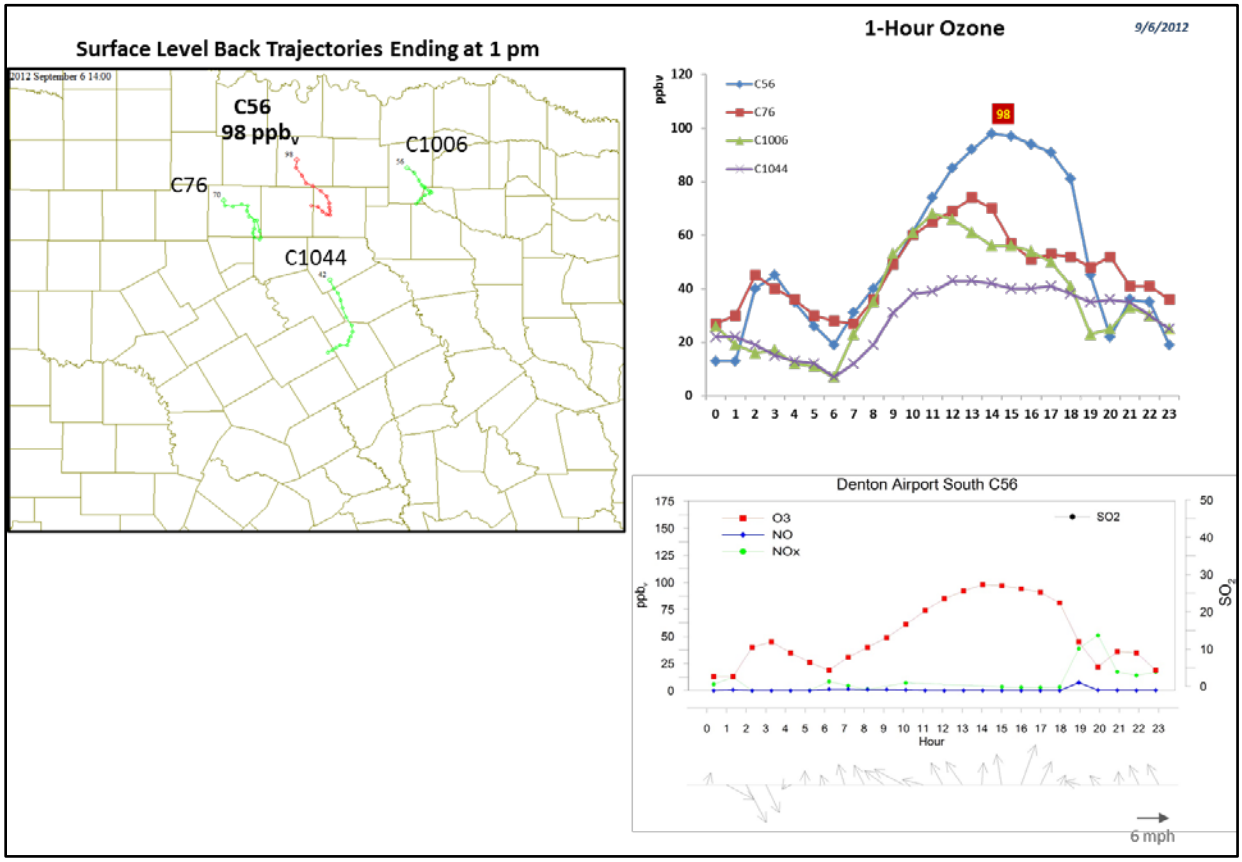

Figure 3-97. September 6, 2012 high ozone day at Denton Airport C56. Left panel: AQPlot back trajectories ending at C56 and four background sites at the time of peak 1-hr ozone was observed. Upper right panel: 1-hour average ozone time series for the C56 and background monitors. Lower right panel: time series of 1-hour ozone, NO, NO_2 and wind vectors at Denton C56 site.

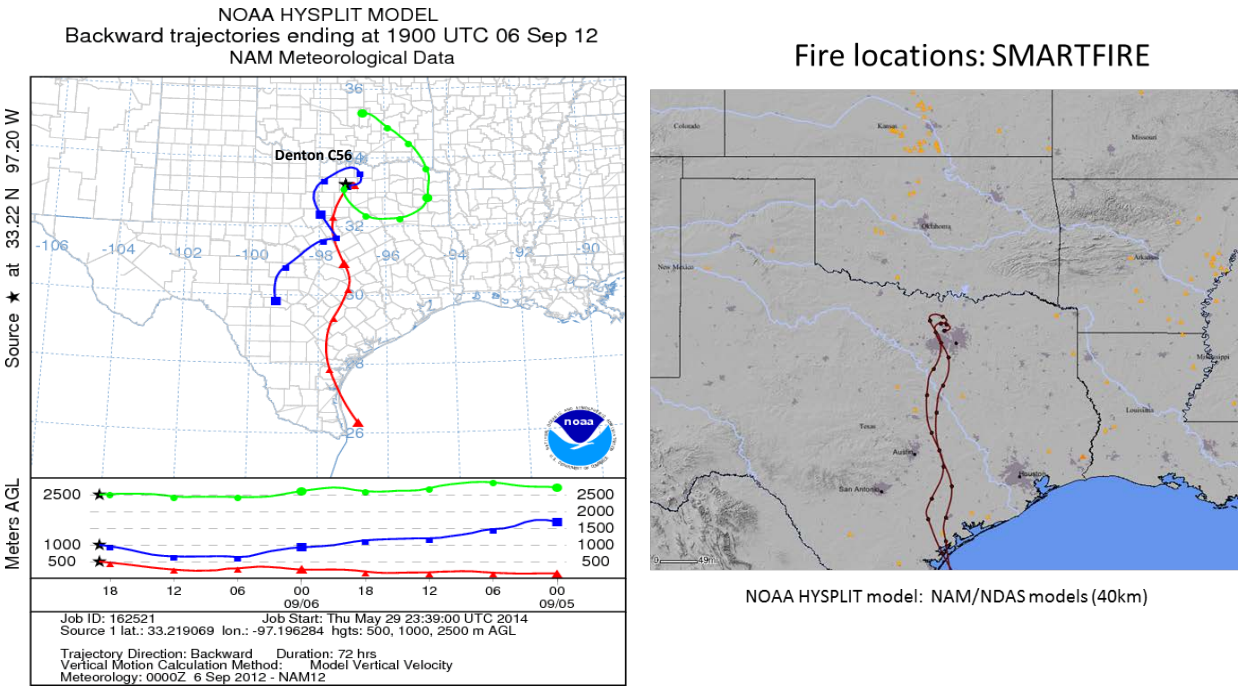

Figure 3-98. 72-hours HYSPLIT back trajectories at Denton Airport C56 (left); SmartFire plots (right) showing fire locations (orange triangles) and with 72-hour HYSPLIT back trajectories from DFW area.

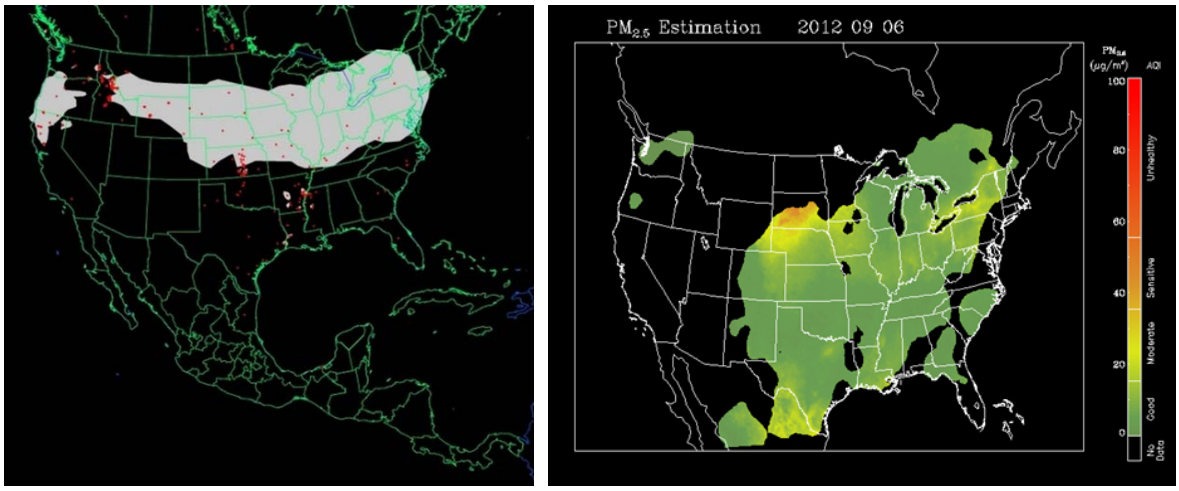

Figure 3-99. Left panel: HMS product showing September 6 fire locations (red dots) and smoke plume (gray area). Right panel: IDEA surface $PM_{2.5}$ estimate based on AOD and surface monitoring data.

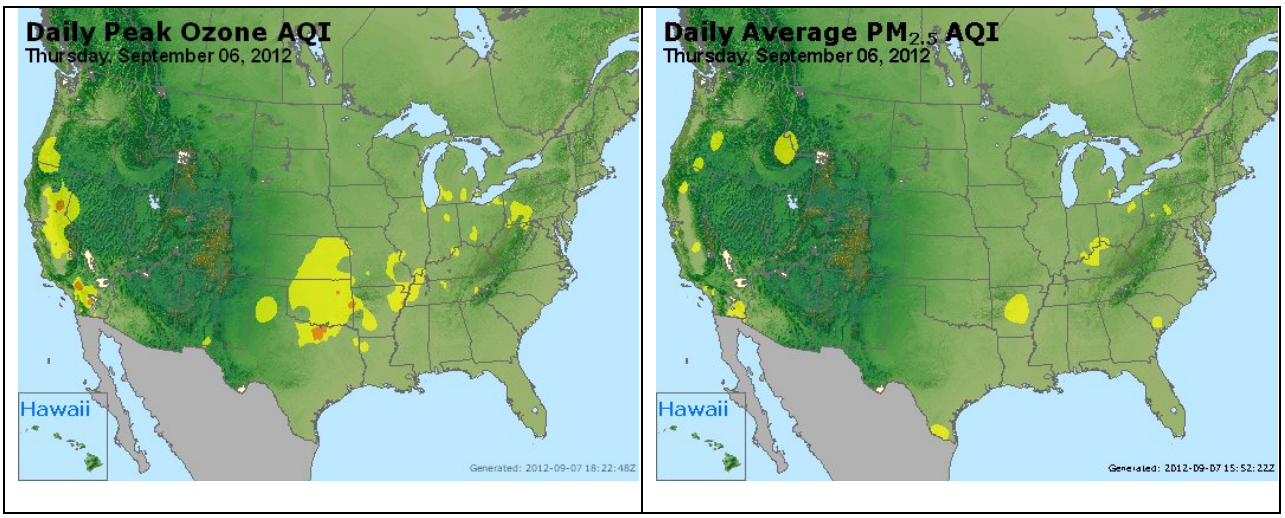

Figure 3-100. Daily average ozone (left) and $PM_{2.5}$ (right) based on observed values. Data from: http://www.airnow.gov/.

The $PM_{2.5}$ time series (Figure 3-103) show that $PM_{2.5}$ values were generally low on September 6. $PM_{2.5}$ at Denton does not exceed ~15 µg m^{-3} on September 6. The only monitors with peaks higher than 20 are C52 and C71, and these peaks occur in the early morning (C52) and the evening (C71) and do not coincide with the high 1-hour ozone values in the DFW area. The NAAPS smoke analysis (Figure 3-102) indicates that there was no smoke over the DFW area on September 6.

There is no evidence that the fires far to the south of the DFW area influenced ozone at Denton on September 6; therefore we do not recommend further analysis of this day.

ENVIRON

Wildfire Emissions Inventory: FINN 2012

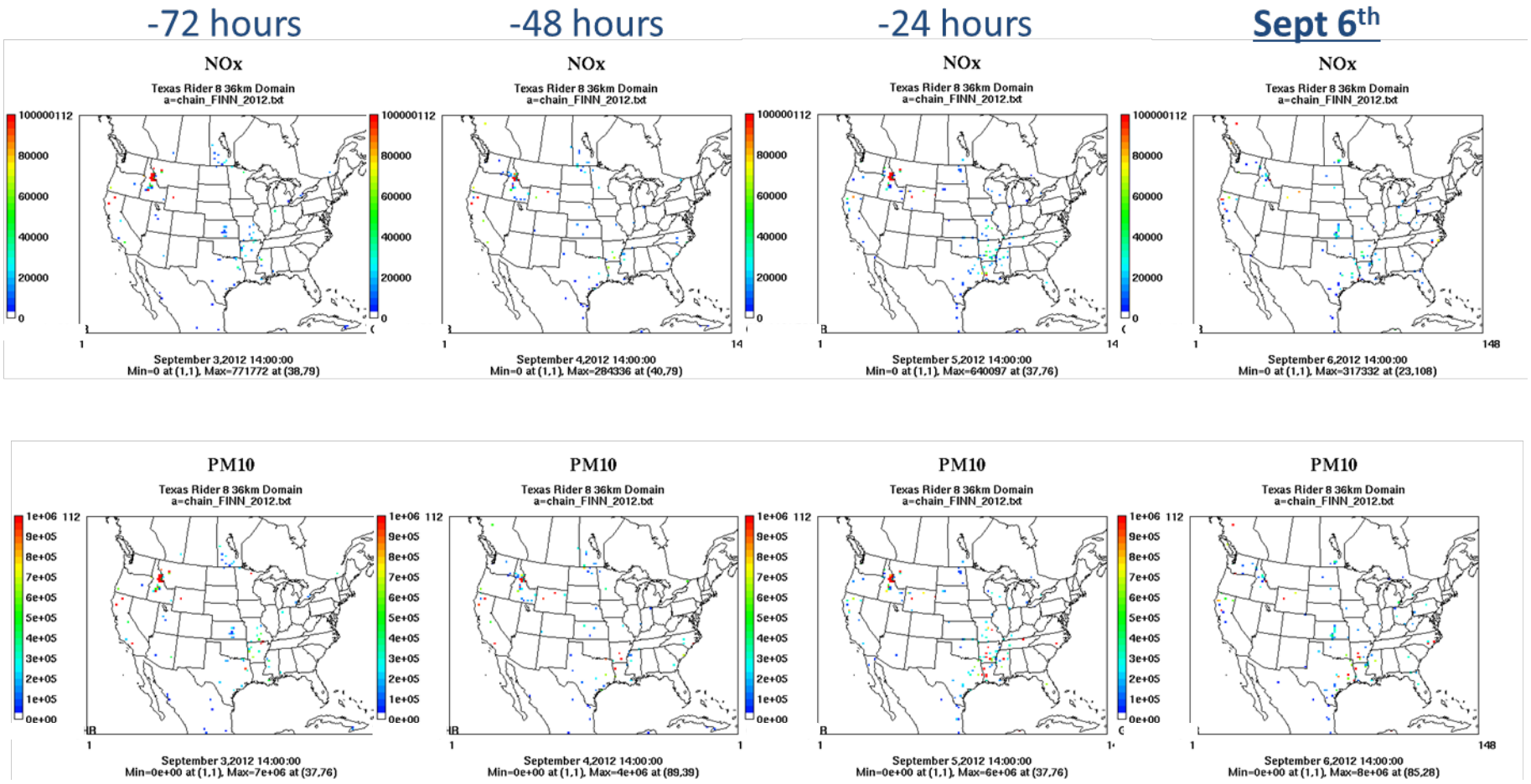

Figure 3-101. September 6, 2012 FINN fire emissions of NOx and PM_{10}.

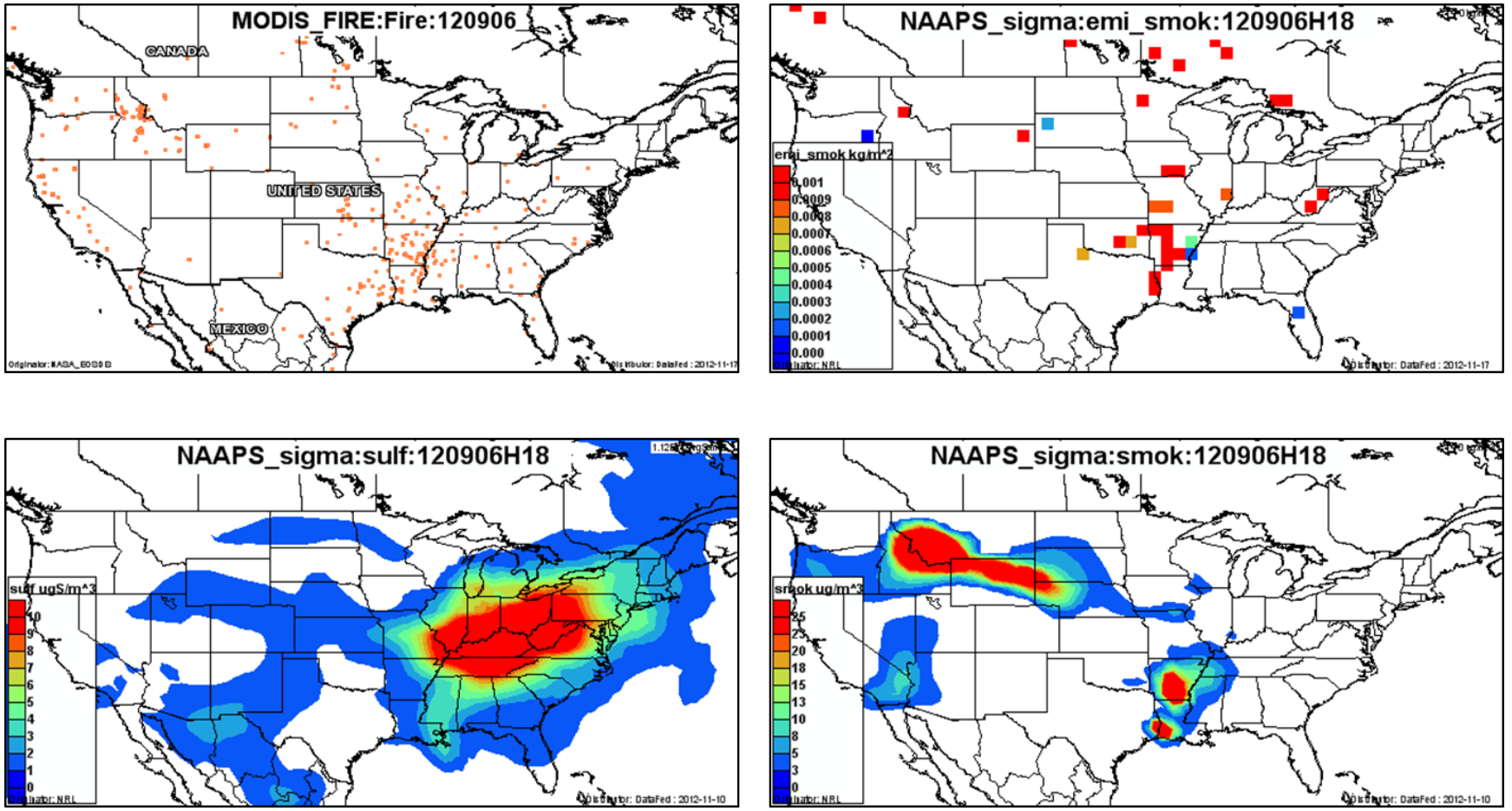

Figure 3-102. September 6, 2012 DataFed analysis. Upper left panel: Locations of active fires from MODIS satellite fire detections. Upper right panel: NAAPS model smoke emissions. Lower left panel: NAAPS model surface layer sulfate concentrations. Lower right panel: NAAPS model surface layer smoke concentrations.

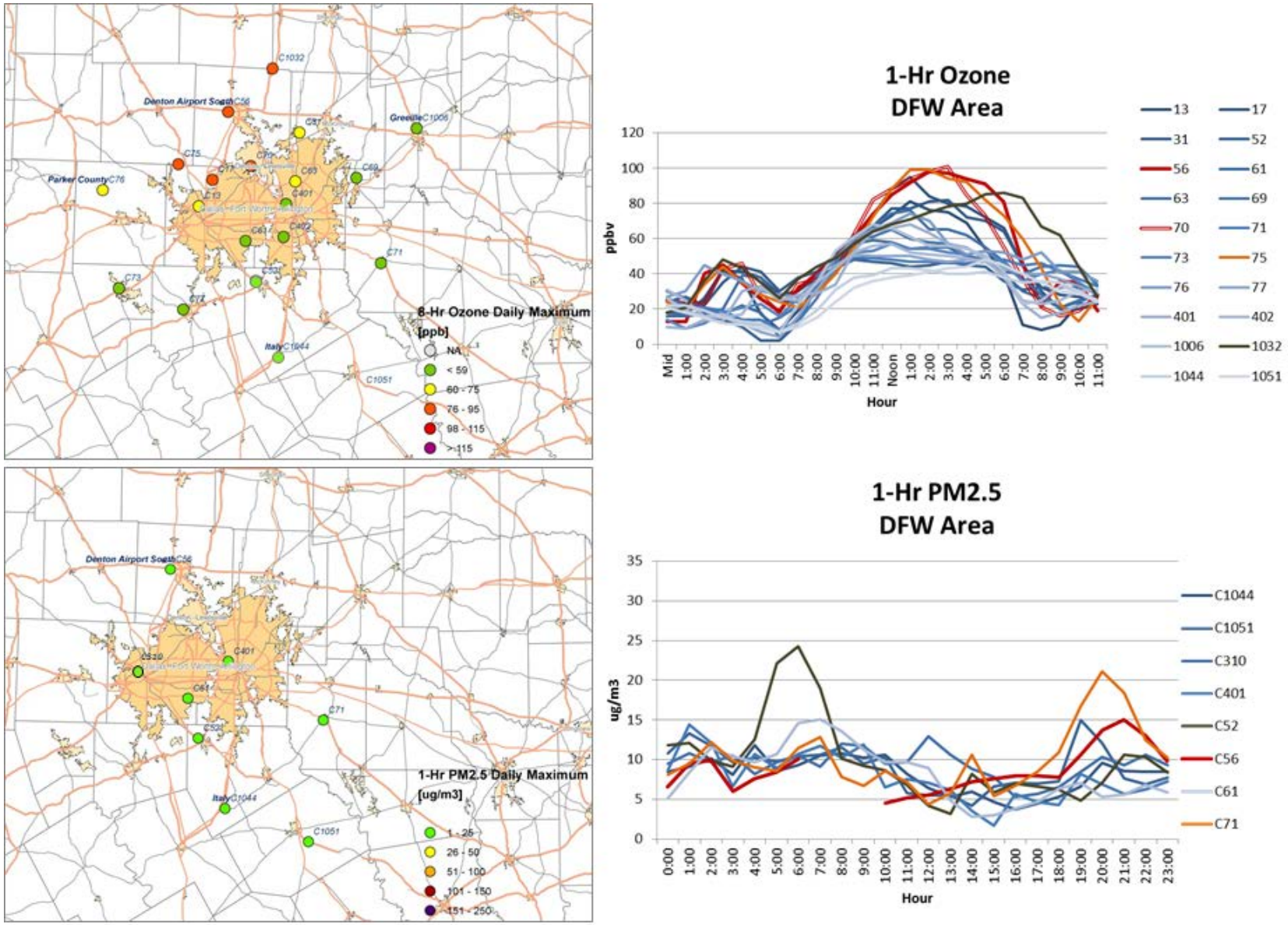

Figure 3-103. Regional ozone (top left and right) and $PM_{2.5}$ (bottom left and right) measurements (DFW area time series).

3.1.13 September 20, 2012

The Manvel Croix Park monitor (C84) recorded its fourth highest MDA8 ozone reading of 87 ppb on September 20 and had a maximum 1-hour ozone reading of 106 ppb, which was the highest in the HGB area (Figure 3-104; Figure 3-110). Winds at the monitor were northeasterly until late afternoon, and the AQPlot back trajectory shows transport from the northeast. The SmartFire and HYSPLIT NAM back trajectories (Figure 3-105) are consistent with one another and with the AQPlot trajectory in showing transport from the northeast in the 72 hours leading up to the high ozone value at Manvel Croix.

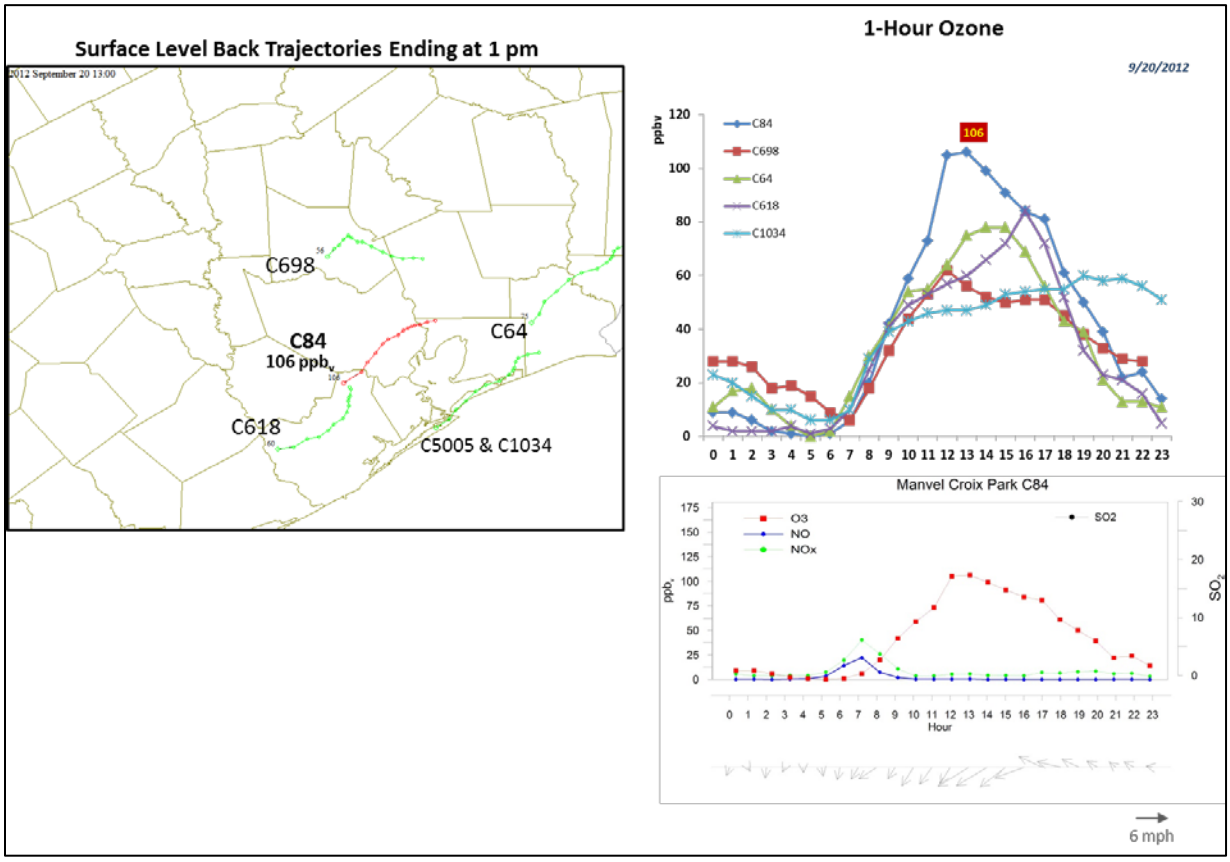

Figure 3-104. September 20, 2012 high ozone day at Manvel Croix C84. Left panel: AQPlot back trajectories ending at C84 and four background sites at the time of peak 1-hr ozone was observed at C84. Upper right panel: 1-hour average ozone time series for the CAMS84 and background monitors. Lower right panel: time series of 1-hour ozone, NO, NO_2 and wind vectors at the Manvel Croix C84.

The SmartFire map shows fires located along the back trajectories near the Texas-Louisiana border (Figure 3-105) as does the DataFed MODIS fire location plot (Figure 3-109). These fires and associated smoke plumes are visible in the HMS product (Figure 3-106) and are also evident in the FINN emissions for September 20 and for -24 hours (Figure 3-108).

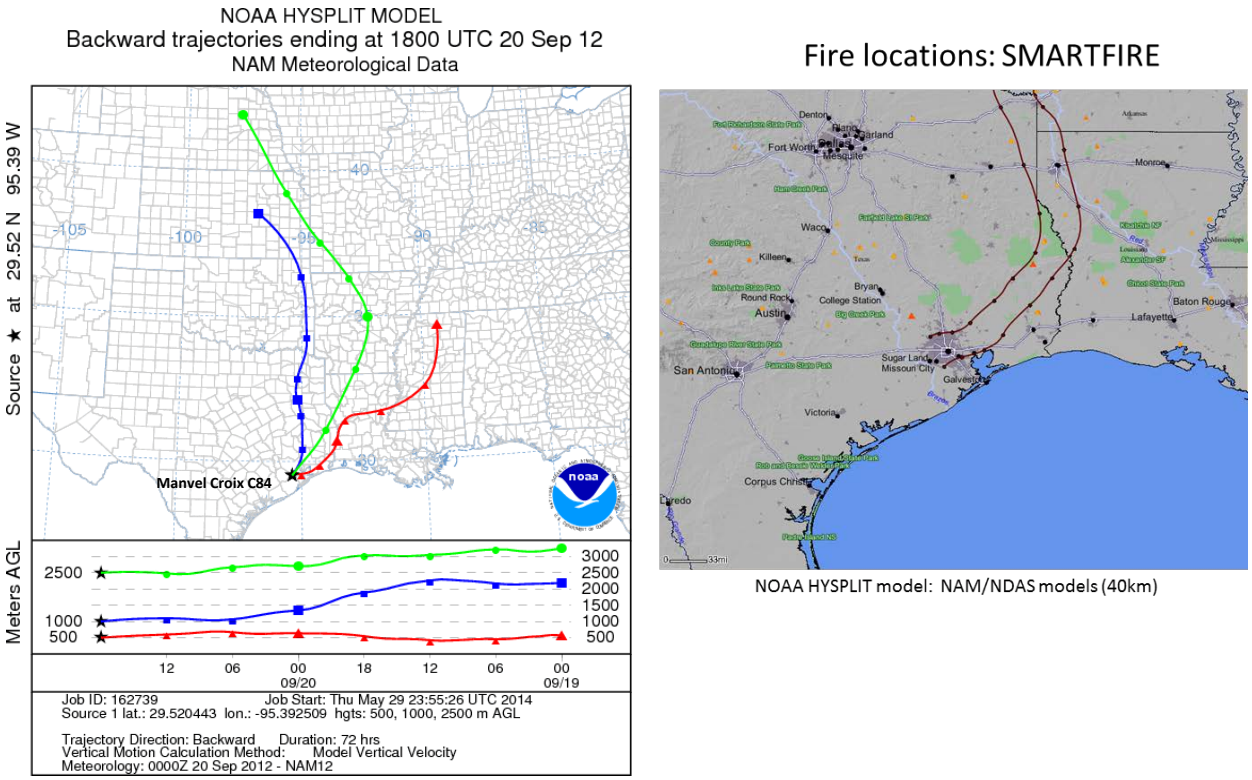

Figure 3-105. 72-hour HYSPLIT back trajectories (NAM 12km) from Manvel Croix Park C84 September 20, 2012; SmartFire plots showing fire locations (orange triangles) and 72-hour HYSPLIT back trajectories (EDAS 40 km; 10m) from two HGB sites C26 and C84 (right).

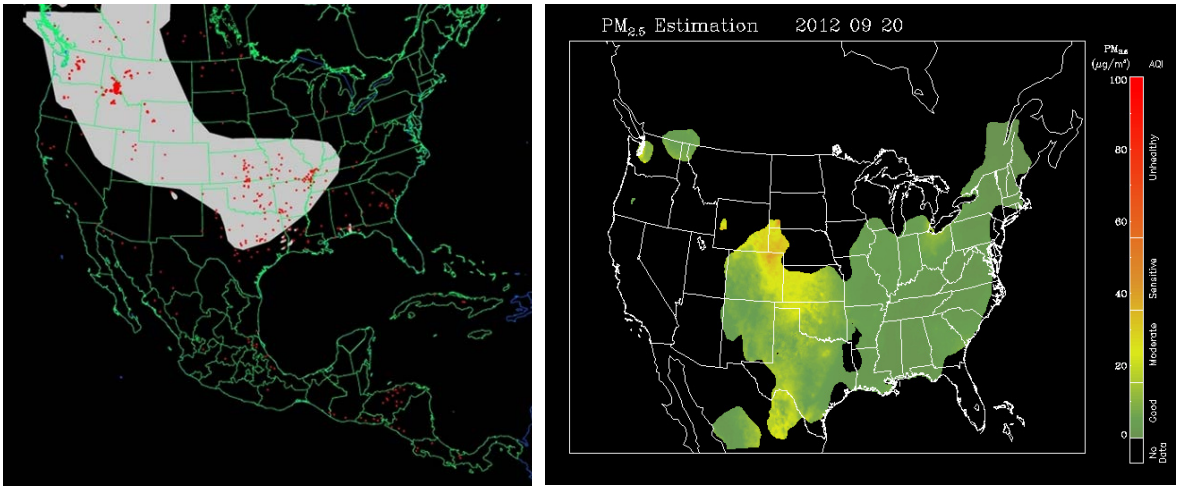

Figure 3-106. Left panel: HMS product showing September 20 fire locations (red dots) and smoke plume (gray area). Right panel: IDEA surface $PM_{2.5}$ estimate based on AOD and surface monitoring data.

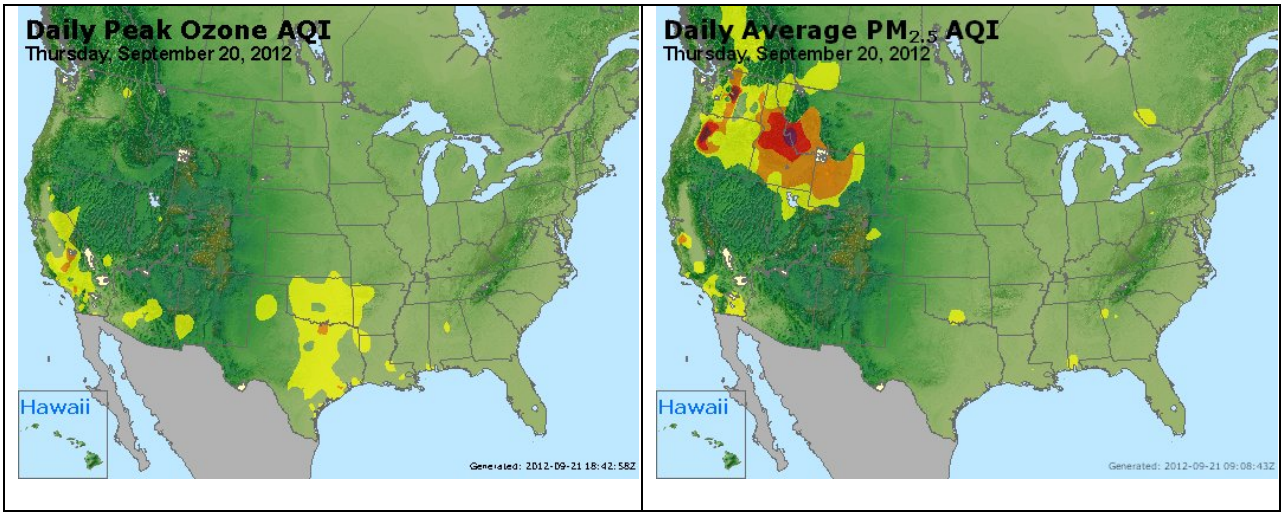

Figure 3-107. Daily average ozone (left) and $PM_{2.5}$ (right) based on observed values. Data from: http://www.airnow.gov/.

Figure 3-110 shows that $PM_{2.5}$ concentrations were low at upwind HGB monitoring sites on September 20. This is consistent with the NAAPS analysis, which shows no smoke in the HGB area (Figure 3-109). The spatial distribution of ozone shows lower MDA8 on the upwind (northeast) side of the HGB area and higher ozone on the downwind (southwest) side of the urban area. The low ozone and $PM_{2.5}$ concentrations in the incoming air mass strongly suggests that plumes from the Louisiana fires did not have a significant impact on the Manvel Croix monitor, but rather that high ozone at the monitor was caused by local emission sources. Therefore, we do not recommend further analysis of September 20 at Manvel Croix.

Wildfire Emissions Inventory: FINN 2012

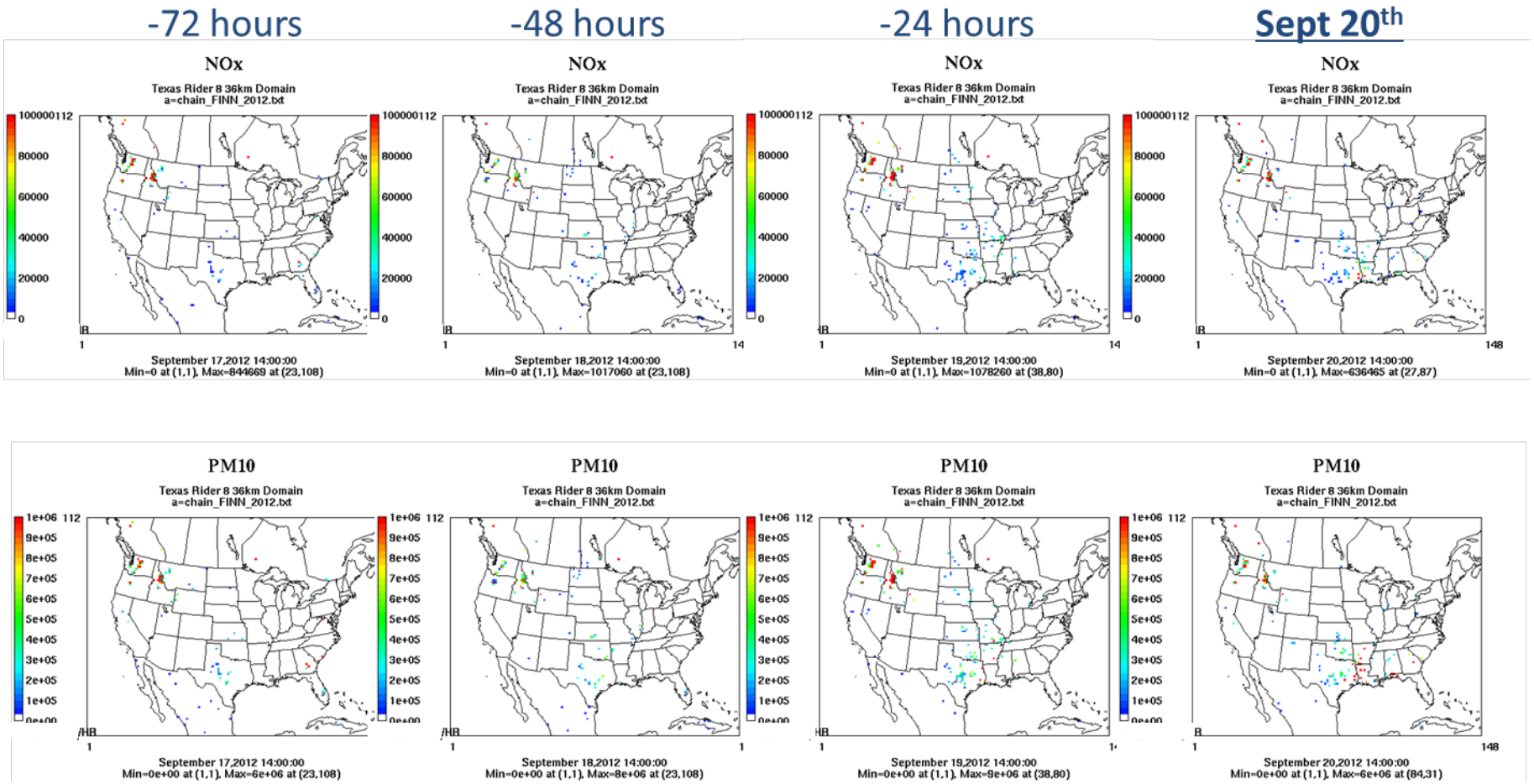

Figure 3-108. September 20, 2012 FINN fire emissions of NOx (top) and PM_{10} (bottom).

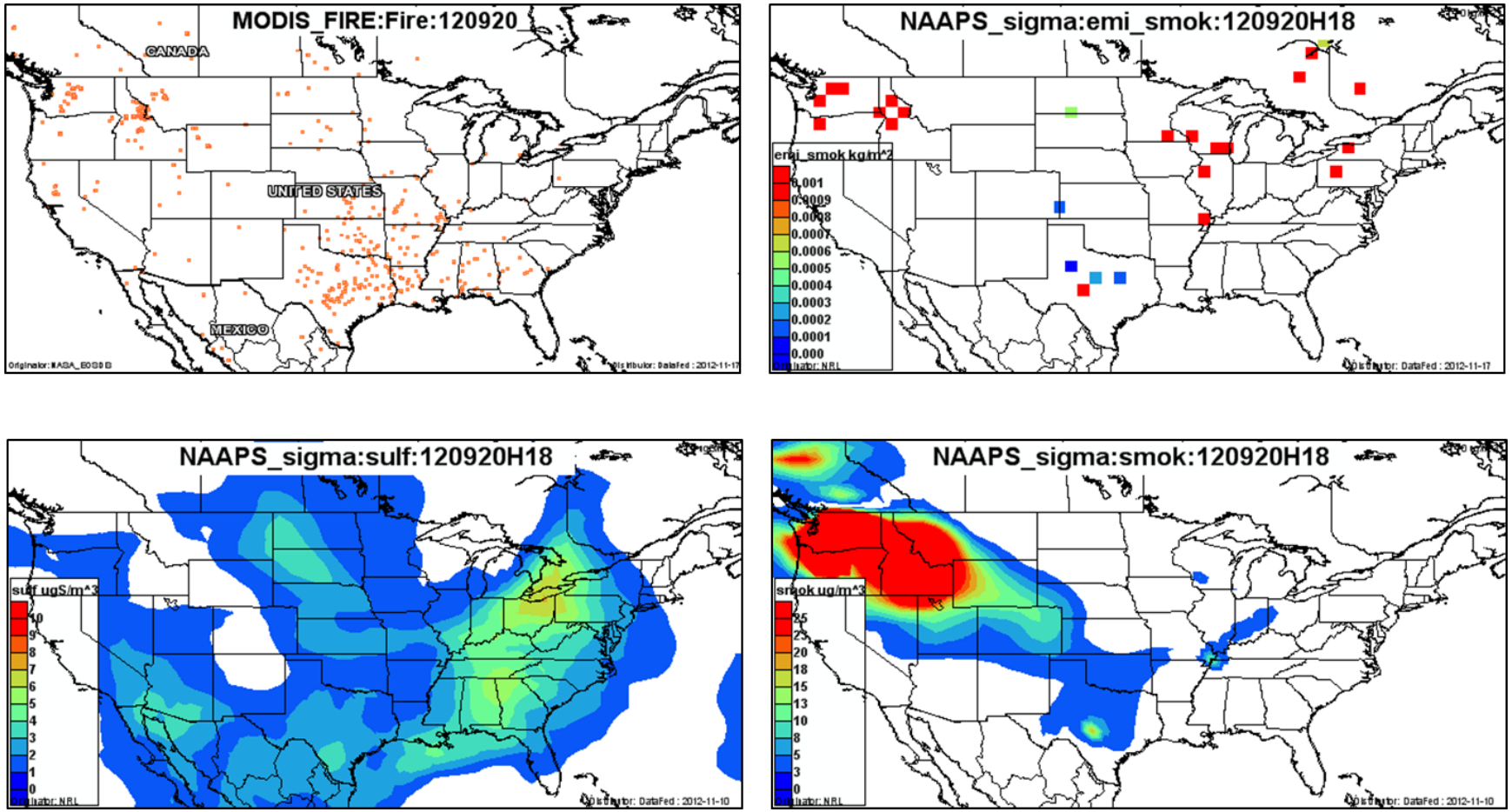

Figure 3-109. September 20, 2012 DataFed analysis. Upper left panel: Locations of active fires from MODIS satellite fire detections. Upper right panel: NAAPS model smoke emissions. Lower left panel: NAAPS model surface layer sulfate concentrations. Lower right panel: NAAPS model surface layer smoke concentrations.

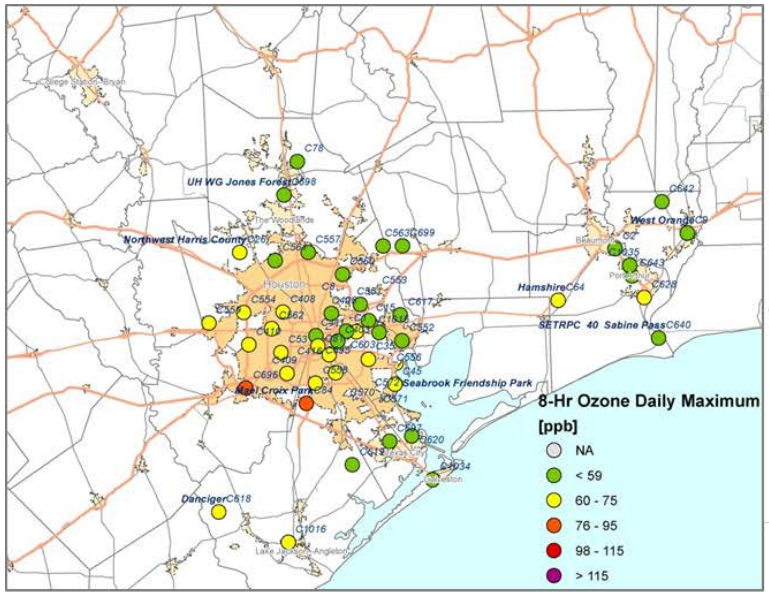

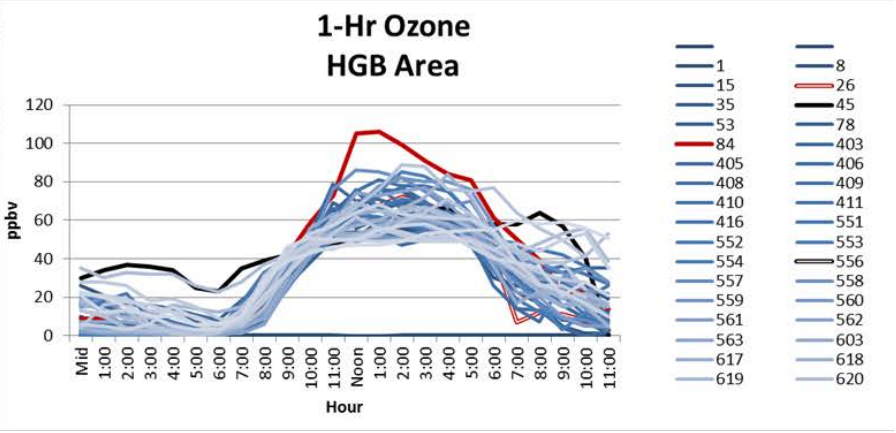

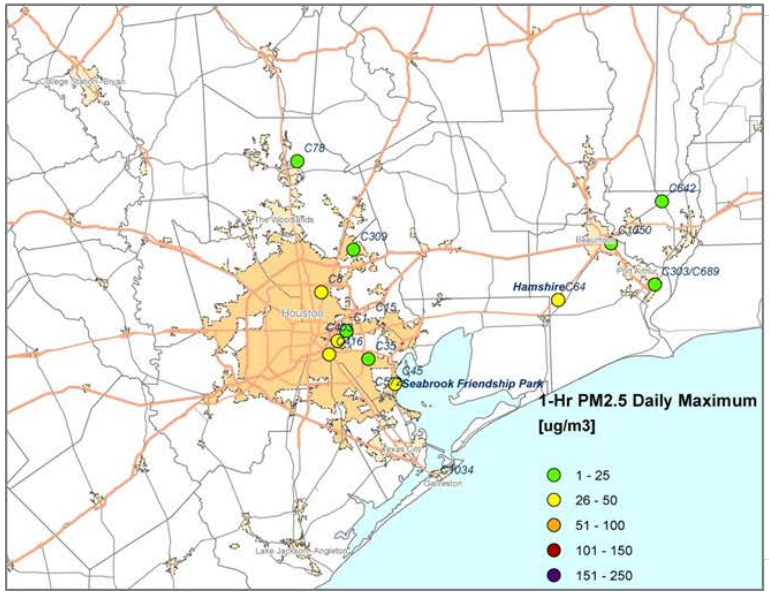

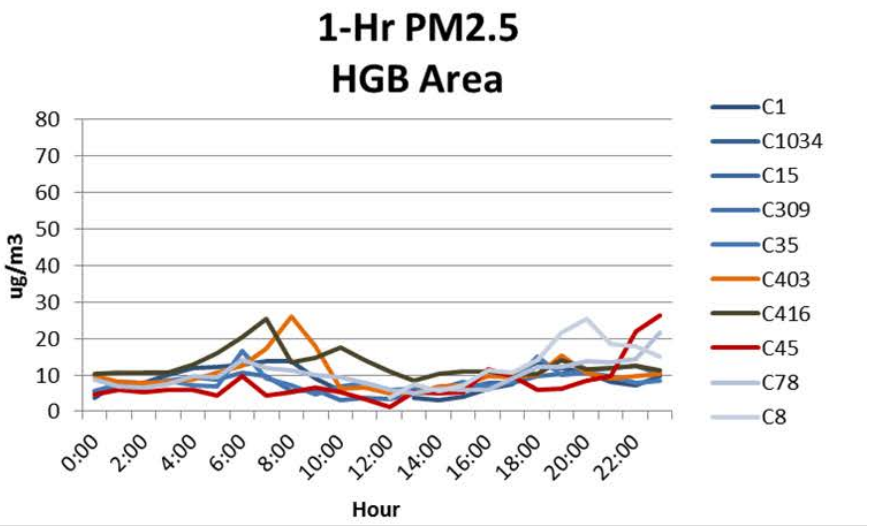

Figure 3-110. Regional ozone (top left and right) and $PM_{2.5}$ (bottom left and right) measurements (HGB area time series).

3.2 2013 Ozone Season

In 2013, there were seventeen distinct days that contributed to the ozone design values in the HGB, DFW and BPA areas. Monitors analyzed on each day are listed in Table 3-2. In this section, we analyze each of these days for each monitor using the methods described in Section 2.

Table 3-2. Monitors analyzed by day: 2013.

Day	Monitor(s) Analyzed
5/7/2013	Sabine Pass
5/13/2013	NW Harris
6/3/2013	Manvel Croix
7/2/2013	Sabine Pass, Manvel Croix
7/3/2013	NW Harris
7/4/2013	Sabine Pass, Manvel Croix
7/5/2013	Denton
7/13/2013	Sabine Pass
8/16/2013	Manvel Croix
8/28/2013	NW Harris
8/30/2013	Grapevine
8/31/2013	Denton
9/4/2013	Denton, Grapevine
9/6/2013	Denton, Grapevine
9/12/2013	Grapevine
9/25/2013	Seabrook, La Porte
10/9/2013	NW Harris

3.2.1 May 7, 2013

On May 7, the Sabine monitor had its 4th highest MDA8 reading (67 ppb) and reached a peak 1-hour average ozone value of 73 ppb. Wind vectors at the Sabine Pass monitor and the AQPlot surface wind back trajectories show that winds were westerly during the morning of May 7 turning to southerly by noon (Figure 3-111). The SmartFire back trajectory and HYSPLIT 500 m and 1,000 m back trajectories both extend westward toward the HGB area and then turn northward. The SmartFire maps shows fires in the region but not in close proximity to the back trajectories. The HMS map shows no smoke in the region (Figure 3-113), but the NAAPS analysis indicates strong maxima of smoke in the BPA area (Figure 3-116). The ozone spatial pattern in Figure 3-117 shows MDA8 values of 75 ppb or lower at all BPA area monitors as well as low values of $PM_{2.5}$. Low values of $PM_{2.5}$ and the lack of a pronounced 1-hour ozone peak at the Sabine Pass monitor indicate that an impact from one or more of the distant fires shown in the SmartFire map is extremely unlikely despite the presence of smoke in the NAAPS analysis. We recommend no further analysis of May 7, 2013.

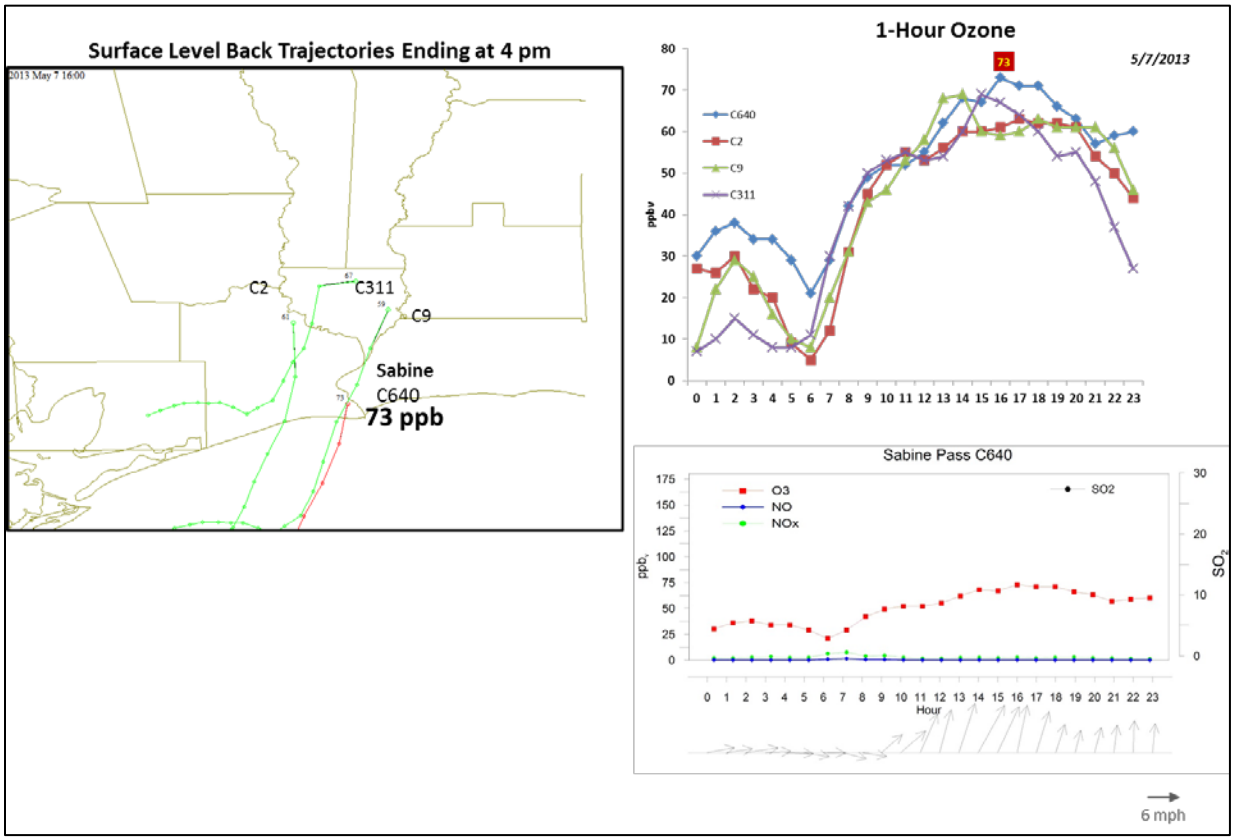

Figure 3-111. May 7, 2013 high ozone day at Sabine Pass C640. Left panel: back trajectories from AQPlot for the HGB monitors for May 7 at the time of peak ozone impact at C640. Upper right panel: 1-hour average ozone time series for the C640 and surrounding BPA monitors. Lower right panel: time series of 1-hour ozone, NO, NO_2 and wind vectors at the Sabine monitor.

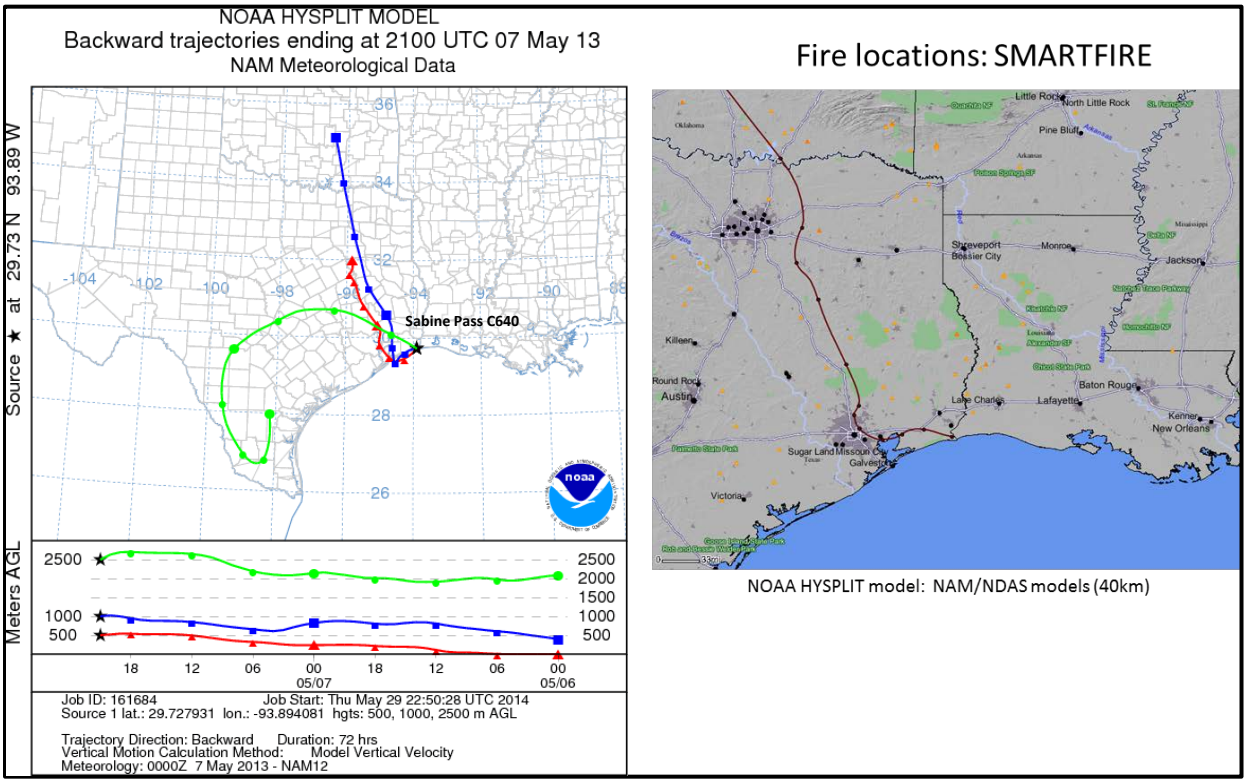

NOAA HYSPLIT model: NAM/NDAS models (40km)

Figure 3-112. 72-hour HYSPLIT back trajectories (NAM 12km) from Sabine Pass C640 ending May 7, 2013; SmartFire plot showing fire locations (orange triangles) and 72-hour HYSPLIT back trajectories (EDAS 40 km) from C640.

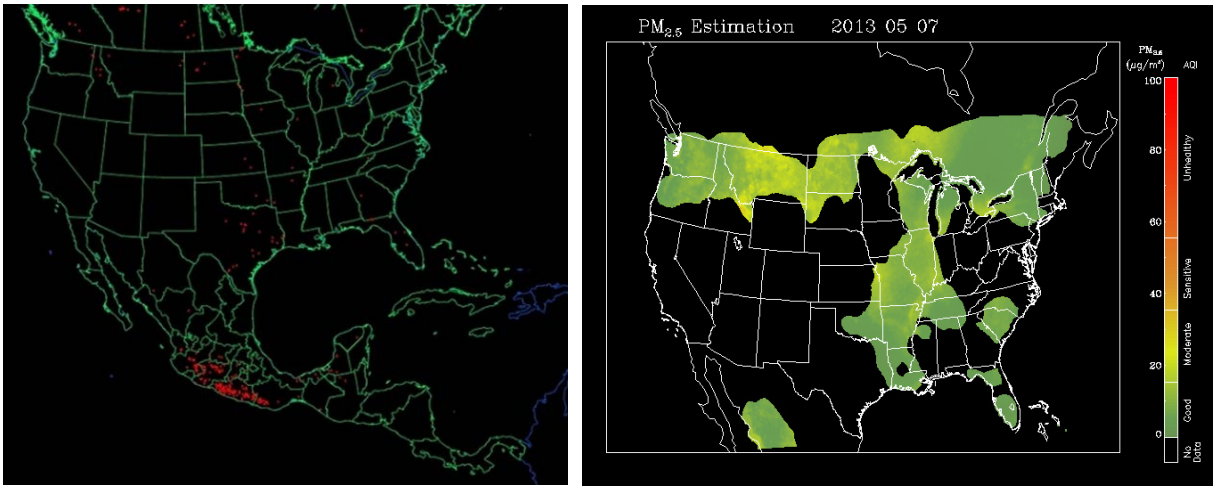

Figure 3-113. Left panel: HMS product showing May 7 fire locations (red dots) and smoke plume (gray area). Right panel: IDEA surface $PM_{2.5}$ estimate based on AOD and surface monitoring data.

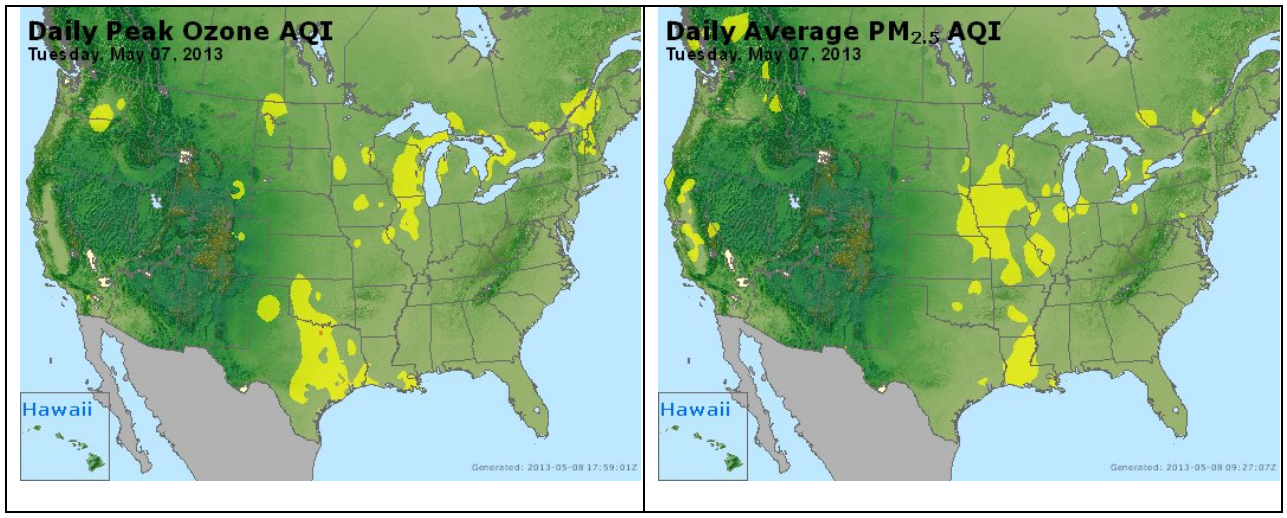

Figure 3-114. Daily average ozone (left) and $PM_{2.5}$ (right) based on observed values. Data from: http://www.airnow.gov/.

ENVIRON

Wildfire Emissions Inventory: FINN 2013

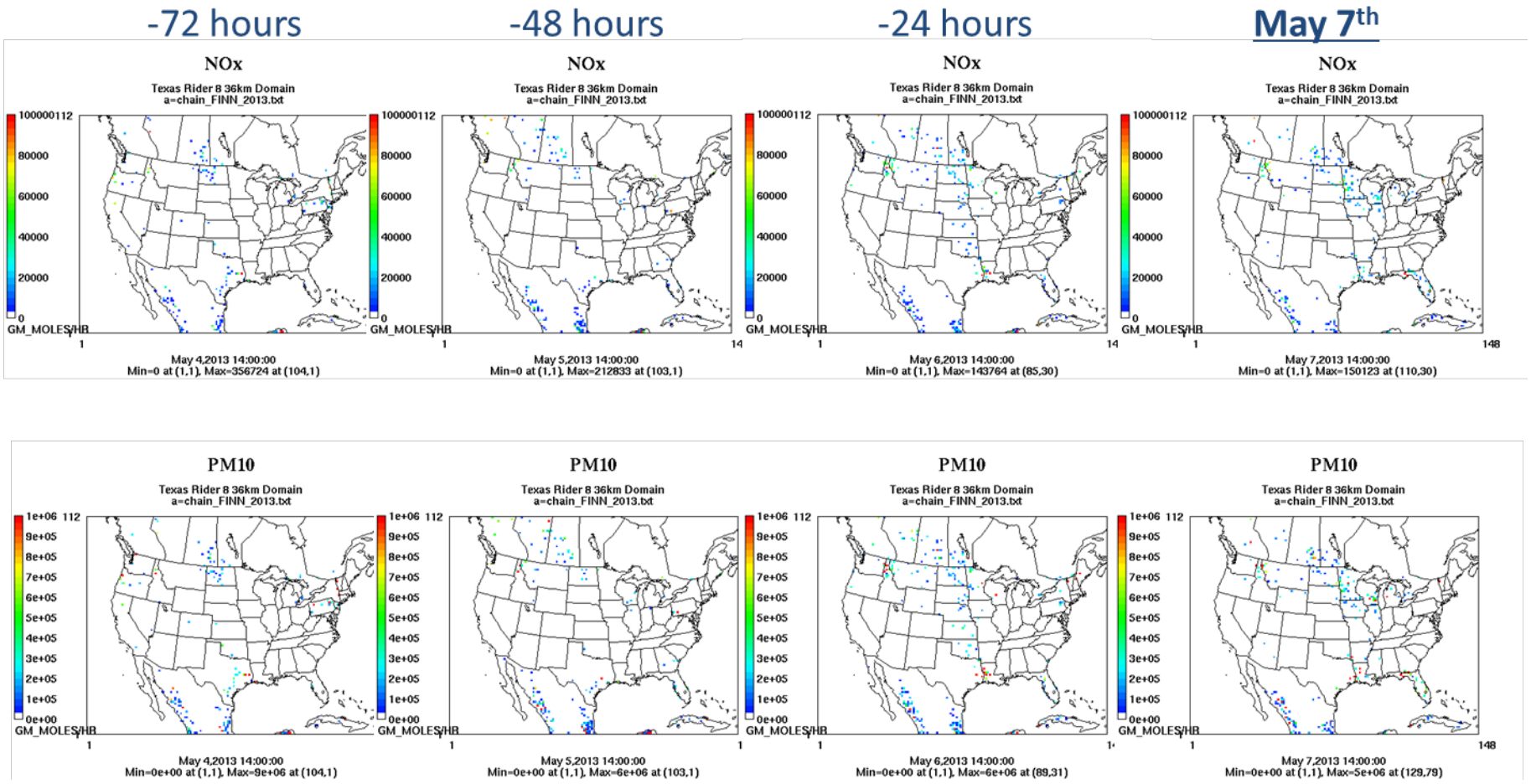

Figure 3-115. May 7, 2013 FINN fire emissions of NOx and PM_{10}.

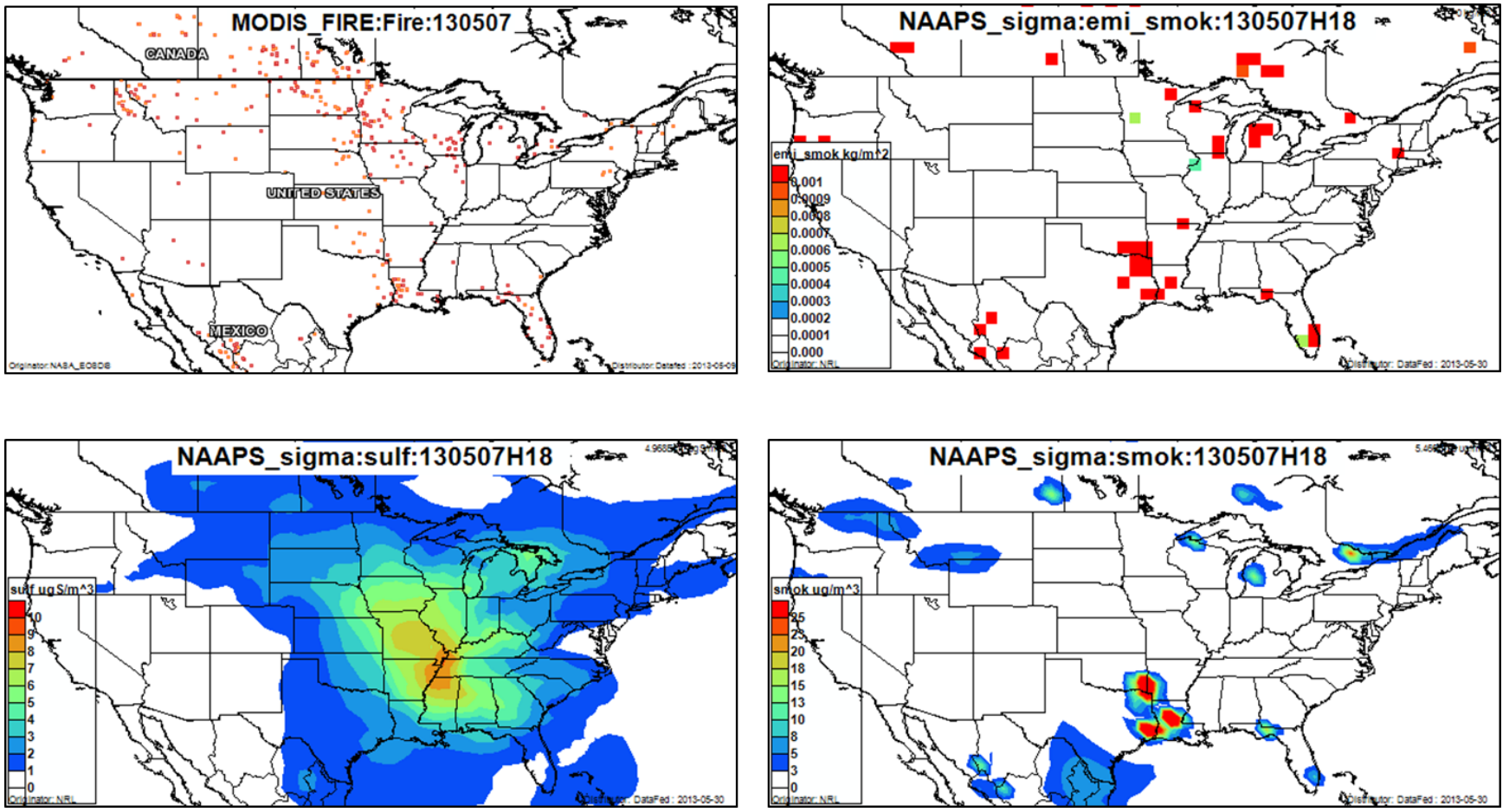

Figure 3-116. May 7, 2013 DataFed analysis. Upper left panel: Locations of active fires from MODIS satellite fire detections. Upper right panel: NAAPS model smoke emissions. Lower left panel: NAAPS model surface layer sulfate concentrations. Lower right panel: NAAPS model surface layer smoke concentrations.

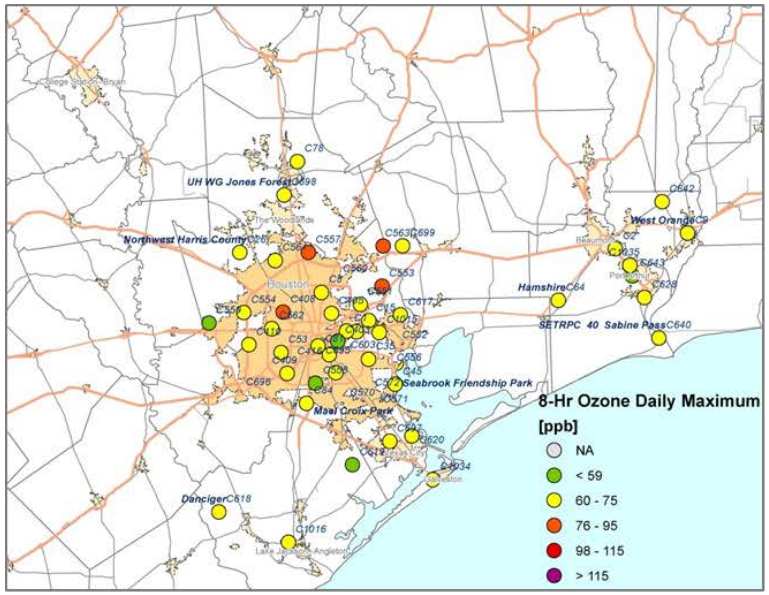

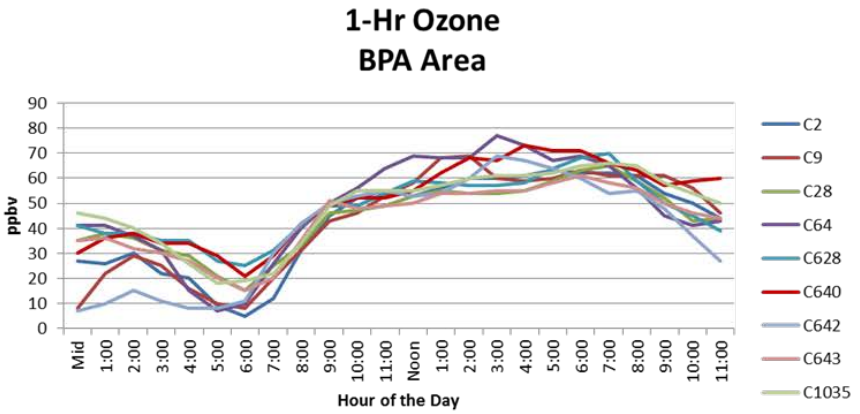

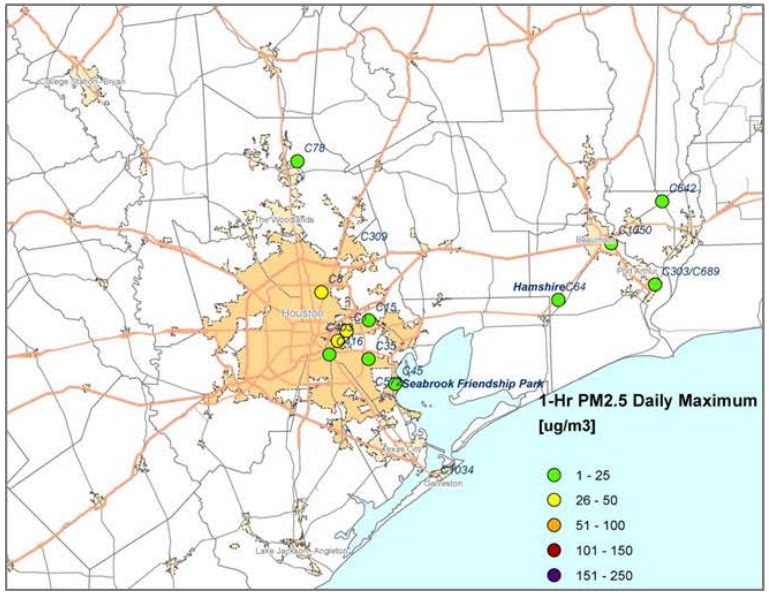

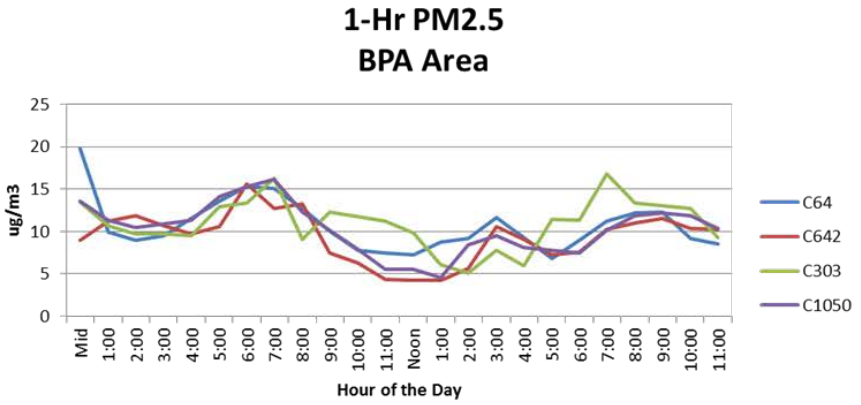

Figure 3-117. Regional ozone (top left and right) and $PM_{2.5}$ (bottom left and right) measurements (HGB area time series).

3.2.2 May 13, 2013

On May 13, the Northwest Harris monitor (C26) recorded its 3rd highest ozone MDA8 value (82 ppb) and had a peak 1-hour value of 98 ppb (Figure 3-118). Wind vectors at the monitor show northerly winds in the early morning shifting to southeasterly by 7 am. There is no peak in NO or NOx coincident with the peak in 1-hour average ozone.

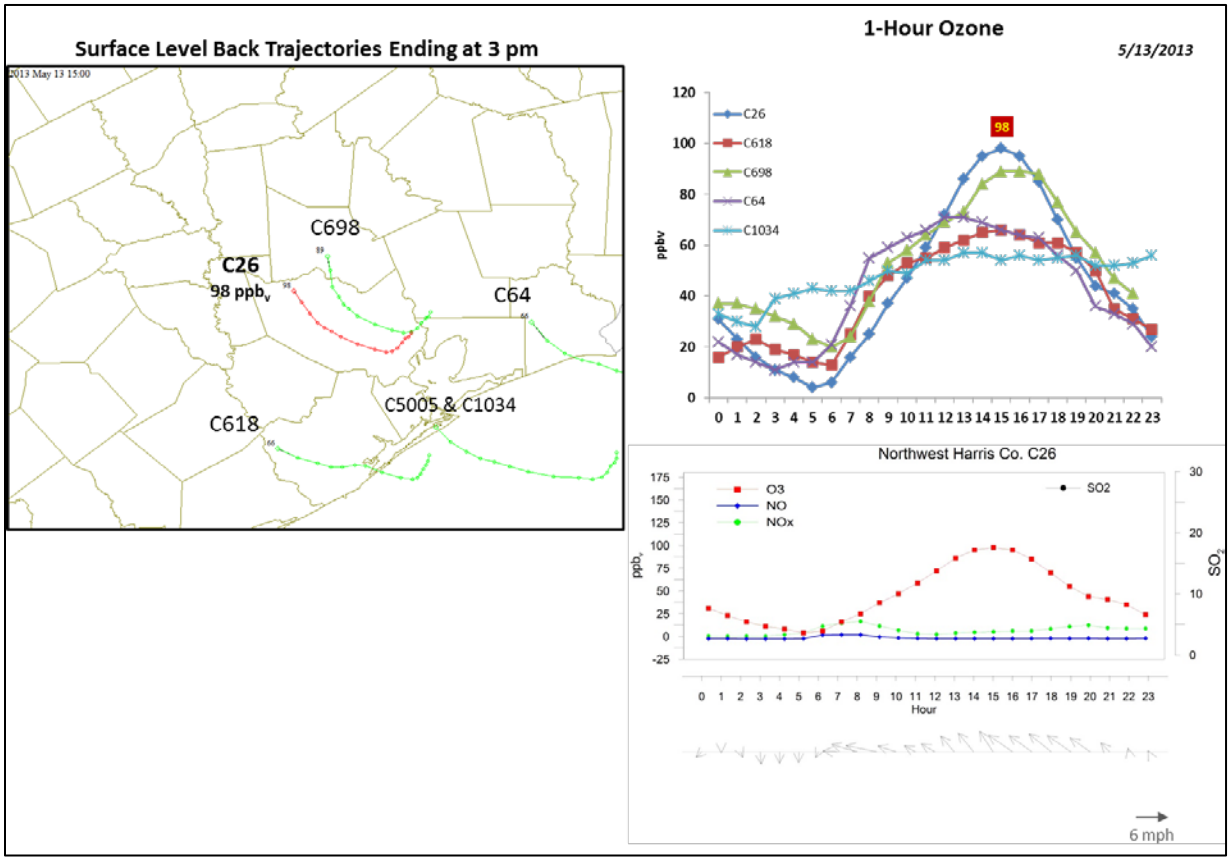

Figure 3-118. May 13, 2013 high ozone day at Northwest Harris Co. C26. Left panel: back trajectories terminating at C26 (red line) and four background HGB monitors (green line) on May 13 at the time of peak ozone impact at C26. Upper right panel: 1-hour average ozone time series for the C26 and surrounding HGB monitors. Lower right panel: time series of 1-hour ozone, NO, NO_2 and wind vectors at the Northwest Harris monitor.

SmartFire and HYSPLIT NAM back trajectories show easterly-southeasterly flow on May 13, with trajectories extending back northward into Northeast Texas and Louisiana (Figure 3-119). The SmartFire map shows fires north and northeast of the Houston urban area and two different fires adjacent to Galveston Bay. The HMS product also shows fires in these locations and indicates that smoke plumes were present north of the HGB area (Figure 3-120). Neither the $PM_{2.5}$ surface analysis (Figure 3-120) nor the $PM_{2.5}$ AQI spatial plot (Figure 3-121) shows enhanced $PM_{2.5}$ over the HGB area.

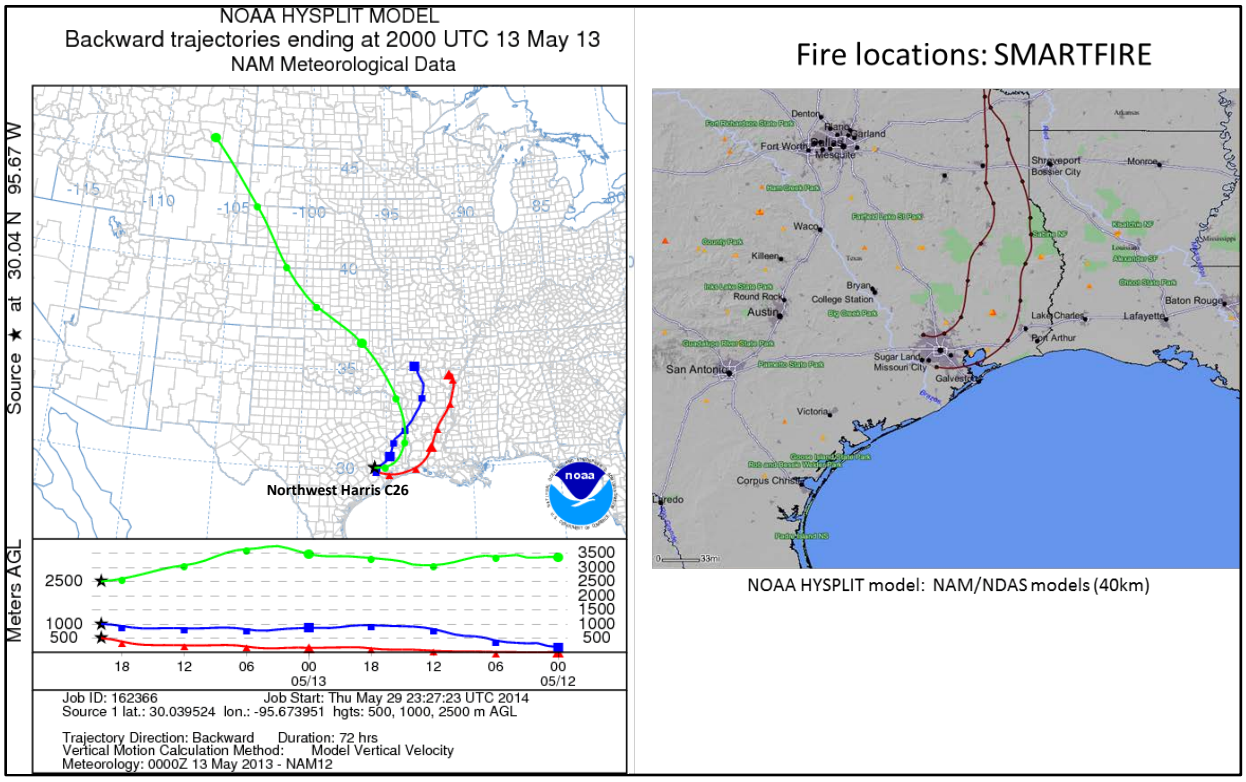

Figure 3-119. 72-hour HYSPLIT back trajectories ending at Northwest Harris C26 at May 13, 2013; Right side: SmartFire plot with nearby fire locations (orange triangles) and 72-hour HYSPLIT back trajectories terminating at HGB sites (C26 and C84).

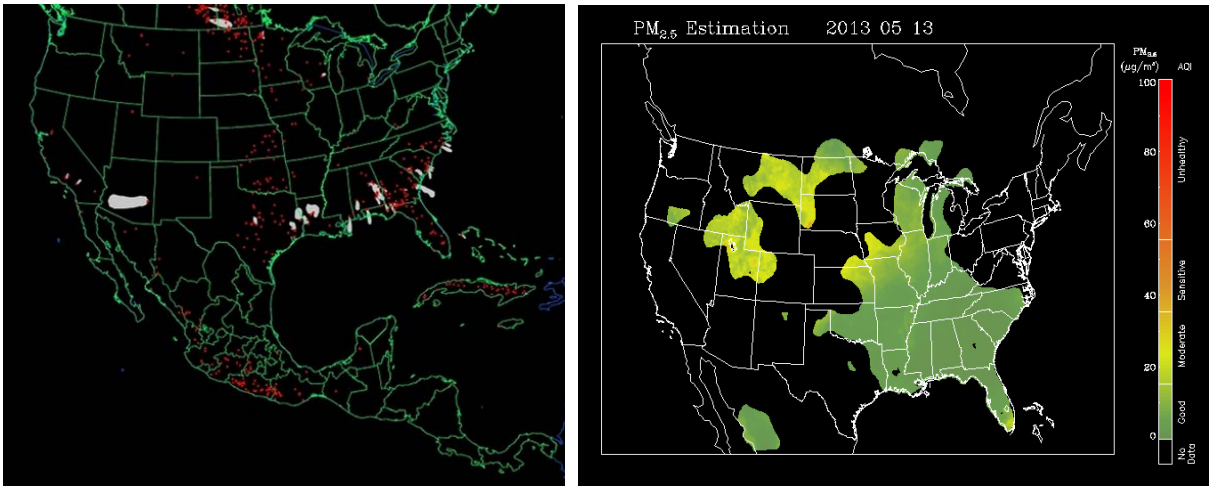

Figure 3-120. Left panel: HMS product showing May 13 fire locations (red dots) and smoke plume (gray area). Right panel: IDEA surface $PM_{2.5}$ estimate based on AOD and surface monitoring data.

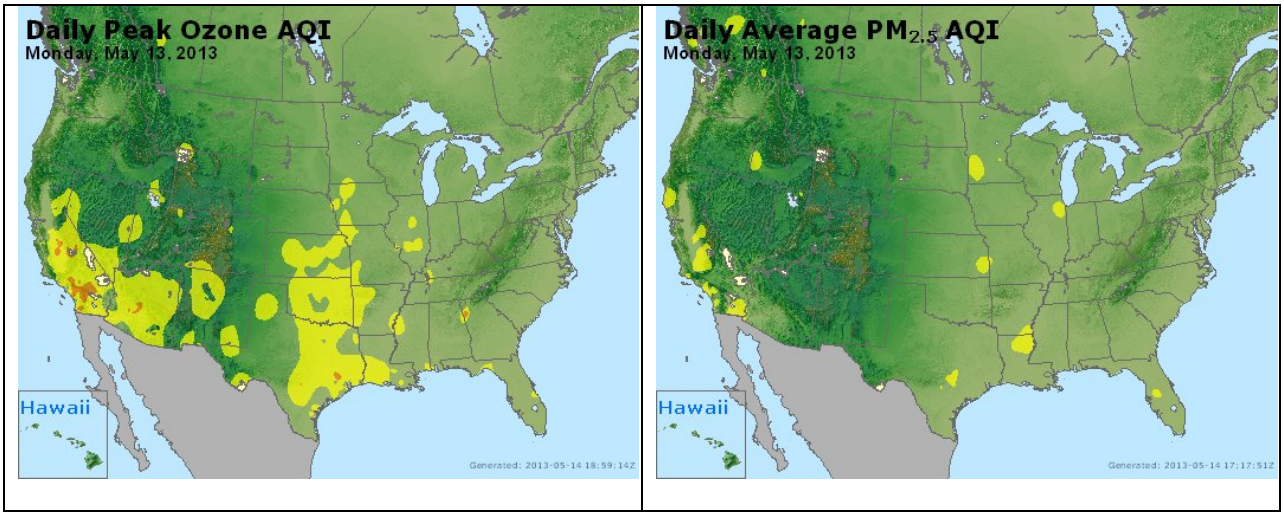

Figure 3-121. Daily average ozone (left) and $PM_{2.5}$ (right) based on observed values. Data from: http://www.airnow.gov/.

The $PM_{2.5}$ time series for May 13 (Figure 3-124) show no evidence of fire plume impacts. $PM_{2.5}$ levels were <20 µg m^{-3} for all HGB monitors during the daylight hours when high ozone occurred at NW Harris. The NAAPS analysis (Figure 3-123) shows the presence of smoke near the Texas-Louisiana border, but this smoke is located to the east of the NW Harris County monitor. Because there is no indication of fire influence on NW Harris County monitor ozone levels, we recommend no further evaluation of May 13, 2013.

Wildfire Emissions Inventory: FINN 2013

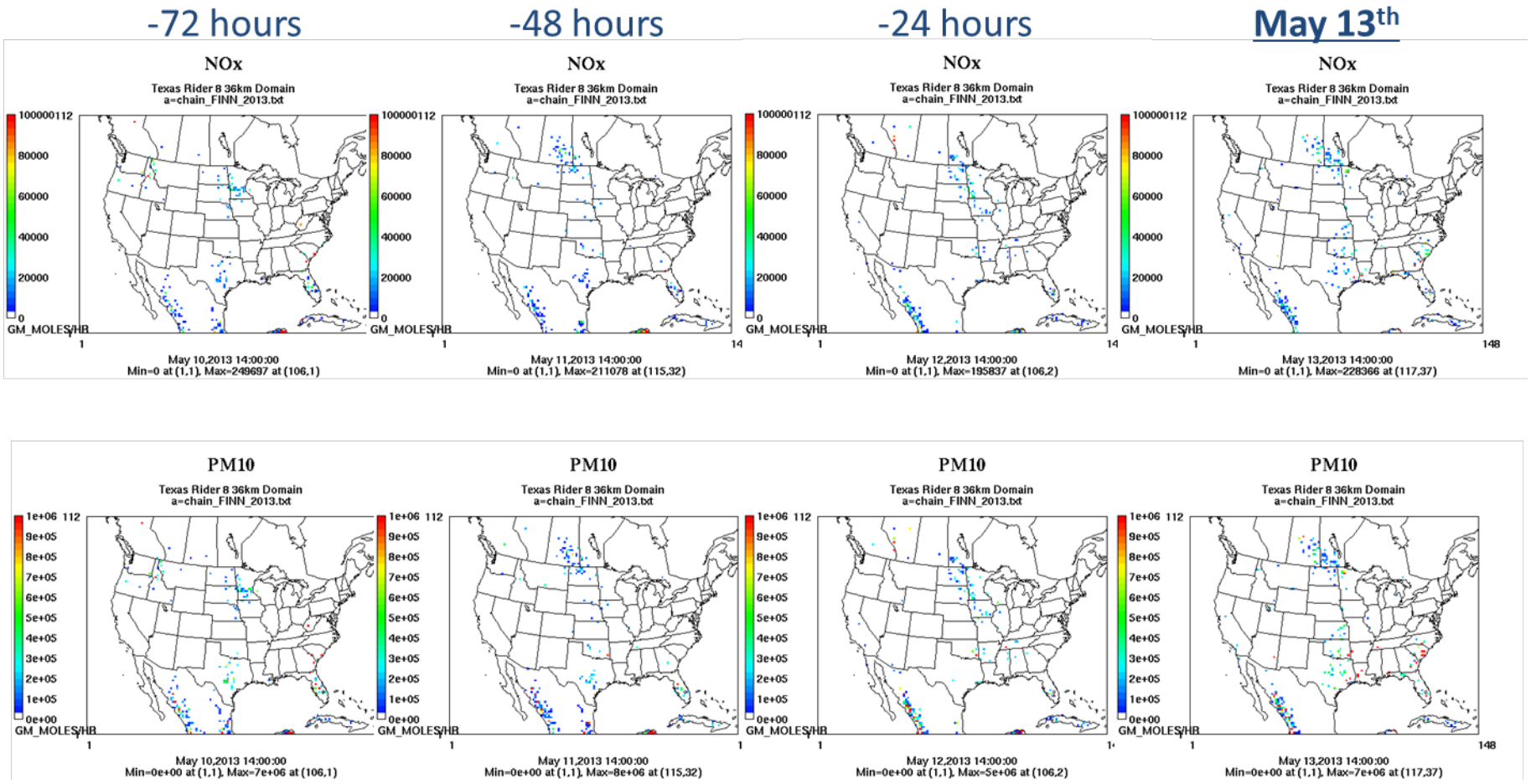

Figure 3-122. May 13, 2013 FINN fire emissions of NOx (top) and PM_{10} (bottom).

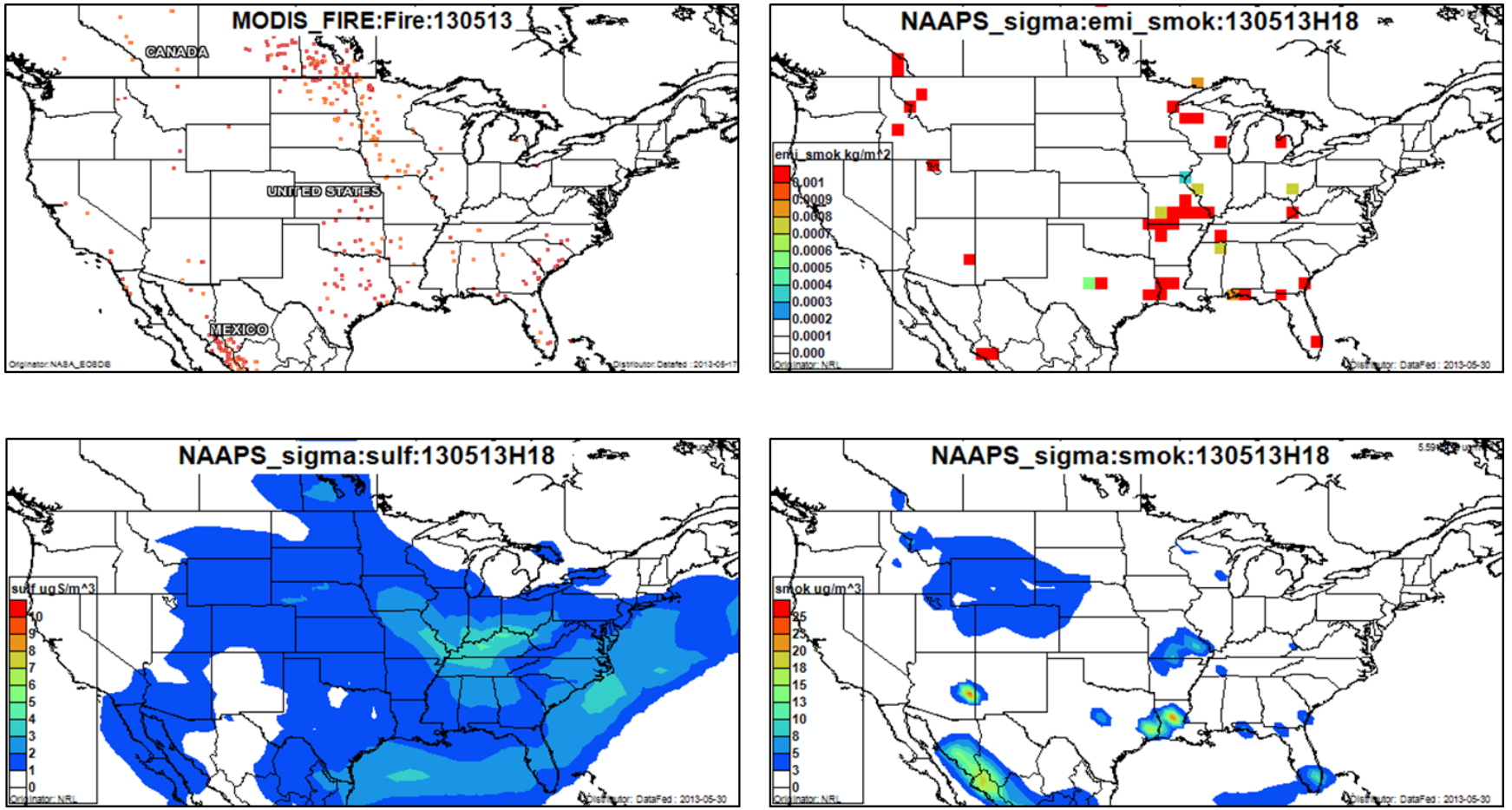

Figure 3-123. May 13, 2013 DataFed analysis. Upper left panel: Locations of active fires from MODIS satellite fire detections. Upper right panel: NAAPS model smoke emissions. Lower left panel: NAAPS model surface layer sulfate concentrations. Lower right panel: NAAPS model surface layer smoke concentrations.

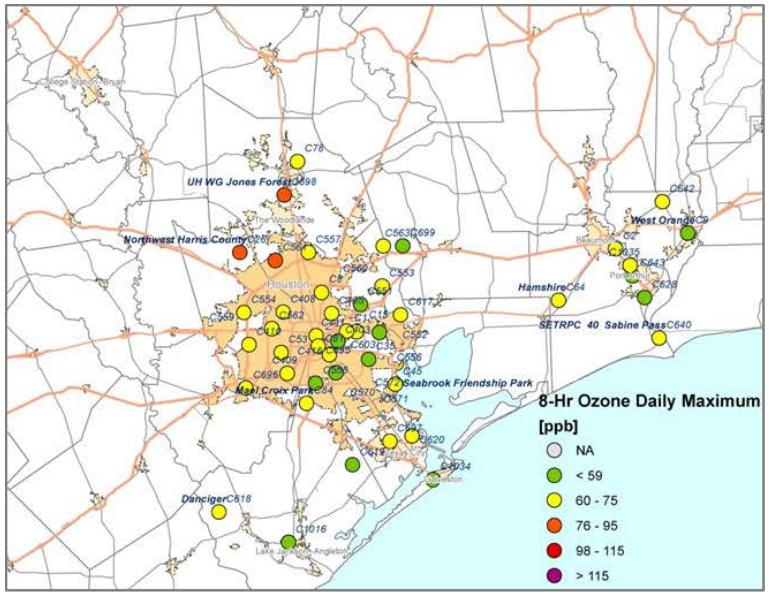

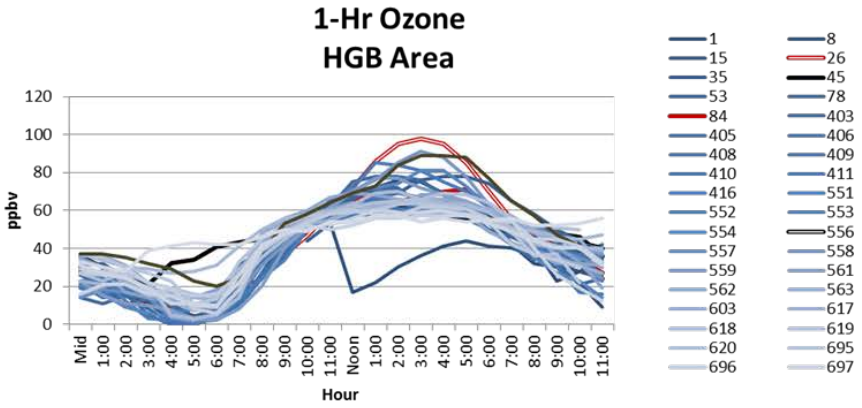

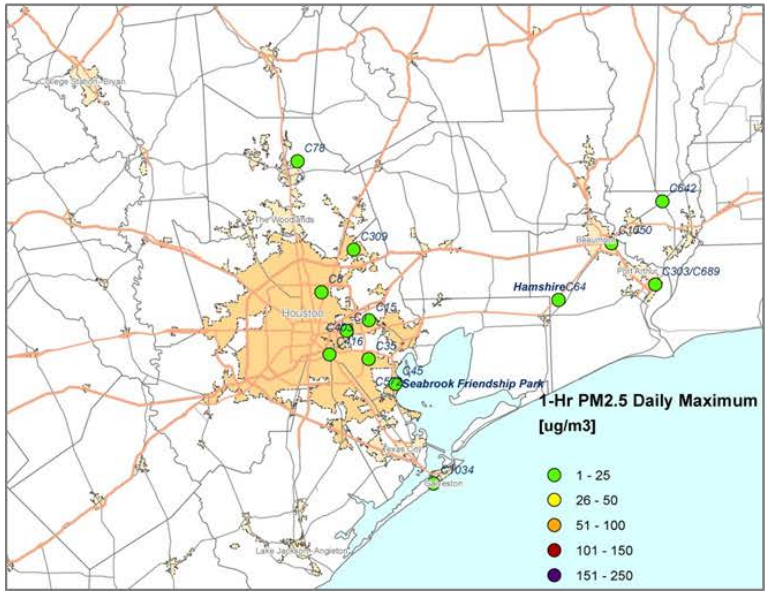

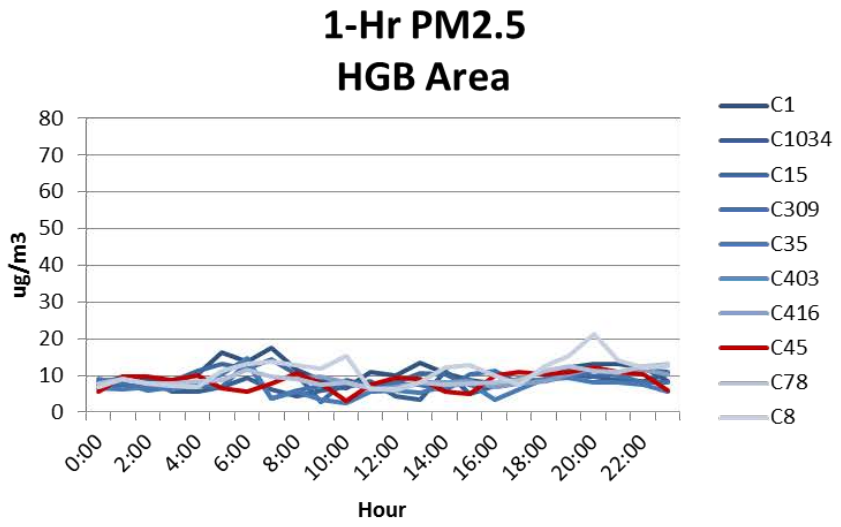

Figure 3-124. Regional ozone (top left and right) and $PM_{2.5}$ (bottom left and right) measurements (HGB area time series).

3.2.3 June 3, 2013

On June 3, 2013, the Manvel Croix (C84) monitor recorded its 3rd high MDA8 value (86 ppb). The MDA1 at Manvel Croix occurred at 3 pm (104 ppb) (Figure 3-125). Background ozone is ~40 ppb. There is a NOx peak during the morning commute period, and NOx data are missing from 8 am-3 pm due to quality control and calibration. NOx is low at 4 pm, one hour after the 1-hour ozone peak at Manvel Croix. Wind vectors at the monitor show northerly winds through 2 pm shifting to southeasterlies by 4 pm and the AQPlot back trajectories in Figure 3-125 show the effect of the sea breeze for all monitors except Hamshire (C64) and Danciger (C618).

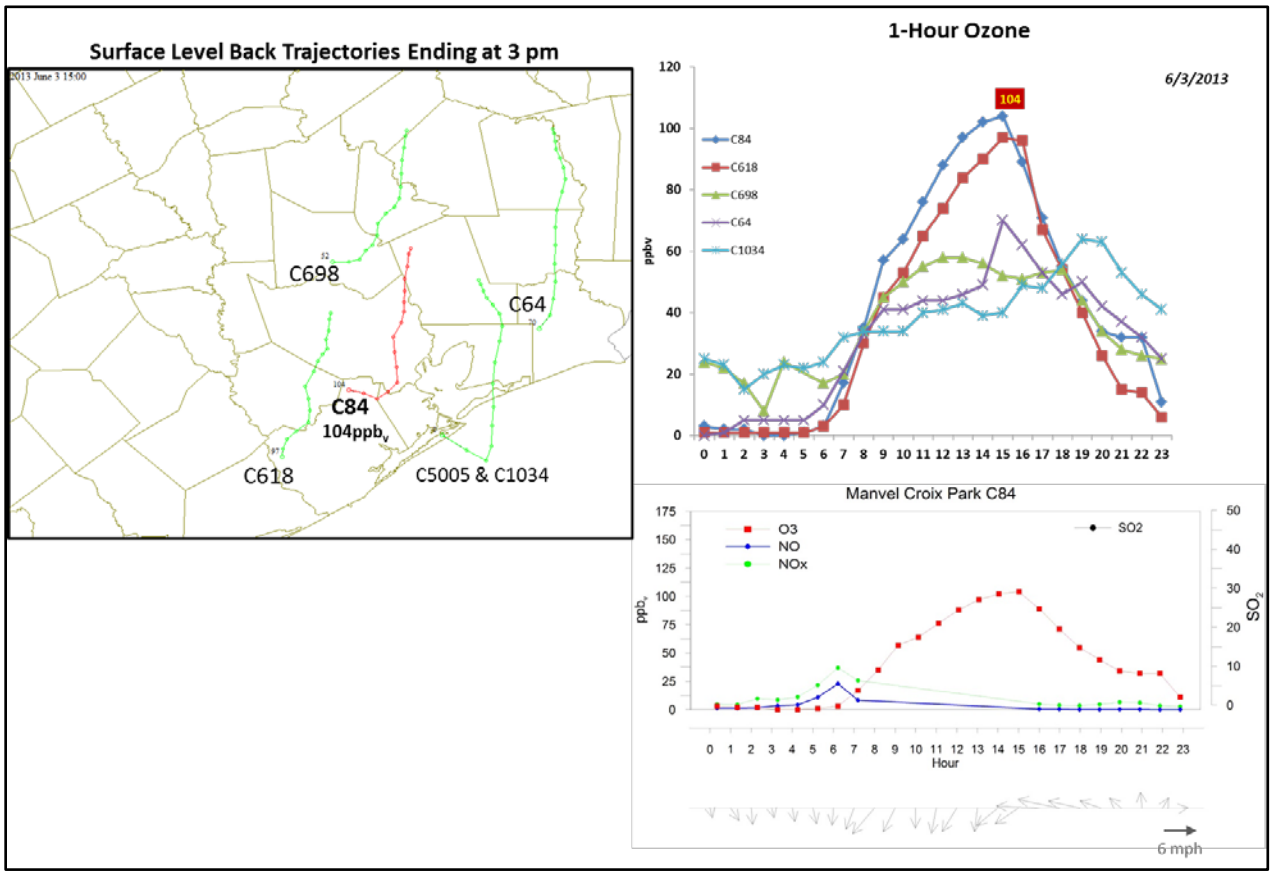

Figure 3-125. June 3, 2013 high ozone day at Manvel Croix C84. Left panel: back trajectories terminating at C84 (red line) and four background HGB monitors (green line) on June 3 at the time of peak ozone impact at C84. Upper right panel: 1-hour average ozone time series for the C84 and surrounding HGB monitors. Lower right panel: time series of 1-hour ozone, NO, NO_2 and wind vectors at the Manvel Croix monitor.

Figure 3-126 shows that back trajectories from the SmartFire tool and the 500 m and 1,500 m back trajectories from HYSPLIT NAM agree that winds were northerly as the air mass approached Manvel Croix, but the HYSPLIT NAM trajectories extend still further northward into Northeast Texas, while the SmartFire trajectory turns southward and moves out over the Gulf of Mexico. The 2,500 m HYSPLIT NAM back trajectory also shows northerly flow on June 3

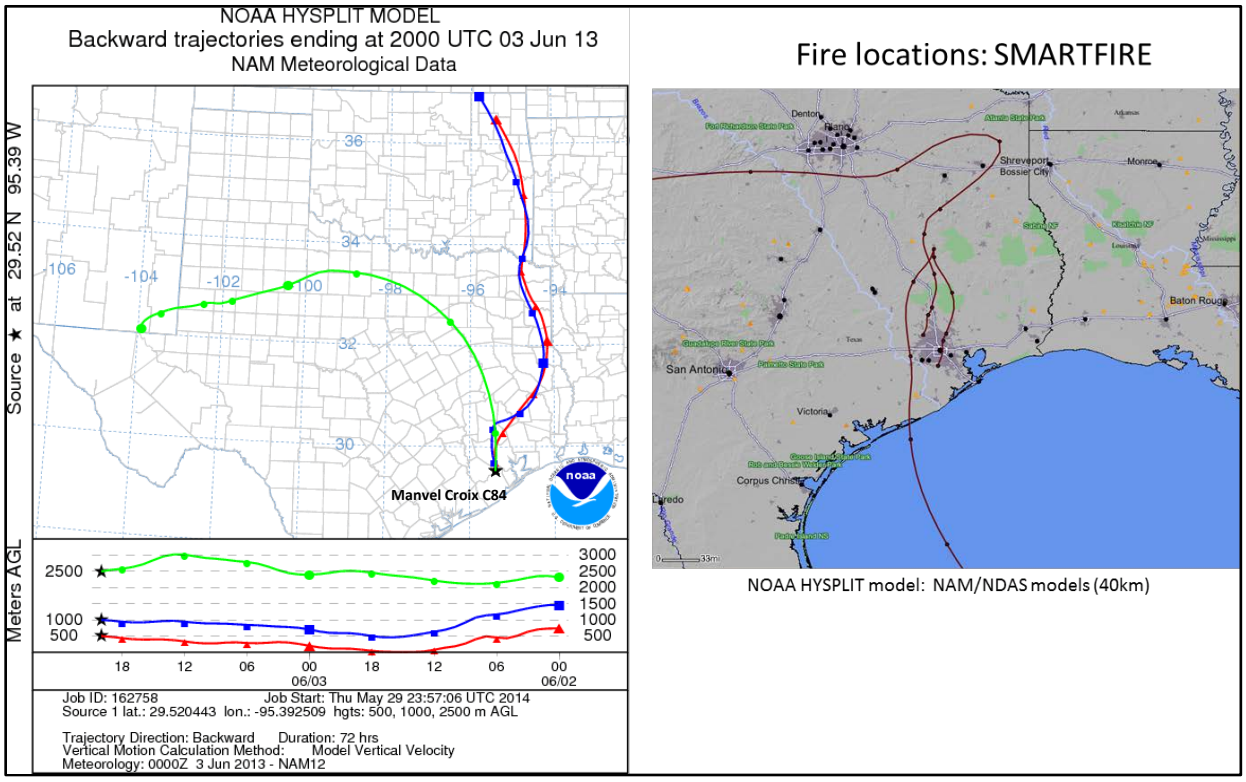

Figure 3-126. 72-hour HYSPLIT back trajectories ending at Manvel Croix C84 on June 3, 2013; Right side: SmartFire plot with nearby fire locations (orange triangles) and 72-hour HYSPLIT back trajectories terminating at HGB sites (C26 and C84).

but extends westward across Texas similar to the SmartFire trajectory for the NW Harris monitor. The back trajectories agree that the winds were northerly on the morning of June 3, but prior to June 3, they disagree on wind direction. Therefore, the back trajectory analysis has limited usefulness for determining the origin of the air mass arriving at Manvel Croix on June 3.

The SmartFire map (Figure 3-126) and the HMS product (Figure 3-127) both show fires along the Texas-Louisiana border and between Houston and Dallas. Although the NAAPS analysis indicates the presence of smoke in the HGB area and BPA areas, the HMS product shows no smoke over East Texas, and the $PM_{2.5}$ AQI plot does not indicate elevated levels of $PM_{2.5}$ over East Texas (Figure 3-128). The FINN emissions show no fires along the paths of either the SmartFire back trajectory for Manvel Croix or the 500 m and 1,500 m back trajectories.

Figure 3-131 shows that $PM_{2.5}$ levels are low (<20 µg m^{-3}) at all monitors in the HGB area. Because there is no evidence of fire plume impact at any monitor, we recommend no further analysis of June 3, 2013.

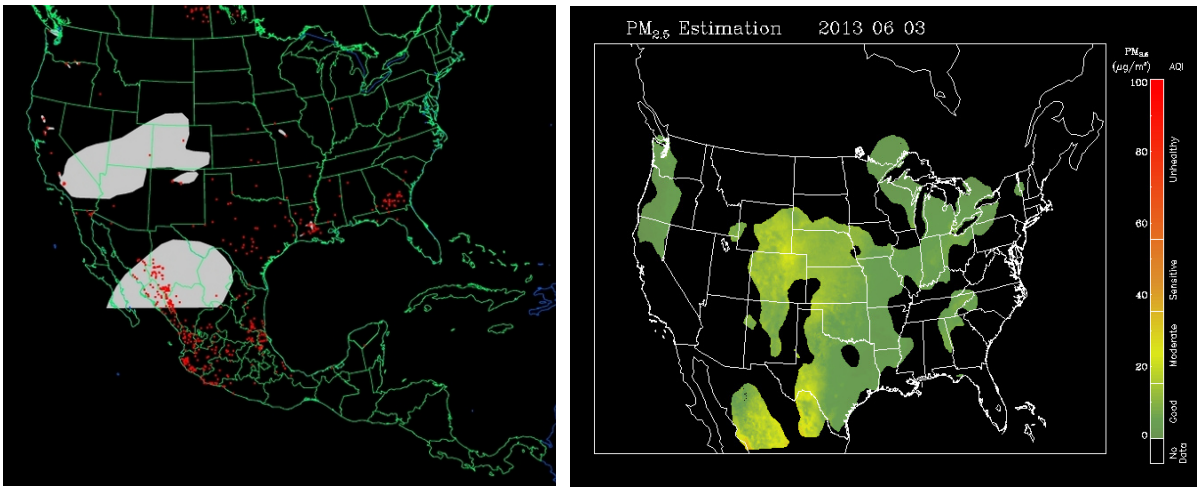

Figure 3-127. Left panel: HMS product showing June 3 fire locations (red dots) and smoke plume (gray area). Right panel: IDEA surface $PM_{2.5}$ estimate based on AOD and surface monitoring data.

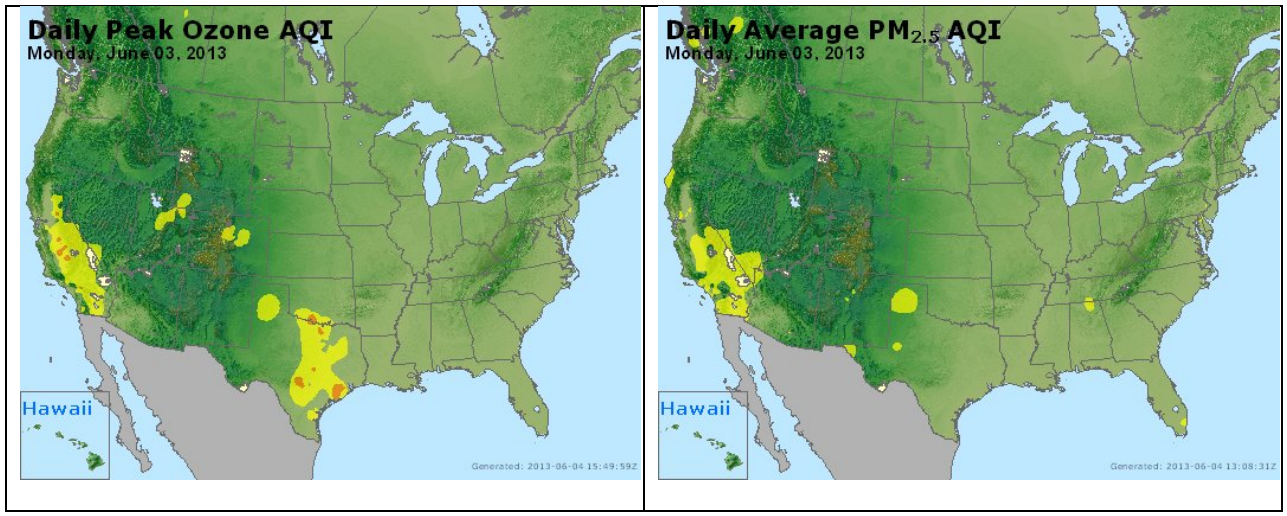

Figure 3-128. Daily average ozone (left) and $PM_{2.5}$ (right) based on observed values. Data from: http://www.airnow.gov/.

Wildfire Emissions Inventory: FINN 2013

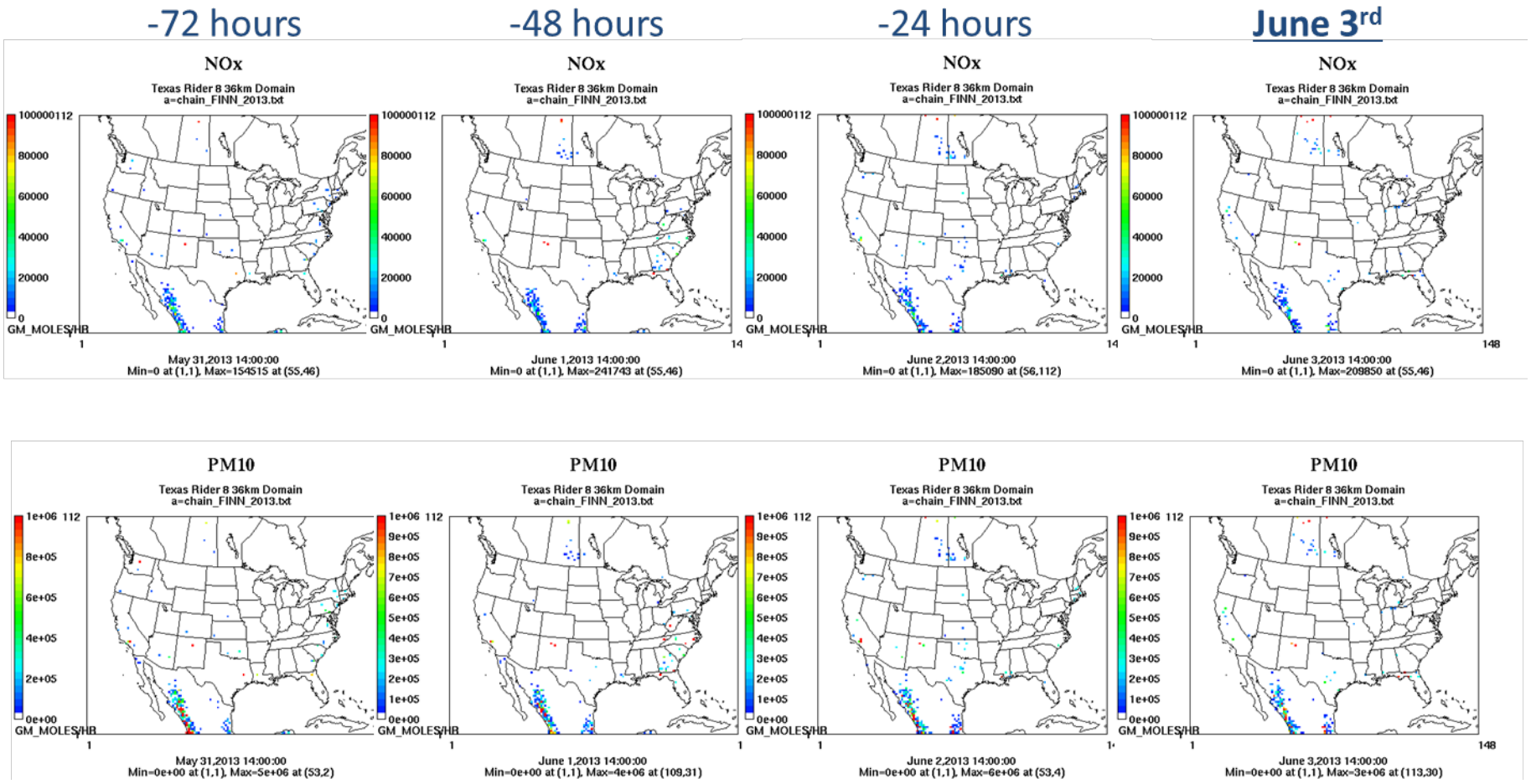

Figure 3-129. June 3, 2013 FINN fire emissions of NOx and PM_{10}.

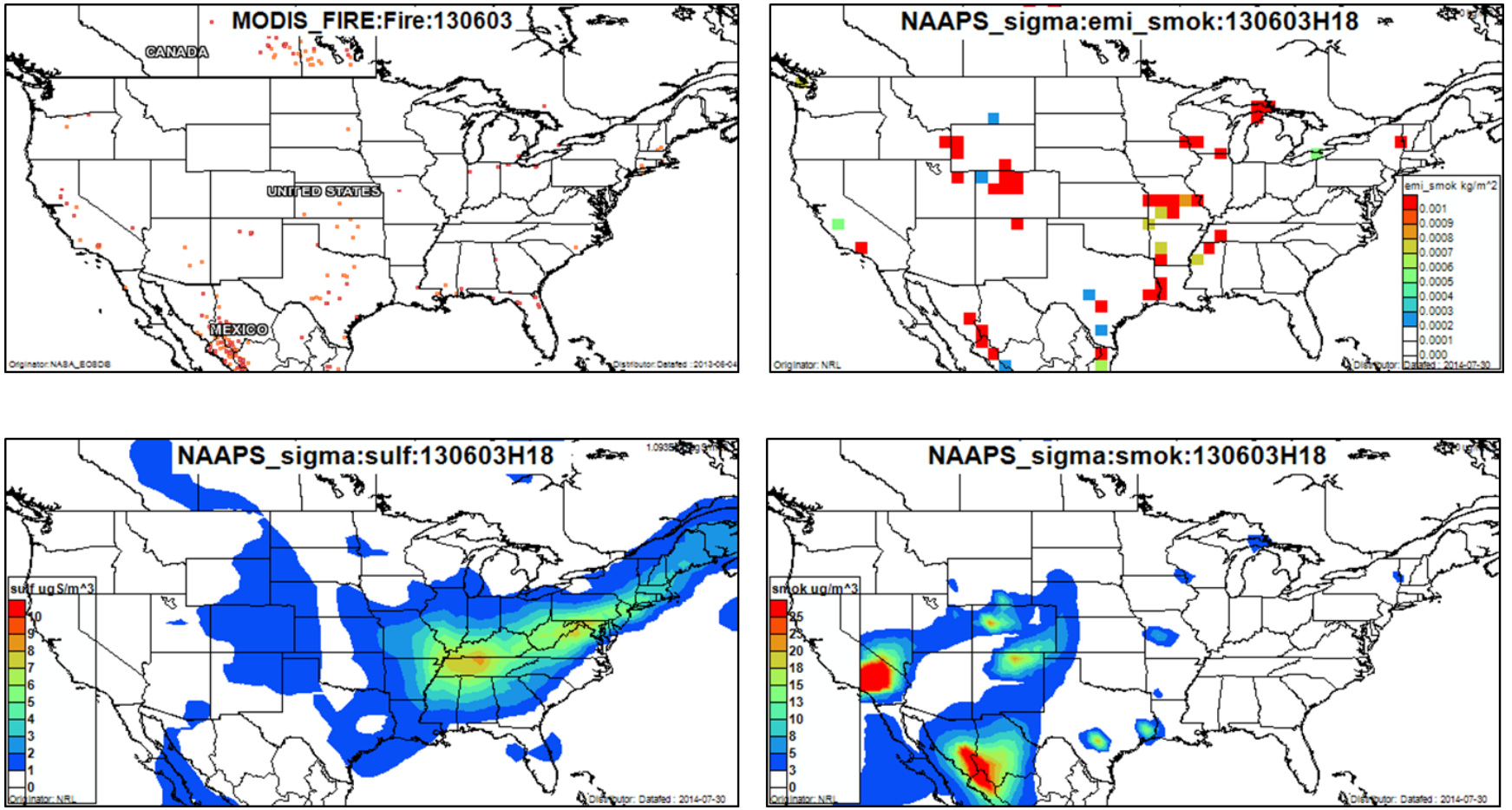

Figure 3-130. June 3, 2013 DataFed analysis. Upper left panel: Locations of active fires from MODIS satellite fire detections. Upper right panel: NAAPS model smoke emissions. Lower left panel: NAAPS model surface layer sulfate concentrations. Lower right panel: NAAPS model surface layer smoke concentrations.

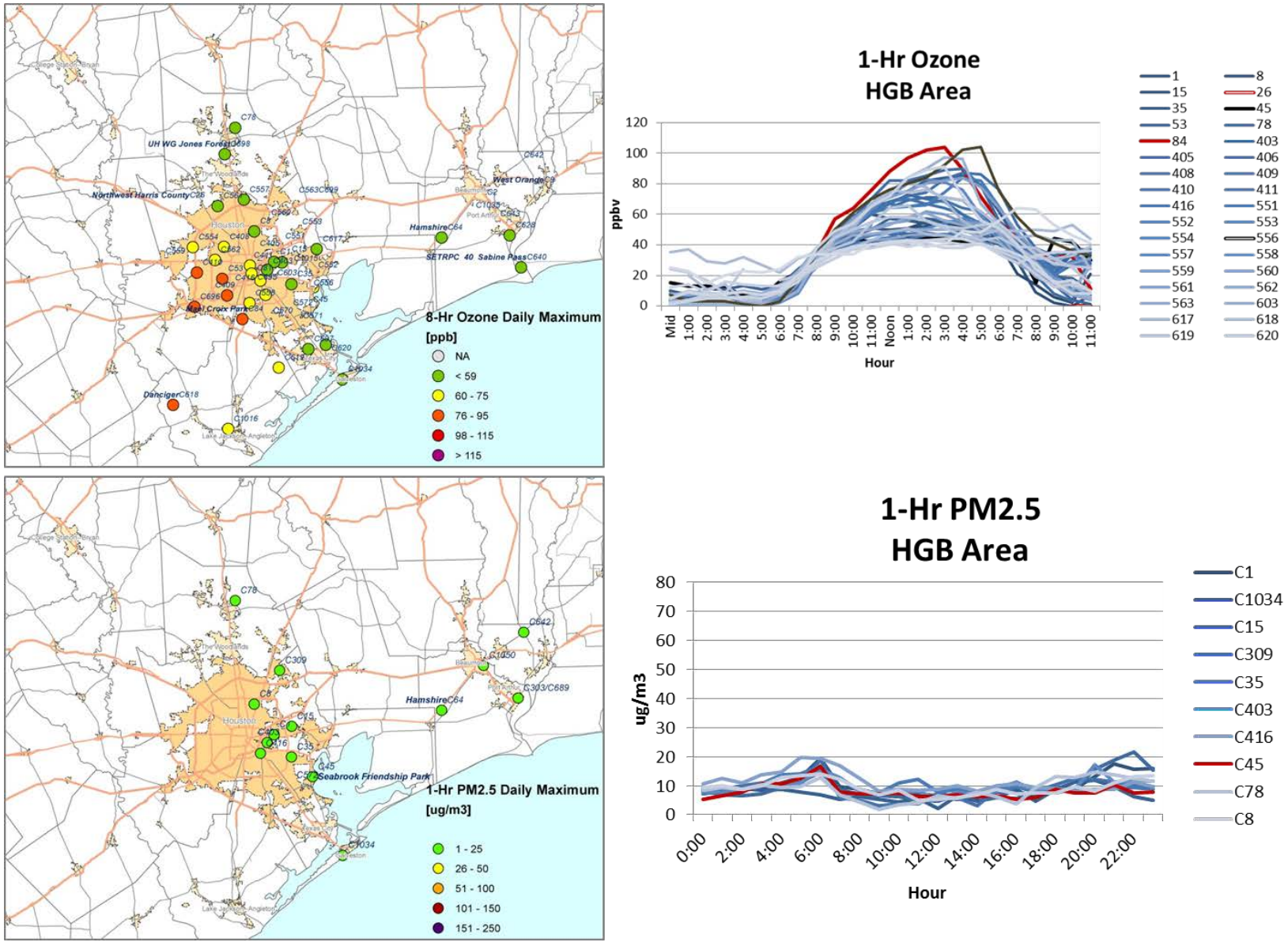

Figure 3-131. Regional ozone (top left and right) and $PM_{2.5}$ (bottom left and right) measurements (HGB area time series).

3.2.4 July 2, 2013

On July 2, 2013, the Manvel Croix Park monitor (C84) recorded its 4th high ozone MDA8 (84 ppb). At Manvel Croix, the peak 1-hour ozone value on July 2 was 92 ppb, which was well above the background level of ~45 ppb (Figure 3-139). Manvel Croix had the highest value of MDA1 ozone of any monitor in the HGB area on July 2, and was the only monitor with MDA8>75 ppb. Inspection of the 1-hour time series for Manvel Croix shows that there is a morning peak in NOx around the time of the morning commute, and that the NOx level fall as ozone rises; NOx then remains low throughout the rest of the day (Figure 3-132). Wind vectors at the monitor show northeasterly winds from 5 am until 3 pm, when the winds shift to southeasterlies. This is consistent with the AQPlot back trajectories, which show recirculating trajectories consistent with a sea breeze for sites nearest the coast (C1034, C618). Because the back trajectories are initiated at the time of Manvel Croix peak ozone at 3 pm, the recirculation that takes place at Manvel in the late afternoon is not apparent on the AQPlot back trajectory; the sea breeze has

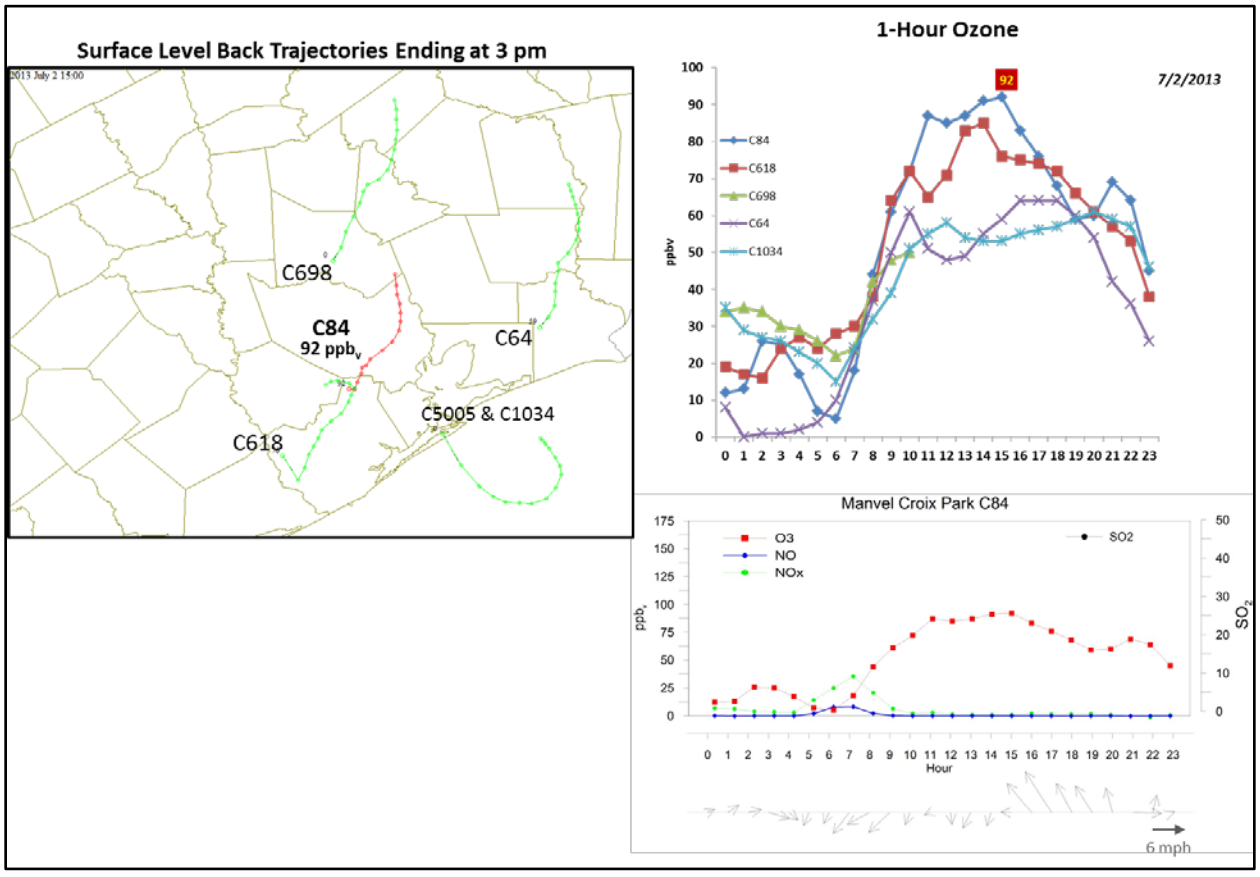

Figure 3-132. July 2, 2013 high ozone day at Manvel Croix C84. Left panel: back trajectories terminating at C84 (red line) and four background HGB monitors (green line) on July 2 at the time of peak ozone impact at C84. Upper right panel: 1-hour average ozone time series for the C84 and surrounding HGB monitors. Lower right panel: time series of 1-hour ozone, NO, NO_2 and wind vectors at the Manvel Croix monitor.

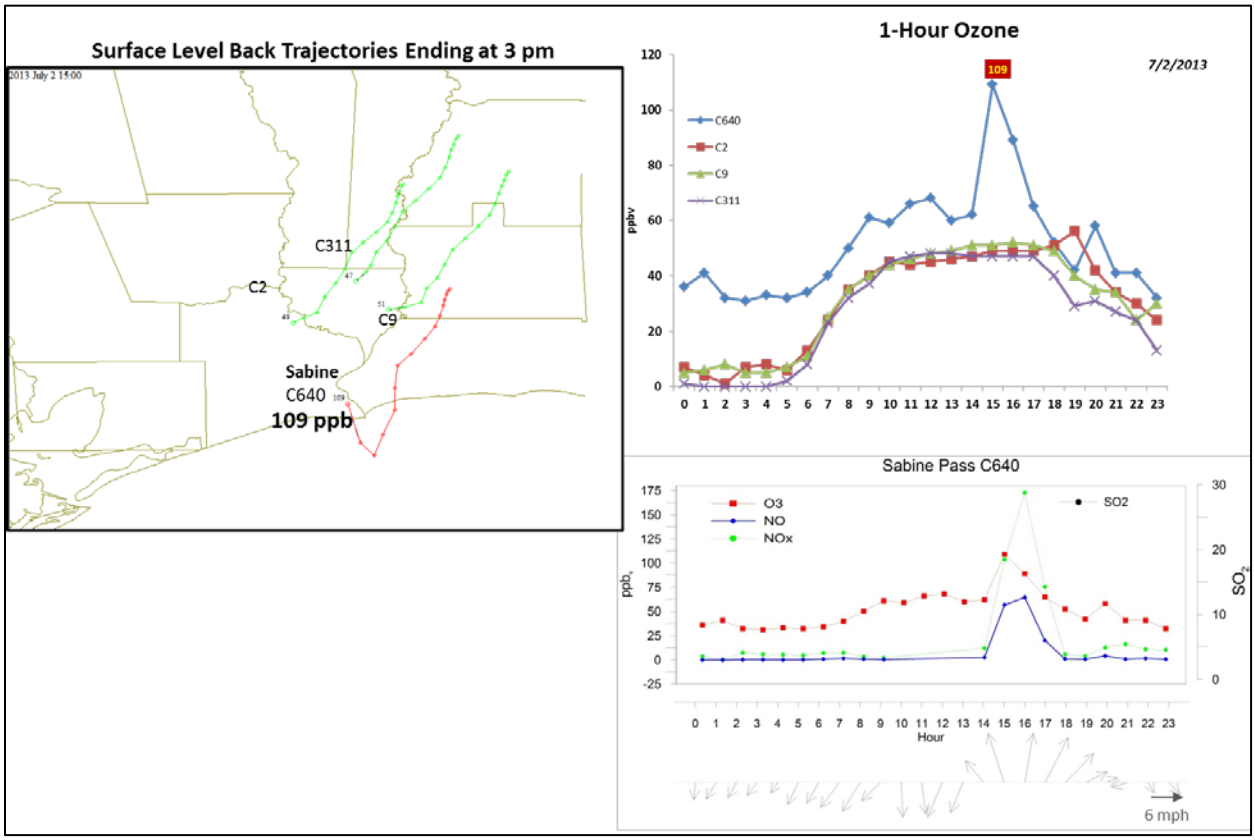

Figure 3-133. July 2, 2013 high ozone day at Sabine Pass C640. Left panel: back trajectories terminating at C640 (red line) and four background BPA monitors (green line) on July 2 at the time of peak ozone impact at C640. Upper right panel: 1-hour average ozone time series for the C640 and surrounding BPA monitors. Lower right panel: time series of 1-hour ozone, NO, NO_2 and wind vectors at the Sabine Pass monitor.

only just penetrated to Manvel Croix by 3 pm. The C698 monitor, located further inland, is unaffected by the sea breeze and shows northeasterly flow, as does the C64 monitor.

Back trajectories for SmartFire and HYSPLIT NAM are consistent with the AQPlot trajectories for the C698 and C64 monitors, showing northeasterly flow into the HGB area on July 2 (Figure 3-134). The SmartFire map shows fires north of the HGB area along the SmartFire and HYSPLIT NAM back trajectories. The HMS product (Figure 3-135) and NAAPS analyses (Figure 3-138) also show fires in this region on July 2, along with a smoke plume that covers all of East Texas. The FINN emissions plots (Figure 3-137) show fire activity north of Houston on July 2 and fires along the back trajectory paths at -72 hours. There are no fires along the back trajectory paths at -24 and -48 hours.

The ozone spatial distribution shows a northeast-southwest gradient across the HGB area consistent with a northwesterly wind direction. There are lower values of MDA8 at sites in the northeast (upwind) of the HGB area and higher values of MDA8 at sites in the southeastern (downwind) part of the HGB area (Figure 3-139). The ozone time series show that only the

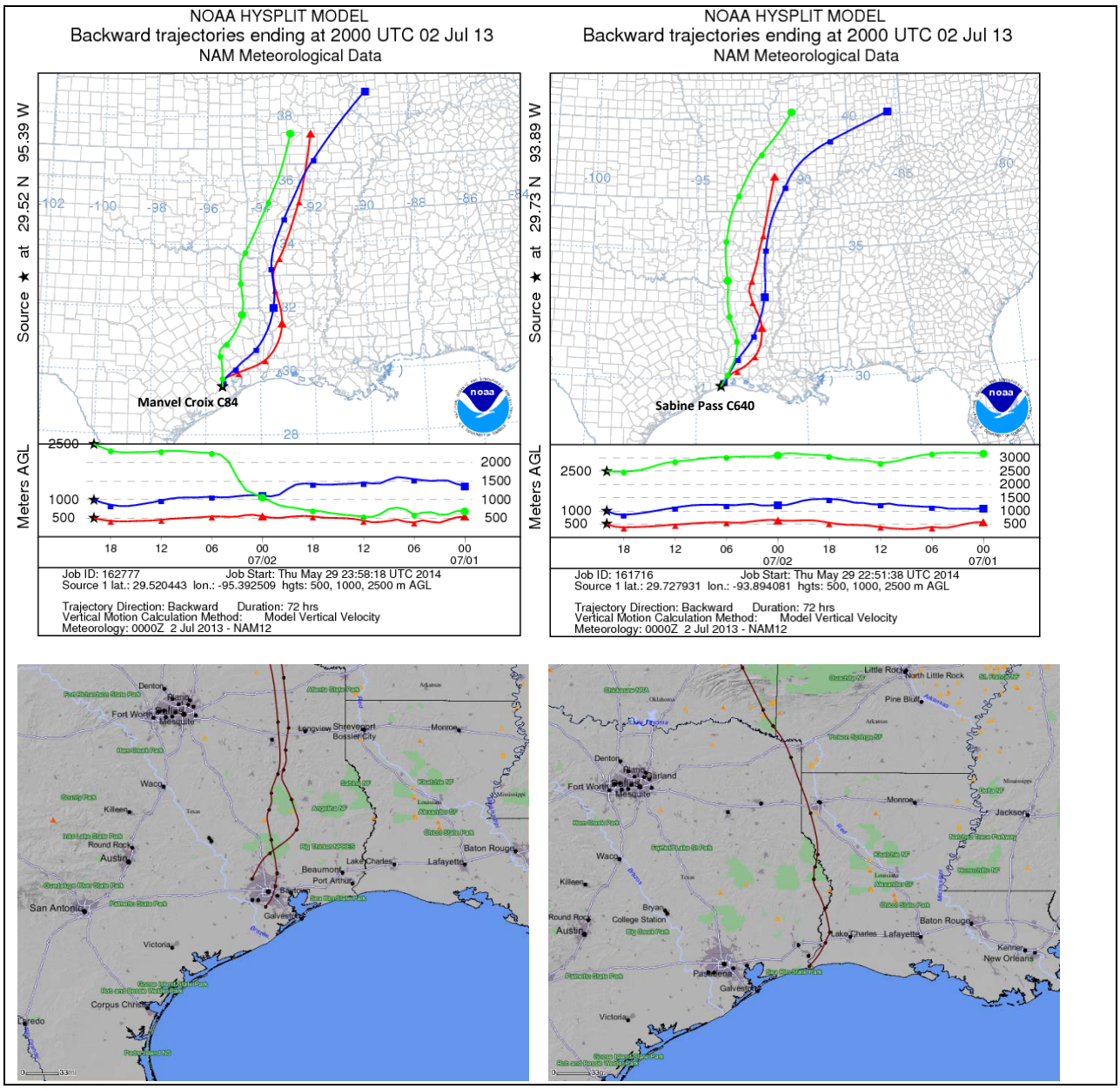

Figure 3-134. 72-hour HYSPLIT back trajectories ending at Manvel Croix C84 (upper left) and Sabine Pass C640 (upper right) on July 2, 2013; Bottom: SmartFire plots with fire locations (orange triangles) and 72-hour HYSPLIT back trajectories terminating at HGB sites (C26 and C84; bottom left) and Sabine Pass C640 in the BPA (bottom right).

Manvel Croix and Danciger (C618) monitors have plume impacts that lift their ozone levels above the rest of the HGB area monitors. The Danciger monitor is located downwind of the Manvel Croix monitor and there is a lag between the onset of high ozone at Manvel Croix and Danciger that is consistent with transport of the HGB urban plume downwind to Danciger.

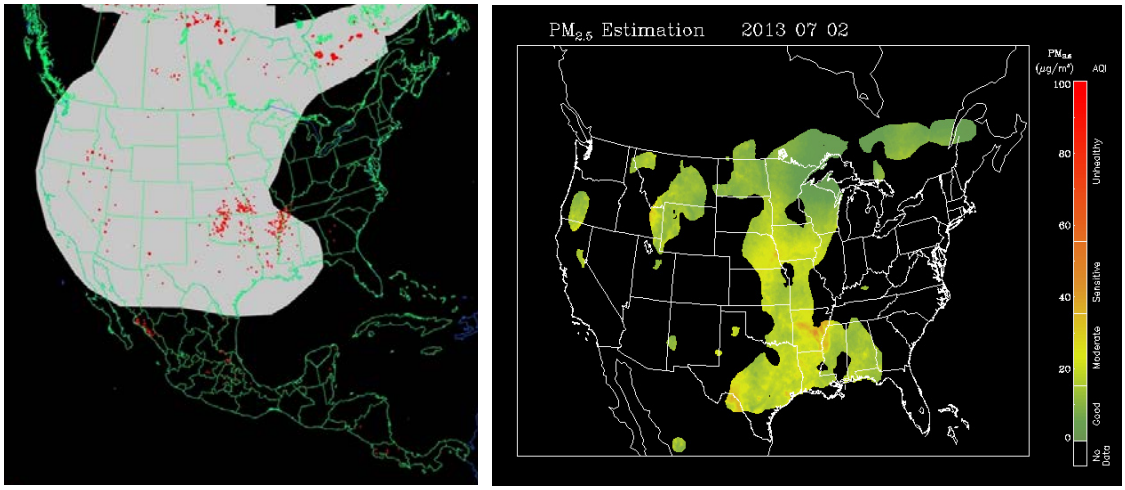

Figure 3-135. Left panel: HMS product showing July 2 fire locations (red dots) and smoke plume (gray area). Right panel: IDEA surface $PM_{2.5}$ estimate based on AOD and surface monitoring data.

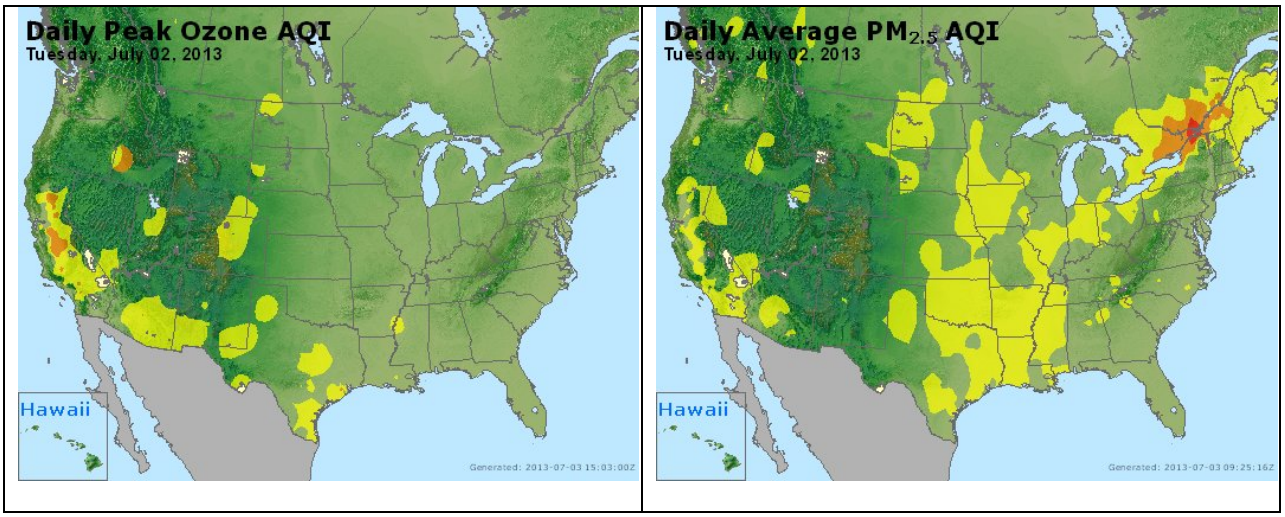

Figure 3-136. Daily average ozone (left) and $PM_{2.5}$ (right) based on observed values. Data from: http://www.airnow.gov/.

The $PM_{2.5}$ time series indicate that $PM_{2.5}$ is low for all sites during the period where ozone is high for the HGB monitors, so that there is no evidence of a fire plume impact. We therefore recommend no further evaluation of July 2 for the Manvel Croix monitor.

The Sabine Pass monitor (C640) had its 2nd high MDA8 (72 ppb) on July 3. Background ozone levels in the BPA area were ~50 ppb on July 2 (Figure 3-140), but the Sabine Pass monitor recorded an MDA1 of 109 ppb (Figure 3-133). This ozone maximum has the characteristics of a plume impact, rising sharply and suddenly above the ozone values at the other BPA monitors.

Coincident with the ozone peak are peaks in NO and NOx, which indicate the presence of fresh combustion emissions in the plume affecting the Sabine Pass monitor.

The AQPlot back trajectories for the BPA area show northeasterly flow for all monitors except Sabine Pass, which has northeasterly flow until 2 pm, when the wind shifts to southeasterly. One hour after the wind shift, the plume impact at Sabine Pass begins. The curvature in the AQPlot back trajectory for the Sabine Pass monitor suggests that a plume containing fresh emissions moved offshore and then came back ashore with the sea breeze causing high ozone at Sabine Pass. A second possibility is that offshore emissions sources contributed to the plume impact.

The SmartFire and HYSPLIT back trajectories show northerly flow leading up to the time of peak ozone at Sabine Pass. The SmartFire map shows no fires in the immediate vicinity of the BPA area, but both sets of trajectories transit the industrial Lake Charles area to the north of the BPA area. There are fires further north in Louisiana in the SmartFire map as well as in the HMS product (Figure 3-135) and the FINN show emissions in northern Louisiana along the back trajectories (Figure 3-137). The FINN, HMS and SmartFire data sets agree that there were no local fires in the BPA area on July 2, which indicates that the cause of the ozone plume, which contained fresh NO `emissions, was likely a local emissions source rather than a distant fire plume.

$PM_{2.5}$ data from BPA area monitors show low levels of $PM_{2.5}$ (<25 µg m^{-3}). There is no evidence of a $PM_{2.5}$ plume that would indicate that high levels of ozone were associated with fire plume emissions. Therefore, we recommend that no further evaluation of July 2 be performed for the Sabine Pass monitor.

Wildfire Emissions Inventory: FINN 2013

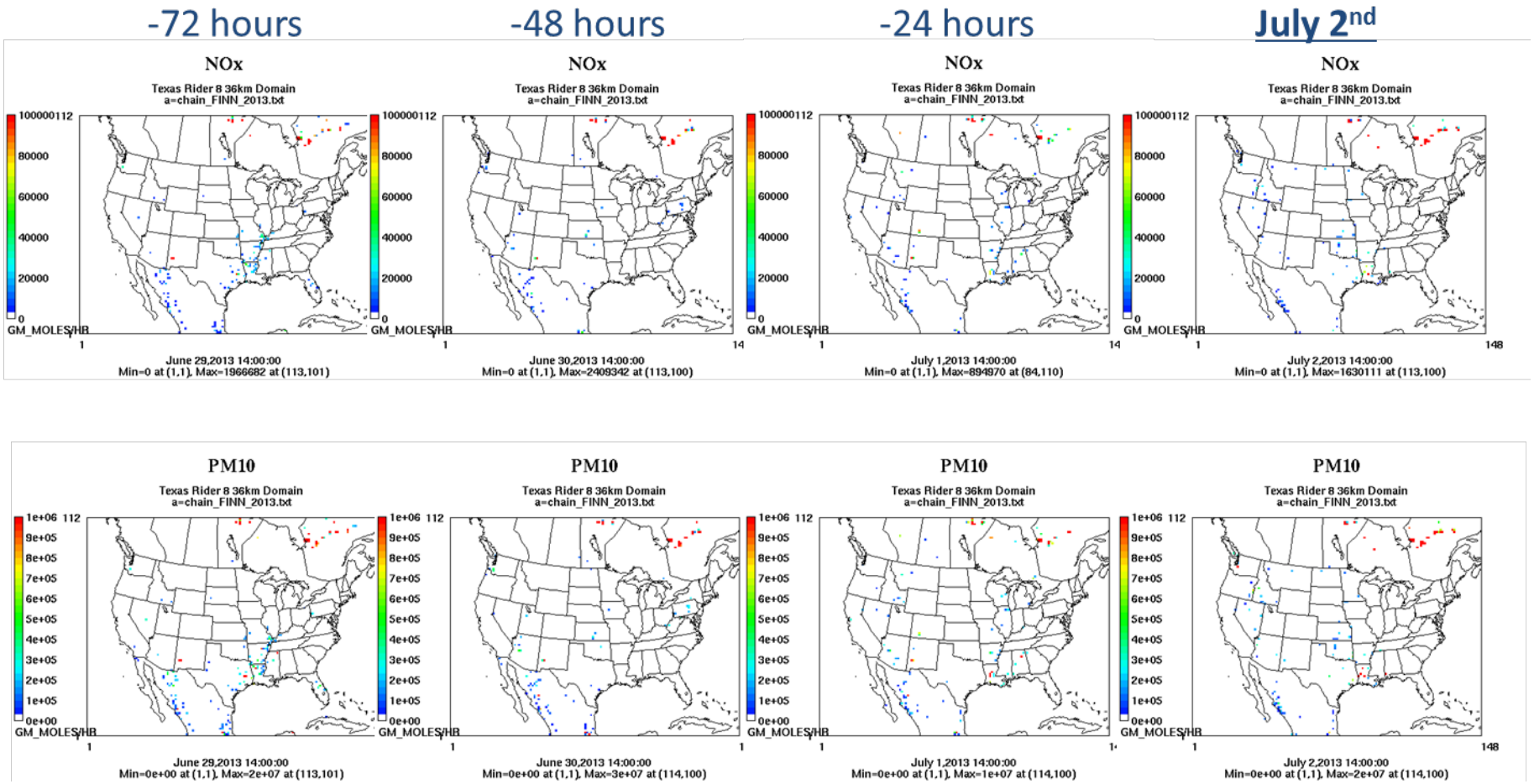

Figure 3-137. July 2, 2013 FINN fire emissions of NOx (top) and PM_{10} (bottom).

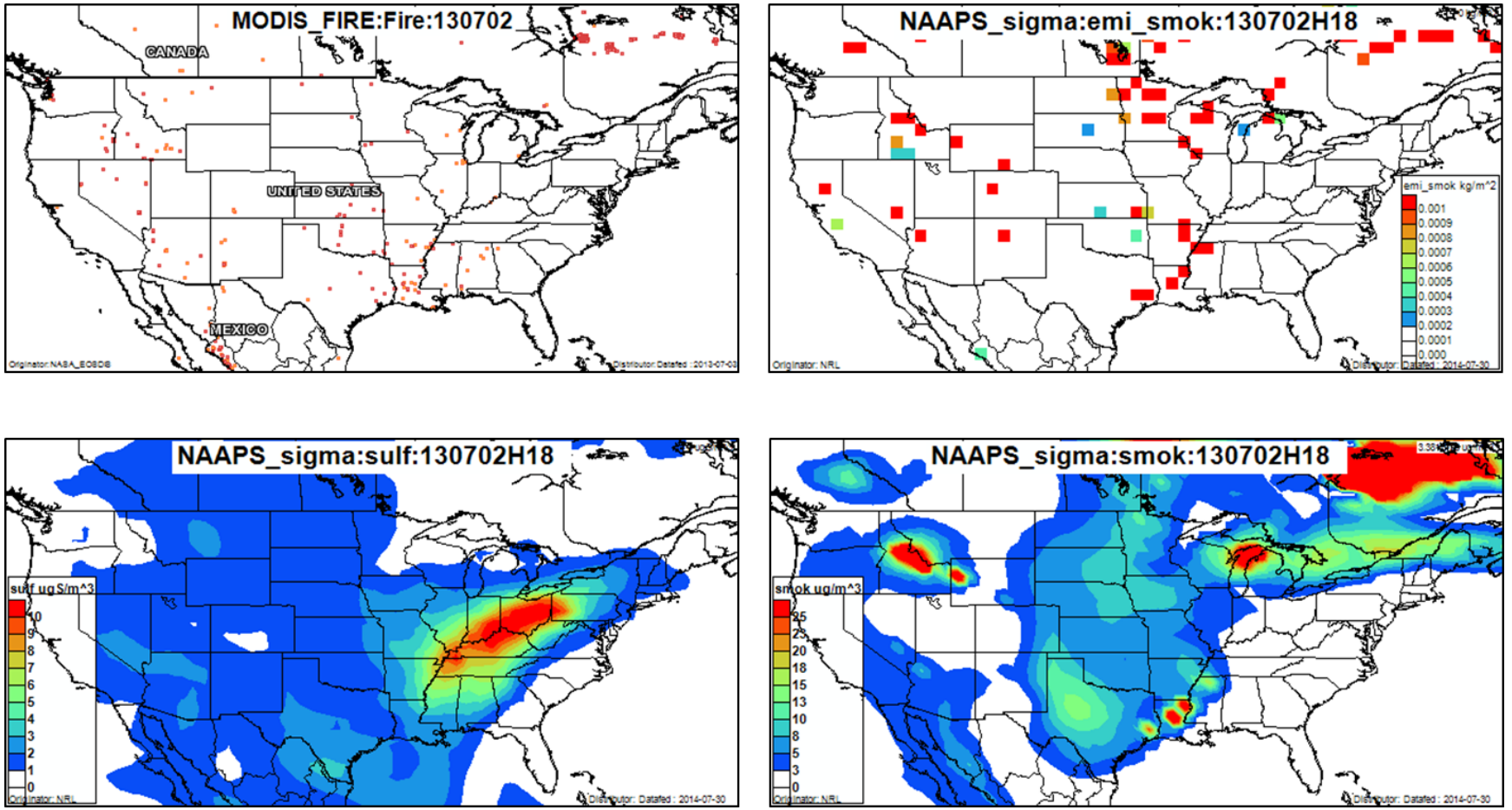

Figure 3-138. DataFed analysis. Upper left panel: Locations of active fires from MODIS satellite fire detections. Upper right panel: NAAPS model smoke emissions. Lower left panel: NAAPS model surface layer sulfate concentrations. Lower right panel: NAAPS model surface layer smoke concentrations.

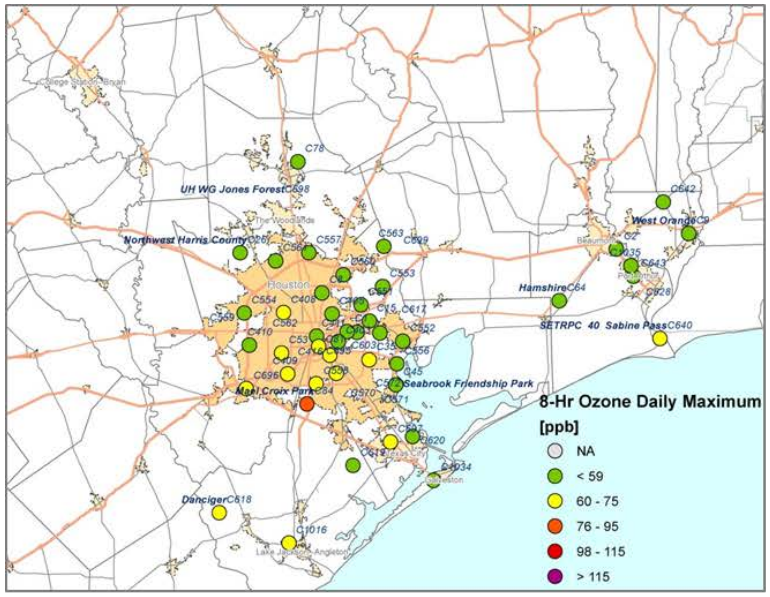

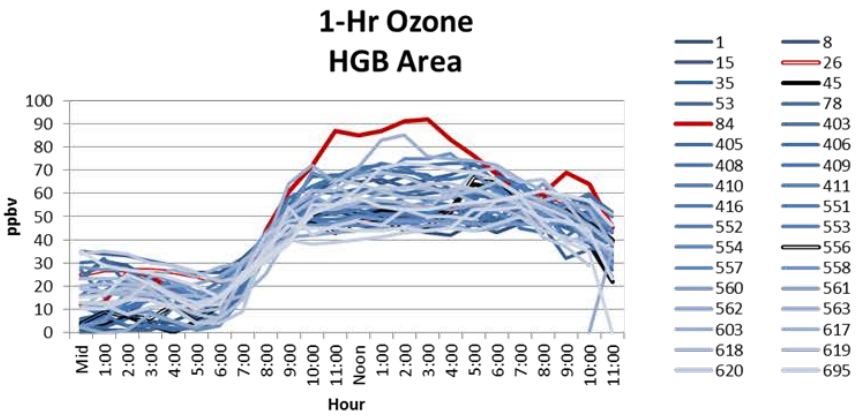

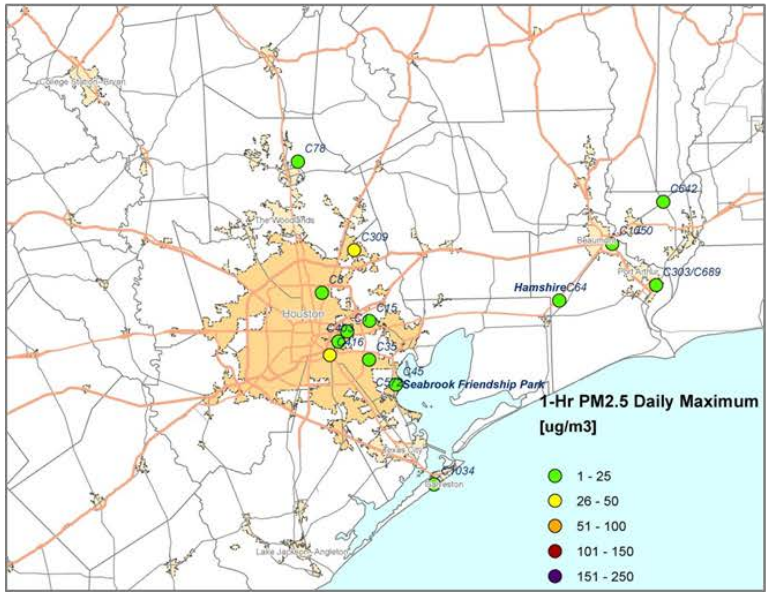

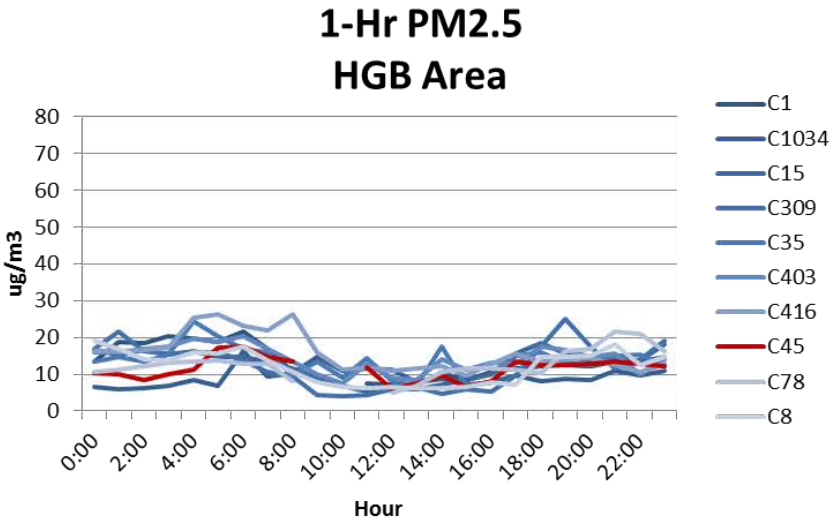

Figure 3-139. Regional ozone (top left and right) and $PM_{2.5}$ (bottom left and right) measurements (HGB area time series).

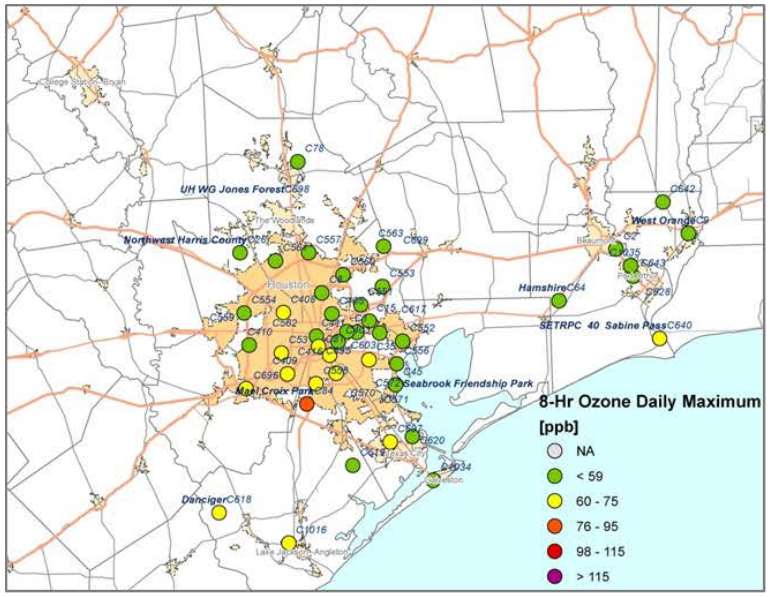

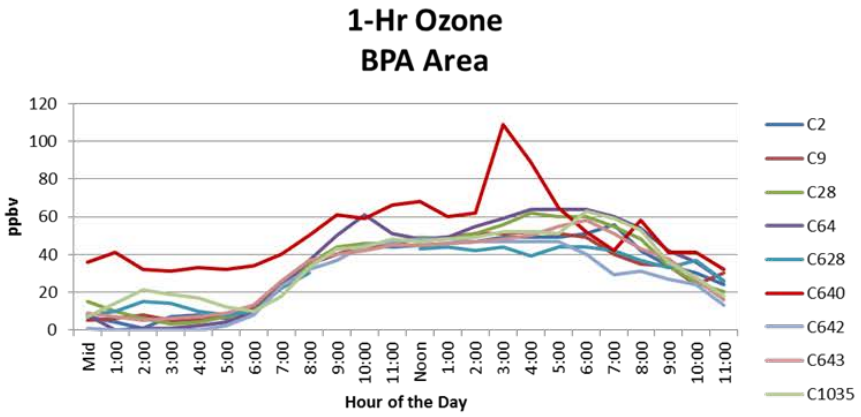

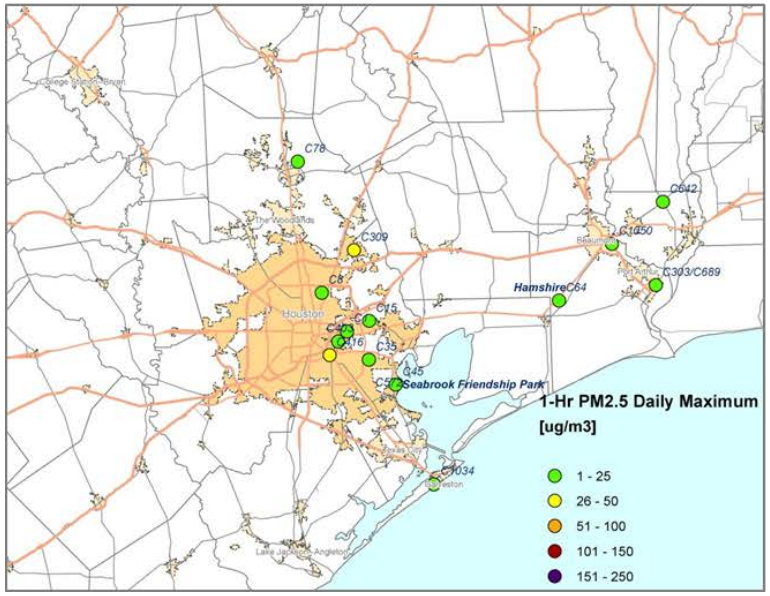

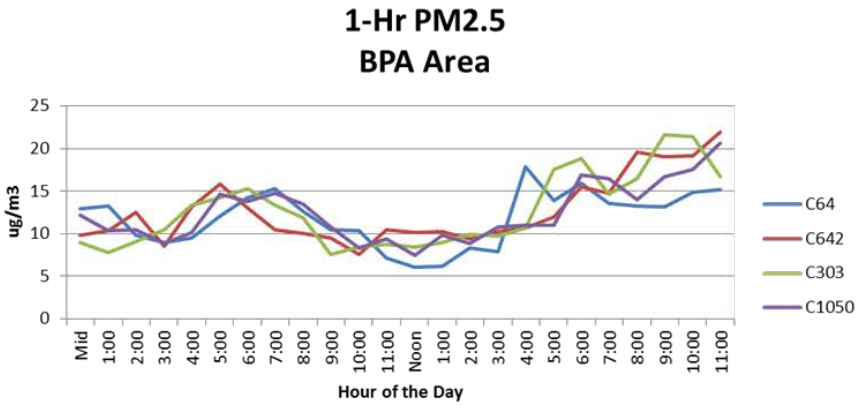

Figure 3-140. Regional ozone (top left and right) and $PM_{2.5}$ (bottom left and right) measurements (BPA area time series).

3.2.5 July 3, 2013

On July 3, 2013, the Northwest Harris Co. monitor (C26) recorded its 4th high MDA8 reading of 80 ppb. The monitor had a late afternoon 1-hour ozone peak of 98 ppb at 4 pm (Figure 3-141). The AQPlot back trajectory for the NW Harris monitor agrees with the C26 wind vectors, showing light early morning winds, shifting to southerlies at 10 am (Figure 3-141). The SmartFire and HYSPLIT NAM 500 m back trajectories show northerly flow leading up to July 3. The back trajectories then show anti-cyclonic motion, curving northeastward across the HGB area before arriving at the monitor. The SmartFire map indicates that there were fires on the eastern outskirts of the HGB area (Figure 3-142). These fires appear in the HMS product (Figure 3-143) and DataFed MODIS fire location plot (Figure 3-146) as well as in the FINN emissions maps for July 3 and for -24 hours (Figure 3-143). The SmartFire map also shows fires at the coast in the BPA area and a second pair of fires northwest of the BPA area. These BPA fires near the Sabine Pass monitor appear in the HMS product, but not in the FINN inventory. All of the HGB and BPA area fires lie in the region traversed by the back trajectories.

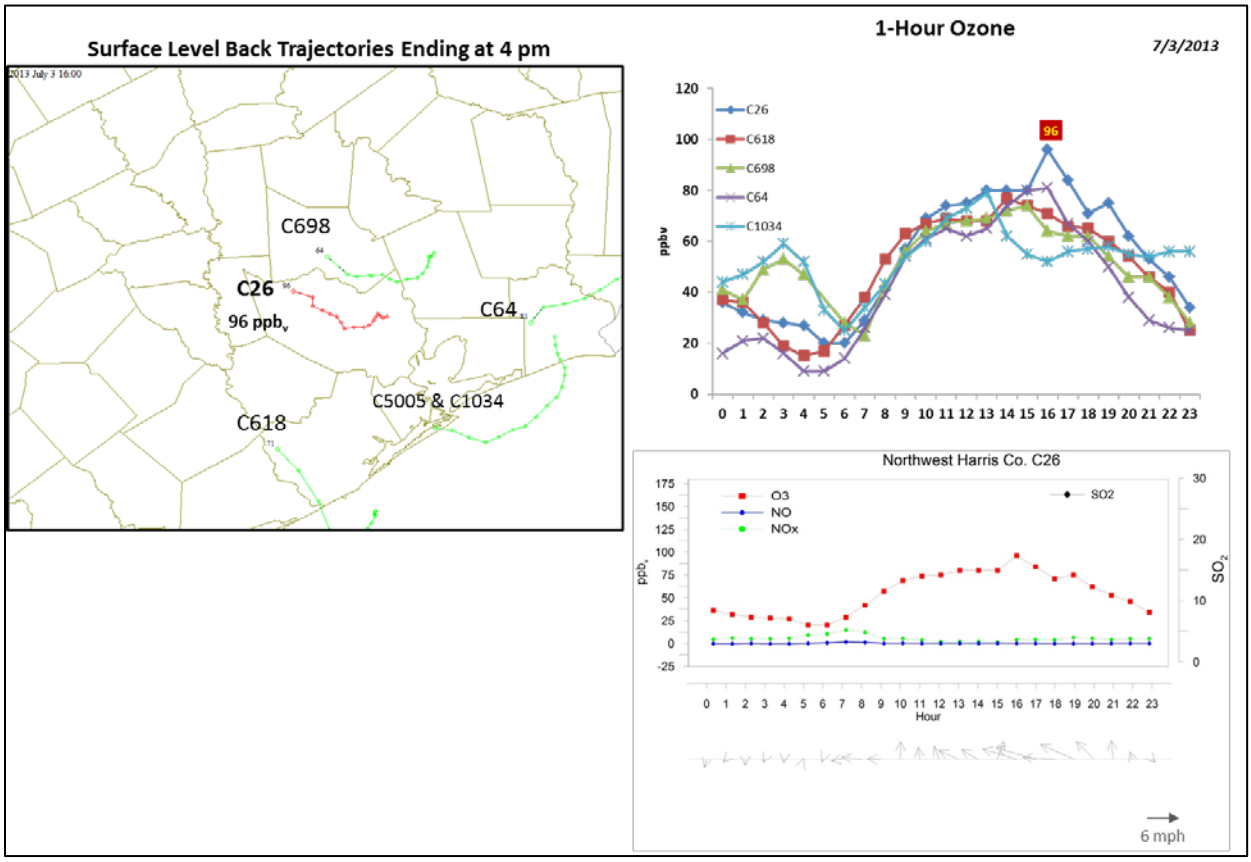

Figure 3-141. July 3, 2013 high ozone day at Northwest Harris C26. Left panel: back trajectories terminating at C26 (red line) and four background BPA monitors (green line) on July 3 at the time of peak ozone impact at C26. Upper right panel: 1-hour average ozone time series for the C26 and surrounding BPA monitors. Lower right panel: time series of 1-hour ozone, NO, NO_2 and wind vectors at the Northwest Harris monitor.

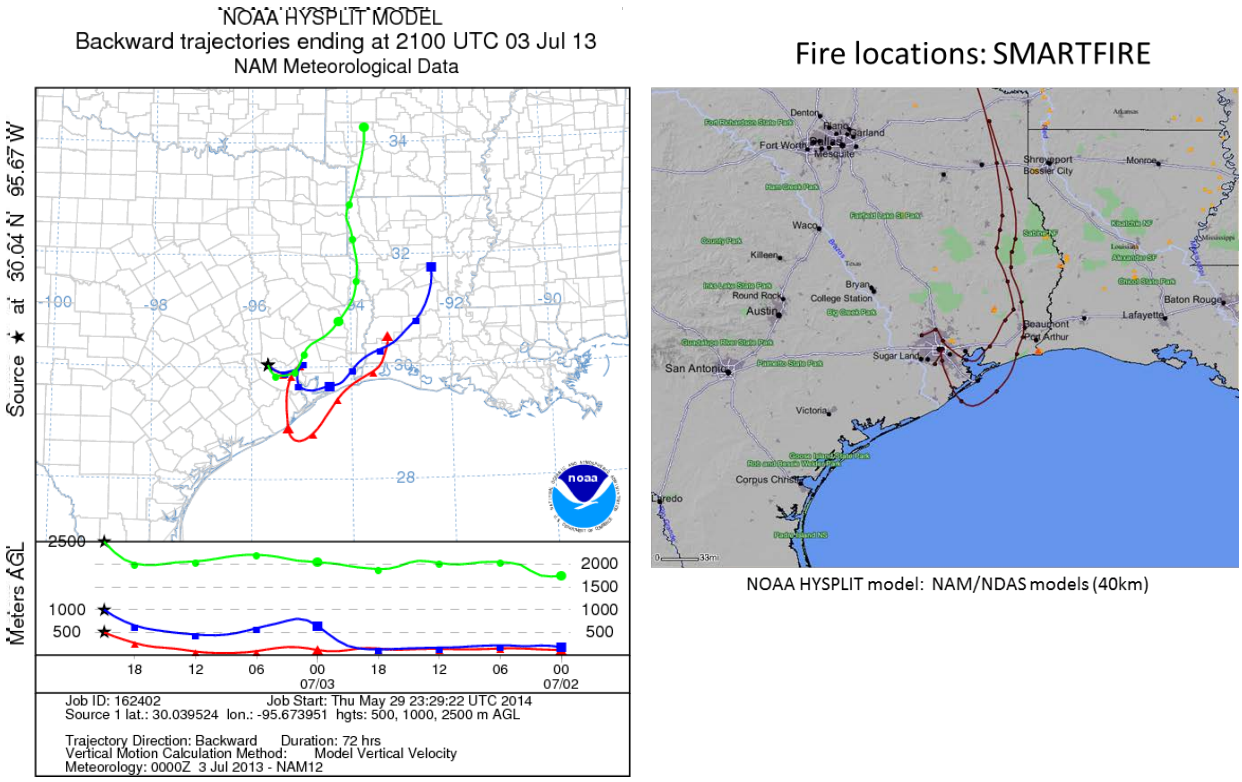

Figure 3-142. 72-hour HYSPLIT back trajectories (NAM 12km) from Northwest Harris C26 ending July 3, 2013; SmartFire plot showing f fire locations (orange triangles) and 72-hour HYSPLIT back trajectories (EDAS 40 km) from C26.

The spatial pattern of MDA8 ozone (Figure 3-147) is consistent with the easterly/southeasterly winds shown in the back trajectories on July 3. Monitors with MDA8>75 ppb are all located in the central and western regions of the HGB urban area. High ozone values above the background occur first at the Park Place (C416) and UH Moody Tower (C695) monitors. Peaks then occur at Lang (C408) and Bayland Park (C53) and finally, ozone peaks appear at the West Houston (C554) and Meyer Park (C561) just before the peak ozone value at NW Harris County at 4 pm. The Harris monitor has a secondary maximum later in the evening at 7 pm. This pattern of 1-hour ozone peaks at monitors located progressively north and west of the urban core is consistent with movement of a plume in southeasterly wind conditions.

Given the generally low levels of $PM_{2.5}$ in the HGB area and the lack of a NOx and/or NO plume at the NW Harris monitor and the ozone spatial pattern, it is likely that the enhancement above background ozone at NW Harris was caused by local emissions sources in the HGB area. However, because the Kingwood (C309) monitor recorded a $PM_{2.5}$ plume impact at 4 pm and this monitor is located along the back trajectory and in the vicinity of the fires shown in Figure 3-142, the possibility of the fires affecting ozone at the NW Harris monitor cannot be excluded. We recommend that July 3, 2013 be investigated further.

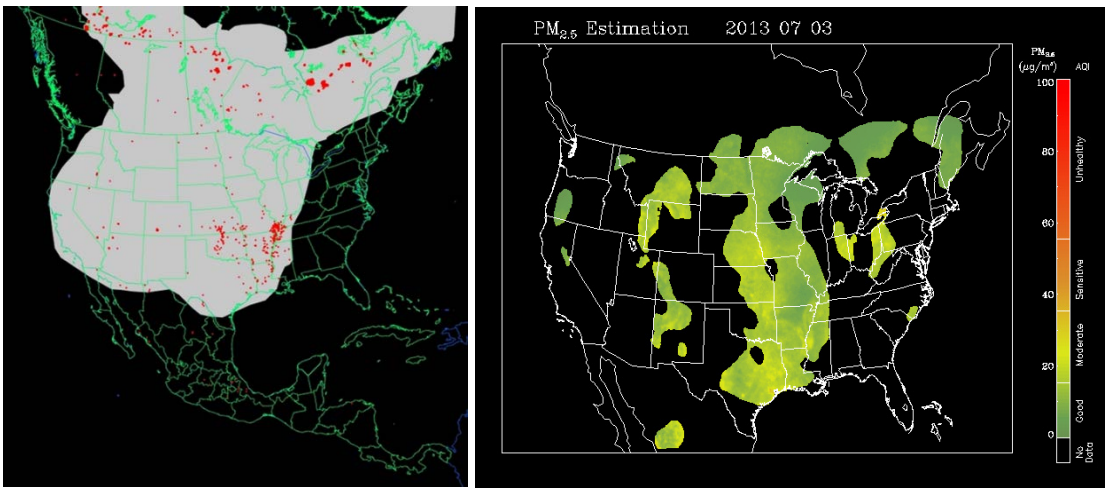

Figure 3-143. Left panel: HMS product showing July 3 fire locations (red dots) and smoke plume (gray area). Right panel: IDEA surface $PM_{2.5}$ estimate based on AOD and surface monitoring data.

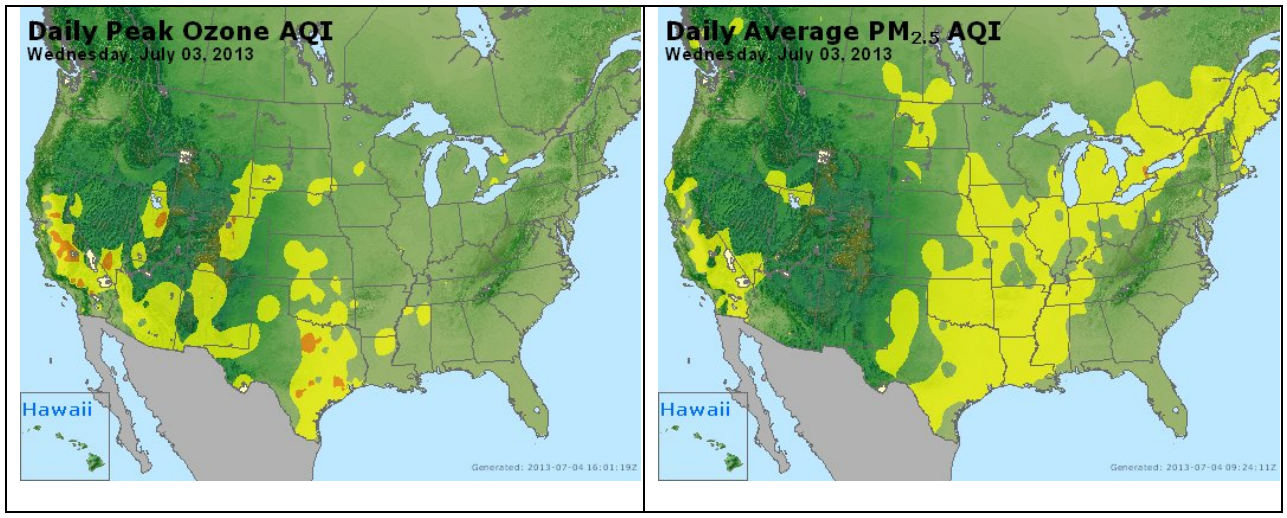

Figure 3-144. Daily average ozone (left) and $PM_{2.5}$ (right) based on observed values. Data from: http://www.airnow.gov/.

ENVIRON

Wildfire Emissions Inventory: FINN 2013

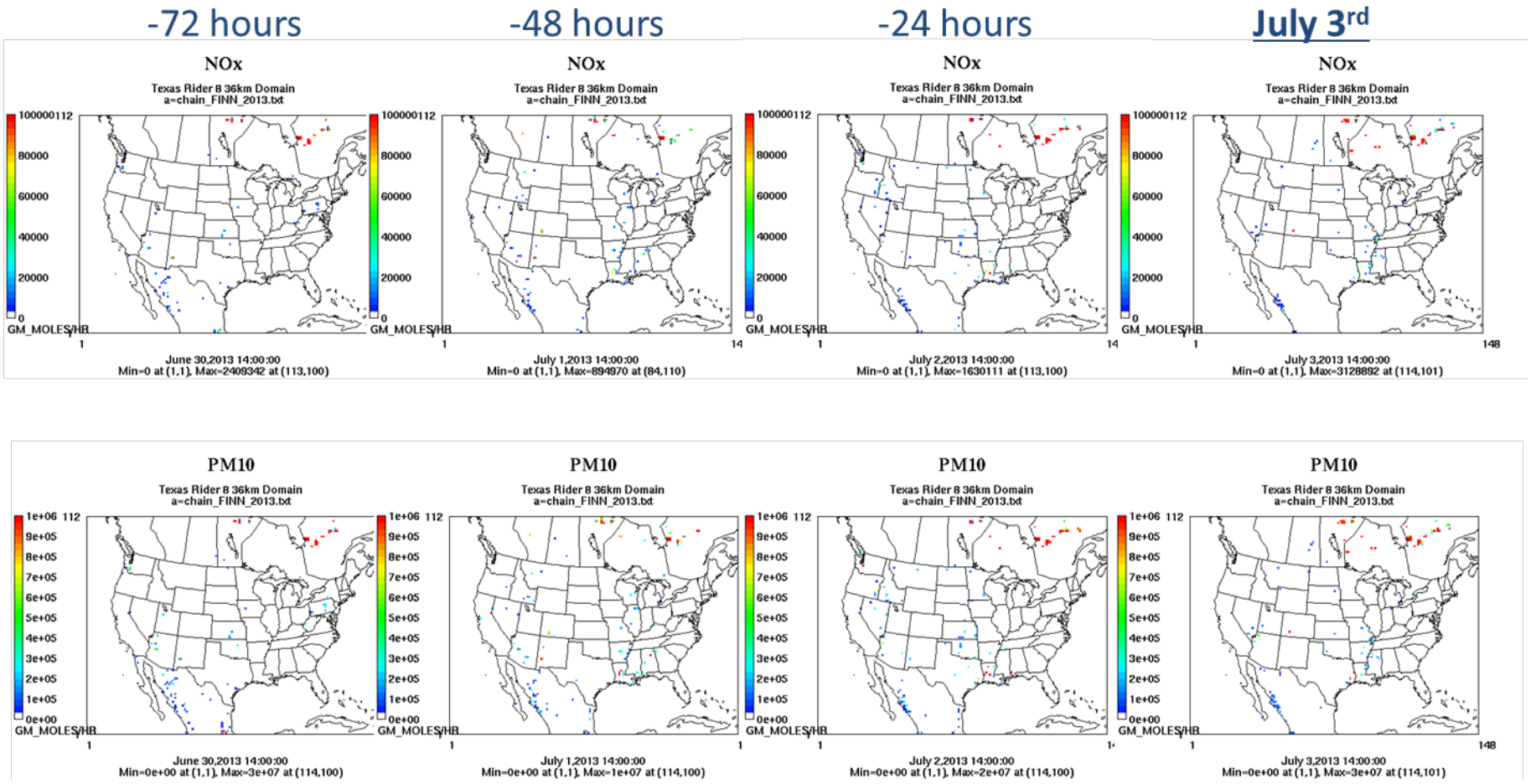

Figure 3-145. July 3, 2013 FINN fire emissions of NOx and PM_{10}.

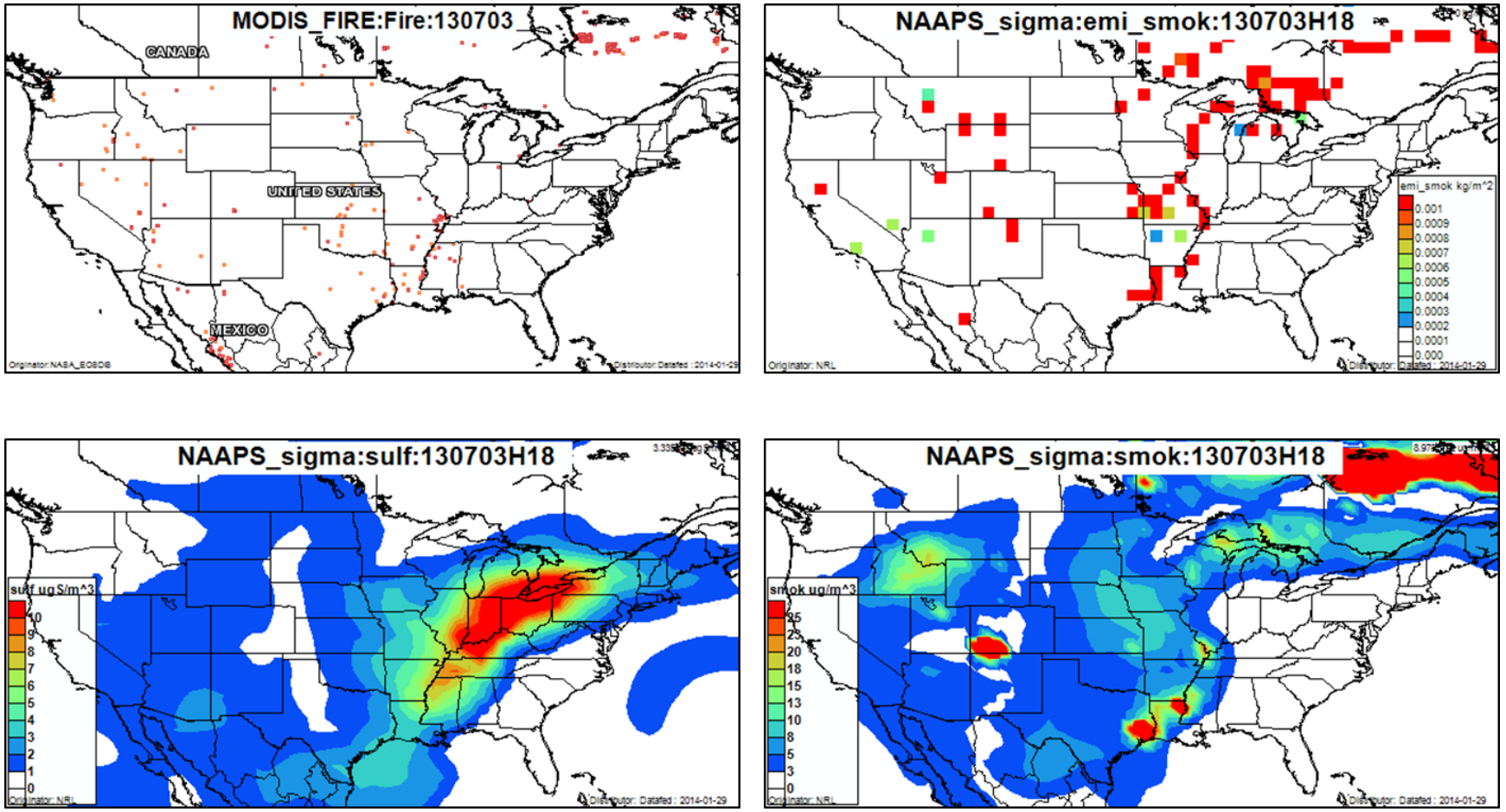

Figure 3-146. July 3, 2013 DataFed analysis. Upper left panel: Locations of active fires from MODIS satellite fire detections. Upper right panel: NAAPS model smoke emissions. Lower left panel: NAAPS model surface layer sulfate concentrations. Lower right panel: NAAPS model surface layer smoke concentrations.

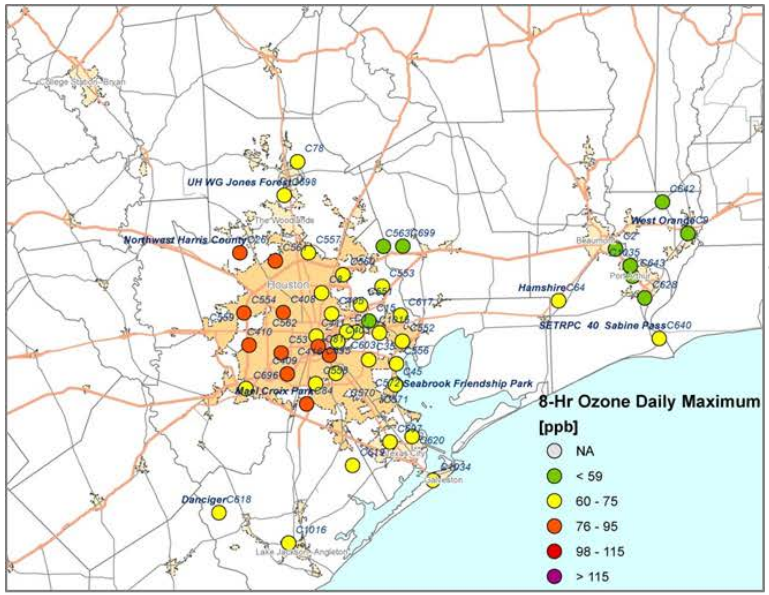

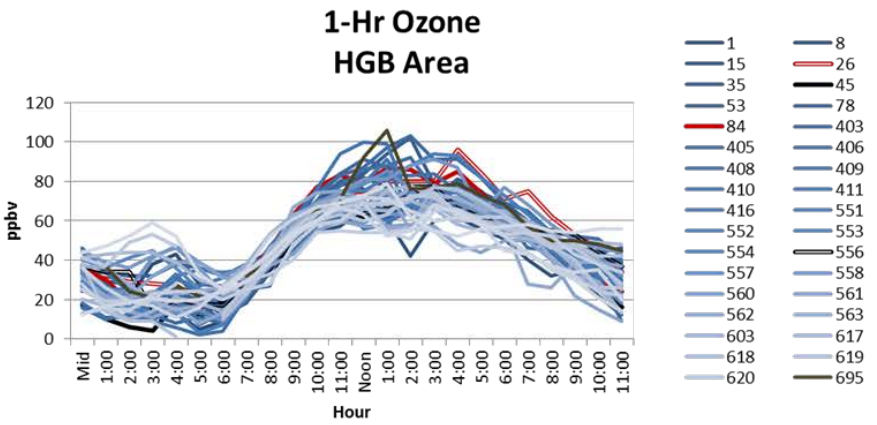

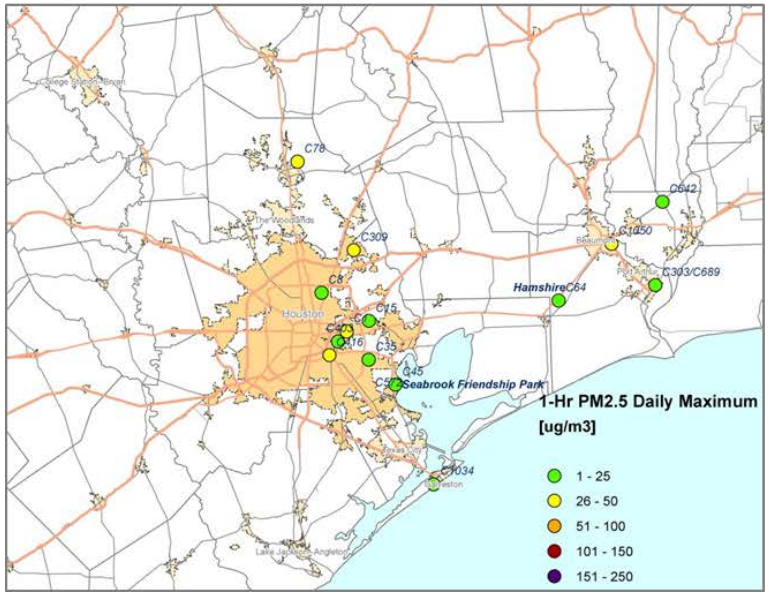

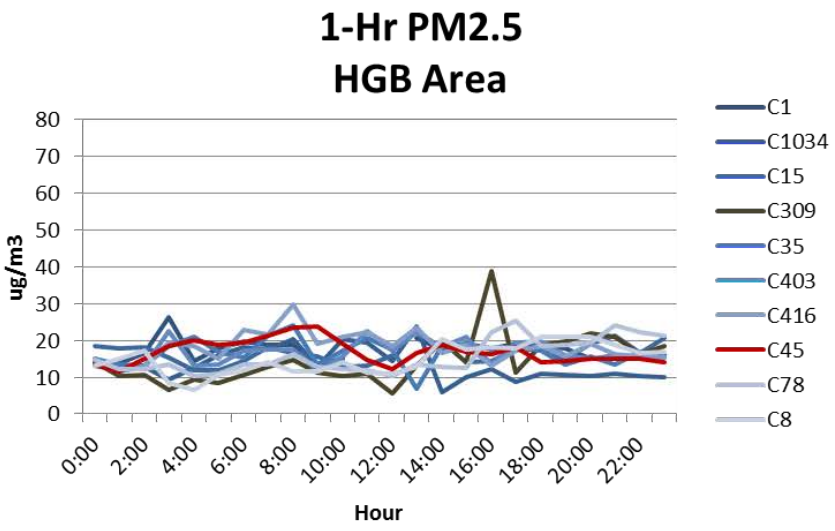

Figure 3-147. Regional ozone (top left and right) and $PM_{2.5}$ (bottom left and right) measurements (HGB area time series).

3.2.6 July 4, 2013

On July 4, the fires present on July 3 at the eastern edge of the HGB urban area are still visible in the SmartFire map (Figure 3-150) and appear in the FINN emissions plot for July 4 (Figure 3-153) and the DataFed MODIS fire location plot (Figure 3-154), but are not present in the HMS product map (Figure 3-151). The HMS product shows the presence of smoke over all of Texas, as does the NAAPS smoke product (Figure 3-154), and background ozone in the HGB area was high (~60 ppb; Figure 3-155).

The Manvel Croix monitor recorded its 2nd high MDA8 value (86 ppb) on July 4, and had a peak 1-hour ozone value of 110 ppb (Figure 3-148). There is no NOx peak at Manvel Croix following the morning commute period. Morning winds were light and northerly and the winds switched to southeasterly at 2 pm. The AQPlot back trajectory and the SmartFire and HYSPLIT NAM back trajectories are consistent in showing stagnant, recirculating flow as air arrives at the monitor (Figure 3-150). The 500 m and 1,000 m HYSPLIT NAM back trajectories agree with the SmartFire and AQplot trajectories in showing shifting low level winds that were east-southeasterly leading

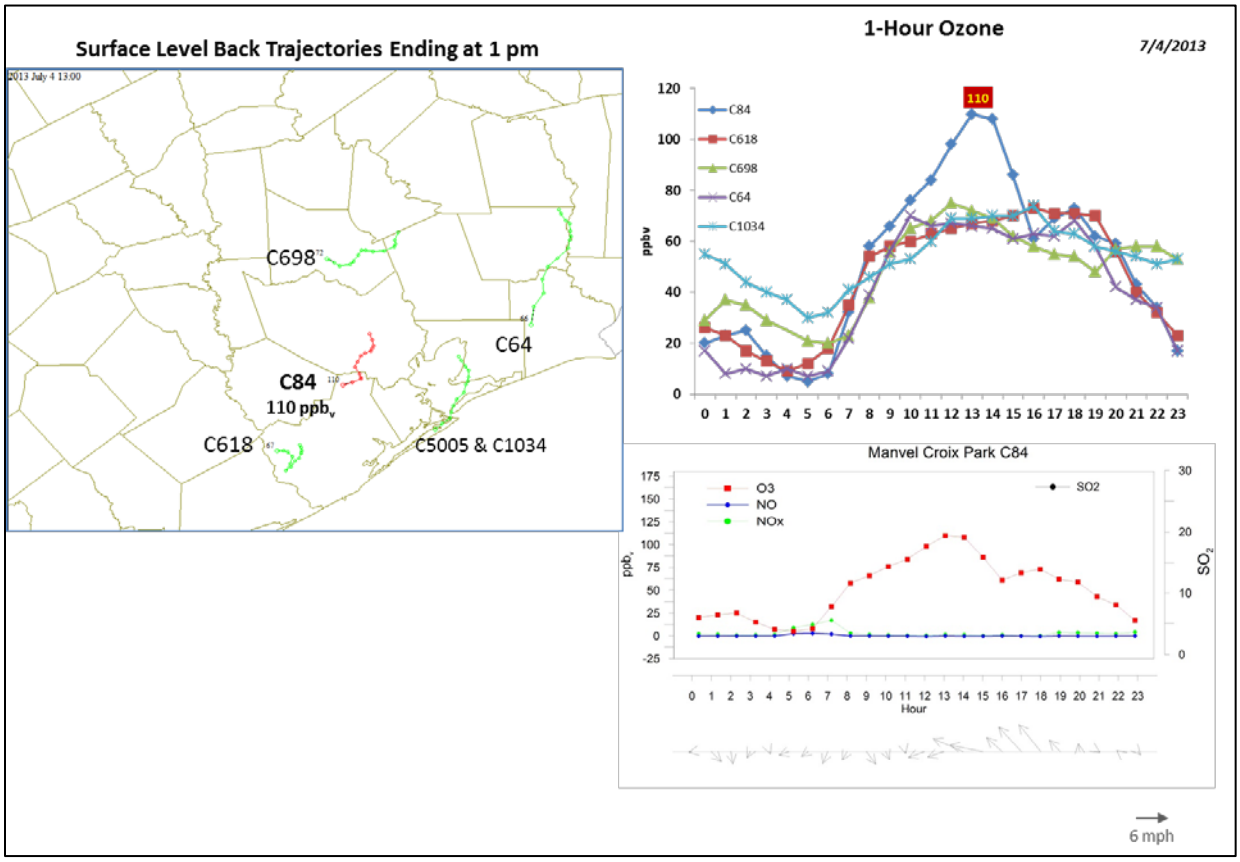

Figure 3-148. July 4, 2013 high ozone day at Manvel Croix C84. Left panel: back trajectories terminating at C84 (red line) and four background HGB monitors (green line) on July 4 at the time of peak ozone impact at C84. Upper right panel: 1-hour average ozone time series for the C84 and surrounding HGB monitors. Lower right panel: time series of 1-hour ozone, NO, NO_2 and wind vectors at the Manvel Croix monitor.

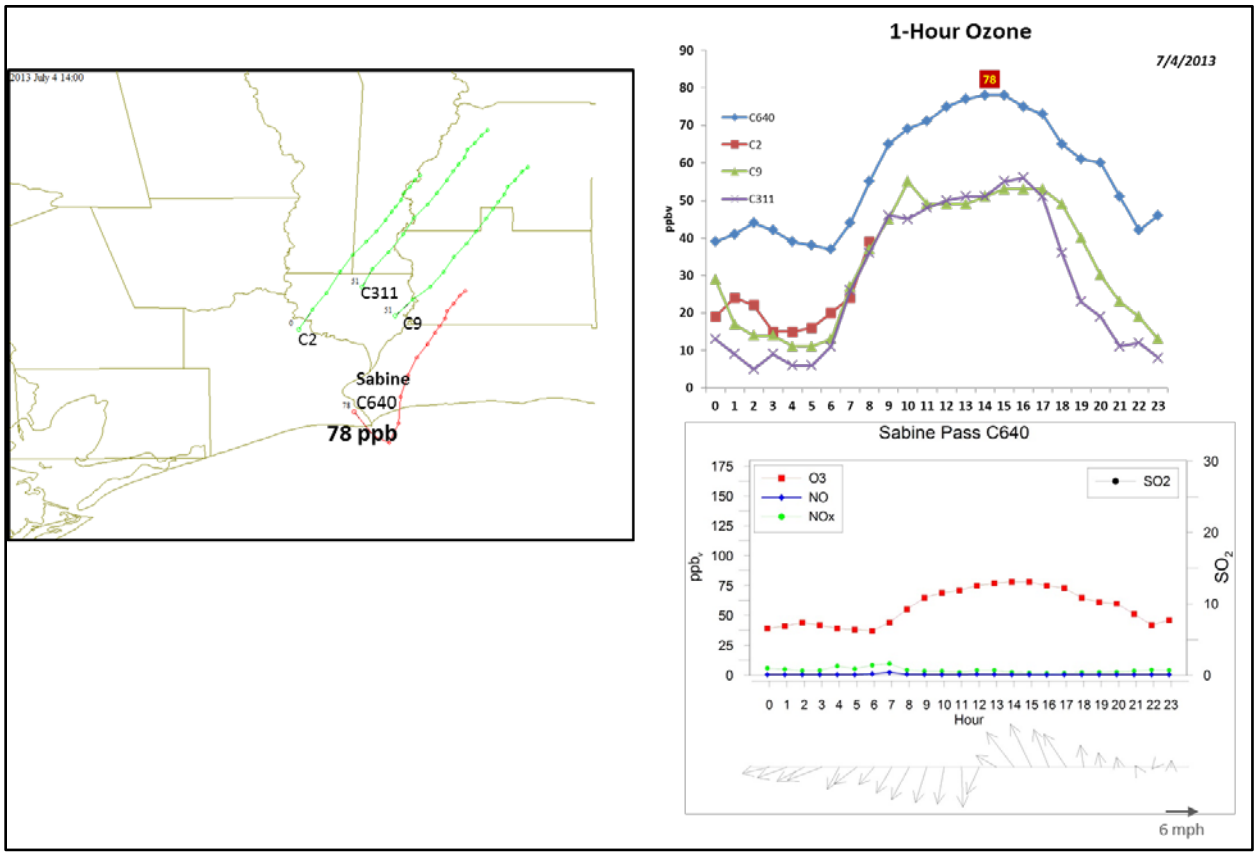

Figure 3-149. July 4, 2013 high ozone day at Sabine Pass C640. Left panel: back trajectories terminating at C640 (red line) and four background BPA monitors (green line) on July 4 at the time of peak ozone impact at C640. Upper right panel: 1-hour average ozone time series for the C640 and surrounding BPA monitors. Lower right panel: time series of 1-hour ozone, NO, NO_2 and wind vectors at the Sabine Pass monitor.

up to the time of the peak 1-hour ozone value on July 4.

The HMS product (Figure 3-151) and NAAPS smoke analysis (Figure 3-154) agree that smoke was present in the HGB area on July 4. The IDEA product (Figure 3-151) and the EPA $PM_{2.5}$ AQI plot (Figure 3-152) also show enhanced levels of $PM_{2.5}$ in the HGB area. Figure 3-155 shows a group of monitors in the west of the HGB urban area with MDA8>75 ppb. Monitors in the eastern part of the HGB area had ozone <75 ppb. The gradient in ozone together with the easterly-southeasterly wind direction suggests that local HGB emissions sources contributed to high ozone at Manvel Croix on July 4th.

Also shown in Figure 3-156 are four monitors with $PM_{2.5}$ values over 50 µg m^{-3}, with the Houston Aldine (C8) monitor and the Houston East (C1) monitors both recording evening $PM_{2.5}$ readings in excess of 100 µg m^{-3}. Given the time of day on July 4th that the high readings occurred, it is possible that they are due to fireworks. However, the high $PM_{2.5}$ readings occurred in the vicinity of the fire on the eastern edge of the HGB area on July 4$^{th.}$ Given the elevated $PM_{2.5}$ levels throughout the region, the sharp ozone maximum at Manvel Croix, the

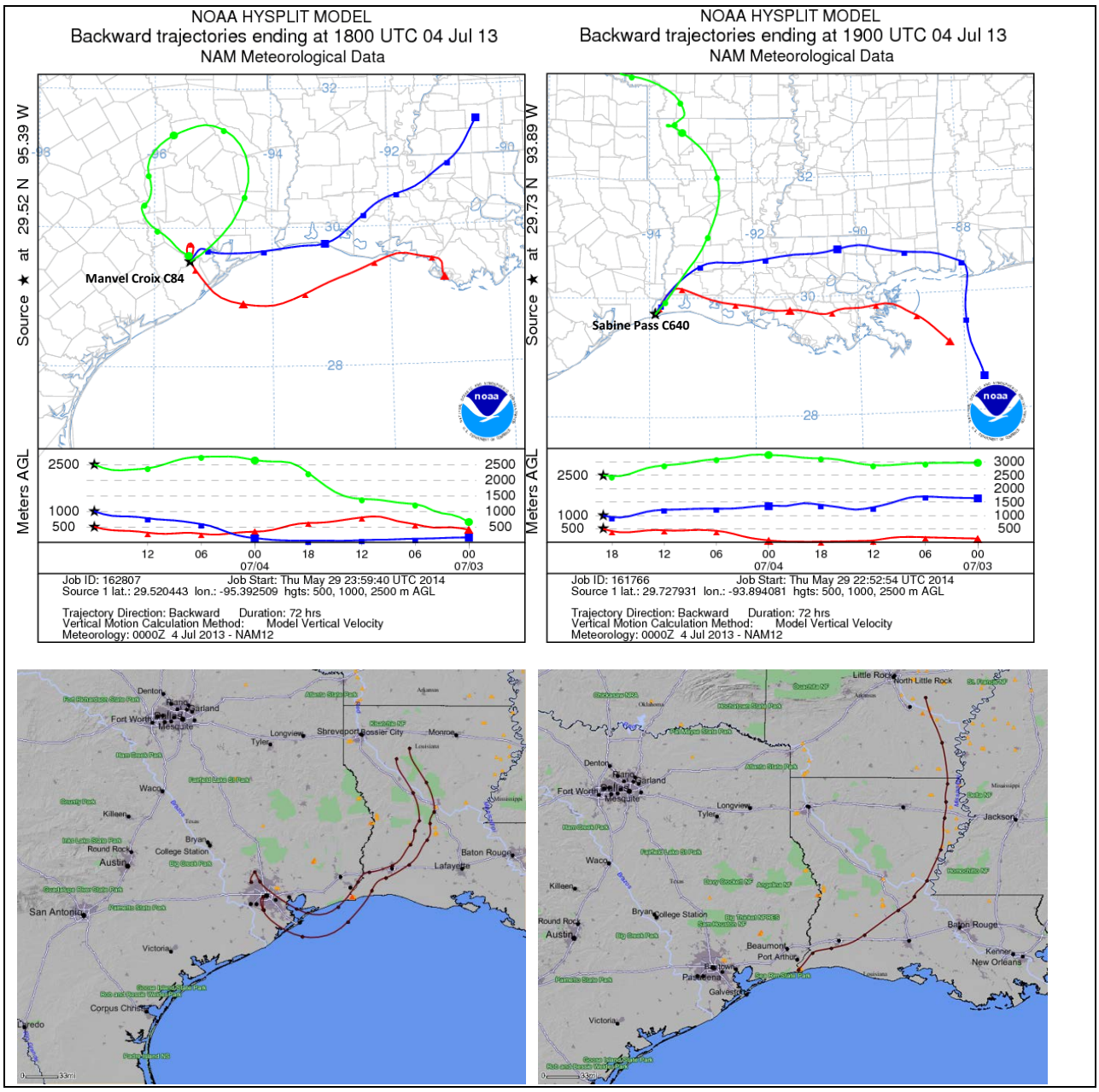

Figure 3-150. 72-hour HYSPLIT back trajectories ending at Manvel Croix C84 (upper left) and Sabine Pass C640 (upper right) at July 4, 2013; Bottom: SmartFire plots with fire locations (orange triangles) and 72-hour HYSPLIT back trajectories terminating at HGB sites (C26 and C84; bottom left) and Sabine Pass C640 in the BPA (bottom right).

presence of a fire within the region, and the stagnant and recirculating winds, it is possible that a plume from the fire affected ozone at the Manvel Croix monitor; the monitor's 1-hour ozone time series has a relatively narrow ozone maximum that is consistent with a plume impact. Therefore, we recommend further analysis of July 4 for the Manvel Croix monitor.

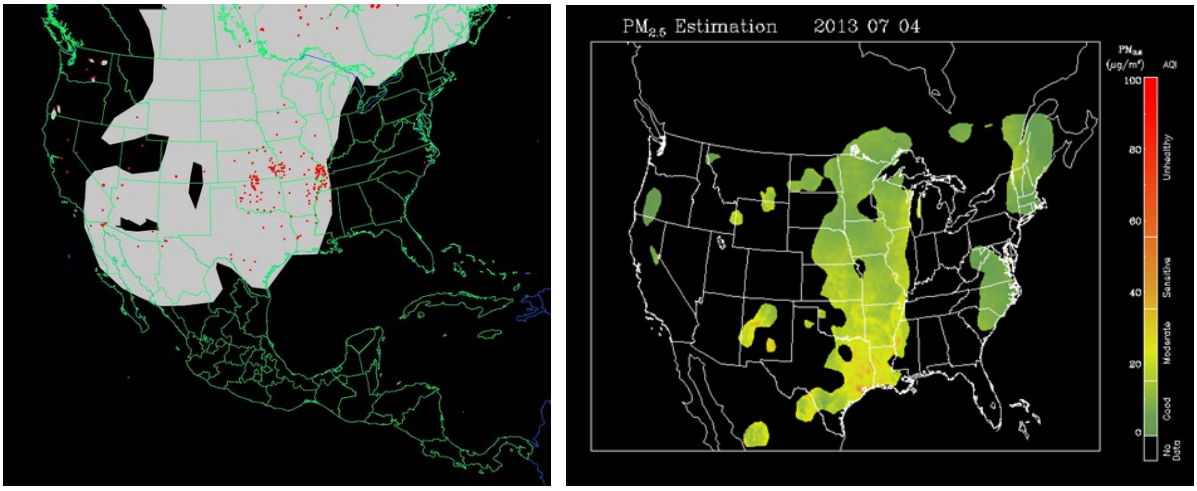

Figure 3-151. Left panel: HMS product showing July 4 fire locations (red dots) and smoke plume (gray area). Right panel: IDEA surface $PM_{2.5}$ estimate based on AOD and surface monitoring data.

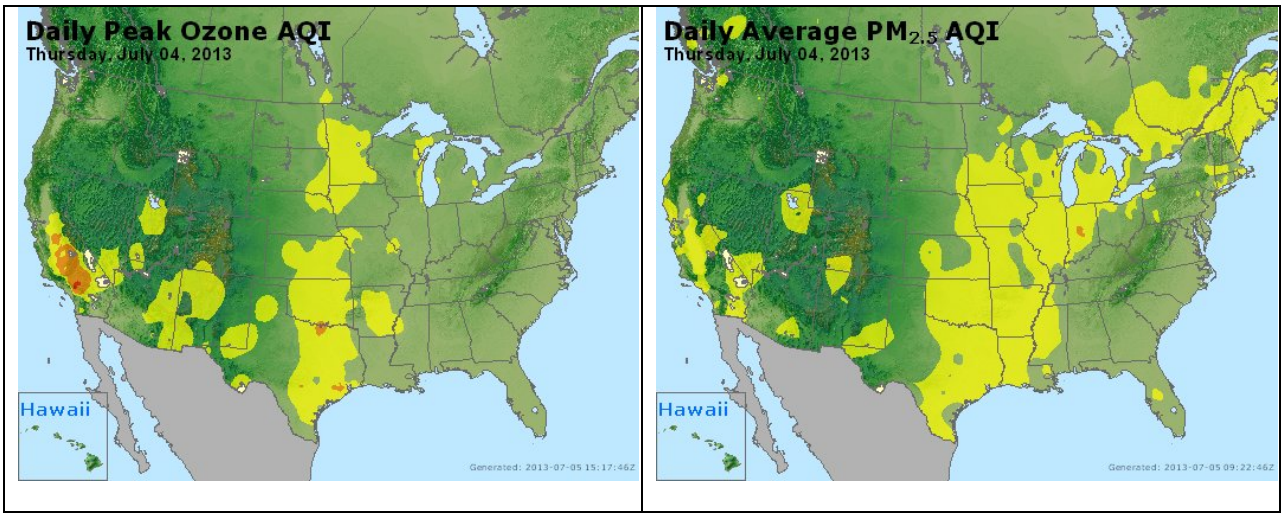

Figure 3-152. Daily average ozone (left) and $PM_{2.5}$ (right) based on observed values. Data from: http://www.airnow.gov/.

The Sabine Pass monitor recorded its highest MDA8 reading for 2013 on July 4 (74 ppb). The SmartFire back trajectory for the Sabine Pass monitor extends northward into Louisiana, where there are a number of fires (Figure 3-150). Figure 3-149 shows that the Sabine Pass monitor had 1-hour ozone that was approximately 20 ppb higher than any other BPA area monitor during the entire day of July 4. There are evening peaks in $PM_{2.5}$ for all of the BPA area monitors, including the C303 monitor, which is the closest $PM_{2.5}$ monitor to the Sabine Pass monitor. There is, however, no NOx peak coincident with high ozone at Sabine Pass. Because of the high values of $PM_{2.5}$ in the area, and the presence of fires along the back trajectories and

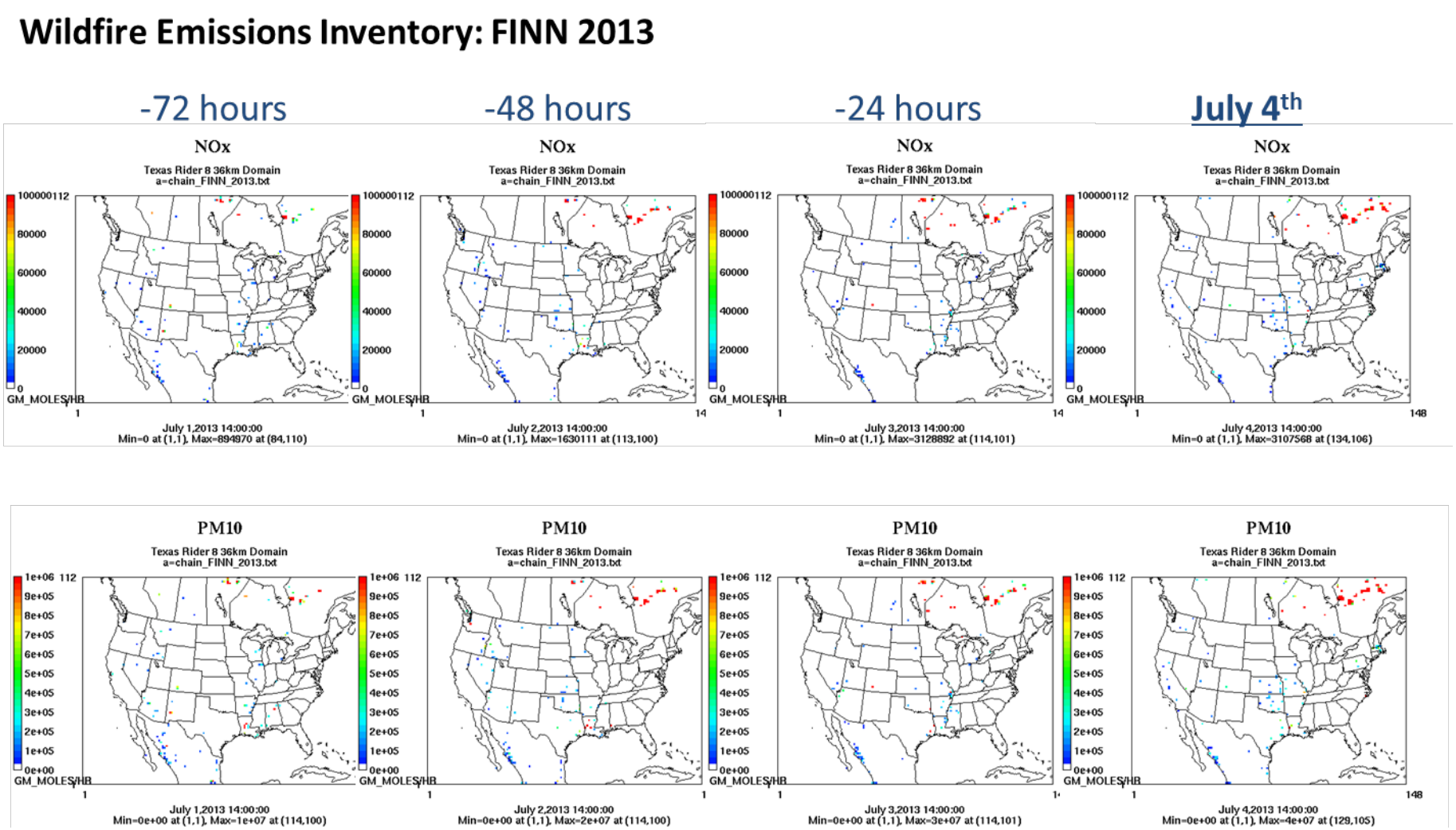

Figure 3-153. July 4, 2013 FINN fire emissions of NOx (top) and PM_{10} (bottom).

smoke in the region as described in the Manvel Croix discussion above, we recommend additional analysis of July 4 for the Sabine Pass monitor.

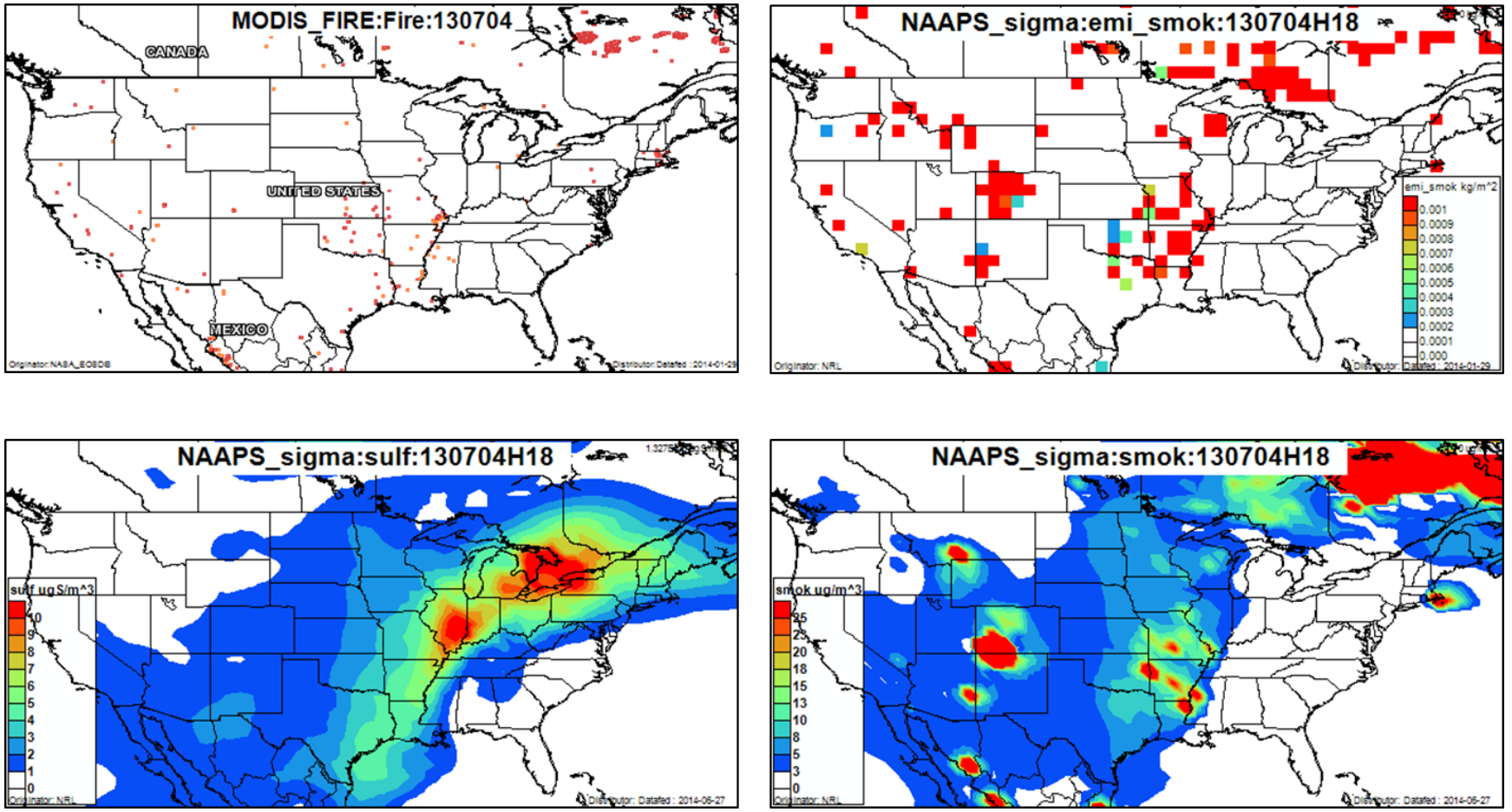

Figure 3-154. July 4, 2013 DataFed analysis. Upper left panel: Locations of active fires from MODIS satellite fire detections. Upper right panel: NAAPS model smoke emissions. Lower left panel: NAAPS model surface layer sulfate concentrations. Lower right panel: NAAPS model surface layer smoke concentrations.

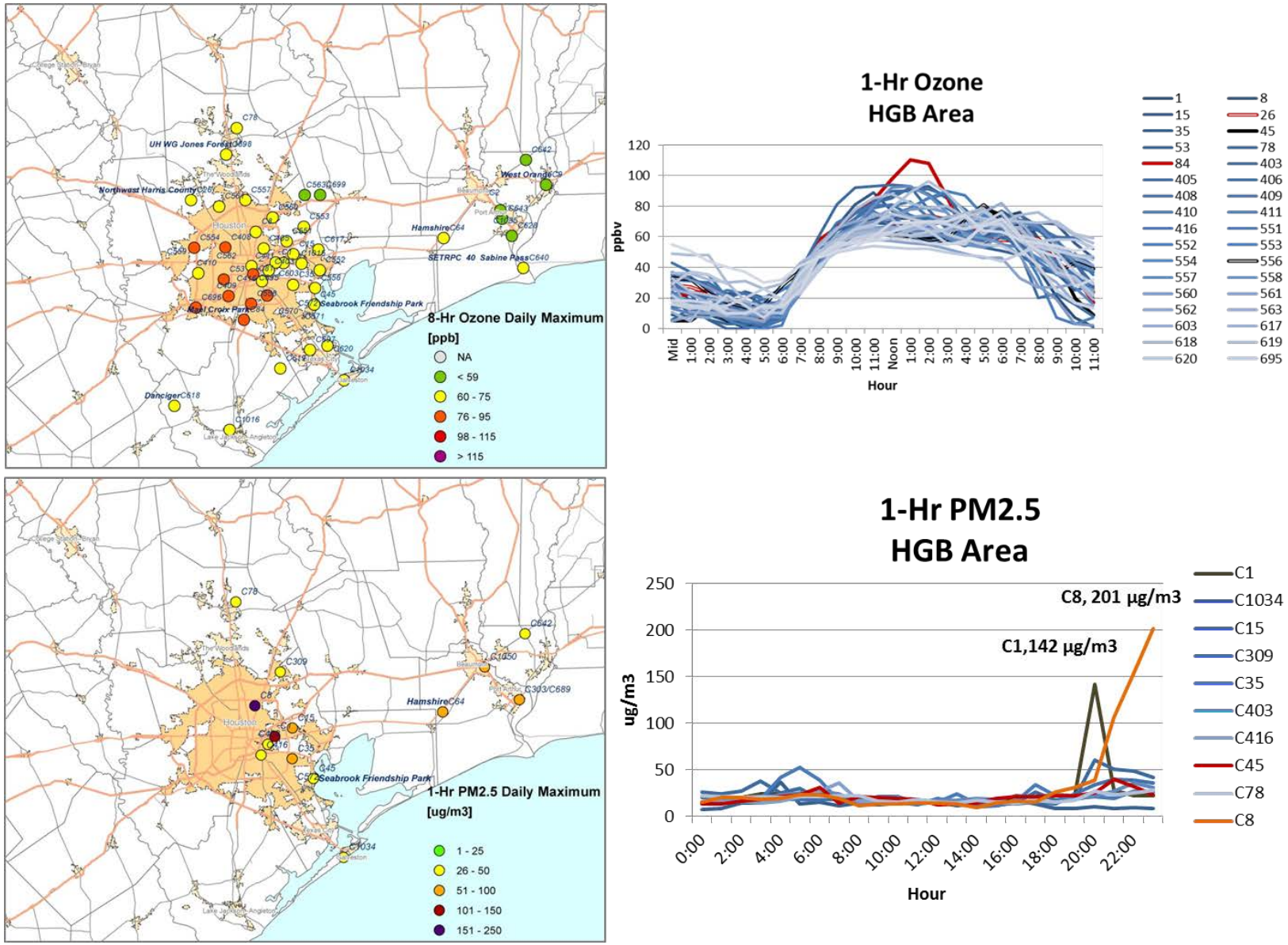

Figure 3-155. Regional ozone (top left and right) and $PM_{2.5}$ (bottom left and right) measurements (HGB area time series).

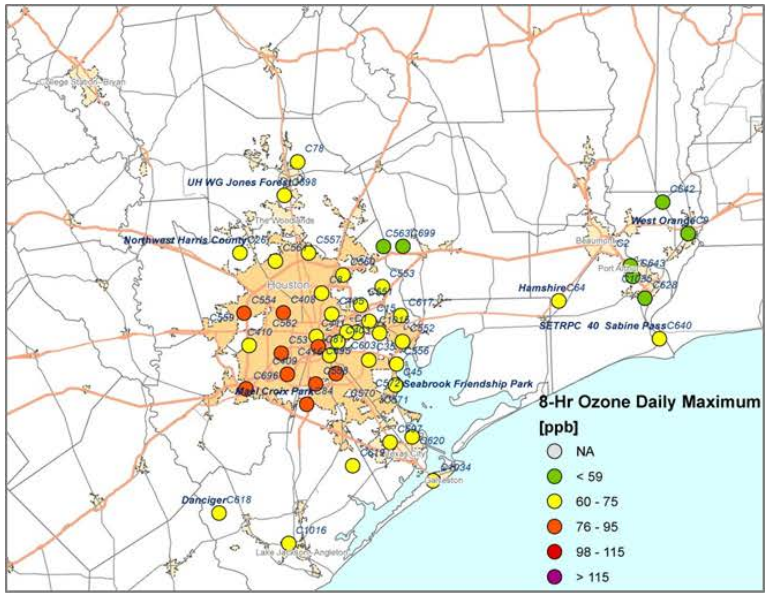

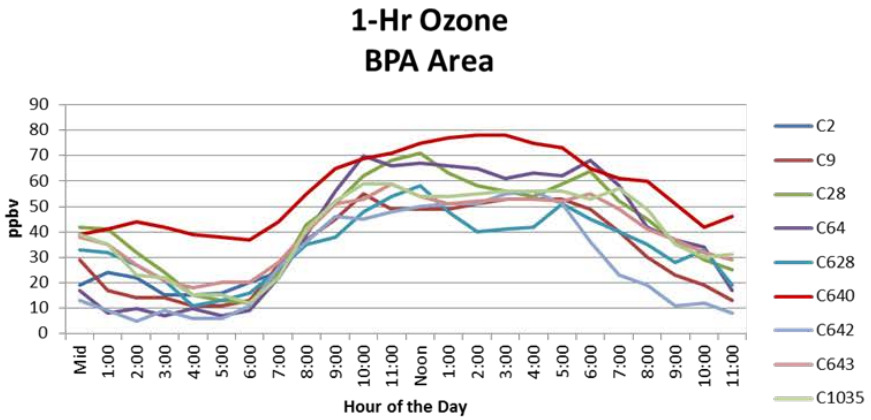

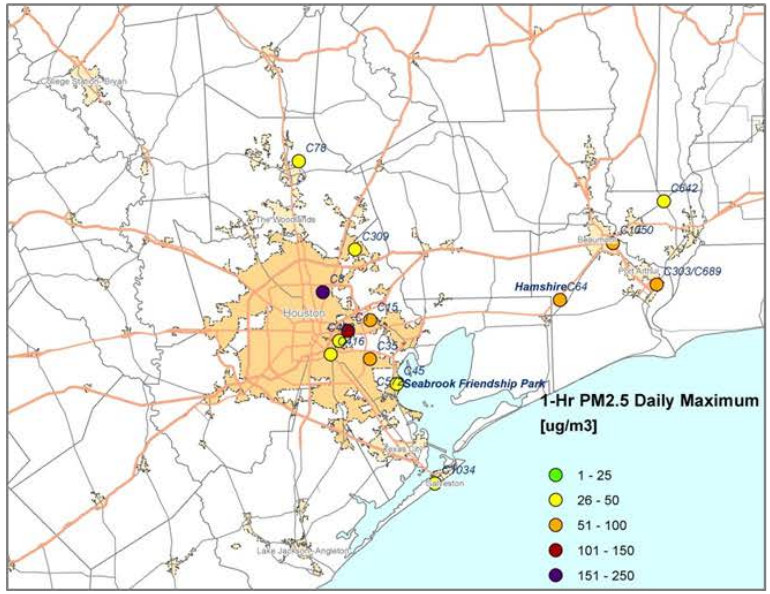

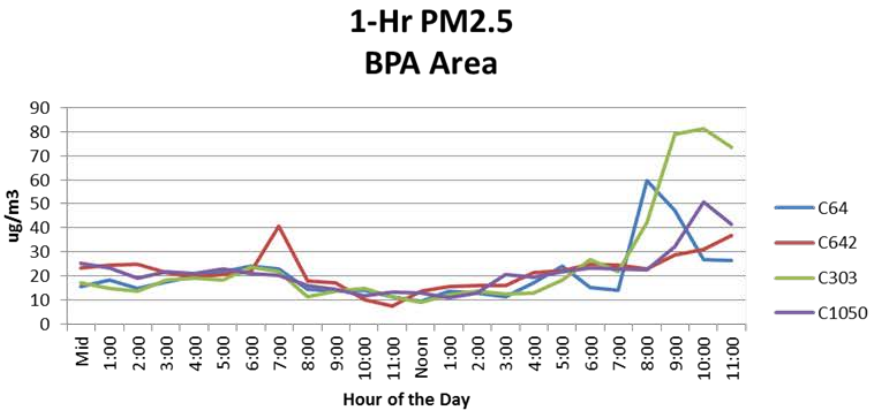

Figure 3-156. Regional ozone (top left and right) and $PM_{2.5}$ (bottom left and right) measurements (BPA area time series).

3.2.7 July 5, 2013

On July 5, the Denton Airport South (C56) had its highest value of the MDA8 during 2013 (90 ppb). The peak 1-hour ozone value occurred in the afternoon (3-4 pm) and was 96 ppb (Figure 3-157). The AQPlot back trajectories (Figure 3-157) show south-southeasterly winds leading up to the hour of peak 1-hour ozone, consistent with the wind vectors at the Denton monitor.

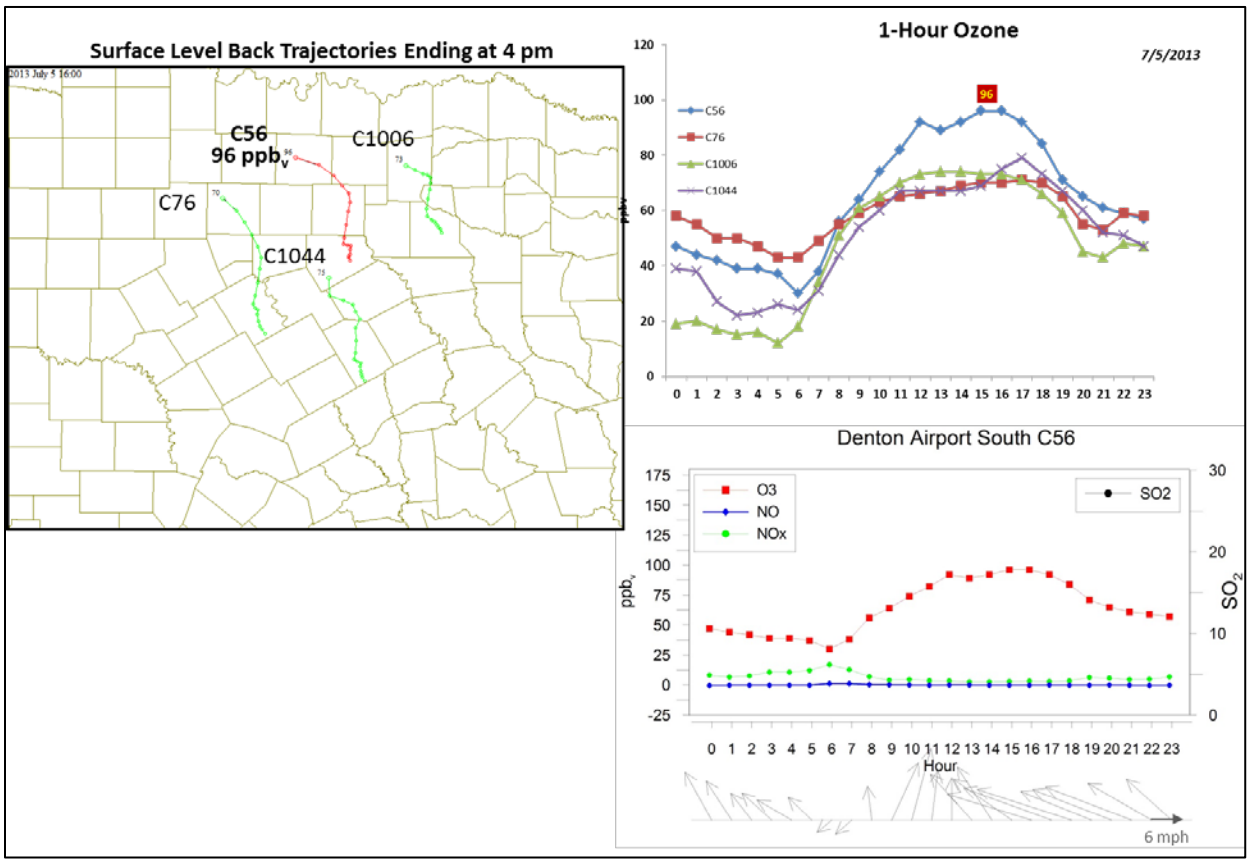

Figure 3-157. July 5, 2013 high ozone day at Denton Airport C56. Left panel: AQPlot back trajectories ending at C56 and four background sites at the time of peak 1-hr ozone was observed. Upper right panel: 1-hour average ozone time series for the C56 and background monitors. Lower right panel: time series of 1-hour ozone, NO, NO_2 and wind vectors at Denton C56 site.

The SmartFire back trajectories (Figure 3-158) also indicate flow from the south-southeast on July 5, with back trajectories extending eastward through Northeast Texas into Louisiana. The HYSPLIT NAM 500 m and 1,000 m back trajectories show southerly flow on July 5, but extend southward toward the Gulf Coast of Texas. The 2,500 m back trajectory extends north, indicating the presence of strong vertical wind shear. The SmartFire map shows that there were no fires along the SmartFire back trajectories on July 5. Although the back trajectory analysis is inconclusive with respect to the origin of the air mass present in DFW on July 5, the SmartFire map shows no fire activity along any of the SmartFire or HYSPLIT NAM back

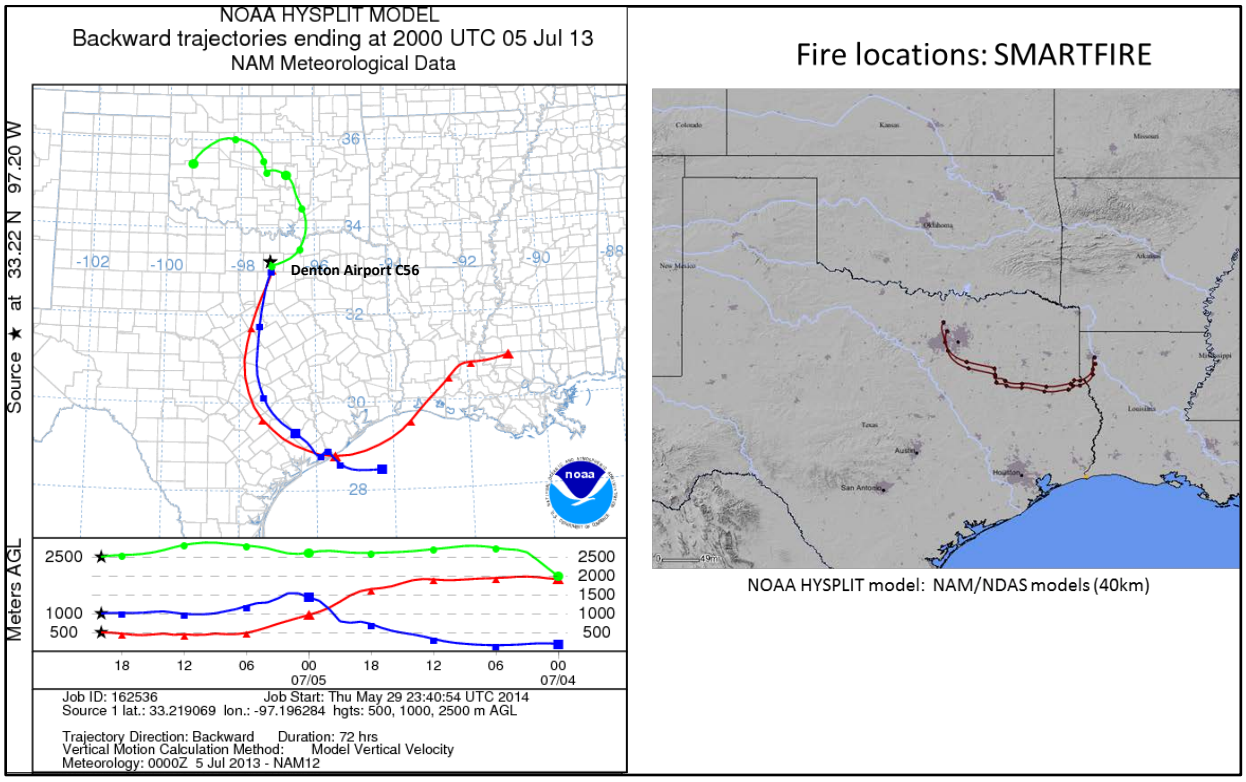

Figure 3-158. 72-hour HYSPLIT back trajectories (NAM 12km) from Denton Airport South (C56) terminating July 5, 2013; SmartFire plot showing fire locations (orange triangles) and 72-hour HYSPLIT back trajectories (EDAS 40 km) from C56.

trajectories. The FINN emissions (Figure 3-161) and the DataFed MODIS fire location (Figure 3-162) plots show a fire south of the DFW area on July 5, and FINN shows fires in Louisiana at -72 hours, when the back trajectories are in their vicinity. The HMS product also shows a fire south of the DFW area and a smoke plume over the DFW region (Figure 3-159). Figure 3-160 shows moderate ozone and $PM_{2.5}$ AQI in the DFW area and both the HMS product (Figure 3-159) and NAAPS smoke analysis (Figure 3-162) indicate the presence of smoke over the DFW area.

The ozone spatial pattern is consistent with a DFW plume impact at Denton on a day with southerly surface winds. The monitors with the highest 1-hour ozone maxima are the northernmost monitors Frisco (C31), Denton, Grapevine Fairway and Pilot Point (C1032) (Figure 3-163). The $PM_{2.5}$ time series for the Denton monitor has a peak during the morning hours and then has relatively low $PM_{2.5}$ during the time of the broad midday ozone maximum. The only monitor that shows a $PM_{2.5}$ peak higher than most DFW monitors on July 5 is the Corsicana monitor (C1051), which is south of the DFW area relatively close to the location of the fire shown on the HMS product and in the FINN emissions. The high $PM_{2.5}$ peak in the late evening at Corsicana is unlikely to be related to the daytime formation of ozone at Denton.

Because there is no $PM_{2.5}$ or NOx peak at Denton coincident with the ozone maximum, there is no evidence of a fire plume impact and we recommend no further evaluation of July 5, 2013.

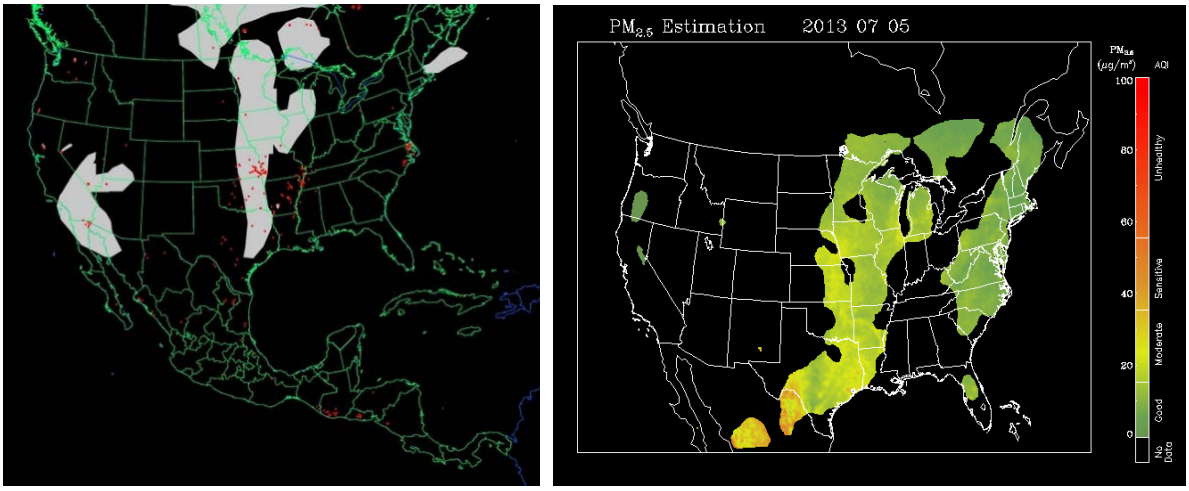

Figure 3-159. Left panel: HMS product showing July 5 fire locations (red dots) and smoke plume (gray area). Right panel: IDEA surface $PM_{2.5}$ estimate based on AOD and surface monitoring data.

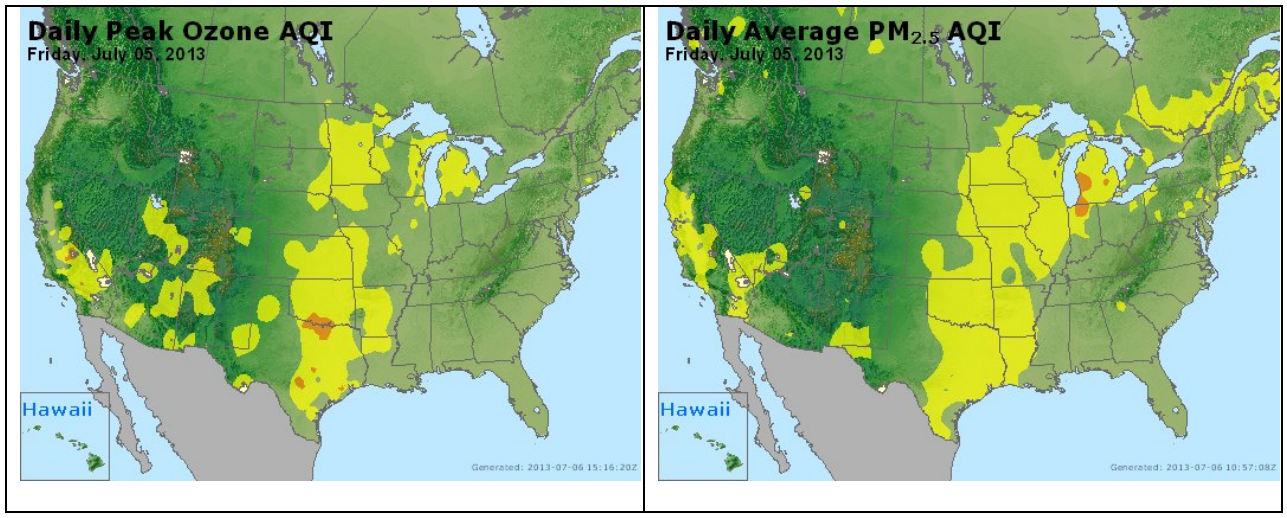

Figure 3-160. Daily average ozone (left) and $PM_{2.5}$ (right) based on observed values. Data from: http://www.airnow.gov/.

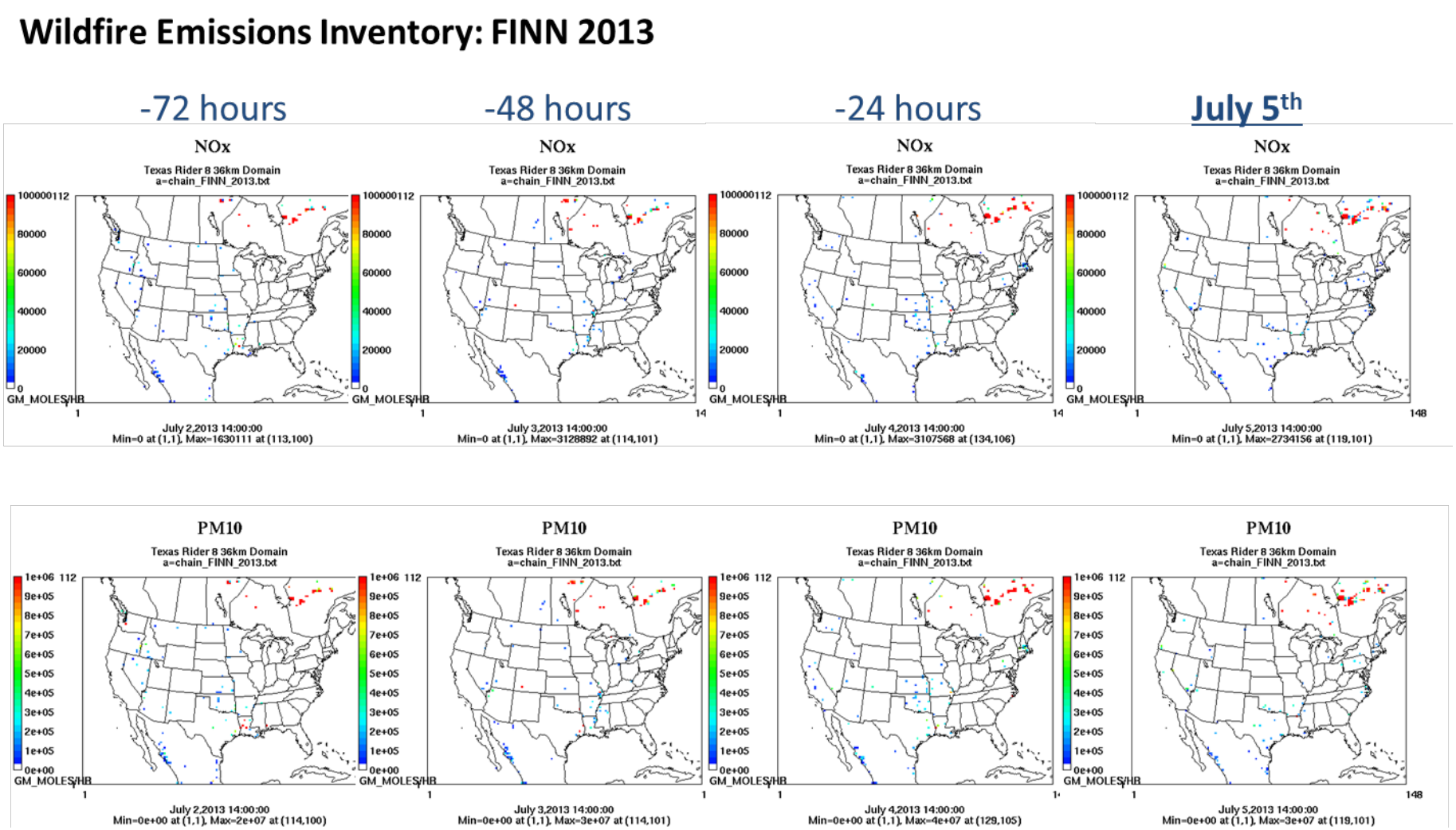

Figure 3-161. July 5, 2013 FINN fire emissions of NOx and PM_{10}.

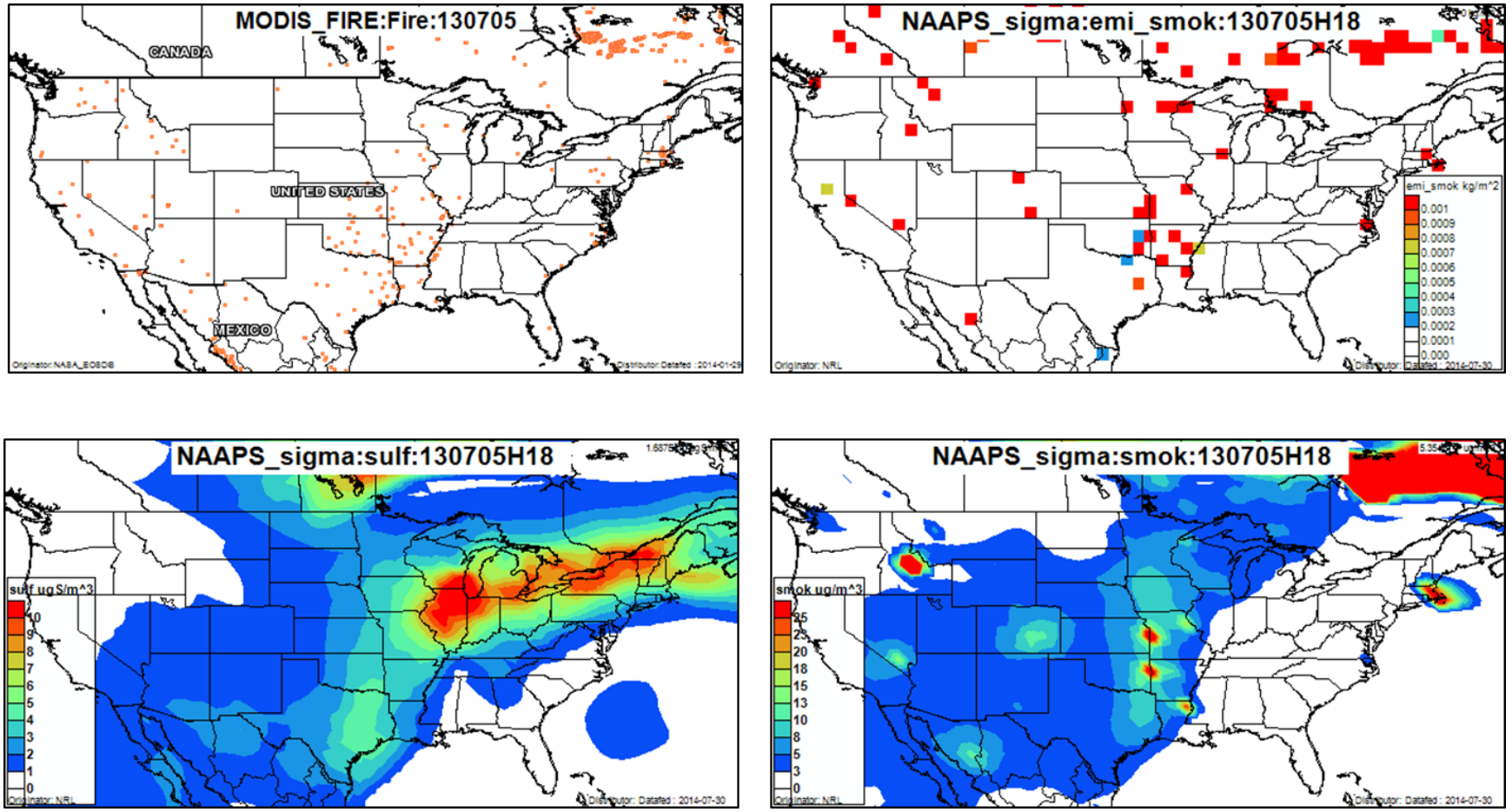

Figure 3-162. July 5, 2013 DataFed analysis. Upper left panel: Locations of active fires from MODIS satellite fire detections. Upper right panel: NAAPS model smoke emissions. Lower left panel: NAAPS model surface layer sulfate concentrations. Lower right panel: NAAPS model surface layer smoke concentrations.

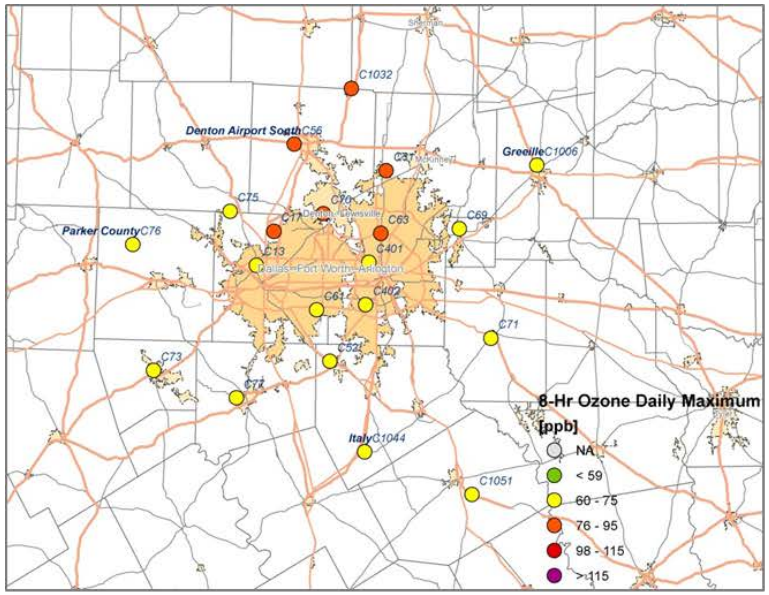

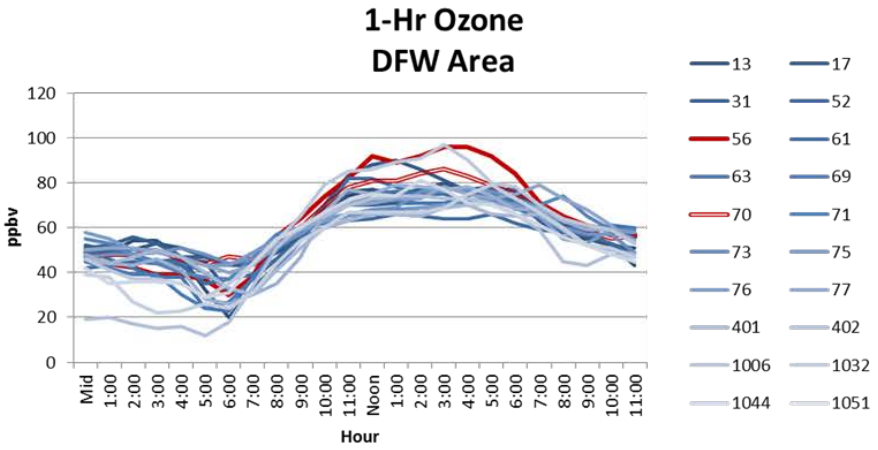

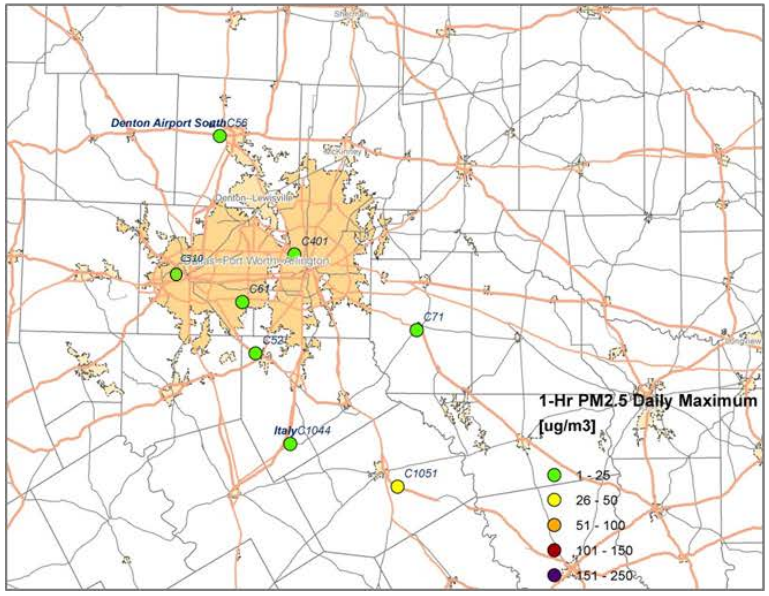

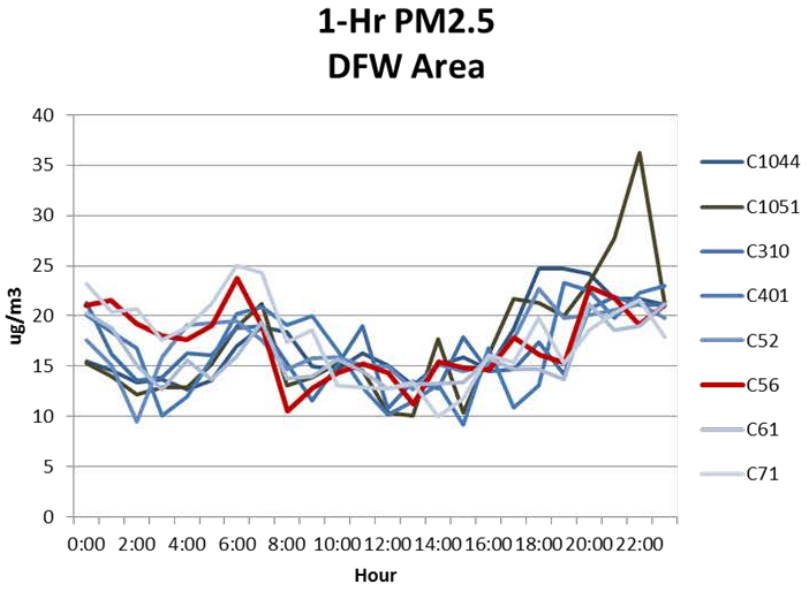

Figure 3-163. Regional ozone (top left and right) and $PM_{2.5}$ (bottom left and right) measurements (DFW area time series).

3.2.8 July 13, 2013

On July 13, the Sabine Pass monitor (C56) had its 3rd highest value of the MDA8 during 2013 (67 ppb). The peak 1-hour ozone value occurred at 1 pm and was 81 ppb (Figure 3-164). Winds at the monitor were northerly throughout the morning leading up to the time of the 1-hour ozone maximum. By 2 pm, the winds shifted to southerly and ozone levels at Sabine Pass began to fall as the sea breeze brought Gulf Air over the monitor. The AQPlot back trajectories (Figure 3-164) end at the time of the 1-hour ozone maximum and show only northerly winds.

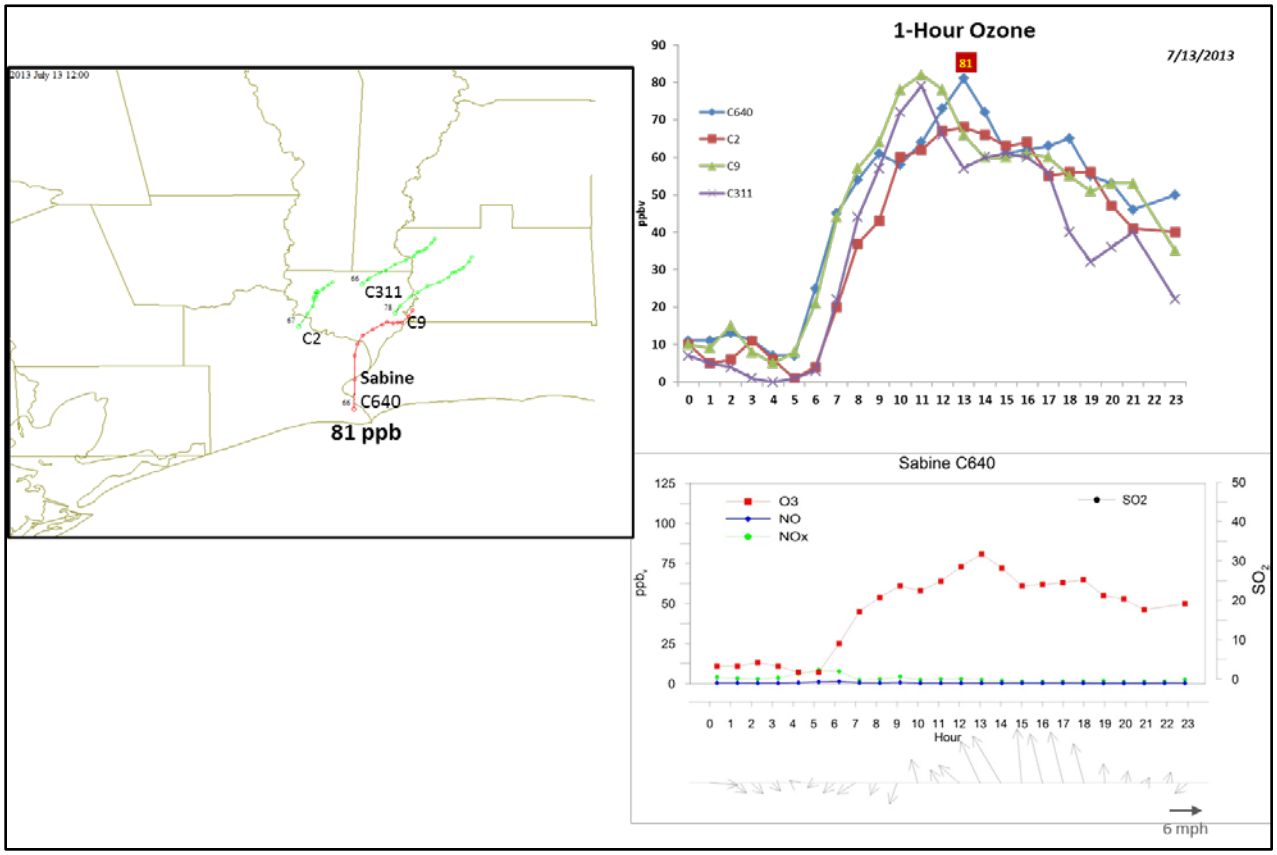

Figure 3-164. July 13, 2013 high ozone day at Sabine Pass C640. Left panel: back trajectories terminating at C640 (red line) and four background BPA monitors (green line) on July 13 at the time of peak ozone impact at C640. Upper right panel: 1-hour average ozone time series for the C640 and surrounding BPA monitors. Lower right panel: time series of 1-hour ozone, NO, NO_2 and wind vectors at the Sabine Pass monitor.

The SmartFire and HYSPLIT NAM back trajectories agree that winds were northerly at Sabine Pass and that air arriving at Sabine Pass on July 13 had recently passed over the HGB area and the Gulf of Mexico. The trajectories show stagnant low level flow influenced by the sea breeze circulation during the 72 hour period preceding the Sabine Pass 1-hour ozone maximum. The 2,500 m HYSPLIT NAM back trajectory extends to the north, and show the presence of strong vertical shear. The SmartFire maps do not show fires in the vicinity of the back trajectories on July 13.

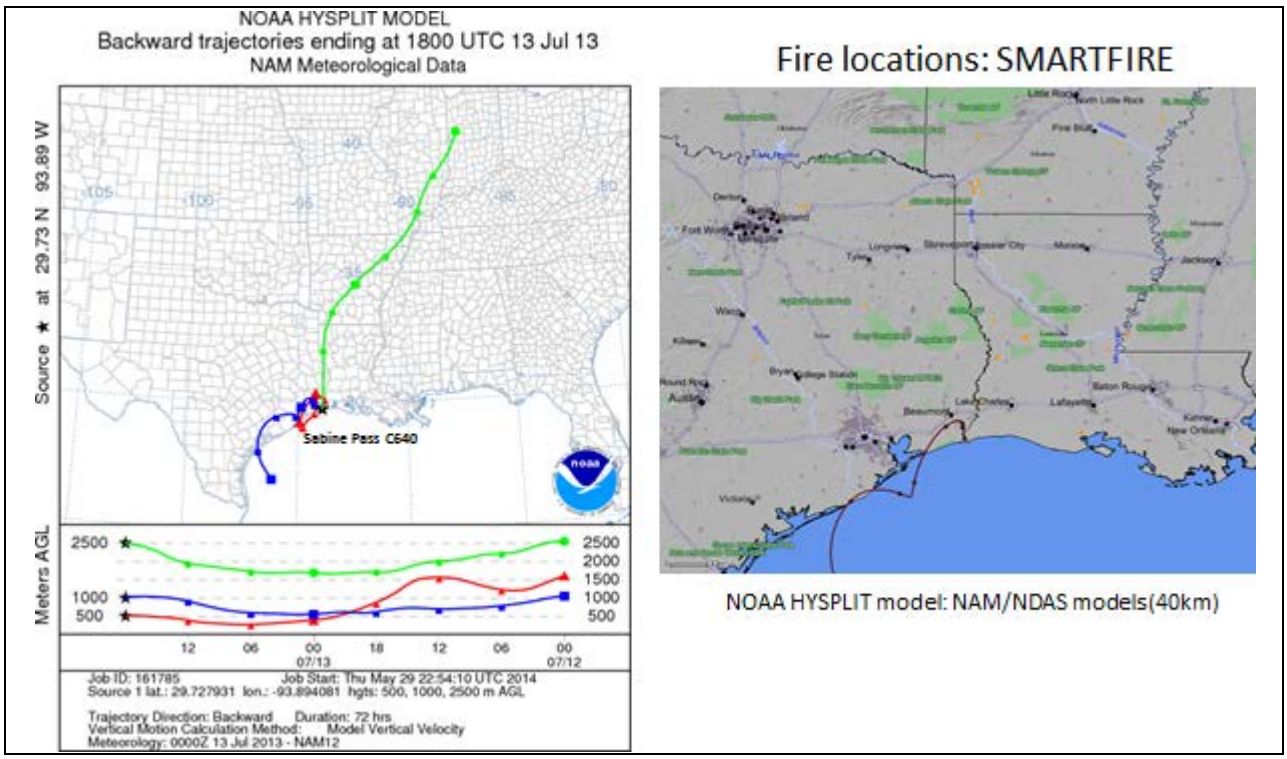

Figure 3-165. 72-hour HYSPLIT back trajectories ending at La Porte Sylvan Beach C556 (upper left) and Sabine Pass C640 (upper right) at July 13, 2013; Bottom: SmartFire plots with fire locations (orange triangles) and 72-hour HYSPLIT back trajectories terminating Sabine Pass C640 in the BPA (bottom right).

The HMS product shows no fires or smoke in the BPA area on July 13 (Figure 3-166), although the NAAPS smoke analysis indicates the presence of smoke over the BPA area (Figure 3-169). The FINN emissions plots (Figure 3-168) show no fires in the vicinity of the SmartFire and 500 m and 1,000 m back trajectories.

The 1-hour $PM_{2.5}$ time series show plume impacts on July 13, but they occur well after the time of the ozone maximum at Sabine Pass (Figure 3-170). Given the lack of fires in the area and the timing of the $PM_{2.5}$ impacts, we conclude that the enhancement of ozone above background at Sabine Pass on July 13 was due to the influence of local emissions and not a fire plume impact. We recommend no further evaluation of July 13, 2013.

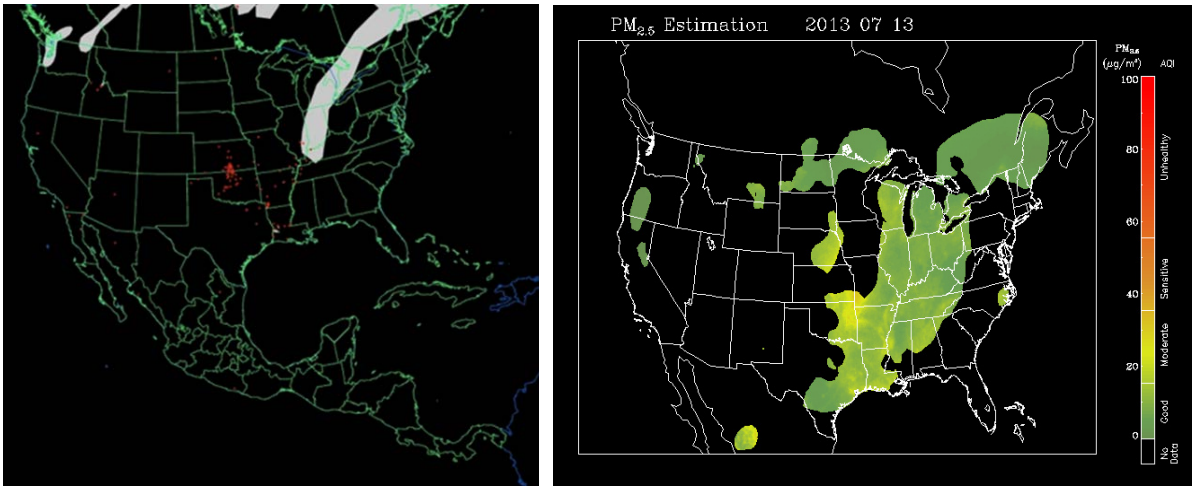

Figure 3-166. Left panel: HMS product showing July 13 fire locations (red dots) and smoke plume (gray area). Right panel: IDEA surface $PM_{2.5}$ estimate based on AOD and surface monitoring data.

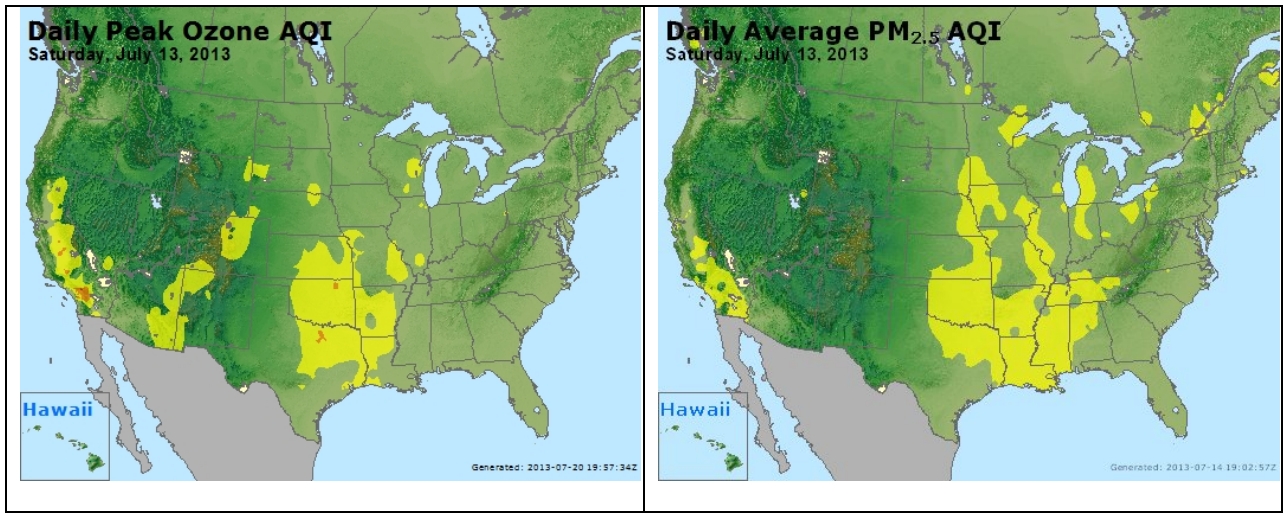

Figure 3-167. Daily average ozone (left) and $PM_{2.5}$ (right) based on observed values. Data from: http://www.airnow.gov/.

ENVIRON

Wildfire Emissions Inventory: FINN 2013

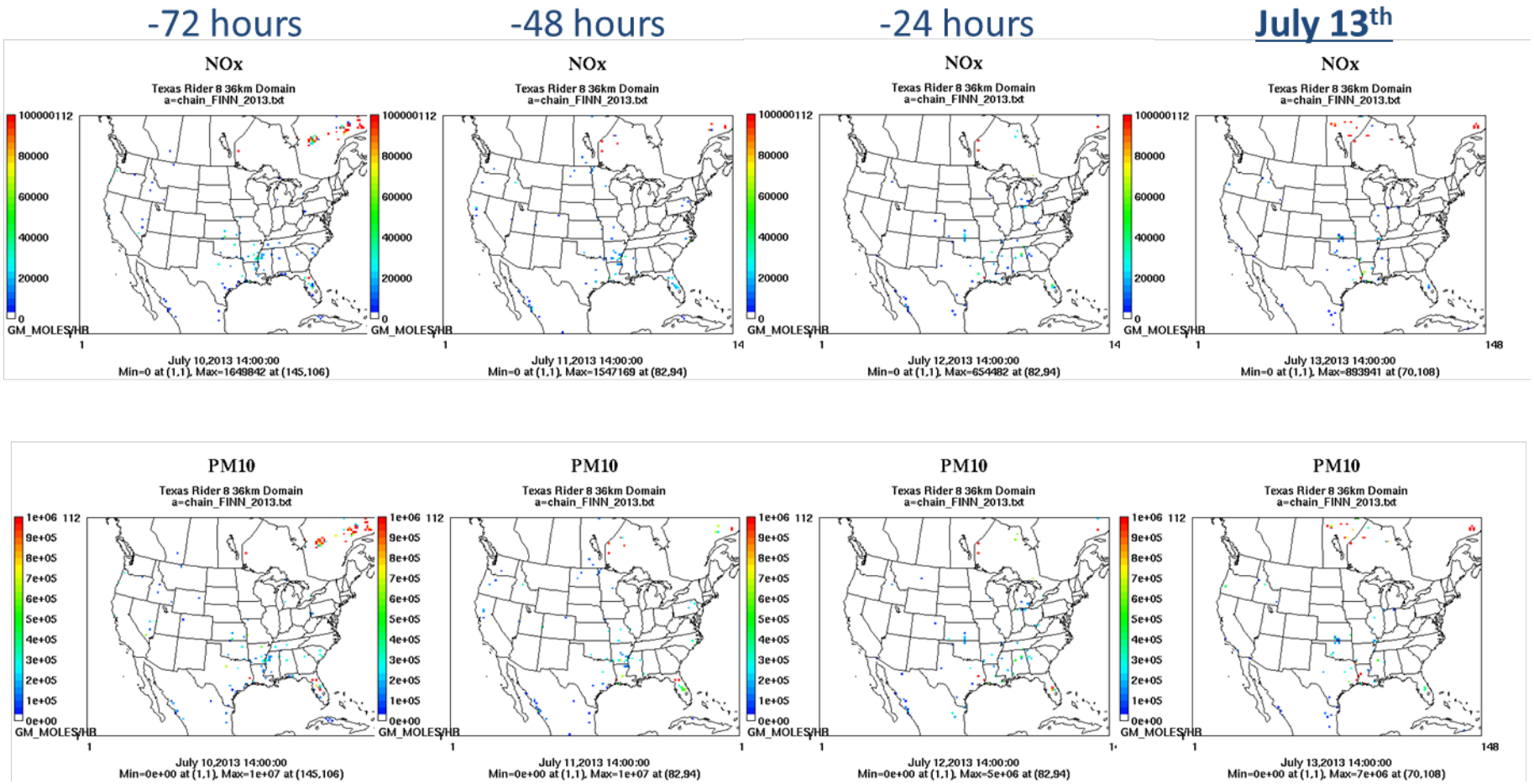

Figure 3-168. July 13, 2013 FINN fire emissions of NOx and PM_{10}.

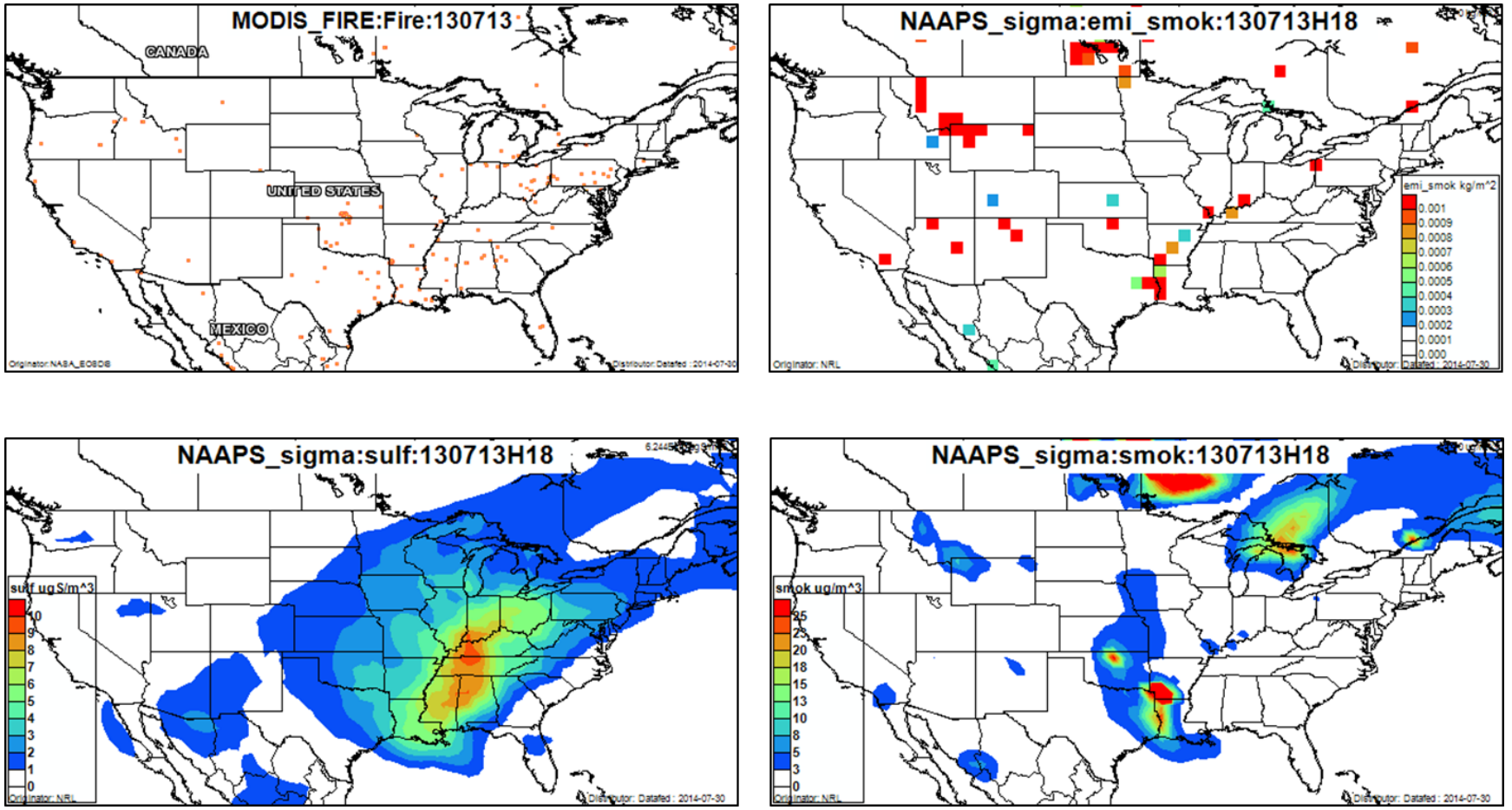

Figure 3-169. July 13, 2013 DataFed analysis. Upper left panel: Locations of active fires from MODIS satellite fire detections. Upper right panel: NAAPS model smoke emissions. Lower left panel: NAAPS model surface layer sulfate concentrations. Lower right panel: NAAPS model surface layer smoke concentrations.

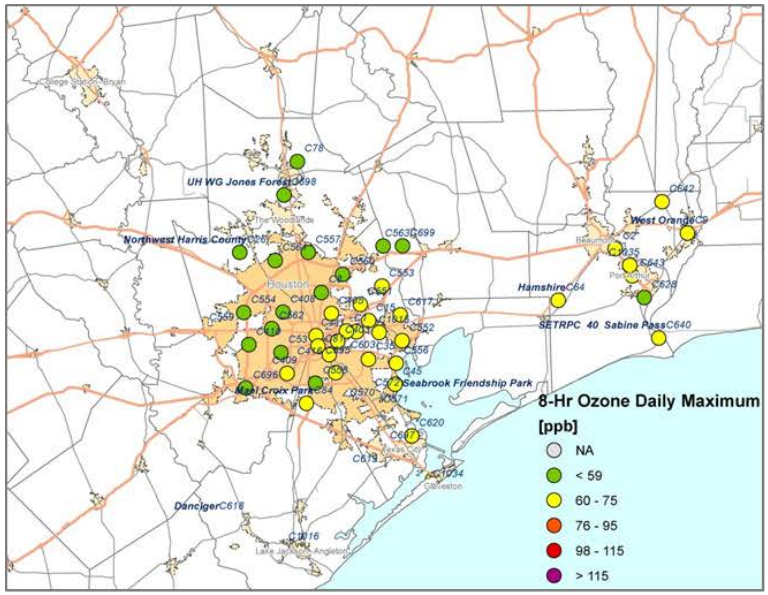

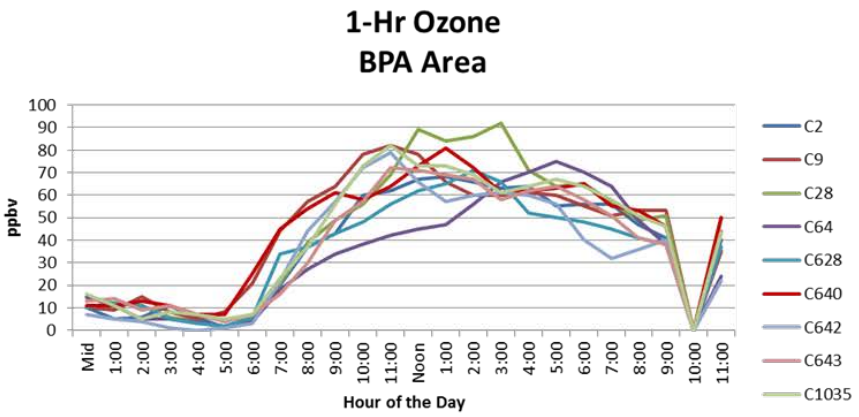

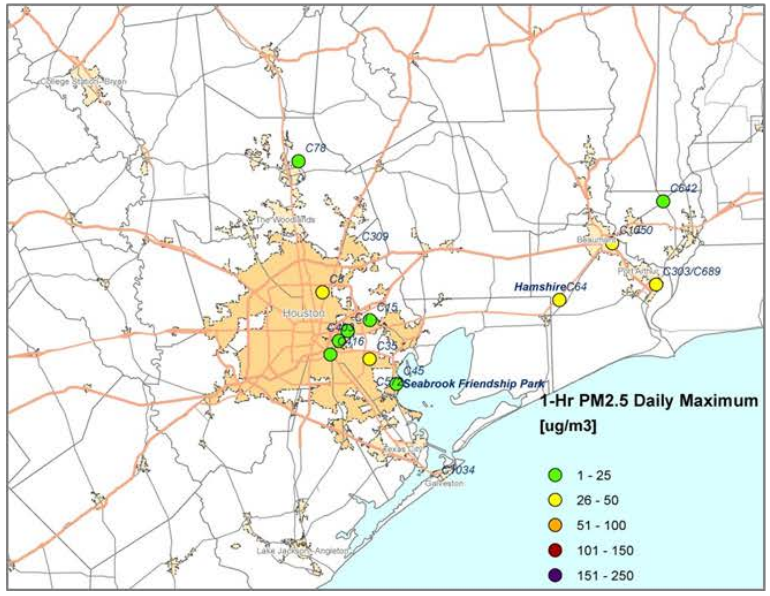

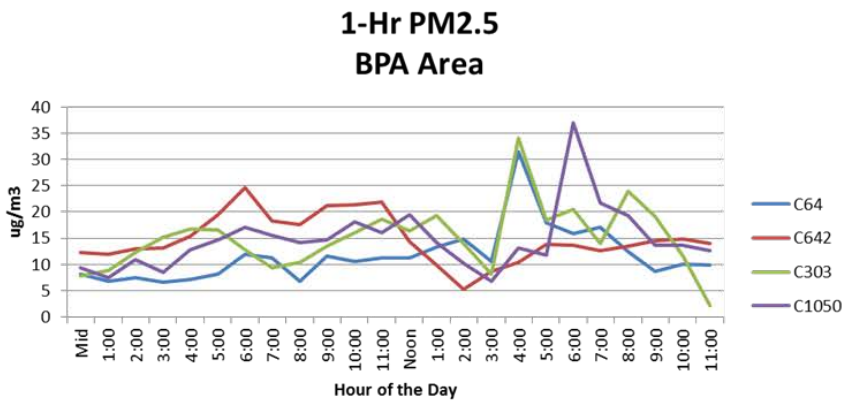

Figure 3-170. Regional ozone (top left and right) and $PM_{2.5}$ (bottom left and right) measurements (BPA area time series).

3.2.9 August 16, 2013

On August 16, 2013 ozone the Manvel Croix monitor (C84) recorded its highest ozone MDA8 value of 2013 (94 ppb) and had a maximum 1-hour average value of 109 ppb (Figure 3-171). Surface wind vectors show northerly winds in the morning shifting to southeasterlies in the early afternoon with northerly winds returning in the evening. There is no significant peak in NO or NOx at Manvel Croix on August 16. The AQplot trajectories show the influence of the sea/bay breeze circulation at the sites near the Gulf coast and Galveston Bay (Figure 3-171). The C698 and C64 monitors show generally northerly winds and are less influenced by the marine circulation.

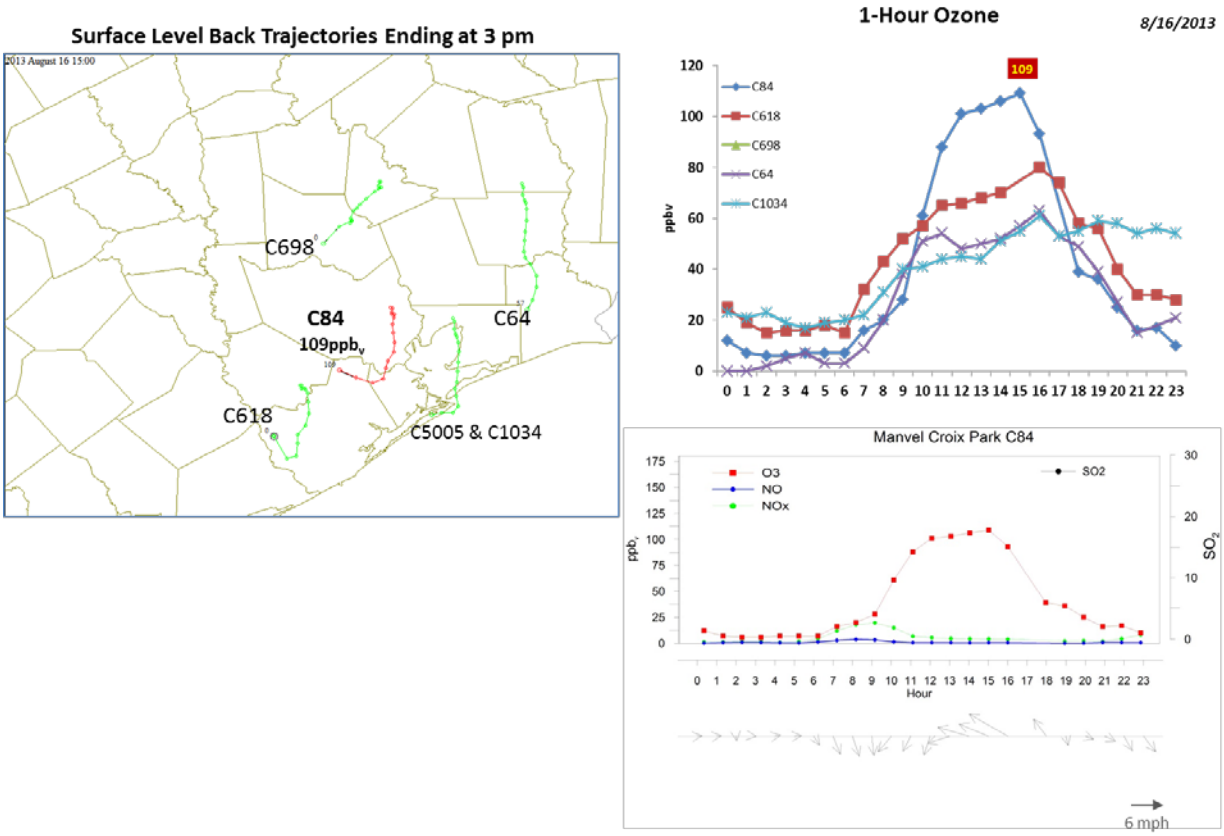

Figure 3-171. August 16, 2013 high ozone day at Manvel Croix Park C84. Left panel: AQPlot back trajectories ending at C84 and four background sites at the time of peak 1-hr ozone was observed. Upper right panel: 1-hour average ozone time series for the C84 and background monitors. Lower right panel: time series of 1-hour ozone, NO, NO_2 and wind vectors at the Grapevine Fairway C84 site.

The SmartFire back trajectories and the HYSPLIT NAM 500 m and 1,000 m trajectories are consistent with one another in showing transport from the northwest during the 72 hours leading up to the time of the ozone maximum at Manvel Croix. (Figure 3-172). These trajectories extend backward into Louisiana. The SmartFire map shows fires (for August 16)

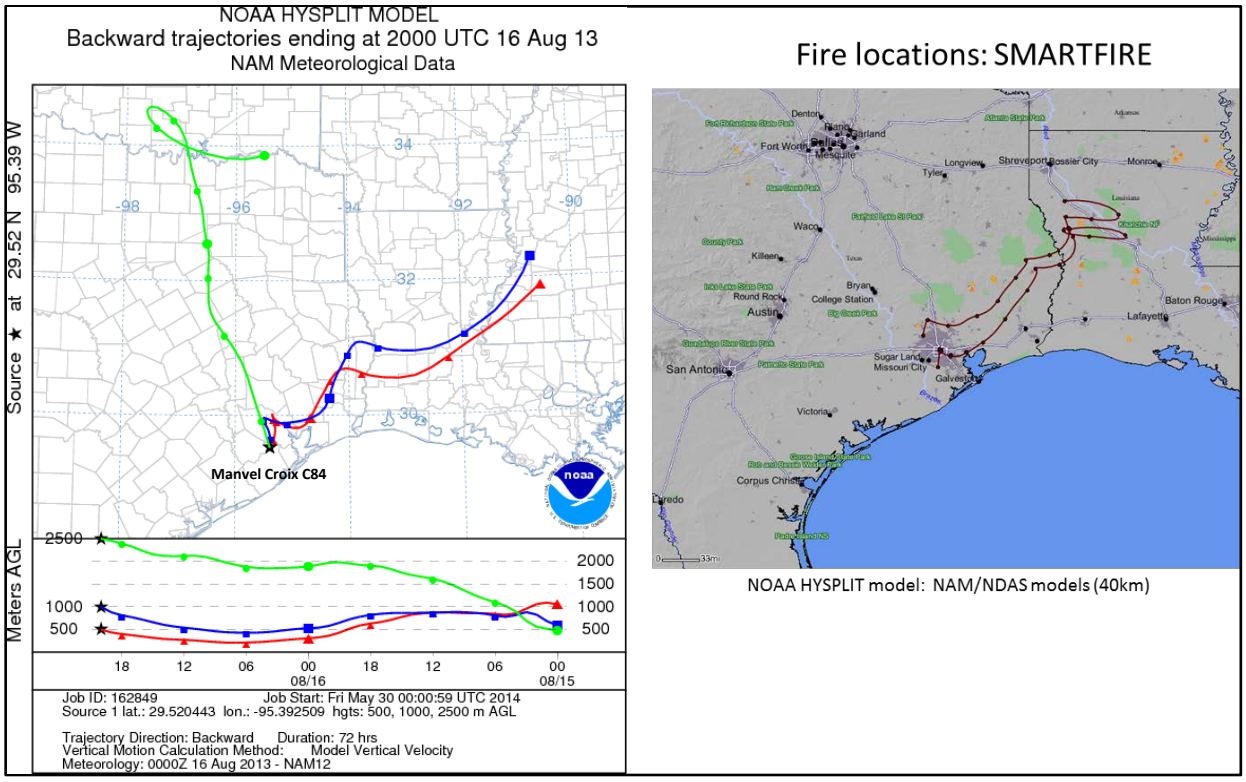

Figure 3-172. 72-hour HYSPLIT back trajectories (NAM 12km) from Manvel Croix Park (C84) terminating August 16, 2013; SmartFire plot showing fire locations (orange triangles) and 72-hour HYSPLIT back trajectories (EDAS 40 km) from C84.

near the Manvel Croix back trajectory's termination in Louisiana. However, the FINN emissions plots show that these fires were not present at -72, -48 or -24 hours, but do appear on August 16. Therefore, these fires could not have influenced the air arriving at Manvel Croix on August 16. The HMS product (Figure 3-173) and DataFed MODIS fire location plot (Figure 3-176) are similar to the SmartFire map in showing fires northeast of the HGB area and in Louisiana on August 16 (Figure 3-173) and the HMS product and the NAAPS analysis (Figure 3-176) show the presence of smoke over East Texas.

The spatial pattern of ozone on August 16 (Figure 3-177) shows that the monitors with the highest MDA8 on August 16 were those located in the HGB urban area on the southwestern side. Monitors on the northern perimeter of the urban area had the lowest MDA8 values on this day. This pattern is consistent with an impact due to local HGB sources at Manvel Croix, which is located downwind of the urban area for northeasterly flow.

$PM_{2.5}$ time series show low values of the MDA1 for all monitors that are upwind of the HGB urban area for northeasterly flow except for C309. All monitors have relatively low values of PM.5 and the only monitor to show a plume impact is C35, which saw a brief period of enhanced $PM_{2.5}$ during the early morning, well before the Manvel Croix ozone maximum.

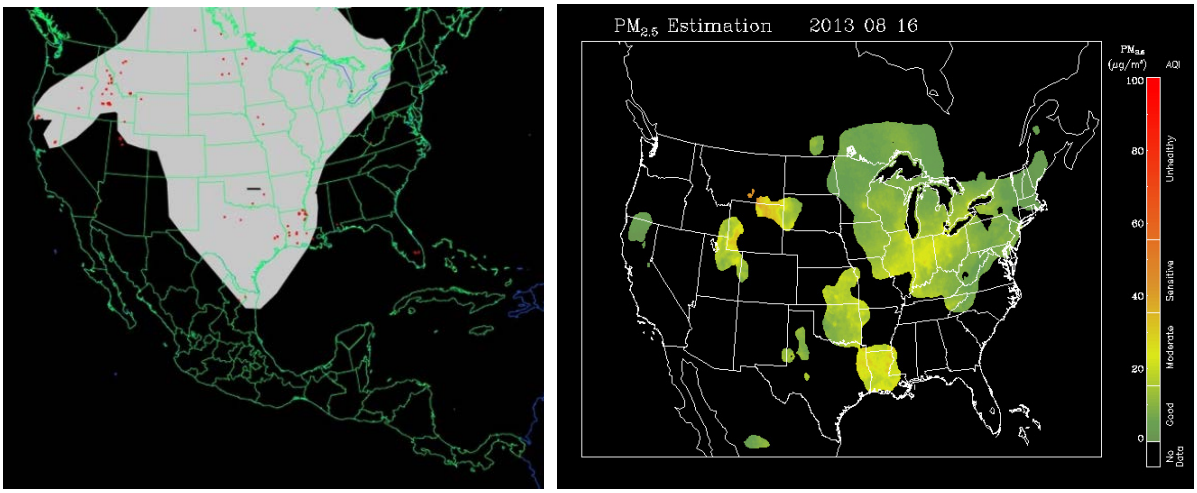

Figure 3-173. Left panel: HMS product showing August 16 fire locations (red dots) and smoke plume (gray area). Right panel: IDEA surface $PM_{2.5}$ estimate based on AOD and surface monitoring data.

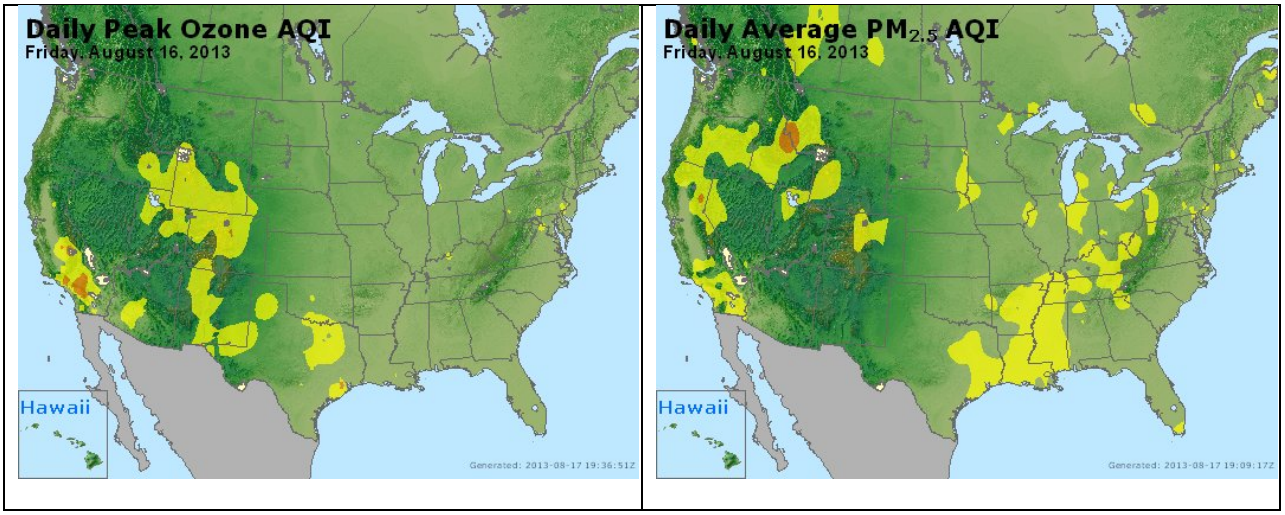

Figure 3-174. Daily average ozone (left) and $PM_{2.5}$ (right) based on observed values. Data from: http://www.airnow.gov/.

Because there is no evidence of a fire plume impact at Manvel Croix, we recommend no further evaluation of August 16, 2013.

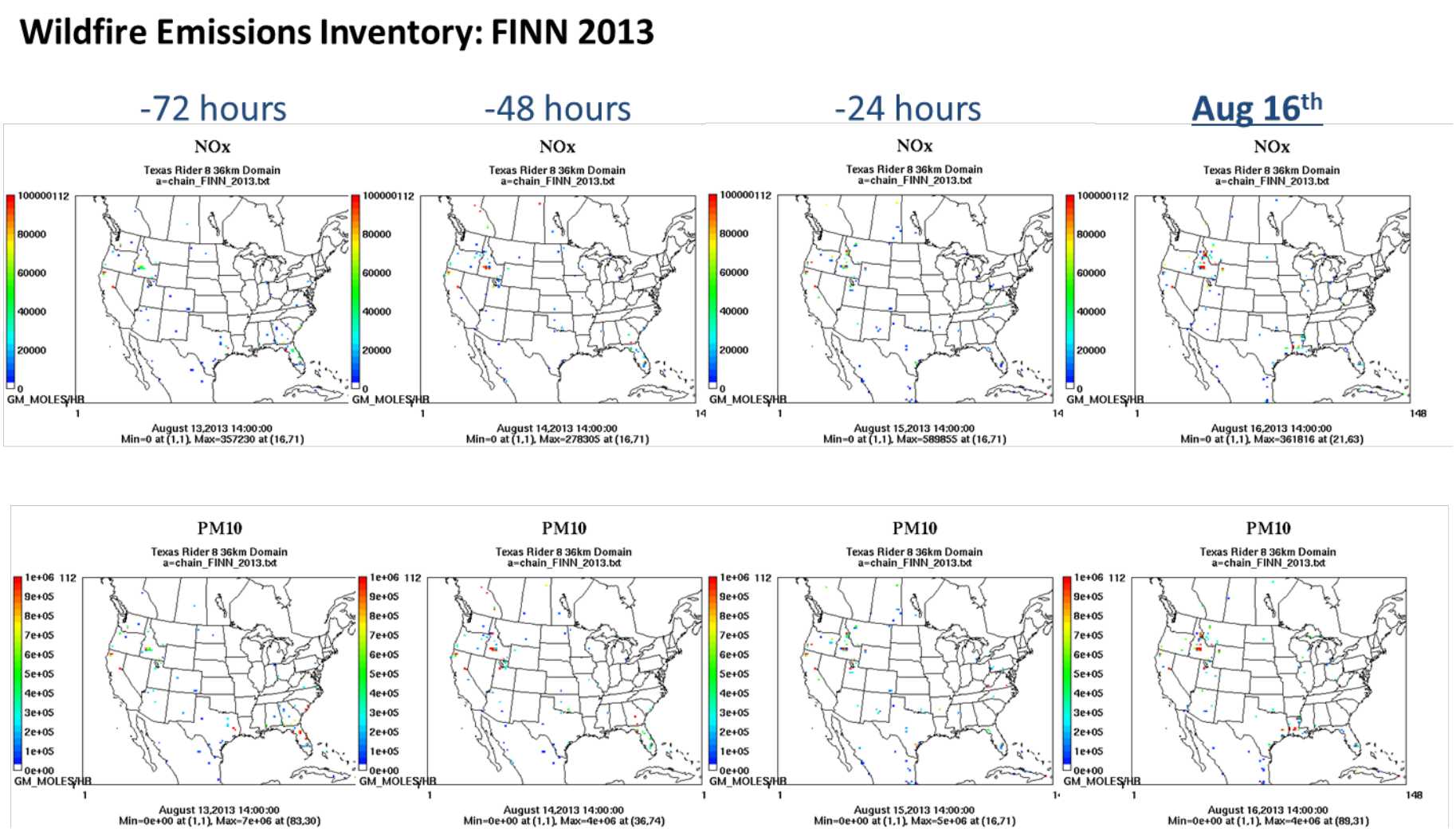

Figure 3-175. August 16, 2013 FINN fire emissions of NOx and PM_{10}.

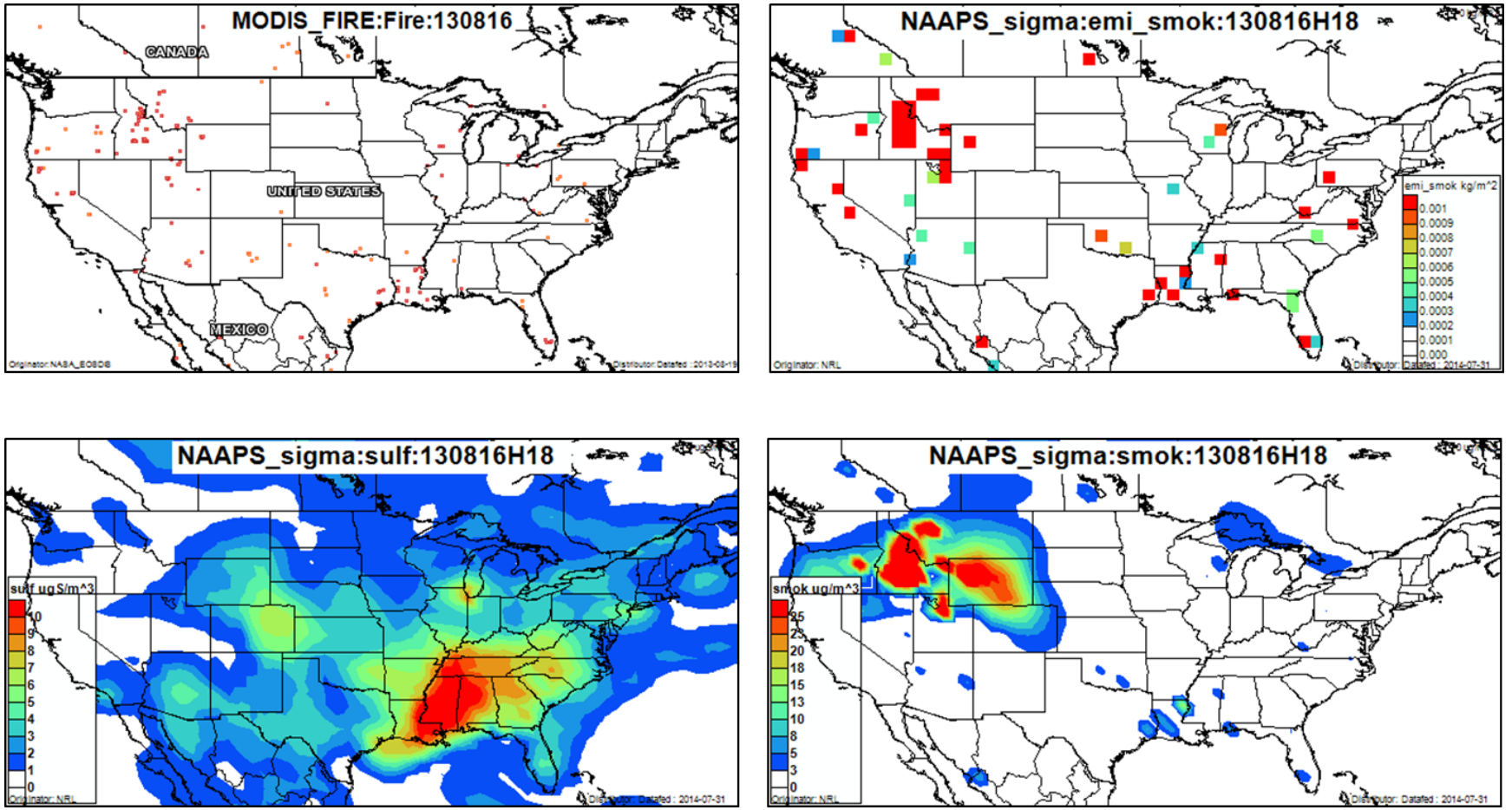

Figure 3-176. August 16, 2013 DataFed analysis. Upper left panel: Locations of active fires from MODIS satellite fire detections. Upper right panel: NAAPS model smoke emissions. Lower left panel: NAAPS model surface layer sulfate concentrations. Lower right panel: NAAPS model surface layer smoke concentrations.

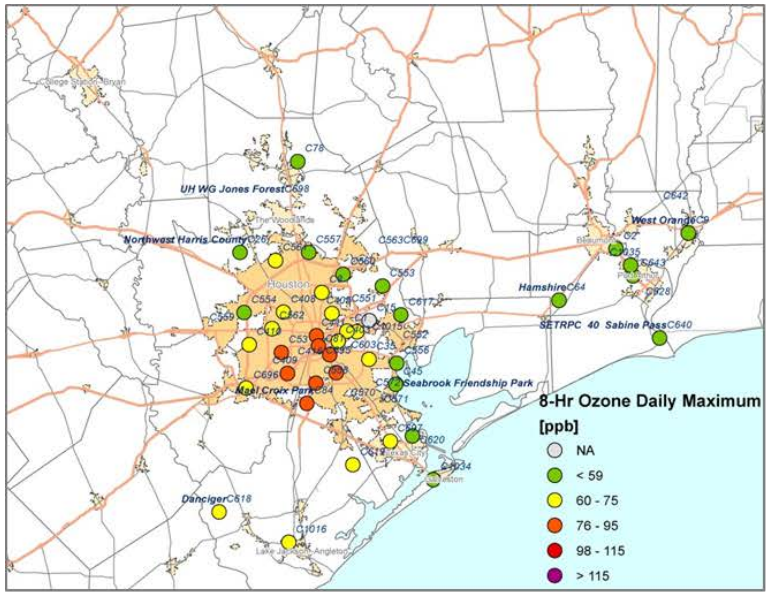

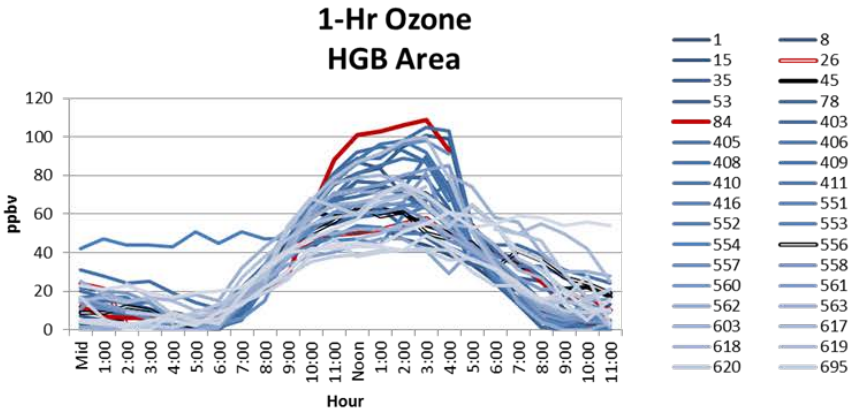

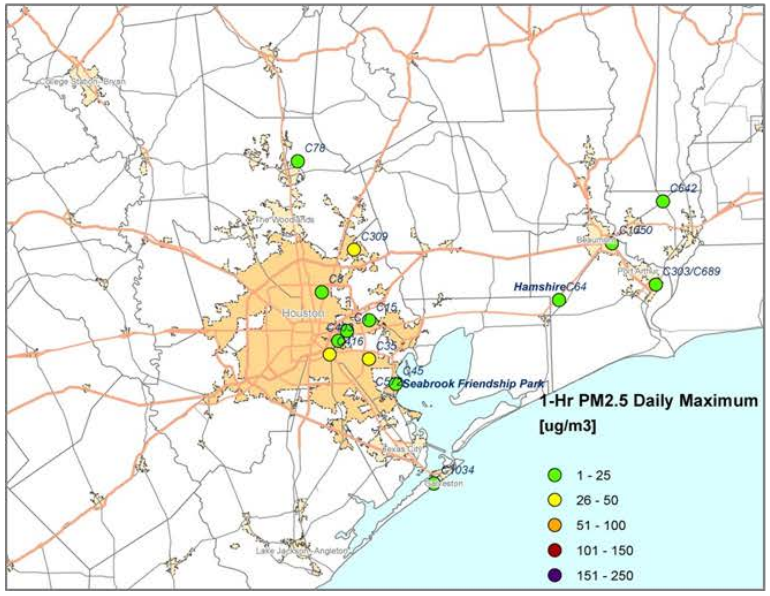

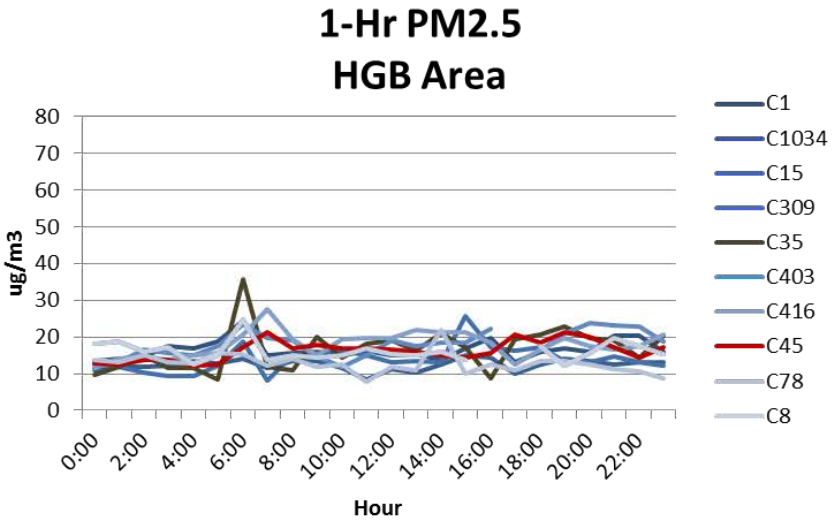

Figure 3-177. Regional ozone (top left and right) and $PM_{2.5}$ (bottom left and right) measurements (HGB area time series).

3.2.10 August 28, 2013

On August 28, the Northwest Harris County monitor had its highest MDA8 reading (83 ppb) of 2013. The wind vectors at the monitor (Figure 3-178) show the influence of the marine circulation, with light northerly winds in the early morning hours followed by a shift to southeasterlies by the afternoon. AQPlot back trajectories also show light, shifting winds with afternoon flow from the southeast at NW Harris.

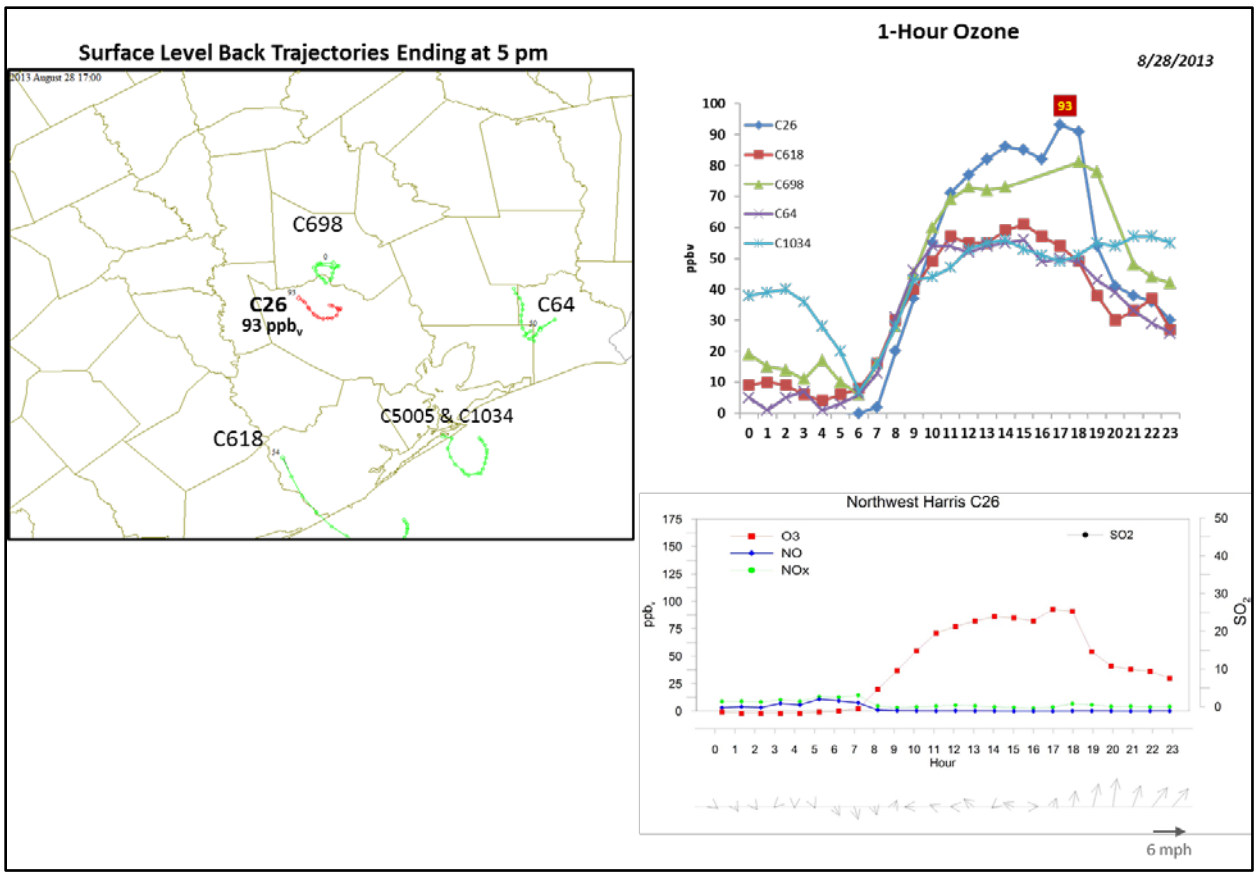

Figure 3-178. August 28, 2013 high ozone day at Northwest Harris Co. C26. Left panel: back trajectories calculated using AQPlot for the HGB monitors at the time of peak ozone impact at C26. Upper right panel: 1-hour average ozone time series for the C26 and surrounding HGB monitors. Lower right panel: time series of 1-hour ozone, NO, NO_2 and wind vectors at the Northwest Harris monitor.

The SmartFire back trajectories also show southerly flow on August 28, with back trajectories eventually extending over the Gulf of Mexico (Figure 3-179). The 500 m HYSPLIT NAM back trajectory is similar to the SmartFire trajectory, while the 1,000 m and 2,500 m HYSPLIT NAM trajectories indicate the presence of vertical wind shear, and have more northerly trajectories. The SmartFire map shows no fires present along the back trajectories on August 28 and the FINN emissions show no fires present along the SmartFire and 500 m HYSPLIT back trajectories during the 72 hour period preceding high ozone at the NW Harris County monitor.

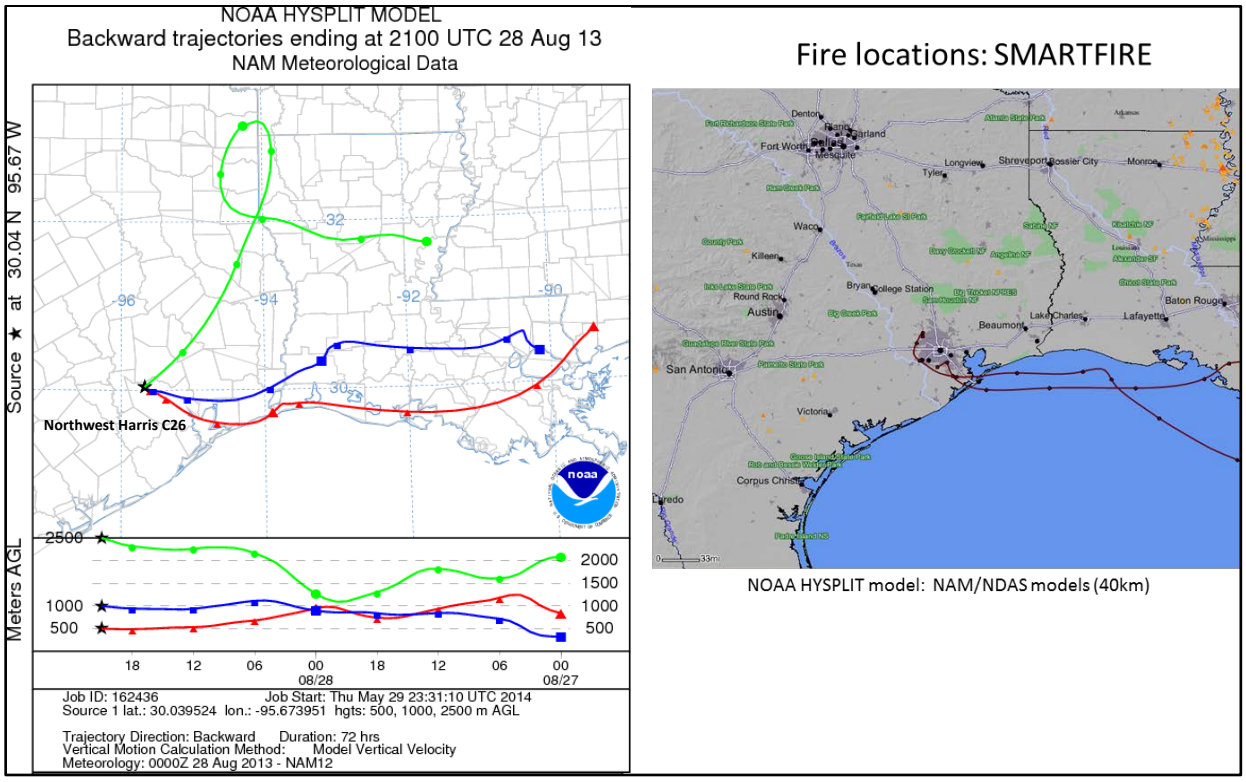

Figure 3-179. 72-hour HYSPLIT back trajectories ending at Northwest Harris C26 at August 28, 2013; Right side: SmartFire plot with nearby fire locations (orange triangles) and 72-hour HYSPLIT back trajectories terminating at HGB sites (C26 and C84).

The HMS product, FINN emissions, DataFed fire location and NAAPS smoke analysis show no fires nor smoke along the back trajectory paths (Figure 3-180), and there is no evidence of a peak in 1-hour average $PM_{2.5}$ or NOx that would indicate a plume impact at the time of the 1-hour ozone peak at the NW Harris County monitor (Figure 3-184). Therefore, we find no evidence of a fire plume impact at the NW Harris County monitor on August 28, 2013, and recommend no further evaluation of this day.

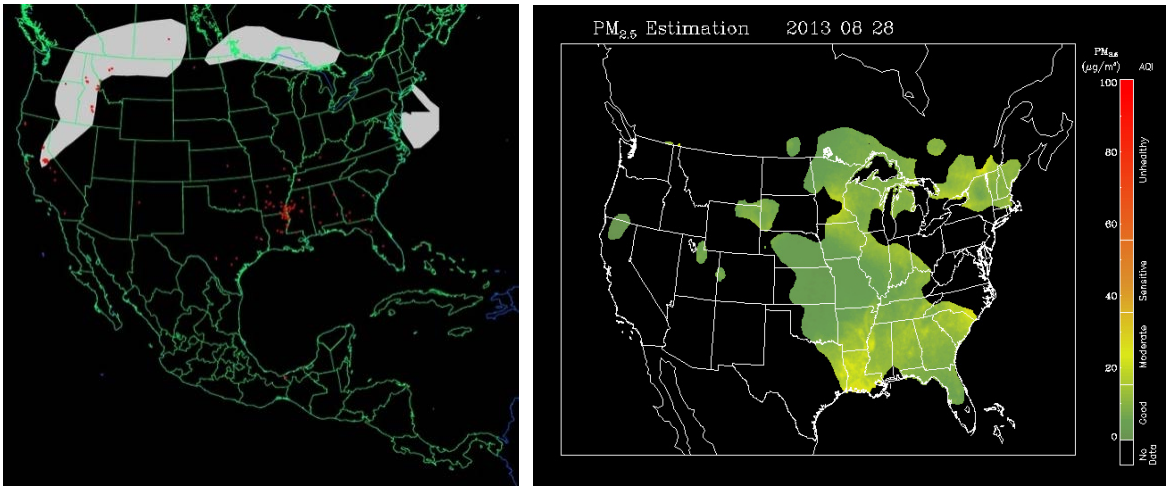

Figure 3-180. Left panel: HMS product showing August 28 fire locations (red dots) and smoke plume (gray area). Right panel: IDEA surface $PM_{2.5}$ estimate based on AOD and surface monitoring data.

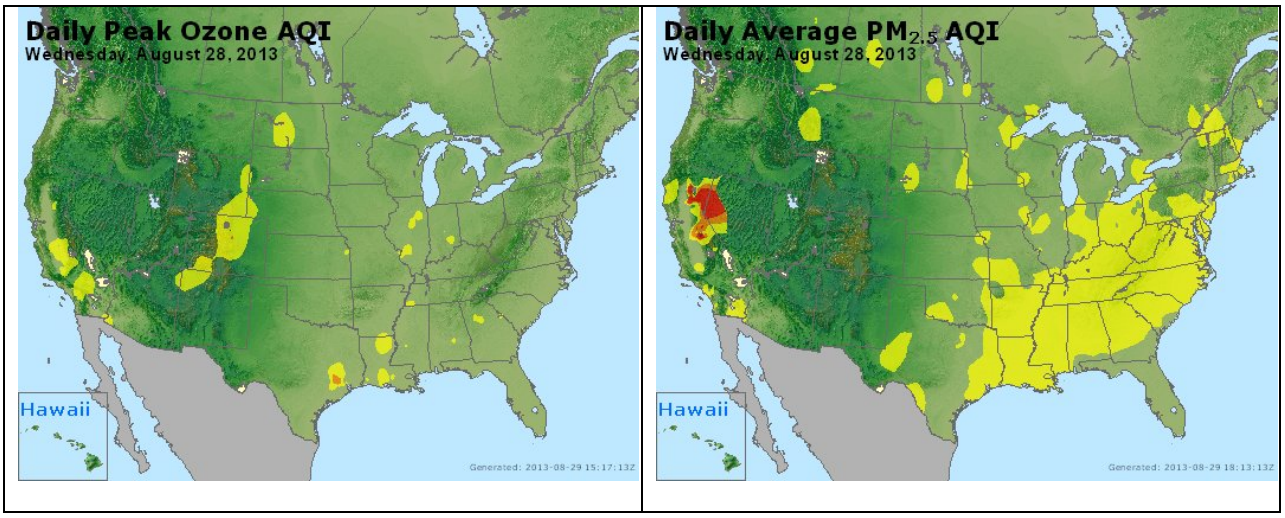

Figure 3-181. Daily average ozone (left) and $PM_{2.5}$ (right) based on observed values. Data from: http://www.airnow.gov/.

Wildfire Emissions Inventory: FINN 2013

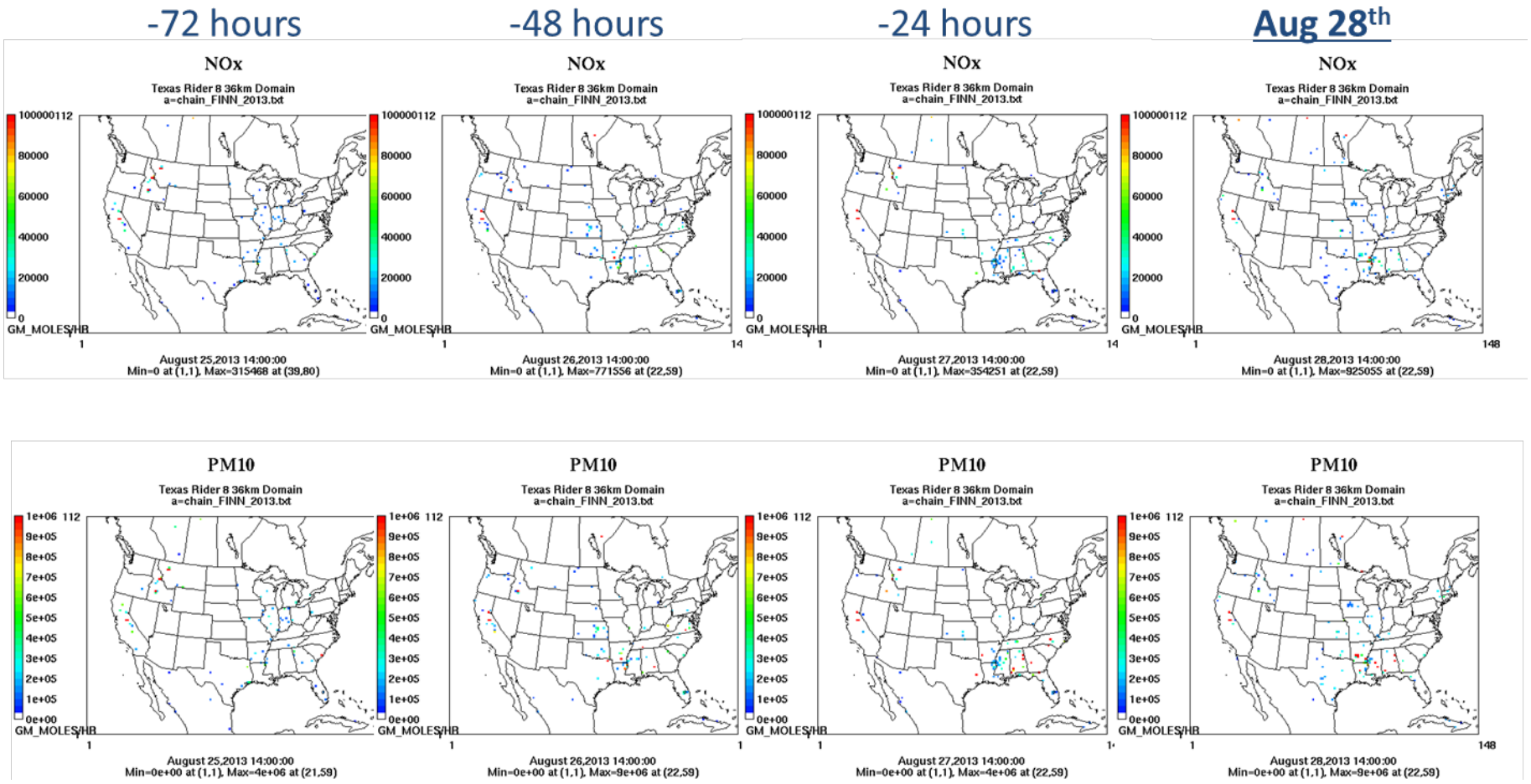

Figure 3-182. August 28, 2013 FINN fire emissions of NOx and PM_{10}.

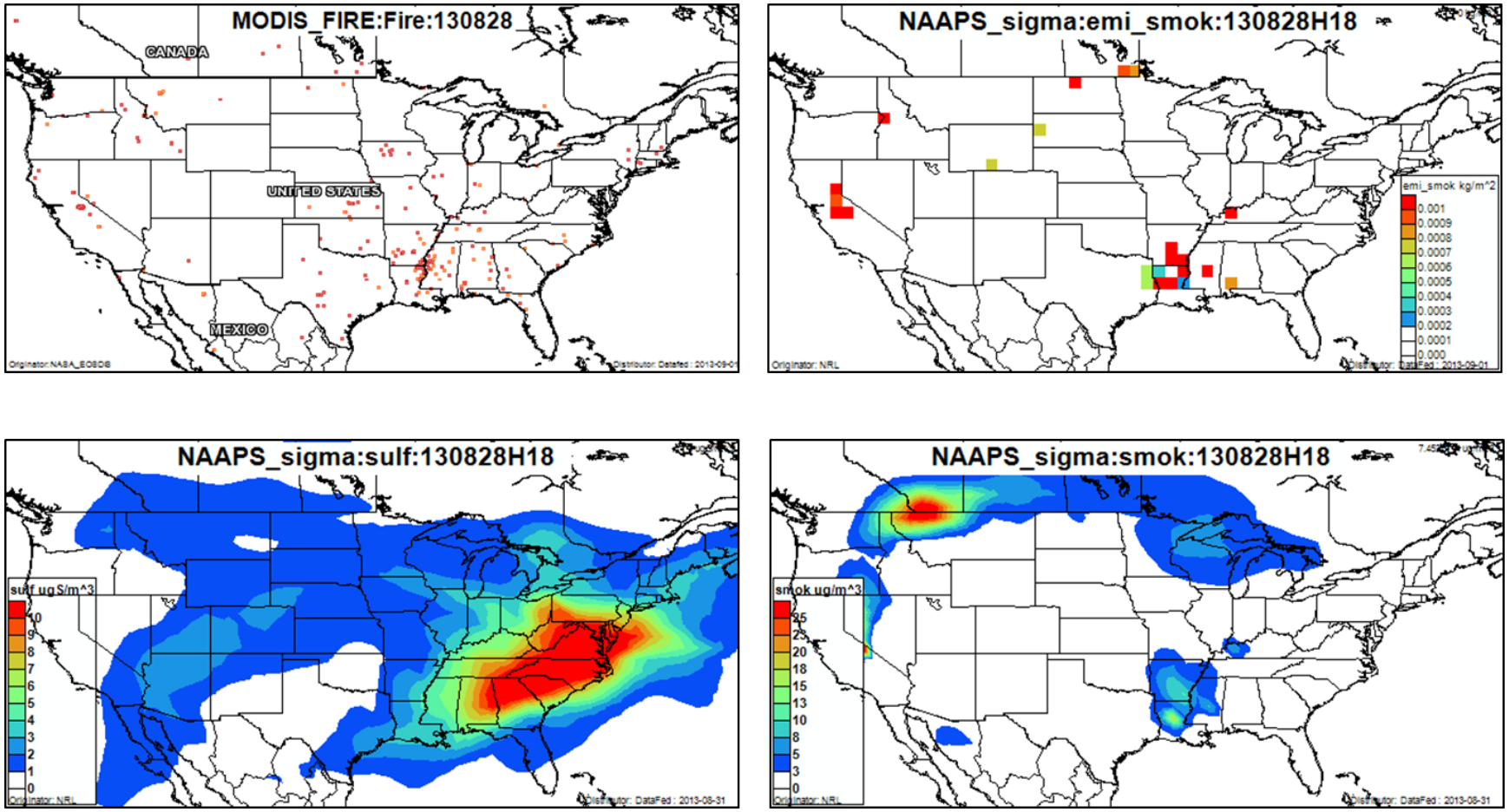

Figure 3-183. August 28, 2013 DataFed analysis. Upper left panel: Locations of active fires from MODIS satellite fire detections. Upper right panel: NAAPS model smoke emissions. Lower left panel: NAAPS model surface layer sulfate concentrations. Lower right panel: NAAPS model surface layer smoke concentrations.

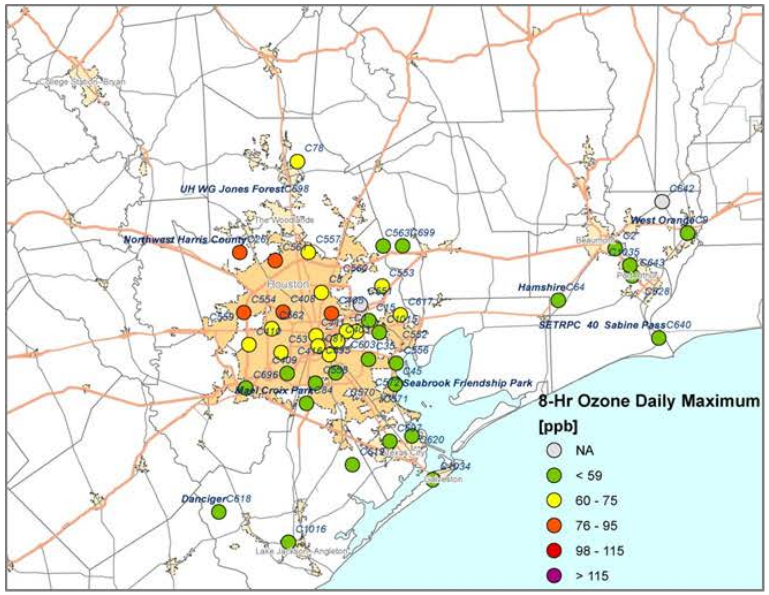

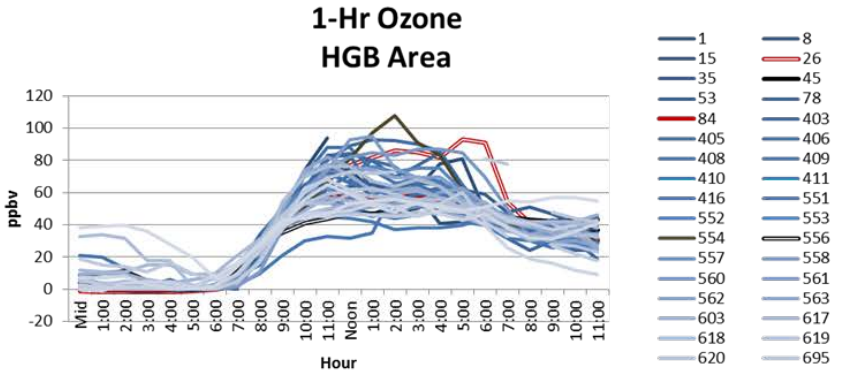

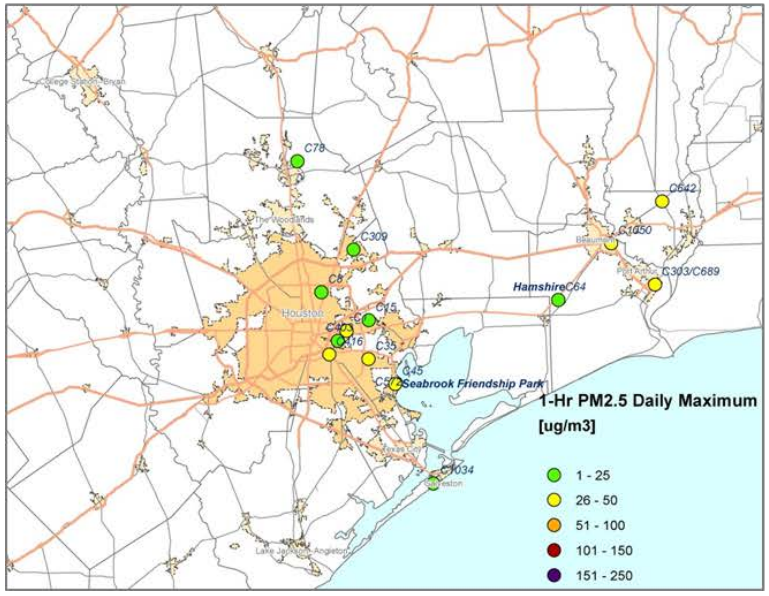

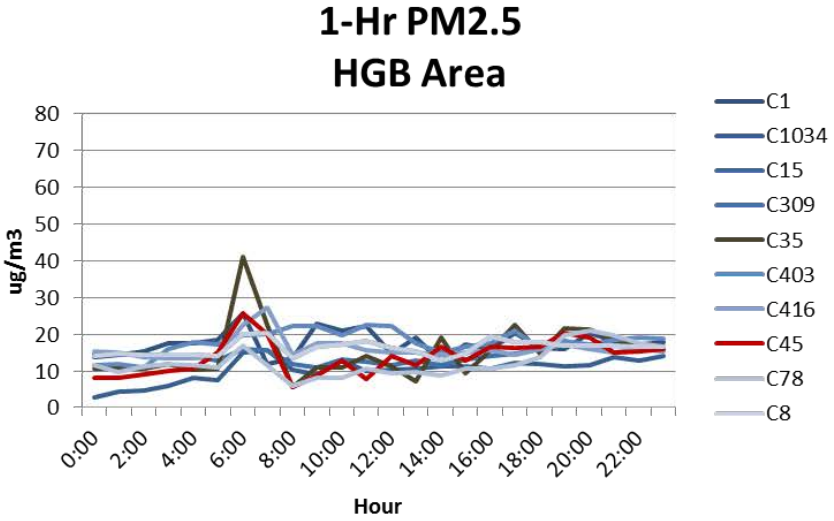

Figure 3-184. Regional ozone (top left and right) and $PM_{2.5}$ (bottom left and right) measurements (HGB area time series).

3.2.11 August 30, 2013

On August 30, the Grapevine Fairway C70 site observed its third highest ozone MDA8 reading of 89 ppb. The background ozone level in the DFW area was ~60 ppb on August 30 (Figure 3-191). The 1-hour ozone peak at Grapevine (95 ppb) was well above the background, but was similar to that of other monitors such as Keller (C17), Denton Airport South (C56) and Dallas North No. 2 (C63). Winds at the Grapevine monitor were south-southeasterly during the daylight hours.

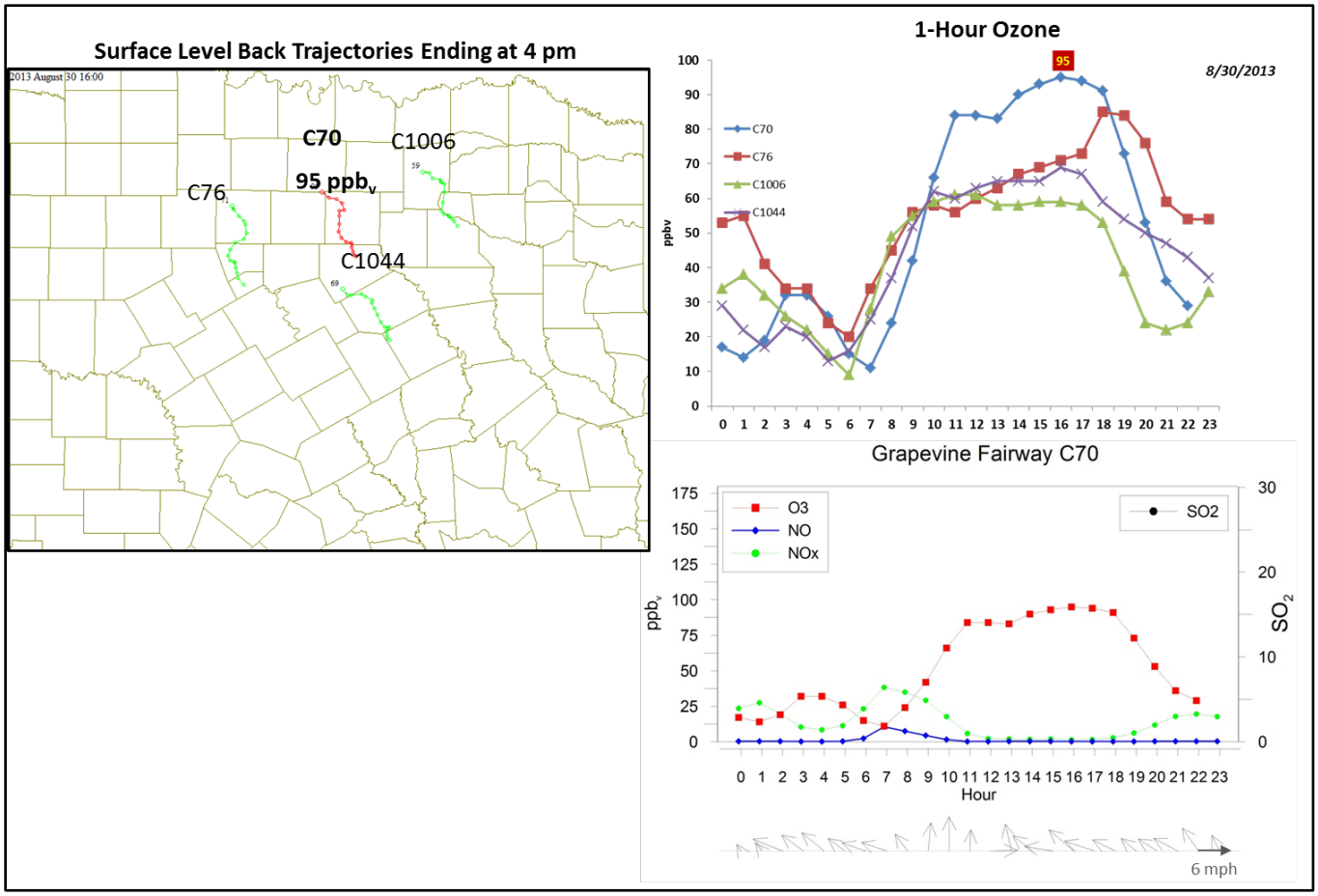

Figure 3-185. August 30, 2013 high ozone day at Grapevine Fairway C70. Left panel: AQPlot back trajectories ending at C70 and four background sites at the time of peak 1-hr ozone was observed. Upper right panel: 1-hour average ozone time series for the C70 and background monitors. Lower right panel: time series of 1-hour ozone, NO, NO_2 and wind vectors at the Grapevine Fairway C70 site.

The SmartFire back trajectories (Figure 3-186) show southerly winds on August 30 and agree well with the HYSPLIT NAM 500 m back trajectory. The SmartFire map and the FINN emissions plots show no fires in the vicinity of either back trajectory on August 30, but the FINN emissions plots for -24 hours and -48 hours do show fires in the vicinity of the NAM 500 m back trajectory. It is possible that emissions from these fires could have reached the DFW area on August 30.

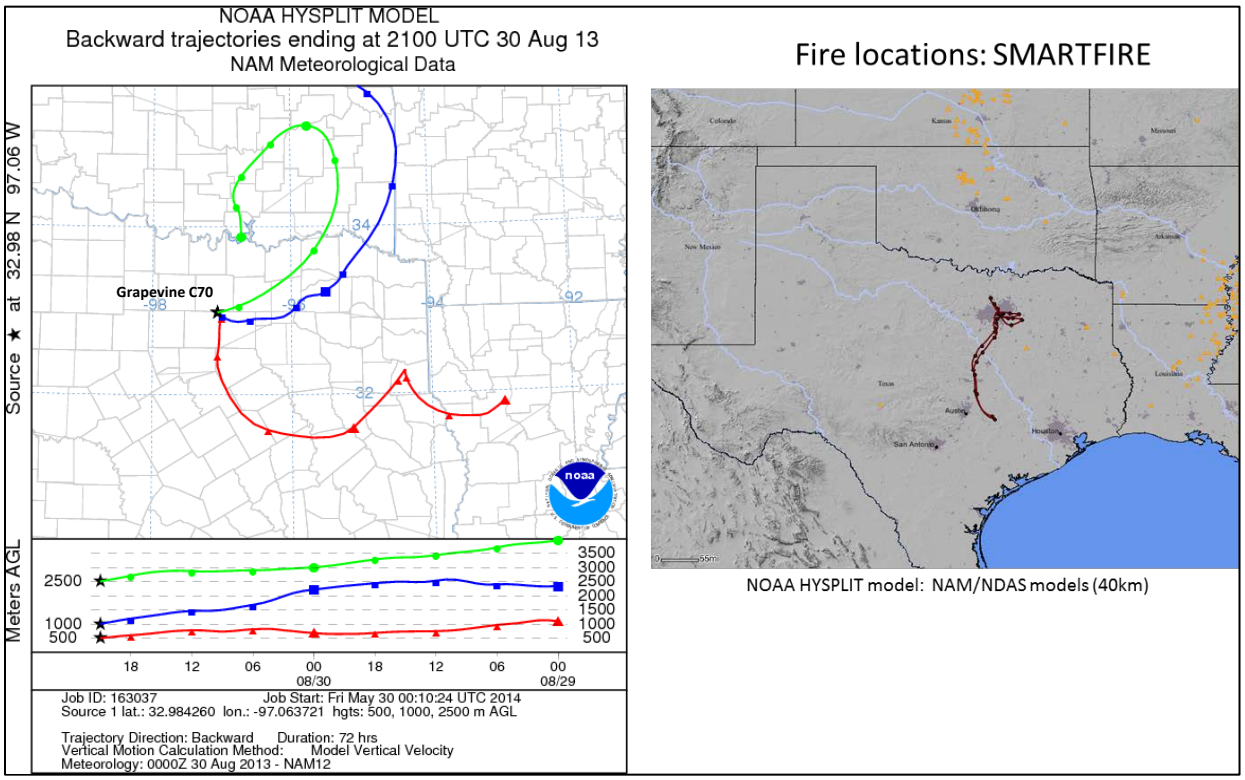

Figure 3-186. 72-hour HYSPLIT back trajectories ending at Grapevine Fairway C70 (left) on August 30, 2013; Right: SmartFire plots with fire locations (orange triangles) and 72-hour HYSPLIT back trajectories terminating at DFW sites (i.e. C56 and C70).

The monitor with the highest $PM_{2.5}$ readings during the time of ozone formation on the morning of August 30 was Dallas Hinton site (C401). A TCEQ quality control audit is in progress for the 8 am reading at Dallas Hinton. However, we note that there was a PM_{10} peak at 9 am at this site (not shown), which suggests the $PM_{2.5}$ peak may be due to the influence of a local source rather than an impact due to a distant fire. The other $PM_{2.5}$ monitors in the DFW area do not have peaks characteristic of a fire plume impact during the period of high ozone at the Grapevine monitor. At 9 pm, however, the Italy monitor (C1044) does show a $PM_{2.5}$ impact that could be a fire plume impact. However, this occurs well after the period of peak 1-hour ozone at Grapevine.

Based on the timing and magnitude of ozone and $PM_{2.5}$ peaks in the DFW area, we conclude that there is no evidence to support an ozone impact due to fire emissions at the Grapevine monitor on August 30. High ozone at Grapevine was likely cause by the influence of local emissions in addition to high levels of background ozone, and we recommend no further evaluation of this day.

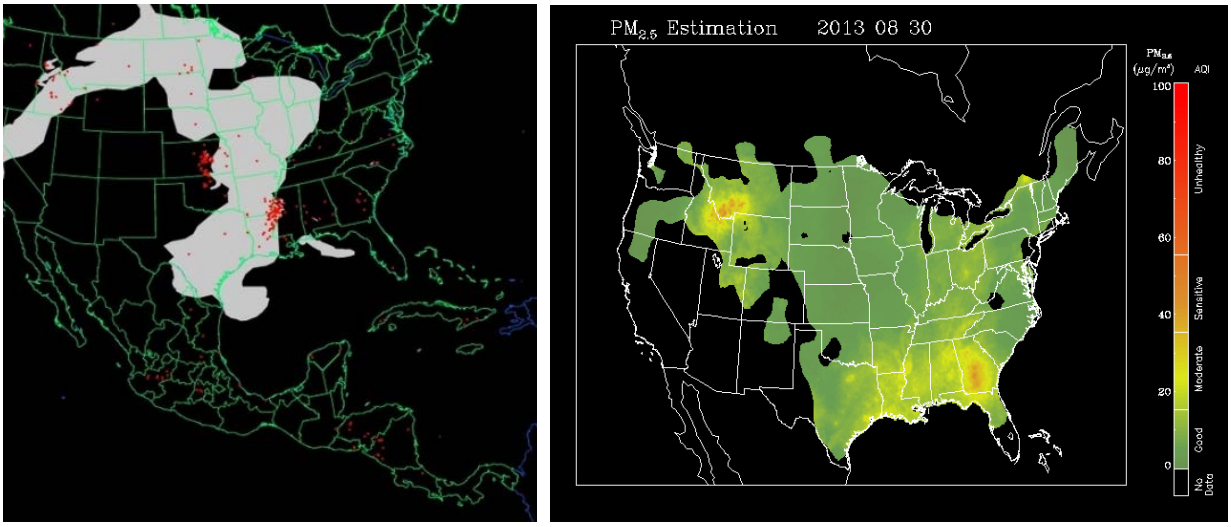

Figure 3-187. Left panel: HMS product showing August 30 fire locations (red dots) and smoke plume (gray area). Right panel: IDEA surface $PM_{2.5}$ estimate based on AOD and surface monitoring data.

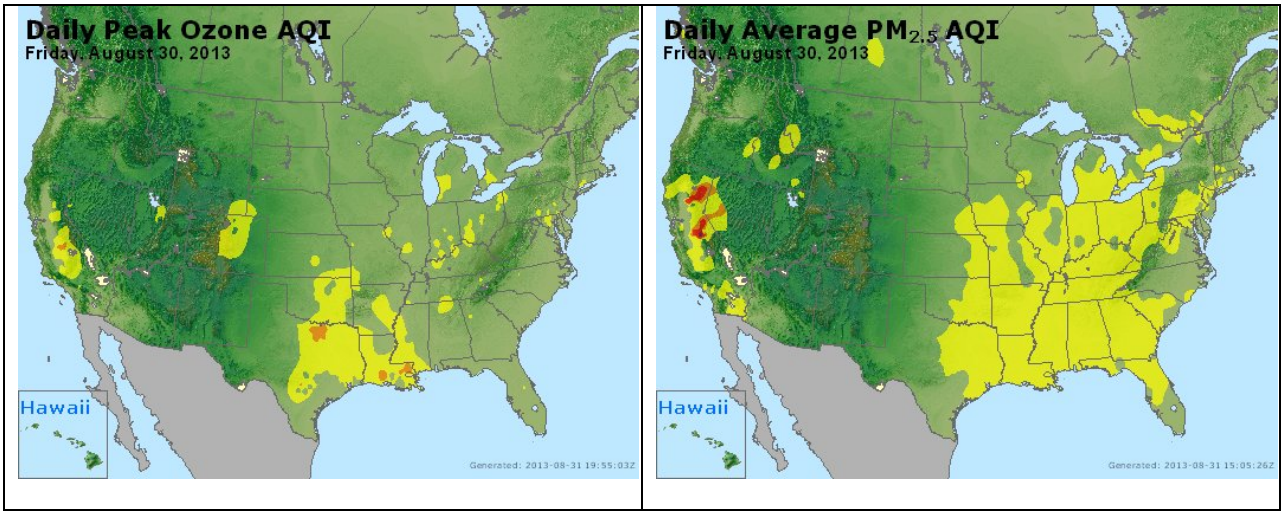

Figure 3-188. Daily average ozone (left) and $PM_{2.5}$ (right) based on observed values. Data from: http://www.airnow.gov/

ENVIRON

Wildfire Emissions Inventory: FINN 2013

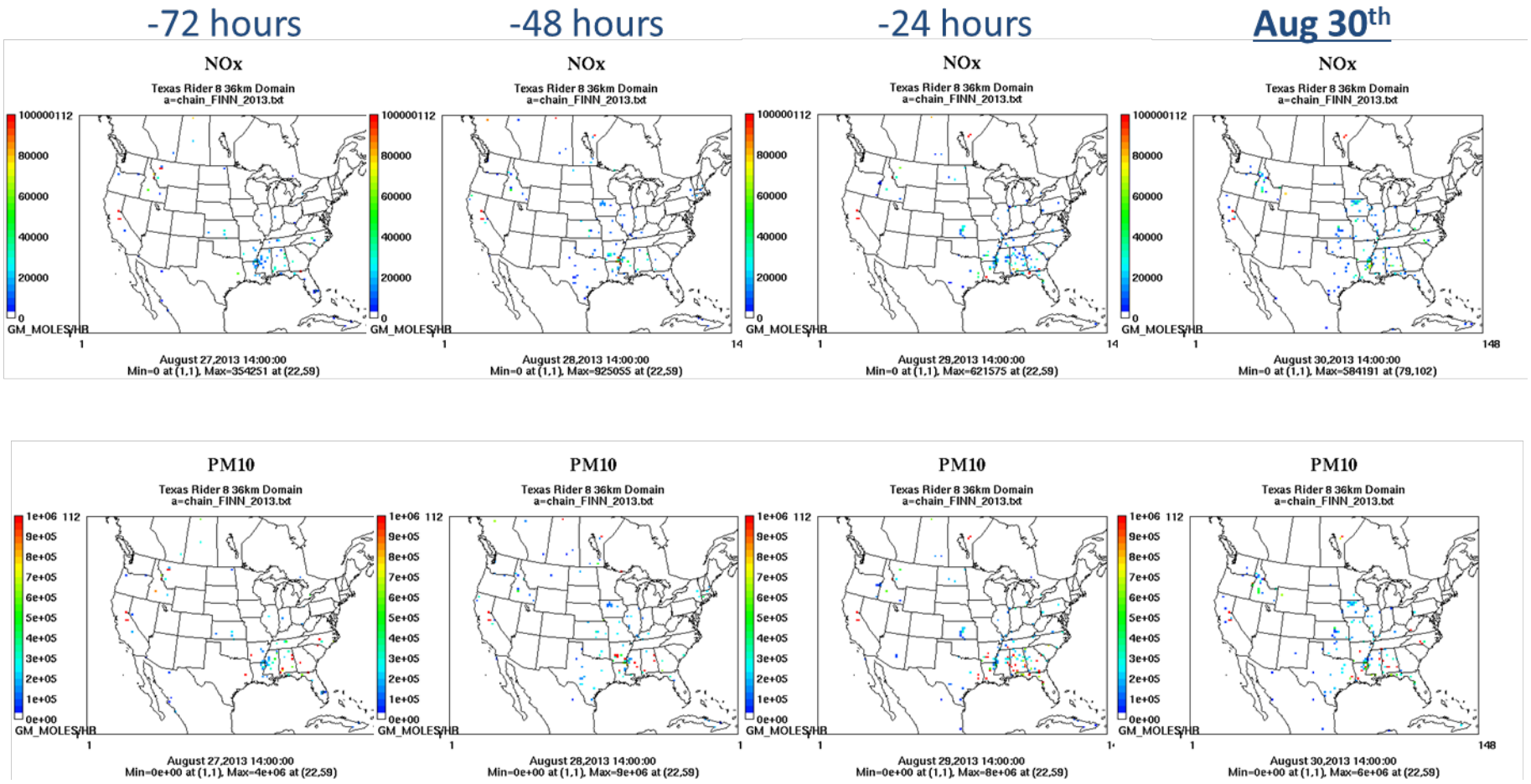

Figure 3-189. August 30, 2013 FINN fire emissions of NOx and PM_{10}.

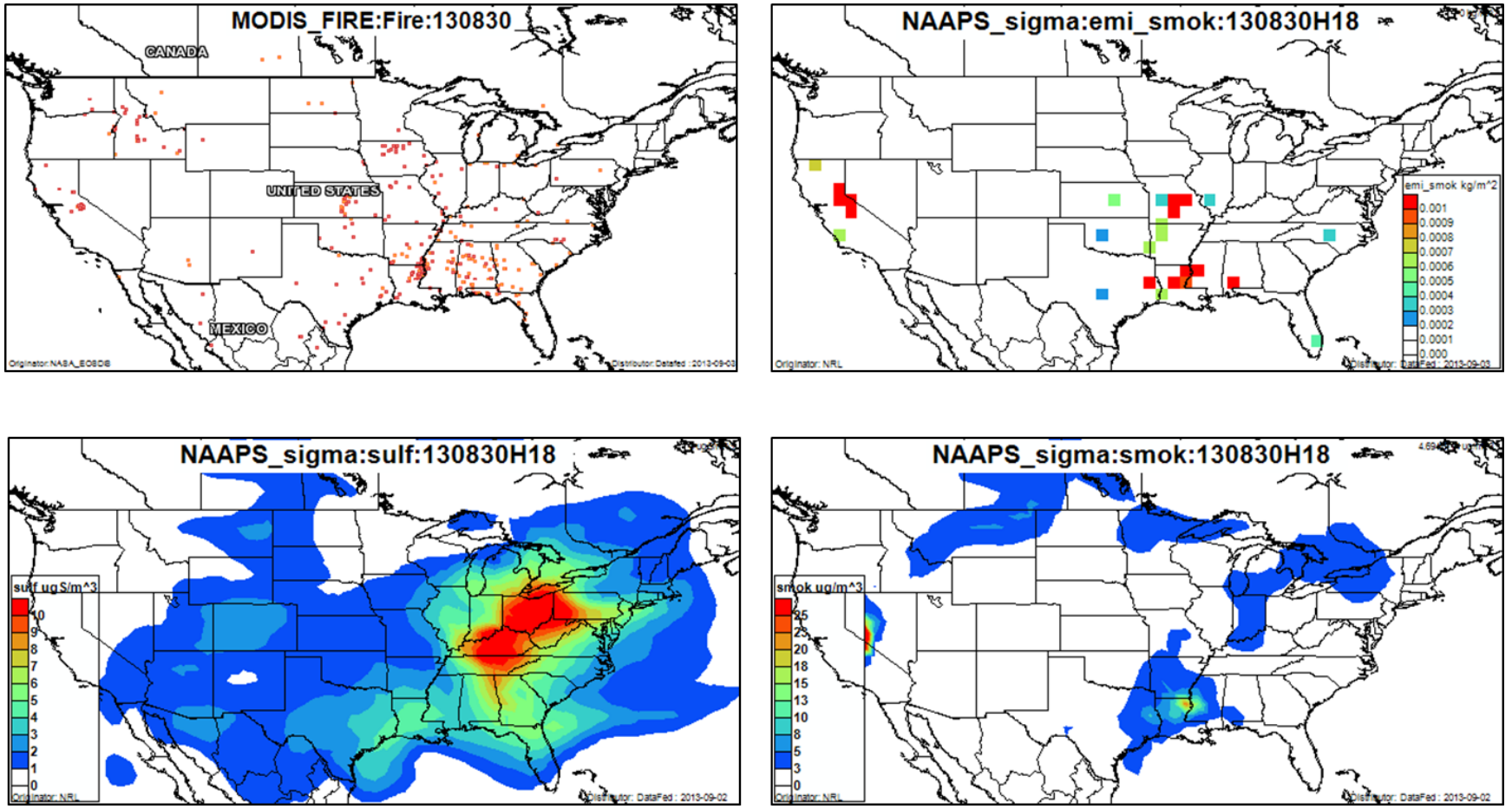

Figure 3-190. August 30, 2013 DataFed analysis. Upper left panel: Locations of active fires from MODIS satellite fire detections. Upper right panel: NAAPS model smoke emissions. Lower left panel: NAAPS model surface layer sulfate concentrations. Lower right panel: NAAPS model surface layer smoke concentrations.

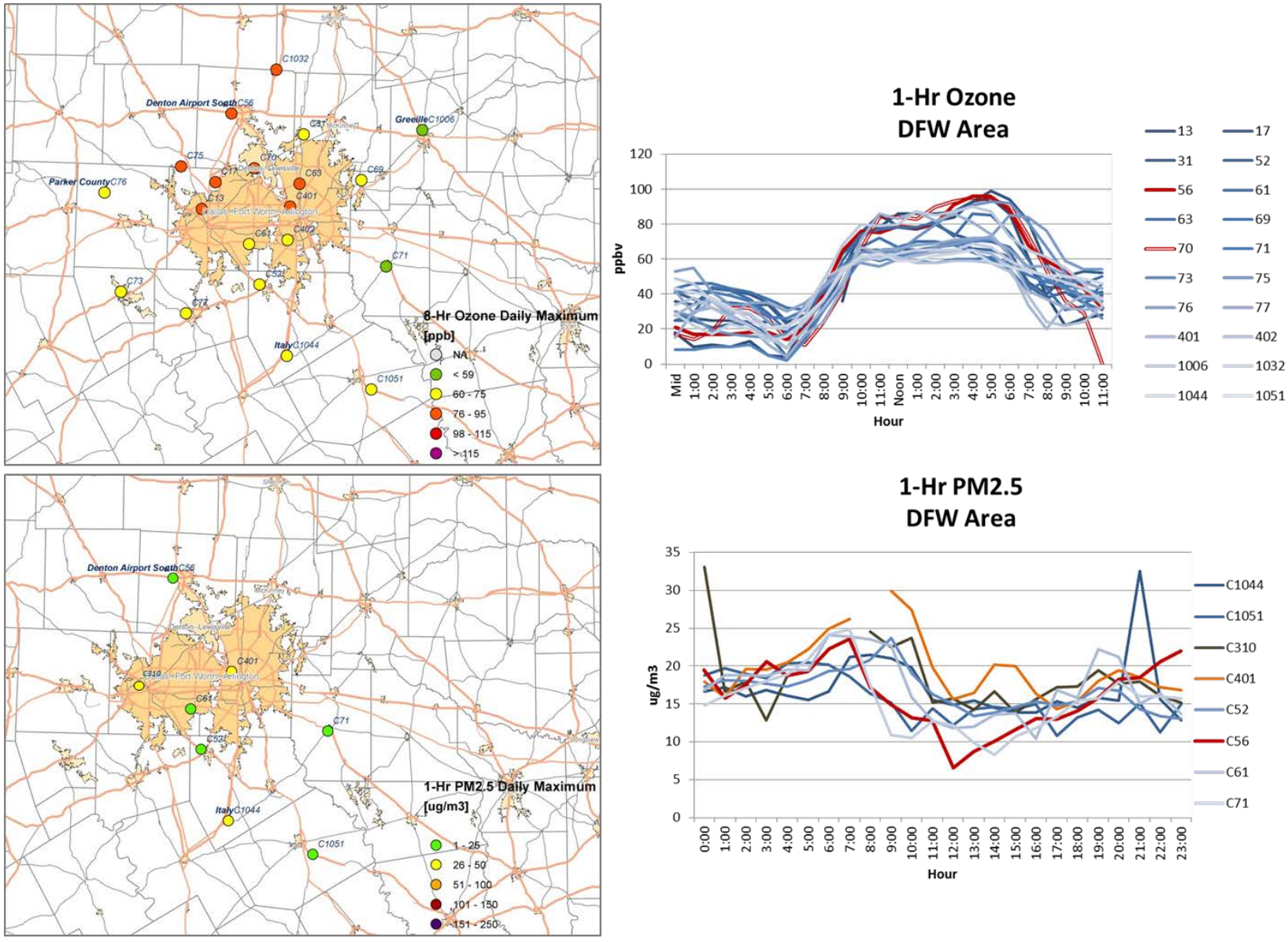

Figure 3-191. Regional ozone (top left and right) and $PM_{2.5}$ (bottom left and right) measurements (DFW area time series).

3.2.12 August 31, 2013

On August 31, the Denton Airport South C56 monitor had its 4th high ozone MDA8 reading of 85 ppb and a 1-hour ozone maximum of 93 ppb. The AQPlot back trajectory is consistent with the monitor wind vectors in showing southerly winds (Figure 3-192). The monitor shows a NOx peak at 3 am, but this peak dissipates by daybreak.

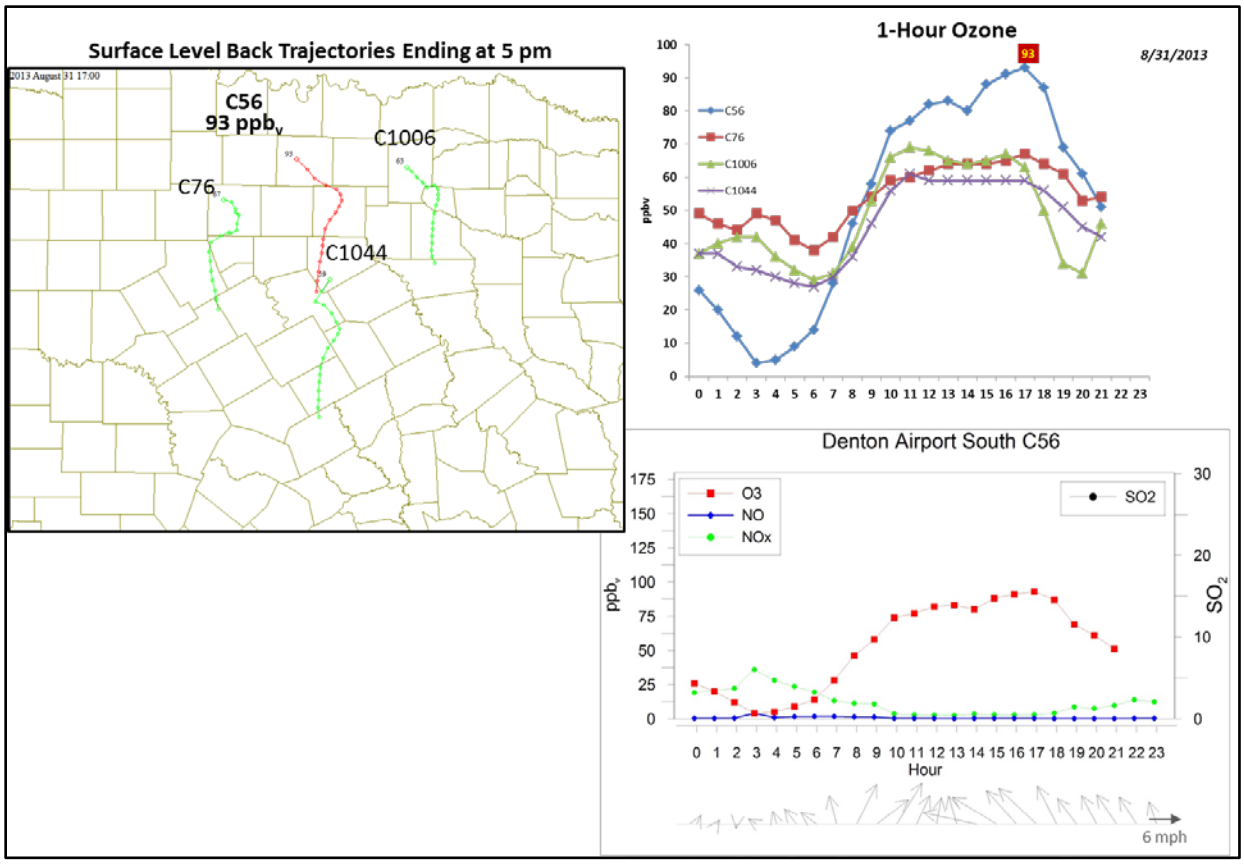

Figure 3-192. August 31, 2013 high ozone day at Denton Airport South C56. Left panel: AQPlot back trajectories ending at C56 and four background sites at the time of peak 1-hr ozone was observed. Upper right panel: 1-hour average ozone time series for the C56 and background monitors. Lower right panel: time series of 1-hour ozone, NO, NO_2 and wind vectors at the Denton Airport South C56 site.

The SmartFire back trajectories and the 500 m HYSPLIT NAM back trajectories are consistent in showing southerly winds on August 31 and back trajectories leading eastward toward the Texas-Louisiana (Figure 3-193). The HYSPLIT 1,000 m and 2,500 m back trajectories indicate the presence of significant vertical wind shear aloft. The SmartFire map shows no fires along the path of the low-level back trajectories on August 31. The FINN emissions plot for August 31 agrees, but the FINN plots for -24, -48 and -72 hours do show fires in the region traversed by the back trajectories.

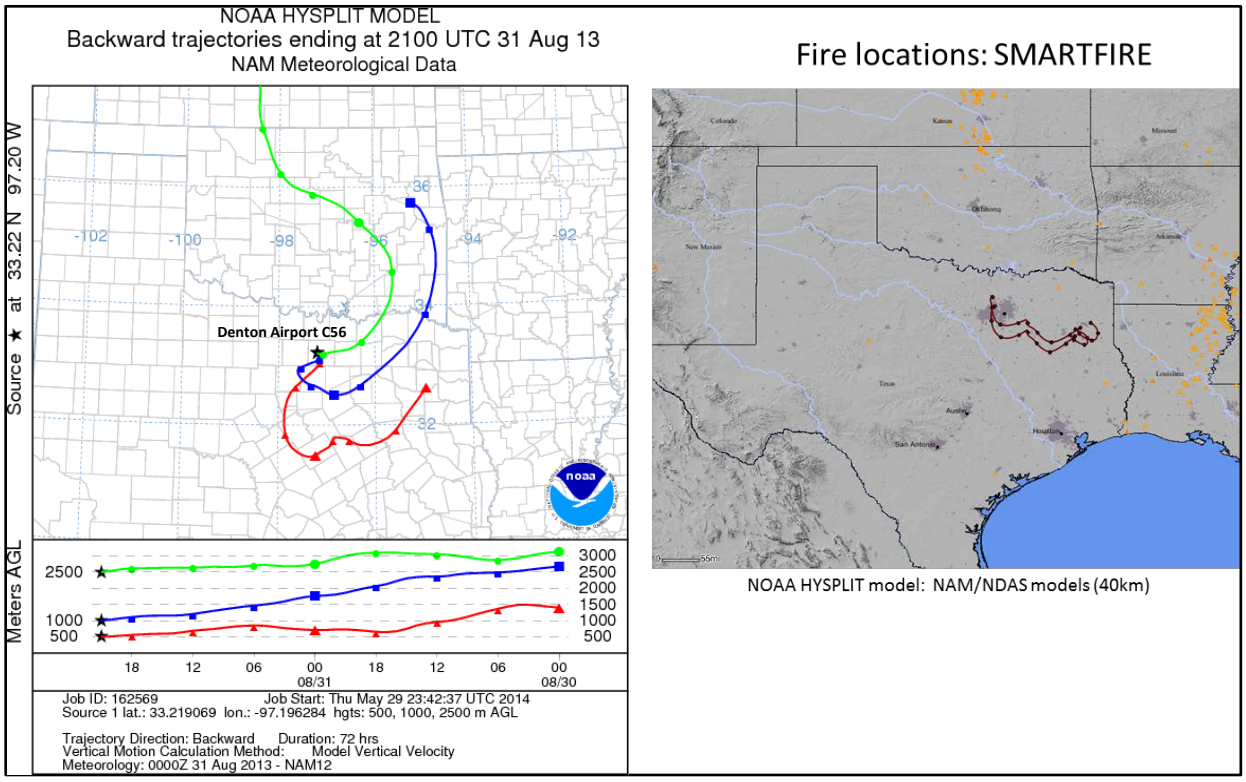

Figure 3-193. 72-hour HYSPLIT back trajectories ending at Denton Airport South C56 on August 31; Right side: SmartFire plot with nearby fire locations (orange triangles) and 72-hour HYSPLIT back trajectories terminating at DFW sites (C56 and C70).

Figure 3-198 shows $PM_{2.5}$ levels for monitors in the DFW area were low during the time of high ozone at the Denton monitor on August 31. If the fire well upwind of the DFW area had influenced ozone at Denton, we would expect to see a broad plume affecting $PM_{2.5}$ readings at multiple DFW area monitors. There is a $PM_{2.5}$ peak at the Corsicana monitor (C1051) that has the shape expected of a peak due to fire emissions, but this peak occurs at 8 pm well after the 1-hour maximum at Denton; the Corsican monitor is located ~90 miles from the Denton monitor.

The ozone spatial pattern shows that monitors in the north of the DFW urban area had higher ozone on August 31 than monitors in the south. This is consistent with the southerly wind flow, which would advect the DFW urban plume northward. The highest 1-hour ozone values at Denton and at the Pilot Point monitor (C1032) occurred at 5 pm, later than the 1-hour ozone maxima at Dallas North No. 2 C63 (11 am) and Keller C17 (1 pm).

Because there is no evidence of a fire plume impact at the time of high ozone at Denton, we recommend no further evaluation of August 31, 2013 at the Denton monitor.

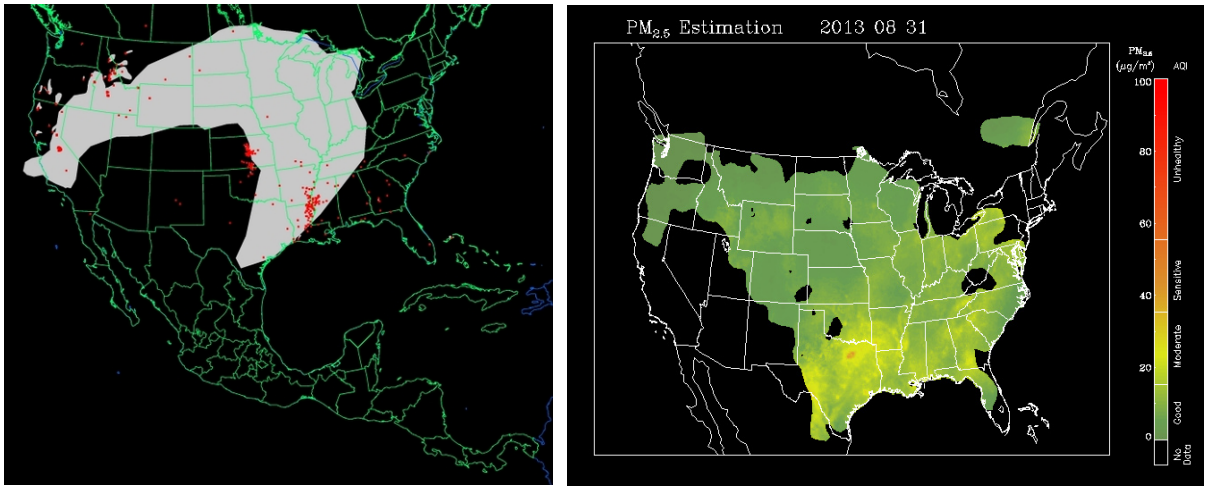

Figure 3-194. Left panel: HMS product showing August 31 fire locations (red dots) and smoke plume (gray area). Right panel: IDEA surface $PM_{2.5}$ estimate based on AOD and surface monitoring data.

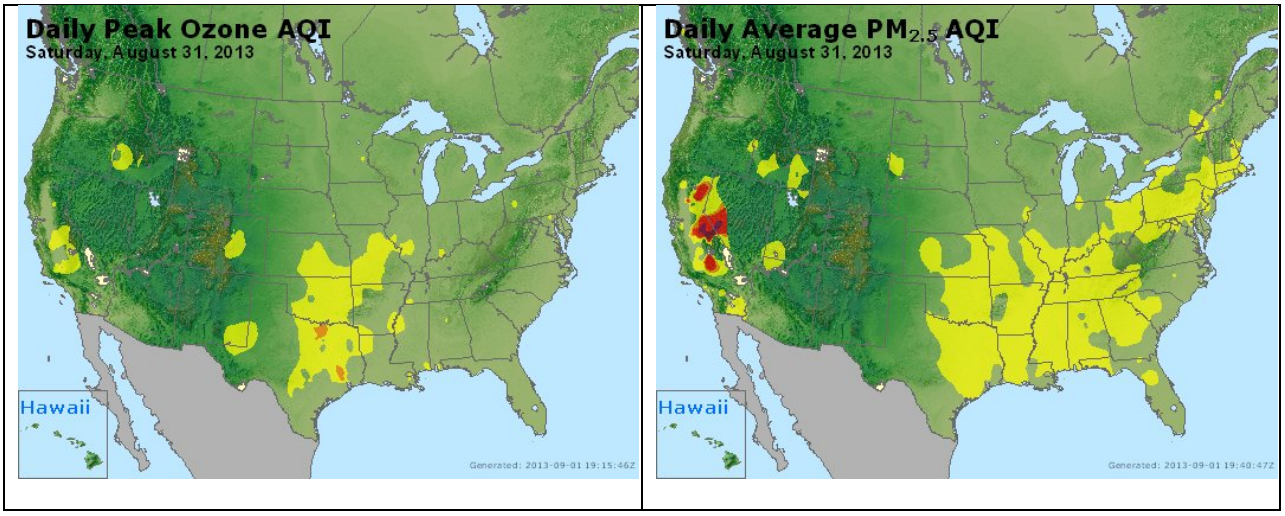

Figure 3-195. Daily average ozone (left) and $PM_{2.5}$ (right) based on observed values. Data from: http://www.airnow.gov/.

ENVIRON

Wildfire Emissions Inventory: FINN 2013

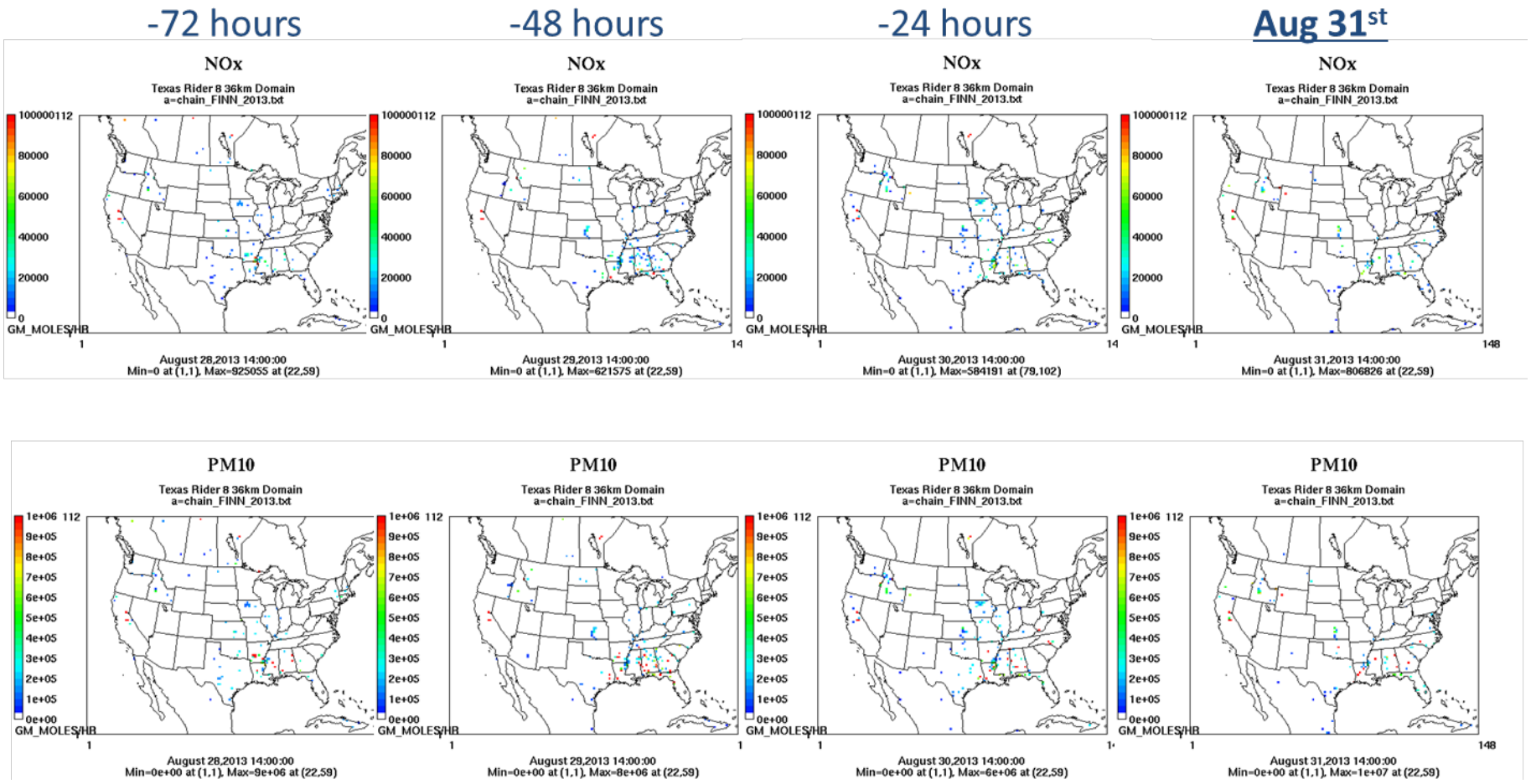

Figure 3-196. August 31, 2013 FINN fire emissions of NOx and PM_{10}.

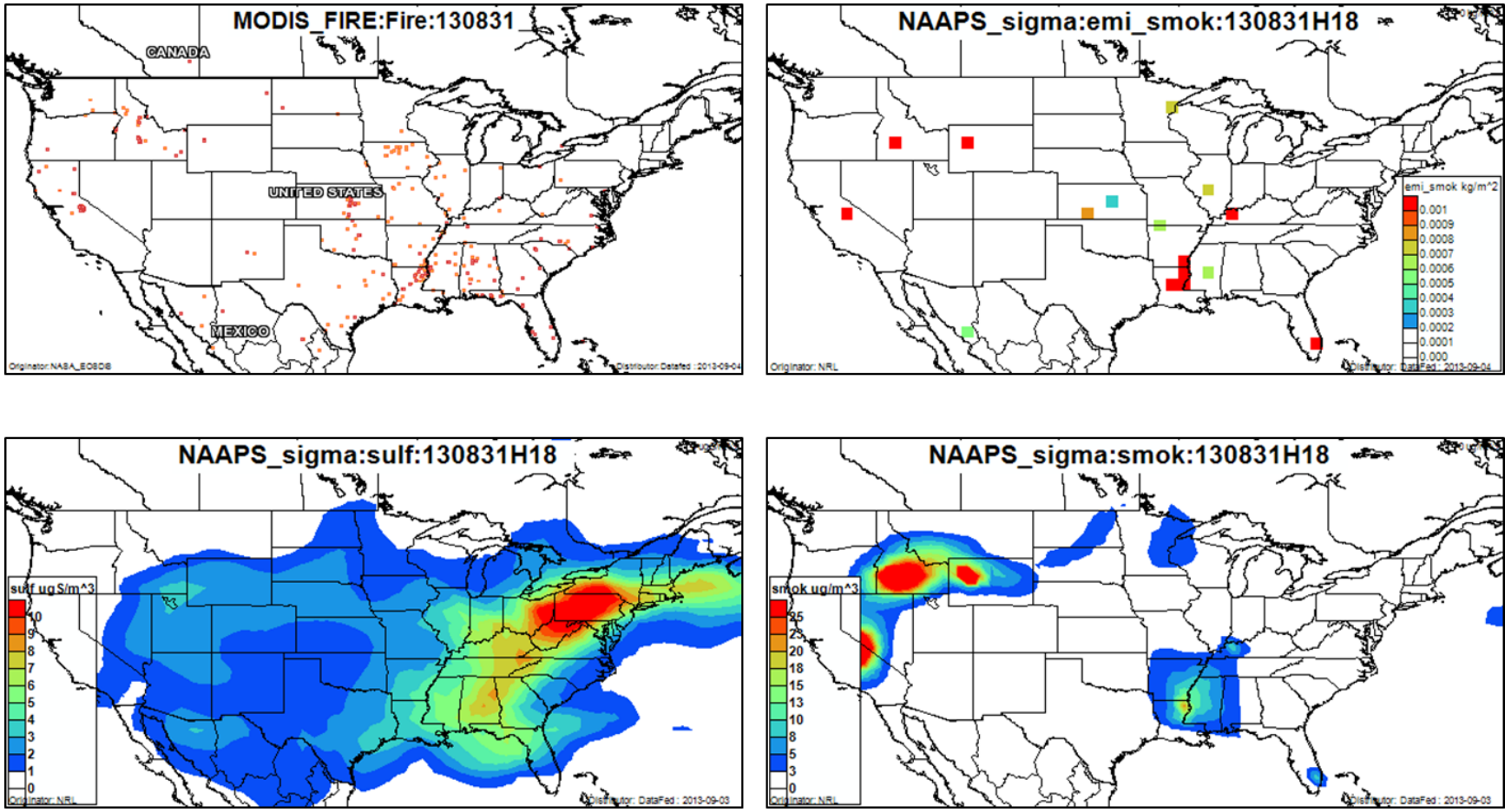

Figure 3-197. August 31, 2013 DataFed analysis. Upper left panel: Locations of active fires from MODIS satellite fire detections. Upper right panel: NAAPS model smoke emissions. Lower left panel: NAAPS model surface layer sulfate concentrations. Lower right panel: NAAPS model surface layer smoke concentrations.

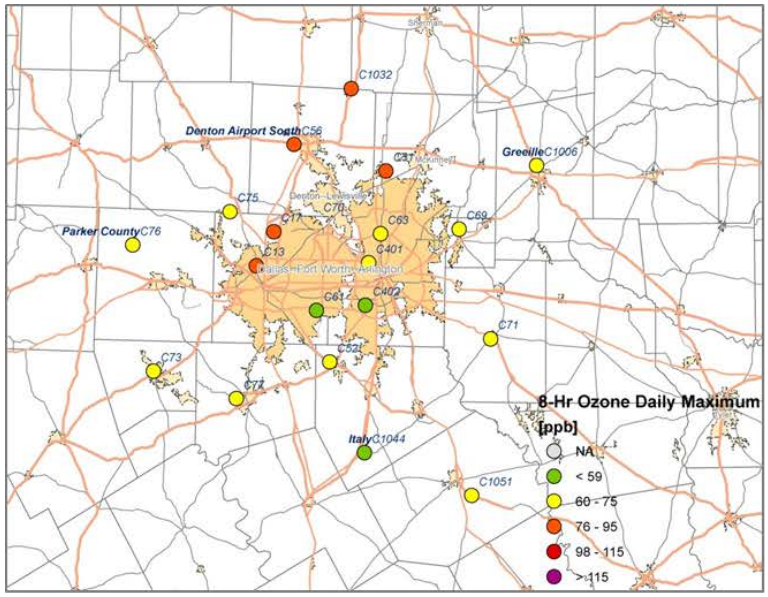

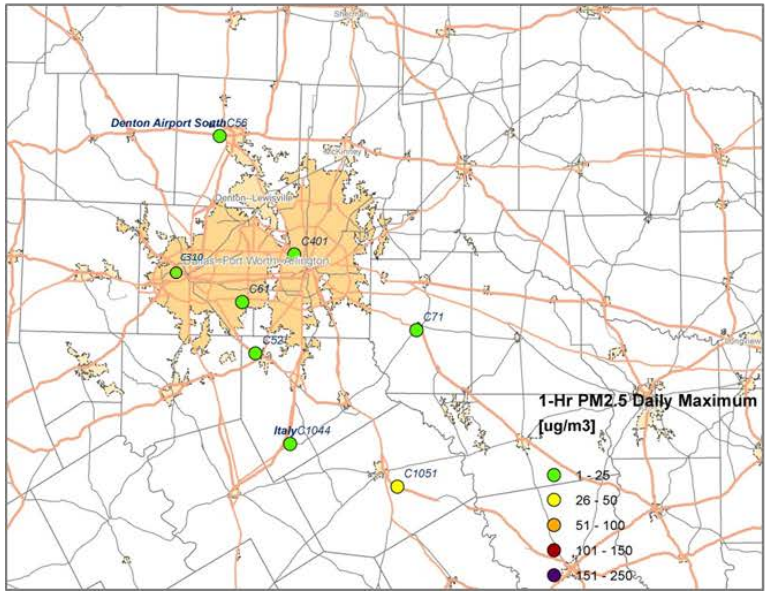

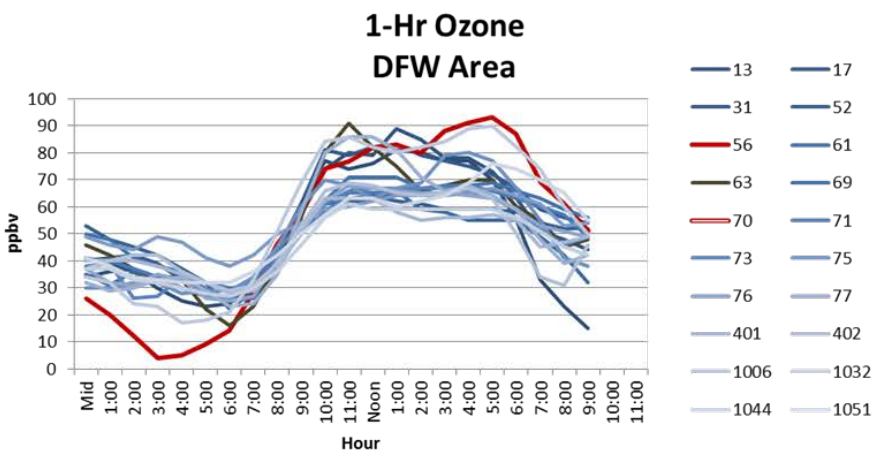

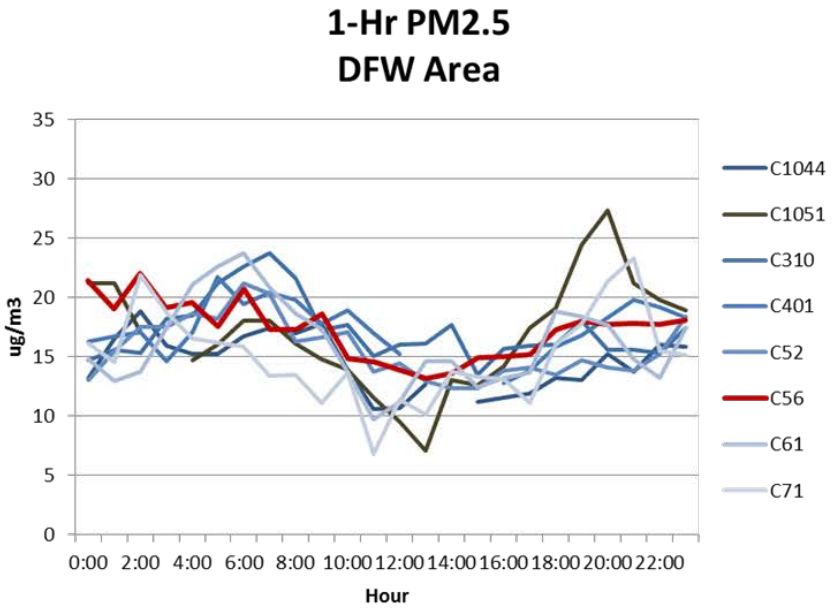

Figure 3-198.August 31, 2013 Regional ozone (top left and right) and $PM_{2.5}$ (bottom left and right) measurements (DFW area time series).

3.2.13 September 4, 2013

On September 4, 2013, the Grapevine Fairway (C70) monitor and the Denton Airport South (C56) monitors both recorded their 2nd high MDA8 value (89 ppb and 87 ppb, respectively. The MDA1 at Grapevine occurred at 11 am (94 ppb) and noon at Denton (92 ppb). Background ozone levels were high, at about 70 ppb (Figure 3-206). The monitors with the highest 1-hour ozone peaks were the Fort Worth NW (C13), Keller (C17) and Granbury (C73) monitors. Wind vectors at the two monitors show northerly winds in the early morning shifting to easterlies by mid-morning and the AQPlot back trajectories in Figure 3-199 and Figure 3-200 show winds to be east-northeasterly at all of the monitors on the morning of September 4.

The SmartFire back trajectories generally agree with the AQ Plot trajectories and wind vectors at the two monitors, showing flow out of the northeast, with back trajectories extending northward into Oklahoma and passing in the vicinity of a number of fires; the fire closest to the DFW area is located near the Texas-Oklahoma border.

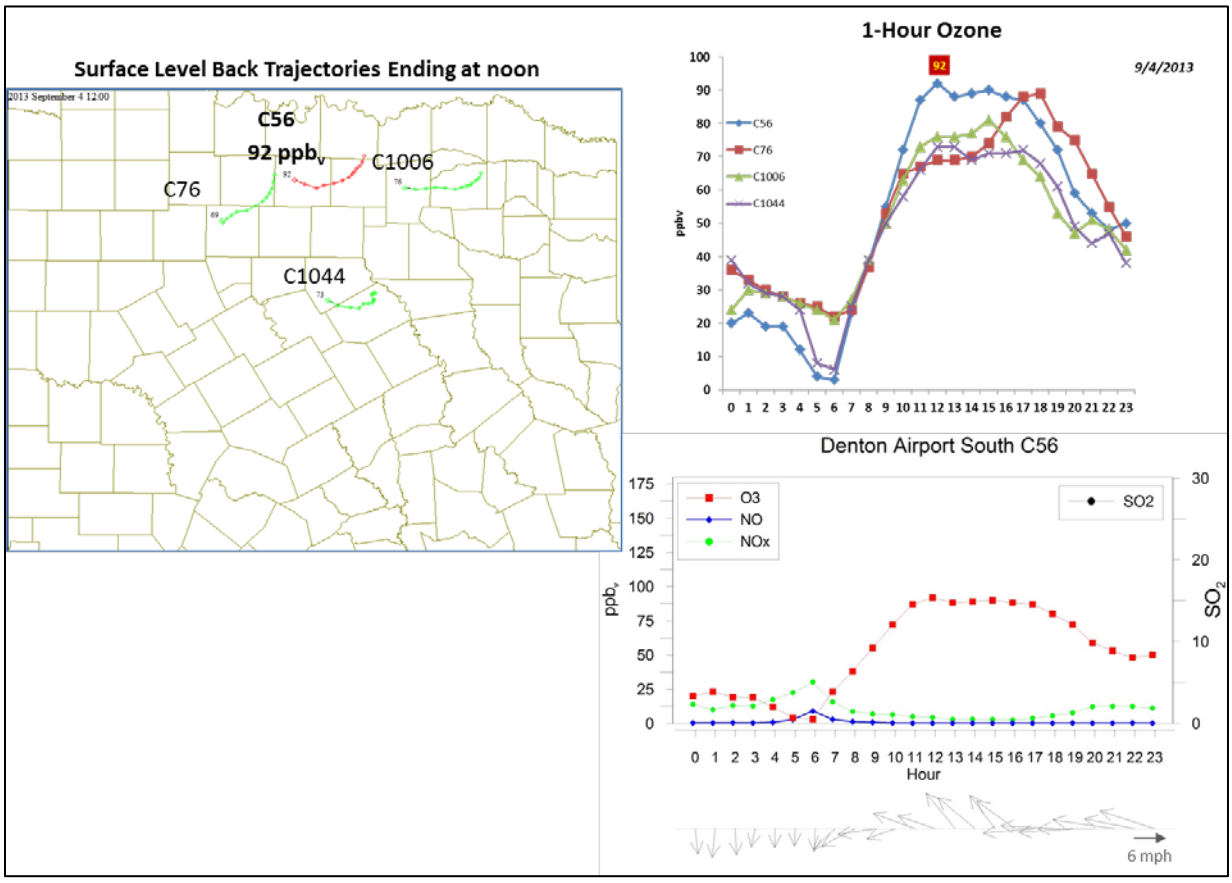

Figure 3-199. September 4, 2013 high ozone day at Denton Airport South C56. Left panel: AQPlot back trajectories ending at C56 and four background sites at the time of peak 1-hr ozone was observed. Upper right panel: 1-hour average ozone time series for the C56 and background monitors. Lower right panel: time series of 1-hour ozone, NO, NO_2 and wind vectors at the Denton Airport South C56 site.

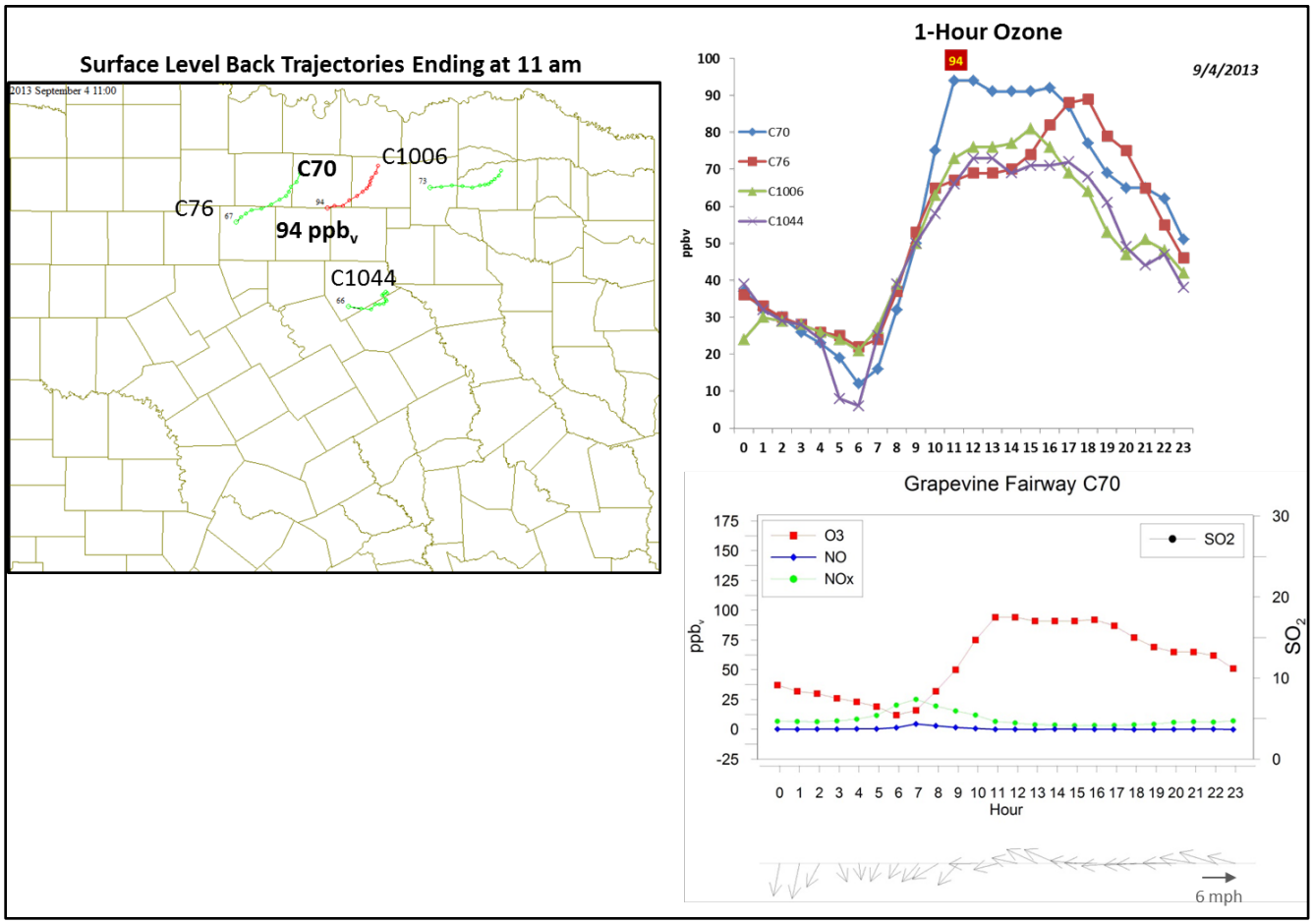

Figure 3-200. September 4, 2013 high ozone day at Grapevine Fairway C70. Left panel: AQPlot back trajectories ending at C70 and four background sites at the time of peak 1-hr ozone was observed. Upper right panel: 1-hour average ozone time series for the C70 and background monitors. Lower right panel: time series of 1-hour ozone, NO, NO_2 and wind vectors at the Grapevine Fairway C70 site.

The HYSPLIT NAM 2,500 m back trajectory also extends northward away from the DFW area, but the 500 m and 1,000 m back trajectories for both the Grapevine and Denton monitors extend to the south, indicating southerly winds. There are no fires to the south of the DFW area, although there are several fires in southern Texas at -48 and -72 hours in the FINN emissions plots (Figure 3-204). Given that the back trajectories estimated by HYSPLIT NAM and SmartFire are very different, the long range back trajectory analysis is inconclusive.

The HMS smoke product shows enhanced AOD throughout East Texas (Figure 3-202), but the NAAPS smoke analysis (Figure 3-205) shows smoke in Northeast Texas only, and no smoke present in the DFW area. The IDEA surface $PM_{2.5}$ product (Figure 3-202) and the EPA $PM_{2.5}$ AQI (Figure 3-203) both show moderate levels of $PM_{2.5}$ over the DFW area.

The pattern of MDA8 ozone in the DFW area shows higher ozone to the west of the DFW area than in the east. This is consistent with the easterly near-surface flow seen in the monitor wind

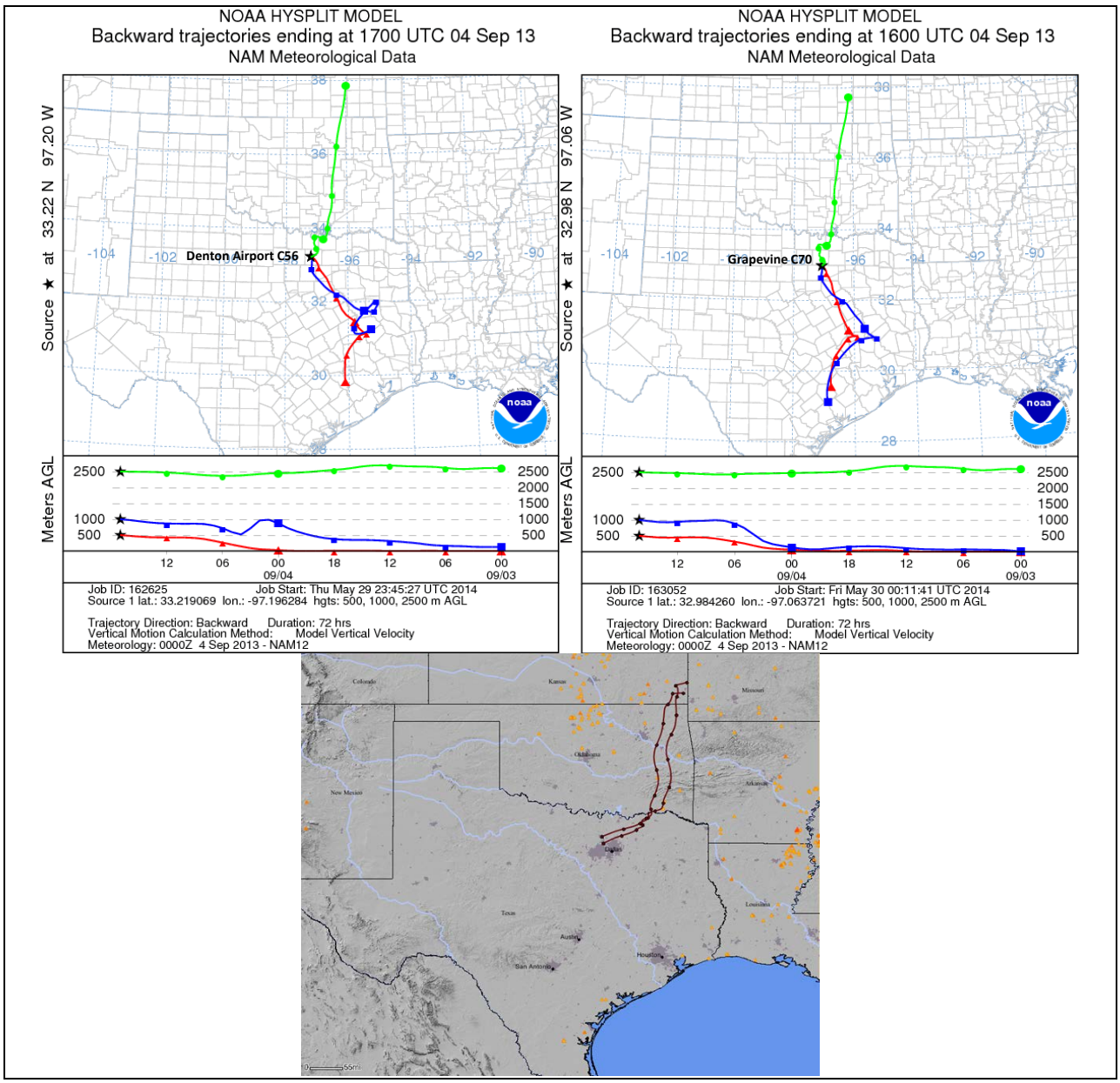

Figure 3-201. 72-hour HYSPLIT back trajectories ending at Danton Airport South C56 (top left) and Grapevine Fairway C70 (top right) on September 4, 2013; Bottom: SmartFire plots with fire locations (orange triangles) and 72-hour HYSPLIT back trajectories terminating at DFW sites (i.e. C56 and C70).

vectors. Easterly winds would bring the DFW urban plume to monitors in the western edge of the metroplex. The C17 and C13 monitors have their peak ozone later in the day than the Grapevine and Denton monitors, and the C73 and C75 monitors' peaks occur later still. This is consistent with a westward-moving urban plume.

The 1-hour $PM_{2.5}$ time series (Figure 3-206) for the Denton monitor has maxima at 8 am and 8 pm. During the time of highest ozone at Denton, the $PM_{2.5}$ values are relatively low. The same

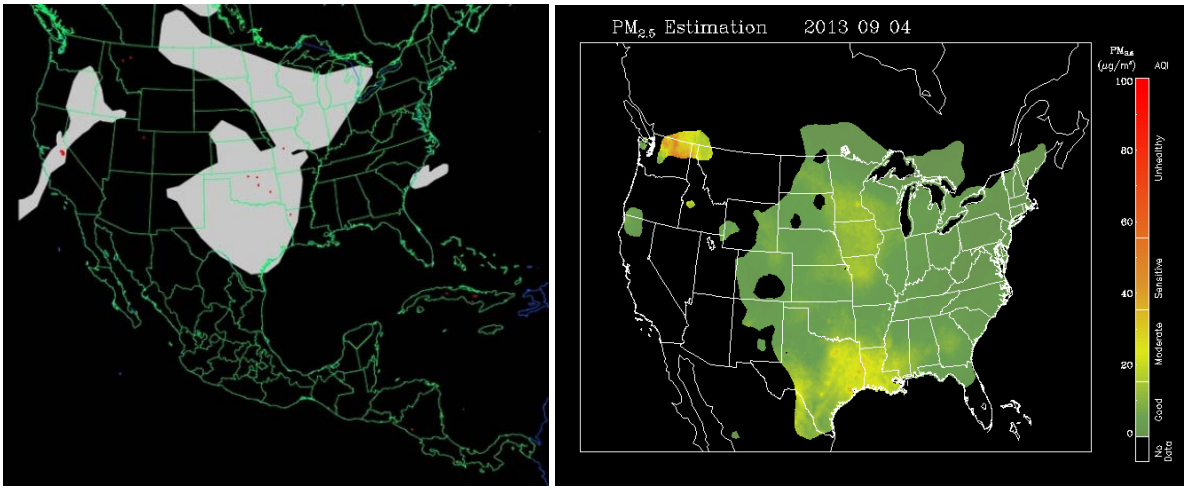

Figure 3-202. Left panel: HMS product showing September 4 fire locations (red dots) and smoke plume (gray area). Right panel: IDEA surface $PM_{2.5}$ estimate based on AOD and surface monitoring data.

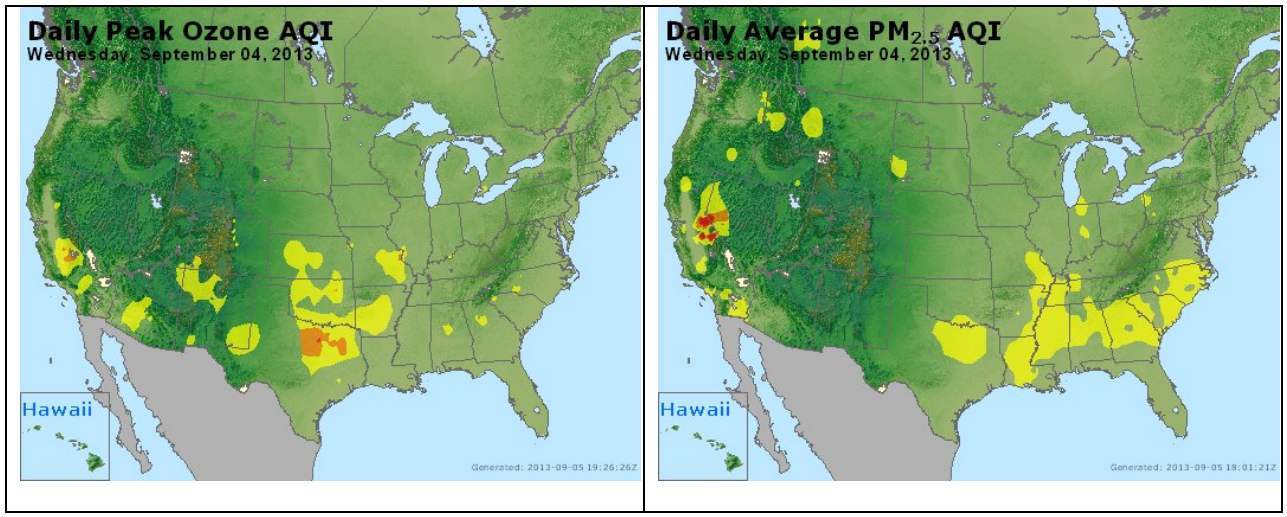

Figure 3-203. Daily average ozone (left) and $PM_{2.5}$ (right) based on observed values. Data from: http://www.airnow.gov/.

is true of $PM_{2.5}$ at the C401 monitor, which is located south of Grapevine. Given the spatial pattern of high ozone and the lack of a $PM_{2.5}$ plume and NOx plume at the time of high ozone at the two monitors, we recommend no further analysis of September 4, 2013.

ENVIRON

Wildfire Emissions Inventory: FINN 2013

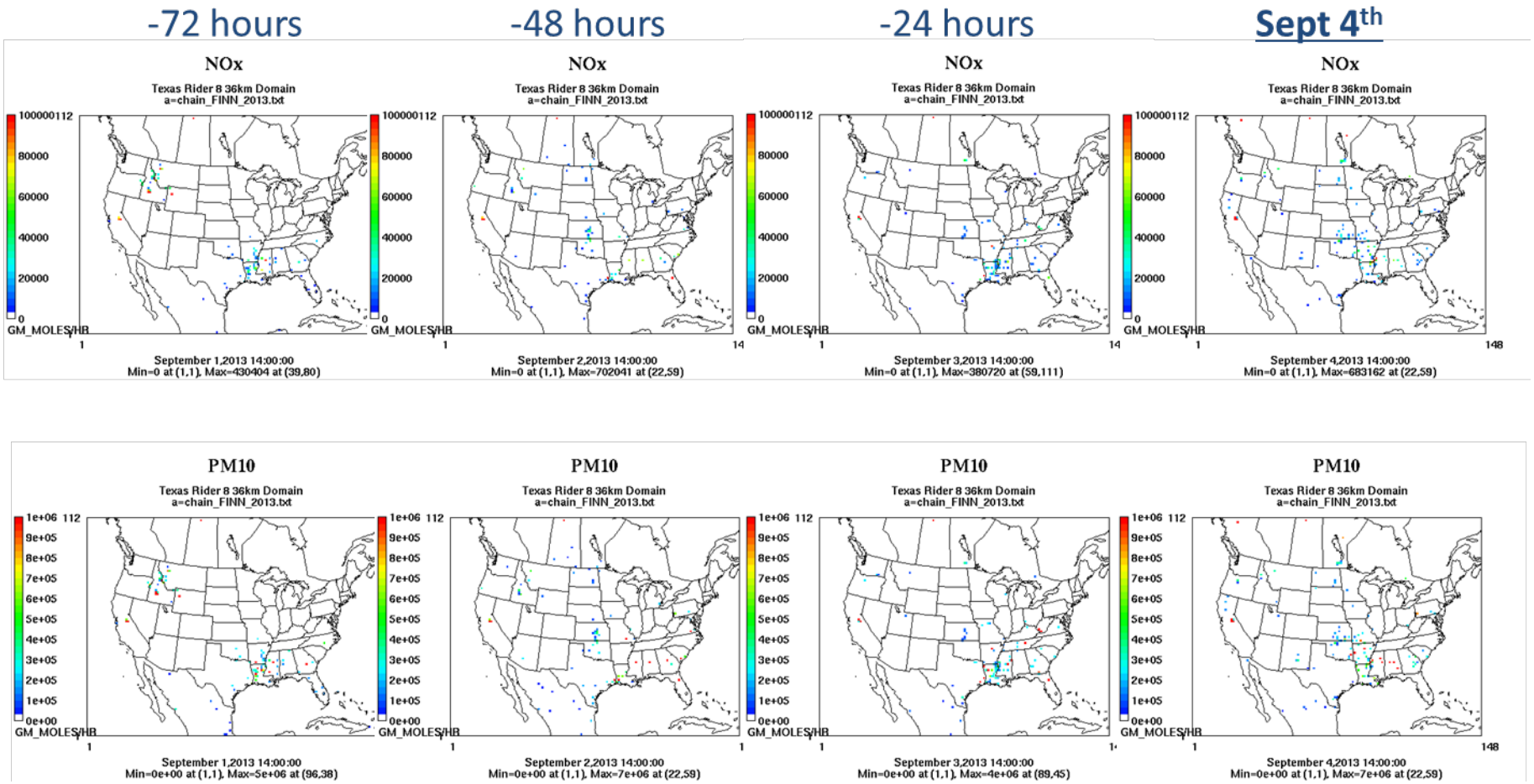

Figure 3-204. September 4, 2013 FINN fire emissions of NOx and PM_{10}.

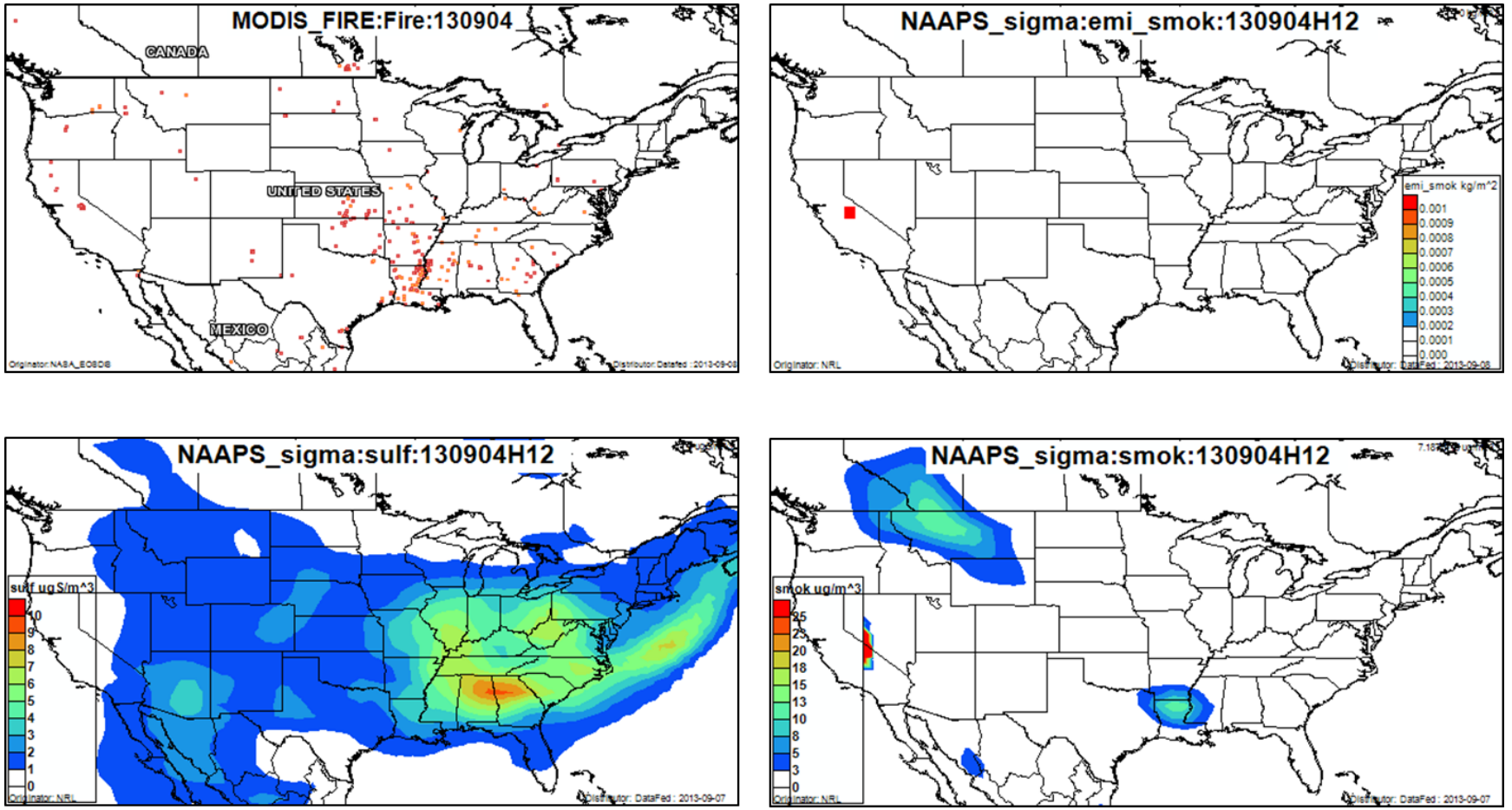

Figure 3-205. September 4, 2013 DataFed analysis. Upper left panel: Locations of active fires from MODIS satellite fire detections. Upper right panel: NAAPS model smoke emissions. Lower left panel: NAAPS model surface layer sulfate concentrations. Lower right panel: NAAPS model surface layer smoke concentrations.

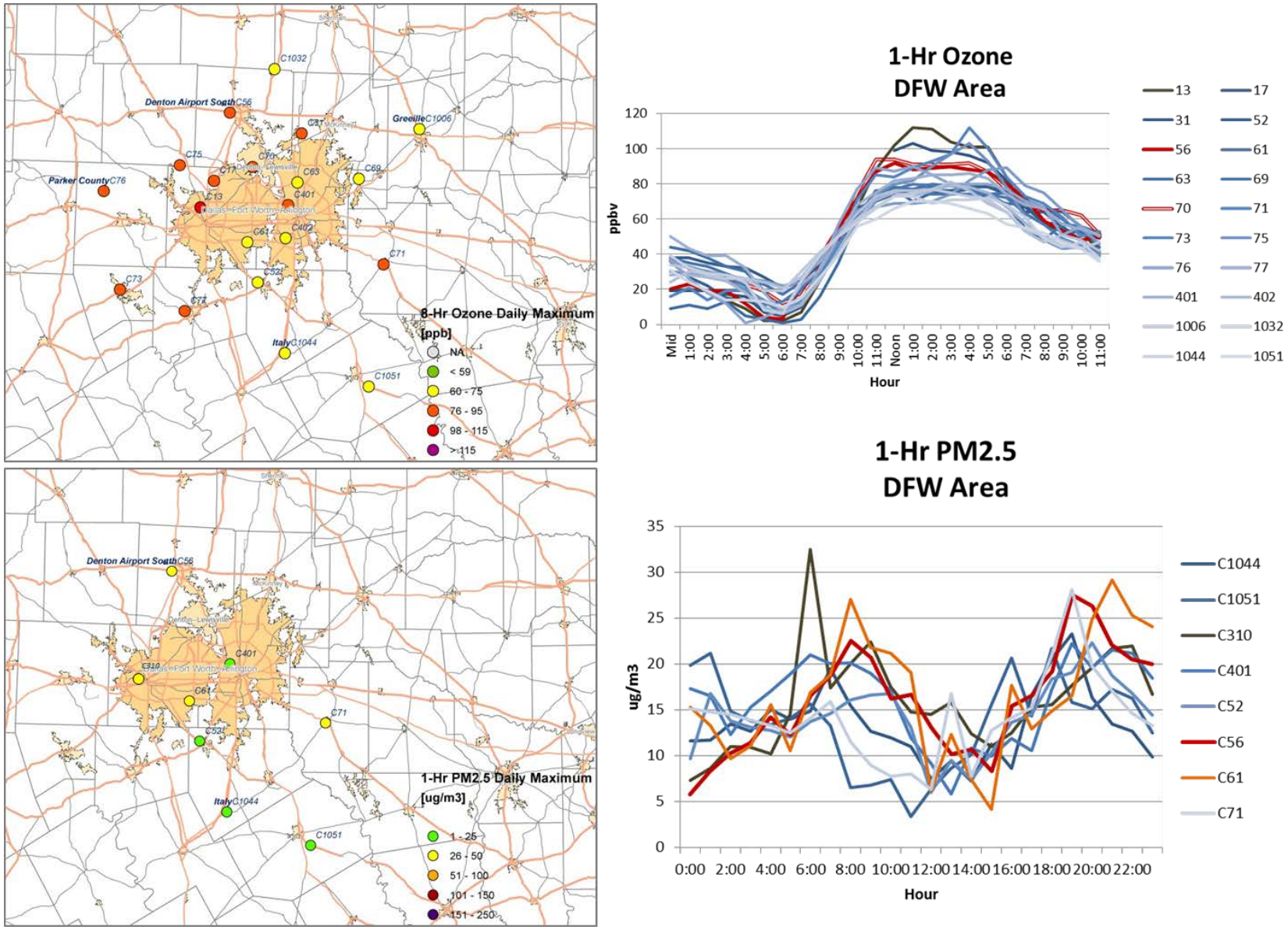

Figure 3-206. Regional ozone (top left and right) and $PM_{2.5}$ (bottom left and right) measurements (DFW area time series).

3.2.14 September 6, 2013

On September 6, the Grapevine Fairway monitor (C70) had its highest MDA8 reading of 2013 (89 ppb) and the Denton Airport South monitor (C56) had its 3rd highest MDA8 (85 ppb). Background ozone was ~60 ppb on September 6 and the monitors had 1-hour ozone peaks well above background (100 ppb and 103 ppb).

Winds were southerly at both monitors during the daylight hours (Figure 3-207; Figure 3-208). The AQPlot back trajectories show transport from the south on September 6.

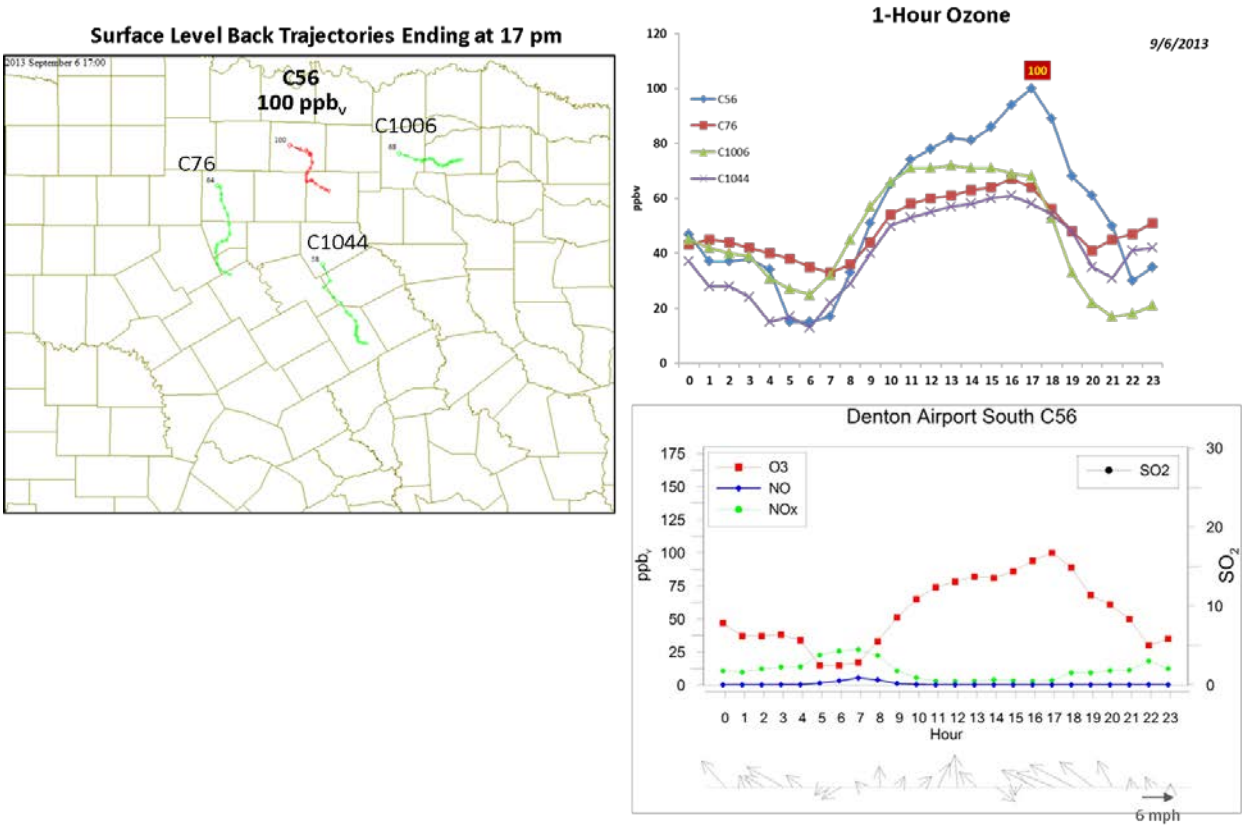

Figure 3-207. September 6, 2013 high ozone day at Denton Airport South C56. Left panel: AQPlot back trajectories ending at C56 and four background sites at the time of peak 1-hr ozone was observed. Upper right panel: 1-hour average ozone time series for the C56 and background monitors. Lower right panel: time series of 1-hour ozone, NO, NO_2 and wind vectors at the Denton Airport South C56 site.

The SmartFire back trajectories do not agree with the HYSPLIT NAM 500 m and 1,000 m back trajectories or with the AQPlot trajectories. The SmartFire back trajectories agree most closely with the 2,500 m HYSPLIT NAM back trajectory, which also extends eastward. The back trajectory analysis is therefore inconclusive. However, the southerly flow shown in the AQPlot near-surface wind back trajectories and the HYSPLIT NAM trajectories is more consistent

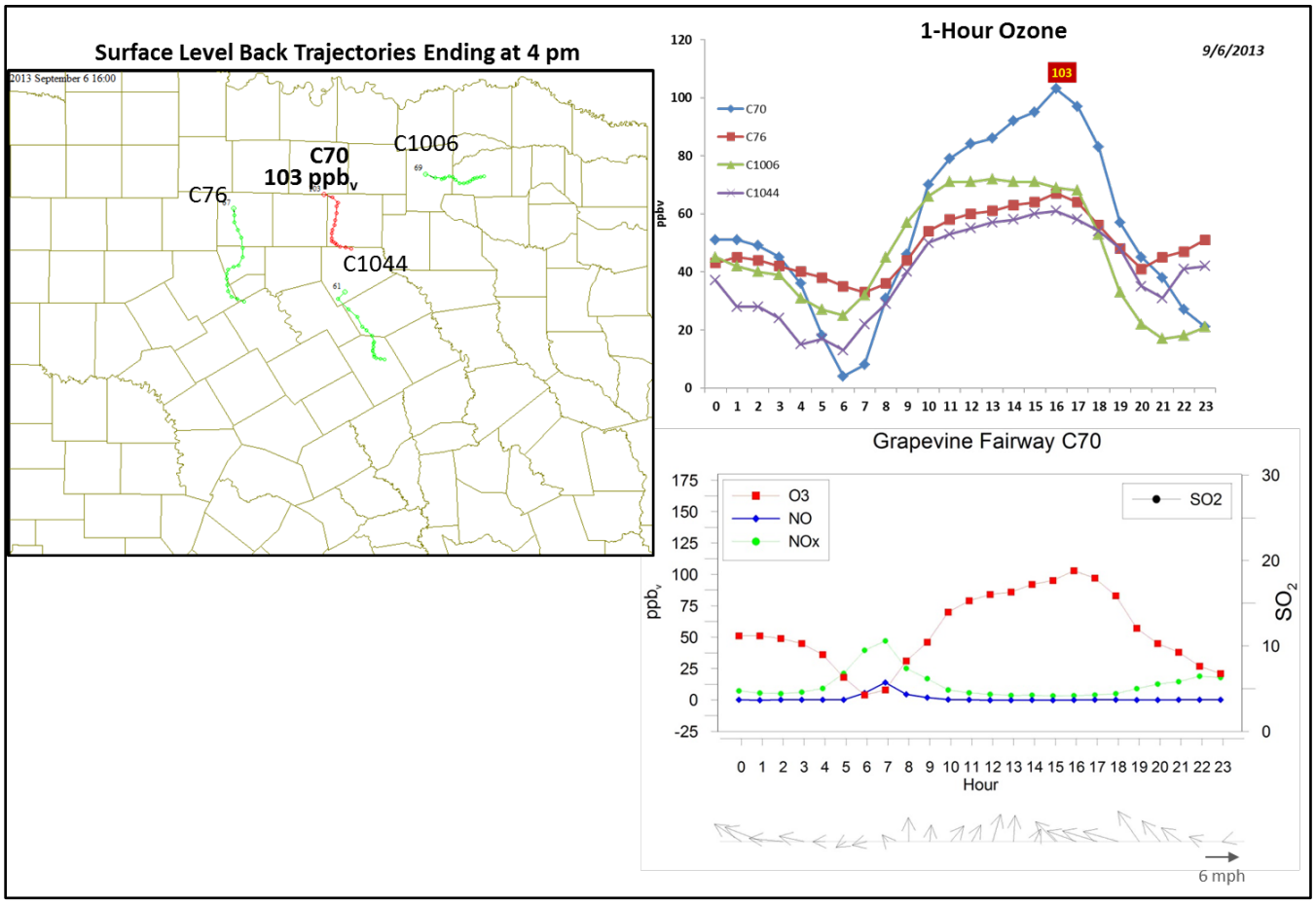

Figure 3-208. September 6, 2013 high ozone day at Grapevine Fairway C70. Left panel: AQPlot back trajectories ending at C70 and four background sites at the time of peak 1-hr ozone was observed. Upper right panel: 1-hour average ozone time series for the C70 and background monitors. Lower right panel: time series of 1-hour ozone, NO, NO_2 and wind vectors at the Grapevine Fairway C70 site.

with the ozone spatial distribution on September 6 (Figure 3-214). Monitors to the north of the DFW urban area have higher ozone than sites located to the south of the DFW area. Monitors in the north (Grapevine, Denton, Keller, Pilot Point) have 1-hour ozone maxima that occur later in the day than other monitors located further south. This pattern is consistent with the advection of the DFW urban plume to the north via southerly winds. Therefore, although the SmartFire trajectories passed over fires in Arkansas and Northeast Texas, we have low confidence in these trajectories, and based on the CAMS wind and ozone data, think it much more likely that the air mass originated south of DFW than to the east. We note that the SmartFire back trajectories are developed with EDAS data that has 40 km horizontal resolution, while the HYSPLIT NAM uses 12 km input meteorology. On this day, when vertical wind shear is critically important, it may be that the lower resolution EDAS analysis is not able to resolve local-scale features that are important in determining the back trajectories.

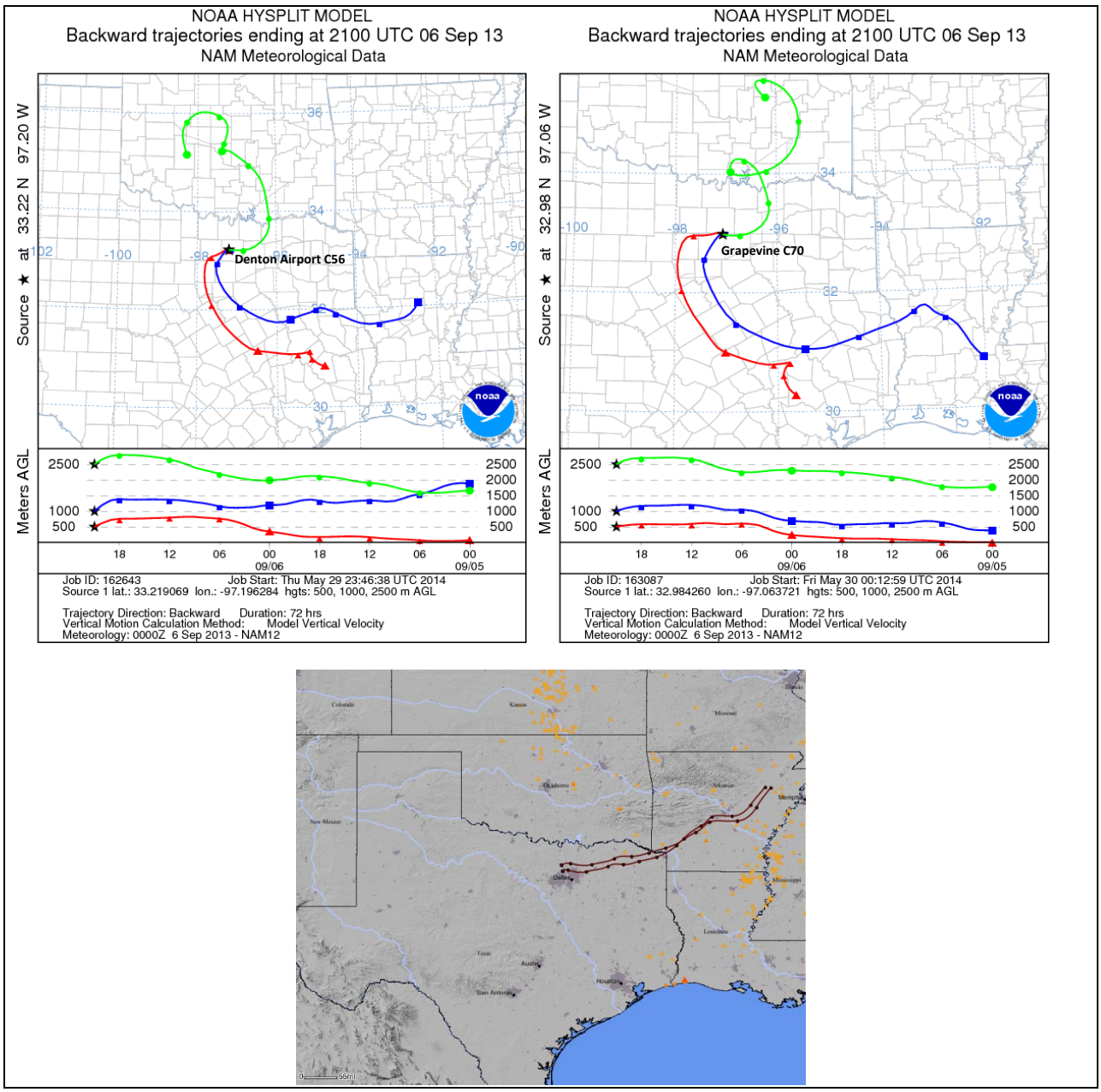

Figure 3-209. 72-hour HYSPLIT back trajectories ending at Denton Airport South C56 (top left) and Grapevine Fairway C70 (top right) on September 6, 2013; Bottom: SmartFire plots with fire locations (orange triangles) and 72-hour HYSPLIT back trajectories terminating at DFW sites (i.e. C56 and C70).

The SmartFire map shows no fires south of the DFW area in the region traversed by the HYSPLIT 500 m back trajectories. The HMS product shows no active fires in Texas on September 6, but does show the presence of smoke over East Texas, including the DFW area. The MODIS fire location plot (Figure 3-213) does show active fires south of DFW and the NAAPS analysis (Figure 3-213) indicates the presence of smoke across East Texas. $PM_{2.5}$ levels at the surface, however, range from moderate to good on the AQI scale (Figure 3-218). The FINN inventory does show

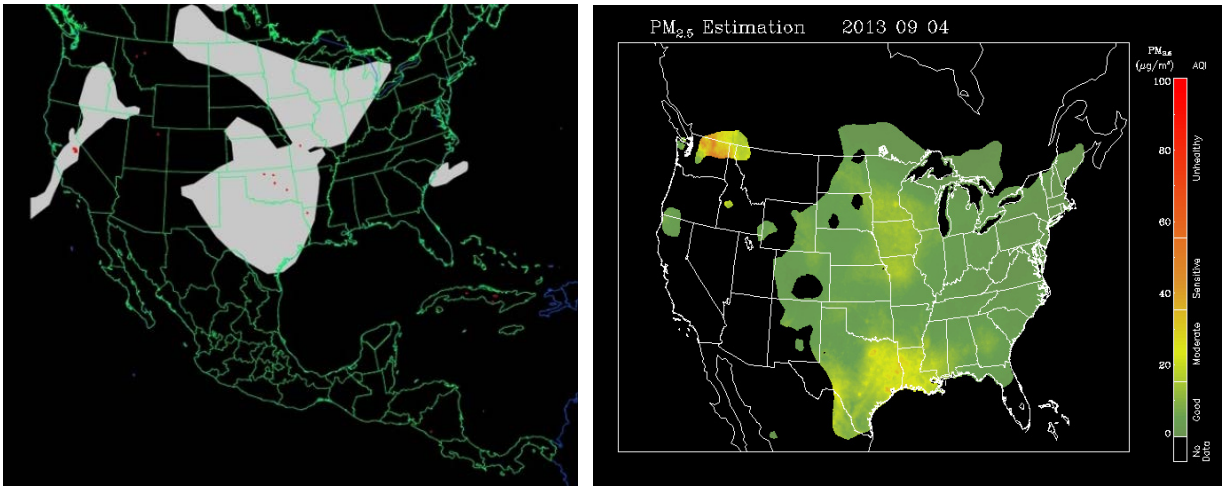

Figure 3-210. Left panel: HMS product showing September 6 fire locations (red dots) and smoke plume (gray area). Right panel: IDEA surface $PM_{2.5}$ estimate based on AOD and surface monitoring data.

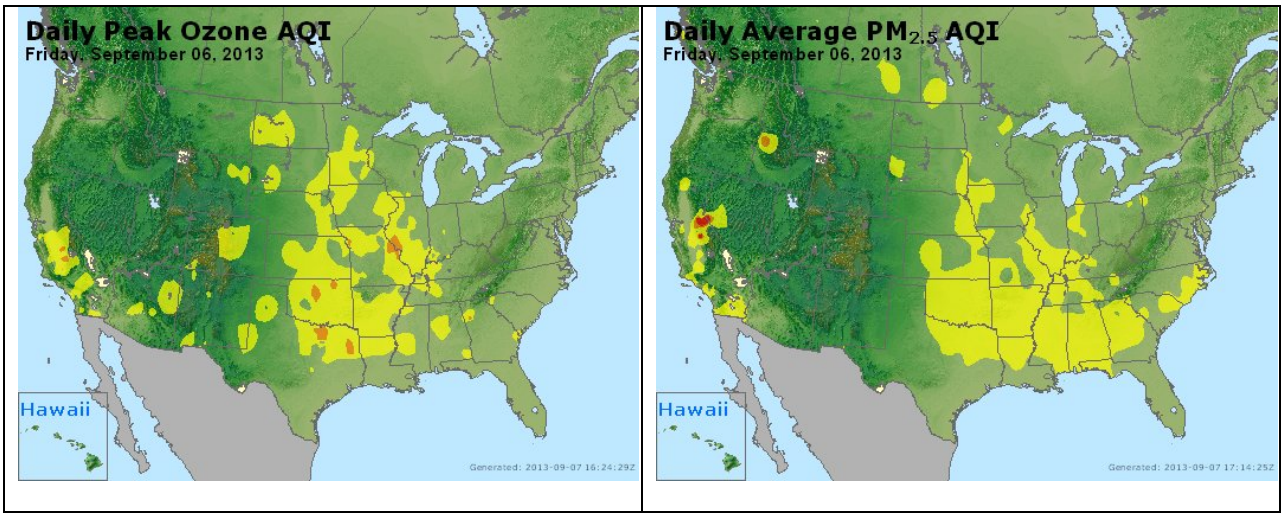

Figure 3-211. Daily average ozone (left) and $PM_{2.5}$ (right) based on observed values. Data from: http://www.airnow.gov/.

fire emissions on September 6 through -72 hours, but these fires were not present in the vicinity of the trajectories at the time when air traversed the fire locations (Figure 3-212). The $PM_{2.5}$ spatial plots show that $PM_{2.5}$ levels were generally low in the DFW area on September 6 (Figure 3-214). The low levels of $PM_{2.5}$ observed at monitors on the southern part of the DFW metroplex are not consistent with northward advection of a distant fire plume. The Denton (C56) monitor has a sharp increase in $PM_{2.5}$ at 2 pm that is likely a plume impact. However, given the lack of evidence of a fire plume impact at other DFW monitors, we hypothesize that the 2 pm plume impact at the Denton monitor is due to local emissions. For all hours except 2 pm, $PM_{2.5}$ levels are relatively low during the time of high 1-hour ozone. There is no NOx peak

during the period of high ozone at either Grapevine or Denton. Although Denton has a NOx peak in the evening, it occurs after ozone levels have declined below 50 ppb. Because there is no evidence that a fire plume from the distant fires along the back trajectories influenced DFW area ozone on September 6, we recommend that no further evaluation of September 6, 2013 be performed.

ENVIRON

Wildfire Emissions Inventory: FINN 2013

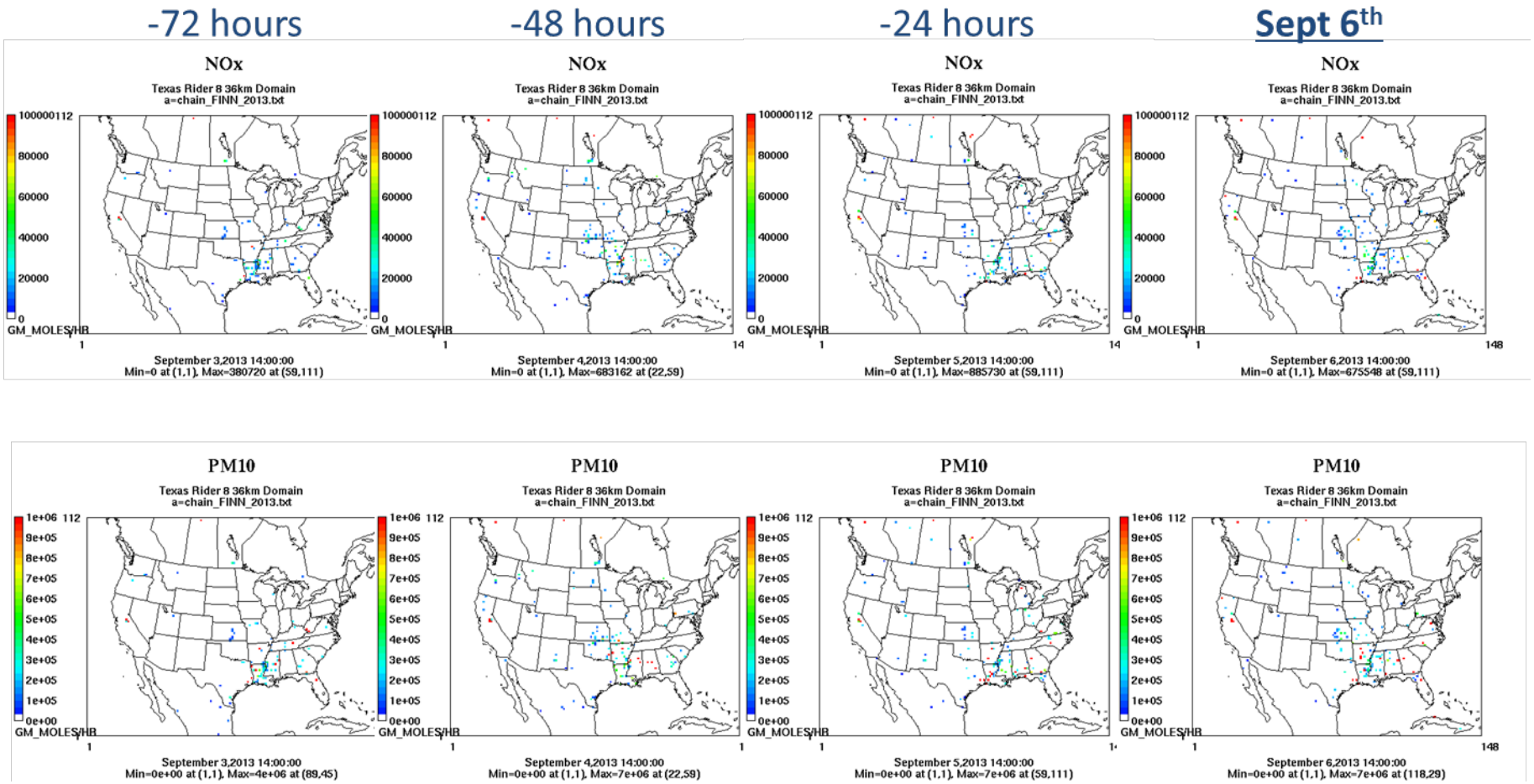

Figure 3-212. September 6, 2013 FINN fire emissions of NOx and PM_{10}.

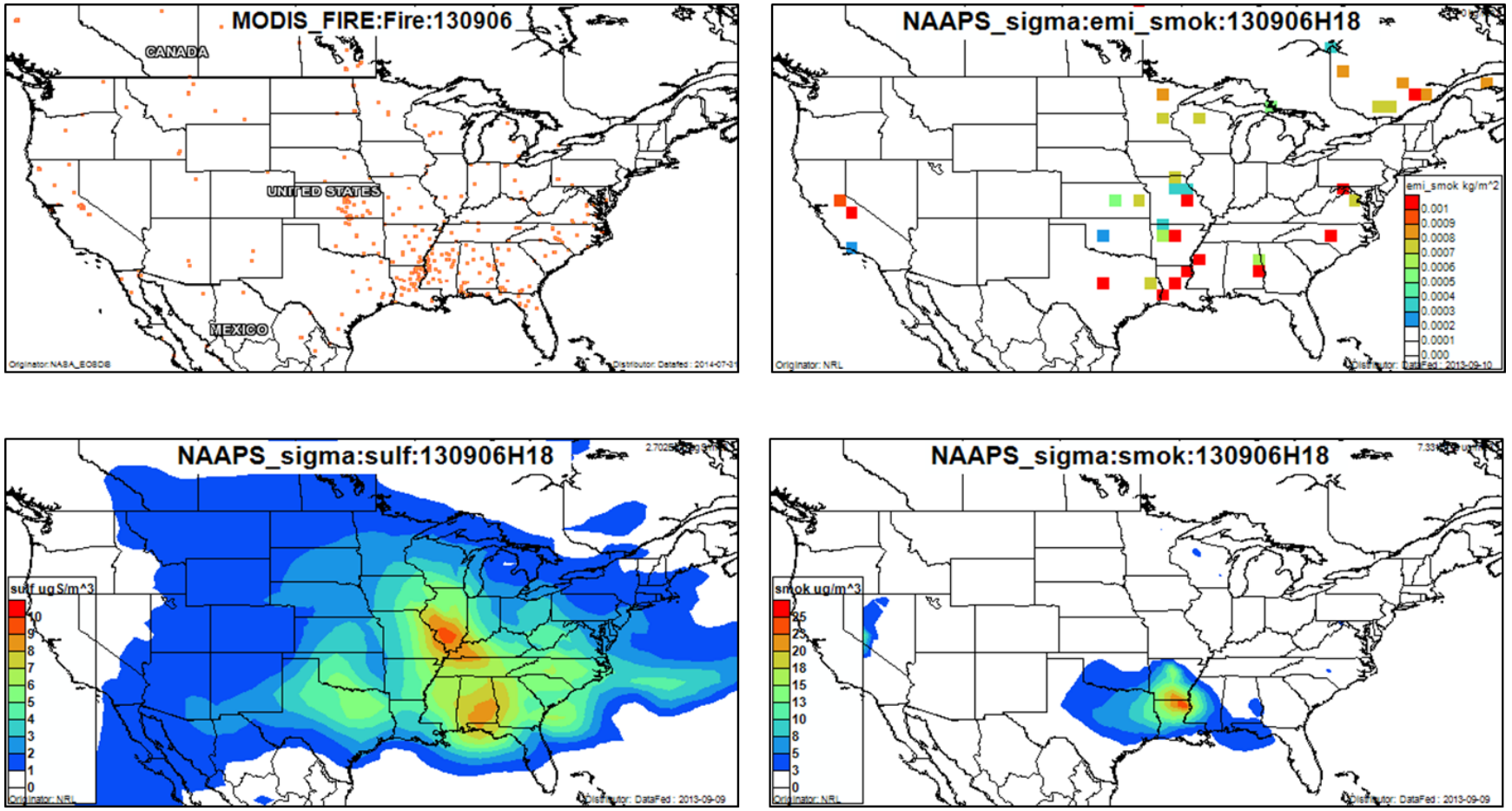

Figure 3-213. September 6, 2013 DataFed analysis. Upper left panel: Locations of active fires from MODIS satellite fire detections. Upper right panel: NAAPS model smoke emissions. Lower left panel: NAAPS model surface layer sulfate concentrations. Lower right panel: NAAPS model surface layer smoke concentrations.

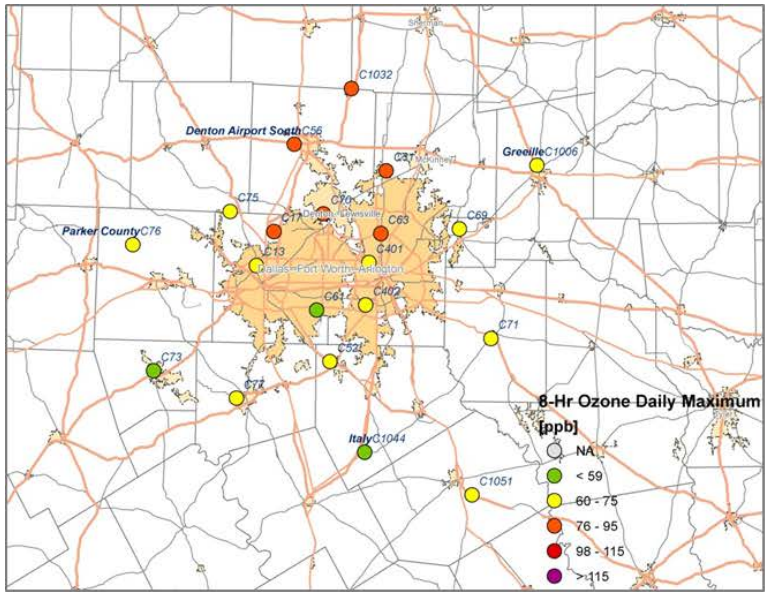

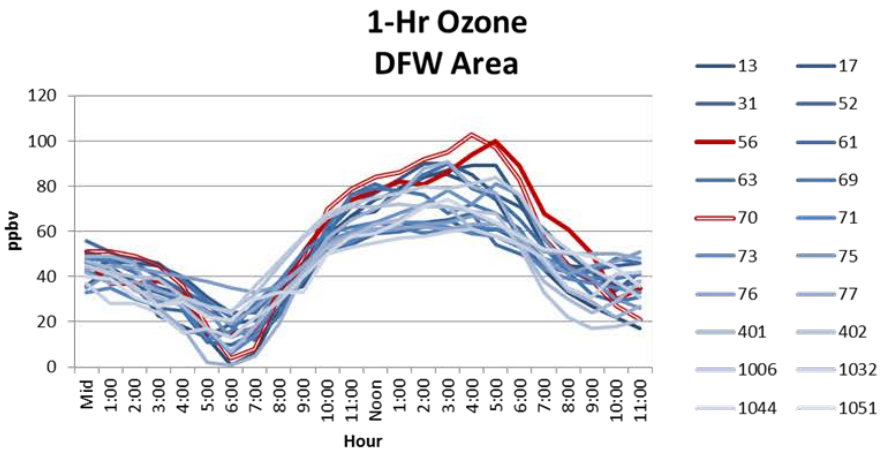

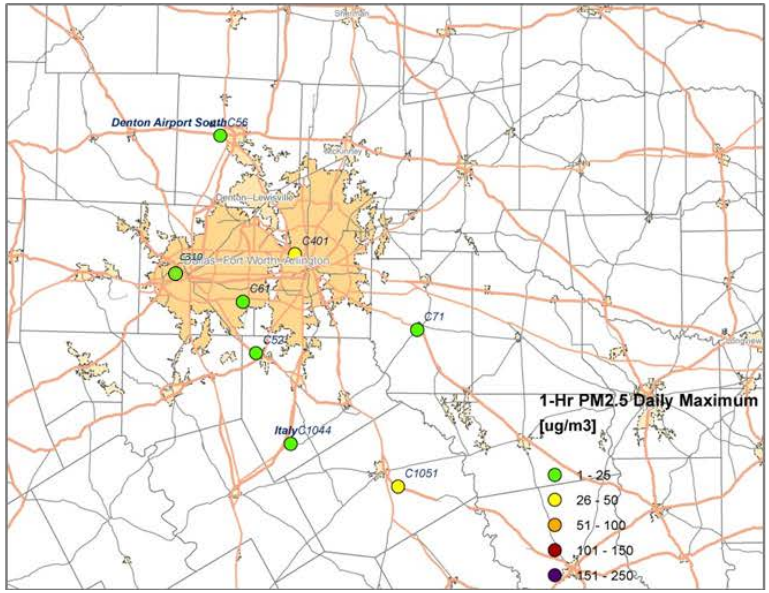

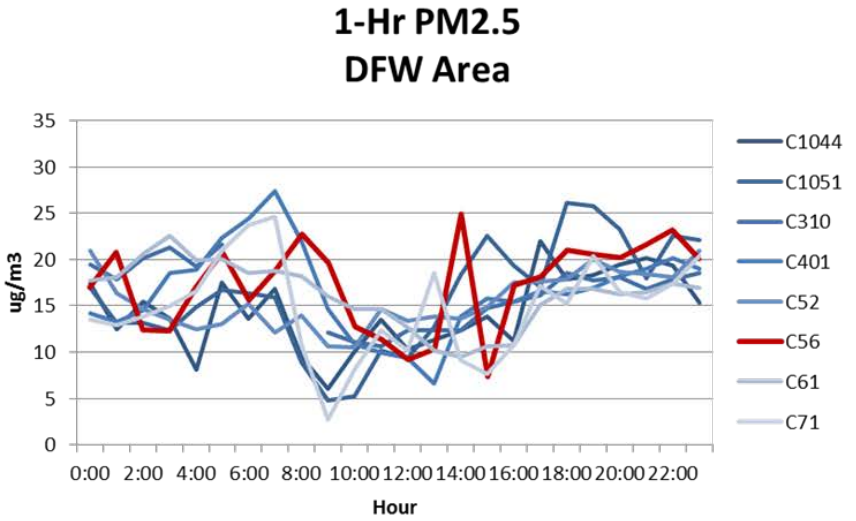

Figure 3-214. Regional ozone (top left and right) and $PM_{2.5}$ (bottom left and right) measurements (DFW area time series).

3.2.15 September 12, 2013

On September 12, the Grapevine Fairway monitor (C70) had its 4th high MDA8 reading of 2013 (83 ppb). Background ozone was ~50 ppb on September 12 (Figure 3-221), and the Grapevine monitor had the highest 1-hour ozone value (96 ppb) of any of the DFW monitors (Figure 3-215). Winds vectors were generally southerly during the daylight hours (Figure 3-215). The AQPlot back trajectories show transport from the south during the morning hours when 1-hour ozone is increasing at the Grapevine monitor on September 12.

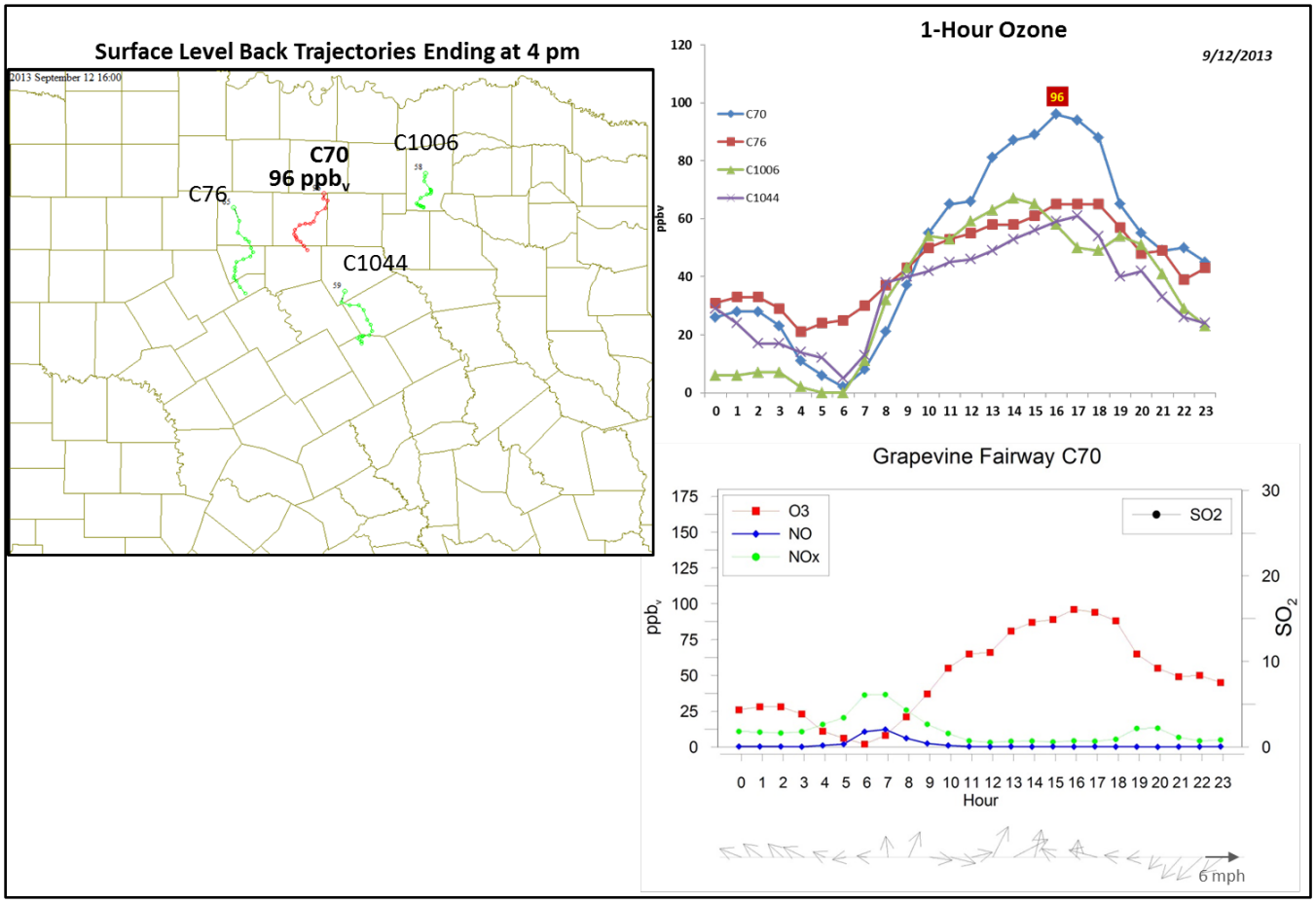

Figure 3-215. September 12, 2013 high ozone day at Grapevine Fairway C70. Left panel: AQPlot back trajectories ending at C70 and four background sites at the time of peak 1-hr ozone was observed. Upper right panel: 1-hour average ozone time series for the C70 and background monitors. Lower right panel: time series of 1-hour ozone, NO, NO_2 and wind vectors at the Grapevine Fairway C70 site.

The SmartFire back trajectories and the HYSPLIT NAM 500 m back trajectory (Figure 3-216) show transport from the southeast leading up to September 12, and a wind shift near the time of the ozone maximum. The SmartFire map shows that the SmartFire back trajectory does not pass near any fires in Texas, but does pass among fires in southern Louisiana. The HYSPLIT NAM 500 m trajectory passes near a fire located south of the DFW area and also passes

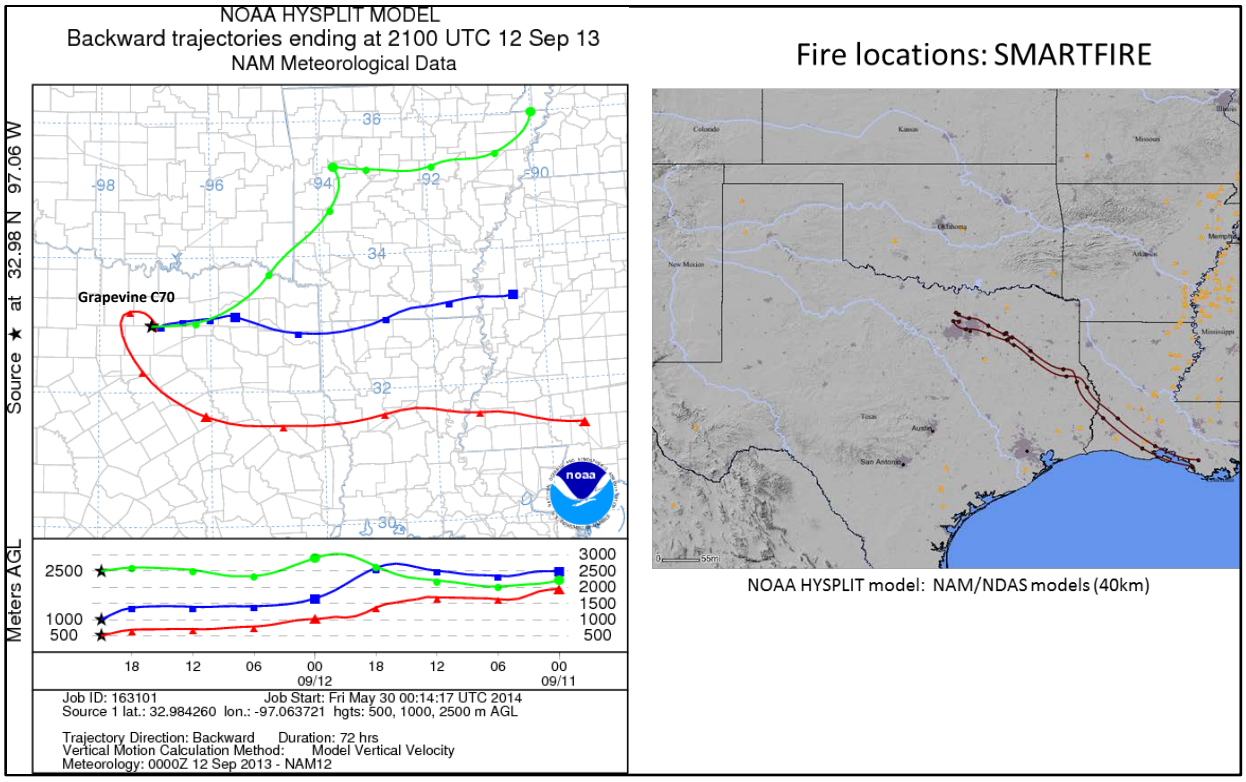

Figure 3-216. 72-hour HYSPLIT back trajectories ending at Grapevine Fairway C70 on September 12, 2013 (left); Right: SmartFire plots with fire locations (orange triangles) and 72-hour HYSPLIT back trajectories terminating at DFW sites (i.e. C56 and C70).

near fires in Louisiana and Mississippi. The fire south of the DFW area is also present in the HMS product (Figure 3-217) and in the FINN fire emissions for September 12 (Figure 3-219). At -24 hours, the fire is south of the DFW area is not present, but there are fires in Louisiana and eastern Mississippi in the vicinity of the back trajectories at -48 and -72 hours.

The ozone spatial pattern (Figure 3-221) is consistent with the southerly wind direction, with lower ozone at monitors south of the DFW urban area and higher ozone within and to the north (downwind) of the urban area. Monitors that are located in the northern part of the urban area (Grapevine, Denton, Pilot Point) have their 1-hour ozone maxima later in the day than the more southerly monitors such as Cleburne.

At all $PM_{2.5}$ monitors south of the DFW area, $PM_{2.5}$ levels are low (<25 µg m^{-3}). The only monitor to rise above 25 µg m^{-3} is the Denton monitor, which has a 7 pm peak that occurs after ozone has begun to decline from its MDA1 value. The low levels of $PM_{2.5}$ observed at monitors on the southern part of the DFW metroplex are not consistent with northward advection of a distant fire plume. There is no NOx plume at the Grapevine monitor at the time of high 1-hour ozone on September 12 (Figure 3-215). Because there is no evidence that a fire plume from the distant fires along the HYSPLIT NAM 500 m and SmartFire back trajectories influenced DFW area ozone, we recommend that no further evaluation of September 12, 2013 be performed.

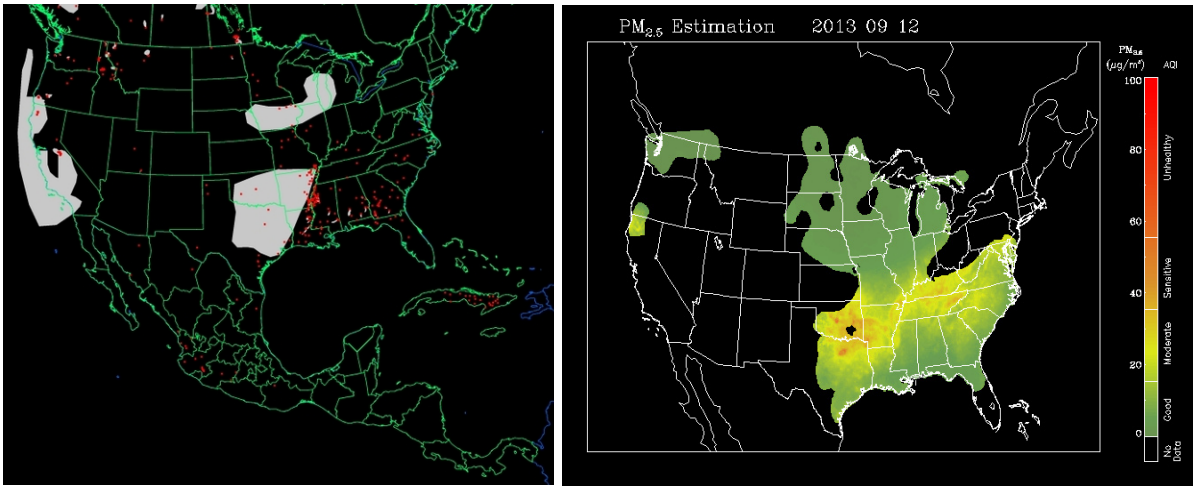

Figure 3-217. Left panel: HMS product showing September 12 fire locations (red dots) and smoke plume (gray area). Right panel: IDEA surface $PM_{2.5}$ estimate based on AOD and surface monitoring data.

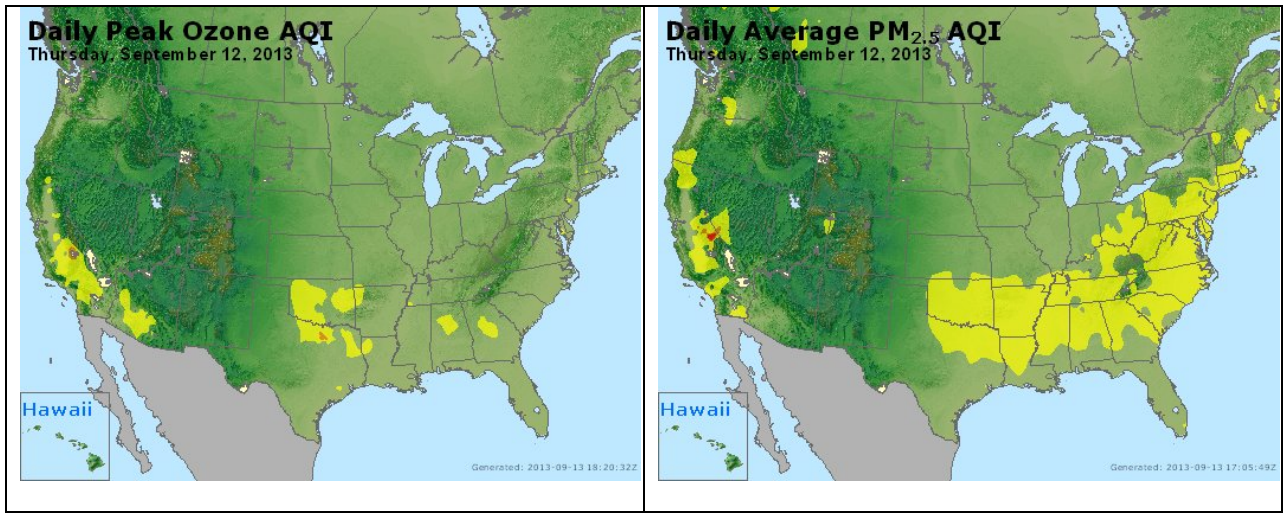

Figure 3-218. Daily average ozone (left) and $PM_{2.5}$ (right) based on observed values. Data from: http://www.airnow.gov/.

Wildfire Emissions Inventory: FINN 2013

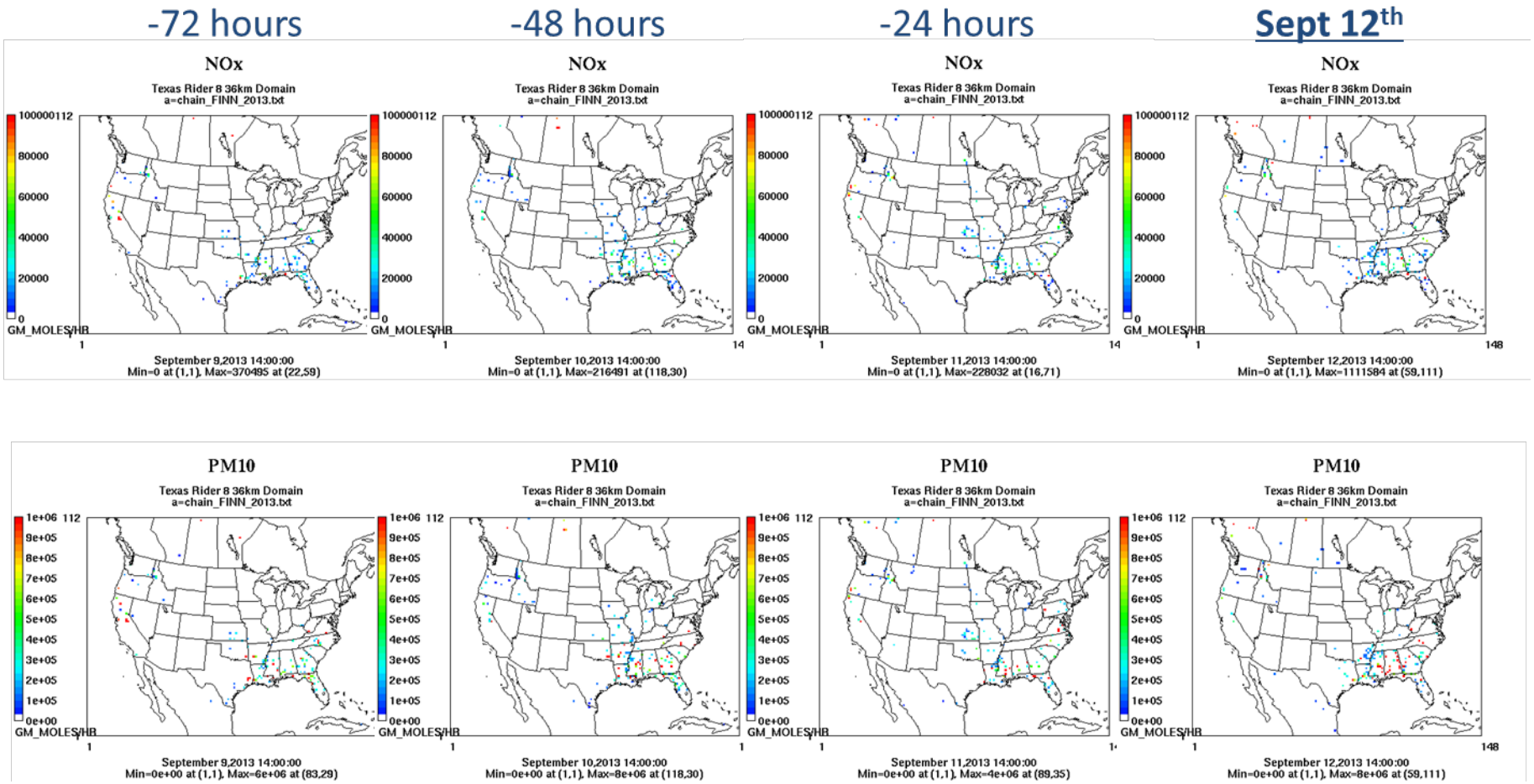

Figure 3-219. September 12, 2013 FINN fire emissions of NOx and PM_{10}.

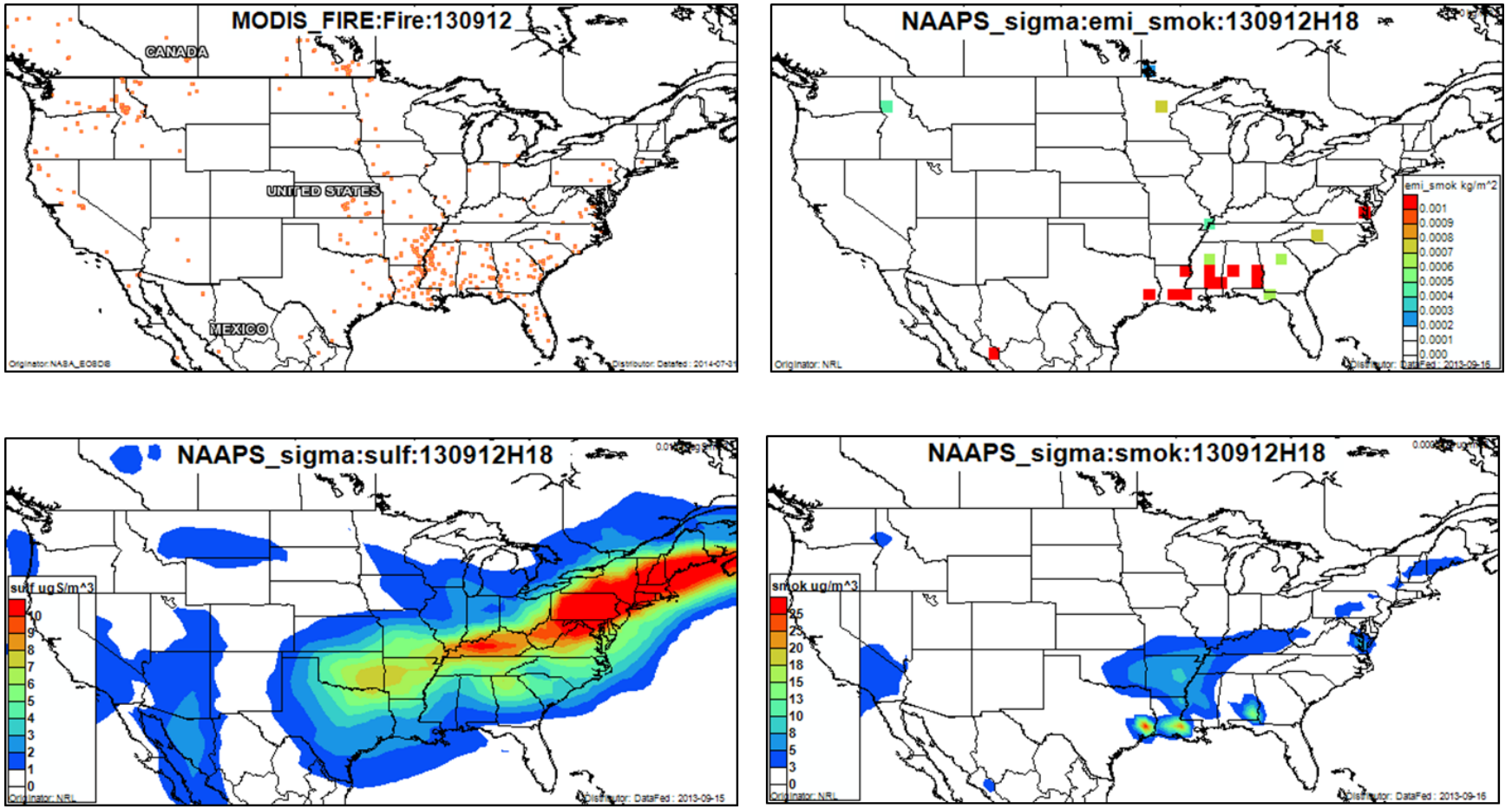

Figure 3-220. September 12, 2013 DataFed analysis. Upper left panel: Locations of active fires from MODIS satellite fire detections. Upper right panel: NAAPS model smoke emissions. Lower left panel: NAAPS model surface layer sulfate concentrations. Lower right panel: NAAPS model surface layer smoke concentrations.

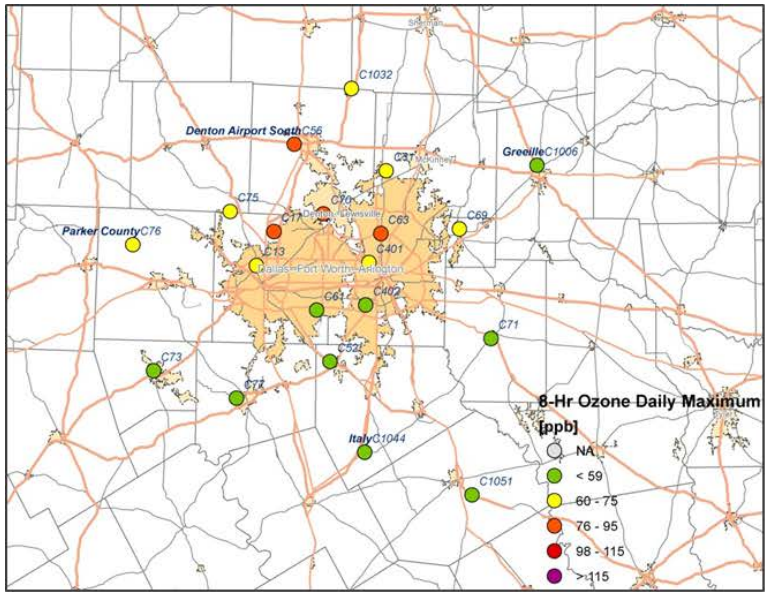

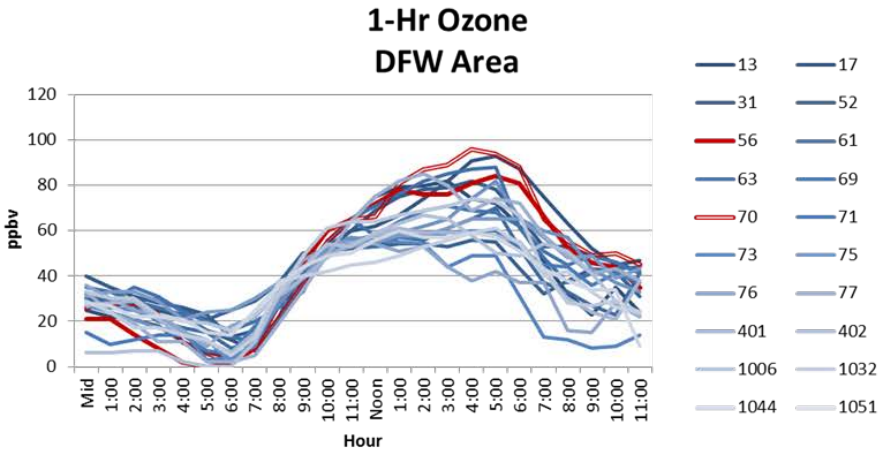

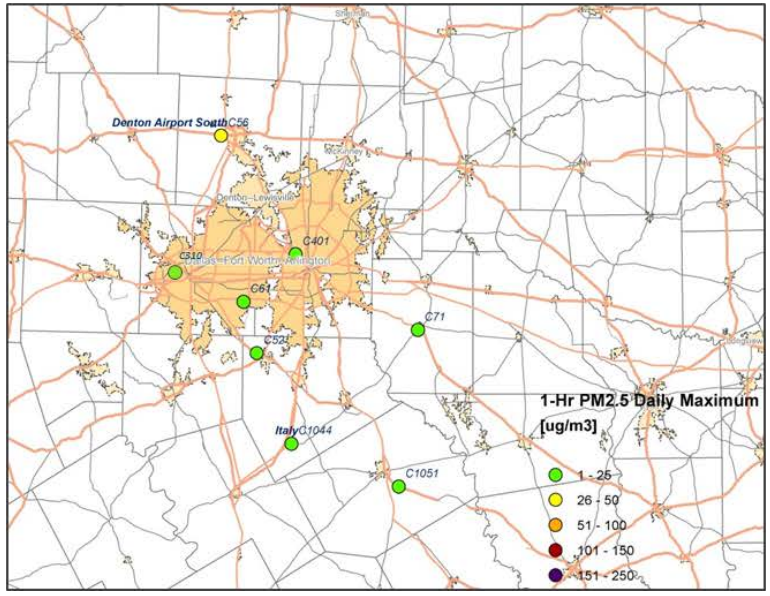

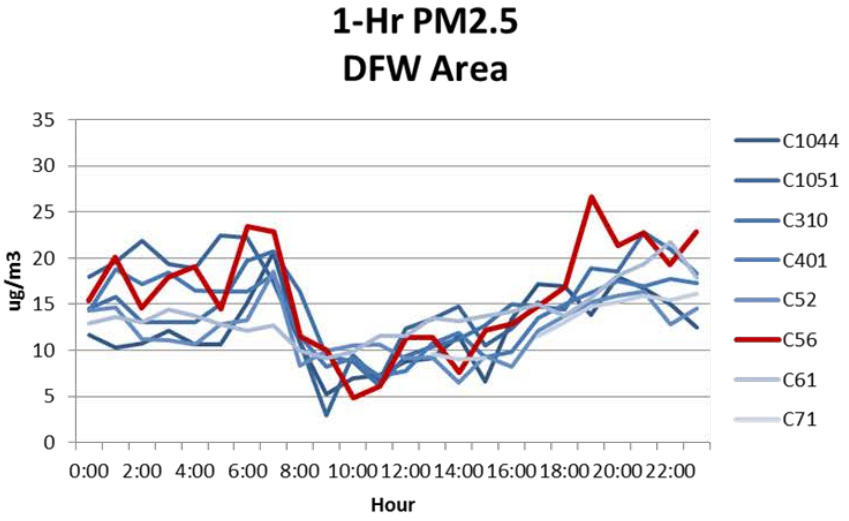

Figure 3-221. Regional ozone (top left and right) and $PM_{2.5}$ (bottom left and right) measurements (DFW area time series).

3.2.16 September 25, 2013

On September 25, 2013, ozone levels were moderately high across East Texas (Figure 3-226), and unusually high values of the MDA8 were monitored at the La Porte Sylvan Beach (C556; 124 ppb) and Seabrook Friendship Park (C45; 104 ppb) sites in the HGB area. These readings were both sites' highest ozone MDA8 in 2013. Figure 3-222 and Figure 3-223 show that the peak 1-hour ozone values at La Porte and Seabrook were 151 ppb and 133 ppb, respectively, and both occurred at noon. The Texas City monitor (C620) also recorded a 1-hour ozone peak at noon, although it was not as high (119 ppb). The 1-hour ozone reading stayed above 100 ppb for 6 hours at La Porte and 5 hours at Seabrook. The Seabrook monitor shows an early morning (6 am) peak in NOx that coincides with the morning commute hours and then dissipates by 9 am. At 10 am, there is a second peak in NOx (~50 ppb) and a smaller peak in NO that coincides with increasing ozone at Seabrook.

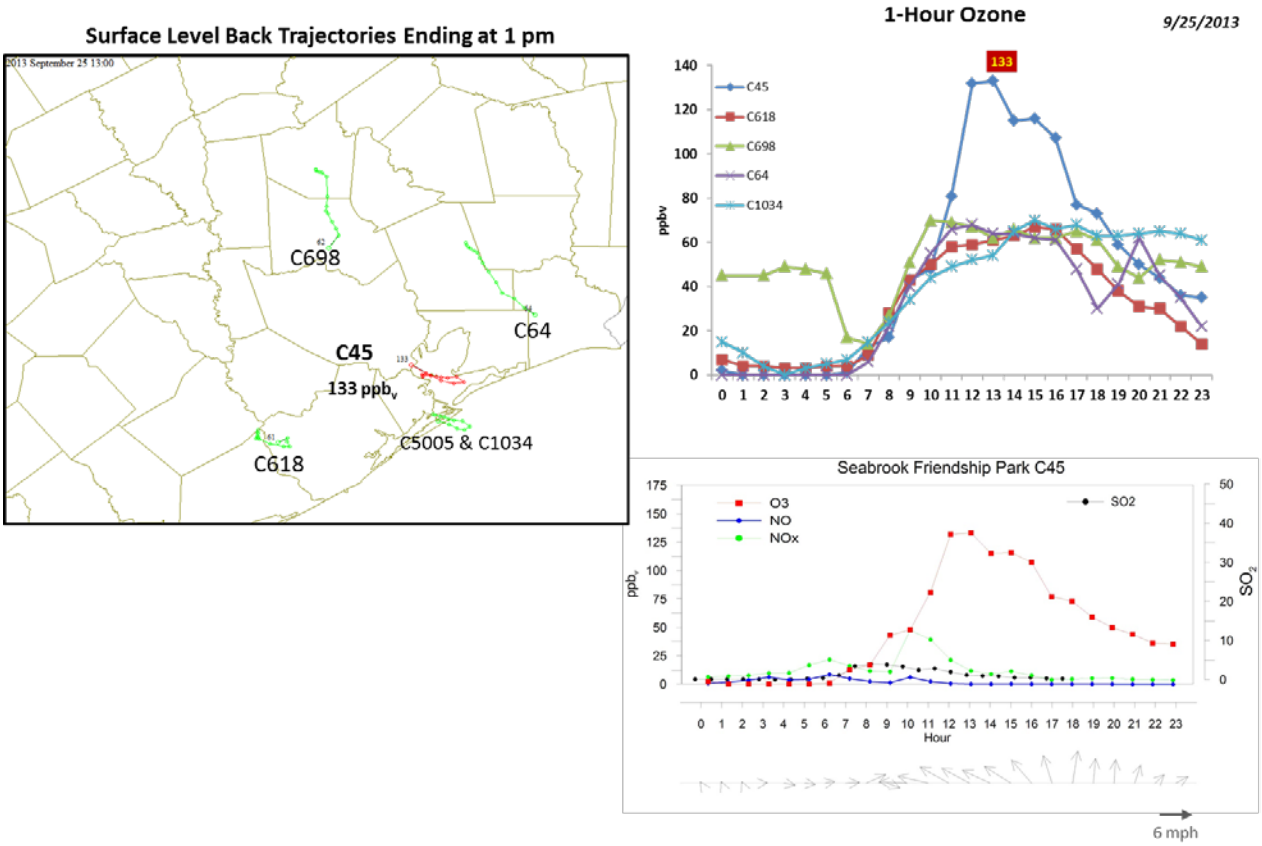

Figure 3-222. September 25, 2013 high ozone day at Seabrook Friendship Park C45. Left panel: back trajectories terminating at C45 (red line) and four other HGB monitors (green lines) on September 25 at the time of peak ozone impact at C45. Upper right panel: 1-hour average ozone time series for C45 and surrounding HGB monitors. Lower right panel: time series of 1-hour ozone, NO, NO_2 and wind vectors at the Seabrook monitor.

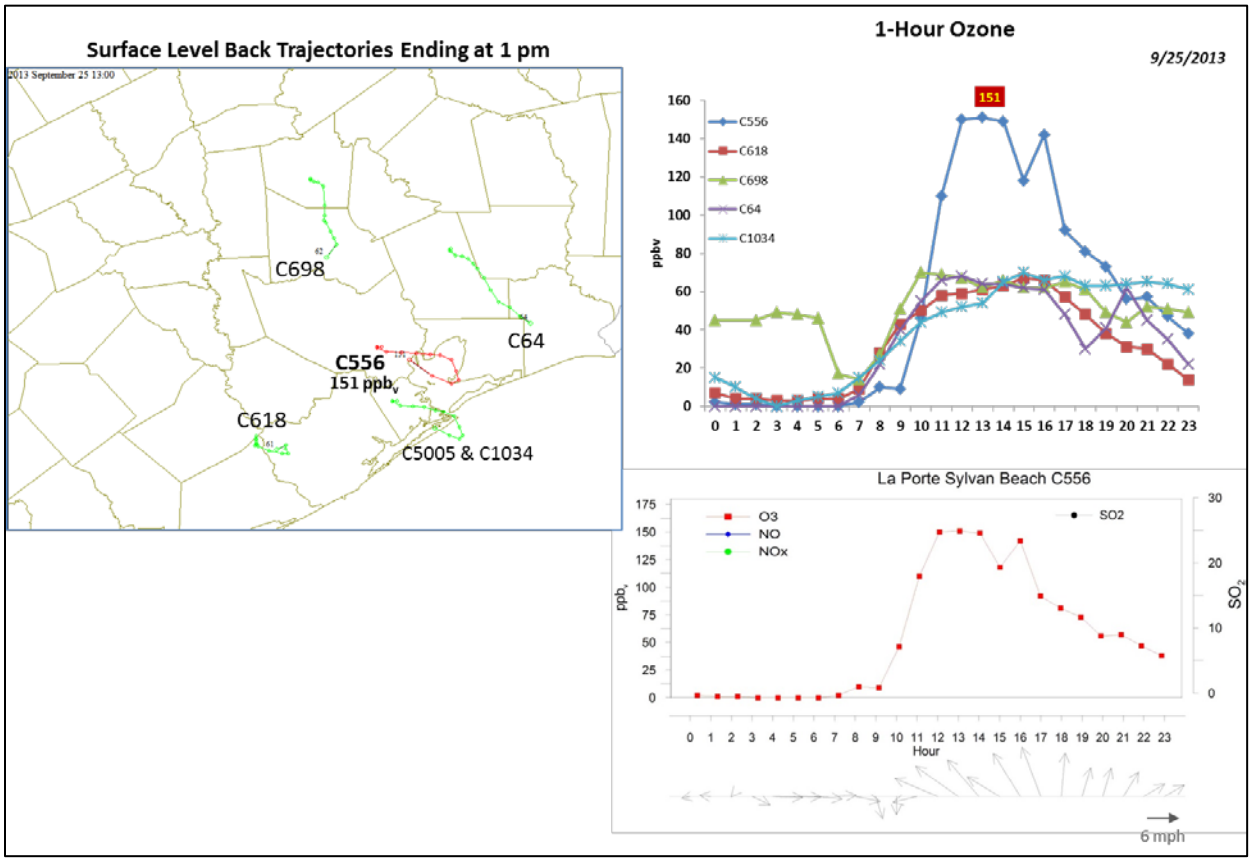

Figure 3-223. September 25, 2013 high ozone day at La Porte Sylvan Beach C556. Left panel: back trajectories terminating at C556 (red line) and four other HGB monitors (green lines) on September 25 at the time of peak ozone impact at C556. Upper right panel: 1-hour average ozone time series for the C556 and surrounding HGB monitors. Lower right panel: time series of 1-hour ozone and wind vectors at the La Porte monitor. SO_2, NO and NOx are not monitored at La Porte.

Both monitors had light winds throughout the night followed by stronger winds from the southeast during the time of rapid ozone formation in the morning. The winds switched to southerly by afternoon, consistent with a sea breeze circulation with onshore flow in the afternoon. The C698 monitor, which is located further inland, shows only northerly winds and no evidence of recirculating flow; this suggests that the marine circulation did not penetrate as far inland as the C698 monitor on September 25. At the La Porte and Seabrook monitors, the AQPlot back trajectories do indicate recirculating wind patterns (Figure 3-222; Figure 3-223).

The SmartFire back trajectory and the HYSPLIT NAM 500 m and 1,000 m back trajectories are consistent in showing northerly flow on September 24. The HYSPLIT NAM and SmartFire back trajectories are based on meteorological data that are too coarse (12 km and 40 km, respectively) to resolve the local scale circulation shown in the AQPlot back trajectories. The SmartFire map shows that there were several fires north and northeast of the HGB area on September 25. The FINN plots show no fire activity along the trajectories at -72 hours. By -24

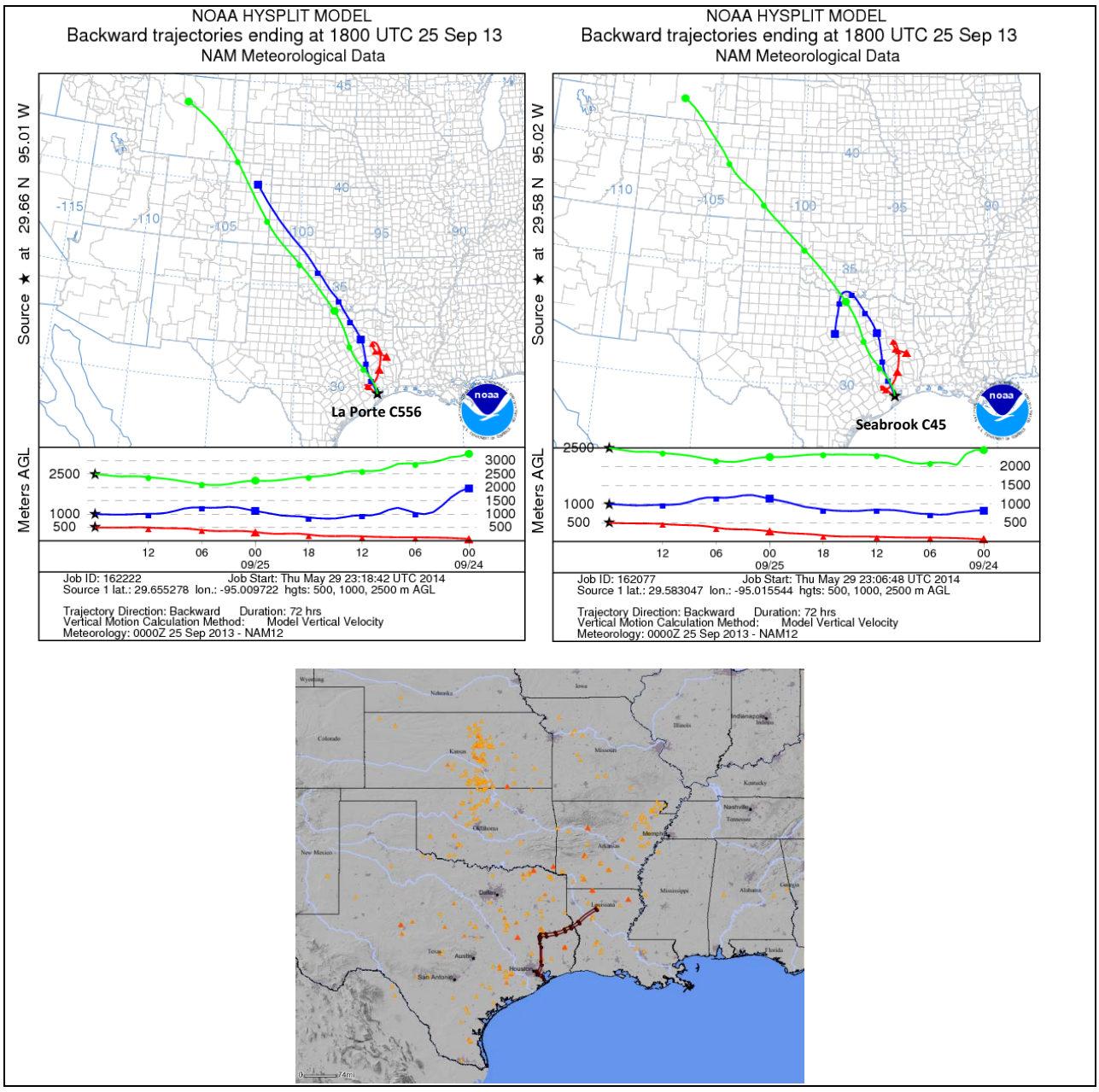

Figure 3-224. 72-hour HYSPLIT back trajectories ending at La Porte Sylvan Beach C556 (top left) and Seabrook Friendship Park C45 (top right) on September 25, 2013; Bottom: SmartFire plots with fire locations (orange triangles) and 72-hour back trajectories terminating at C556 and C45.

hours, fire activity in East Texas increased dramatically, and fires are visible north of the HGB area. These fires appear on the DataFed MODIS fire location plot and their emissions are apparent in the NAAPS smoke emission product. The NAAPS smoke analysis shows a smoke plume north of the HGB area. On September 25, the FINN emissions map shows fires with relatively high PM and NOx emissions just north of the HGB urban area. These fires are also

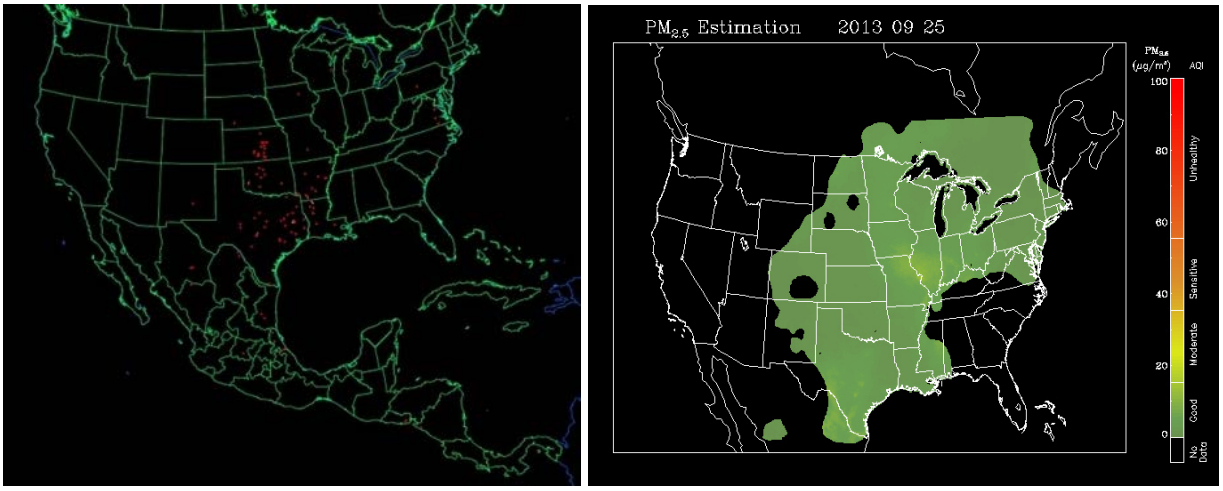

Figure 3-225. Left panel: HMS product showing September 25 fire locations (red dots) and smoke plume (gray area). Right panel: IDEA surface $PM_{2.5}$ estimate based on AOD and surface monitoring data.

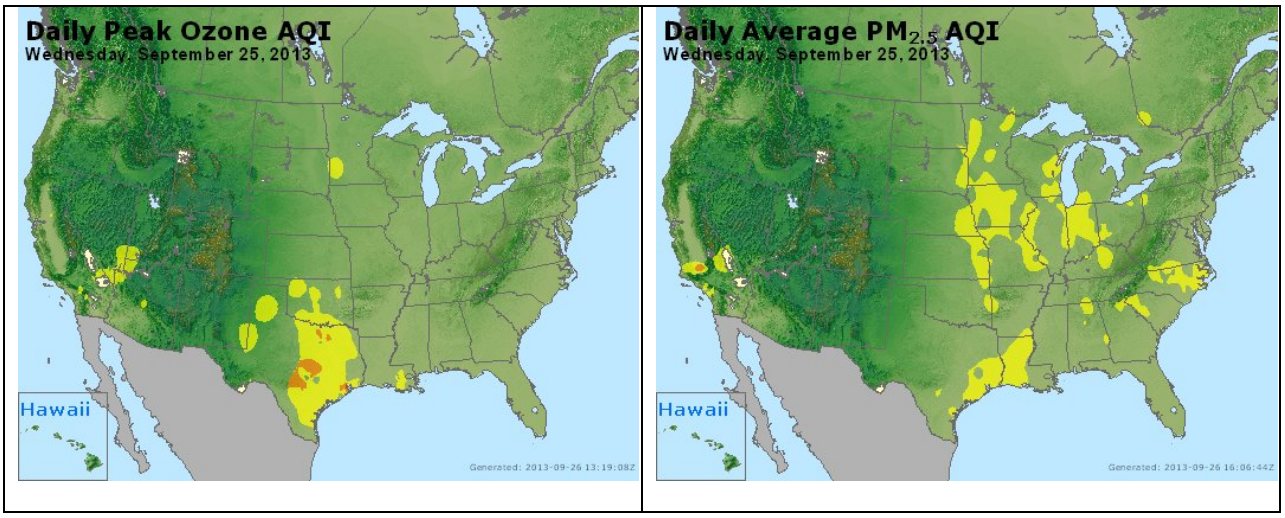

Figure 3-226. Daily average ozone (left) and $PM_{2.5}$ (right) based on observed values. Data from: http://www.airnow.gov/.

visible on the HMS product map, although there is no evidence of a smoke plume (Figure 3-225). The $PM_{2.5}$ AQI is moderate, despite the fire activity in East Texas (Figure 3-226). The ozone spatial plots indicate that ozone MDA8>75 ppb at most monitors south of a line oriented southwest-northeast and running parallel to Interstate 69 (Figure 3-229). The sites that had the highest ozone peaks with maxima at noon (La Porte, Seabrook, and Texas City 34th St.) are all located adjacent to Galveston Bay in the area affected by the marine circulation shown in the AQPlot back trajectories.

The $PM_{2.5}$ time series show maxima at most HGB monitors during the morning hours. The Seabrook monitor September 25 $PM_{2.5}$ data for 10 am-11pm have been rejected by TCEQ validators so it is not possible to know whether there was a $PM_{2.5}$ peak that coincided with the NOx and/or ozone peaks.

Because of the presence of sizable nearby fires that were generally upwind of the monitors and the presence of a NOx peak at Seabrook during the morning ozone increase, we recommend further investigation of September 25, 2013 for both La Porte and Seabrook. For both of these sites, the 1-hour ozone was unusually high. The high MDA1 values, which far exceeded those measured at other HGB monitors on this day, are consistent with the impact of a plume. The La Porte and Seabrook monitors are located near a large number of industrial emissions sources, so additional analysis is required to determine the source of the plume impacts. PM filter analysis should be performed to determine whether the signature of biomass burning is evident at HGB monitors on September 25. Photochemical modeling may also be useful, but we note that the first step in the modeling process will be to ensure that the model can simulate the sea breeze circulation noted in the AQPlot back trajectories and the monitor wind vectors. This local-scale circulation may be difficult for a mesoscale meteorological model to reproduce when running at resolution of 4 km.

Wildfire Emissions Inventory: FINN 2013

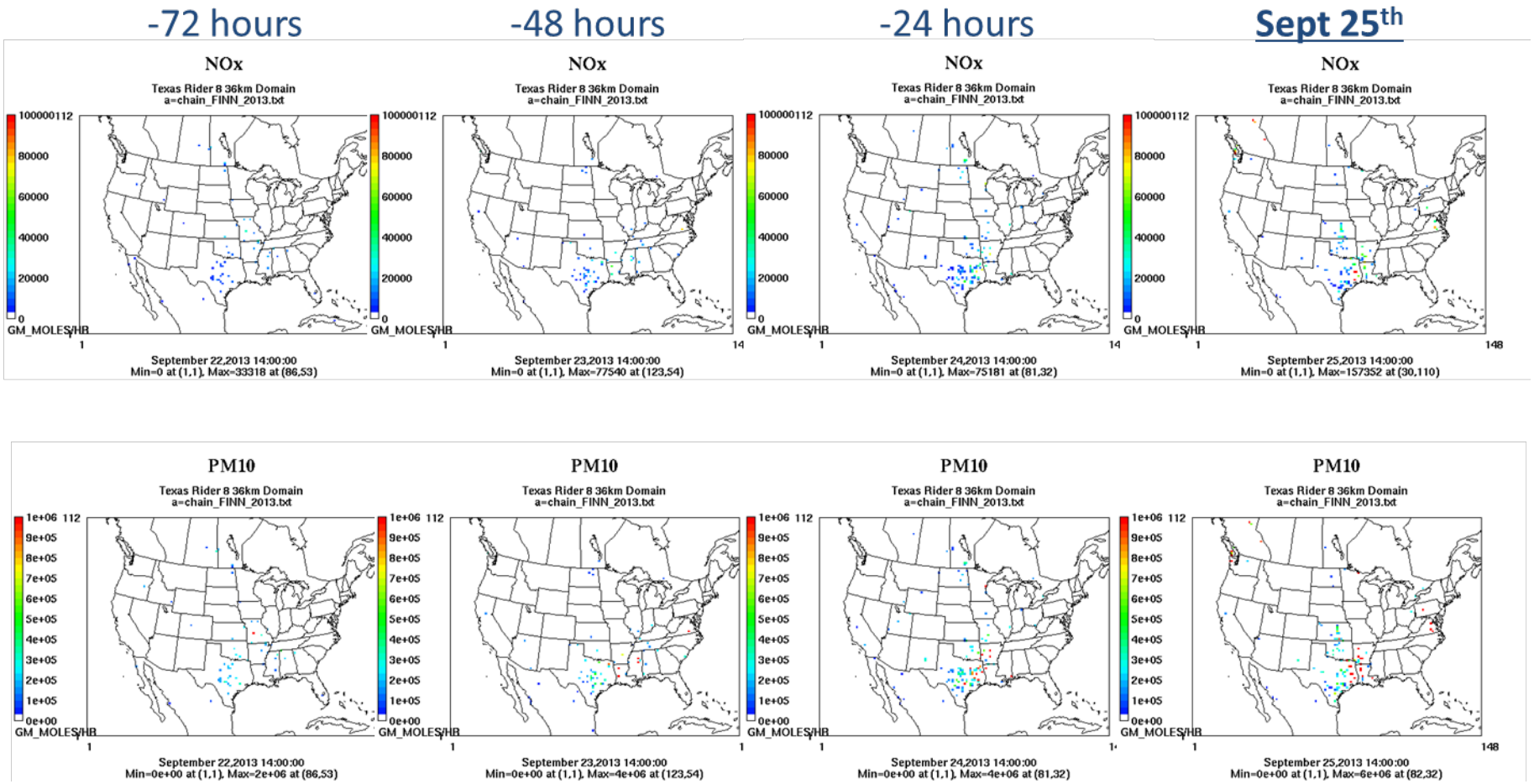

Figure 3-227. September 25, 2013 FINN fire emissions of NOx and PM_{10}.

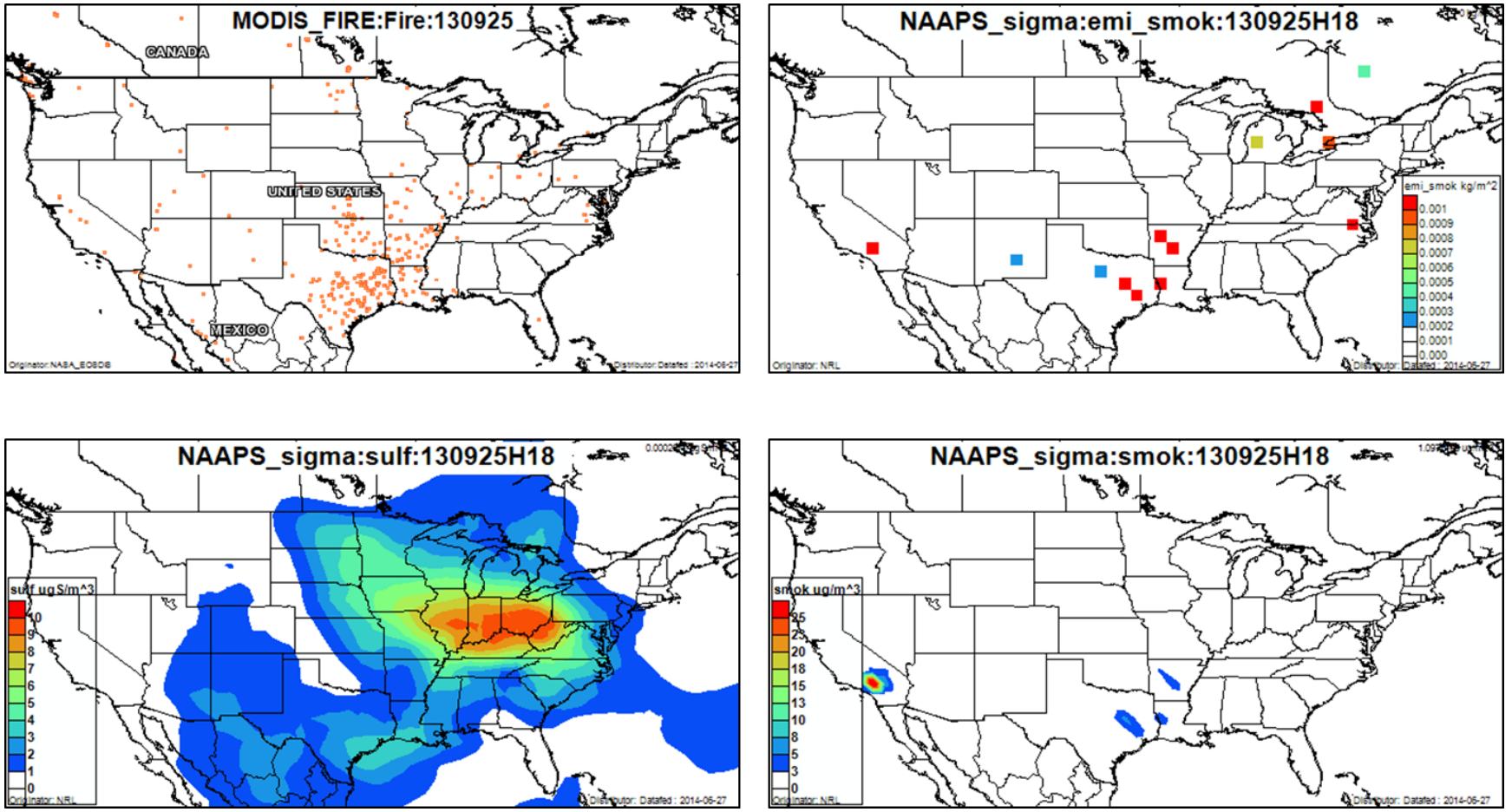

Figure 3-228. September 25, 2013 DataFed analysis. Upper left panel: Locations of active fires from MODIS satellite fire detections. Upper right panel: NAAPS model smoke emissions. Lower left panel: NAAPS model surface layer sulfate concentrations. Lower right panel: NAAPS model surface layer smoke concentrations.

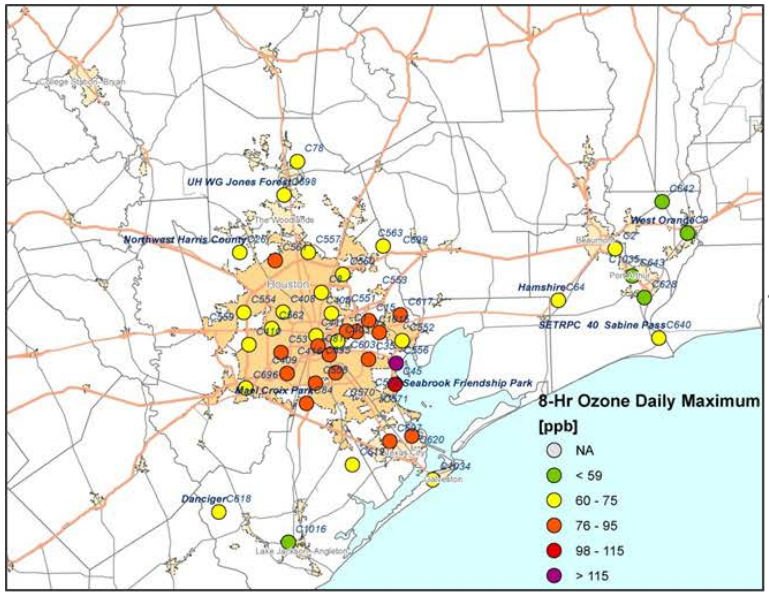

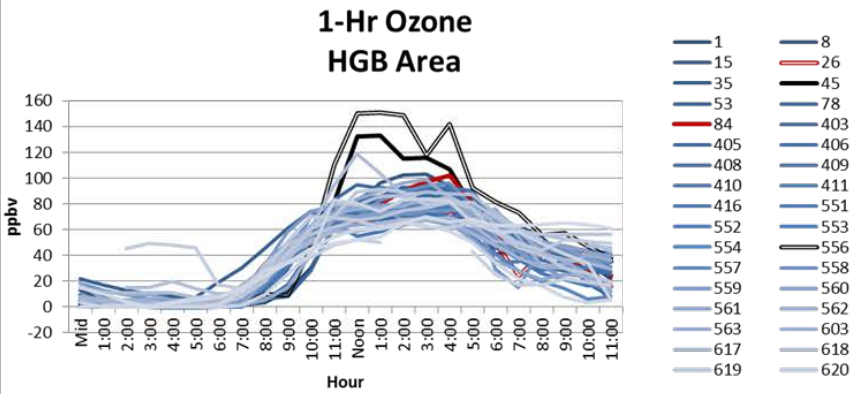

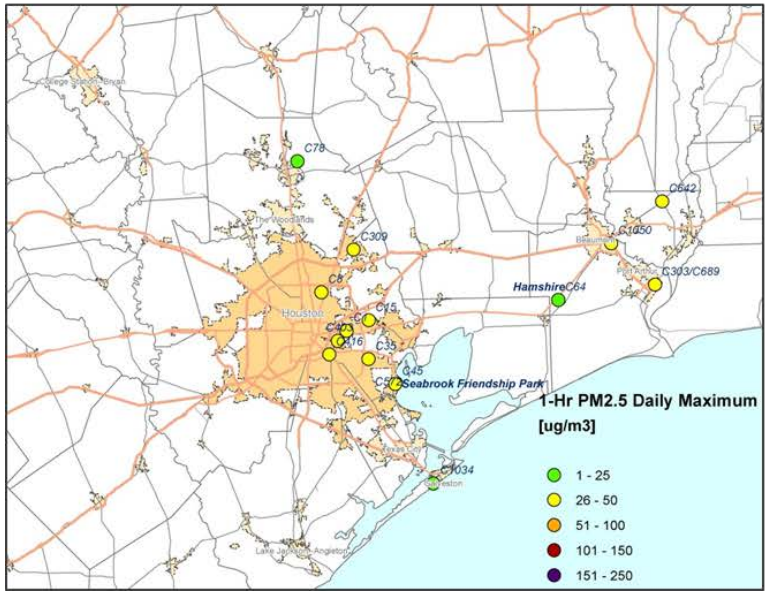

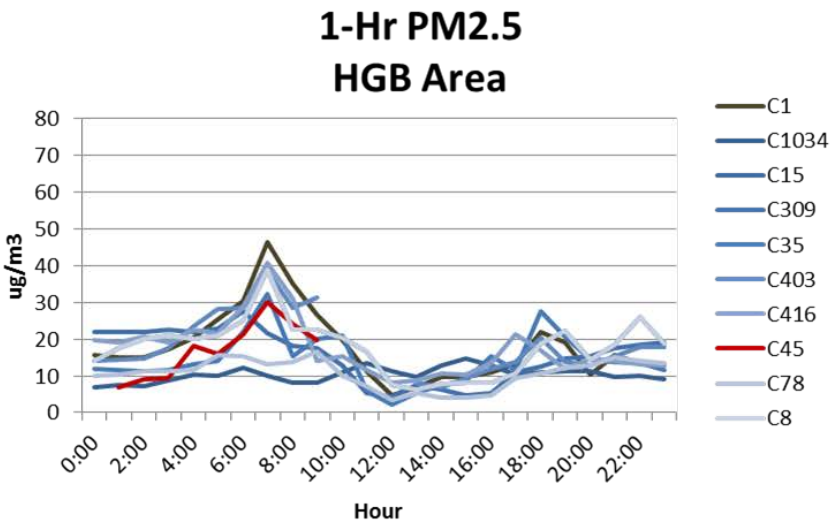

Figure 3-229. Regional ozone (top left and right) and $PM_{2.5}$ (bottom left and right) measurements (HGB area time series)

3.2.17 October 9, 2013

On October 9, 2013, the NW Harris County monitor (C26) monitor recorded its 2nd high MDA8 value (82 ppb). The MDA1 at NW Harris occurred at 4 pm (94 ppb) (Figure 3-230). Background ozone in the HGB area was ~50 ppb (Figure 3-236). There is a small NOx peak during the morning commute period, but there is no NOx peak during the mid-day hours when the 1-hour ozone has its highest values. Wind vectors at the NW Harris County monitor show light northerly winds in the early morning shifting to light southeasterlies by mid-morning and the AQPlot back trajectories in Figure 3-230 show winds to be southeasterly at all of the monitors on the early afternoon of October 9.

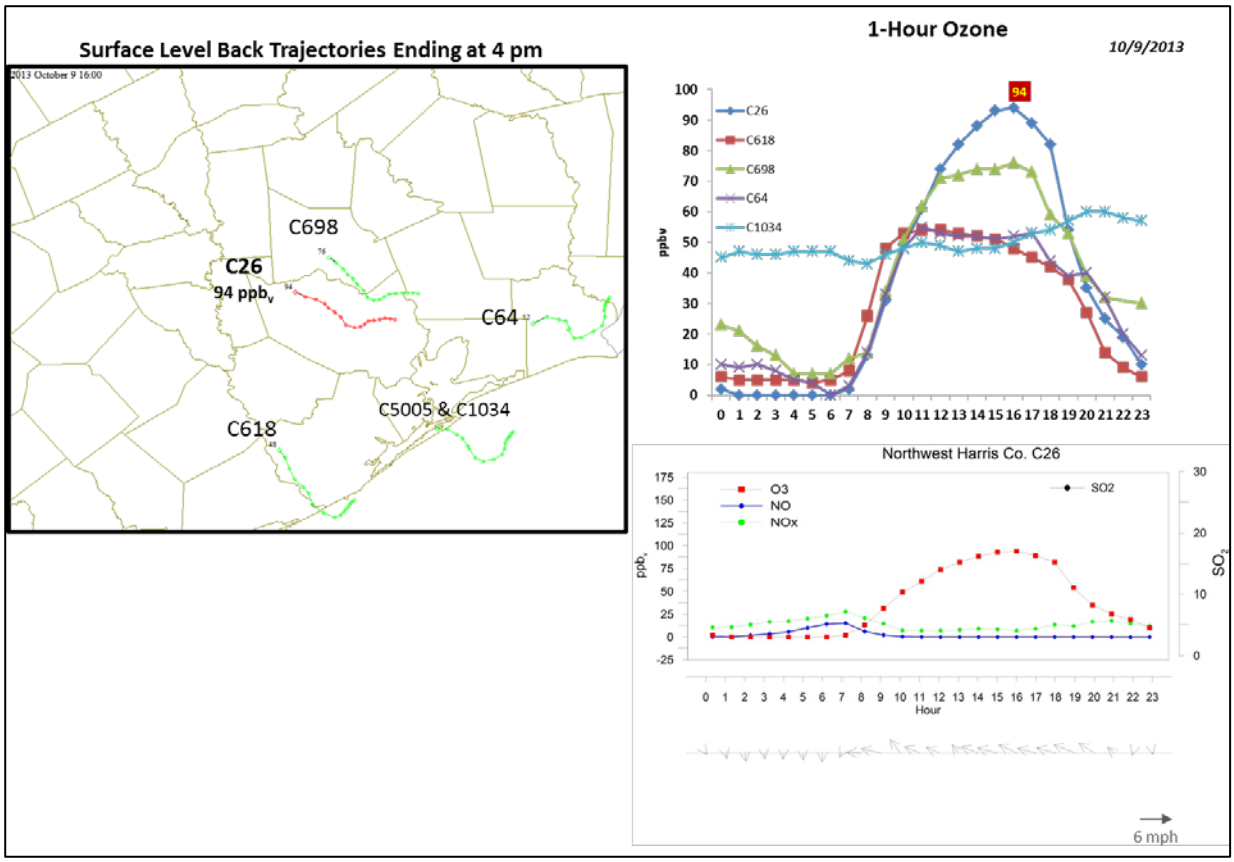

Figure 3-230. October 9, 2013 high ozone day at Northwest Harris Co. C26. Left panel: back trajectories calculated using AQPlot for the HGB monitors at the time of peak ozone impact at C26. Upper right panel: 1-hour average ozone time series for the C26 and surrounding HGB monitors. Lower right panel: time series of 1-hour ozone, NO, NO_2 and wind vectors at the Northwest Harris monitor.

The HYSPLIT NAM 500 m and 1,000 m back trajectories are consistent with the AQPlot trajectories in showing southeasterlies leading up to the time of the 1-hour ozone maximum at

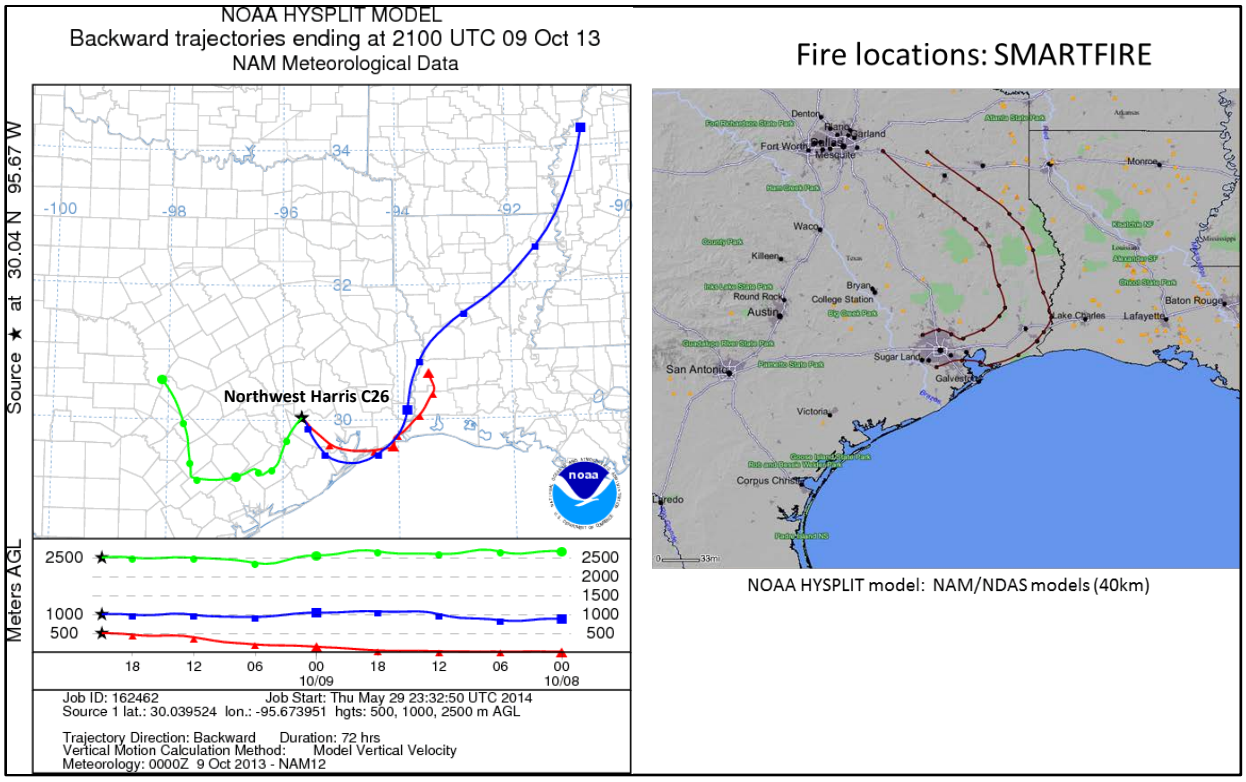

Figure 3-231. 72-hour HYSPLIT back trajectories (NAM 12km) from Northwest Harris C26 terminating October 9, 2013; SmartFire plot showing fire locations (orange triangles) and 72-hour HYSPLIT back trajectories (EDAS 40 km) terminating at C26.

the NW Harris County monitor (Figure 3-231). The SmartFire back trajectory shows anti-cyclonic motion similar to the HYSPLIT NAM trajectories, but takes a different path through the HGB area before arriving at the NW Harris monitor. The SmartFire map shows that there is a fire just north of the HGB urban area, but the trajectories pass to the south of it. The SmartFire plot also shows fires in Northeast Texas and eastern Louisiana. The HMS product (Figure 3-232) also indicates that fires are present in these areas on October 9, and FINN emissions plots show fires north of Houston and in Northeast Texas and eastern Louisiana from -48 hours through October 9 (Figure 3-234).

The ozone spatial pattern is consistent with southeasterly flow transporting the HGB urban plume northward, following the trajectories predicted by the AQPlot and HYSPLIT tools. Monitors with the highest values of the MDA8 are located on the northwestern perimeter of the HGB urban area: Mercer Arboretum (C557), Meyer Park (C561), and NW Harris County. Monitors on the southeastern part of the HGB urban area (C620) generally had lower ozone than those located in the northern and northwestern parts.

$PM_{2.5}$ values throughout the HGB area were relatively low (i.e., <25 µg m^{-3}) except during the morning commute hours (Figure 3-236). The $PM_{2.5}$ time series shows no evidence of a fire plume that coincides with the high ozone values and there is no NOx plume coincident with the

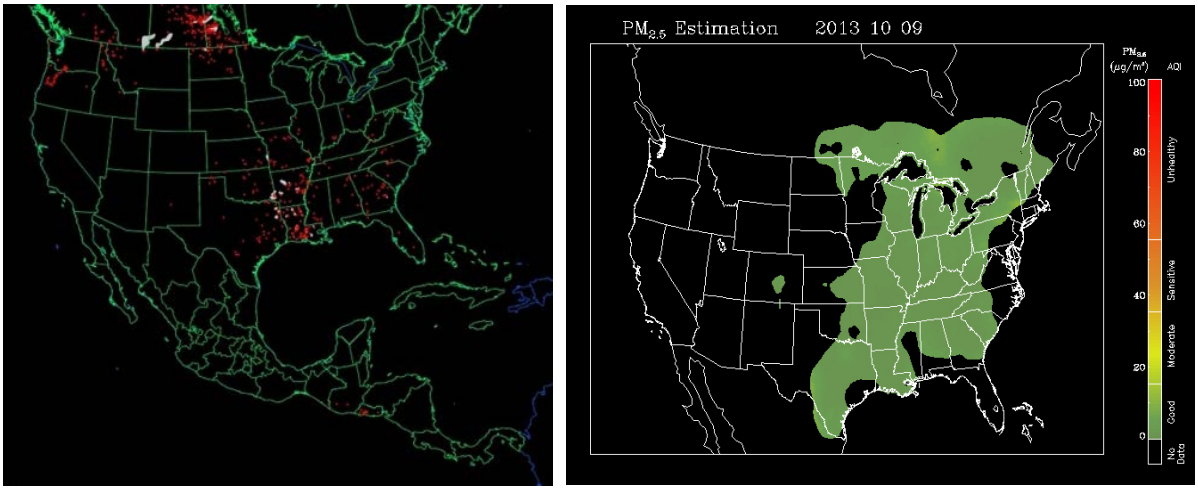

Figure 3-232. Left panel: HMS product showing October 9 fire locations (red dots) and smoke plume (gray area). Right panel: IDEA surface $PM_{2.5}$ estimate based on AOD and surface monitoring data.

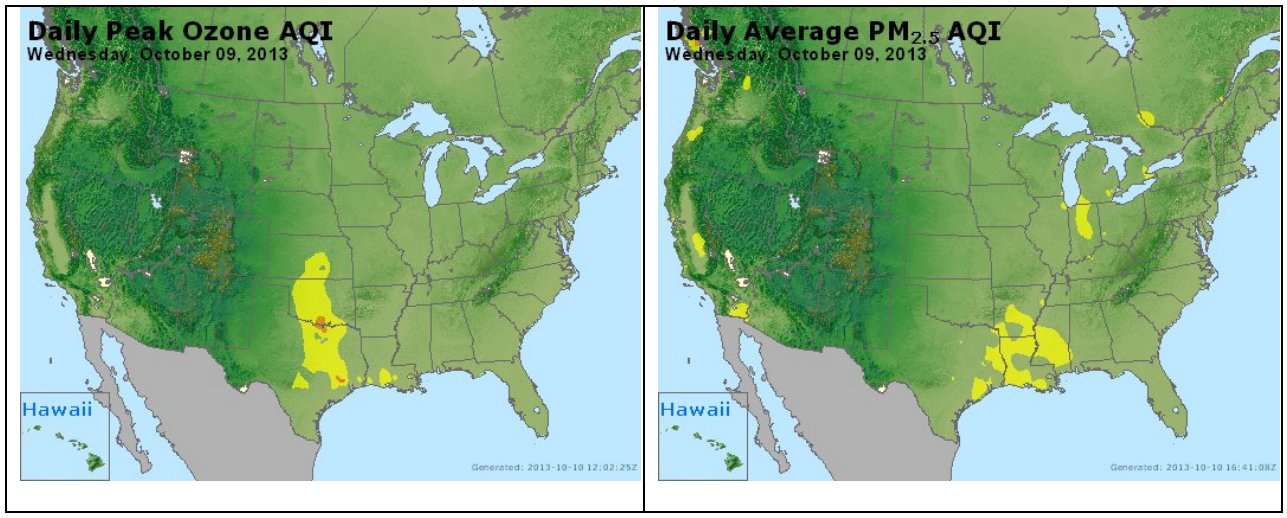

Figure 3-233. Daily average ozone (left) and $PM_{2.5}$ (right) based on observed values. Data from: http://www.airnow.gov/.

high ozone values measured at midday at NW Harris County. Therefore, we recommend no further evaluation of October 9, 2013.

ENVIRON

Wildfire Emissions Inventory: FINN 2013

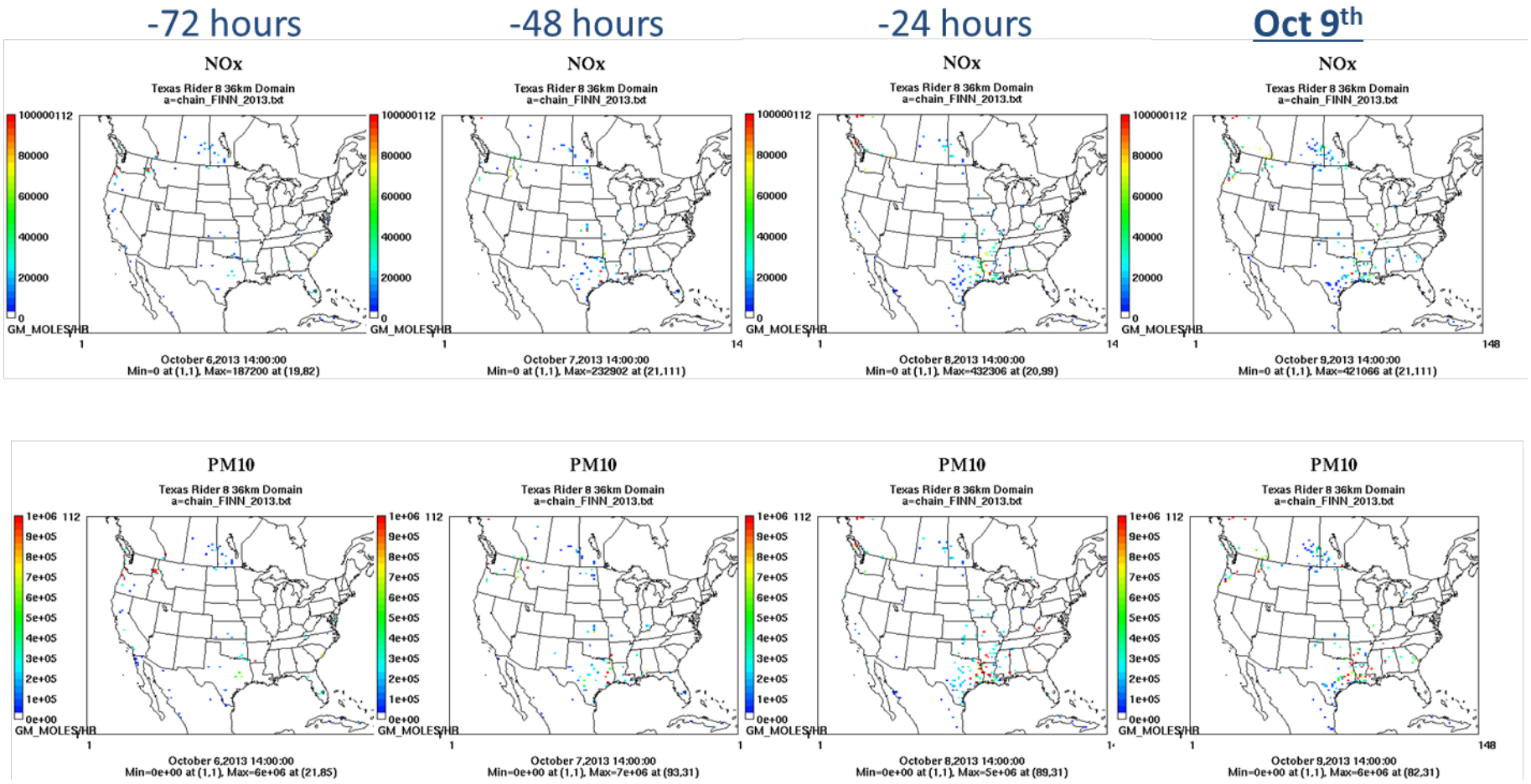

Figure 3-234. October 9, 2013 FINN fire emissions of NOx and PM_{10}.

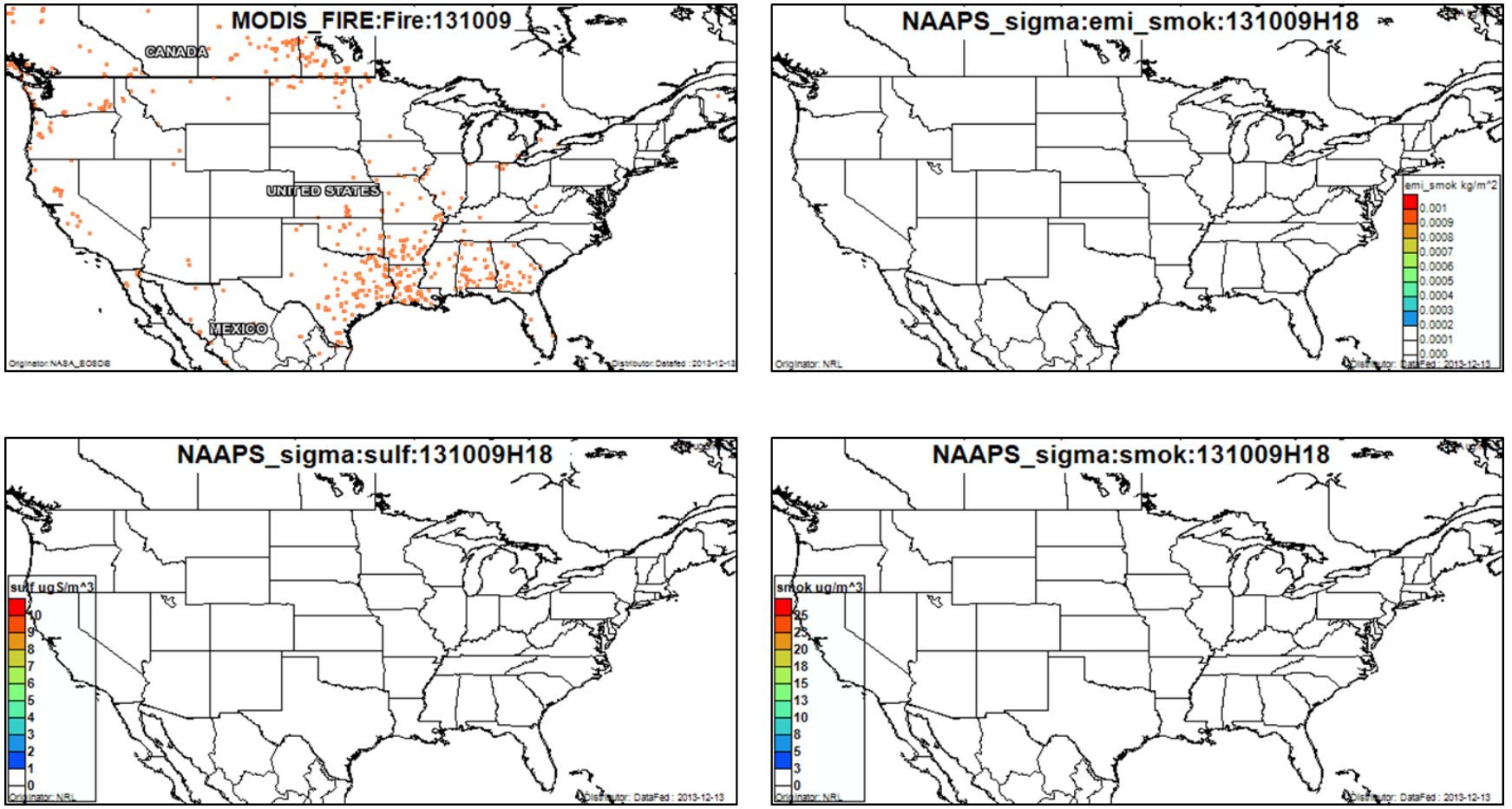

Figure 3-235. October 9, 2013 DataFed analysis. Upper left panel: Locations of active fires from MODIS satellite fire detections. Upper right panel: NAAPS model smoke emissions. Lower left panel: NAAPS model surface layer sulfate concentrations. Lower right panel: NAAPS model surface layer smoke concentrations.

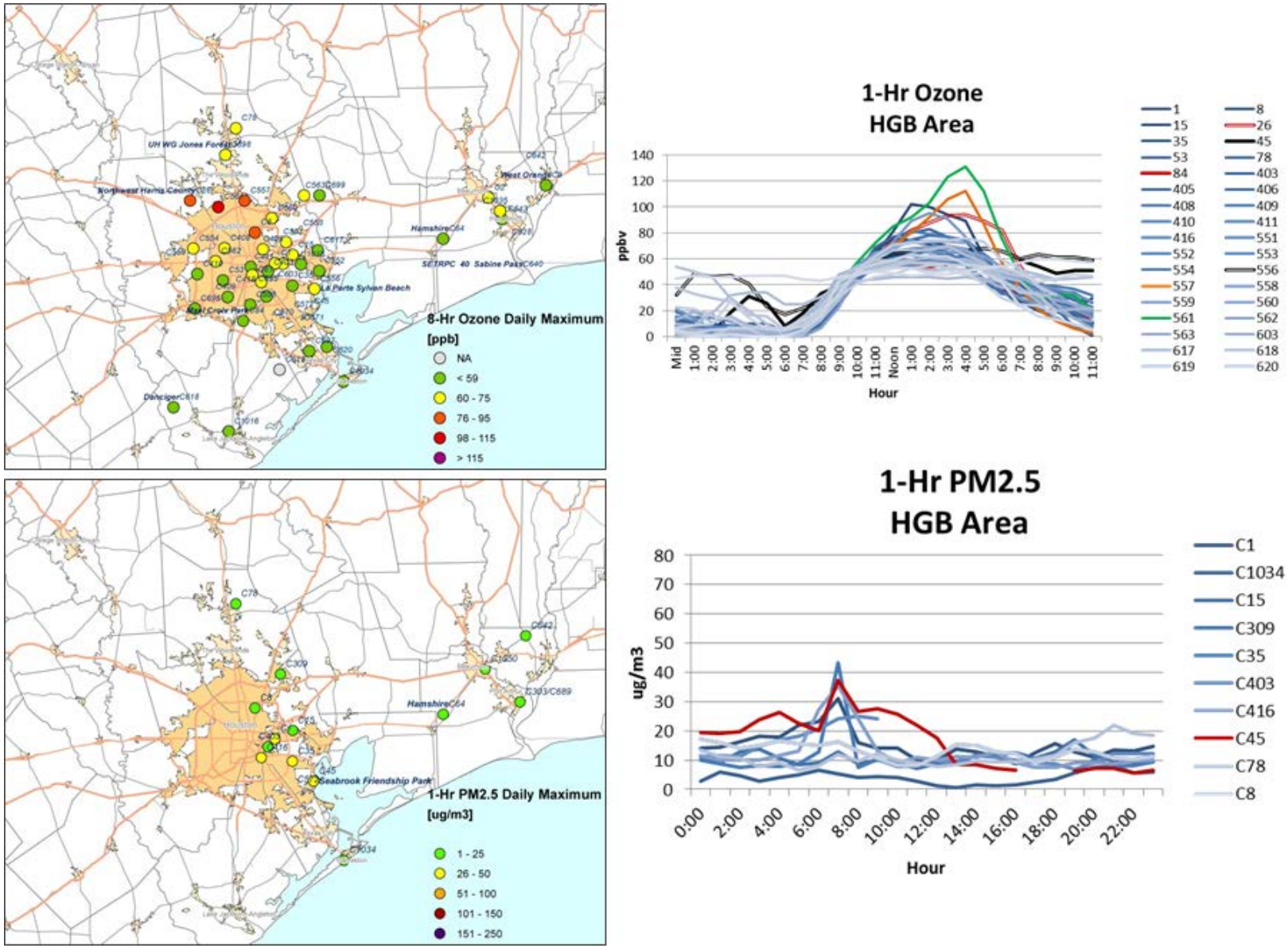

Figure 3-236. Regional ozone (top left and right) and $PM_{2.5}$ (bottom left and right) measurements (HGB area time series).

3.3 Summary of High Ozone Day Analysis

In Sections 3.1 and 3.2, we reviewed the four highest 8-hour ozone days in 2012 and 2013 at the monitors with the highest and second-highest design values in the HGB and DFW areas as well as the monitor with the highest design value in the BPA area and two days selected by the TCEQ at the Seabrook and La Porte monitors in the HGB area. For each of these high ozone days, we evaluated the potential for fire emissions to have influenced monitored ozone. We reviewed available ambient monitoring data, model data, emission inventories and satellite products, and determined whether emissions from fires are likely to have contributed to high ozone at monitors with high ozone on each day. For each day we reviewed, we provided a recommendation as to whether further analysis of the day is warranted to establish whether a fire plume impact occurred and, if an impact occurred, what the contribution of the fire emissions was to monitored ozone.

We recommended further evaluation for days for which the following criteria were true:

1. Modeled back trajectories indicate a fire was located upwind of the monitor during the 72-hour period prior to the monitor's daily 1-hour ozone maximum

   and

2. $PM_{2.5}$ readings consistent with a plume impact occurred at least one monitor in the area (not required to be at the monitor with high ozone since not all ozone monitoring sites measure PM)

   or

3. NOx readings consistent with a plume impact occur together with the ozone peak at the monitor. NOx peaks that occur during early morning and/or evening commute hours are not considered unless the ozone peak occurs together with the NOx peak.

The results are summarized in Table 3-3. We identified 2 days in 2012 (June 25, June 27) and 3 days in 2013 (July 3-4, September 25) as days on which fire emissions may have affected ozone at one or more monitors and for which further analysis is recommended. All days recommended for further study based on the high ozone day analysis results and the criteria above are highlighted in yellow in Table 3-3.

The days highlighted in yellow in Table 3-3 were determined in Section 3 to show a causal relationship between fires and high ozone at one or more monitors. For each of these days, we performed additional analyses, which are described in Sections 4-6. These additional analyses are aimed at confirming the causal relationship (Section 4) and determining whether these days satisfy the EER criteria of concentrations above historical fluctuations (Section 5) and the "but-for" test (Section 6).

Table 3-3. Summary of high ozone day analysis.

2012 Day	Monitor(s) Analyzed	Further Evaluation Required?	Upwind Fire?	PM2.5 Peak?	NOx Peak?	PM Filters Available?
3/24/2012	Sabine Pass, Seabrook, La Porte	No				
3/25/2012	Sabine Pass	No				
3/26/2012	NW Harris	No				
5/17/2012	Denton, NW Harris	No				
5/21/2012	Manvel Croix	No				
5/22/2012	Sabine Pass	No				
6/1/2012	NW Harris	No				
6/24/2012	Grapevine Fairway	No				
6/25/2012	Denton, Grapevine Fairway, Manvel Croix	Yes Grapevine/Denton; No Manvel	Yes	Yes	No	FRM only, (Hinton)
6/26/2012	Sabine Pass, Grapevine Fairway, Manvel Croix	No				
6/27/2012	Denton, Grapevine Fairway, NW Harris	Yes Grapevine/Denton; No NW Harris	Yes	No[1]	No	No
9/6/2012	Denton	No				
9/20/2012	Manvel Croix	No				
2013 Day	**Monitor(s) Analyzed**	**Further Evaluation Required?**				**PM Filters Available?**
5/7/2013	Sabine Pass	No				
5/13/2013	NW Harris	No				
6/3/2013	Manvel Croix	No				
7/2/2013	Manvel Croix, Sabine Pass	No				
7/3/2013	NW Harris	Yes	Yes	Yes	No	Clinton (SC), Galveston (SC), Freeport (SA)
7/4/2013	Sabine Pass, Manvel Croix	Yes; Yes	Yes	Yes	No	Clinton (SC), Galveston (SC)
7/5/2013	Denton	No				
7/13/2013	Sabine Pass	No				
8/16/2013	Manvel Croix	No				
8/28/2013	NW Harris	No				
8/30/2013	Grapevine	No				
8/31/2013	Denton	No				
9/4/2013	Denton, Grapevine	No				
9/6/2013	Grapevine, Denton	No				
9/12/2013	Grapevine	No				
9/25/2013	La Porte, Seabrook	Yes for both	Yes	No[1]	Yes	Aldine (SM), Clinton (AN,SC), Galveston (AN)
10/9/2013	NW Harris	No				

PM Filter availability (Richard Tropp, DRI, personal communication, 2014):
SC: Sampled & analyzed - remainder can be reanalyzed for carbon and/or levoglucosan
SA: Sampled - available for analysis (levoglucosan only - no carbon)
AN: Sampled & analyzed - nothing left to reanalyze
SM: Sampled - carbon results available, uncertain if enough sample remains for levoglucosan

[1]$PM_{2.5}$ data are missing for the Seabrook monitor for the period of high ozone on September 25, 2012 and from several DFW area monitors on June 27, 2013.

4.0 ANALYSIS OF SPECIATED $PM_{2.5}$ DATA

Speciated $PM_{2.5}$ data can be used to determine whether emissions from fires influenced a monitor. The presence of the sugar anhydride levoglucosan (1,6-anhydro-β-D-glucopyranose) is a marker that is specific to biomass burning (e.g. Simoneit et al., 1999; Cheng et al., 2013; Zhang et al., 2013). Levoglucosan is released when cellulose or starches burn, but is not released during the combustion of fossil fuels. The ratio of levoglucosan to other species (e.g. mannosan, see Cheng et al., 2013) can be used to distinguish among different types of biomass burning.

The work plan for this project called for the Desert Research Institute (DRI) to analyze filters collected at DFW and HGB area monitors for the presence of levoglucosan and mannosan in order to provide a definitive conclusion as to whether fire emissions influenced ozone at DFW and HGB monitors on days analyzed in Section 3. No filters were available for the BPA area (Richard Tropp, DRI, personal communication, 2014). Due to a sampler loader malfunction, DRI was unable to carry out this analysis during the time frame of this study.

Therefore, we reviewed the 2012-2013 speciated $PM_{2.5}$ data for the HGB and DFW areas available through the TCEQ's Texas Air Monitoring Information System (TAMIS) Web Interface. Two sites monitored speciated $PM_{2.5}$ in the HGB area during 2012-2013: Deer Park #2 (CAMS 35) and Aldine (CAMS 8). In the DFW area, the Convention Center, Hinton (CAMS 401) and Midlothian (CAMS 52) sites monitored speciated $PM_{2.5}$. The Convention Center and Hinton sites are located in Dallas, while the Midlothian site is south of the DFW urban area. The BPA area did not have speciated PM data available for2012-2013.

Here, we present time series for organic carbon (OC) and elemental carbon (EC) for each monitor for the years 2009-2013. This represents the entire available data record for the DFW and HGB monitors. Elevated values of OC and EC are found in fire plumes (e.g. Cheng et al., 2013), but, unlike levoglucosan, OC and EC are not unique to biomass burning. For example, EC (soot) is emitted by the combustion of fossil fuels. Therefore, the presence of a plume of EC or OC at a monitor may indicate the presence of a fire plume, but not all EC and OC plumes are related to fires. EC and OC are measured by two different methods: thermal optical reflectance (TOR) and thermal optical transmittance (TOT), and we present time series for both measurement methods for EC and OC. EC_TOT is well-correlated to EC_TOR and the same is true for OC_TOT and OC_TOR.

Figure 4-1 shows the OC time series for the Houston Deer Park #2 and Houston Aldine monitors. The Deer Park and Aldine monitors both show OC_TOR and OC_TOT peaks on June 26, 2012, July 3, 2013 and September 25, 2013. The September 25, 2013 peak is far more pronounced for Aldine than for Deer Park. The EC time series (Figure 4-2) show a similar result. June 26, 2012 and July 3, 2013 show large peaks for Deer Park, while the peaks for these two days are visible but not as large at Aldine. At Aldine, however, the September 25, 2013 has higher amplitude than at Deer Park. The EC and OC results are therefore reasonable consistent for these two HGB area monitors.

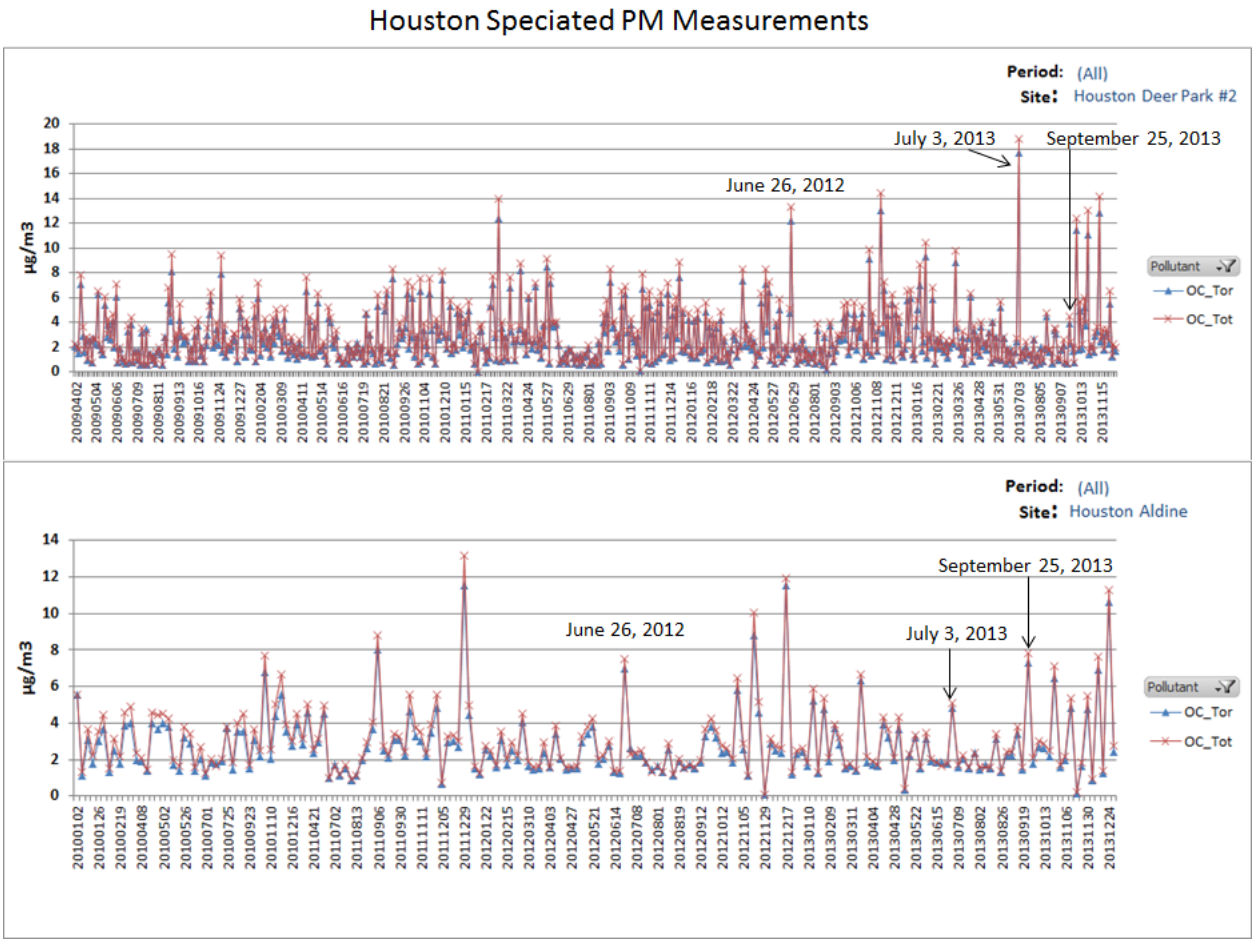

Figure 4-1. Organic carbon measurements for Houston area monitors. Entire data record through 2013 is shown for each monitor.

OC and EC time series for the DFW area monitors Convention Center, Dallas Hinton and Midlothian OFW are shown in Figure 4-3 and Figure 4-4, respectively. For OC, the most pronounced peak during 2012-2013 comes on June 26, 2012 and the same is true for EC. No other high ozone day analyzed in Section 3 stood out as consistently among the DFW area monitors.

Based on the time series shown in Figure 4-1-Figure 4-4, the EC and OC measurements are consistent with potential fire impacts on June 26, 2012 in DFW, July 3, 2013 in HGB and September 25, 2013 in HGB. The PM sampling for the monitors occurs on a 3 or 6 day cycle depending on the monitor. For example, the DFW Convention Center monitor sampled ambient air on June 23, June 26 and June 29, 2012. No information is available about days between the sampling days. To be conservative, therefore, we assume that EC and OC values on June 25, 2012 and June 27, 2012 were also consistent with fire impacts and that July 4, 2013 as well as July 3, 2013 had high EC and OC values.

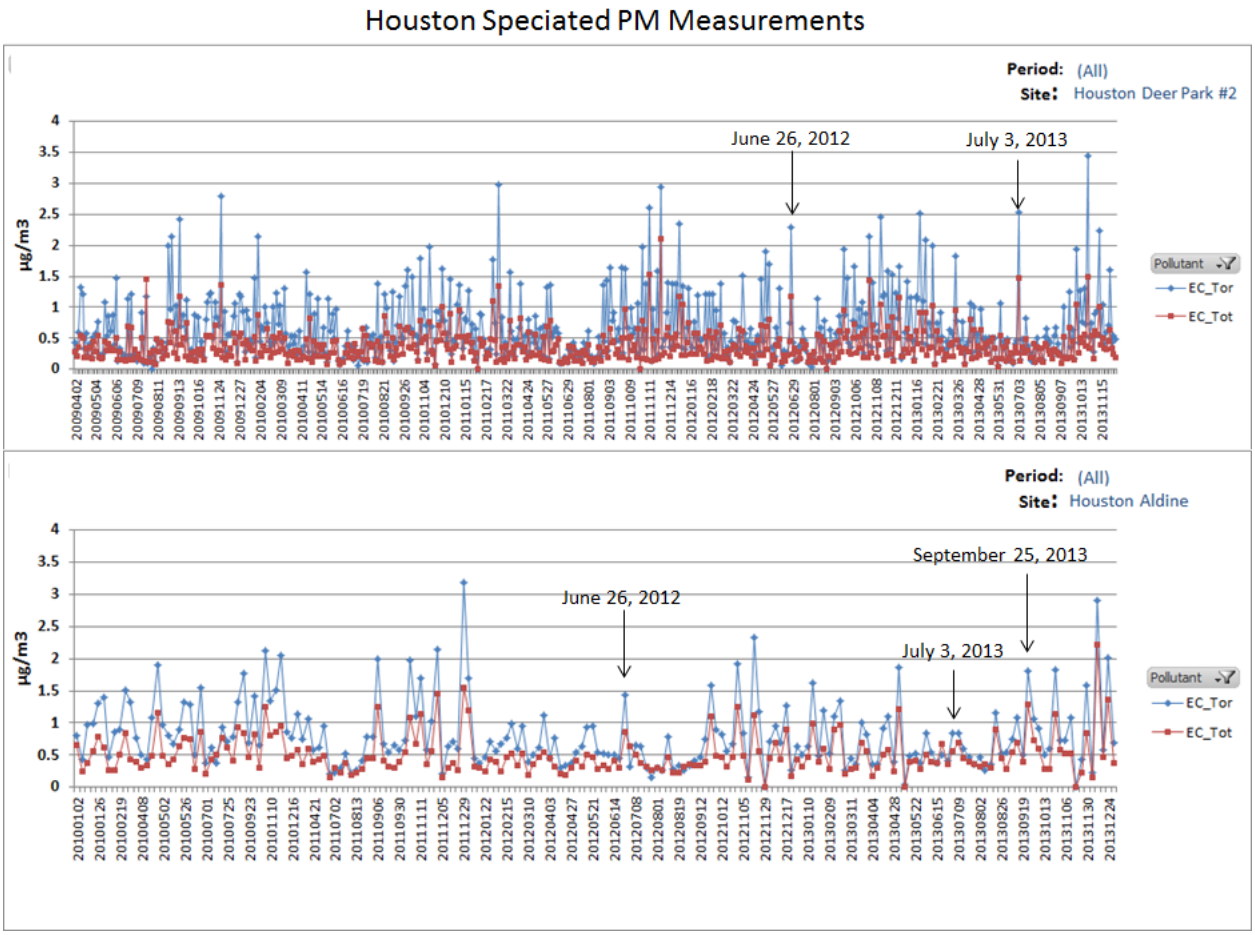

Figure 4-2. Elemental carbon measurements for Houston area monitors. Entire data record through 2013 is shown for each monitor.

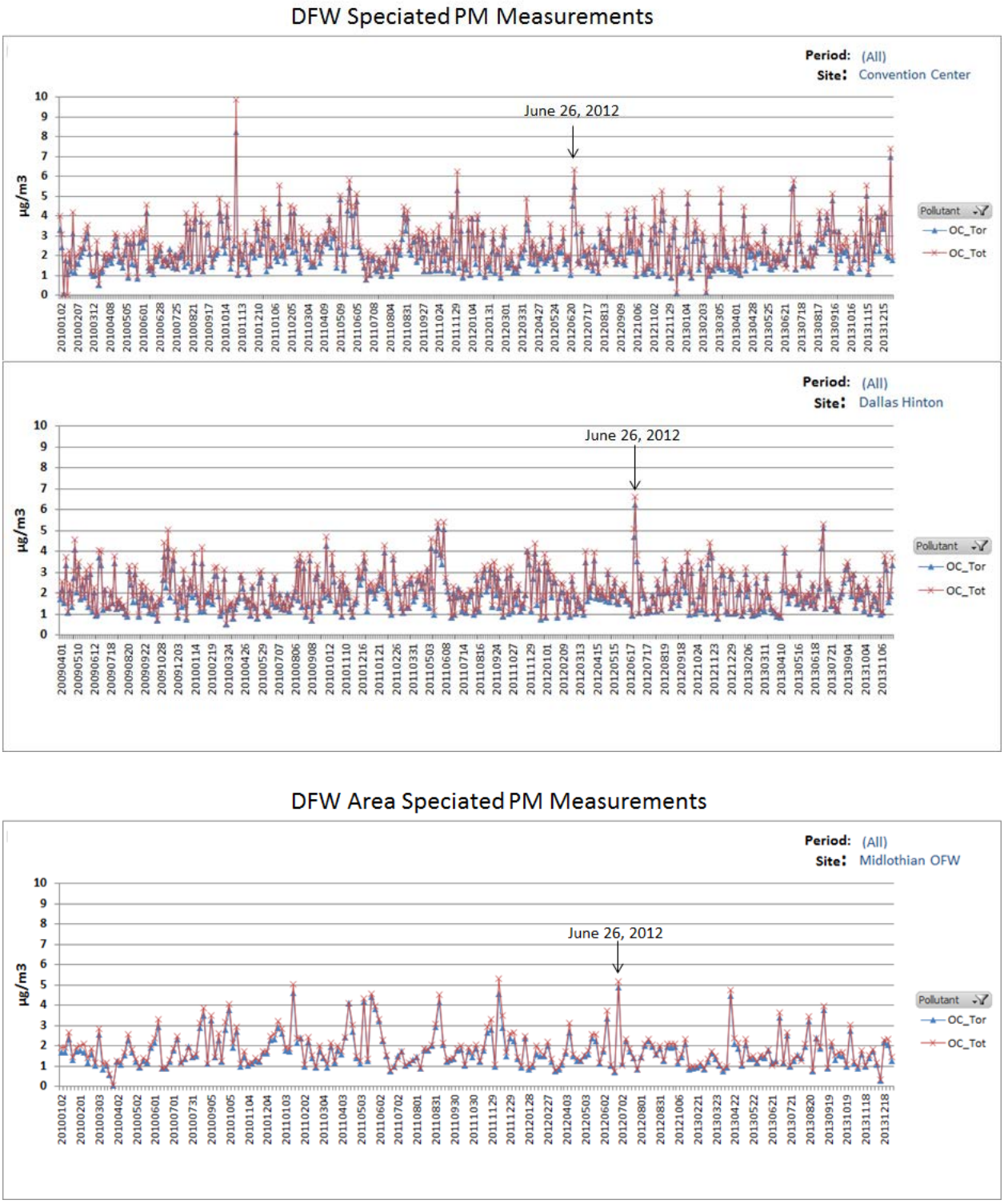

Figure 4-3. Organic carbon measurements for DFW area monitors. Entire data record through 2013 is shown for each monitor.

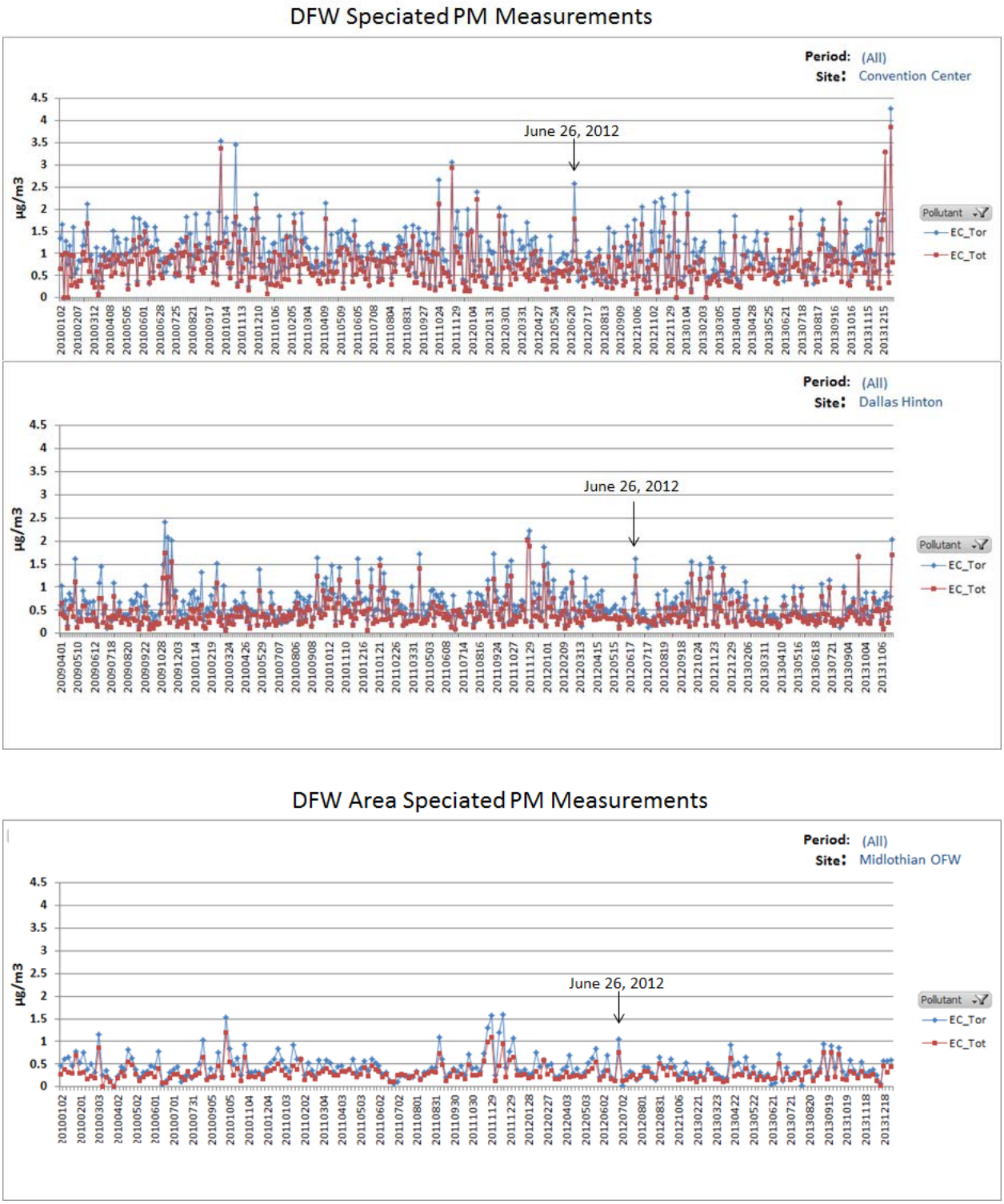

Figure 4-4. Elemental carbon measurements for DFW area monitors. Entire data record through 2013 is shown for each monitor.

5.0 COMPARISON OF 2012-2013 HIGH OZONE VALUES WITH HISTORICAL DATA

In the high ozone day analysis described in Section 3, we identified 2 days in 2012 (June 25, June 25) and 3 days in 2013 (July 3-4, September 25) for which fire emissions may have affected ozone at one or more monitors and for which further analysis is recommended. We then evaluated the possibility that each of these high ozone days may be considered an exceptional event based on whether the value of the MDA8 ozone on that day was among the highest values at that monitor since 2006. We chose 2006 as the start date for this analysis because this is the year of the TCEQ's oldest ozone modeling episode currently used in the development of the Texas State Implementation Plan for ozone. We assume that before this date, emissions would have been sufficiently different from 2012-2013 emissions that a comparison could not be made on an even basis because ozone would have been higher in earlier years due to higher local emissions and transported background ozone (e.g. Berlin et al., 2014).

For each monitor analyzed, we present time series of the MDA8 ozone for the entire calendar year for each year from 2006-2013 in Figure 5-1 through Figure 5-7. Days with unusually high ozone in 2012-2013 are indicated on the plots. The figures show a number of days during 2012-2013 when ozone was very high. For example, on September 25, 2013, the La Porte monitor had its highest value of MDA8 ozone during the entire 2006-2013 period (Figure 5-2).

Since all of the days recommended for additional evaluation in Table 3-3 had unusually high ozone based on inspection of Figure 5-1-Figure 5-7, we examined the frequency distribution of MDA8 at each monitor and determined the value of the 95th percentile MDA8 ozone for the 2006-2013 period (Figure 5-8-Figure 5-12) consistent with the Preamble to the Exceptional Event Rule[3] (40 CFR Parts 50 and 51) that notes that the EPA requires less supporting evidence for classifying events that exceed the 95th percentile of historical values as exceptional than for events that only exceed the 75th percentile. EPA guidance recommends evaluating ozone data by season when screening for exceptionally high values. However, the MDA8 time series for sites in the HGB and BPA areas (Figure 5-1-Figure 5-5) show significant sub-seasonal variation. Ozone is generally higher in summer than in winter, similar to the DFW area, but the sites near the Gulf of Mexico have July ozone values that are generally lower than those of June and August. This is due to the southerly flow off the Gulf of Mexico which tends to bring in clean marine air to the HGB and BPA areas in July. In the determination of whether a July event is exceptional, inclusion of data from June and/or August will compare the July event against days when the background ozone levels are generally higher than in July and will make the test more stringent for July days than in they were compared only against other July days. Therefore, only data from the month during which the high ozone event occurred were used in the frequency distribution charts. The vertical red line on each frequency distribution plot shows the 95th percentile value for each monitor for that month based on 2006-2013 data, and the dated black arrows shows the bin in which the MDA8 ozone lies for each day recommended for further evaluation. Bins are defined such that the value listed on the chart represents the upper bound of the bin so that the 90 ppb bin represents values from 90-81 ppb.

[3] http://www.epa.gov/ttn/caaa/t1/fr_notices/exeventfr.pdf

For the Seabrook and La Porte monitors, September 25, 2013 was recommended for further evaluation. Figure 5-8 shows that the MDA8 ozone value for September 25 exceeded the 95th percentile at both monitors, so that September 25 was an exceptionally high value of MDA8 ozone relative to other MDA8 values during the 2006-2013 period for both Seabrook and La Porte. Note that the La Porte monitor had several periods of missing data in September and has fewer observed values than the Seabrook monitor.

At Manvel Croix Park, July 4, 2013 was recommended for further analysis. On July 4, the MDA8 ozone at Manvel Croix exceeded the 95th percentile of the MDA8 during the period 2006-2013 (Figure 5-9). For the NW Harris County monitor, July 3, 2013 and June 27, 2012 were recommended for further analysis. Figure 5-10 shows that both of these days had MDA8 ozone that exceeded the 95th percentile.

Figure 5-11 shows the frequency distribution for the Denton and Grapevine monitors. For the both monitors, the two days recommended for further analysis are June 25, 2012 and June 27, 2012. For the Denton monitor, June 27 exceeds the 95th percentile value, while June 25 does not. Both June 25, 2012 and June 27, 2012 exceed the 95th percentile threshold for the Grapevine Fairway monitor. At the Sabine Pass monitor, July 4th was recommended for further evaluation, and the MDA8 ozone value for this day exceeds the 95th percentile value (Figure 5-12).

In summary, the following days pass the test of having exceptionally high MDA8 ozone relative to historical fluctuations: June 25, 2012 (Grapevine Fairway), June 27, 2012 (Grapevine Fairway and Denton), July 3, 2013 (NW Harris County), July 4, 2013 (Manvel Croix, Sabine Pass) and September 25, 2013 (Seabrook and La Porte).

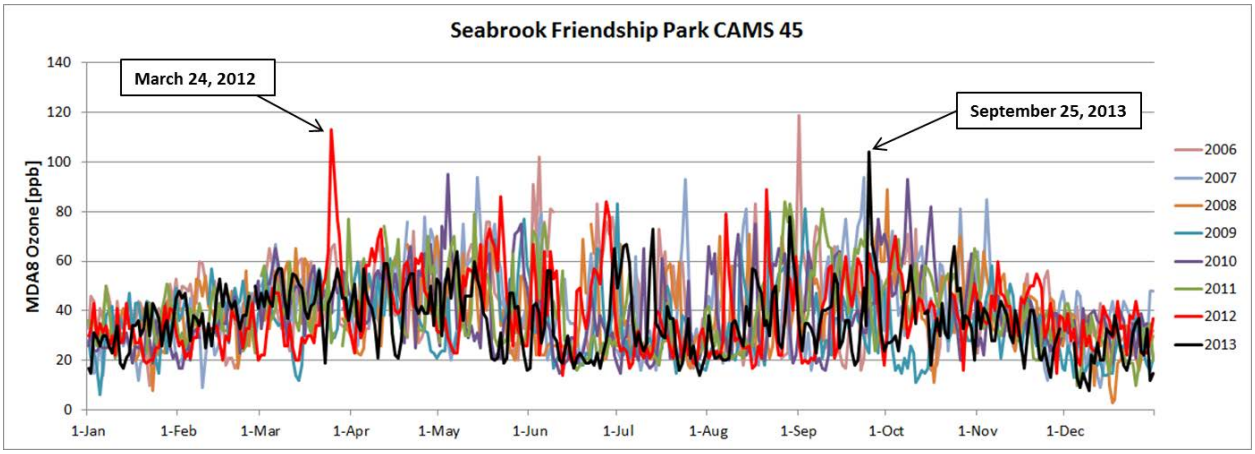

Figure 5-1. Seabrook daily maximum 8-hour ozone for each year from 2006-2013.

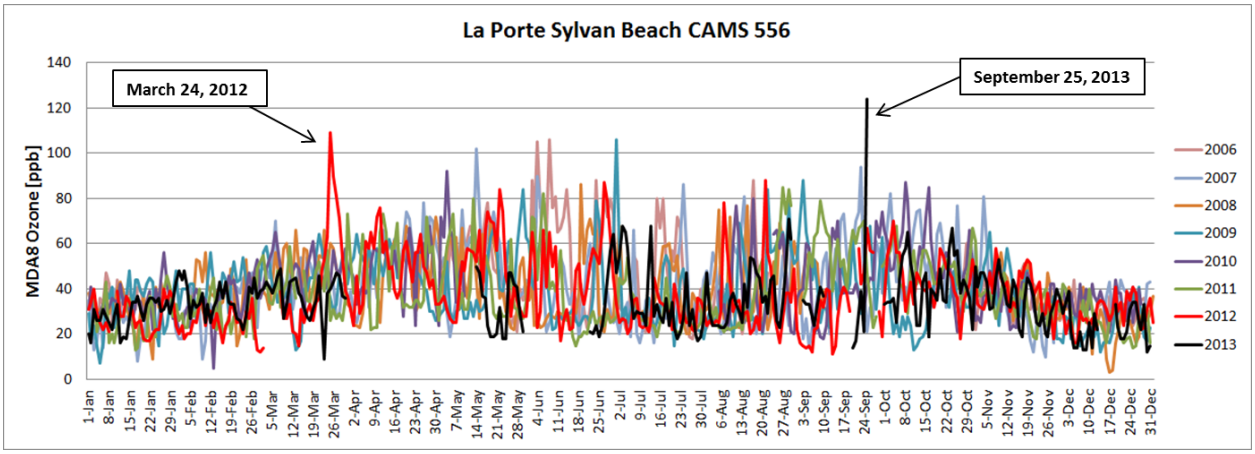

Figure 5-2. La Porte daily maximum 8-hour ozone for each year from 2006-2013.

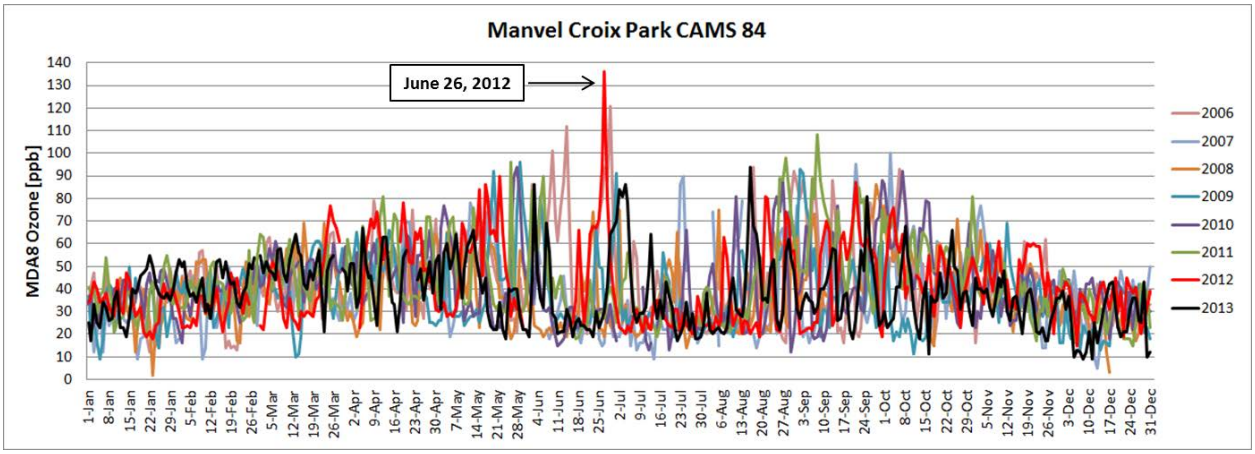

Figure 5-3. Manvel Croix daily maximum 8-hour ozone for each year from 2006-2013.

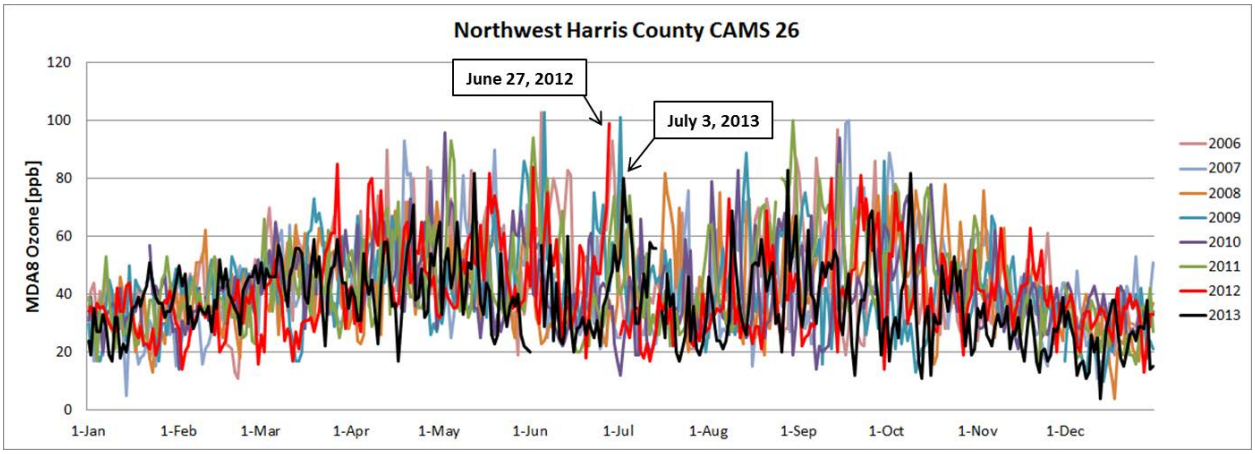

Figure 5-4. Northwest Harris County daily maximum 8-hour ozone for each year from 2006-2013.

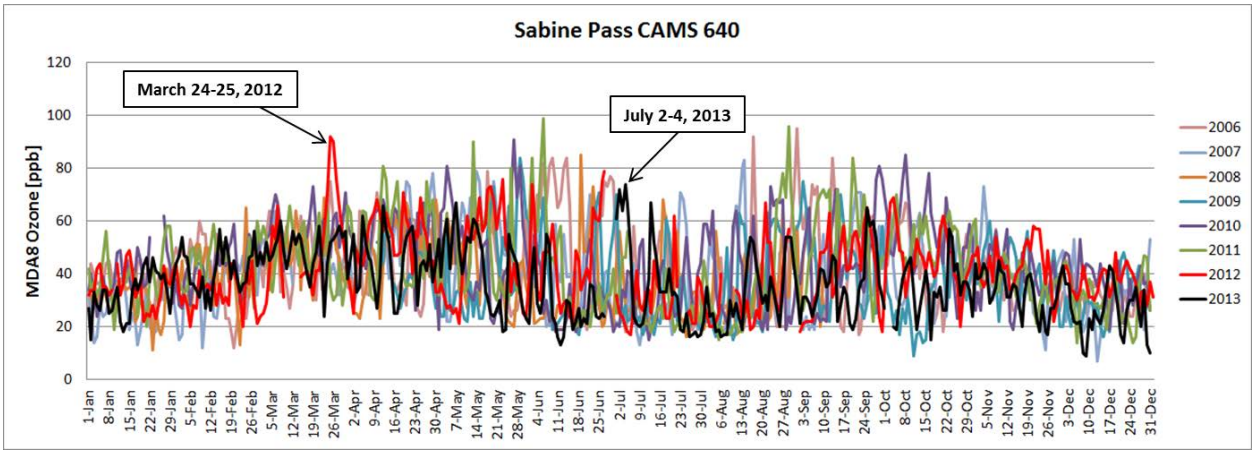

Figure 5-5. Sabine Pass daily maximum 8-hour ozone for each year from 2006-2013.

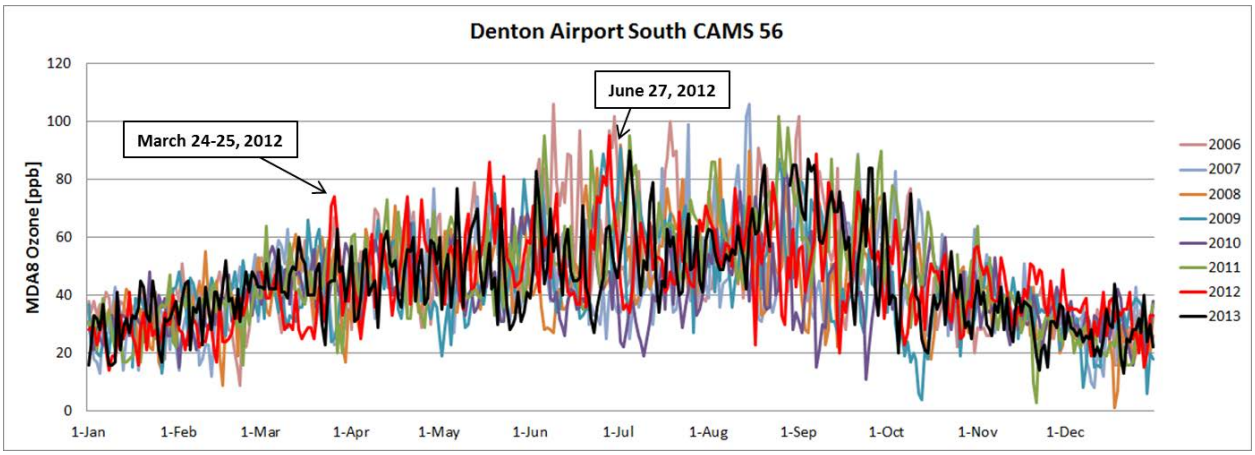

Figure 5-6. Denton Airport South daily maximum 8-hour ozone for each year from 2006-2013.

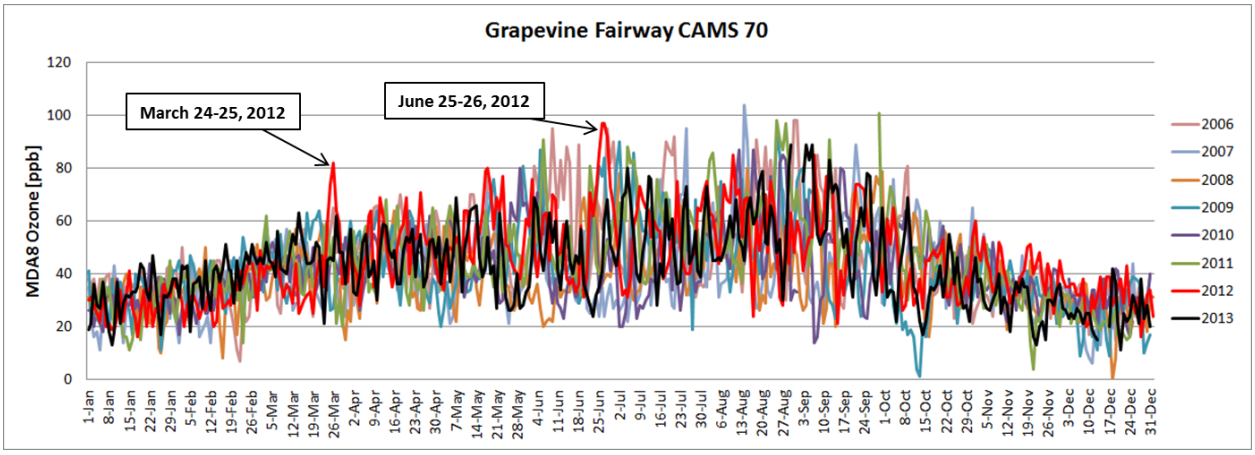

Figure 5-7. Grapevine Fairway daily maximum 8-hour ozone for each year from 2006-2013.

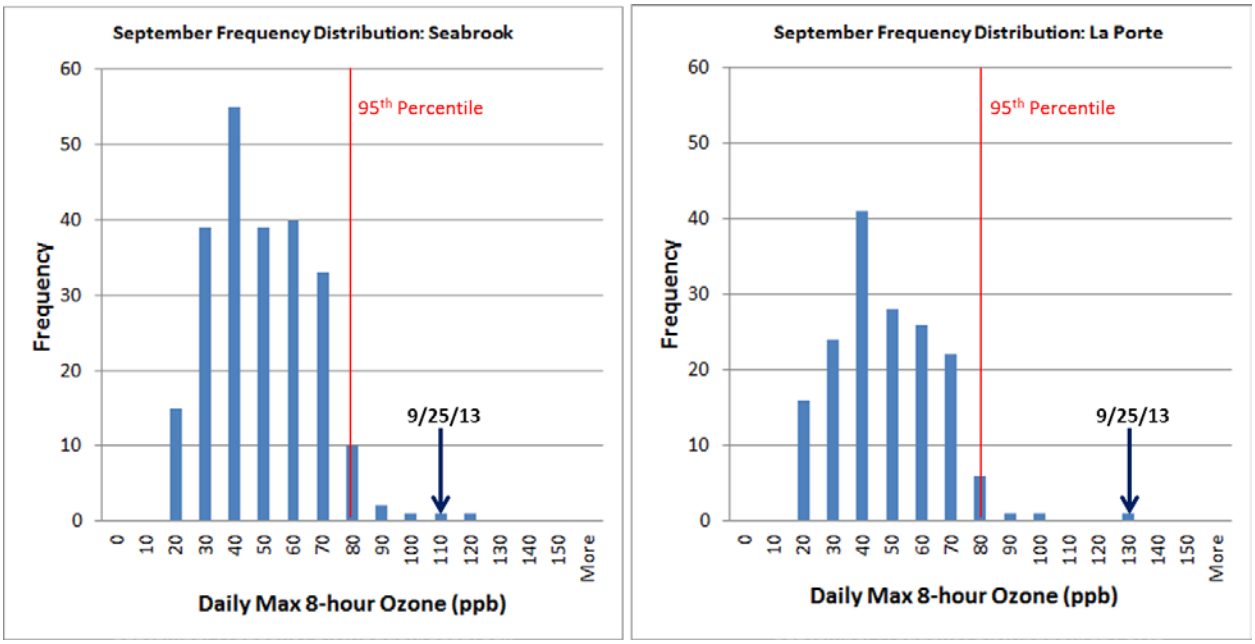

Figure 5-8. Frequency distribution for September MDA8 for Seabrook and La Porte monitors for the 2006-2013 ozone seasons. Vertical red line shows the 95th percentile value of the MDA8 for this period.

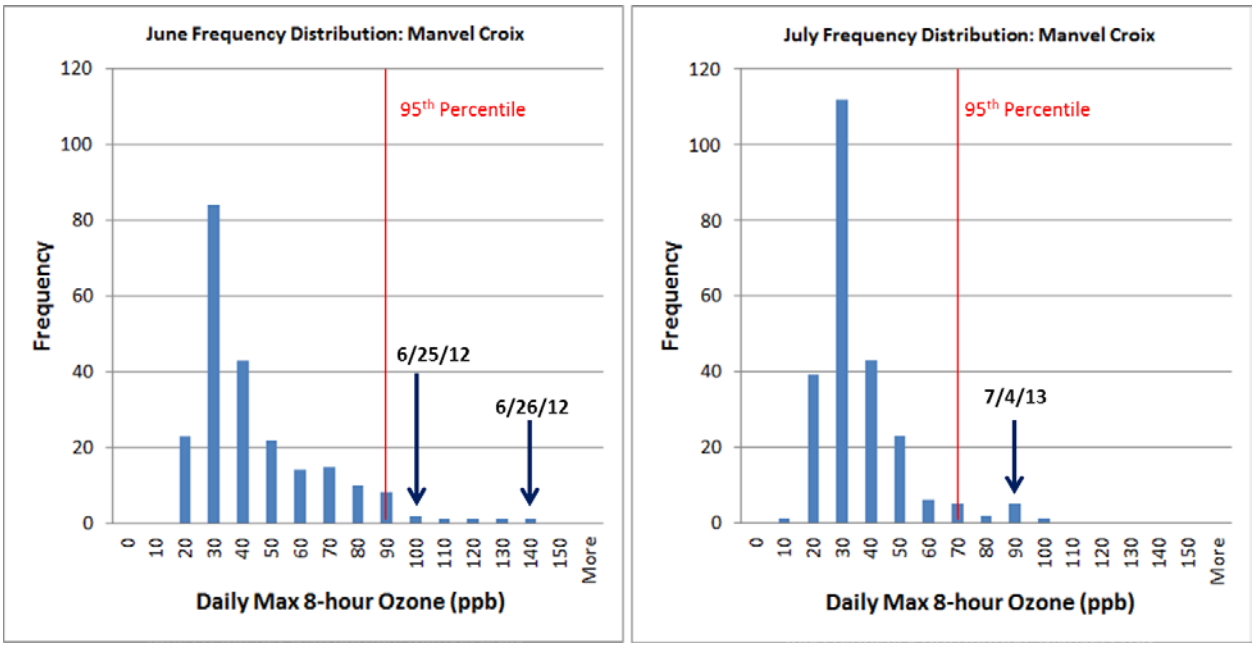

Figure 5-9. Frequency distribution for June (left) and July (right) MDA8 for the Manvel Croix monitors for the 2006-2013 ozone seasons. Vertical red line shows the 95th percentile value of the MDA8 for this period.

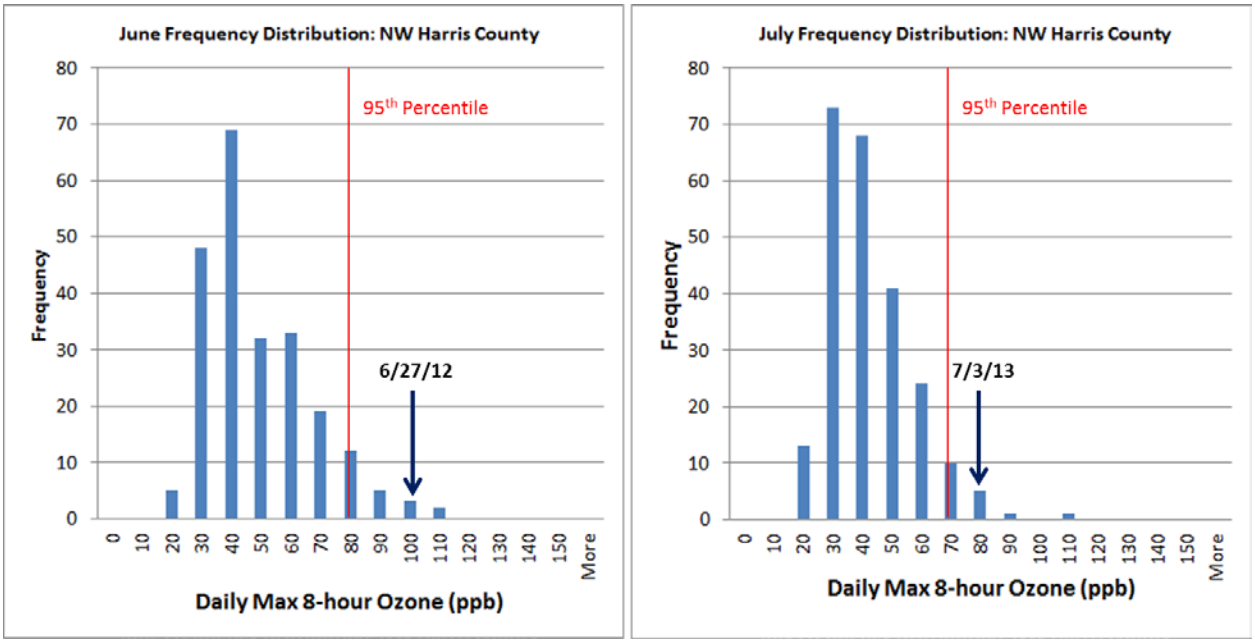

Figure 5-10. Frequency distribution for June (left) and July (right) MDA8 for the NW Harris County monitor for the 2006-2013 ozone seasons. Vertical red line shows the 95th percentile value of the MDA8 for this period.

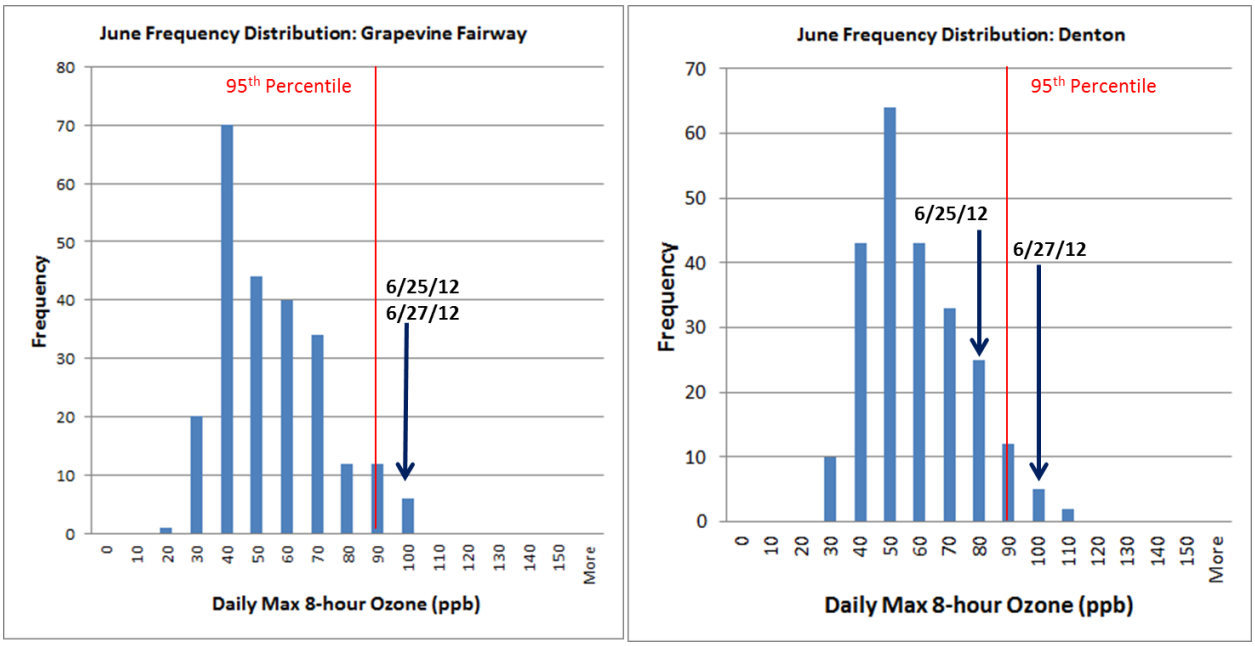

Figure 5-11. June frequency distribution for MDA8 ozone for Denton Airport South and Grapevine Fairway monitors for the 2006-2013 ozone seasons. Vertical red line shows the 95th percentile value of the MDA8 for this period.

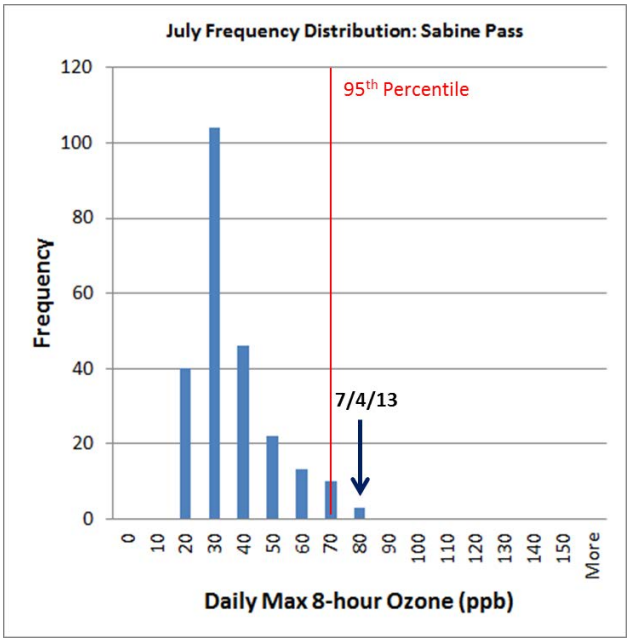

Figure 5-12. Frequency distribution for MDA8 for the Sabine Pass monitor for the 2006-2013 ozone seasons. Vertical red line shows the 95th percentile value of the MDA8 for this period.

6.0 PHOTOCHEMICAL MODELING

The following days met the first three EER criteria shown on p. 30: June 25, 2012 (Grapevine Fairway), June 27, 2012 (Grapevine Fairway and Denton), July 3, 2013 (NW Harris County), July 4, 2013 (Manvel Croix, Sabine Pass) and September 25, 2013 (Seabrook and La Porte). To assess whether these days pass the "but-for" criterion, we evaluated the contribution of fire emissions to the MDA8 for each monitor and day using a photochemical grid model. The Comprehensive Air Quality Model with Extensions (CAMx, ENVIRON, 2014a) photochemical grid model was used to determine whether an exceedance or violation would have occurred at the monitors of interest without the ozone impacts of the fire emissions. We modeled the episode June 24-27, 2012 and two 2013 episodes: July 3-4 and September 25. In this section, we describe the configuration of the model for the 2012 and 2013 episodes, the evaluation of the model and the ozone impacts of the fire emissions on MDA8 at the monitors of interest.

6.1 2012 Ozone Model

6.1.1 CAMx Model Configuration

An ozone model for the period June 24-27, 2012 was developed using modeling inputs provided by the TCEQ. Although only June 25 and 27 are on the list of high ozone days in Table 3-3, we include June 24-27 because modeling the full period allows us to compare model predictions against the results of the high ozone day analysis for days and monitors determined not to show a clear, causal connection between high ozone and fire emissions and requires little additional effort.

The modeling grid system is shown in Figure 6-1 and is comprised of nested 36/12/4 km modeling domains with a 4 km grid focused on East Texas. A 10-day spinup period prior to June 24 was modeled in addition to the episode of interest. The TCEQ provided ozone season day anthropogenic emissions and day-specific biogenic emissions as well as model-ready meteorological inputs developed using the Weather Research and Forecasting model (WRF; Skamarock et al;., 2005). The TCEQ has evaluated the WRF modeling, so no performance evaluation of the WRF meteorological inputs was done as part of this study.

To evaluate the impact of fire emissions on theMDA8 at monitors in Table 3-3, two CAMx runs were made. The first CAMx run contains the FINN fire emissions and the second run is identical to the first except that it has no fire emissions. By subtracting the ozone predicted from the two runs, we obtain the ozone impact of the fire emissions.

6.1.2 Processing of FINN Fire Emissions for Use in CAMx

FINN fire emissions data for both episodes were extracted for the full extent of the TCEQ's 36/12/4 km nested grid system. Fire locations were mapped from latitude/longitude coordinates to the RPO Lambert Conformal Projection. Any fire location within 5 km of another fire was assumed to be part of the same fire event. A fire event is therefore defined as a cluster of points meeting this criterion. The fire emissions for the two episodes were then reformatted into the Emissions Processing System version 3 (EPS3) input format. The daily fire emissions

Figure 6-1. 36/12/4 km CAMx nested modeling grids for the ozone modeling of June 2012. 36 km grid is outlined in black. The 12 km is grid outlined in green, and the 4 km grid is outlined in blue. TCEQ figure from http://www.tceq.texas.gov/airquality/airmod/rider8/modeling/domain.

were processed using an updated version of the Emissions Processor System (EPS3) version 3.20. Each fire event was treated as a point source. A plume profile was calculated for each point in order to distribute the emissions vertically using the methodology outlined in the WRAP 2002 Phase II report (WRAP, 2005). In the WRAP algorithm, fires are assigned to one of five fire size classes. Three plume parameters – the top and bottom of the plume and the fraction of emissions in layer 1 – are computed from tables of buoyancy efficiencies and maximum top and bottom plume heights, which are functions of the fire size class and/or hour of the day.

The diurnal profiles, parameters, and equations needed to compute the plume attributes were obtained from the WRAP report and are incorporated into the PSTFIR routine in EPS3. The only variable not directly available from the NCAR dataset and required by EPS3 is the fire size. In the WRAP report, fire sizes were classed in terms of virtual acres, which are estimated using the equation below:

$$Acreage_{virtual} = Acreage_{actual} * \sqrt{FuelLoading / Normalizer}$$

WRAP normalized wildfires to 13.8 tons per acre (tpa) and prescribed fires to 5.0 tpa. The five fire classes are shown in Table 6-1. Because it is not possible to determine from satellite data

whether a particular fire is a wildfire or a prescribed burn, all points were conservatively treated as wildfires. The virtual area for each fire event was set to the sum of the virtual areas from the cluster of points defining the fire event.

Table 6-1. Fire Classes used by WRAP.

Fire Class	MinVirtual Area [acres]	Max Virtual Area [acres]
1	>= 0	<10
2	10	100
3	100	1000
4	1000	5000
5	5000	

In order to distribute the emissions in the vertical , a fraction of the hourly emissions is assigned to the lowest layer; the remainder is distributed among multiple point sources at the same (x,y) location with each point assigned to a different CAMx layer between the plume bottom and plume top, weighted by the thickness of the layer. The fraction in layer 1 and the plume bottom and top are dependent on the hour of the day and size of the fire. All fire emissions are output into a day-specific point source file and flagged with a negative stack height so that no plume rise calculation is performed in CAMx.

Each emissions record includes the FIPS code, SCC, optional IDs, date, location, virtual area, and emissions rate for each species. The NCAR data lists country and state for each fire, but not its county. The FIPS codes within the US consisted of the state FIPS followed by "000". Fires outside the US used a two letter country identifier followed by the state or province number, if available. The SCC was set to 2810001000 (wildfires) for all records. Temporal allocation of the fire emissions was performed by applying a single diurnal profile to all fires. The profile, shown in Figure 6-2, allocates the daily emissions total across the 24 hour day such that emissions from fires are largest in the afternoon and lowest at night.

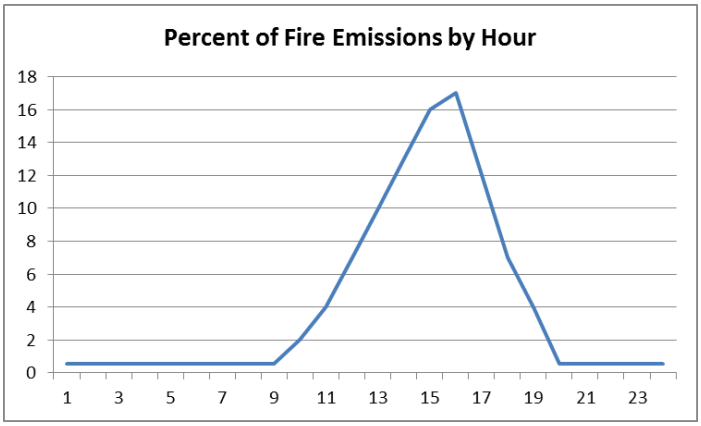

Figure 6-2. Diurnal Profile Used for Temporal Allocation of Fire Emissions.

Emissions plots were generated and reviewed in order to verify the fire emissions processing. MODIS fire location data were used to confirm that the fires had been correctly located within the modeling domain.

6.1.3 CAMx Model Performance Evaluation for Surface Layer Ozone

The CAMx model surface layer ozone for both runs was evaluated against 1-hour average ozone measured at TCEQ CAMS sites during the June 24-27, 2012 episode days (Figure 6-3 through Figure 6-9). We evaluated the model at the sites that are listed in Table 1-3. At the Denton and Grapevine monitors in the DFW area, the model captures the peak ozone values reasonably well on June 24 and June 27. CAMx overestimates peak ozone at both monitors on June 25 and on June 26th as well at the Denton monitor. The magnitude of the peak is well-simulated at Grapevine on June 26, but the morning rise in ozone occurs too early in the model and the modeled peak leads the observed peak in time by an hour. For both monitors, the model greatly overestimates the magnitude of the nighttime ozone minimum on June 25 and June 26, but tracks the observed ozone somewhat better on the night of June 27. The ozone time series for the runs with and without fire emissions are very similar, with the largest differences between them coming in the early morning hours of June 27.

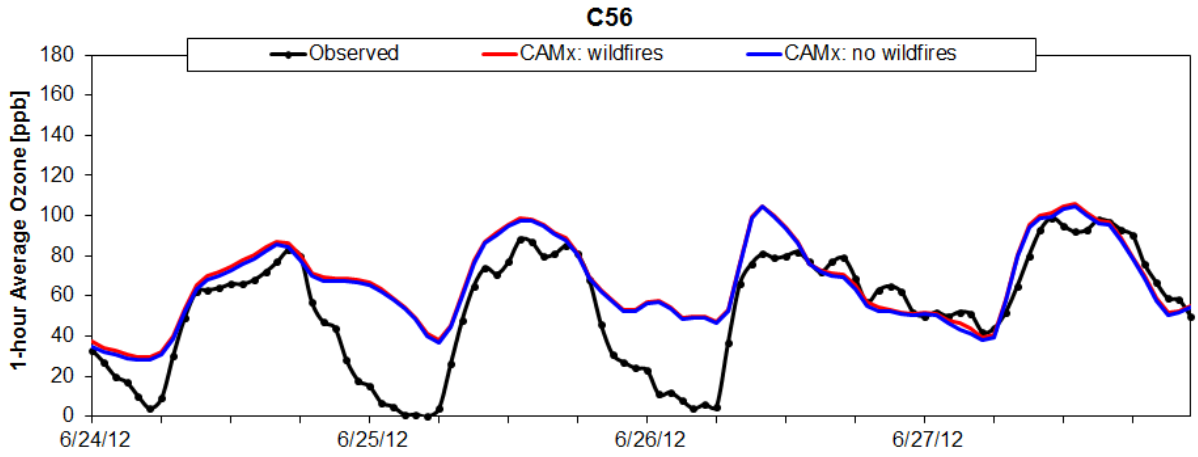

Figure 6-3. Denton observed 1-hour ozone (black) versus modeled 1-hour average surface layer ozone for the CAMx run with fire emissions (red) and the CAMx run with no fire emissions (blue).

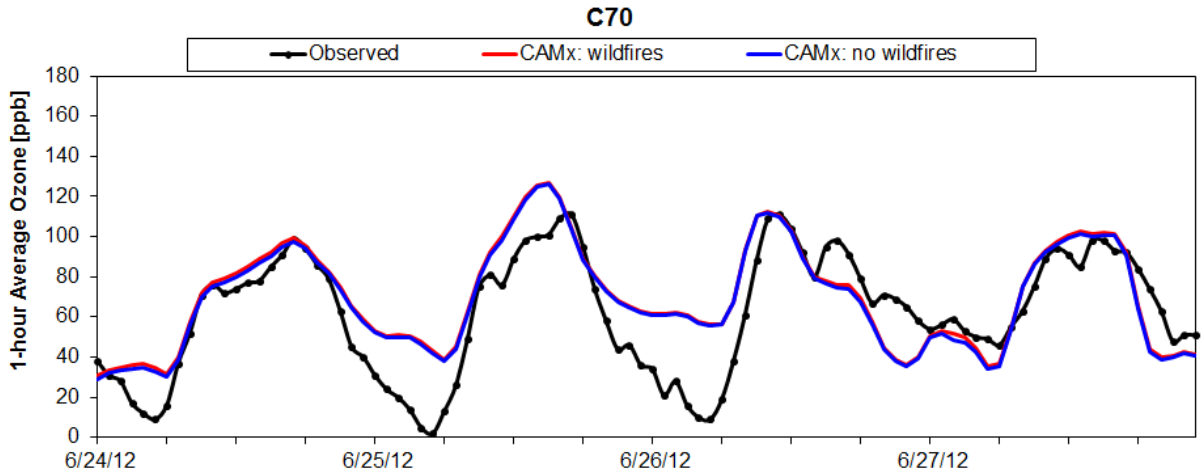

Figure 6-4. Grapevine observed 1-hour ozone (black) versus modeled 1-hour average surface layer ozone for the CAMx run with fire emissions (red) and the CAMx run with no fire emissions (blue).

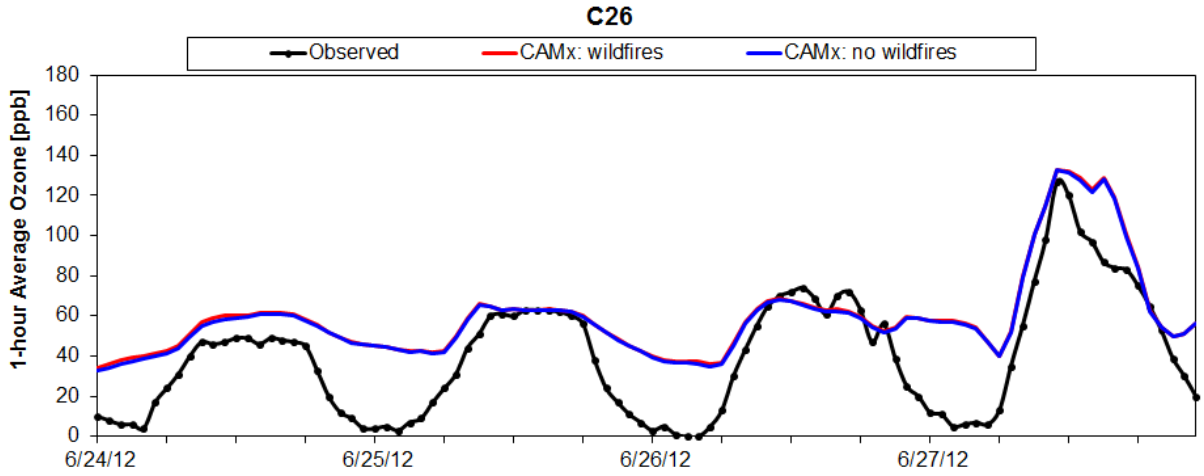

Figure 6-5. NW Harris County observed 1-hour ozone (black) versus modeled 1-hour average surface layer ozone for the CAMx run with fire emissions (red) and the CAMx run with no fire emissions (blue).

As for the Denton and Grapevine monitors, nighttime ozone is overestimated at the NW Harris County monitor (Figure 6-5).

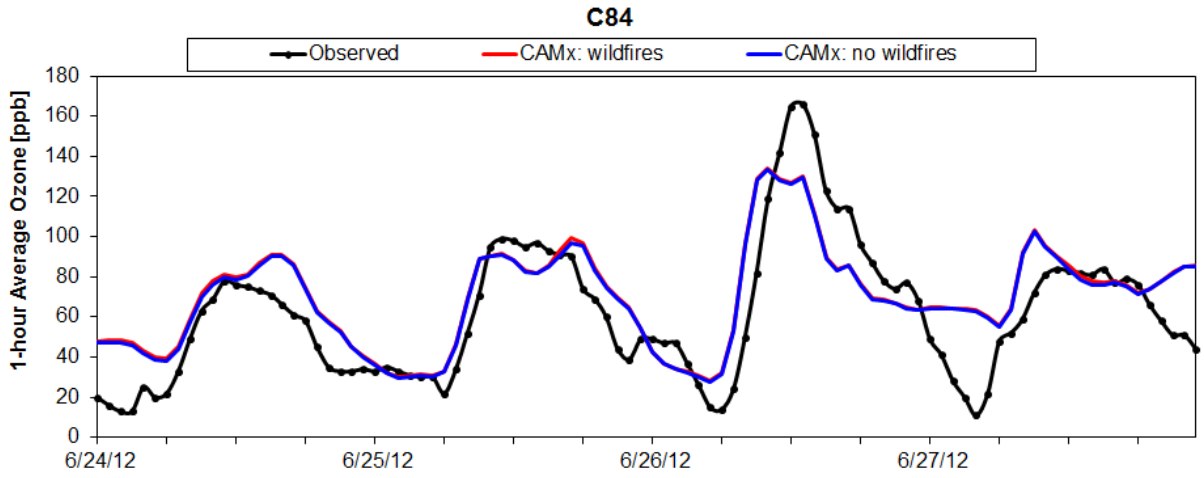

Figure 6-6. Manvel Croix observed 1-hour ozone (black) versus modeled 1-hour average surface layer ozone for the CAMx run with fire emissions (red) and the CAMx run with no fire emissions (blue).

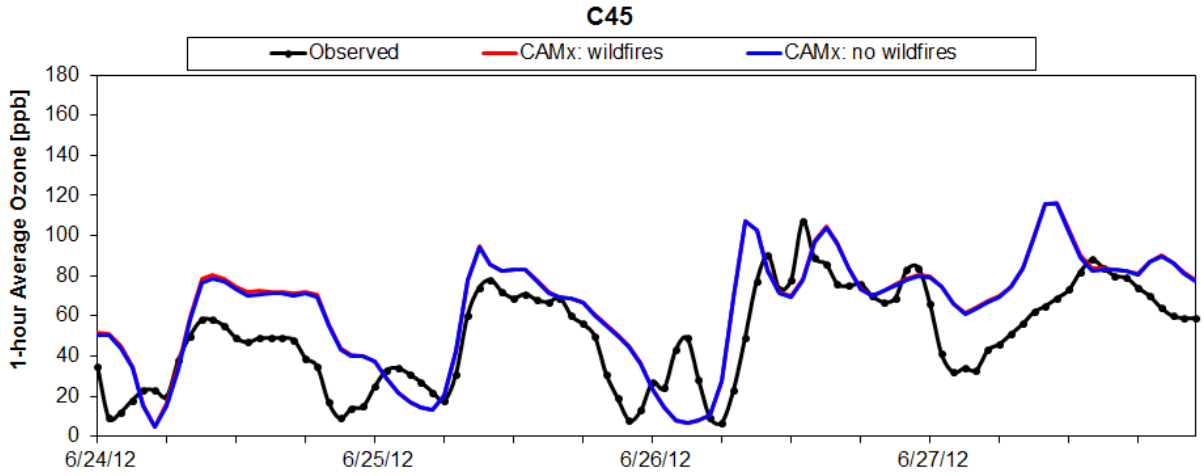

Figure 6-7. Seabrook observed 1-hour ozone (black) versus modeled 1-hour average surface layer ozone for the CAMx run with fire emissions (red) and the CAMx run with no fire emissions (blue).

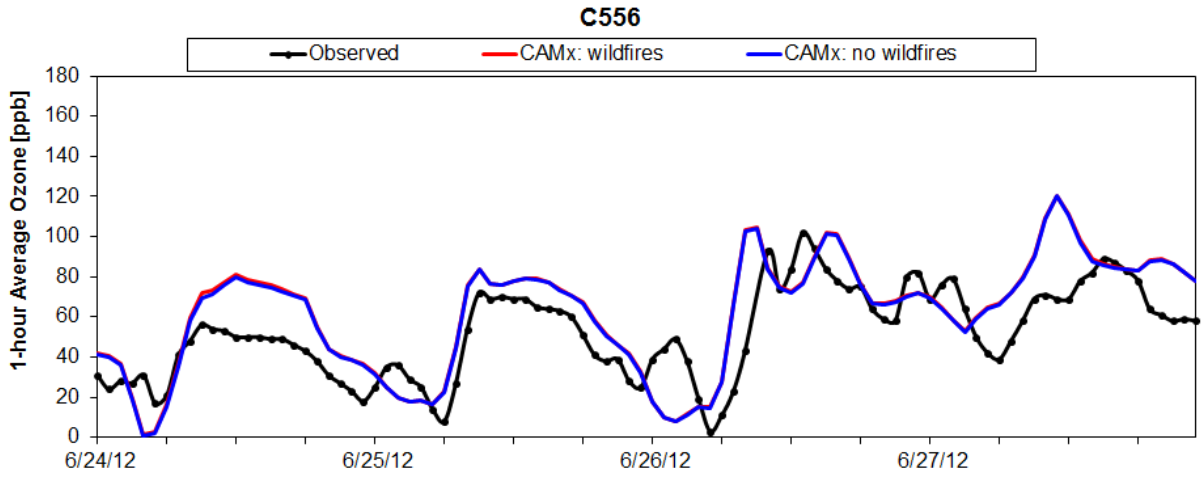

Figure 6-8. La Porte observed 1-hour ozone (black) versus modeled 1-hour average surface layer ozone for the CAMx run with fire emissions (red) and the CAMx run with no fire emissions (blue).

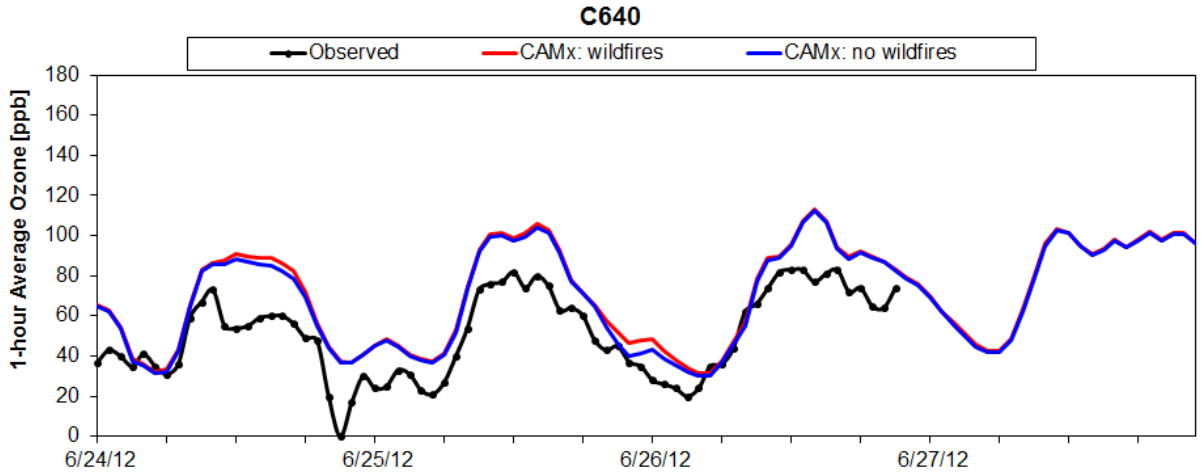

Figure 6-9. Sabine Pass observed 1-hour ozone (black) versus modeled 1-hour average surface layer ozone for the CAMx run with fire emissions (red) and the CAMx run with no fire emissions (blue).

6.1.4 Ozone Impacts from Fire Emissions: June 24-27, 2012

Figure 6-10 shows the MDA8 ozone impacts for July 24, 2012 within the 4 km modeling grid. The MDA8 ozone impacts were obtained by taking the difference between the CAMx runs with and without fire emissions. On June 24, impacts to MDA8 ozone are less than 2 ppb at the Grapevine and Denton monitors and the HGB area monitors. The location of fires with relatively large NOx emissions is indicated by blue shading, where the presence of NOx emissions from the fire titrates ozone. For example, there is a fire in Tyler County to the north of the HGB and BPA areas. Downwind of the region of suppressed ozone caused by the fire

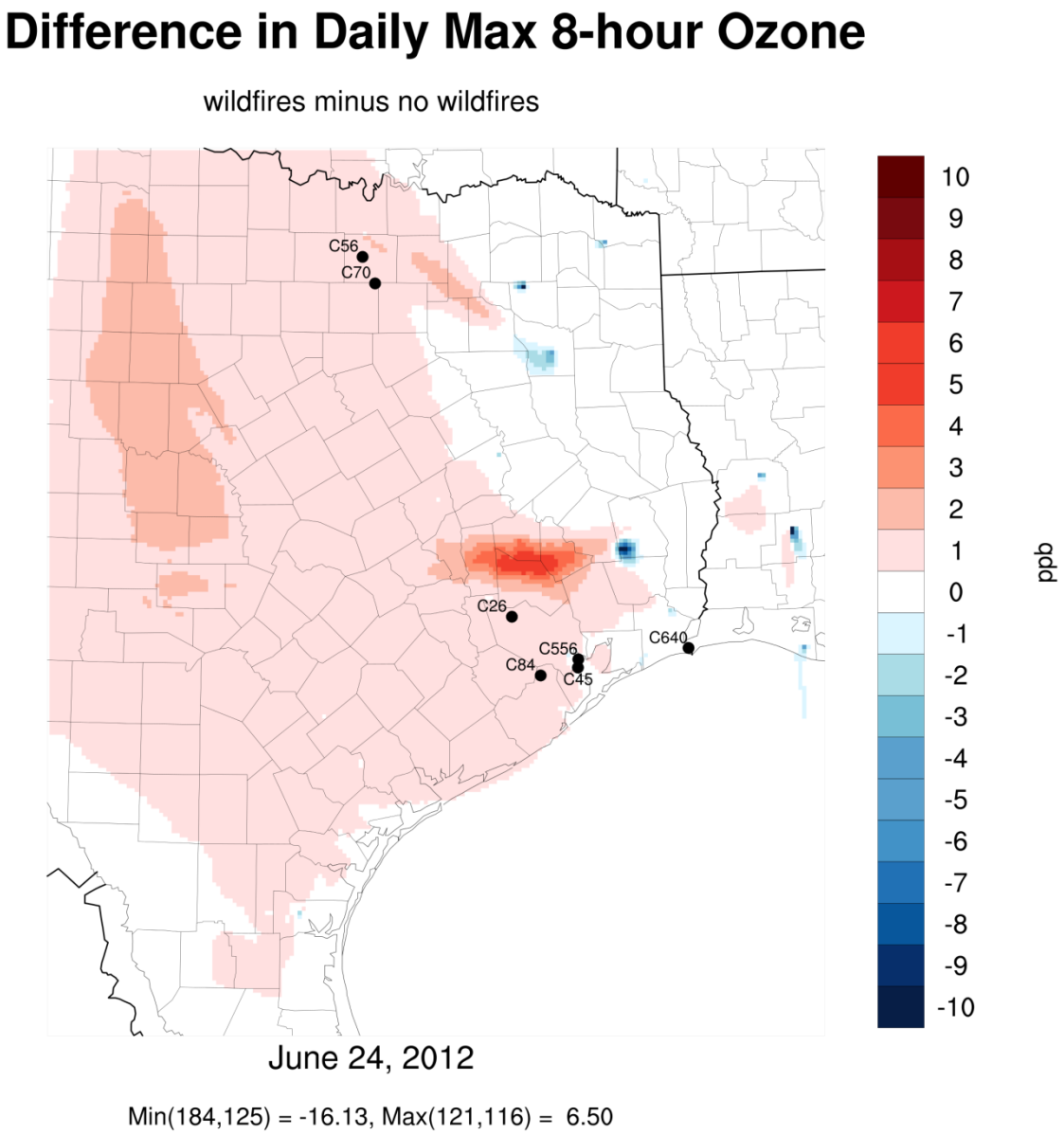

Figure 6-10. June 24, 2012 difference in MDA8 between CAMx run with fire emissions and CAMx run with no fire emissions.

NOx emissions is a plume of enhanced ozone. The plume passes to the north of the NW Harris County monitor (C26). Fire emissions contributed less than 1 ppb to the MDA8 at the Sabine Pass monitor on June 24.

Figure 6-11 shows an impact of <1 ppb to the MDA8 for the Manvel Croix monitor (C84) in the HGB area. Impacts to the MDA8 are ≤ 2 ppb at both the Grapevine Fairway (C70) (and Denton Airport South (C56) monitors. East of the DFW area, there is a plume emanating from a fire in Wood County (the fire location is indicated by an area where ozone is suppressed due to the

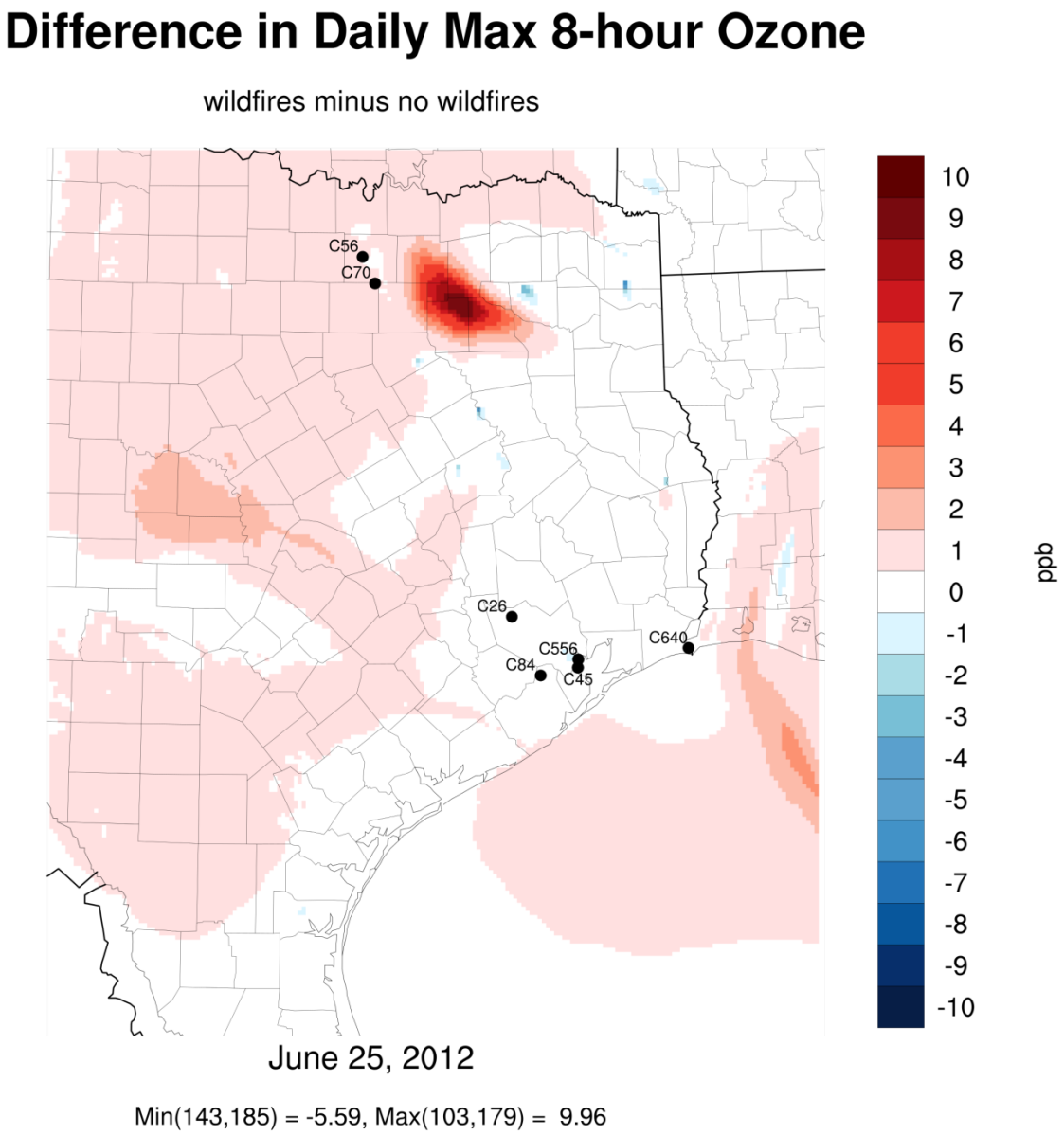

Figure 6-11. June 25, 2012 difference in MDA8 between CAMx run with fire emissions and CAMx run with no fire emissions.

fire). The peak impacts from the fire are 10 ppb and occur ~100 km from the C56 and C70 monitors.

On June 26, fire impacts on the MDA8 are <1 ppb for all DFW and HGB monitors (Figure 6-12). Fire impacts are larger at Sabine Pass (< 3 ppb), and there is an area of enhanced ozone just offshore of the BPA area.

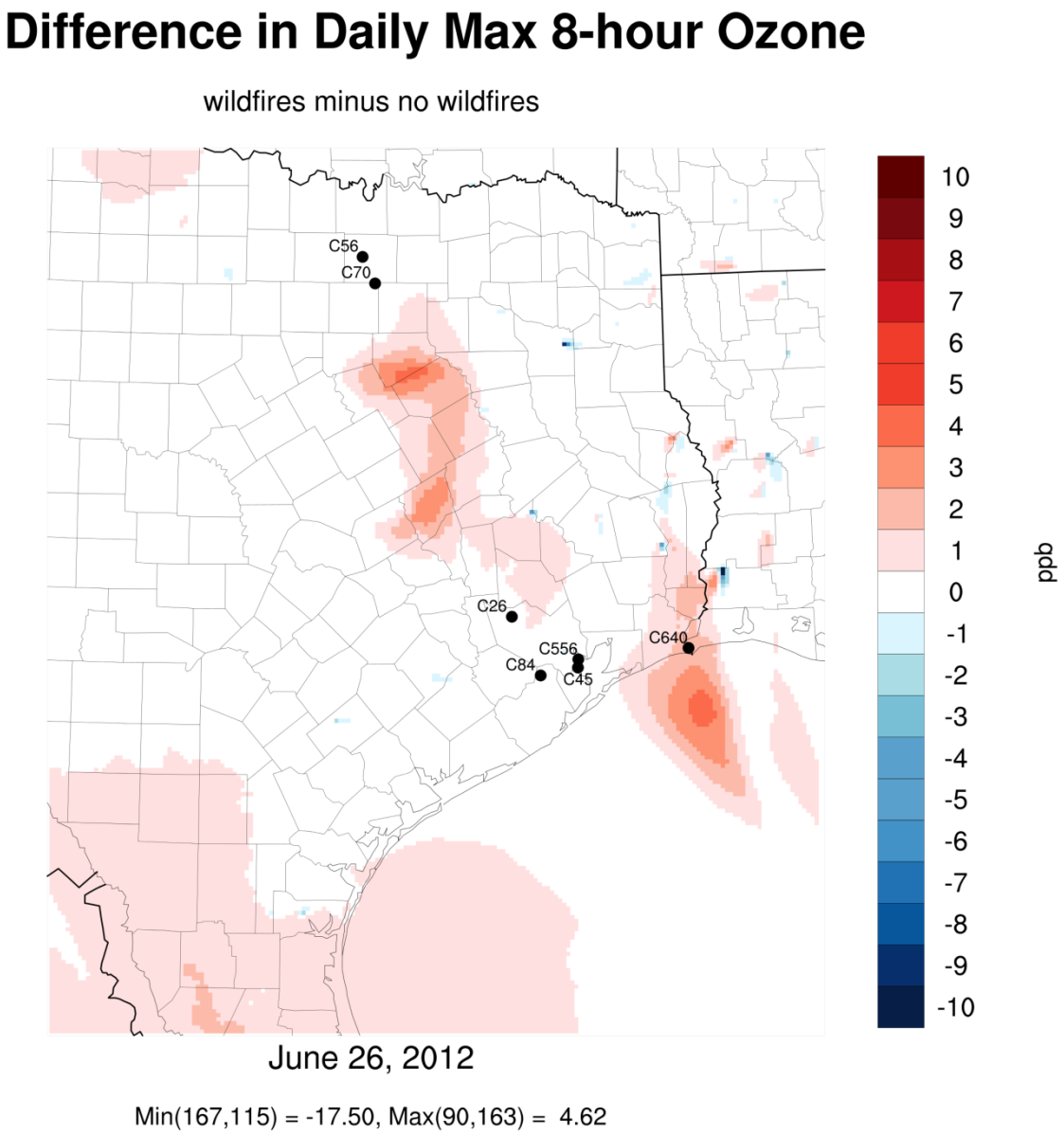

Figure 6-12. June 26, 2012 difference in MDA8 between CAMx run with fire emissions and CAMx run with no fire emissions.

On June 27 (Figure 6-13), fire emissions have an impact on the MDA8 that is ≤ 2 ppb at Grapevine Fairway and Denton Airport South. In the HGB area, the effect of fire emissions is smaller than in the DFW area, with impacts on the MDA8 that are ≤ 1 ppb at the NW Harris County. As on June 26, there is an area offshore of the BPA area where ozone is enhanced due to fire emissions.

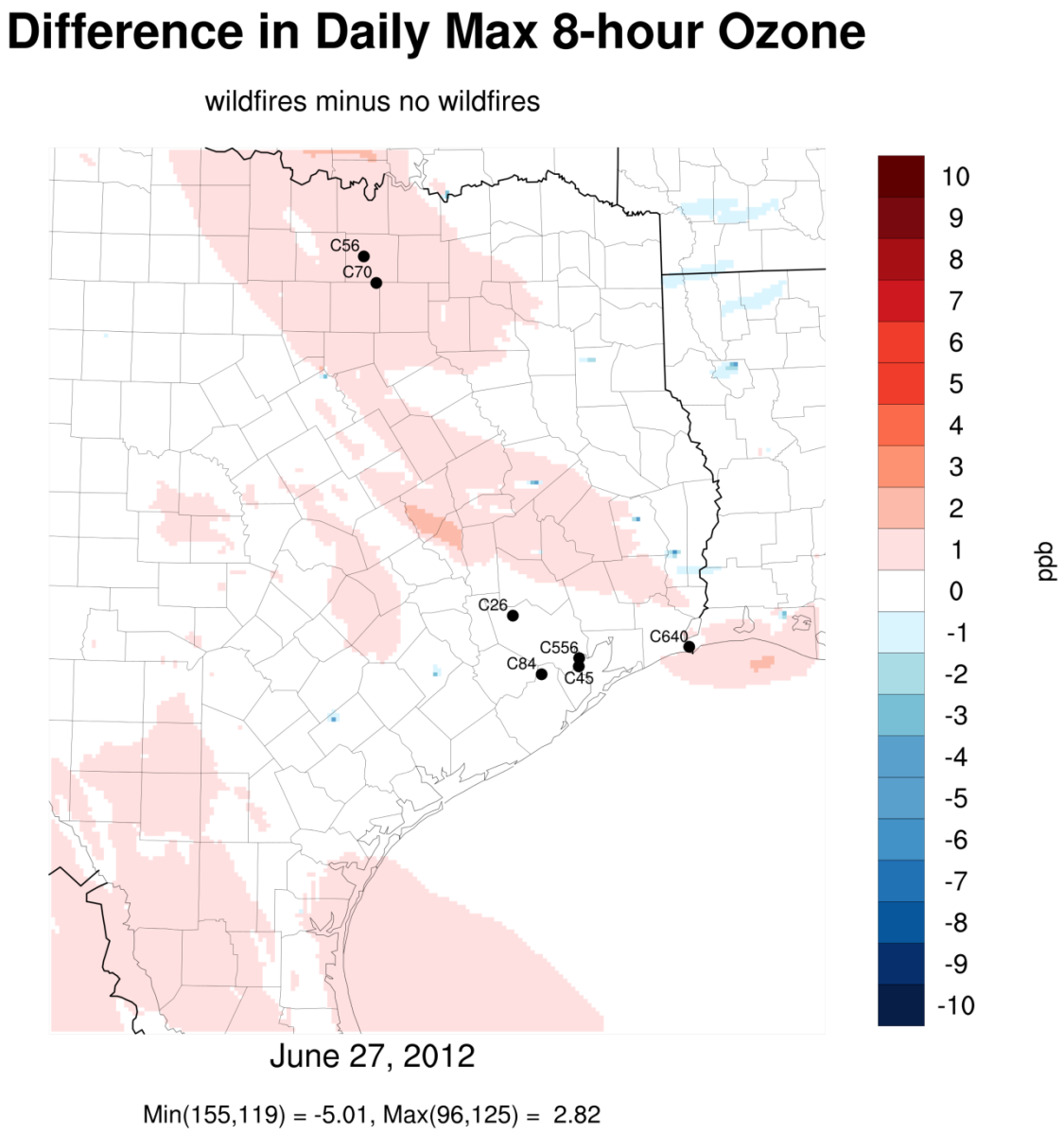

Figure 6-13. June 27, 2012 difference in MDA8 between CAMx run with fire emissions and CAMx run with no fire emissions.

6.2 2013 Ozone Model

The TCEQ Near Real Time Ozone Model platform (Johnson et al., 2013) was used to model the two 2013 episodes. To model the July and September, 2013 episodes, ENVIRON developed meteorological inputs for CAMx by running the WRF model in hindcast mode and used an emission inventory for a typical 2012 ozone season day for 2012 developed by the TCEQ. This 2012 typical day emission inventory was augmented by the TCEQ with 2013 oil and gas emissions for the State of Texas. The FINN fire emission inventory for the 2013 episodes was

processed in the same manner as for the 2012 episode. The 36/12/4 km nested CAMx model grids are shown in blue in Figure 6-14.

6.2.1 WRF Model Configuration

The WRF model was run for the two 2013 episodes in a configuration developed by ENVIRON for the TCEQ's Near-Real-Time ozone model. A summary of the WRF model configuration is provided in Table 6-2. The WRF modeling domains are shown in red in Figure 6-14. The 36 km RPO grid is used for the outermost modeling grid. The 12 km domain was developed for use in AQRP Project 14-016 and is larger than the TCEQ's 12 km modeling grid in order to encompass 2013 NOAA and NCAR aircraft flight paths The 4 km grid is focused on Houston, because the two 2013 episodes modeled here have high ozone days in the HGB and BPA areas only.

Table 6-2. Summary of WRF configuration.

WRF version	3.6
Horizontal Resolution	36/12/4 km
Microphysics	WSM6
Longwave Radiation	RRTMG
Shortwave Radiation	RRTMG
Surface Layer Physics	MM5 similarity
LSM	Noah
PBL scheme	Yonsei University (YSU)
Cumulus parameterization	36/12 km: Kain-Fritsch 4km: none
Boundary and Initial Conditions Data Source	12 km NAM analysis
Analysis Nudging Coefficients (s^{-1})	36/12 km: 3-D 4 km: None
Winds	$3x10^{-4}$
Temperature	$3x10^{-4}$ (above BL only)
Water Vapor Mixing Ratio	$3x10^{-4}$ (above BL only)
Observation Nudging Coefficients (s^{-1})	36/12/4 km: None
Winds	None
Temperature	None
Water Vapor Mixing Ratio	None
Miscellaneous Notes	Using KF-RRTMG interaction which feeds back subgrid cloud information to radiation scheme (36/12 km only)

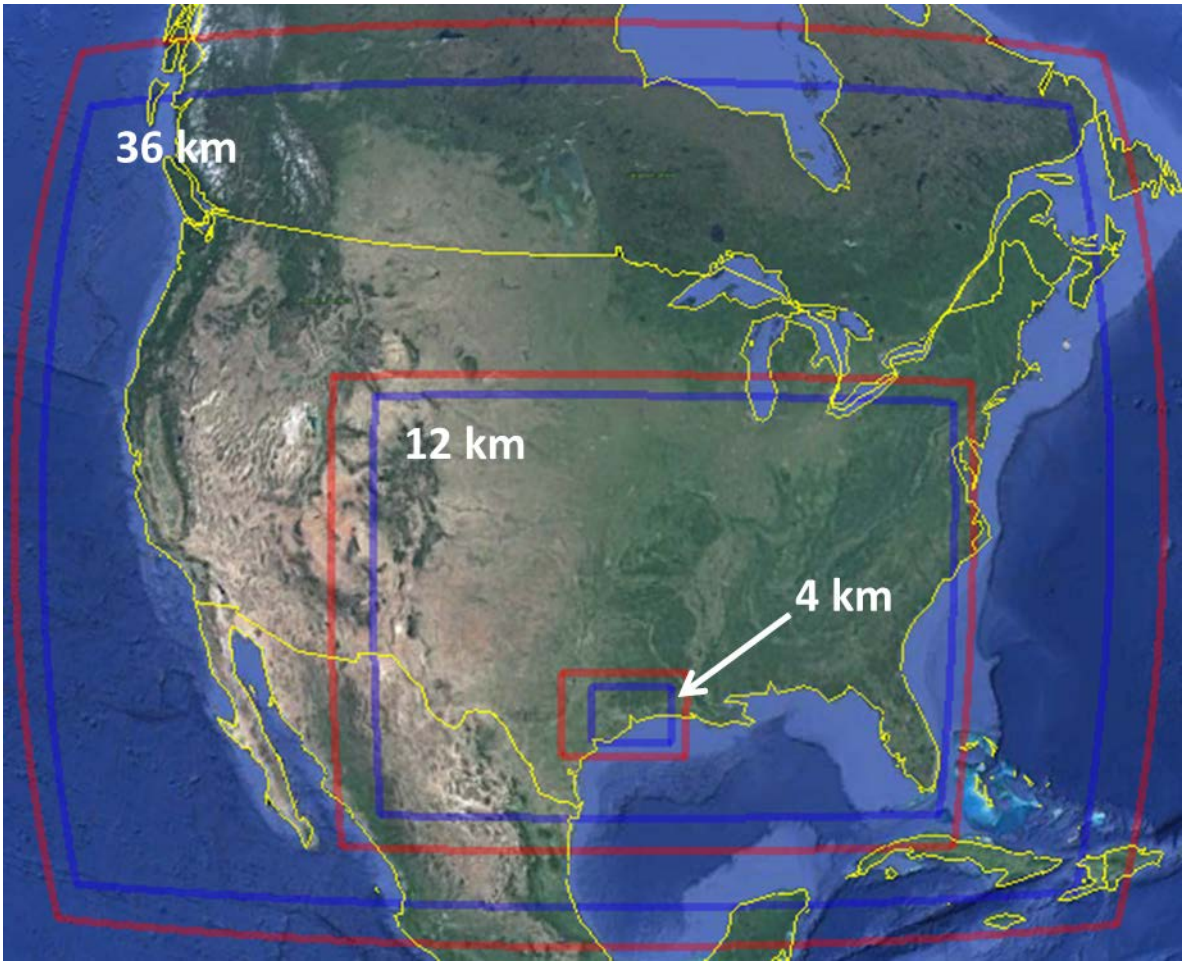

Figure 6-14. WRF (red) and CAMx (blue) 36/12/4 km modeling domains used in the modeling of 2013.

Both of the 2013 episodes were run with a 10 day spinup period before the first episode day (July 3 and September 25). The WRF model was run in 5-day chunks. Once the model run was completed, we evaluated the model against CAMS monitor surface wind speed and direction data during the episode days. We focus the evaluation on winds and temperatures for the monitors that are being tested against the "but-for" criterion in this section.

6.2.2 WRF Model Performance Evaluation

In Figure 6-15 through Figure 6-24, we present the model performance evaluation of the WRF run against CAMS wind speed and wind direction measurements. Temperature was also evaluated, but the results are not shown here for the sake of brevity. The wind speed time series for both the July and September episodes indicate that WRF consistently overestimates wind speeds. This will cause the ozone model to underestimate ozone, as the WRF model will tend to produce more dispersion of ozone and precursors than is observed. The wind direction plots show that WRF does not show good skill in predicting shifts in wind direction. For s

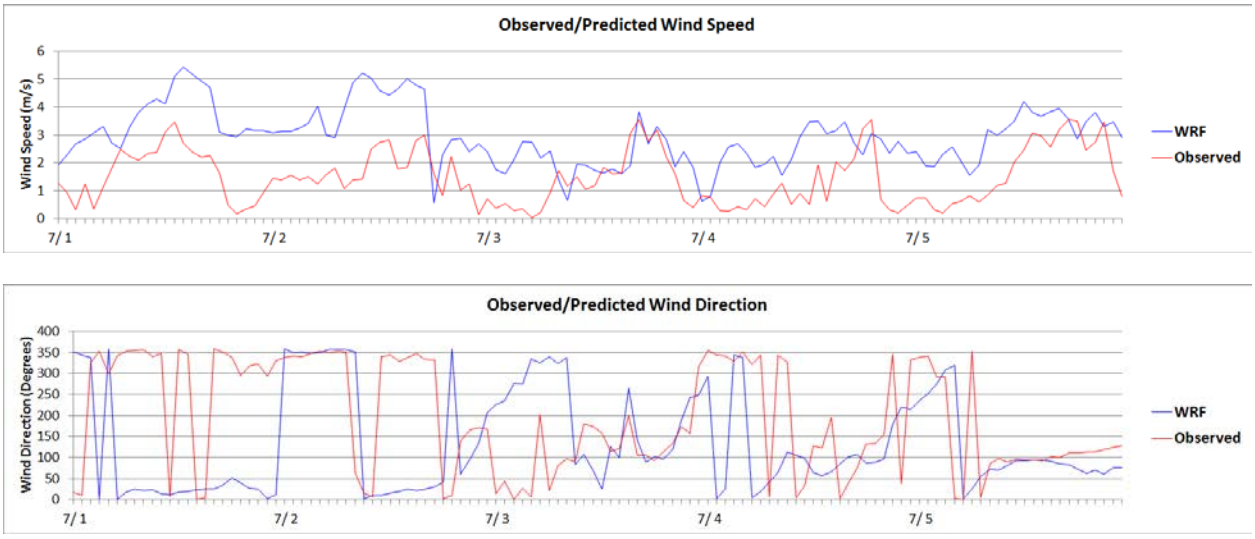

Figure 6-15. Northwest Harris County wind speed (upper panel) and wind direction (lower panel) for July 2013 episode.

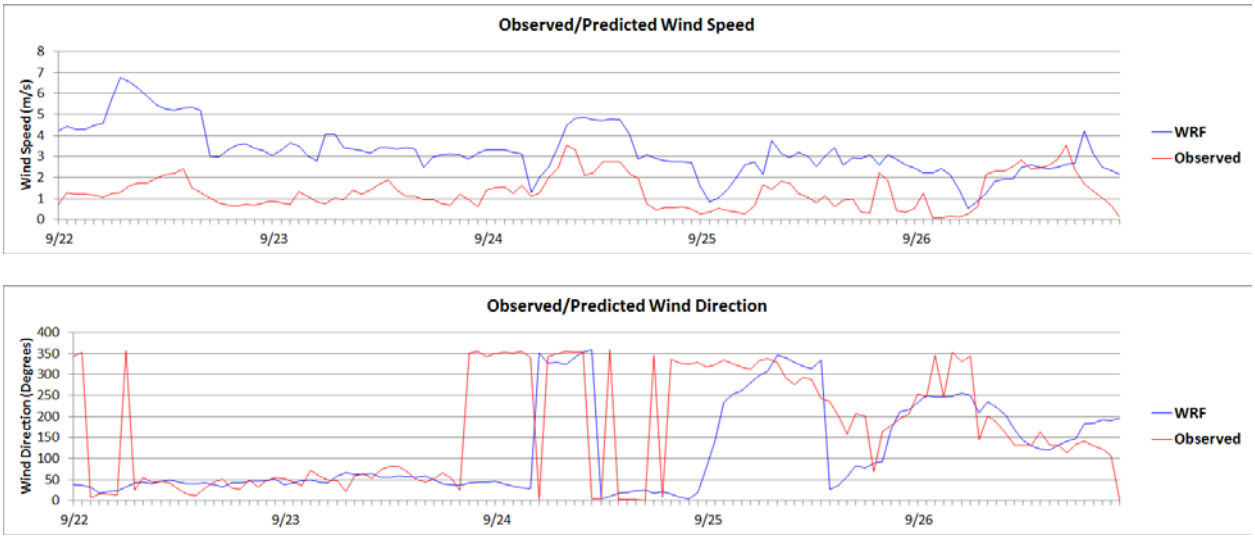

Figure 6-16. Northwest Harris County wind speed (upper panel) and wind direction (lower panel) for September 2013 episode.

example, on September 25, both the La Porte and Seabrook monitors saw an abrupt wind shift during midday as the sea breeze circulation transitioned to onshore winds at the monitors. The lower panel of Figure 6-20 and Figure 6-22 show that the WRF model captures the shift from northwesterly to southeasterly winds that appears in the observed winds, but the wind shift is delayed by four hours in the model. This type of sea breeze circulation occurs on spatial scales comparable to the model resolution and is very difficult to capture accurately. There is no monitor for which wind direction is well-simulated for the entire July or September episode, and we may expect the WRF model's overestimate of wind speeds and mis-timing of wind shifts to have a negative impact on the ozone model's performance.

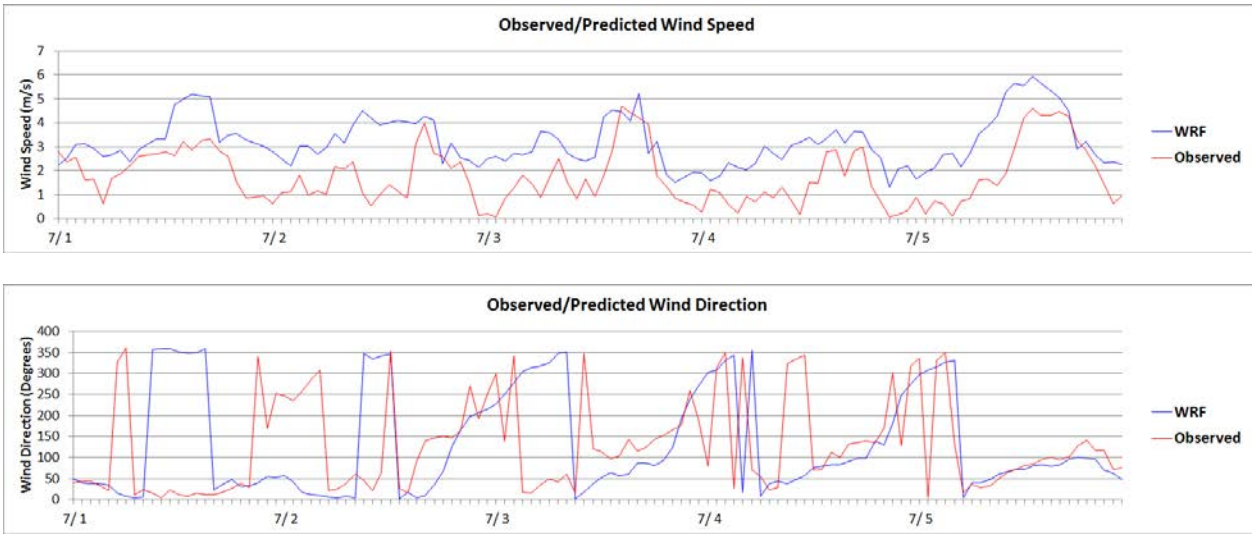

Figure 6-17. Manvel Croix wind speed (upper panel) and wind direction (lower panel) for July 2013 episode.

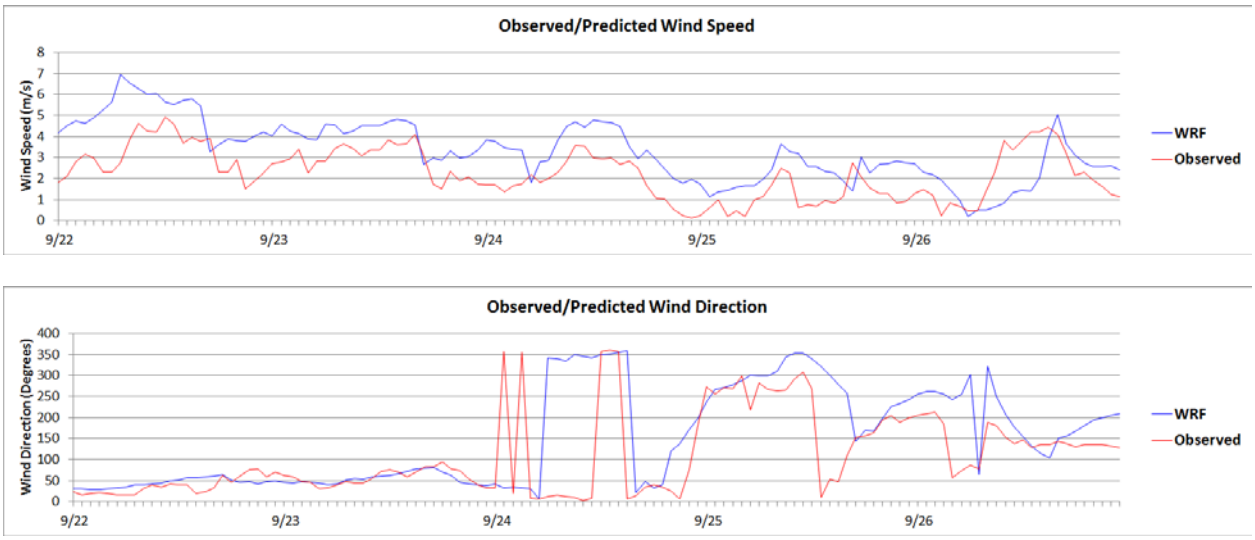

Figure 6-18. Manvel Croix wind speed (upper panel) and wind direction (lower panel) for September 2013 episode.

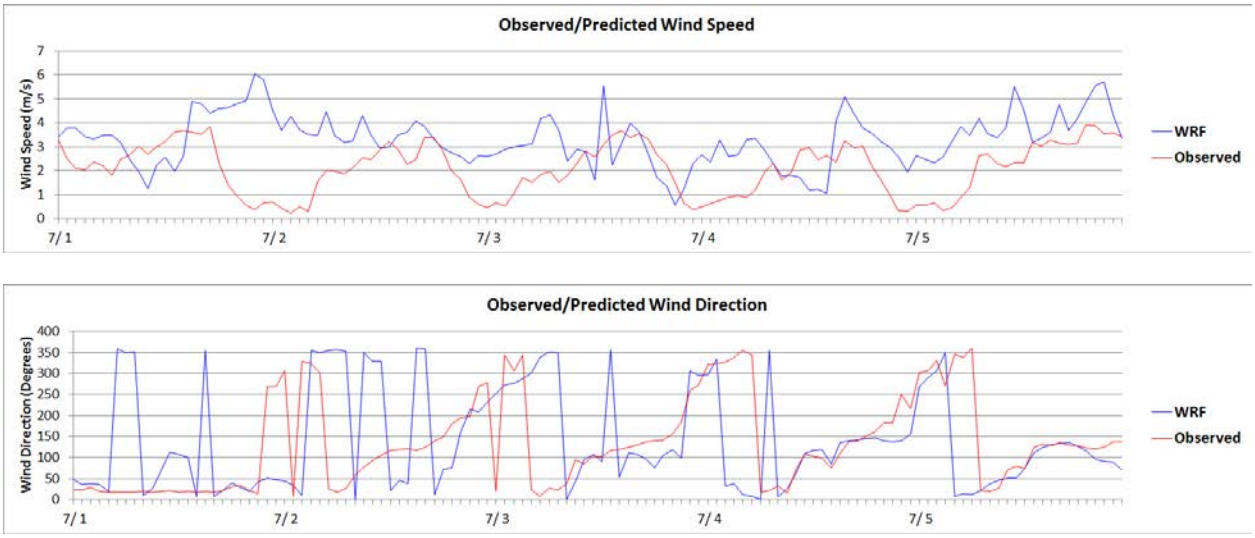

Figure 6-19. Seabrook wind speed (upper panel) and wind direction (lower panel) for July 2013 episode.

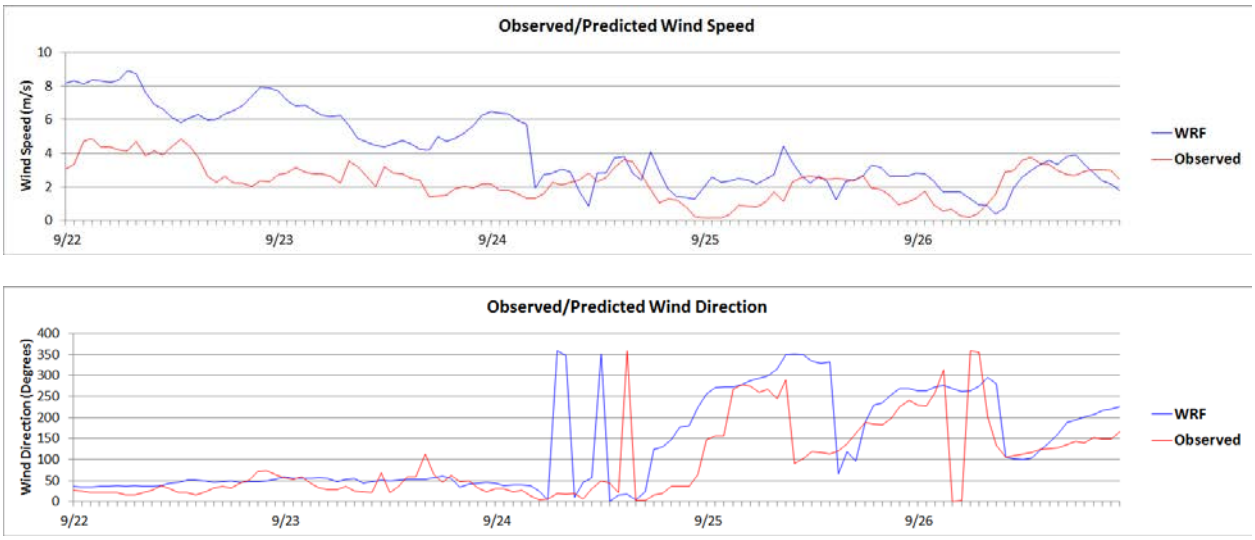

Figure 6-20. Seabrook wind speed (upper panel) and wind direction (lower panel) for September 2013 episode.

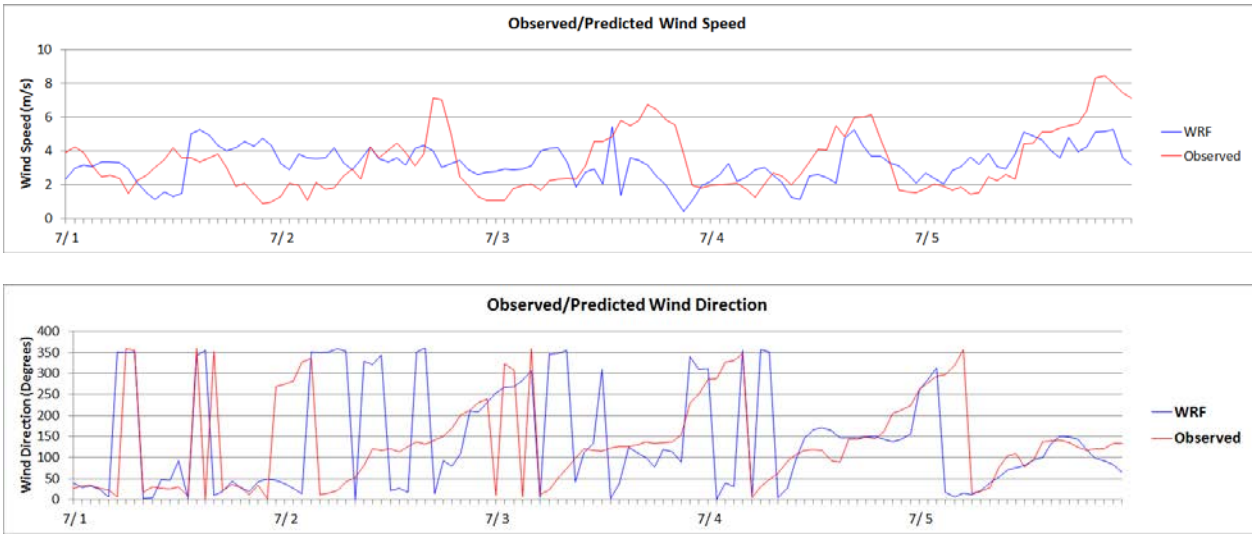

Figure 6-21. La Porte wind speed (upper panel) and wind direction (lower panel) for July 2013 episode.

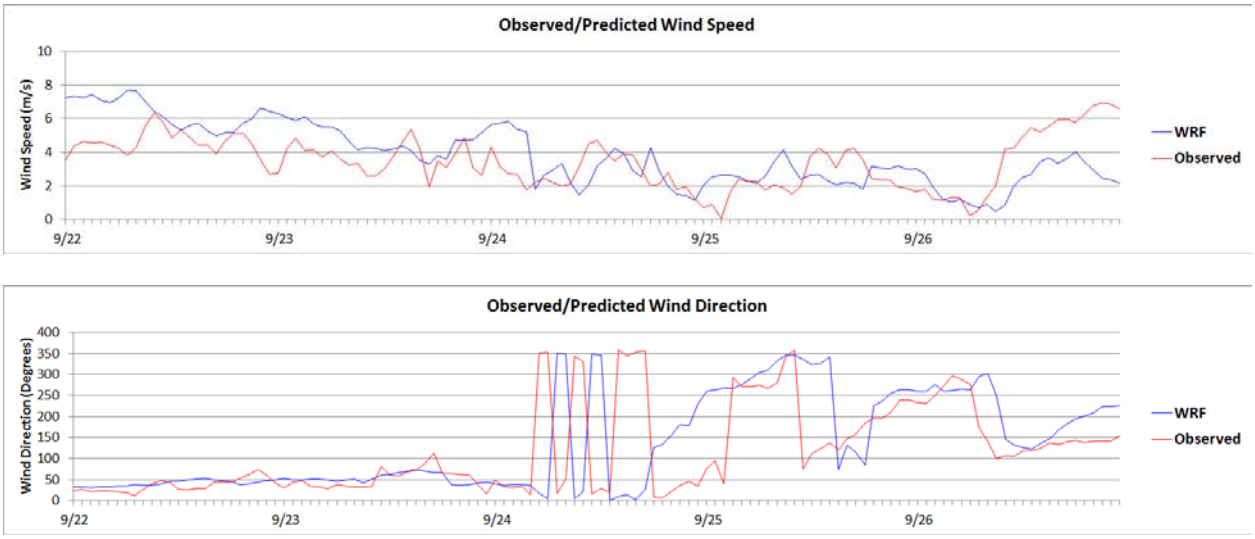

Figure 6-22. La Porte wind speed (upper panel) and wind direction (lower panel) for September 2013 episode.

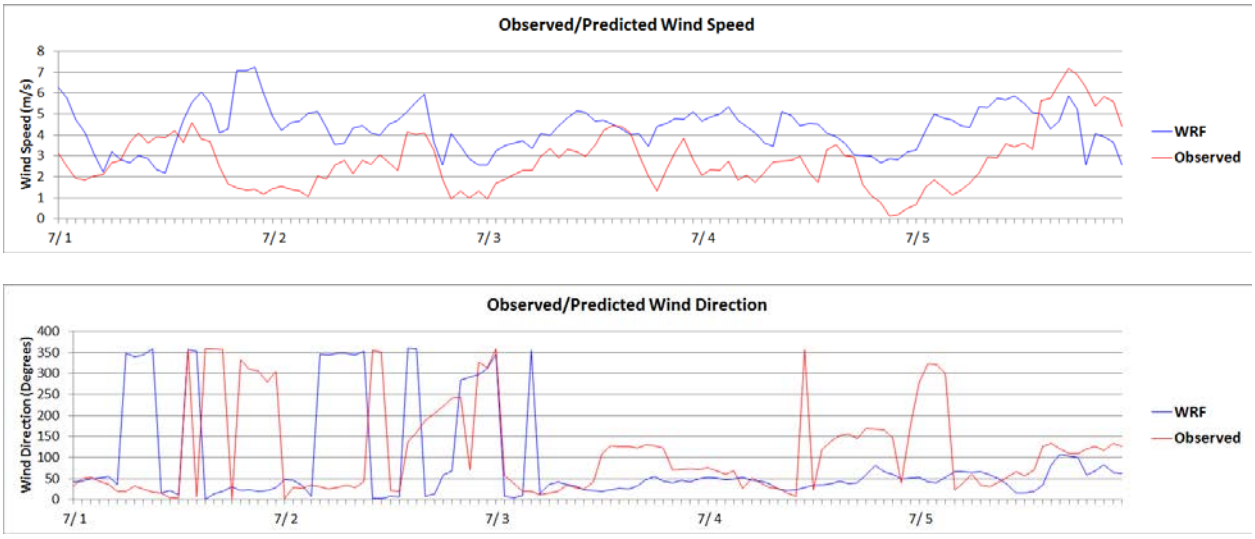

Figure 6-23. Sabine Pass wind speed (upper panel) and wind direction (lower panel) for July 2013 episode.

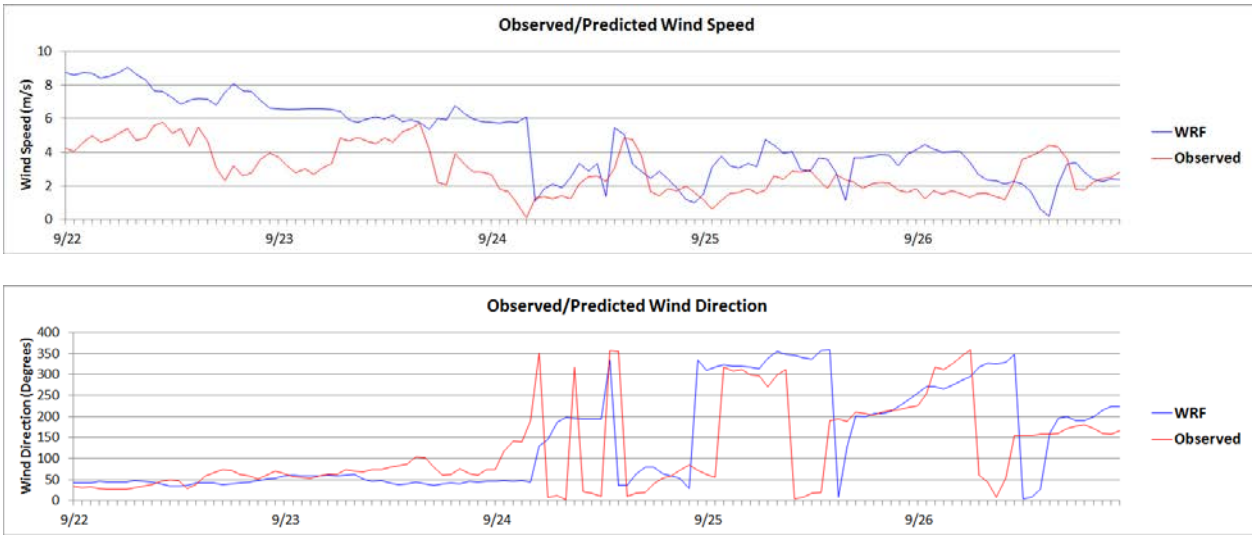

Figure 6-24. Sabine Pass wind speed (upper panel) and wind direction (lower panel) for September 2013 episode.

6.2.3 CAMx Model Performance Evaluation for Surface Layer Ozone: July 3-4, 2013

The CAMx model surface layer ozone for both runs was evaluated against 1-hour average ozone measured at TCEQ CAMS sites during the July 3-4, 2013 episode days (Figure 6-25 through Figure 6-29). We evaluated the model at HGB and BPA sites within the 4 km modeling domain that are highlighted in yellow in Table 3-3.

At the NW Harris County monitor (Figure 6-26), both CAMx runs show much less variability over the course of the two day period than the observed ozone. The nighttime ozone minima are far lower in the observations than in the model runs. On July 4, the model simulates the

background ozone relatively well, but misses the midday peak apparent in the observations. On July 5th, the modeled morning increase in ozone occurs earlier than in the observed ozone time series, and the morning peak is too high in the model. During the entire two day period, the run with fires has higher ozone than the run without fires, which indicates a persistent modeled impact on ozone due to fire emissions.

At Manvel Croix (Figure 6-26), fire impacts are evident on July 4th. In both model runs, the peak 1-hour ozone is underestimated. The emission inventory used for the 2013 modeling is a typical ozone season day emission inventory for the year 2012. On July 3 at 11 pm, the Shell Deer Park Refinery had an upset event that lasted through 10 pm on July 5[4]. During this event, process gas was routed to the facility's olefins flare system, resulting in emissions of several highly reactive volatile organic compounds (HRVOCs) including 3,606 lbs ethylene, 1,524 lbs propylene, and 1,054 lbs 1,3 butadiene. Based on the back trajectories shown in Figure 3-150, the Shell Deer Park Refinery was upwind of the Manvel Croix monitor on July 4, so it is possible that the HRVOC release could have influenced ozone at Manvel Croix, and this contribution could not be simulated in a model that uses a typical day emission inventory. As at the NW Harris county monitor, CAMx overestimates nighttime ozone values and fire emissions increased ozone slightly throughout the episode in the CAMx run with fires relative to the CAMx run without fires.

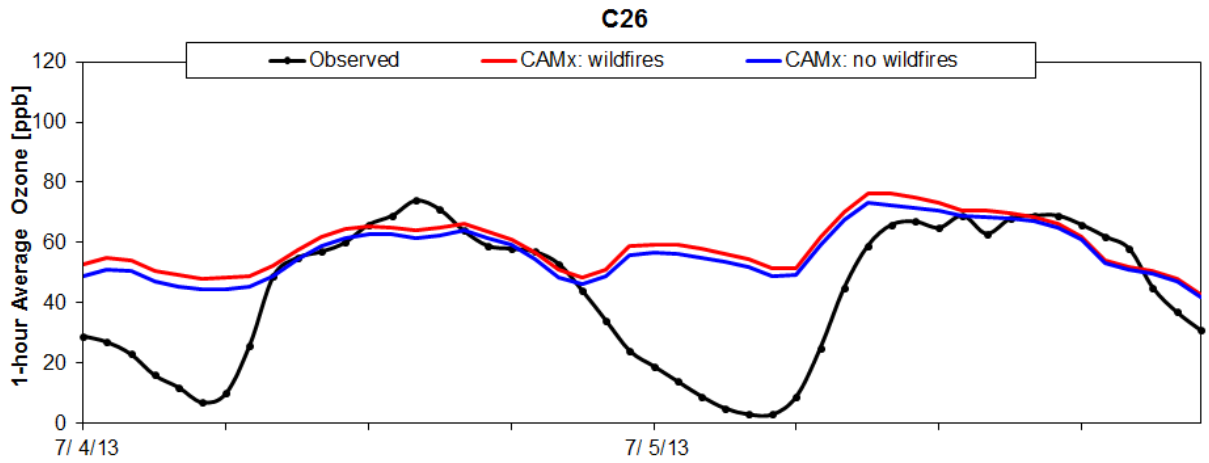

Figure 6-25. NW Harris County observed 1-hour ozone (black) versus modeled 1-hour average surface layer ozone for the CAMx run with fire emissions (red) and the CAMx run with no fire emissions (blue).

[4] http://www11.tceq.texas.gov/oce/eer/index.cfm?fuseaction=main.getDetails&target=185156

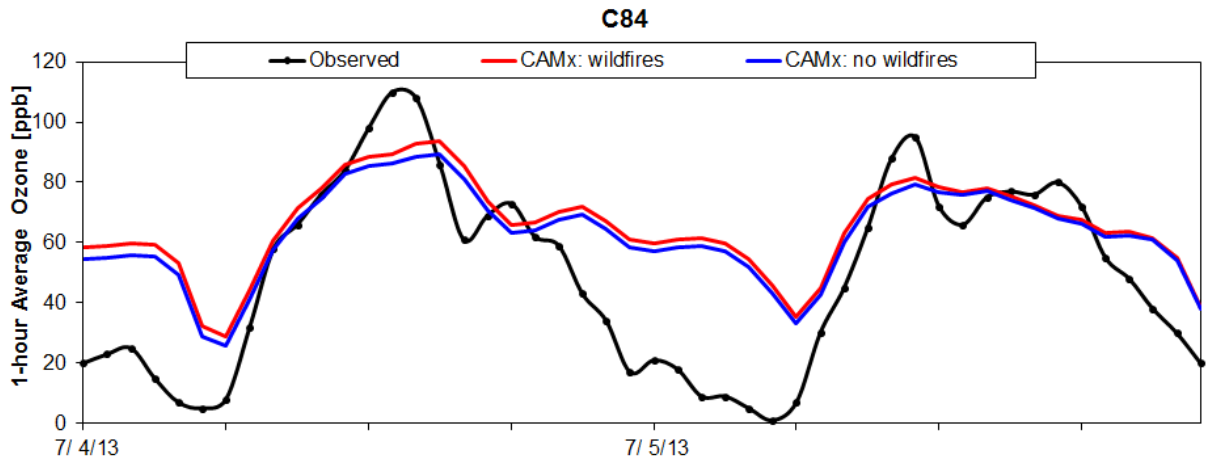

Figure 6-26. Manvel Croix observed 1-hour ozone (black) versus modeled 1-hour average surface layer ozone for the CAMx run with fire emissions (red) and the CAMx run with no fire emissions (blue).

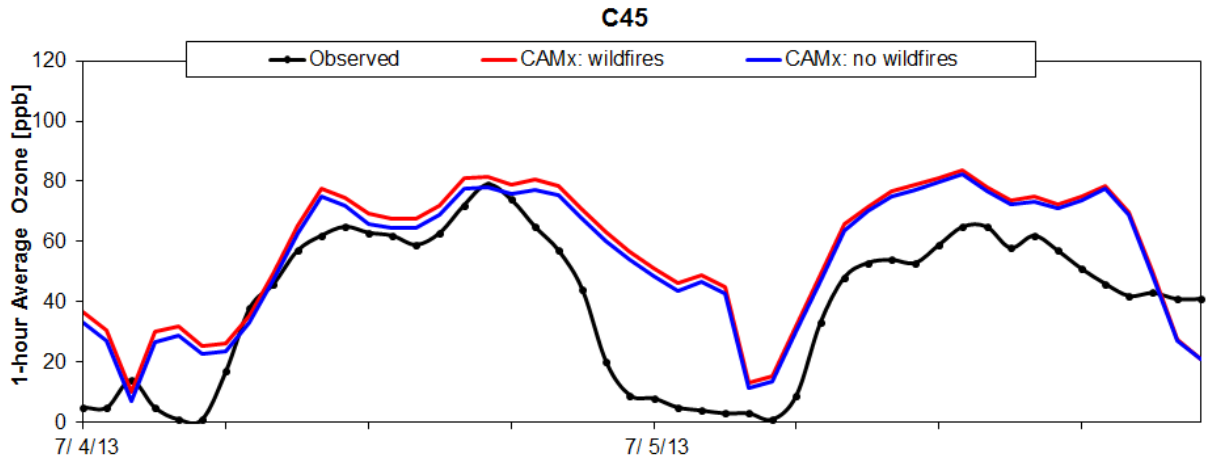

Figure 6-27. Seabrook observed 1-hour ozone (black) versus modeled 1-hour average surface layer ozone for the CAMx run with fire emissions (red) and the CAMx run with no fire emissions (blue).

CAMx performance at the Seabrook (Figure 6-27) and La Porte monitors (Figure 6-28) was similar. At both monitors, CAMx overestimates ozone throughout the period, and impacts from fire emissions increase ozone in the CAMx run with fires relative to the run without fires. At the Sabine Pass monitor (Figure 6-28), the model underestimates peak ozone on July 4, which is also the period of greatest impact to ozone from fire emissions. On July 5, the model underestimates peak ozone, although the nighttime ozone is well-simulated on both July 4 and July 5.

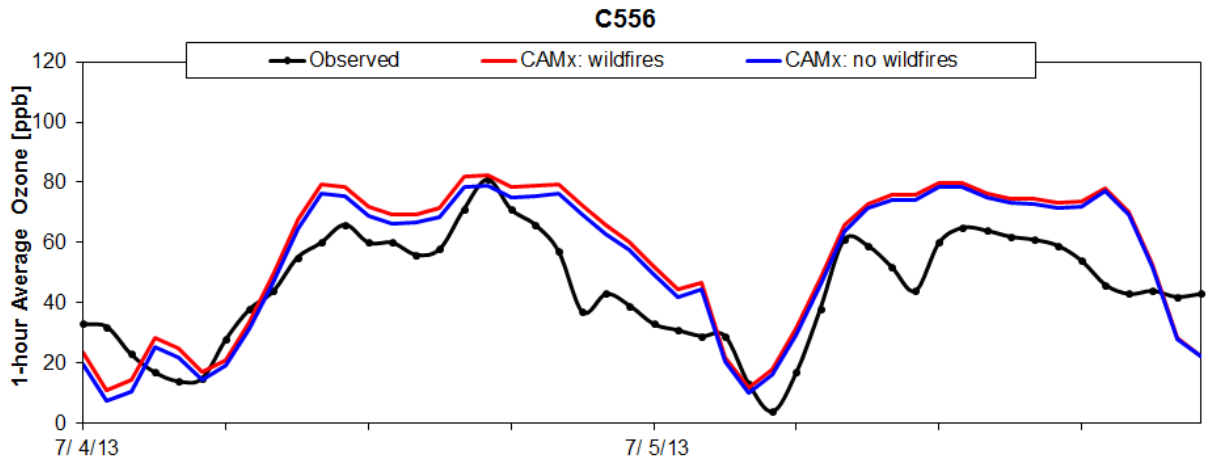

Figure 6-28. La Porte observed 1-hour ozone (black) versus modeled 1-hour average surface layer ozone for the CAMx run with fire emissions (red) and the CAMx run with no fire emissions (blue).

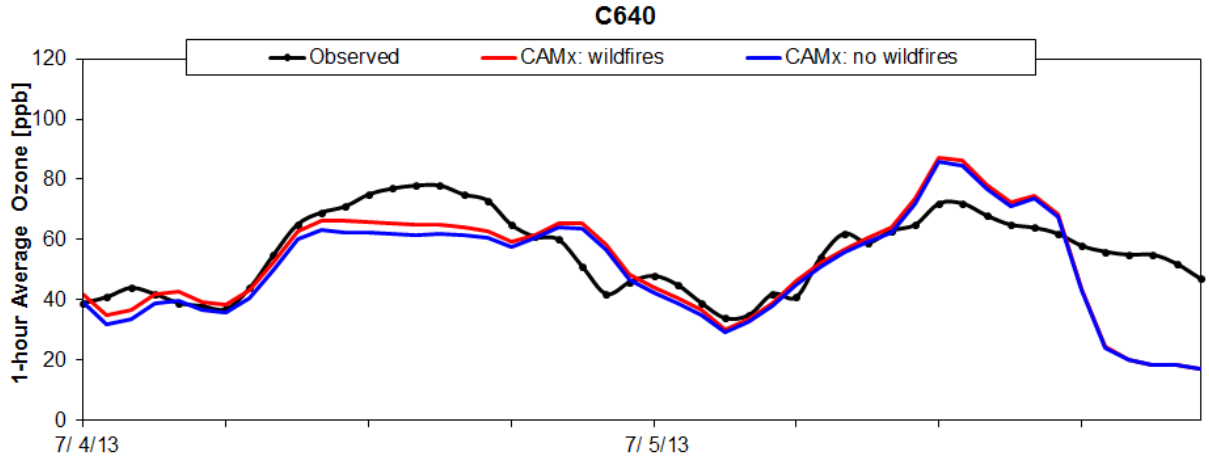

Figure 6-29. Sabine Pass observed 1-hour ozone (black) versus modeled 1-hour average surface layer ozone for the CAMx run with fire emissions (red) and the CAMx run with no fire emissions (blue).

6.2.4 Ozone Impacts from Fire Emissions: July 3-4, 2013

Below, we show the impacts on the MDA8 ozone from fire emissions for the July 3-4, 2013 episode.

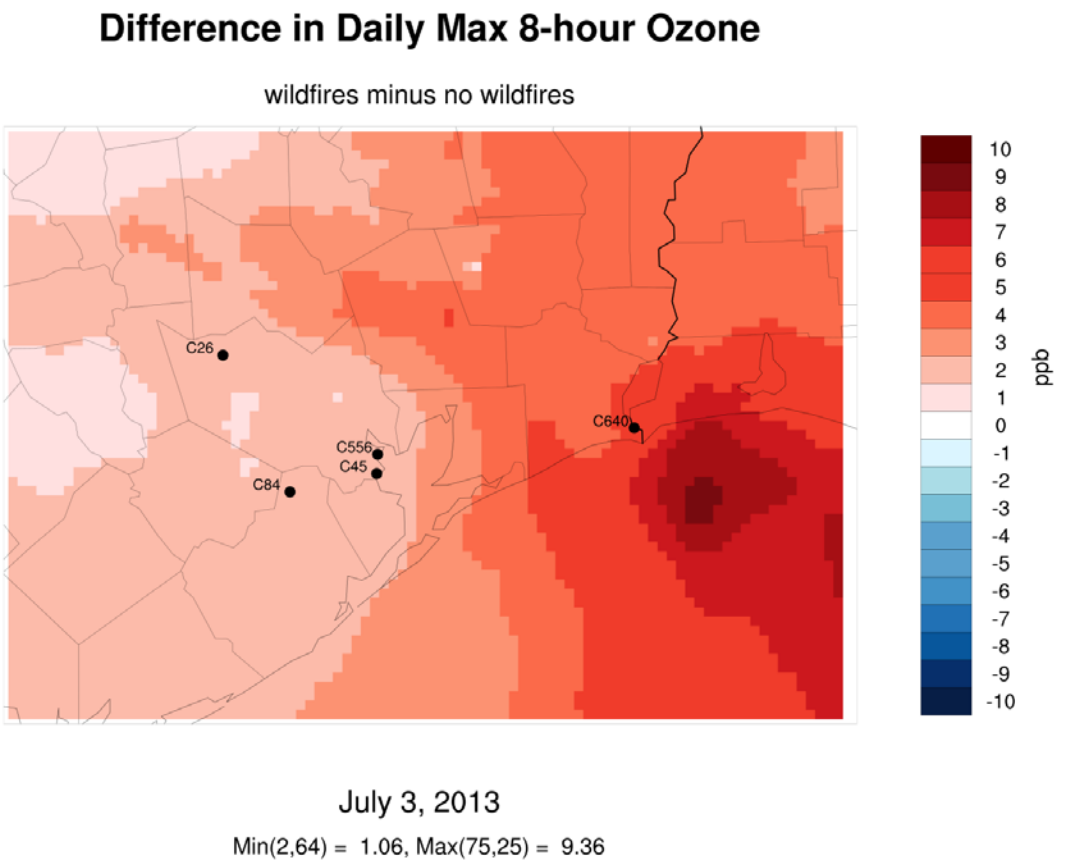

Figure 6-30. July 3, 2013 difference in MDA8 between CAMx run with fire emissions and CAMx run with no fire emissions.

On July 3, there are ozone impacts from fires across the 4 km modeling domain (Figure 6-30). At the NW Harris County (C26) monitor, the impacts of fire emissions on the MDA8 are ≤ 3 ppb. Impacts are 3 ppb or less at all of the HGB monitors shown in Figure 6-30. There is an area of ozone that is enhanced due to fire emissions over the Gulf of Mexico to the southeast of the BPA area, and fire emission impacts in this plume reach a maximum of 9 ppb.

Impacts on HGB monitor MDA8 are larger on July 4 than on July 3 (Figure 6-31). At the Manvel Croix monitor (C84), fire impacts on the MDA8 are ≤ 4 ppb and impacts are ≤ 4 ppb at the Sabine Pass monitor (C640). As on July 3, fire impacts are apparent across the 4 km domain on July 4. This is consistent with the HMS product and NAAPS smoke analyses, both of which showed smoke across the region of the 4 km modeling domain on July 3 and July 4.

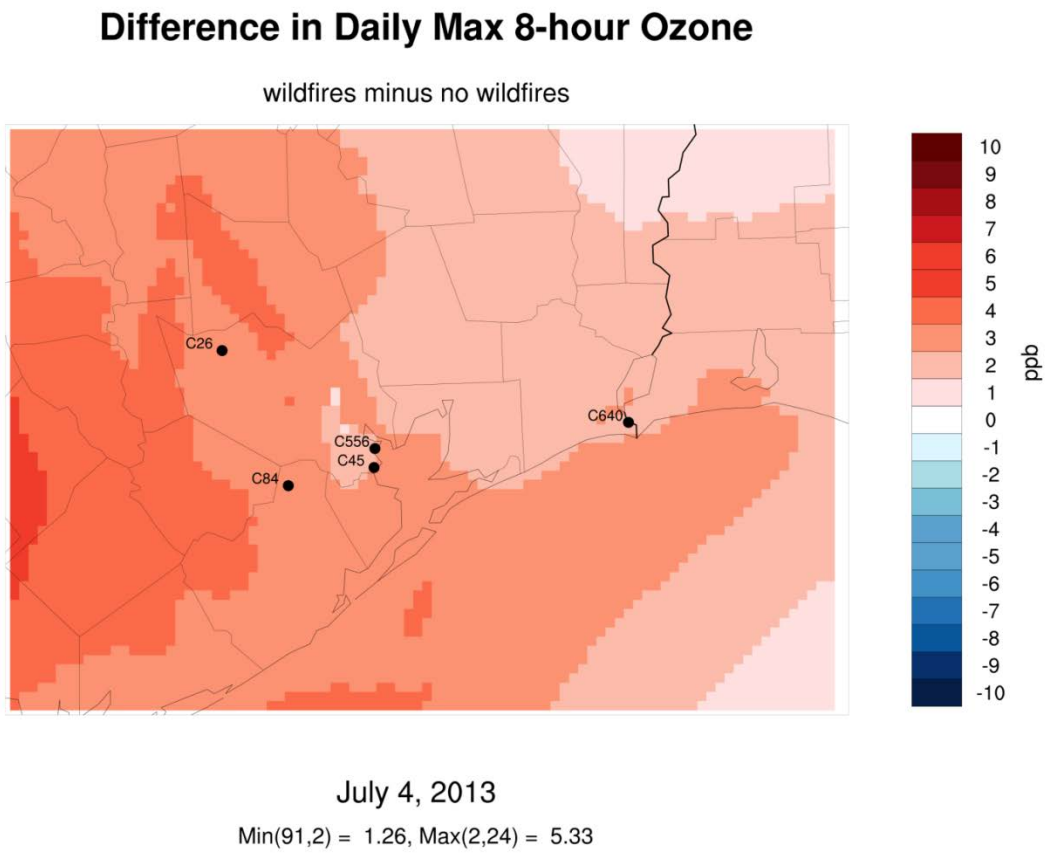

Figure 6-31. July 4, 2013 difference in MDA8 between CAMx run with fire emissions and CAMx run with no fire emissions.

6.2.5 CAMx Model Performance Evaluation for Surface Layer Ozone: September 25 2013

The CAMx model surface layer ozone for both runs was evaluated against 1-hour average ozone measured at TCEQ CAMS sites during the September 25, 2013 episode day (Figure 6-32 through Figure 6-36). We evaluated the model at HGB and BPA sites within the 4 km modeling domain.

At the NW Harris County monitor (Figure 6-32), the modeled ozone time series shows less variability than the observed profile. Modeled ozone is 40 ppb higher than observed ozone during the early morning of September 25. The modeled peak ozone value is similar to the observed peak, but the modeled peak occurs several hours too early in both model runs. At Manvel Croix (Figure 6-33), the same is true: the modeled peak occurs well before the observed peak. There is a late (7 pm) secondary maximum in the model runs that does not occur in the observed time series.

At the Seabrook and La Porte monitors (Figure 6-34, Figure 6-35), the model underestimates the observed peak values of ozone by ~55 ppb. Fire impacts are apparent in the afternoon hours at both monitors.

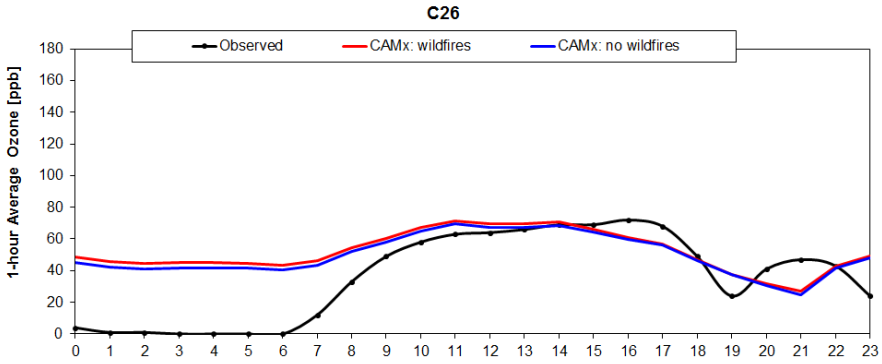

Figure 6-32. Northwest Harris County observed 1-hour ozone (black) versus modeled 1-hour average surface layer ozone for the CAMx run with fire emissions (red) and the CAMx run with no fire emissions (blue).

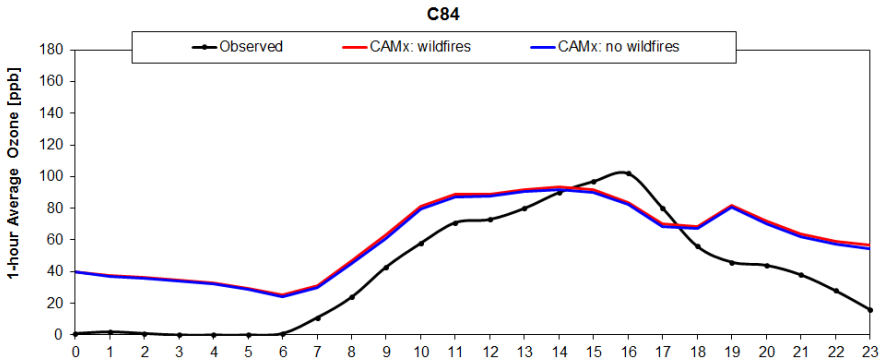

Figure 6-33. Manvel Croix observed 1-hour ozone (black) versus modeled 1-hour average surface layer ozone for the CAMx run with fire emissions (red) and the CAMx run with no fire emissions (blue).

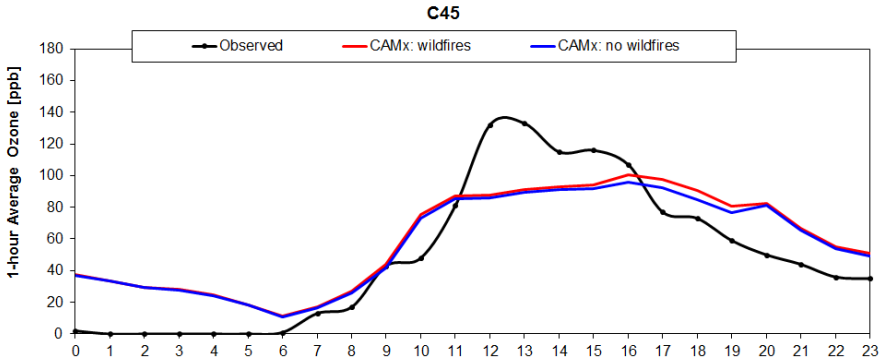

Figure 6-34. Seabrook observed 1-hour ozone (black) versus modeled 1-hour average surface layer ozone for the CAMx run with fire emissions (red) and the CAMx run with no fire emissions (blue).

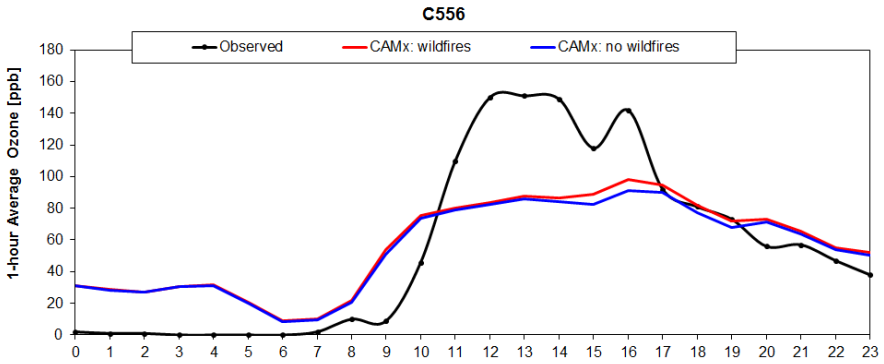

Figure 6-35. La Porte observed 1-hour ozone (black) versus modeled 1-hour average surface layer ozone for the CAMx run with fire emissions (red) and the CAMx run with no fire emissions (blue).

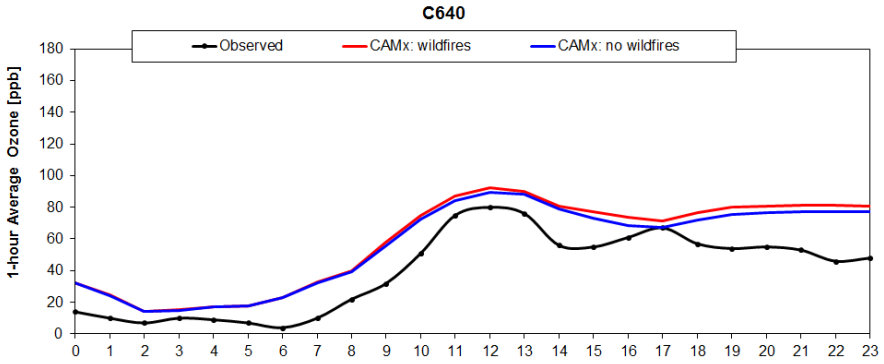

Figure 6-36. Sabine Pass observed 1-hour ozone (black) versus modeled 1-hour average surface layer ozone for the CAMx run with fire emissions (red) and the CAMx run with no fire emissions (blue).

At the Sabine Pass monitor (Figure 6-36), both model runs overestimate ozone throughout the day. Following the noon peak, observed ozone tapers off slowly over the course of the afternoon, while the modeled ozone remains high. Fire impacts on ozone are more pronounced later in the day at Sabine Pass.

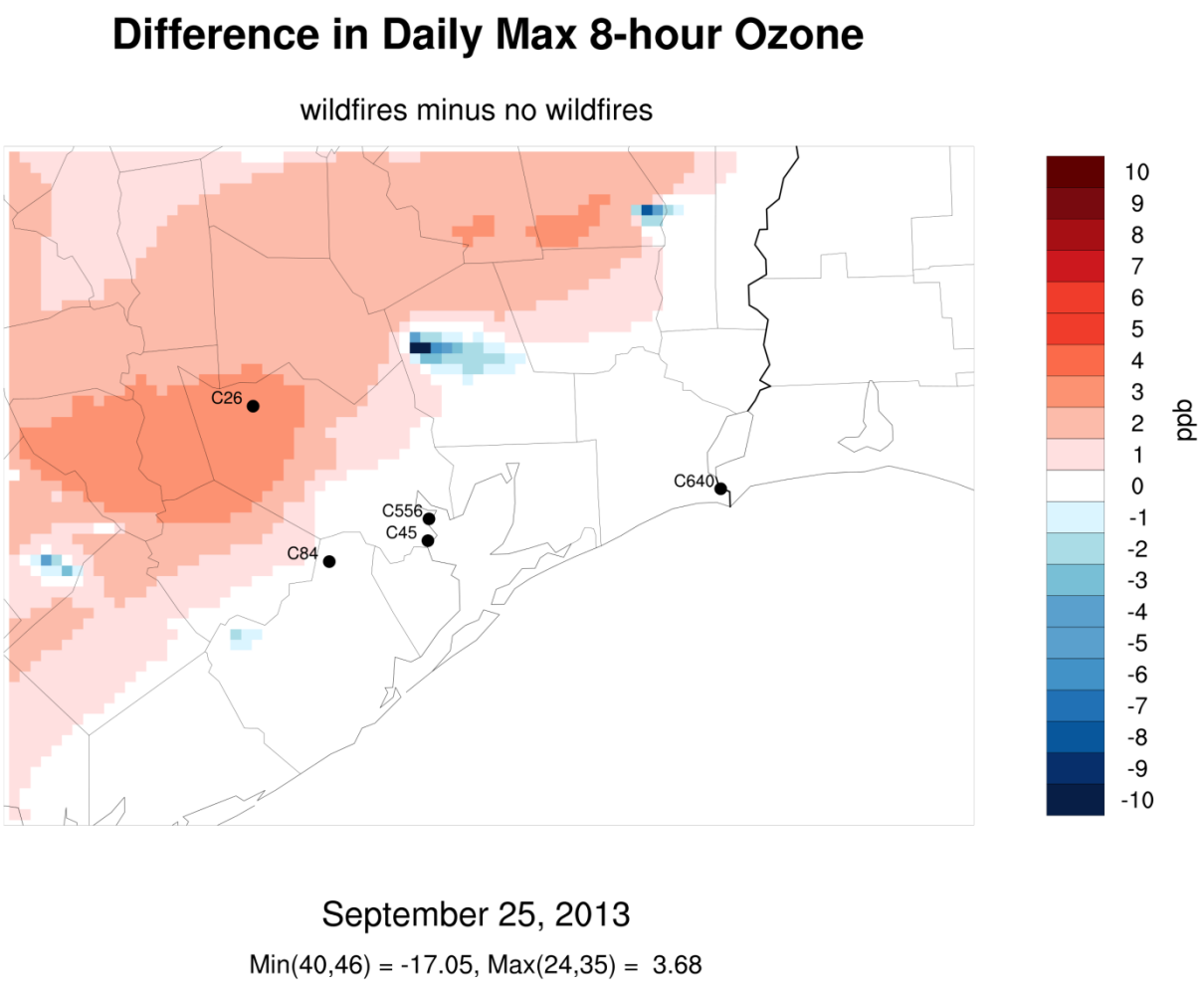

Figure 6-37. September 25, 2013 difference in MDA8 between CAMx run with fire emissions and CAMx run with no fire emissions..

6.2.6 Ozone Impacts from Fire Emissions: September 25, 2013

On September 25, 2013, ozone impacts due to fire emissions are apparent as a northeast-southwest oriented band across the modeling domain (Figure 6-37). Several active fires are visible within the 4 km modeling domain. The Seabrook and La Porte monitors are south of the region of the fire plume and have impacts that are ≤ 1 ppb.

6.3 Effect of Modeled Ozone Impacts on Design Values

In Table 6-3, we summarize the ozone modeling results. The maximum modeled impact on the MDA8 for each monitor/day is shown. The modeled impacts on the MDA8 range from 1-4 ppb. The modeled impact at each monitor was subtracted from the observed MDA8 in order to calculate the MDA8 that would have occurred but for the presence of the fire emissions and their effect on ozone. Next, we determined whether the lower value of the MDA8 (with fire impacts subtracted) would affect the value of the 4th high MDA for the year. For the Northwest Harris County monitor and the Manvel Croix monitors, the 4th high value was lowered for the year 2013. The reduction in the 4th high MDA8 resulted in a 1 ppb reduction of the 2013 design value. For Manvel Croix, the 2013 design value was reduced from 87 ppb to 86 ppb when fire impacts were subtracted from the July 4, 2013 MDA8. For the NW Harris County monitor, the 2013 design value was reduced from 82 ppb to 81 ppb when fire impacts were subtracted from the July 3, 2013 MDA8. For all other monitors listed in Table 6-3, there was no change to the 4th high MDA8 value for that year and therefore no change to the 2013 design value.

Table 6-3. Effect of modeled ozone impacts of fire emissions on 2013 design values.

Date	Monitor Name	Observed MDA8 (ppb)	Maximum Modeled Impact on MDA8 from (ppb)	MDA8 but for the fire emissions (ppb)	Change in 4th high MDA8?	Change in 2013 Design Value (ppb)	Resulting 2013 Design Value (ppb)
6/25/2012	Grapevine Fairway	97	2	95	No	0	86
6/25/2012	Denton Airport South	81	2	79	No	0	87
6/27/2012	Grapevine Fairway	92	2	90	No	0	86
6/27/2012	Denton Airport South	95	2	93	No	0	87
7/3/2013	Northwest Harris Co.	80	3	77	Yes	-1	81
7/4/2013	Manvel Croix	86	4	82	Yes	-1	86
7/4/2013	Sabine Pass	74	4	70	No	0	75
9/25/2013	Seabrook	104	1	103	No	0	77
9/25/2013	La Porte	124	1	123	No	0	78

The photochemical modeling results indicate that none of the monitors/days shown in Table 6-3 meet the EER “but-for” criterion.

7.0 SUMMARY AND RECOMMENDATIONS

The purpose of this study was to assess whether the 2012 and 2013 design values for the HGB, BPA, and DFW areas may have been influenced by wildfire emissions, and whether any days contributing to the design value might be excluded from comparison with the NAAQS under the EER. We reviewed the four highest 8-hour ozone days in 2012 and 2013 at the monitors with the highest and second-highest design values in the HGB and DFW areas as well as the monitor with the highest design value in the BPA area and two additional days selected by the TCEQ at the Seabrook and La Porte monitors in the HGB area.

For each of these high ozone days, we evaluated the potential for fire emissions to have influenced monitored ozone. We reviewed available ambient monitoring data, model data, emission inventories and satellite products, and determined whether emissions from fires are likely to have contributed to the MDA8 at monitors with high ozone on each day. For each day we reviewed, we determined whether a clear, causal connection between fire emissions and high monitored ozone was apparent. For each day where a clear, causal relationship with upwind fire(s) was evident, we determined whether the measured MDA8 was in excess of historical fluctuations by analyzing the frequency distribution of MDA8 ozone at that monitor for the period 2006-2013 and assessing whether the day in question had MDA8 above the 95th percentile. Finally, we used a photochemical model to quantify the contribution of fire emissions to ozone at each monitor in order to determine whether the "but-for" EER criterion was met. The results of the analysis are shown in Table 7-1, which lists all 2012-2013 days with fire influence that met the "clear, causal relationship" criterion and notes whether each day met the remaining two EER criteria.

Table 7-1. Comparison of high ozone days showing clear, causal relationship with fire emissions with the remaining three EER criteria.

Date	Monitor Name	CAMS Number	Area	2013 Design Value (ppb)	Exceptional Event Rule Criteria			
					Fire(s) Present Upwind?	Clear Causal Relationship?	Concentration in Excess of Historical Backgound?	Passes "But-For" Test?
6/25/2012	Grapevine Fairway	70	DFW	86	Yes	Yes	Yes	No
6/25/2012	Denton Airport South	56	DFW	87	Yes	Yes	No	No
6/27/2012	Grapevine Fairway	70	DFW	86	Yes	Yes	Yes	No
6/27/2012	Denton Airport South	56	DFW	87	Yes	Yes	Yes	No
7/3/2013	Northwest Harris Co.	26	HGB	82	Yes	Yes	Yes	No
7/4/2013	Manvel Croix	84	HGB	87	Yes	Yes	Yes	No
7/4/2013	Sabine Pass	640	BPA	75	Yes	Yes	Yes	No
9/25/2013	Seabrook	45	HGB	77	Yes	Yes	Yes	No
9/25/2013	La Porte	556	HGB	78	Yes	Yes	Yes	No

All days listed in Table 7-1 met the "concentration in excess of historical fluctuation" criterion except for June 25, 2012 at Denton. Because the 95th percentile criterion is not a bright line test

for determining whether a day can be considered to be an exceptional event[5], this does not rule out June 25, 2012 at Denton, but indicates that EPA may require a more extensive demonstration for June 25th than it would for a day that exceeds the 95th percentile.

The photochemical modeling results showed that none of the 2012 or 2013 days evaluated in this study passed the EER "but-for" test. Modeled impacts on MDA8 ozone due to fire emissions were sufficiently small that no violations or exceedances of the NAAQS would be removed by subtracting the modeled ozone impacts of fire emissions from the observed MDA8. However, it is important to note the uncertainties inherent in photochemical modeling of fires and their impact on ozone.

The modeled ozone impacts of fires depend on accurate characterization of fire emissions and simulation of the transport, chemical transformation, and fate of emitted ozone precursors and the ozone that forms from them. Fire emissions contain uncertainties in both their magnitude and their chemical composition (e.g. Wiedinmyer et al. 2011; Jaffe and Wigder, 2012). The chemical composition of the emissions plays a role in the photochemistry of the resulting fire plume and therefore the resulting ozone impact.

The chemistry of ozone production in fire plumes is an area of active research. Measurement campaigns in which aircraft made transects through fire plumes and measured ozone and other trace gases have produced a range of results regarding the magnitude of ozone production in fire plumes (e.g. Bertschi et al., 2004; Alvarado et al; 2010). Jaffe and Wigder (2012) note that there is not a clear relationship between the quantity of ozone precursor emissions released into the atmosphere and the ozone produced in the plume downwind of the fire. Wigder et al. (2013) hypothesize that plume rise and the altitude of subsequent plume transport can affect ozone production in the plume because temperatures are lower at higher altitudes.

The interaction of fire plumes with anthropogenic emissions is not well understood. Singh et al. (2012) and Wigder et al. (2013) found enhanced ozone in fire plumes that mixed with air containing urban emissions. The presence of aerosols (smoke) in the fire plume can reduce the amount of sunlight available to initiate photochemistry, inhibiting ozone formation (e.g. Parrington et al., 2013). The TCEQ's SIP modeling is focused on ozone and does not include simulation of aerosols, so this "aerosol shading" mechanism is absent in our modeling of 2012 and 2013.

Photochemical modeling is one method of carrying out a "but-for" analysis for a candidate exceptional event, and other methods are available. For example, ozone concentrations at a given monitor on a high ozone day can be compared to ozone at that monitor on days when ozone was low but weather conditions were similar. By comparing days with comparable weather, the contribution of fire emissions to ozone at the monitor on a high ozone day can be estimated though comparison with ozone values on all other days with similar weather, implicitly making an assumption that the presence of the fire is the only source of difference.

[5] http://www.epa.gov/ttn/caaa/t1/fr_notices/exeventfr.pdf

Because all available methods of carrying out the "but-for" analysis have limitations, a weight of evidence approach may be indicated in which multiple analysis methods are carried out and the results compared. The conclusions from such a comparison would take into account the uncertainties inherent in each method.

The photochemical modeling performed in this study could be refined through the use of day-specific emission inventories. The WRF meteorological modeling of 2013 should be evaluated in more detail and sensitivity testing to determine whether a configuration can be found that better simulates the surface wind shifts on high ozone days should be performed Meteorological model evaluation for 2013 will be undertaken as part of Texas Air Quality Research Program (AQRP) Project 14-016. We did not evaluate the 2012 WRF meteorological model inputs to CAMx, but this should be done as well and further testing undertaken if problems with model performance are found.

The work plan for this project allowed for the Desert Research Institute (DRI) to analyze particulate matter (PM) filters collected at DFW and HGB area monitors for the presence of the biomass burning markers levoglucosan and mannosan in order to provide a definitive conclusion as to whether fire emissions influenced ozone at DFW and HGB monitors on days of interest. No filters were available for the BPA area (Richard Tropp, DRI, personal communication, 2014). Due to equipment malfunction, DRI was unable to carry out this analysis during the time frame of this study. Laboratory analysis of available PM filters for levoglucosan and mannosan will provide an unambiguous determination as to whether a fire plume was present at each monitor for which data are available and should be carried out when possible.

Summary of Recommendations

- Perform PM filter analysis for levoglucosan/mannosan for days listed in Table 7-1
- Carry out a "but-for" analysis using alternate method(s) and compare with photochemical modeling results
- Review the representation of chemistry of ozone formation within fire plumes in CAMx and evaluate whether updates to the model are required to allow accurate simulation of fire plumes in the TCEQ's SIP modeling
- Refine photochemical modeling analysis through the use of day-specific emissions and improvement of WRF model performance in simulating surface winds in the 2013 episodes
- Evaluate WRF model performance for 2012 and improve if necessary

8.0 TECHNICAL SYSTEMS AUDIT

As part of the assessment and oversight procedures, a technical systems audit was performed, as stated in the project Quality Assurance Project Plan (QAPP; ENVIRON, 2014b). A thorough, systematic qualitative audit of facilities, equipment, personnel, training, procedures, record keeping, data validation, data management, and reporting was carried out by ENVIRON. The purpose of the technical systems audit was to assess whether project personnel and equipment were functioning properly and that all procedures were implemented as prescribed in the QAPP and the project Work Plan. The technical systems audit was carried out by Lan Ma, a Senior Associate at ENVIRON's Novato Office. Ms. Ma did not participate in the project up until the time when she carried out the technical systems audit during the last week of July, 2014. By the end of July, the project technical work was completed and the work had been presented to the TCEQ project manager at a meeting at TCEQ headquarters in Austin, TX.

To assist her carrying out the audit, Ms. Ma was provided with the charts shown in Table 8-1 through Table 8-3 below, which indicate the person responsible for each technical task, the data used in each task, the person responsible for quality assurance (QA) of each task, and the percentage of data that were audited. She was also provided with the presentation given to TCEQ summarizing the project results, and a draft of the final report. She then carried out a series of interviews of personnel listed in Table 8-1 through Table 8-3 and documented her findings, which are shown in Section 8.2.

8.1 Quality Control Flow

The charts shown in Table 8-1 through Table 8-3 provide a schematic showing how QA was performed during this project and were provided to the auditor prior to the beginning of the audit.

Table 8-1. Quality assurance flow for high ozone day analysis.

Quality Assurance Flow	Data Used in High Ozone Day Analysis						
	Monitor Data	Back Trajectories			Fire Locations/Emissions		Satellite/Analysis/Model Products
	CAMS Data	AQPlot	HYSPLIT	SmartFire	FINN Emissions	SmartFire	HMS, NAAPS, EPA, AQI, NWS Maps
Prepared by	Thomas Pavlovic	Thomas Pavlovic	Justin Zagunis	Thomas Pavlovic	Ed Tai	Thomas Pavlovic	Thomas Pavlovic, Sue Kemball-Cook
Used in	Time series, spatial plots	Back trajectory plots			Spatial Plots, ozone modeling	Fire location maps	Maps of AOD, PM, ozone, smoke, fire location
QA by	Sue Kemball-Cook, Lynsey Parker	Sue Kemball-Cook, Lynsey Parker	Sue Kemball-Cook, Lynsey Parker	Sue Kemball-Cook, Lynsey Parker	Thomas Pavlovic, Sue Kemball-Cook, Lynsey Parker	Sue Kemball-Cook, Lynsey Parker	Sue Kemball-Cook, Lynsey Parker
Data Audited	100%	100%	100%	100%	100%	100%	100%

Table 8-2. Quality assurance flow for the analysis of speciated PM data and evaluation of whether MDA8 ozone on a given high ozone day was exceptional compared to historical values.

Quality Assurance Flow	Speciated PM Analysis and Historical Ozone Analysis	
	Speciated CAMS PM Data	MDA8 Frequency Distribution Plots
Prepared by	Thomas Pavlovic	Sue Kemball-Cook
Used in	Time series of organic carbon and elemental carbon	Assessment of whether days contributing to 2013 DVs had exceptionally high MDA8 ozone compared to historical values at each monitor
QA by	Sue Kemball-Cook	Lynsey Parker
Data Audited	100%	100%

Table 8-3. Quality assurance flow for photochemical modeling.

Quality Assurance Flow	Data Used in Photochemical Grid Modeling			
	CAMS Data (Ozone, Winds, Temperatures)	2012 WRF Model Data	2013 WRF Model Data	2012/2013 CAMx Model Data
Prepared by	Lynsey Parker	TCEQ	DJ Rasmussen	DJ Rasmussen
Used in	Evaluating WRF and CAMx performance against observed data	WRF model outputs were used as inputs to the CAMx photochemical model	WRF model outputs were used as inputs to the CAMx photochemical model	Evaluating MDA8 ozone impacts of fire emissions
QA by	Jeremiah Johnson, Sue Kemball-Cook	Jeremiah Johnson, Sue Kemball-Cook	Jeremiah Johnson, Sue Kemball-Cook	Jeremiah Johnson, Sue Kemball-Cook
Data Audited	100%	25%	50%	100%

8.2 Auditor's Statement

As part of the procedure stated in the Quality Assurance Project Plan (QAPP), I conducted a third-party, technical audit for the project by interviewing six key staff on data handling, modeling procedures, and quality assurance. Below is a summary of findings.

The identification of high ozone days was performed objectively without reviewing other parameters such as wild fire events. The ozone time-series plots, AQPlot and HYPLIT back trajectories, and SmartFire plots were developed independently to reduce errors. A trained staff with knowledge of the local meteorological conditions and of model performance and constraints conducted a detailed review of the plots for all days of interest. This was crucial especially because back trajectories from different models sometimes did not agree, a trained staff was able to qualitatively evaluate if there were any real or inconclusive correlations.

The fire locations from the FINN and SmartFire databases and satellite maps captured different range of resolution and details of wild fire events, but these locations were qualitatively compared as a high-level QA. The FINN emissions data had to be converted to a different map

projection and grouped to 1km or 5km zones. QA was performed by plotting the outputs in PAVE to ensure fires events occurred at reasonable locations after the data was processed.

The speciated PM analysis was used a marker for biomass burning events. However, at the time of the audit interviews, this data quality assurance had not been thoroughly carried out.

Input data for the WRF model were obtained from a third party. A model performance evaluation compared the predicted temperature and winds against the observations for the Houston area for 2013. For all days of interest, the evaluation showed that model outputs matched relatively well with observation after time zone and averaging periods were adjusted. Again, such adjustment required experience with the background of the model as well as the collection and reporting of the observed data. A trained staff was able to resolve the initial differences during this QA procedure. Similarly, CAMx modeling output were also evaluated by comparing to observed ozone data for all days of interest. Plots were made to visually QA for reasonableness. NOx output were also used as a QA by geo-locating with expected emissions sources such as fires and road-ways, which further assures the performance of the models.

In conclusion, the QA process was performed by experienced and professional staff who understood the constraints of various models and differences across models; they were able to explain well the trends observed or the lack thereof. They also adopted various methods of QA to reduce systematic errors and increase the quality of the procedures. After conducting the auditing interviews, I am satisfied with the steps carried out to ensure the quality of the procedures and the data.

Signature: 

Date: August 8, 2014

Name: Lan Ma

Title: Senior Associate
ENVIRON International Corporation

9.0 ACKNOWLEDGEMENTS

We thank Jim Mackay of the TCEQ for providing 2012 and 2013 anthropogenic emissions and to Doug Boyer of the TCEQ for providing 2012 WRF meteorological inputs and biogenic emissions.

We thank John Simko and Mark Ruminski of the NOAA/NESDIS Satellite Analysis Branch for providing the archived HMS maps and Christine Wiedinmyer of NCAR for supplying the FINN fire emission inventories for 2012 and 2013.

We acknowledge the NOAA Air Resources Laboratory (ARL) for the provision of the HYSPLIT READY website (http://www.ready.noaa.gov) used in this study.

10.0 REFERENCES

Alvarado, M.J., Logan, J.A., Mao, J., et al. 2010. Nitrogen oxides and PAN in plumes from boreal fires during ARCTAS-B and their impact on ozone: An integrated analysis of aircraft and satellite observations. *Atmos. Chem. and Phys.* 10, 9739−9760.

Berlin, S., A.O. Langford, M. Estes, M. Dong and D.D. Parrish (2013). Magnitude, Decadal Changes, and Impact of Regional Background Ozone Transported into the Greater Houston, Texas, Area. *Env. Sci. Tech*. 47, 13,985−13,992. dx.doi.org/10.1021/es4037644.

Bertschi, I.B., Jaffe, D.A., 2005. Long-range transport of ozone, carbon monoxide and aerosols to the NE Pacific troposphere during the summer of 2003: observations of smoke plumes from Asian Boreal fires. *J. Geophys. Res*. 110, D05303. doi:10.1029/2004JD005135.

Cheng, Y., G. Engling, K.-B. He, F.-K. Duan, Y.-L. Ma, Z.-Y. Du, J.-M. Liu, M. Zheng, and R. J. Weber. 2013. Biomass burning contribution to Beijing aerosol. *Atmos. Chem. Phys*., 13, 7765–7781, 2013. www.atmos-chem-phys.net/13/7765/2013/ doi:10.5194/acp-13-7765-2013

Draxler, R.R. and Rolph, G.D. (2013). HYSPLIT (HYbrid Single-Particle Lagrangian Integrated Trajectory) Model access via NOAA ARL READY Website (http://www.arl.noaa.gov/HYSPLIT.php). NOAA Air Resources Laboratory, College Park, MD.

Duncan, B.N., Prados, A.I., Lamsal, L., Liu, Y., Streets, D., Gupta, P., Hilsenrath, E., Kahn, R., Nielsen, J.E., Beyersdorf, A., Burton, S., Fiore, A.M., Fishman, J., Henze, D., Hostetler, C., Krotkov, N.A., Lee, P., Lin, M., Pawson, S., Pfister, G., Pickering, K.E., Pierce, B., Yoshida, Y., Ziemba, L., Satellite Data of Atmospheric Pollution for U.S. Air Quality Applications: Examples of Applications, Summary of Data End-User Resources, Answers to FAQs, and Common Mistakes to Avoid. 2014. *Atmos. Env* (2014), doi: 10.1016/j.atmosenv.2014.05.061.

ENVIRON, 2014a. The User's Guide to the Comprehensive Air Quality Model with Extensions Version 6.10. Available from Environ International Corporation, 773 San Marin Drive, Novato, CA. 94998 and at http://www.camx.com.

ENVIRON, 2014b. Quality Assurance Project Plan for WO582-11-10365-FY14-19. Prepared for Jonathan Steets. April.

US EPA, Developing Spatially Interpolated Surfaces and Estimating Uncertainty, Environmental Protection Agency, Research Triangle Park, NC. Emissions, Monitoring, and Analysis Div., Technical Report, Nov 2004.

US EPA, The Air Quality Index, http://airnow.supportportal.com/link/portal/23002/23002/Article/16115/How-are-your-ozone-maps-calculated, Accessed May 2014.

Hu, Y., Odman, M. T., Chang, M. E., Jackson, W., Lee, S., Edgerton, E. S., ... & Russell, A. G. (2008). Simulation of air quality impacts from prescribed fires on an urban area. *Env. Sci. & Tech*, 42(10), 3676-3682.

Jaffe, D., D. Chand, W. Hafner, A. Westerling, and D. Spracklen (2008), Influence of fires on O(3) concentrations in the western US, *Env. Sci. & Tech*., 42(16), 5885-5891.

Jaffe, D. and Wigder, N., (2012). Ozone production from wildfires: A critical review. *Atmos. Env.*, 51 (2012) 1-10.

Johnson, J., P. Karamchandani, G. Wilson, and G. Yarwood, (2013). TCEQ Ozone Forecasting System. Prepared for Mark Estes, TCEQ. November.

Junquera , V., M.M. Russell, W. Vizuete, Y. Kimura, and D. Allen (2005), Wildfires in eastern Texas in August and September 2000: Emissions, aircraft measurements, and impact on photochemistry, *Atmos. Env*., 39(27), 4983-4996.

McDonald, S. and F. Mercado, 2006. Using AQPlot to Compare MM5 Wind Fields to Observed Data. TCEQ presentation available at http://www.tceq.texas.gov/assets/public/implementation/air/am/committees/pmt_set/20060523/20060523-mcdonad-AQPlot_mm5_wind.pdf .

NOAA, About the SSD Fire and Smoke Program, http://www.ssd.noaa.gov/PS/FIRE/about.html, 2014a, Accessed May 2014.

NOAA, Center for Satellite Applications and Research (STAR), http://www.star.nesdis.noaa.gov/star/index.php, 2014b, Accessed May 2014.

Simoneit, B., J.J. Schauer, C.G. Nolte, D.R. Oros, V.O. Elias, M.P. Fraser, W.F. Rogge, and G.R. Cass. Levoglucosan, a tracer for cellulose in biomass burning and atmospheric particles. *Atmos. Env.* Volume 33, Issue 2, January 1999, Pages 173–182

Singh, H.B., Anderson, B.E., Brune, W.H., Cai, C., Cohen, R.C., Crawford, J.H., Cubison, M.J., Czech, E.P., Emmons, L., Fuelberg, H.E., Huey, G., Jacob, D.J., Jimenez, J.L., Kaduwela, A., Kondo, Y., Mao, J., Olson, J.R., Sachse, G.W., Vay, S.A., Weinheimer, A., Wennberg, P.O., Wisthaler, A., 2010. Pollution influences on atmospheric composition and chemistry at high northern latitudes: boreal and California forest fire emissions. *Atmos. Env*. 44, 4553e4564.

van Donkelaar, A., R. V. Martin, M. Brauer, R. Kahn, R. Levy, C. Verduzco, and P. J. Villeneuve. 2010. Global estimates of ambient fine particulate matter concentrations from satellite-based aerosol optical depth: Development and application, *Environ. Health Perspec.*, doi:10.1289/ehp.0901623.

Wiedinmyer, C., S. K. Akagi, R. J. Yokelson, L. K. Emmons, J. A. Al-Saadi, J. J. Orlando, and A. J. Soja (2011), The Fire INventory from NCAR (FINN): a high resolution global model to

estimate the emissions from open burning, *Geoscientific Model Development*, 4(3), 625-641.

Zhang, H., Hoff, R.M., Engel-Cox, J.A. 2009: The relation between Moderate Resolution Imaging Spectroradiometer (MODIS) aerosol optical depth and $PM_{2.5}$ over the United States: a geographical comparison by EPA regions, *J. Air & Waste Manage. Assoc*.

Zhang, Y. D. Obrist, B. Zielinska and A. Gertler. 2013. Particulate emissions from different types of biomass burning. *Atmos. Env*., 72, Pages 27–35.